به نام خدا

مرکز دانلود رایگان
مهندسی متالورژی و مواد

www.Iran-mavad.com

CORROSION OF WELDMENTS

The Materials Information Society

Corrosion of Weldments

Edited by
J. R. Davis
Davis & Associates

ASM International®
Materials Park, OH 44073-0002
www.asminternational.org

First printing, December 2006

Comments, criticisms, and suggestions are invited, and should be forwarded to ASM International.

Prepared under the direction of the ASM International Technical Books Committee, Yip-Wah Chung, FASM, Chair (2005–2006).

ASM International staff who worked on this project include Charles Moosbrugger, Product Developer; Diane Grubbs, Editorial Assistant; Madrid Tramble, Senior Production Coordinator; Diane Wilkoff, Production Coordinator; Scott Henry, Senior Manager of Product and Service Development; Bonnie Sanders, Manager of Production and Eleanor Baldwin, Research Librarian.

Library of Congress Cataloging-in-Publication Data

Corrosion of weldments / edited by J. R. Davis.
p. cm.
Includes bibliographical references and index.
ISBN-13: 978-0-87170-841-0
ISBN-10: 0-87170-841-8
1. Steel, Structural—Welding. 2. Steel, Structural—Corrosion. 3. Welded joints. I. Davis, J. R. (Joseph R.)

TS227.2.C68 2006
671.5′2—dc22

2006051209

SAN: 204-7586

ASM International®
Materials Park, OH 44073-0002
www.asminternational.org

Printed in the United States of America

Contents

Preface . . . . . **vii**

Chapter 1 Basic Understanding of Weld Corrosion **1**
Factors Influencing Corrosion of Weldments 1
Weld Microstructures 1
Forms of Weld Corrosion 3
Welding Practice to Minimize Corrosion 10

Chapter 2 Corrosion of Carbon Steel and Low-Alloy Steel Weldments **13**
Classification of Steels and Their Welding Characteristics 13
Carbon Steels 13
Low-Alloy Steels 14
Corrosion Considerations for Carbon and Low-Alloy Steel Weldments 15
Corrosion of Carbon Steel Weldments 19
Influence of Weld Microstructure 19
Residual Stress 19
Geometrical Factors 19
Preferential HAZ Corrosion 20
Preferential Weld Metal Corrosion 21
Mitigation of Preferential Weldment Corrosion 21
Galvanic Corrosion 23
Environmentally Assisted Cracking (EAC) 24
Wet Hydrogen Sulfide Cracking 25
Stress-Corrosion Cracking 25
Hydrogen-Induced Cracking 33
Effect of Welding Practice on Weldment Corrosion 35

Chapter 3 Corrosion of Austenitic Stainless Steel Weldments **43**
Grade Designations 43
Standard Grades 43
Nonstandard Grades 43
Properties 47
General Welding Considerations 48
Corrosion Behavior 48
Intergranular Corrosion 49

Preferential Attack Associated with Weld Metal Precipitates . . . 52
Pitting and Crevice Corrosion . . . 53
Stress-Corrosion Cracking . . . 58
Microbiologically Induced Corrosion . . . 62
Other Factors Influencing Corrosion of Weldments . . . 66

Chapter 4 Corrosion of Ferritic Stainless Steel Weldments . . . 77
Grade Classifications . . . 77
Properties . . . 79
General Welding Considerations . . . 80
Corrosion Behavior . . . 82
Hydrogen Embrittlement . . . 82
Intergranular Corrosion . . . 83
Avoiding Intergranular Corrosion . . . 84
Example 1: Leaking Welds in a Ferritic Stainless Steel Wastewater Vaporizer . . . 87
Example 2: Weld Failure Due to Intergranular Corrosion and Cracking in a Heat-Recovery Steam Generator . . . 89

Chapter 5 Corrosion of Duplex Stainless Steel Weldments . . . 99
Duplex Stainless Steel Development and Grade Designations . . . 99
Microstructure and Properties . . . 100
General Welding Considerations . . . 103
Corrosion Behavior of Weldments . . . 105
Corrosion Behavior of Alloy 2205 Weldments . . . 109

Chapter 6 Corrosion of Martensitic Stainless Steel Weldments . . . 115
Grade Designations . . . 115
Standard Grades . . . 115
Nonstandard Grades . . . 116
Properties . . . 117
General Welding Considerations . . . 118
Corrosion Behavior . . . 118

Chapter 7 Corrosion of High-Nickel Alloy Weldments . . . 125
Types of Corrosion-Resistant Alloys (CRAs) . . . 125
General Welding Considerations . . . 130
Welding Metallurgy of CRAs Containing Molybdenum . . . 132
Welding Metallurgy of Ni-Cu, Ni-Cr, and Ni-Cr-Fe CRAs . . . 134
Corrosion Behavior . . . 134
Phase Stability of Nickel-Base Alloys and Corrosion Behavior . . . 137

Chapter 8 Corrosion of Nonferrous Alloy Weldments . . . 143
Aluminum and Aluminum Alloys . . . 143
General Welding Considerations . . . 143
Corrosion Behavior of Aluminum Alloy Weldments . . . 144
Copper and Copper Alloys . . . 155
General Welding Considerations . . . 155
Corrosion Behavior of Copper Weldments . . . 155

Titanium and Titanium Alloys 156
General Welding Considerations 157
Corrosion Behavior of Titanium and Titanium Alloy Weldments 158
Zirconium and Zirconium Alloys 160
General Welding Considerations 161
Corrosion Behavior of Zirconium and Zirconium Alloy Weldments 162
Tantalum and Tantalum Alloys 164
General Welding Considerations 164
Corrosion Behavior of Tantalum and Tantalum Alloy Weldments 164

Chapter 9 Corrosion of Dissimilar Metal Weldments 169
Factors Influencing Joint Integrity 169
Corrosion Behavior 173

Chapter 10 Weld Corrosion in Specific Industries and Environments . . 177
Corrosion of Weldments in Petroleum Refining and Petrochemical Operations 177
Fabricability Considerations 177
Wet H_2S Cracking 178
Hydrogen-Induced Disbonding 181
Liquid Metal Embrittlement 181
Stress-Corrosion Cracking of Weldments in BWR Service 183
BWR Piping Systems 183
Stress-Corrosion Cracking of Pipe Weldments 183
Model for IGSCC 184
Weld Residual Stresses 185
Mitigation of IGSCC in Boiling Water Reactors 187
Materials Solutions 188
Tensile Stress Reduction Solutions 189
Environmental Solutions 190
Corrosion in the Pulp and Paper Industry 191
Pulp Production 191
Corrosion of Weldments in Pulp Bleach Plants 196

Chapter 11 Monitoring and Testing of Weld Corrosion 203
Corrosion Monitoring 203
Direct Testing of Coupons 203
Electrochemical Techniques 206
Nondestructive Testing Techniques 207
Corrosion Testing 208
Tests for Intergranular Corrosion 209
Tests for Pitting and Crevice Corrosion 213
Tests for SCC 213
Tests for MIC 215

Index 217

Preface

Welding is one of the most important processes for fabricating metallic structures. The study of welding metallurgy has long been addressed by academia, industry, and organizations such as the American Welding Society and the Edison Welding Institute in the United States and The Welding Institute in the United Kingdom. Similarly, extensive research has been carried out on the fundamentals of corrosion and the various types of corrosion that can render a structure useless. *Corrosion of Weldments* explores both of these important disciplines and describes how the welding process can influence both microstructural and corrosion behavior. Hydrogen-induced cracking of steel weldments, sensitization and subsequent intergranular corrosion of stainless steel weldments, sulfide stress cracking of pipeline steel weldments, microbiologically induced corrosion of weldments, and stress-corrosion cracking of weldments are addressed in detail. Although emphasis has been placed on carbon steels and stainless steels, nonferrous alloys such as high-nickel alloys, aluminum alloys, and titanium alloys also are covered. Weld corrosion in some important industries and environments also is reviewed as are methods for monitoring corrosion and testing of weldments.

As always I would like to acknowledge the support of the ASM editorial and production staffs during work on this project. In particular, I would like to thank Project Editor Charles Moosbrugger for his help and patience. I hope our combined efforts will result in a lasting contribution to the technical literature.

Joseph R. Davis
Davis & Associates
Chagrin Falls, Ohio

ASM International is the society for materials engineers and scientists, a worldwide network dedicated to advancing industry, technology, and applications of metals and materials.

ASM International, Materials Park, Ohio, USA
www.asminternational.org

Publication title	Product code
Corrosion of Weldments	05182G

To order products from ASM International:

Online Visit www.asminternational.org/bookstore

Telephone 1-800-336-5152 (US) or 1-440-338-5151 (Outside US)

Fax 1-440-338-4634

Mail Customer Service, ASM International
9639 Kinsman Rd, Materials Park, Ohio 44073-0002, USA

Email CustomerService@asminternational.org

In Europe American Technical Publishers Ltd.
27-29 Knowl Piece, Wilbury Way, Hitchin Hertfordshire SG4 0SX, United Kingdom
Telephone: 01462 437933 (account holders), 01462 431525 (credit card)
www.ameritech.co.uk

In Japan Neutrino Inc.
Takahashi Bldg., 44-3 Fuda 1-chome, Chofu-Shi, Tokyo 182 Japan
Telephone: 81 (0) 424 84 5550

Corrosion of Weldments
J.R. Davis, editor, p 1-12
DOI:10.1361/corw2006p001

CHAPTER 1

Basic Understanding of Weld Corrosion

CORROSION FAILURES OF WELDS occur in spite of the fact that the proper base metal and filler metal have been selected, industry codes and standards have been followed, and welds have been deposited that possess full weld penetration and have proper shape and contour. It is not unusual to find that, although the wrought form of a metal or alloy is resistant to corrosion in a particular environment, the welded counterpart is not. Further welds can be made with the addition of filler metal or can be made autogenously (without filler metal). However, there are also many instances in which the weld exhibits corrosion resistance superior to that of the unwelded base metal. There also are times when the weld behaves in an erratic manner, displaying both resistance and susceptibility to corrosive attack.

Factors Influencing Corrosion of Weldments

It is sometimes difficult to determine why welds corrode; however, one or more of the following factors often are implicated:

- Weldment design
- Fabrication technique
- Welding practice
- Welding sequence
- Moisture contamination
- Organic or inorganic chemical species
- Oxide film and scale
- Weld slag and spatter
- Incomplete weld penetration or fusion
- Porosity
- Cracks (crevices)
- High residual stresses
- Improper choice of filler metal
- Final surface finish

Metallurgical Factors. The cycle of heating and cooling that occurs during the welding process affects the microstructure and surface composition of welds and adjacent base metal. Consequently, the corrosion resistance of autogenous welds and welds made with matching filler metal may be inferior to that of properly annealed base metal because of:

- Microsegregation
- Precipitation of secondary phases
- Formation of unmixed zones
- Recrystallization and grain growth in the weld heat-affected zone (HAZ)
- Volatilization of alloying elements from the molten weld pool
- Contamination of the solidifying weld pool

Corrosion resistance can usually be maintained in the welded condition by balancing alloy compositions to inhibit certain precipitation reactions, by shielding molten and hot metal surfaces from reactive gases in the weld environment, by removing chromium-enriched oxides and chromium-depleted base metal from thermally discolored (heat tinted) surfaces, and by choosing the proper welding parameters.

Weld Microstructures

Weldments exhibit special microstructural features that need to be recognized and understood in order to predict acceptable corrosion service life of welded structures (Ref 1). This

chapter describes some of the general characteristics associated with the corrosion of weldments. The role of macrocompositional and microcompositional variations, a feature common to weldments, is emphasized in this chapter to bring out differences that need to be realized in comparing corrosion of weldments to that of wrought materials. More extensive presentations, with data for specific alloys, are given in the chapters which immediately follow.

Weldments inherently possess compositional and microstructural heterogeneities, which can be classified by dimensional scale. On the largest scale, a weldment consists of a transition from wrought base metal through an HAZ and into solidified weld metal and includes five microstructurally distinct regions normally identified (Ref 2) as the fusion zone, the unmixed region, the partially melted region, the HAZ, and the unaffected base metal. This microstructural transition is illustrated in Fig. 1. The unmixed region is part of the fusion zone, and the partially melted region is part of the HAZ, as described below. Not all five zones are present in any given weldment. For example, autogenous (that is, no filler metal) welds do not have an unmixed zone.

The fusion zone is the result of melting which fuses the base metal and filler metal to produce a zone with a composition that is most often different from that of the base metal. This compositional difference produces a galvanic couple, which can influence the corrosion process in the vicinity of the weld. This dissimilar-metal couple can produce macroscopic galvanic corrosion.

The fusion zone itself offers a microscopic galvanic effect due to microstructural segregation resulting from solidification (Ref 3). The fusion zone also has a thin region adjacent to the fusion line, known as the unmixed (chilled) region, where the base metal is melted and then quickly solidified to produce a composition similar to the base metal (Ref 4). For example, when type 304 stainless steel is welded using a filler metal with high chromium-nickel content, steep concentration gradients of chromium and nickel are found in the fusion zone, whereas the unmixed zone has a composition similar to the base metal (Fig. 2).

Heat-Affected Zone. The HAZ is the portion of the weld joint which has experienced peak temperatures high enough to produce solid-state microstructural changes but too low to cause any melting. Every position in the HAZ relative to the fusion line experiences a unique thermal experience during welding, in terms of both maximum temperature and cooling rate. Thus, each position has its own microstructural features and corrosion susceptibility.

The partially melted region is usually one or two grains into the HAZ relative to the fusion line. It is characterized by grain boundary liquation, which may result in liquation cracking. These cracks, which are found in the grain boundaries one or two grains below the fusion line, have been identified as potential initiation sites for hydrogen-promoted underbead cracking in high-strength steel.

Unaffected Base Metal Finally, that part of the workpiece that has not undergone any metallurgical change is the unaffected base metal. Although metallurgically unchanged, the unaffected base metal, as well as the entire weld joint, is likely to be in a state of high residual transverse and longitudinal shrinkage stress,

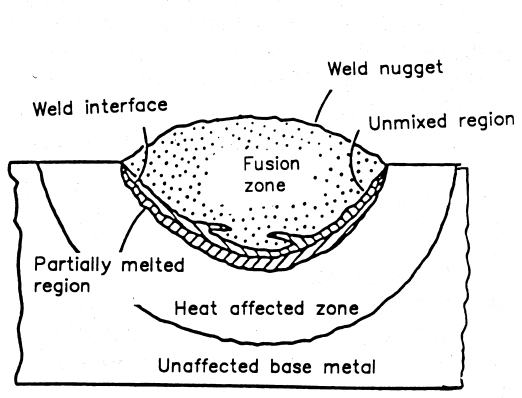

Fig. 1 Schematic showing the regions of a heterogeneous weld. Source: Ref 2

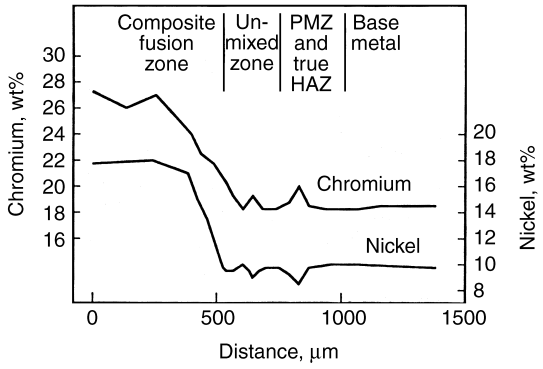

Fig. 2 Concentration profile of chromium and nickel across the weld fusion boundary region of type 304 stainless steel. Source: Ref 4

depending on the degree of restraint imposed on the weld.

Microstructural Gradients. On a fine scale, microstructural gradients exist within the HAZ due to different time-temperature cycles experienced by each element of material. Gradients on a similar scale exist within solidified multi-pass weld metal due to bead-to-bead variations in thermal experience. Compositional gradients on the scale of a few microns, referred to as microsegregation, exist within individual weld beads due to segregation of major and trace elements during solidification (Ref 3).

Forms of Weld Corrosion

Weldments can experience all the classical forms of corrosion, but they are particularly susceptible to those affected by variations in microstructure and composition. Specifically, galvanic corrosion, pitting, stress corrosion, intergranular corrosion, hydrogen cracking, and microbiologically influenced corrosion must be considered when designing welded structures.

Galvanic Couples. Although some alloys can be autogenously welded, filler metals are more commonly used. The use of filler metals with compositions different from the base material may produce an electrochemical potential difference that makes some regions of the weldment more active. For example, Fig. 3 depicts weld metal deposits that have different corrosion behavior from the base metal in three aluminum alloys (Ref 5).

For the majority of aluminum alloys, the weld metal and the HAZ become more noble relative to the base metal, as demonstrated in Fig. 3(a) and (b) for a saltwater environment (Ref 5). Certain aluminum alloys, however, form narrow anodic regions in the HAZ and are prone to localized attack. Alloys 7005 and 7039 are particularly susceptible to this problem (Fig. 3c).

There are a number of other common weld deposit/base metal combinations that are known to form galvanic couples. It is common practice to use austenitic stainless steel welding consumables for field repair of heavy machinery, particularly those fabricated from high-strength low-alloy steel. This practice leaves a cathodic stainless steel weld deposit in electrical contact with the steel. In the presence of corrosive environments, hydrogen is generated at the austenitic weld metal cathode, which is capable of maintaining a high hydrogen content without cracking. However, the cathodic behavior of the austenitic weld deposit may increase the susceptibility for stress-corrosion cracking (SCC) in the HAZ of the high-strength steel. A 40% thermal expansion mismatch between the austenitic stainless steel and ferritic base metal produces a significant residual stress field in the weldment; this residual stress field also con-

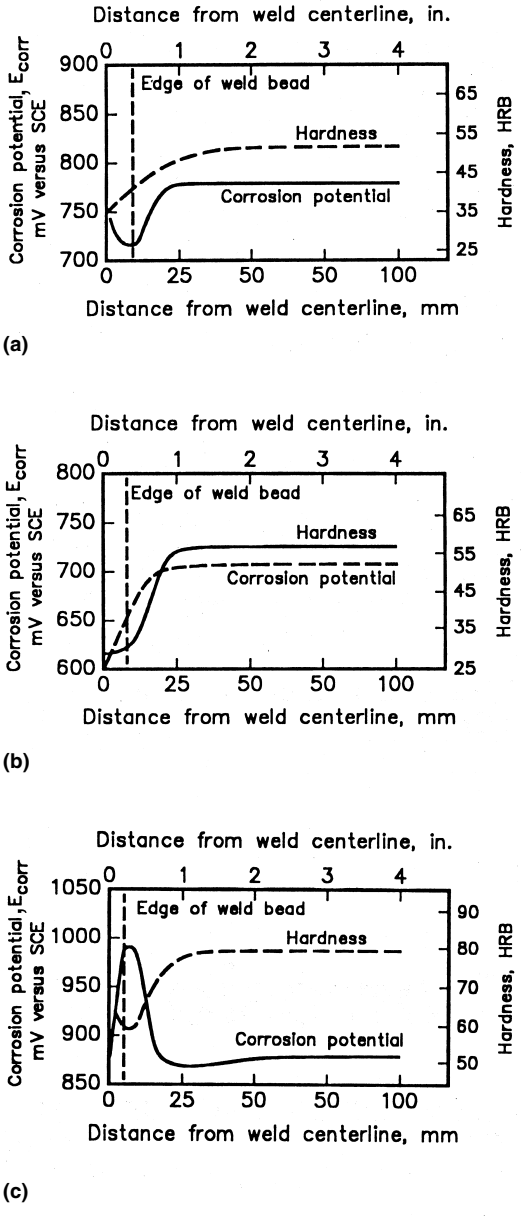

Fig. 3 Effect of welding heat on microstructure, hardness, and corrosion potential of three aluminum alloy welded assemblies. (a) Alloy 5456-H321 base metal with alloy 5556 filler. (b) Alloy 2219-T87 base metal with alloy 2319 filler. (c) Alloy 7039-T651 base metal with alloy 5183 filler. Source: Ref 5

tributes to cracking susceptibility. A similar, but more localized, behavior may explain the correlation between SCC susceptibility and the presence of retained austenite in high-strength steel weld deposits.

Another common dissimilar metal combination involves the use of high-nickel alloys for weld repair of cast iron. Fe-55Ni welding electrodes are used to make weld deposits that can hold in solid solution many of the alloying elements common to cast iron. Furthermore, weld deposits made with Fe-55Ni welding consumables have an acceptable thermal expansion match to the cast iron. Because cast iron is anodic to the high-nickel weld deposit, corrosive attack occurs in the cast iron adjacent to the weld deposit. It is suggested that cast iron welds made with high-nickel deposits be coated (painted) to reduce the susceptibility to selective corrosion attack.

Plain carbon steel weldments can also exhibit galvanic attack. For example, the E6013 welding electrode is known to be highly anodic to A285 base metal in a seawater environment (Ref 6). It is important to select a suitable filler metal when an application involves a harsh environment.

Weld Decay of Stainless Steel. During welding of stainless steels, local sensitized zones (i.e., regions susceptible to corrosion) often develop. Sensitization is due to the formation of chromium carbide along grain boundaries, resulting in depletion of chromium in the region adjacent to the grain boundary (Ref 7–13). This chromium depletion produces very localized galvanic cells (Fig. 4). If this depletion drops the chromium content below the necessary 12 wt% that is required to maintain a protective passive film, the region will become sensitized to corrosion, resulting in intergranular attack. This type of corrosion most often occurs in the HAZ. Intergranular corrosion causes a loss of metal in a region that parallels the weld deposit (Fig. 5). This corrosion behavior is called weld decay (Ref 12).

The formation of sufficient chromium carbide to cause sensitization can be described by the C-shaped curves on the continuous cooling diagram illustrated in Fig. 6. The figure shows susceptibility to sensitization as a function of temperature, time, and carbon content (Ref 14). If the cooling rate is sufficiently great (curve A in Fig. 6), the cooling curve will not intersect the given C-shaped curve for chromium carbide and the stainless steel will not be sensitized. By decreasing the cooling rate, the cooling curve (curve B) eventually intersects the C-shape

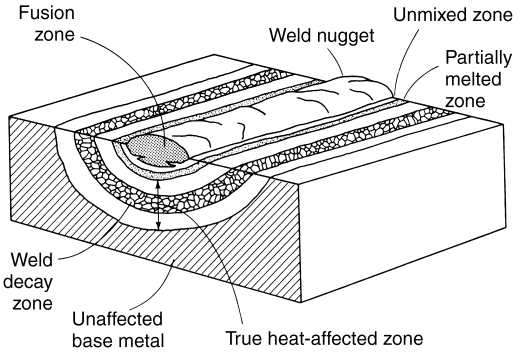

Fig. 5 Intergranular corrosion (weld decay) of stainless steel weldments

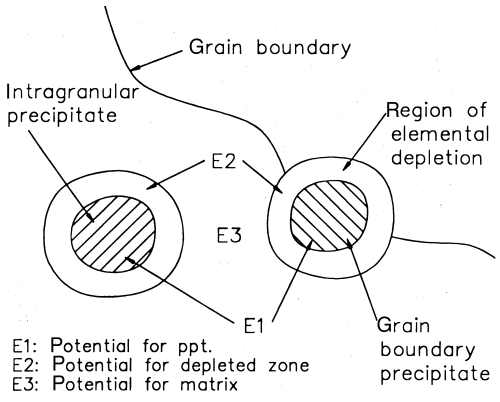

Fig. 4 Depleted regions adjacent to precipitates. These regions cause an electrochemical potential (E) difference that can promote localized corrosion at the microstructural level.

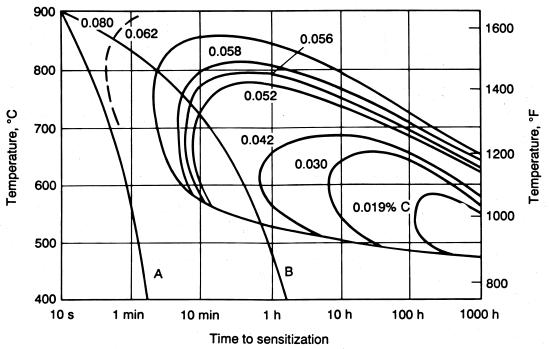

Fig. 6 Time-temperature-sensitization curves for type 304 stainless steel in a mixture of $CuSO_4$ and HSO_4 containing copper. Source: Ref 14. Curves A and B indicate high and medium cooling rates, respectively.

nucleation curve, indicating that sensitization may occur. At very low cooling rates, the formation of chromium carbide occurs at higher temperature and allows for more nucleation and growth, resulting in a more extensive chromium-depleted region.

The minimum time required for sensitization as a function of carbon content in a typical stainless steel alloy is depicted in Fig. 7. Because the normal welding thermal cycle is completed in approximately two minutes, for this example the carbon content must not exceed 0.07 wt% to avoid sensitization. Notice that the carbide nucleation curves of Fig. 6 move down and to longer times with decreasing carbon content, making it more difficult to form carbides for a given cooling rate.

The control of stainless steel sensitization may be achieved by using:

- A postweld high-temperature anneal and quench to redissolve the chromium at grain boundaries, and hinder chromium carbide formation on cooling
- A low-carbon grade of stainless steel (e.g., 304L or 316L) to avoid carbide formation
- A stabilized grade of stainless steel containing titanium (alloy 321) or niobium (alloy 327), which preferentially form carbides and leave chromium in solution. (There is the possibility of knife-line attack in stabilized grades of stainless steel.)
- A high-chromium alloy (e.g., alloy 310)

Role of Delta Ferrite in Stainless Steel Weld Deposits. Austenitic weld deposits are frequently used to join various ferrous alloys. It has been well established that it is necessary to have austenitic weld deposits solidify as primary ferrite, also known as a δ ferrite, if hot cracking is to be minimized (Ref 15, 16). The amount and form of ferrite in the weld metal can be controlled by selecting a filler metal with the appropriate chromium and nickel equivalent. A high chromium-to-nickel ratio favors primary ferrite formation, whereas a low ratio promotes primary austenite (Fig. 8). An optimum condition can be attained for ferrite contents between 3 and 8 vol% in the weld deposit. Ferrite contents above 3 vol% usually guarantee primary ferrite formation and thus reduce hot cracking susceptibility. However, ferrite above 10 vol% can degrade mechanical properties at low- or high-temperature service. At low temperatures, excess ferrite can promote crack paths when the temperature is below the ductile-brittle transition temperature. At high temperatures, continuous brittle σ phase may form at the interface between the austenite and the ferrite. The ferrite content can be confirmed using magnetic measuring equipment (Ref 15, 16).

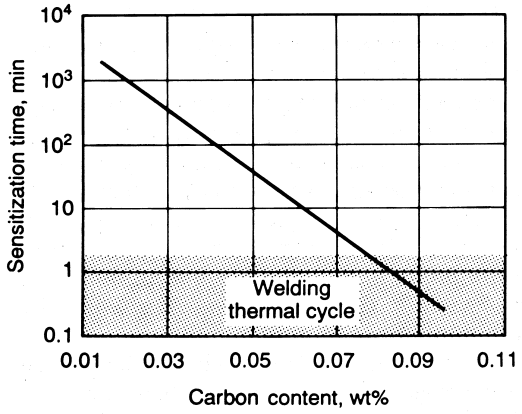

Fig. 7 Minimum sensitization time from a time-temperature-sensitization diagram as a function of carbon content for a typical 300-series stainless steel alloy. Source: Ref 14

Figure 8 can be used to predict the type of ferrite (primary or eutectic) and the ferrite content when a difference exists between the stainless steels being joined, such as when welding type 304 to type 310 stainless steel (Ref 17). This diagram shows the compositional range for the desirable primary solidification mode. The dotted lines on the diagram indicate the various transitions in the primary solidification phase. Because not all ferrite is primary ferrite (i.e., some is a phase component of a ferrite-austenite eutectic), this diagram can be used to ensure that ferrite is the first solid (primary) phase to form. This condition occurs when the weld deposit has a composition in the range labeled FA in Fig. 8. Because primary ferrite is the preferable microstructure, use of this diagram should reduce problems of hot cracking during welding. Also, the corrosion behavior of stainless steel weld deposits and castings is measurably different depending on whether the stainless steel has a microstructure generated with primary ferrite or primary austenite (Ref 18–24). Thus, knowledge of the weld metal ferrite content and form is necessary in order to be able to properly characterize and predict corrosion behavior.

Pitting is a form of localized attack caused by a breakdown in the thin passive oxide film that protects material from the corrosion process. Pits are commonly the result of a con-

centration cell established by a variation in solution composition that is in contact with the alloy material. Such compositional variations result when the solution at a surface irregularity is different from that of the bulk solution composition. Once a pit has formed, it acts as an anode supported by relatively large cathodic regions. Pitting has a delay time prior to nucleation and growth, and nucleation is very site-selective and microstructure-dependent. Pits are often initiated at specific microstructural features in the weld deposit (Ref 25). Pitting occurs when the material/solution combination achieves a potential that exceeds a critical value, known as the pitting potential. The tendency for a given alloy/solution combination to pit can often be characterized by critical potentials for pitting and repassivation determined by a cyclic potentiodynamic polarization technique.

Pits develop more readily in metallurgically heterogeneous materials. For example, when austenitic stainless steel is heated to temperatures where sensitization takes place (Ref 25, 26), the resulting chromium-depleted region is subject to pitting. Pits may also initiate at the austenite-ferrite interfaces in stainless steel weld metal.

Although weld metal has a higher probability of being locally attacked because of microsegregation in the dendritic structure, filler metals are now available that have better pitting resistance than their respective base metals; information about these filler metals can be obtained from consumable suppliers. However, even when the proper filler metal is used, pitting may still occur in the unmixed zone.

Duplex stainless steels, with ferrite contents in the range of 40 to 50 vol%, are often used to decrease the tendency of stress-corrosion cracking in chromium-nickel high-alloy steels. The welding practice for duplex stainless steels must be given special attention (Ref 19, 21, 23, 24, 26) to avoid reduction in corrosion resistance. The combination of a low carbon content and a carefully specified nitrogen addition have been reported to improve resistance to pitting corrosion, SCC, and intergranular corrosion in the as-welded condition. The low carbon content helps avoid sensitization, while the addition of nitrogen slows the precipitation kinetics associated with the segregation of chromium and molybdenum during the welding process (Ref 1). On rapid cooling from high temperature, nitrogen also has been reported to form deleterious pre-

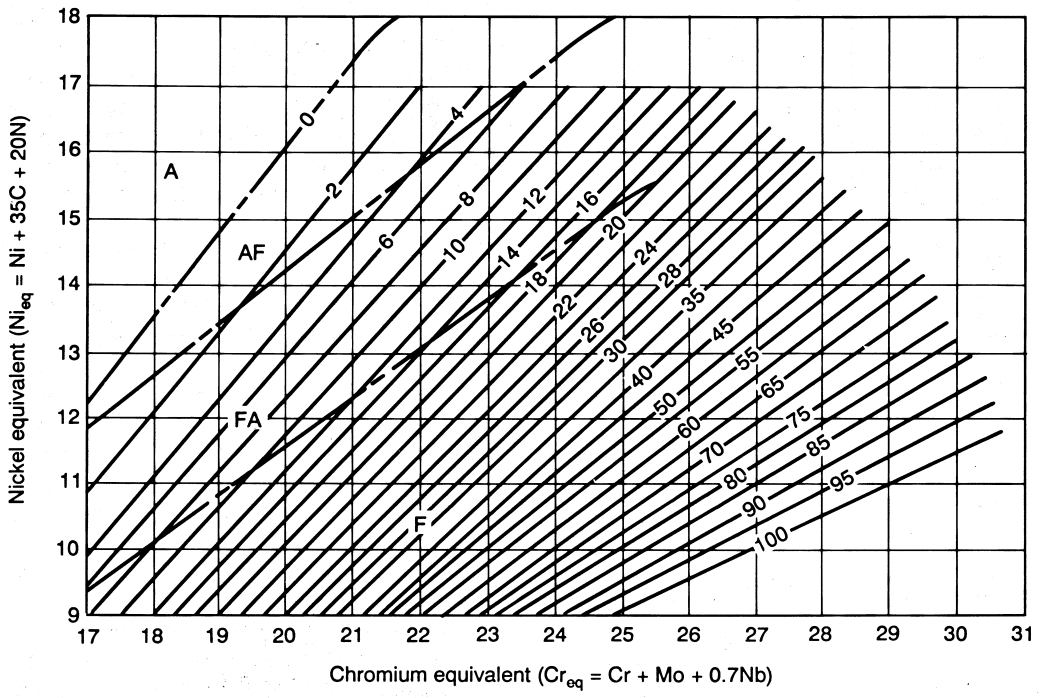

Fig. 8 Welding Research Council (WRC-1988) diagram used to predict weld metal ferrite content. Source: Ref 17

cipitates (for example, Cr_2N) in the ferrite, thus reducing the corrosion resistance (Ref 27). Nitrogen also increases the formation of austenite in the HAZ and weld metal during cooling. A minimum pitting corrosion rate is achieved at a ferrite content of about 50 vol%.

Stress-Corrosion Cracking. Weldments can be susceptible to SCC under specific environmental conditions. This cracking requires the proper combination of corrosive media, susceptible microstructure, and tensile stress. Welds are often loaded in tension (due to residual stress) to a level approaching the yield strength of the base metal. A weld, with its various heterogeneous microstructural features, thus becomes an excellent candidate for SCC.

Stress-corrosion cracks have an anodic crack tip and often leave apparent corrosion products along the fracture. Cracking is often characterized by crack branching and usually has a delay time prior to crack initiation, with initiation occurring at corrosion pits. Increasing the ferrite content in stainless steel weld metal reduces SCC susceptibility. Approximately 50 vol% ferrite gives optimum SCC resistance.

Welding parameters influence the amount and distribution of residual stress, because the extent of the stressed region and the amount of distortion are directly proportional to the size of the weld deposit; this deposit is directly related to the heat input. The thermal experience of welding is often very localized, resulting in strains that can cause distortion and residual stress. These residual stresses can be important in the initiation and propagation of environmentally assisted cracking. The use of small weld deposits reduces the stress and thus reduces the susceptibility of environmentally enhanced cracking.

It is known that postweld heat treatment can reduce SCC by redistributing the localized load and by reducing the magnitude of the residual tensile stress available to induce corrosion cracking (Ref 28). In one study on a cast austenitic stainless steel, postsolidification heat treatments were also shown to modify the local composition gradients, significantly altering the susceptibility of the solidified microstructure to SCC (Ref 29).

Hydrogen-Induced Cold Cracking. Cold cracking is the term used for cracks that occur after the weld has solidified and cooled; it occurs in either the HAZ or the weld metal of low-alloy and other hardenable steels. Because these cracks occur under conditions of restraint, they are often referred to as restraint cracks. Cracking may occur several hours, days, or weeks after the weld has cooled; consequently, the term *delayed cracking* is also used. On the basis of location, cracks are often described as toe cracking, root cracking, or underbead cracking.

For cold cracks to occur in steels, three principal factors must be present: atomic hydrogen, HAZ or portion of the weld metal that is susceptible to hydrogen embrittlement, and a high tensile stress resulting from restraint. Controlling one or more of these factors may reduce the occurrence of cold cracking. The basic relationships among the variables responsible for cold cracking and the methods of controlling these variables are summarized in Fig. 9 and 10.

In steels, cracking in the base metal is often attributed to high carbon, alloy, or sulfur content. Control of this cracking requires the use of low-hydrogen electrodes, high preheat, sufficient interpass temperature, and greater penetration through the use of higher currents and larger electrodes. The susceptibility of the microstructure to cold cracking relates to the solubility of hydrogen and the possibility of supersaturation. Austenite, in which hydrogen is highly soluble, is least susceptible to cold cracking, and martensite, in which the solubility of hydrogen is lower, is most susceptible, because the rapid cooling necessary for the austenite-to-martensite transformation traps the hydrogen in a state of supersaturation in the martensite. For this reason rapid cooling rates must be avoided.

Cracking Due to Environments Containing Hydrogen Sulfide. High-strength steel pipes used in drilling and completion of oil and gas wells may exhibit delayed failure in environments containing hydrogen sulfide. This type of failure is referred to as sulfide stress cracking. The basic cause of sulfide stress cracking is embrittlement resulting from hydrogen absorbed into steel during corrosion in sour environments. The presence of hydrogen sulfide in the environment promotes hydrogen absorption into steel, thereby making the environment more severe and thus more likely to cause hydrogen embrittlement. Although hydrogen sulfide gas, like gaseous hydrogen, can cause embrittlement, water ordinarily must be present for sulfide stress cracking to occur.

The susceptibility to sulfide stress cracking increases with increasing hydrogen sulfide concentration or partial pressure and decreases with increasing pH. The ability of the environment to cause sulfide stress cracking decreases markedly above pH 8 and below 101 Pa (0.001 atm) partial

pressure of hydrogen sulfide. The cracking tendency is most pronounced at ambient temperature and decreases with increasing temperature. For a given strength level, tempered martensitic steels have better sulfide stress cracking resistance than normalized-and-tempered steels, which in turn are more resistant than normalized steels. Untempered martensite demonstrates poor resistance to sulfide stress cracking. It is generally agreed that a uniform microstructure of fully tempered martensite is desirable for sulfide stress cracking resistance.

The effect of alloying elements on the sulfide stress cracking resistance of carbon and low-alloy steels is controversial, except for one element. Nickel is detrimental to sulfide stress cracking resistance. Steels containing more than 1% Ni are not recommended for service in sour environments.

The sulfide stress cracking susceptibility of weldments appears to be greater than that of the base metal, and the high hardness and residual stresses resulting from welding are believed to increase the susceptibility. In a laboratory study of the sulfide stress cracking resistance of submerged-arc weldments in a hydrogen sulfide saturated aqueous solution of 0.5% acetic acid and 5% sodium chloride, no failures were observed for the welds with hardness values below 191 HB; all of the welds with hardness values of 225 HB (20 HRC) or higher failed. It should be noted that sulfide stress cracking occurred in the weldments having hardnesses lower than 22 HRC. Steels with hardness values less than 22 HRC are considered acceptable for sour service.

NACE International issued a standard (Ref 30) for metallic materials (including steels) resistant to sulfide stress cracking for oil-

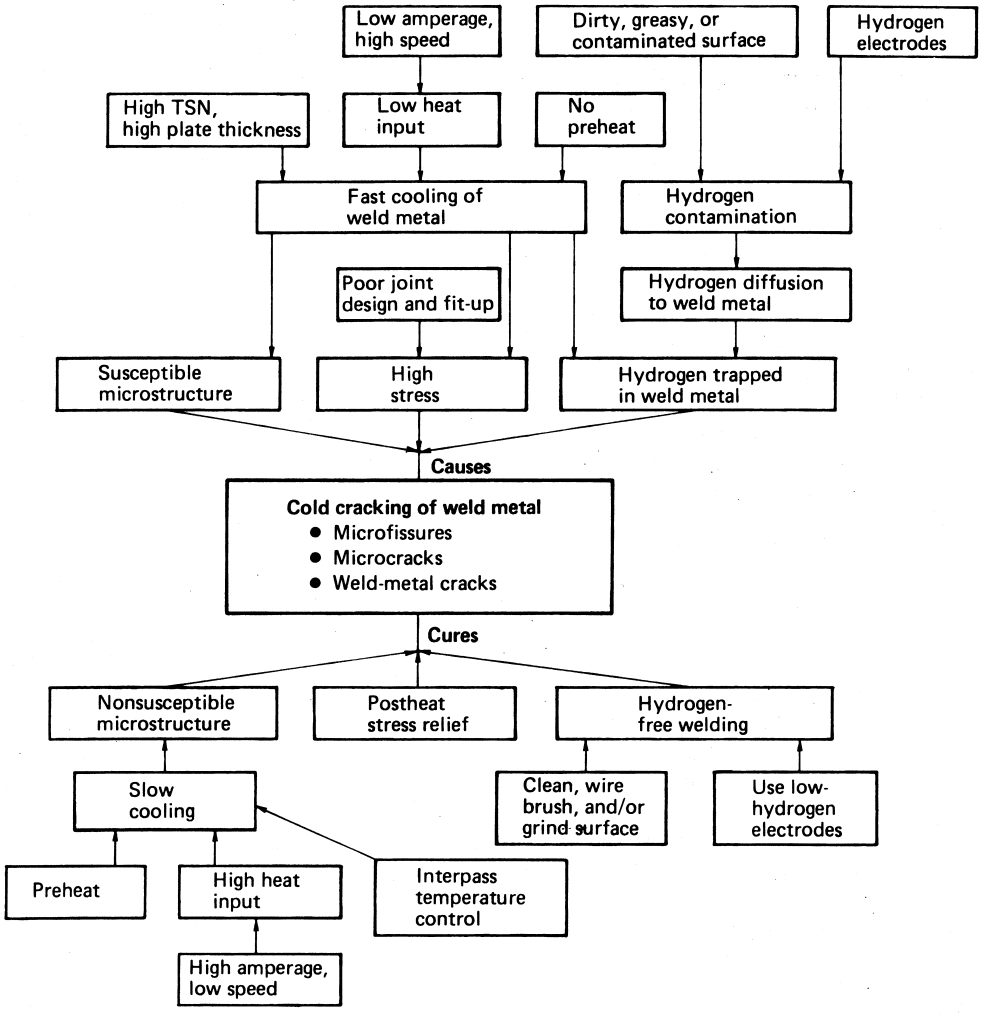

Fig. 9 Causes and cures of hydrogen-induced cold cracking in weld metal. Thermal severity number (TSN), which is four times the total plate thickness capable of removing heat from the joint, is thus a measure of the member's ability to serve as a heat sink.

field equipment. This standard covers metallic-material requirements for sulfide stress cracking resistance for petroleum production, drilling, gathering, and transmission equipment and for field-processing facilities to be used in hydrogen sulfide bearing hydrocarbon service. Guidelines for dealing with the hydrogen stress cracking that occurs in refineries and petrochemical plants have also been developed by the American Petroleum Institute (Ref 31).

Microbiologically Influenced Corrosion (MIC) is a phenomenon in which microorganisms play a role in the corrosion of metals. This role may be to initiate or accelerate the corrosion process. For example, water and some organic media may contain certain microorganisms that can produce a biofilm when exposed to a metal surface. The resulting nonuniform coverage may lead to a concentration cell and eventually initiate corrosion. In addition, the metabolic process of the microorganism can produce a localized acid environment that changes the corrosion behavior of the exposed metal by, for example, altering anodic and cathodic reactions, destroying protective films, or creating corrosive deposits (Ref 32).

In austenitic stainless steel weldments, the effects of MIC are usually observed as pitting on or adjacent to welds (Ref 33, 34). MIC attacks either γ or α phases, and chlorides are sometimes found in a pit, even when the water has extremely low chloride content. Pits are found in regions of the HAZ at the fusion line, and in the base metal near the weld for reasons not well understood. There is some evidence that MIC takes place along with SCC weldments of austenitic stainless steel. Welding design and plant operation can minimize MIC attack, mainly by preventing an acceptable environment for microorganisms.

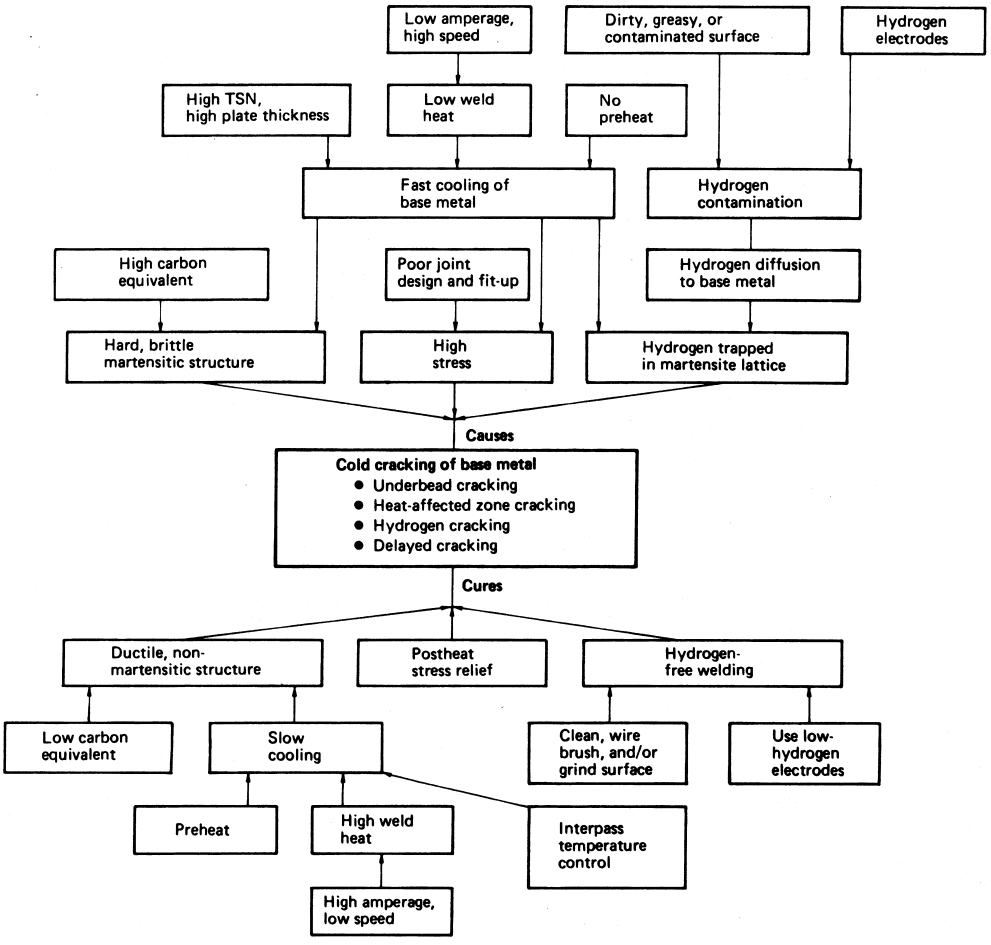

Fig. 10 Causes and cures of hydrogen-induced cold cracking in base metal

Heat-Tint Oxide Formation. The welding process, especially with poor gas shielding, can produce a variation in the thickness of the passivating oxide. The variation in oxidation will result in a gradient in the degree of chromium depletion adjacent to a stainless steel weld. This behavior will cause some tendency for localized corrosion (Ref 1). An indication of this problem can be seen by the heat-tint oxide formation (Ref 35).

Welding Practice to Minimize Corrosion

Several methods are available to minimize corrosion in weldments (Ref 36). The most important of these are discussed below.

Material and Welding Consumable Selection. Careful selection of materials and welding consumables can reduce the macro- and micro-compositional differences across the weldment and thus reduce the galvanic effects.

Surface Preparation. A properly selected cleaning process can reduce defects that are often sites for corrosive attack in aggressive environments. However, the cleaning process can also be a source of trouble. For example, any mechanically cleaned surface (i.e., cleaned by sand blasting or grinding) can leave impurities on the surface. The type of wire brush used can also be an important consideration (Ref 36). Stainless steel brushes are generally preferred because they do not form corrosion products capable of holding moisture.

Welding design should promote deposits that have relatively flat beads with low profiles and have minimal slag entrapment. A poor design can generate crevices that trap stagnant solutions, leading to pitting and crevice corrosion. Irregular weld deposit shapes can promote turbulent flow in a tubular product and result in erosion corrosion.

Welding Practice. Complete penetration is preferred to avoid underbead gaps. Slag should be removed after each pass with a power grinder or power chipping tool. If the welding method uses flux, the geometry of the joint must permit thorough flux removal, because many flux residues are hydrophilic and corrosive.

Weld Surface Finishing The weld deposit should be inspected visually immediately after welding. Maximum corrosion resistance usually demands a smooth uniformly oxidized surface that is free from foreign particles and irregularities (Ref 34). Deposits normally vary in roughness and in degree of weld spatter, a concern that can be minimized by grinding. For smooth weld deposits, wire brushing may be sufficient. For stainless steel, however, brushing disturbs the existing passive film and may aggravate corrosive attack.

Surface Coating When a variation in composition across the weld metal can cause localized attack, it may be desirable to use protective coatings. The coating needs to cover both the weldment and the parent metal and often requires special surface preparation.

Postweld Heat Treatment. A postweld heat treatment can be an effective way to reduce corrosion susceptibility. This improved corrosion resistance is accomplished through a reduction in residual stress gradients that influence SCC growth. Postweld heat treatment can assist in the transport of hydrogen from the weldment and reduce susceptibility to hydrogen cracking. The treatment can also reduce compositional gradients (i.e., microsegregation) and corresponding microgalvanic cells.

Preheat and Interpass Temperature. The selection and use of proper preheat treatment and interpass temperature may prevent hydrogen cracking in carbon and low-alloy steel.

Passivation Treatment. A passivation treatment may increase the corrosion resistance of stainless steel welded components.

Avoidance of Forming Crevices. Slag that is still adhering to the weld deposit and defects such as lack of penetration and microfissures can result in crevices that can promote a localized concentration cell, resulting in crevice corrosion. Proper selection of welding consumables, proper welding practice, and thorough slag removal can alleviate this form of corrosion damage.

Removing Sources of Hydrogen. Through proper selection of welding consumables (that is, low-hydrogen shielded metal arc welding electrodes), proper drying of flux, and welding clean surfaces, the hydrogen pickup can be drastically reduced.

ACKNOWLEDGMENT

Portions of this chapter were adapted from A. Wahid, D.L. Olson, D.K. Matlock, and C.E. Cross, Corrosion of Weldments, *Welding, Brazing, and Soldering,* Vol 6, *ASM Handbook,* ASM International, 1993, p 1065–1069

REFERENCES

1. O.I. Steklov et al., Method of Evaluating the Influence of Non-Uniformity of Welded Joint Properties on Corrosion, *Svar. Proiz.,* Vol 19 (No. 9), 1972, p 34–36
2. W.F. Savage, New Insight into Weld Cracking and a New Way of Looking at Welds, *Weld. Des. Eng.,* Dec 1969
3. R.G. Buchheit, Jr., J.P. Moran, and G.E. Stoner, Localized Corrosion Behavior of Alloy 2090—The Role of Microstructural Heterogeneity, *Corrosion,* Vol 46 (No. 8), 1990, p 610–617
4. W.A. Baeslack III, J.C. Lippold, and W.F. Savage, Unmixed Zone Formation in Austenitic Stainless Steel Weldments, *Weld. J.,* Vol 58 (No. 6), 1979, p 168s–176s
5. J.E. Hatch, Ed., *Aluminum: Properties and Physical Metallurgy,* ASM International, 1984, p 283
6. C.A. Arnold, "Galvanic Corrosion Measurement of Weldments," presented at NACE Corrosion/80, Chicago, March 1980
7. M.W. Marshall, Corrosion Characteristics of Types 304 and 304L Weldments, *Weld. J.,* Vol 38 (No. 6), 1959, p 247s–250s
8. M.E. Carruthers, Weld Corrosion in Type 316 and 316L Stainless Steel and Related Problems, *Weld. J.,* Vol 38 (No. 6), 1959, p 259s–267s
9. K.E. Pinnow and A. Moskowitz, Corrosion Resistance of Stainless Steel Weldments, *Weld. J.,* Vol 49 (No. 6), 1970, p 278s–284s
10. T.J. Moore, Time-Temperature Parameters Affecting Corrosion of 18Cr-8Ni Weld Metals, *Weld. J.,* Vol 39 (No. 5), 1960, p 199s–204s
11. J. Honeycombe and T.G. Gooch, Intergranular Attack in Welded Stress-Corrosion Resistant Stainless Steel, *Weld. J.,* Vol 56 (No. 11), 1977, p 339s–353s
12. T.G. Gooch and D.C. Willingham, Weld Decay in AISI 304 Stainless Steel, *Met. Const. Brit. Weld. J.,* Vol 3 (No. 10), 1971, p 366
13. T.G. Gooch, Corrosion of AISI Type 304 Austenitic Stainless Steel, *Brit. Weld. J.,* Vol 15 (No. 7), 1968, p 345
14. R.M. Davidson, T. DeBold, and M.J. Johnson, *Metals Handbook,* Vol 13, 9th ed., ASM International, 1987, p 551
15. D.J. Kotecki, Understanding Delta Ferrite, *Weld. Des. Fabr.,* Vol 63 (No. 12), 1990, p 33–36
16. D.J. Kotecki, Ferrite Control in Duplex Stainless Steel Weld Metal, *Weld. J.,* Vol 65 (No. 10), 1987, p 273s–278s
17. T.A. Siewert, C.N. McCowan, and D.L. Olson, Ferrite Number Prediction to 100FN in Stainless Steel Weld Metal, *Weld. J.,* Vol 67 (No. 12), 1988, p 289s–298s
18. W.A. Baeslack III, D.J. Duquette, and W.F. Savage, The Effect of Ferrite Content on Stress Corrosion Cracking in Duplex Stainless Steel Weld Metals at Room Temperature, *Corrosion,* Vol 35 (No. 2), 1979, p 45–54
19. W.A. Baeslack III, D.J. Duquette, and W.F. Savage, Technical Note: Stress Corrosion Cracking in Duplex Stainless Steel Weldments, *Weld. J.,* Vol 57 (No. 6), 1978, p 175s–177s
20. D.H. Sherman, D.J. Duquette, and W.F. Savage, Stress Corrosion Cracking Behavior of Duplex Stainless Steel Weldments in Boiling $MgCl_2$, *Corrosion,* Vol 31 (No. 10), 1975, p 376–380
21. T.G. Gooch, Weldability of Duplex Ferritic-Austenitic Stainless Steels, *Duplex Stainless Steels,* ASM, 1983, p 573–602
22. A Backman and B. Lundqvist, Properties of a Fully Austenitic Stainless Steel Weld Metal for Severe Corrosion Environments, *Weld. J.,* Vol 56, 1977, p 23s–28s
23. H. Menendez and T.M. Devine, The Influence of Microstructure on the Sensitization Behavior of Duplex Stainless Steel Welds, *Corrosion,* Vol 46 (No. 5), 1990, p 410–417
24. T. Ogawa and T. Koseki, Effect of Composition Profiles on Metallurgy and Corrosion Behavior of Duplex Stainless Steel Weld Metals, *Weld. J.,* Vol 68 (No. 5), 1989, p 181s–191s
25. A Garner, The Effect of Autogeneous Welding on Chloride Pitting Corrosion in Austenitic Stainless Steels, *Corrosion,* Vol 35 (No. 3), 1979, p 108–114
26. T.A. DeBold, J.W. Martin, and J.C. Tverberg, Duplex Stainless Offers Strength and Corrosion Resistance, *Duplex Stainless Steel,* ASM International, 1983, p 169–189
27. N. Sridhar and J. Kolts, Effects of Nitro-

gen on the Selective Dissolution of a Duplex Stainless Steel, *Corrosion,* Vol 43 (No. 11), 1987, p 646–651
28. K.N. Krishnan and K.P. Rao, Room-Temperature Stress Corrosion Cracking Resistance of Post-Weld Heat-Treated Austenitic Weld Metals, *Corrosion,* Vol 46 (No. 9), 1990, p 734–742
29. G.L. Berry, Jr., D.L. Olson, and D.K. Matlock, Influence of Microcompositional Gradients on Stress Corrosion Crack Propagation, *Mat. Eng. Sci.,* Vol A148, 1991, p 1–6
30. "Sulfide Stress Cracking Resistant Metallic Material for Oil Field Equipment," NACE MR0175/ISO 15156 (latest revision), Material Requirement, NACE International
31. "Controlling Weld Hardness of Carbon Steel Refinery Equipment to Prevent Environmental Cracking," Recommended Practice 942, 2nd ed., American Petroleum Institute, 1982
32. S.C. Dexter, Localized Biological Corrosion, *Metals Handbook,* Vol 13, 9th ed., ASM, 1987, p 114–120
33. G.J. Licina, *Sourcebook of Microbiologically Influenced Corrosion in Nuclear Power Plants,* NP5580, Electric Power Research Institute, 1988
34. S.W. Borenstein, "Microbiologically Influenced Corrosion Failures of Austenitic Stainless Steel Welds," Paper 78, Corrosion 88, NACE, 1988
35. S. Turner and F.P.A. Robinson, The Effect of the Surface Oxides Produced During Welding on the Corrosion Resistance of Stainless Steels, *Corrosion,* Vol 45 (No. 9), 1989, p 710–716
36. F.C. Brautigam, Welding Practices that Minimize Corrosion, *Chem. Eng.,* Jan 17, 1977, p 145–147

SELECTED REFERENCES

- B. Mishra, D.L. Olson, and C. Lensing, The Influence of Weld Microstructural Features on Corrosion Behavior, *The Third Pacific Rim International Conference on Advanced Materials and Processing (PRICM 3),* TMS, 1998, p 2303–2308
- D.L. Olson, A.N. Lasseigne, M. Marya, and B. Mishra, Weld Features that Differentiate Weld and Plate Corrosion, *Practical Failure Analysis,* Vol 3 (No. 5), Oct 2003, p 43–57

Corrosion of Weldments
J.R. Davis, editor, p 13-41
DOI:10.1361/corw2006p013

CHAPTER 2

Corrosion of Carbon Steel and Low-Alloy Steel Weldments

CARBON AND LOW-ALLOY STEELS are by far the most frequently welded metallic materials. Welded assemblies fabricated from carbon and low-alloy steels can be found in virtually all heavy industrial applications including the petroleum and petrochemical industry, land transportation industry, pulp and paper industry, chemical processing industry, electrical power industry, and the building industry, to name only a few.

In addition, much of the welding metallurgy research, including an understanding of the solidification of welds, microstructure of the weld and heat-affected zone (HAZ), solid-state phase transformations during welding, control of toughness in the HAZ, the effects of preheating and postweld heat treatment (PWHT), and weld discontinuities, has been directed toward ferrous alloys, and in particular carbon and low-alloy steels.

Classification of Steels and Their Welding Characteristics

Carbon and low-alloy steels cover a wide variety of compositions and properties. Steels are most often classified according to their carbon and/or alloy content. The various classifications have become known under assorted designations, such as plain-carbon steel, carbon-manganese steel, medium-carbon steel, low-alloy steel, high-strength low-alloy steel, and microalloyed steel. The boundaries between all the above classes are often diffuse, they frequently overlap, and they are sometimes arbitrary (Table 1).

Carbon Steels

Carbon steels are defined as those steels containing up to 2% C, 1.65% Mn, 0.60% Si, and 0.60% Cu, with no deliberate addition of other elements to obtain a desired alloying effect. The weldability of these steels greatly depends on their carbon and manganese contents and impurity levels.

Low-carbon steels contain up to approximately 0.30 wt% C and up to about 1.65 wt% Mn. Most as-rolled steel used for welded applications consist of low-carbon steel. This group encompasses steels that can have wide variations in weldability. For example, at low carbon levels (less than 0.15% C), the steels are nonhardening and weldability is excellent. The bulk of the steels in this carbon range are used for flat-rolled products (sheet and strip), which may contain up to 0.5% Mn. Most of these steels are now aluminum-killed, continuous-cast product supplied in the cold-rolled and annealed condition. The lower available oxygen in the killed sheet makes it easier to arc weld without porosity formation. Typical uses for these steels are

Table 1 Carbon steels classified according to carbon content

Carbon, %				
Low-carbon steel	Mild steel	Medium-carbon steel	High-carbon steel	Ref
≤0.15	0.15–0.30	0.30–0.50	0.50–1.00	1
≤0.15	0.15–0.35	0.35–0.60	0.60–1.0	2
<0.30	. . .	0.30–0.60	>0.6	3
≤0.30	≤0.25	0.30–0.60	0.60–1.00	4

automobile body panels, appliances, and light-walled tanks.

In the range of 0.15 to 0.30% C (sometimes termed mild steels), the steels are generally easily welded, but because hardening is a possibility, precautions such as preheating may be required at higher manganese levels, in thicker sections, or at high levels of joint restraint. Much of the steel in this carbon range is used for rolled structural plate and tubular products. These steels are generally killed or semi-killed and are usually supplied in the hot-rolled condition. The presence of surface scale (iron oxide) from the high-temperature rolling process increases the likelihood of porosity formation during welding and may require the use of welding electrodes with higher levels of deoxidizers, or removal of the scale prior to welding. Some carbon steel plate may be heat-treated (normalized or quenched and tempered) to enhance properties. In such cases, careful selection of the welding consumable must be made in order to match the base metal properties. Welding heat input may have to be controlled so as not to diminish the properties in the HAZ of the base metal, or PWHT may be necessary to restore the strength and/or toughness of the HAZ.

Medium-carbon steel—steel that contains 0.30 to 0.60% C—can be successfully welded by all of the arc welding processes, provided suitable precautions are taken. The higher carbon content of these steels, along with manganese from 0.6 to 1.65%, makes these steels more hardenable. For this reason, they are commonly used in the quenched and tempered condition for such applications as shafts, couplings, gears, axles, crankshafts, and rails. Because of the greater likelihood of martensite formation during welding, and the higher hardness of the martensite formed, preheating and postheating treatments are necessary. Low-hydrogen consumables and procedures should also be used to reduce the likelihood of hydrogen-induced cracking. The higher strength level of these steels may require the use of an alloyed electrode to match the base metal properties. It may also be necessary to PWHT the part in order to restore the strength and/or toughness of the HAZ.

High-carbon steel—steel that contains 0.60 to 2.00% C—has poor weldability because of the likelihood of formation of a hard, brittle martensite upon weld cooling. Steels of this type are used for springs, cutting tools, and abrasion-resistant applications. Low-hydrogen consumables and procedures, preheating, interpass control, and stress relieving are essential if cracking is to be avoided. Austenitic stainless steel electrodes are sometimes used to weld high-carbon steels. These electrodes will reduce the risk of hydrogen-induced cracking but may not match the strength of the high-carbon steel base metal.

Welding Processes. All of the arc welding processes are suitable for welding carbon steels. Choosing the best process to use for a particular application must take into account not only the material characteristics (sensitivity to porosity or cracking and the required mechanical properties), but also the details of the joint (plate thickness, joint design, welding position, and location) and weld economics (deposition rates and efficiencies, cost of labor, cost of consumables, capital cost of equipment, number of spare parts required, operator skills or training needed, setup and cleanup cost, and so on). Table 2 provides a guide that can be used to select welding processes for carbon steels.

Low-Alloy Steels

Low-alloy steels constitute a category of ferrous materials that exhibit mechanical properties superior to plain carbon steels as the result of additions of such alloying elements as nickel, chromium, and molybdenum. Total alloy content can range from 2.07% up to levels just below that of stainless steels, which contain a minimum of approximately 11% Cr. For many alloy steels, the primary function of the alloying elements is to increase hardenability in order to optimize mechanical properties and toughness after heat treatment. In some cases, however, alloy additions are used to reduce environmental degradation under certain specified service conditions. Composition ranges for selected low-alloy steels are listed in Table 3.

High-strength low-alloy (HSLA) steels are designed to provide better mechanical properties than those of conventional carbon steels. These steels generally have yield strengths of 290 to 550 MPa (42 to 80 ksi). They are also generally of the carbon-manganese type, with very small additions of niobium and vanadium to ensure both grain refinement and precipitation hardening. The term microalloyed steels is often used in reference to these materials. Fabricators usually weld these steels in the as-rolled or the normalized condition. The weldability of most HSLA steels is similar to that of mild steel.

Quenched-and-tempered steels are heat treated to provide yield strengths of 345 to 1035

MPa (50 to 150 ksi). ASTM A 514 and A 517 are well-known examples of this category of steel. Other examples include the HY-80, HY-100, and HY-130 Ni-Cr-Mo steels covered by military specifications. Weldments fabricated from these materials generally do not need further heat treatment except for a PWHT (stress relief) in some special applications. For example; HY-100 and HY-130 require controls on the filler-metal carbon content, preheat/interpass minimums and maximums, heat input, and postweld soaks to achieve the desired military mechanical properties.

Heat-treatable low-alloy (HTLA) steels are usually reaustenitized, then quenched and tempered after welding. These are relatively hardenable steels that in their quenched-and-tempered condition develop yield strengths well above 965 MPa (140 ksi). Weld metals usually cannot develop acceptable combinations of strength and toughness at these levels in the as-welded or stress-relieved condition. Therefore, it is necessary to reaustenitize and then quench and temper the entire weldment after welding. These steels are often referred to by their SAE designations (for example, SAF 4140 and SAE 4340).

Thermal-mechanical-controlled processing (TMCP) steels are a relatively recent addition to the family of steels. These steels are generally produced with a combination of controlled rolling followed by accelerated cooling or in-line direct quenching. This processing allows the steelmaker to develop a combination of high strength and high toughness while maintaining good weldability. The weldability is good because the alloy content of these steels can be kept very lean, with carbon contents generally below 0.06 wt%. Yield strength levels as high as 700 MPa (100 ksi) and above are possible with these steels. Generally, they can be welded without preheat. However, at the high strength levels, preheat may be required in order to prevent cracking in the weld metal.

Chromium-molybdenum steels are extensively used for elevated-temperature applications in the power and petroleum refinery industries. The chromium content of these steels varies from 0.5 to 9%, and the molybdenum content from 0.5 to 1.0% (Table 3). They are usually supplied in the normalized-and-tempered or the quenched-and-tempered condition.

Because these materials have reasonable hardenability, adequate precautions must be taken to avoid weld-related hydrogen-induced cracking (Ref 5). The service application frequently imposes additional requirements on the welding of these steels. For example, in the power industry, these materials are required for their creep resistance, and the weld metal and HAZ must provide adequate creep properties. The corrosion environment in refineries requires that the maximum HAZ hardness be limited to avoid corrosion cracking.

Welding Processes. All of the common arc welding processes can be used with low-alloy steels. Shielded metal arc, gas-tungsten arc, gas-metal arc, flux-cored arc, and submerged arc welding processes are used for most applications.

Electroslag and electrogas processes can be used to weld some of the low-alloy structural and pressure vessel steels, although restrictions may be imposed by some codes.

Corrosion Considerations for Carbon and Low-Alloy Steel Weldments

Carbon and low-alloy steels used for structural applications are not commonly utilized in severe corrosion environments. However, they are used in moderate corrosive service conditions such as those in oil refinery facilities and sour gas/oil pipelines. The presence of a weld often leads to a reduction in corrosion caused by the following circumstances (Ref 6):

- Compositional variations in the base metal, HAZ, and weld metal that results in a condition favoring galvanic corrosion. Galvanic corrosion is discussed in the section "Corrosion of Carbon Steel Weldments" in this chapter
- Susceptibility to hydrogen-containing environments which leads to cracking. See the section "Environmentally Assisted Cracking" in this chapter for more detailed information
- Presence of welding residual stresses that lead to stress-corrosion cracking (SCC). See the section "Environmentally Assisted Cracking" in this chapter for more detailed information
- Hydrogen-induced cracking of the weldment. Hydrogen in welding can result from improperly baked or stored electrodes, moisture in the flux, or the presence of moisture and other impurities on the components to be welded. See the section "Hydrogen-Induced Cracking" in this chapter for more detailed information
- Presence of weld discontinuities, such as surface flaws, which act as preferential sites for local corrosion attack

Table 2 Process selection guidelines for arc welding carbon steels

Parameters	SMAW	GMAW	FCAW	GTAW/PAW	SAW	EGW/ESW	SW
Usability	Very adaptable, all-position process. Can be used outdoors. Gives excellent joint accessibility. Very portable. Can be used on carbon steels down to 18 gage. Joint preparation is required on thicknesses over 3.2 mm ($^1/_8$ in). Unlimited upper thickness but other processes (GMAW, FCAW, or SAW) are usually more economical.	An all-position process in the short arc or pulsed mode. Moderately adaptable, but use limited outside where loss of shielding is possible. Usable on steel down to <0.25 mm (<0.010 in.) thick. Above 4.8 mm ($^3/_{16}$ in.), requires joint preparation. No upper limit of plate thickness.	All-position process. Equipment similar to GMAW, but self-shielded version has better portability and is usable outdoors. Minimum plate thickness is 18 gage. For self-shielded material above 6.4 mm ($^1/_4$ in.), requires joint preparation. With CO_2 shielding, materials above 13 mm ($^1/_2$ in.), requires joint preparation. There is no upper limit on plate thickness.	An all-position process with fair joint accessibility. Limited outdoor use. Can weld very thin material in all positions; GTAW—<0.13 mm (<0.005 in.) min. thickness, joint prep. over 3.2 mm ($^1/_8$ in.); PAW—<0.13 mm (<0.005 in.) min. thickness, joint prep over 6.4 mm ($^1/_4$ in.). No upper limit on thickness but other processes are more efficient.	Limited to flat and horizontal position. Semiautomatic version has some adaptability but process is most often mechanized and has limited portability. Minimum material thickness is 1.6 mm ($^1/_{16}$ in.) (mechanized). Joint preparation is required on material above 13 mm ($^1/_2$ in.) thick. The process lends itself to welding thick materials.	Limited to vertical or near-vertical. O.K. outside. Fair portability. Used on plate 9.5 to 102 mm ($^3/_8$ to 4 in.) thick.	All position. O.K. outside. Fair portability. Used on plate 1.0 mm (0.04 in.) and above. No joint preparation required.
Cost factors	A low-deposition-rate process (up to 9 kg/h, or 20 lb/h) with low deposit efficiency (typically 65%). Low operator factor. Equipment cost is low and spare parts are minimal. Welding speeds are generally low. Housekeeping is required to deslag and dispose of flux and electrode stubs.	Deposition rates (to 16 kg/h, or 35 lb/h) are higher than SMAW. Deposition efficiency (90–95%) and operator factor (typical 50%) are also higher. Equipment and spare parts costs refer to are moderate to high (pulsed arc power supplies are higher cost). Welding speeds are moderate to higher (buried arc CO_2 can weld at over 2540 mm/min (100 in./min). Cleanup is minimal.	Deposition rates (up to 18 kg/h, or 40 lb/h) are higher than GMAW. Deposition efficiencies (80–90%) are lower but operator factors (50%) are similar to GMAW. Equipment cost is moderate. Good out-of-position deposition rates can be achieved with conventional power sources. Welding speeds are moderate to high. Slag and spatter removal and disposal is required.	Low deposition rates (up to 5.4 kg/h, or 12 lb/h) but high deposition efficiency (99%). If automated, the operator factor is high. Equipment and spare parts costs are moderate to high, depending on complexity (PAW is slightly more expensive). Cleanup is generally unnecessary due to no flux or spatter.	Deposition rates are very high (over 45 kg/h, or 100 lb/h with multiwire systems). Deposition efficiency is 99% but that does not include the flux (a 1 : 1 flux-to-wire ratio is common). Because the process is usually mechanized, operator factors are high. Cost is moderate for single-wire systems. High welding speeds are achievable. Higher housekeeping costs result from the need to handle the slag and unfused flux.	High joint completion rate. High deposition efficiency (solid wires—99%, cored wires lower). High operator factor. High equipment and setup costs.	Equipment cost is moderate.
Weld metal quality	Strongly dependent on the skill of the welder. Lack of fusion or slag inclusions are potential problems. The relatively small beads usually result in a high percentage of refining in multipass welds, and very good toughness is achievable with some electrodes.	Very good quality. Porosity or lack of fusion can be a problem. Less tolerant of rust and millscale than flux-using processes. Very good toughness is achievable.	Good quality. Weld metal toughness is fair to good (best with basic electrodes). Slag inclusions are a potential problem.	High quality, but requires clean plate. Excellent toughness possible due to small bead size (high refined weld metal, finer grain size).	Very good. Good weld metal toughness is possible. Handles rust and millscale well with proper flux selection. High-dilution process.	Large columnar grain structure results in only fair toughness. High dilution of baseplate (up to 35% for EGW, up to 50% for ESW).	Minimal weld size. Usually fine-grained due to fast cooling. Weld structure is as cast.

SMAW, shielded metal arc welding; GMAW, gas metal arc welding; FCAW, flux-cored arc welding; GTAW, gas tungsten arc welding; PAW, plasma arc welding; SAW, submerged arc welding; EGW, electrogas welding; ESW, electroslag welding; SW, stud arc welding

(continued)

Table 2 (continued)

Parameters	SMAW	GMAW	FCAW	GTAW/PAW	SAW	EGW/ESW	SW
Effect on base metal	Low heat inputs can cause rapid HAZ cooling. Flux coatings are a potential source of hydrogen.	Generally a low-hydrogen process.	Flux core can contribute hydrogen.	A low-hydrogen process. Low heat inputs can cause rapid HAZ cooling.	Higher heat inputs can result in large HAZ and possible deterioration of baseplate properties (especially quenched and tempered plate). Flux is a source of hydrogen.	High heat input results in large HAZ and grain growth. Not recommended for quenched-and-tempered steels unless reheat treatment is to be done. Slow welds cooling allows hydrogen to escape weld area.	Causes rapid cooling of HAZ.
General comments	Very versatile, low-cost process. Especially strong on nonroutine or repair jobs. Usually not economical on standard thick welds or on repetitive jobs that can be mechanized.	Relatively versatile. Equipment more costly, complex, and less portable than SMAW. Easily mechanized. A clean process with higher deposition rates and efficiencies than SMAW.	Relatively versatile (self-shielded version can be used outside). Higher deposition rates than GMAW (higher fumes also). Welds easily out-of-position. Readily mechanized.	Extremely good welds in all positions. Requires more preparation. Low deposition rates limit process to thinner plates.	A high-deposition, high-penetration process, but thin material can be welded at high speeds. Easily mechanized. Natural for welding thicker plates. Housekeeping and position limitation can be a problem.	High joint completion rate, but limited to vertical. Used mainly on long vertical welds. High heat input can limit baseplates.	Specialized process for attaching studs to steel plate. Usually more economical than drilling and tapping.

SMAW, shielded metal arc welding; GMAW, gas metal arc welding; FCAW, flux-cored arc welding; GTAW, gas tungsten arc welding; PAW, plasma arc welding; SAW, submerged arc welding; EGW, electrogas welding; ESW, electroslag welding; SW, stud arc welding

Table 3 Composition and carbon equivalent of selected low-alloy steels

Steel designations			Composition, wt%										Carbon equivalent, %
SAE	ASTM	MIL-STD	C	Mn	P	S	Si	Ni	Cr	Mo	V	Nb	
High-strength low-alloy steels													
...	A 242, A 572, A 588	...	0.10–0.25	0.50–1.5	<0.04	<0.05	0.20–0.35	0–0.75	0–0.75	0–0.25	0–0.05	0–0.04	0.25–0.75
Quenched-and-tempered steels													
...	A 508, A 517	S-16216 (HY-80)	0.10–0.30	0.20–1.5	<0.04	<0.05	0.20–0.35	0–3.4	0–1.5	0–0.5	0–0.05	0–0.04	0.35–1.10
Heat-treatable low-alloy steels													
4140, 4340	...	...	0.30–0.50	0.50–1.0	<0.04	<0.05	0.15–0.30	0–3.0	0.50–1.0	0.15–0.25	...	...	0.55–1.20
Thermal-mechanical-controlled processing steels													
...	A 841		0.04–0.15	0.70–1.5	<0.03	<0.03	0.20–0.35	...	0–0.25	0–0.05	0–0.05	0–0.03	0.20–0.50
Chromium-molybdenum steels													
...	A 217, A 387	...	0.10–0.20	0.50–0.70	<0.035	<0.04	0.15–0.50	...	0.50–9.0	0.50–1.0	...	...	0.38–2.0

Corrosion of Carbon Steel Weldments

The corrosion behavior of carbon steel weldments produced by fusion welding is dependent on a number of factors. Corrosion of carbon steel weldments can be due to metallurgical effects, such as preferential corrosion of the HAZ or weld metal, or it can be associated with geometrical aspects, such as stress concentration at the weld toe, or creation of crevices due to joint design. Additionally, specific environmental conditions can induce localized corrosion such as temperature, conductivity of the corrosive fluid, or thickness of the liquid corrosive film in contact with the metal. In some cases, both metallurgical and geometric factors will influence behavior, such as in SCC. Preferential weldment corrosion of carbon steels has been investigated since the 1950s, commencing with the problems on ice breakers, but the problem continues today in different applications (Ref 7).

This section describes issues related to corrosion of carbon steel weldments and remedial measures that have proven successful in specific cases; however, it is still difficult to predict whether attack will be concentrated on the HAZ, weld metal, or both areas in susceptible conditions. Care is also required in transfer of remedial measures to different applications because of the complexity of interacting factors that may lead to additional problems. Frequently, therefore, corrective measures need to be applied once a problem is identified, but laboratory testing is recommended for applications where preferential attack is anticipated.

Influence of Weld Microstructure

Consideration must be given to the compositional effects of the base metal and welding consumable and to the different welding processes used. The base metal experiences temperatures ranging from ambient at a distance away from the weld to the melting point at the fusion boundary during welding. Therefore, metallurgical transformations occur across the weld metal and HAZ, and these microstructures can significantly alter the intrinsic corrosion rate of the steel. Fusion welding produces a weld metal that, due to the high cooling rate, is effectively a chill casting containing a high density of lattice defects and segregation of elements (Ref 8). A wide range of microstructures can be developed in a weldment based on cooling rates, and these microstructures are dependent on energy input, preheat, metal thickness (heat sink effects), weld bead size, and reheating effects due to multipass welding. As a result of their different peak temperatures, chemical compositions, and weld inclusions (oxides and sulfides), weld metal microstructures are usually significantly different from those of the HAZ and base metal. Similarly, corrosion behavior can also vary, but in cases where corrosion mitigation measures are correctly applied, for example, coating or cathodic protection or inhibition, these will normally be adequate to prevent preferential corrosion of carbon steel weldments.

Another important factor to note is that for a given composition, hardness levels will be lowest for high heat inputs, such as those produced by submerged arc weldments, and will be highest for low-energy weldments (with faster cooling rates) made by, for example, the shielded metal arc, gas tungsten arc, and metal inert-gas processes. Note that in comparing the heat input, it is necessary to account for the arc efficiency to compare processes. Depending on the welding conditions, weld metal microstructures generally tend to be fine grained with basic flux and somewhat coarser with acid or rutile (TiO_2) flux compositions.

Residual Stress

During welding, the base metal, HAZ, and underlying weld passes experience stresses due to thermal expansion and contraction. On solidification, high levels of residual stress, often close to the material yield stress, remain as a result of weld shrinkage. Stress-concentration effects as a result of geometrical discontinuities, such as weld reinforcement (excess weld metal) and lack of full weld penetration (dangerous because of the likelihood of crevice corrosion and the possibility of fatigue cracking), are also important because of the possibility of SCC in some environments.

Geometrical Factors

It should be recognized that excess root penetration can interrupt fluid flow close to the wall of a pipe in high-flow-rate operation, leading to impingement corrosion downstream of the weld. Alternatively, in low-velocity oil and gas systems where the water content is entrained in the bulk fluid, such excess penetration can cause flow disruption and water dropout, allowing pooling of water downstream of the weld, which can lead to increased corrosion of the weldment or adjacent base metal (Ref 9).

Preferential HAZ Corrosion

A wide range of HAZ microstructures can be produced because, close to the fusion boundary, the HAZ transformation to austenite on heating will be followed on cooling by transformation to give either a ferrite-carbide microstructure or martensite, depending on material composition, peak temperature, and cooling rate. Farther from the weld, the material will be exposed to a lower peak temperature, so only partial reaustenization occurs, and those areas heated below the ferrite-to-austenite transformation temperature (Ac_1) will not be significantly affected, other than by some carbide coarsening and tempering. Despite these variations, in the majority of applications, there is little influence on the corrosion performance, and preferential HAZ corrosion is relatively rare. Where preferential HAZ attack has been reported, it is more common in carbon and carbon-manganese steels than in higher-alloy grades (Ref 8).

An example of preferential corrosion in the HAZ of a carbon steel weldment is shown in Fig. 1. This phenomenon has been observed in a wide range of aqueous environments, the common link being that the environments are fairly high in conductivity, while attack has usually, but not invariably, occurred at pH values below approximately 7 to 8.

Preferential HAZ corrosion in seawater was reported in the 1960s and attributed to the presence of low-temperature transformation products such as martensite, lower bainite, or retained austenite (Ref 11). Therefore, steel compositions favoring increased hardenability (e.g., increase in manganese content) may lead to increased localized corrosion, but microalloyed steels are not susceptible. *Tramline corrosion* is a term applied to preferential HAZ corrosion concentrated at the fusion boundaries and has been observed in acidic aqueous environments such as acid mine waters.

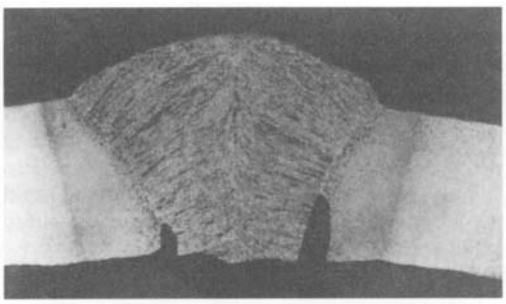

Fig. 1 Preferential corrosion in the HAZ of a carbon steel weldment after service in an aqueous environment. 5×. Source: Ref 10

There is clearly a microstructural dependence, and studies on HAZs show corrosion to be appreciably more severe when the material composition and welding parameters are such that hardened structures are formed. It has been known for many years that hardened steel may corrode more rapidly in acid conditions than fully tempered material, apparently because local microcathodes on the hardened surface stimulate the cathodic hydrogen evolution reaction. The rate of corrosion is usually governed by the cathodic (reduction) rate when other limiting factors are not present, and therefore, it is a factor in acidic environments but less so in neutral or alkaline conditions. On this basis, it is proposed that water treatments ensuring alkaline conditions should be less likely to induce HAZ corrosion, but even at a pH near 8, hydrogen ion (H^+) reduction can account for approximately 20% of the total corrosion current; pH values substantially above this level would be needed to suppress the effect completely. Furthermore, if such treatments may be useful to control preferential HAZ corrosion when it has not been anticipated, it is considered to be more reliable to avoid the problem through design. Avoidance through selection of appropriate material or welding procedure, for example, to minimize hardness, is the preferred remedial approach, because PWHT may necessitate temperatures high enough for normalizing to gain full benefit, which is usually impractical (Ref 8).

In some oil and gas production environments, preferential weldment corrosion may lead to enhanced HAZ attack or weld metal corrosion. In the late 1980s, studies of the problems associated with preferential weldment corrosion in sweet oil and gas production systems were undertaken (Ref 12). In some cases, the HAZ was attacked, while in other cases, the weld metal was preferentially corroded. Where enhanced HAZ corrosion was observed, the composition was more influential than the microstructure; however, hardened transformed microstructures suffered increased corrosion. The PWHT at 590 °C (1100 °F) for stress relief was beneficial in reducing HAZ attack (Ref 9), despite the previous comments.

HAZ/Fusion Line Corrosion of Welded Line Pipe. There is a particular case of preferential weldment corrosion worth highlighting in

respect to electric-resistance-welded/high-frequency-induction-welded (ERW/HFI) pipe, where attack of the seam weld HAZ/fusion line can occur in aqueous environments or when exposed to the water phase in a mixed-phase system due to flow conditions or water dropout at low points. This grooving corrosion has been attributed to inclusions within the pipe material being exposed at the pipe surface and modified by the weld thermal cycle (Ref 11). A normalizing heat treatment can reduce or prevent occurrence. However, the major remedial action is the selection of a cleaner alloyed steel (Ref 13). Corrosion is due to electrochemical potential differences (galvanic corrosion) between the HAZ/fusion line and the parent material, attributed to the unstable MnS inclusions produced during the welding cycle. It is highlighted that the potential difference may only be of the order of perhaps 30 to 70 mV, but the low surface area ratio of anode to cathode results in high corrosion rates (between 1 to 10 mm, or 0.04 to 0.4 in., per year). Mitigation against this form of corrosion was achieved through modified steel composition in the 1970s; the addition of copper plus reduced sulfur to minimize MnS formation and the addition of calcium, nickel, or titanium to stabilize the remaining sulfur eliminates the potential difference. Such corrosion has become less common in recent years, due to awareness of these issues and remedial measures.

Preferential Weld Metal Corrosion

The weld metal in a carbon-manganese steel may suffer preferential corrosion, but again, if quality corrosion mitigation is in place for the main structure, such as coating or cathodic protection, this preferential attack is also normally prevented. However, there are cases where coating failure or inefficient inhibition can then lead to localized corrosion.

It is probable that similar microstructural considerations also apply to the preferential corrosion of weld metal, but in this case, the situation is further complicated by the presence of deoxidation products, their type and number depending largely on the flux system employed. Consumable type plays a major role in determining weld metal corrosion rate, and the highest rates of metal loss are normally associated with shielded metal arc electrodes using a basic coating. In seawater, for example, the corrosion rate for a weld made using a basic-flux-coated consumable may be three times as high as for weld metal from a rutile-flux-coated consumable. Fewer data are available for submerged arc weld metals, but it would appear that they are intermediate between basic and rutile flux shielded metal arc electrodes and that a corrosion rate above that of the base steel can be expected. In many cases, the underlying cause of the problem is the electrochemical potential difference between the weld metal and the adjacent parent steel, as discussed subsequently.

Preferential weld metal corrosion of carbon and low-alloy steels used for pipelines and process piping systems in carbon dioxide (CO_2)-containing media has been observed increasingly in recent years. In particular, this has been on weldments made by the manual metal arc (MMA) process using electrodes containing nickel or nickel plus copper. One comprehensive study examined the link between preferential weld metal corrosion and electrode composition (Ref 7). Corrosion tests were conducted on weldments produced in X52, X60, and X65 grade pipe materials in CO_2-containing media. Greatest resistance to preferential weld metal corrosion was obtained for autogenous root deposits or for welds deposited using consumables without significant alloying additions (matching filler metals). The addition of 1% Ni was detrimental, as was 1% Si. The addition of 0.5% Mo or 0.6 to 0.7% Cr to the weld metal had no consistent beneficial effect with respect to preferential weld metal corrosion. Preferential weld metal corrosion also increased with increasing hardness, increasing grain size, an increasing level of aligned second phase, and a decreasing level of microstructure refinement of the root by subsequent passes. Details of the welding consumables and significant alloying elements are given in Table 4. Figure 2 shows the average calculated electrochemical impedance spectroscopy (EIS) corrosion rates between 5 and 10 days from a low chloride (0.35 g/L NaCl) test.

Mitigation of Preferential Weldment Corrosion

Optimized process selection and welding procedures will assist in achieving good-quality welds, ensuring full weld penetration and minimizing excessive weld reinforcement; postweld dressing by grinding (a costly method) can be effective in minimizing the geometric effects.

A stress-relieving heat treatment may be effective in reducing residual stress (internal

weld shrinkage stress) and metal hardness to safe levels in most cases of concern regarding environmentally assisted cracking (SCC and sulfide stress cracking).

A PWHT stress relief has also been reported to be beneficial in reducing HAZ attack (Ref 8). However, in other cases, avoidance through selection of appropriate material or welding procedure is the preferred remedial approach, because PWHT may necessitate temperatures high enough for normalizing to gain full benefit, which is usually impractical (Ref 8).

Mitigation of preferential weld metal corrosion may be achieved in some cases via alloying additions to make the weld metal cathodic to the adjacent base metal. It must be noted that although the weld becomes cathodic to the base material, accelerated corrosion of the base metal

Table 4 Welding details for the preferential weld metal corrosion study

Weld number	Weld type (target dilution)	Parent steel grade	Welding process(a)	AWS consumable designation (closest)	Significant alloying elements	Alloying element in weld metal%
W41	Matching filler	X52/A333-6	MMA	E7018	None	. . .
W21	Matching filler	X52/A333-6	TIG	ER70S-6	None	. . .
W39	Matching filler	X65	TIG	ER70S-6	None	. . .
W25	High Si (20%)	X52/A333-6	TIG	ER70S-6	1.05%Si	0.55(Si)
W20	High Ni (30%)	X52/A333-6	MMA	E8018-C3	1%Ni	0.58(Ni)
W26	Low Ni (50%)	X52/A333-6	TIG	ER80S-Ni1	1%Ni	0.41(Ni)
W29	High Cr (20%)	X60 (0.5%Cr)	MMA	E8010-G	0.6%Cr	0.67(Cr)
W31	Low Cr (50%)	X52/A333-6	TIG	ER80S-G	0.6–0.7%Cr	0.34(Cr)
W43	High Cr (20%)	X52/A333-6	MMA	E8010-G	0.6%Cr	0.57(Cr)
W33	Mo addition (20%)	X52/A333–6	MMA	E7015–A1	0.5%Mo	0.32(Mo)
W35	Autogenous	X52/A333-6	TIG	. . .	. . .	. . .
W37A	Autogenous	X65	TIG	. . .	. . .	. . .

(a) MMA, manual metal arc; TIG, tungsten inert gas. Source: Ref 7

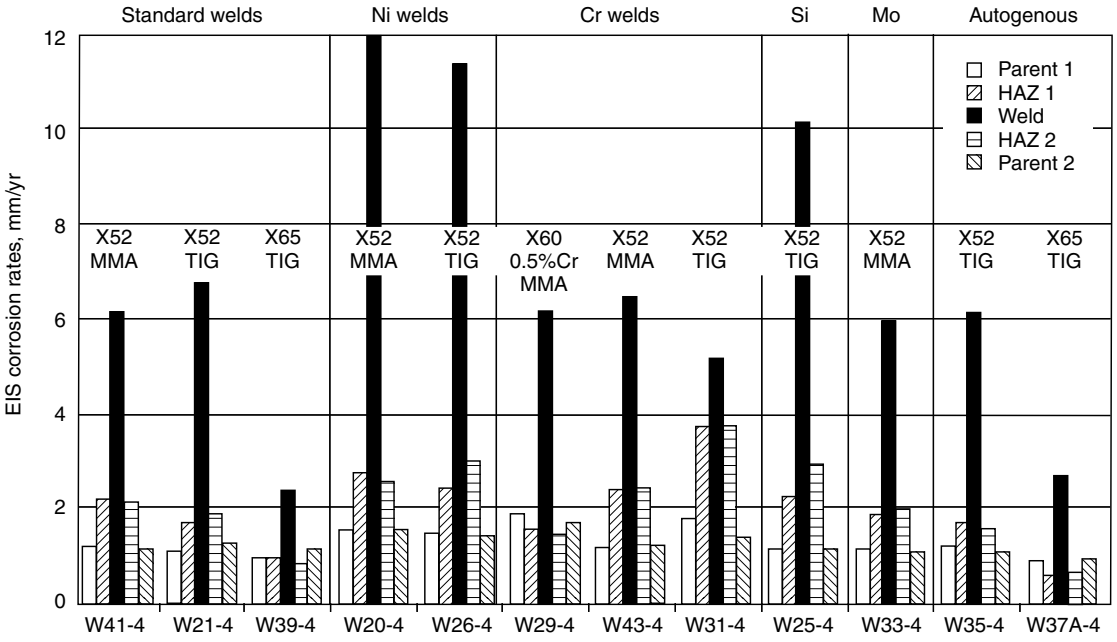

Fig. 2 Average EIS calculated corrosion rate during the period of 5–10 days; tests conducted in low chloride solution at 60 °C (140 °F) Source: Ref 7

is unlikely, because the anode-to-cathode surface area ratio becomes very high. However, care is required in extrapolating remedial measures proven in one environment, because they may not be efficient in different conditions. For example, the factors influencing such localized corrosion in sweet oil and gas environments are complex, and the use of nickel-containing weld metal for the root, successful in mitigating attack in seawater injection systems, has led to incidents of preferential attack in particular systems operated at temperatures of approximately 70 to 80 °C (160 to 175 °F) (Ref 14).

However, when introducing measures to avoid weld metal corrosion, care must be taken to avoid enhanced corrosion of the adjacent HAZ, due again to galvanic effects, particularly where the environment has relatively low conductivity, such as freshwater (Ref 11).

In summary, preferential weldment corrosion of carbon steels has been observed in diverse applications, from plate steels in the marine industry to pipe and process equipment, piping tankage, pressure vessels (Ref 15), and similar equipment in the oil and gas sectors. Some typical case histories are presented as follows, but mitigation in most cases requires an assessment of the particular environment and materials involved and will likely necessitate some testing to evaluate the performance in service.

Galvanic Corrosion

Some of the earliest problems of weld metal corrosion related to ships in arctic waters, where ice abraded the paint to expose bare steel and damaged the anodes, thus rendering the cathodic protection system ineffective. In these cases, it was observed that enhanced corrosion of the weld metal was due to electrochemical potential differences between the weld metal and the base metal, such that the weld metal is anodic in the galvanic couple. Further detailed studies were undertaken in the late 1980s to assess more modern steels and welding consumables in arctic waters off Canada (Ref 16). Both HAZ and weld metal attack were observed, and the general conclusions were that for steels between 235 and 515 MPa (34 and 75 ksi) minimum yield strength with high manganese content (1.4%) in the parent steel, resulted in enhanced preferential HAZ attack, but this could be reduced via increased heat input during welding. Generally, the rate of weld metal attack was dependent on the nickel and copper contents of the welding consumable and was less influenced by parent steel composition, although a steel with copper, nickel, and chromium additions led to a more noble parent steel, hence accelerating weld metal attack. It was noted that parent steel with low silicon content led to increased weld metal corrosion, supporting the earlier findings that silicon <0.2% can be detrimental, but the opposite was observed for silicon in the weld metal.

It is highlighted that, as for the autogenous seam weld in ERW/HFI pipe, the difference in corrosion potential for the separated regions (parent steel, HAZ, and weld metal) may be only a few tens of millivolts, but due to the low surface area ratio of anode to cathode in conductive solutions, the attack on the anodic weld metal or HAZ may be very high. Also, ongoing corrosion of the parent steel will continue, and if this rate is unacceptable, mitigation or protection methods are required for the base material in addition to consideration of ways to control the enhanced localized attack at the weldments. Generally, such weld metal attack has occurred in high-conductivity media, and the measures described to ensure the weld metal is cathodic (more noble) relative to the base metal have been successful. However, this may not be successful in different environmental conditions.

Industrial Case Studies of Galvanic Corrosion. In one case, premature weld failures were experienced in a 102 mm (4 in.) ASTM A53 pipe that was used to transfer a mixture of chlorinated hydrocarbons and water. During construction, the pipeline was fabricated with E7010-Al welding electrodes (see Table 5 for the compositions of all materials discussed in these examples). Initial weld failures and subsequent tests showed the following welding electrodes to be anodic to the A53, grade B, base metal: E7010-Al, E6010, E6013, E7010-G, and E8018-C2. Two nickel-base electrodes—Inco-Weld A (American Welding Society, or AWS, A5.11, class ENiCrFe-2) and Incoloy welding electrode 135—were tested; they were found to be cathodic to the base metal and to prevent rapid weld corrosion. The corrosion rates of these various galvanic couples are listed in Table 6.

Another example is the failure of low-carbon steel welds in seawater service at 25 °C (75 °F). Fabrications involving ASTM A285, grade C, plate welded with E6013 electrodes usually start to fail in the weld after 6 to 18 months in seawater service at this temperature. Welds

made with E7010 electrodes do not fail. Tests were conducted in seawater at 50 °C (120 °F) using A285, grade C, plate welded with E6010, E7010-Al, and E7010-G. It was determined that E7010-Al was the best electrode to use in seawater and that E6010 and E7010-G were not acceptable (although they were much better than E6013), because they were both anodic to the base metal. A zero resistance ammeter was used to determine whether the electrodes were anodic or cathodic to the base metal.

In another case, welds made from E7010-Al electrodes to join ASTM A285, grade C, base metal were found to be anodic to the base metal when exposed to raw brine, an alkaline-chloride (pH > 14) stream, and raw river water at 50 °C (120 °F). When E7010-G was exposed to the same environment, it was anodic to the base metal in raw brine and raw river water and was cathodic to ASTM A285, grade C, in the alkaline-chloride stream. When the base metal was changed to ASTM A53, grade B, and A106, grade B, it was found that E7010-Al weld metal was cathodic to both when exposed to raw brine at 50 °C (120 °F).

Finally, routine inspection of a column in which a mixture of hydrocarbons was water washed at 90 °C (195 °F) revealed that E7016 welds used in the original fabrication were corroding more rapidly than the ASTM A285, grade C, base metal. Corroded welds were ground to sound metal, and E7010-Al was used to replace the metal that was removed. Approximately 3 years later, during another routine inspection, it was discovered that the E7010-Al welds were being selectively attacked. Tests were conducted that showed E7010-Al and E7016 weld metals to be anodic to A285, grade C, while E7018 and E8018-C2 would be cathodic. Corrosion rates of these various galvanic couples are given in Table 7.

These examples demonstrate the necessity for testing each galvanic couple in the environment for which it is intended. Higher-alloy filler metals can sometimes be used to advantage to prevent rapid preferential weld corrosion.

Environmentally Assisted Cracking (EAC)

Environmentally assisted cracking is common in the refining and power-generation industries where components frequently operate in aggressive environments. Environmentally assisted cracking or degradation can take many forms, ranging from local thinning caused by global corrosion attack, to SCC and hydrogen damage. The form of cracking or degradation depends on a number of factors, including the material, chemical composition and microstructure, weld metal and HAZ properties (including hardness), weld geometry, level of welding residual stresses, operating conditions, and environment.

Table 5 Compositions of carbon steel base metals and some filler metals subject to galvanic corrosion

See Tables 6 and 7 for corrosion rates of galvanic couples.

	Composition, wt%						
Metal	C	Mn	Si	Cr	Ni	Fe	Others
Base metals							
ASTM A53, grade B	0.30	1.20	. . .	. . .	. . .	bal	. . .
ASTM A285, grade C	0.22	0.90	. . .	. . .	. . .	bal	. . .
Filler metals							
E6010	No specific chemical limits						
E6013	No specific chemical limits						
E7010-A1	0.12	0.60	0.40	. . .	. . .	bal	0.4–0.65Mo
E7010-G	. . .	1.00(a)	0.80(a)	0.30(a)	0.50(a)	bal	0.2Mo, 0.1V
E7016	. . .	1.25(b)	0.90	0.20(b)	0.30(b)	bal	0.3Mo, 0.08V(b)
E7018	. . .	1.60(c)	0.75	0.20(c)	0.30(c)	bal	0.3Mo, 0.08V(c)
E8018-C2	0.12	1.20	0.80	. . .	2.0–2.75	bal	. . .
ENiCrFe-2 (Inco Weld A)	0.10	1.0–3.5	1.0	13.0–17.0	bal	12.0	1–3.5Mo, 0.5Cu, 0.5–3(Nb + Ta)
Incoloy welding electrode 135	0.08	1.25–2.50	0.75	26.5–30.5	35.0–40.0	bal	2.75–4.5Mo, 1–2.5Cu

(a) The weld deposit must contain only the minimum of one of these elements. (b) The total of these elements shall not exceed 1.50%. (c) The total of these elements shall not exceed 1.75%. Source: Ref 15

Wet Hydrogen Sulfide Cracking

Corrosion of carbon and low-alloy steels by aqueous hydrogen sulfide (H_2S) solutions or sour waters can result in one or more types of EAC. Two of the more prevalent forms of EAC affecting weldment corrosion are hydrogen-induced cracking (HIC) and sulfide stress cracking (SSC). It should be noted that there are actually two forms of HIC. The first form is cracking due to exposure to wet H_2S as described in this section. A second form—weld-related HIC—is described later in this chapter. Additional information on EAC due to wet H_2S environments can be found in Chapter 10, "Weld Corrosion in Specific Industries and Environments."

Hydrogen-induced cracking, which has been observed in both high- and low-strength steels even under nonstressed conditions, occurs primarily in the low-strength steels that are exposed to a hydrogen-containing environment. Because of its rapid cooling and solidification, weld metal forms a structure of dendrites and has oxide inclusions dispersed in the form of fine globules. It has been confirmed that weld metals, even when used without a filler metal of special chemistry, do not develop HIC up to a maximum hardness of 280 HV. In comparison, HIC has been observed primarily in the base metal and HAZ (Ref 17, 18).

Sulfide stress cracking is the failure of steel caused by the simultaneous action of stress and hydrogen absorbed from corrosion by aqueous H_2S. Susceptibility to SSC is a function of a number of variables, two of the more important are strength or hardness of the steel and the level of tensile stresses. Sulfide stress cracking is normally associated with high-strength steels and alloys—yield strength greater than 550 MPa (80 ksi)—and with high-hardness (>22 HRC) structures in weld HAZs. Non-postweld heat treated weldments are particularly problematic, because they often contain both high HAZ hardness and high residual tensile stresses that can initiate SSC and promote crack propagation. Resistance to SSC is usually improved through the use of PWHT and through the use of lower-carbon-equivalent plate steels and quenched-and-tempered wrought steels.

Table 6 Corrosion rates of galvanic couples of ASTM A53, grade B, base metal and various filler metals in a mixture of chlorinated hydrocarbons and water

The areas of the base metal and the deposited weld metal were equal.

	Base metal corrosion rate		Filler metal corrosion rate	
Filler metal	mm/yr	mils/yr	mm/yr	mils/yr
E6010	0.4	15	0.9	35
E6013	0.18	7	0.9	35
E7010-A1	1.3	50	4.3	169
E7010-G	1.7	68	2.8	112
E8018-C2	0.36	14	1.7	66
Inco Weld A	0.48	19	0.013	0.5
Incoloy welding electrode 135	0.36	14	<0.0025	<0.1

Source: Ref 15

Table 7 Corrosion rates of galvanic couples of ASTM A285, grade C, base metal and various filler metals at 90 °C (195 °F) in water used to wash a hydrocarbon stream

	Base metal corrosion rate		Filler metal corrosion rate	
Filler metal	mm/yr	mils/yr	mm/yr	mils/yr
E7010-A1	0.69	27	0.81	32
E7016	0.46	18	0.84	33
E7018	1.3	50	1.2	48
E8018-C2	2.2	85	1.04	41

Source: Ref 15

Stress-Corrosion Cracking

Stress-corrosion cracking is a term used to describe service failures in engineering materials that occur by slow, EAC propagation. The observed crack propagation is the result of the combined and synergistic interaction of mechanical stress and corrosion reactions.

SCC Due to Welding Residual Stresses. There is no doubt that residual welding stresses can contribute to SCC in specific environments in which such failure represents a hazard. This is the case for failure by both active path and hydrogen embrittlement mechanisms, and, in the latter case, failure may be especially likely at low-heat-input welds because of the enhanced susceptibility of the hardened structures inevitably formed. The following example describes SCC that resulted from residual welding stresses.

Stress-Corrosion Cracking of C-Mn Steel in a CO_2 Absorber in a Chemical Plant (Ref 19). The source of cracking in the circumferential weld of a JIS-SM50B carbon-manganese

steel pipe used in a CO_2 absorber was investigated; the absorber had been in service for 18 years. The seam had been weld-repaired twice, and the repair welds had been locally stress relieved.

The longitudinal seems of the same vessel showed no tendency toward SCC. However, these weld seams had been furnace stress relieved.

The vessel was 37.4 m (123 ft) long, 45 mm (1.8 in.) thick, and 3.9 m (13 ft) in outside diameter and was made of carbon-manganese steel conforming to Japanese specification JIS-SM50B. It was welded with E-7018 AWS-classified welding electrodes. The compositions of the parent metal and weld metal are listed in Table 8.

Background. A CO_2 absorber is used to remove CO_2 from the process gas so the gas can be reused in the chemical plant. Carbon dioxide is removed by passing it through a solution (Table 9) flowing downward from the top of the vessel (Fig. 3). The process gas is allowed to rise in the solution. The solution absorbs CO_2 from the process gas, and the gas exiting the top of the vessel is free of CO_2. The temperature of the solution during this process is approximately 125 °C (260 °F).

Circumstances Leading to Failure. Stress corrosion is caused by the presence of external or internal stresses in addition to the corrosive medium. The following condition produced these factors in this case:

- After welding, the circumferential seam was heat treated by local stress relieving that does not ensure complete removal of residual stresses.
- The seam had been repaired twice without being stress relieved adding considerable residual stresses to the weld and nearby region.
- The solution passing through the vessel contained CO_2-CO-H_2O, KHCO, and Cl^- ions, which induce SCC in carbon steels at temperatures greater than 100 °C (212 °F).

Nondestructive Evaluation. The vessel was shortened to remove the cracked circumferential weld and welded again. Two plates, 850 by 120 by 45 and 250 by 100 by 45 mm (35 by 5 by 1.8 and 10 by 4 by 1.8 in.), from the cut portion with weld in the center were sent for evaluation.

Weld seams on one side of each plate were clearly visible. No cracks were visible after cleaning the plates with acetone.

The plates were ground flat to facilitate radiographic examination. Both plates were checked for internal cracks. Several branched cracks in the weld and HAZ of the longer plate were reported. These cracks were parallel to the weld and branched severely into the base metal.

Liquid penetrant testing was conducted on both surfaces of the plates. A large number of branching cracks were noticed in the weld and HAZ. However, these cracks were seen only on the inner surface of the vessel.

Ultrasonic examination revealed a few cracks in the weld as well as in the HAZ. These cracks were 2 to 3 mm (0.08 to 0.12 in.) deep measured from the inner surface.

Microstructural Analysis. One section of the small plate was polished, etched with 3% nital, and examined at 5 × magnification. All cracks were in the HAZ of the weld, extending and branching into the base metal just adjacent to this zone. The depth of the cracks was 10 to 12 mm (0.4 to 0.5 in.). Two repair beads, one 10 to 12 mm (0.4 to 0.5 in.) deep and another 2 to 3 mm (0.08 to 0.12 in.), deep were also seen adjacent to the original weld (Fig. 4). Uniform grain structure was observed in the base metal, with coarser grains visible in the HAZ. The cracks propagating into the base metal followed a predominantly transgranular path (Fig. 5).

Mechanical Properties. Hardness measurements were taken on the base metal, original

Table 8 Absorber vessel chemical analysis results

	Composition, %								
Material	C	Mn	Si	S	P	As	Sn	Pb	Sb
Weld	0.049	0.62	0.56	0.028	0.017	0.0014	0.0025	0.001	nil
Parent metal	0.18	1.47	0.35	0.022	0.018	0.0021	0.0030	0.001	nil
JIS-SM50B	0.18 (max)	1.50 (max)	0.55 (max)	0.04 (max)	0.04 (max)	. . .	. . .	. . .	. . .

weld, two repair welds, and their HAZs using the Vicker's diamond pyramid method at a load of 10 kg (approximately 22 lb). The results were within specification and are given in Table 10.

Impact Toughness. Charpy V-notch impact testing was conducted at 0 °C (32 °F) and at room temperature to determine the toughness of the weld, HAZ, and base metal. Specimens were taken from the top and bottom of the weld, HAZ and base metal. The results met the material specifications and are given in Table 11.

Simulation Tests. To evaluate the susceptibility of the weld to SCC, two U-bend specimens (80 by 20 by 3 mm, or 3.2 by 0.8 by 0.12 in.), machined from the same material with weld in the center and bent to a radius of 5 mm (0.2 in.), were exposed to the same operating conditions inside the vessel (ASTM G30). These specimens were checked with liquid pen-

Table 9 Solution used to remove CO_2 from the process gas

Component	Value
K_2CO_3%	18
Diethylene amine (DEA), %	2.7
KHCO, %	13.8
As_2O_3 %	0.91
Aqueous K_2CO_3 %	27.5
Chloride, ppm	97.8
Iron, ppm	19.1
Suspended matter, ppm	11.9

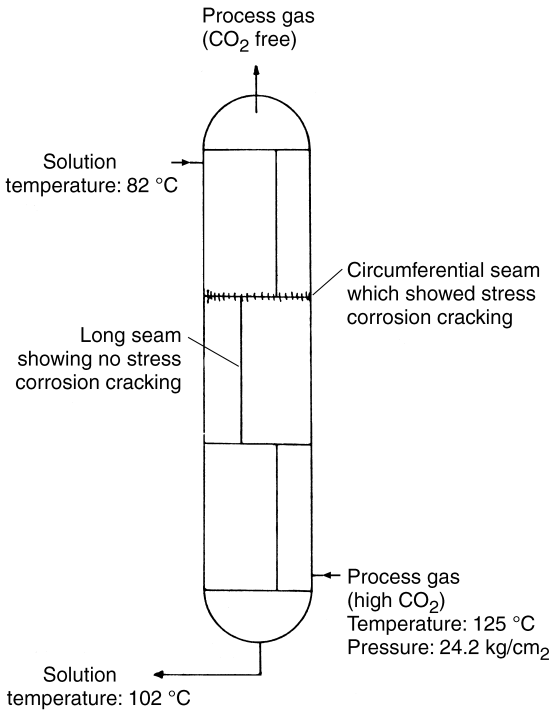

Fig. 3 Absorber vessel used to remove CO_2 from the process gas

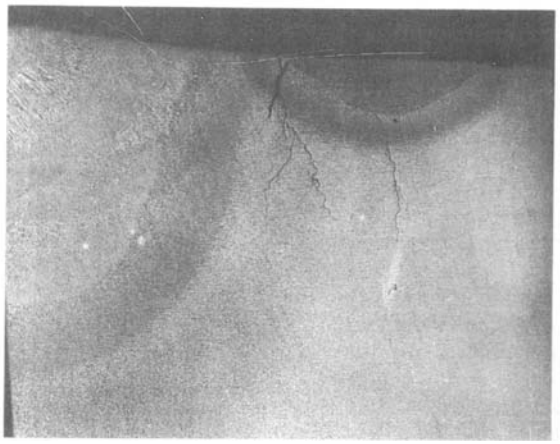

Fig. 4 Macrophotograph showing branching crack in a plate sample. 5×

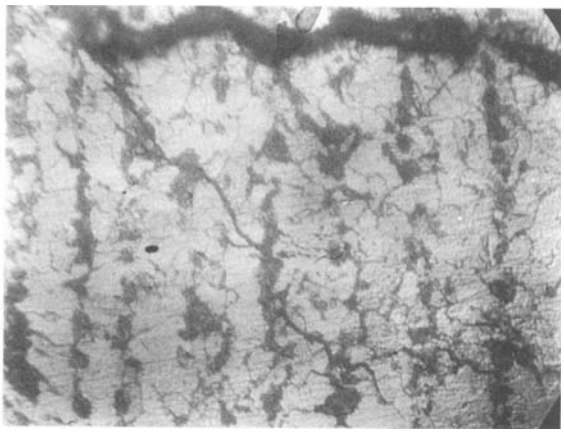

Fig. 5 Microphotograph of the crack, showing transgranular path through the base metal. 500×

Table 10 Absorber vessel hardness results

Location	Hardness, HV
Original weld (inner side)	176–181
Original weld (outer side)	180–187
First repair weld (10–12 mm deep)	206–221
Second repair weld (2–3 mm deep)	276–279
HAZ of first repair weld	195–206
HAZ of second repair weld	203–209
HAZ of original weld	161–170
Base metal	150–160

etrant prior to insertion in the vessel. After 1 year, the specimens were removed and examined. Liquid penetrant examination of these specimens also showed multidirectional cracks in the weld and the HAZ.

Discussion. Nondestructive testing revealed severe branching of the cracks on the inner side of the plates. This type of cracking is generally representative of SCC. Microexamination of the cracks revealed that propagation was transgranular, further supporting the possibility of SCC. The results of the simulation test confirmed this mode of failure.

The vessel was in service at a temperature of 125 °C (255 °F) in the presence of carbonate ions and CO_2-CO-H_2O. In this environment, carbon steel is very susceptible to SCC.

All the cracks were progressing through the HAZ of the weld. It appears that the cracks originated in this zone and subsequently propagated into the base metal and weld. The weld joint under consideration was locally stress relieved on site, while other joints were stress relieved inside a furnace. The vessel was also repaired to a depth of 10 to 12 mm (0.4 to 0.5 in.) once and to an additional 2 to 3 mm (0.08 to 0.12 in.) the following year. After these repairs, no stress relieving was done. This further enhanced the stress conditions in the HAZ and aggravated the SCC.

Conclusion and Recommendations. The basic cause of failure was stress corrosion caused by locked-in residual stresses resulting from improper and inadequate stress relieving.

To avoid SCC the welding seams should be furnace heat treated at a temperature of 600 to 640 °C (1110 to 1180 °F) for a minimum of 1 h per inch of section thickness.

SCC Due to Nitrates. Carbon and low-alloy steels are also known to fail by SCC when exposed to solutions containing nitrates (NO_3^-). Refrigeration systems using a 30% magnesium nitrate ($Mg(NO_3)_2$) brine solution, for example, are commonly contained in carbon steel. In this case, pH adjustment is important, as is temperature. Failures in the HAZ due to SCC have been reported when brine temperatures have exceeded 30 °C (90 °F) during shutdown periods. To avoid these failures, carbon steel is being replaced with type 304L stainless. Others have stress-relieved welded carbon steel systems and have operated successfully, although elevated-temperature excursions are discouraged.

SCC in Oil Refineries. Monoethanolamine (MEA) is an absorbent used to remove acid gases containing H_2S and CO_2 in oil refining operations. Recent failures in several refineries have shown that cracks can be parallel or normal to welds, depending on the orientation of principal tensile stresses. Cracking has been reported to be both transgranular and intergranular.

Before 1978, postweld stress relief of carbon steel weldments in MEA systems was performed only when the metal temperature of the equipment was expected to exceed 65 °C (150 °F) and the acid gas contained more than 80% CO_2 or when temperatures were expected to exceed 95 °C (200 °F) in any acid gas concentration.

Currently, any equipment containing MEA at any temperature and at any acid gas concentration is being postweld stress relieved. This is the result of surveys conducted by several refineries to define the extent of the SCC problem in this environment. These inspection programs showed that leaks were widespread, and were found in vessels that ranged in age from 2 to 25 years. However, there were no reports of cracking in vessels that had been postweld stress relieved. In addition, it was found that all concentrations of MEA were involved and that MEA solutions were usually at relatively low temperatures (below 55 °C, or 130 °F). Equipment found to suffer from cracking included tanks, absorbers, carbon treater drums, skimming drums, and piping. The following example of a metallurgical investigation conducted

Table 11 Absorber vessel Charpy V-notch impact test results

	Energy absorbed, J (ft · lbf)					
	Base metal		HAZ		Weld	
Temperature	Top	Bottom	Top	Bottom	Top	Bottom
0 °C (32 °F)	60(44)	54(40)	46(34)	52(38)	156(115)	136(100)
	54(40)	45(33)	. . .	. . .	. . .	. . .
Room temperature	. . .	. . .	. . .	. . .	187(138)	122(90)

by one oil refinery illustrates the problem of SCC of carbon steel in amine service (Ref 20).

Leaking Carbon Steel Weldments in a Sulfur Recovery Unit. In December 1983, two leaks were discovered at a sulfur recovery unit. More specifically, the leaks were at pipe-to-elbow welds in a 152 mm (6 in.) diameter line operating in lean amine service at 50 °C (120 °F) and 2.9 MPa (425 psig). Thickness measurements indicated negligible loss of metal in the affected areas, and the leaks were clamped. In March 1984, 15 additional leaks were discovered, again at pipe-to-elbow welds of lean amine lines leading to two major refining units. The piping had been in service for approximately 8 years.

Investigation. Metallurgical examination of several of the welds revealed that leaking occurred at what appeared to be stress-corrosion cracks originating from the inside surface. Cracks were present in weld metal and base metal approximately 5 mm (0.2 in.) away from the weld, and they passed through the HAZ as shown in Fig. 6. In other cases, stress-corrosion cracks also originated in the HAZ. The cracks typically ran parallel to the weld (Fig. 7).

Brinell hardness values, obtained by conversion of Knoop microhardness readings, were 133 to 160 (pipe base metal), 160 to 230 (weld metal), 182 to 227 (HAZs), and 117 to 198 (elbow base metal). The pipe base metal had an equiaxed fine-grain microstructure typical of low-carbon steel, and the elbow base metal had a nonequiaxed microstructure typical of hot-finished fittings. Carbon contents ranged from 0.25 to 0.30% by weight. Cracking was intergranular, as shown in Fig. 8 and 9.

The refinery operators immediately embarked on a program of visual inspection of all amine lines. As of June 1985, a total of 35 leaks in lean amine piping had been discovered. All leaks were at cracks in or around pipe-to-elbow welds, except for two leaks at welds that connected a tee and reducer, respectively. Piping size ranged from 76 to 305 mm (3 to 12 in.). Service temperature ranged from 40 to 60 °C (100 to 140 °F), with most leaks having occurred in lines carrying lean amine at 55 °C (130 °F). Pressures ranged from atmospheric to 2.9 MPa (425 psig), with most leaks having occurred between 2.8 and 2.9 MPa (400 and 425 psig). All piping had been in service for approximately 8 years, except two leaks at piping welds that had been in service for only 4 years.

As had been generally accepted industry practice, the specifications called for stress relieving or PWHT of piping and vessels in amine service at temperatures above 95 °C (200 °F). Therefore, it was highly unlikely that any of the leaking welds had received PWHT. Further metallurgical examination of leaking welds from various lines conclusively confirmed that the leaking originated at stress-corrosion cracks. No leaks were found in rich amine piping. The characteristics of the mode of fracture suggested that the failure mechanism was a form of caustic SCC.

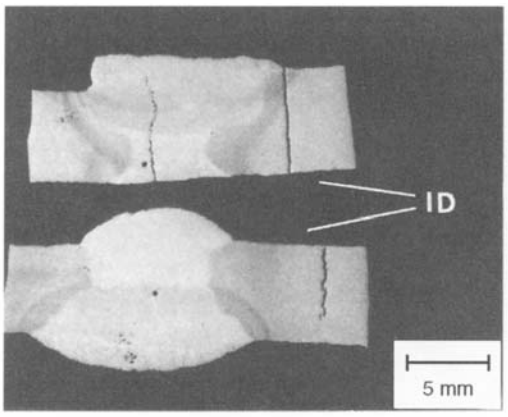

Fig. 6 Cross sections of pipe-to-elbow welds showing stress-corrosion cracks originating from the inside surface of the weld metal and the base metal. ID, inside diameter. Source: Ref 20

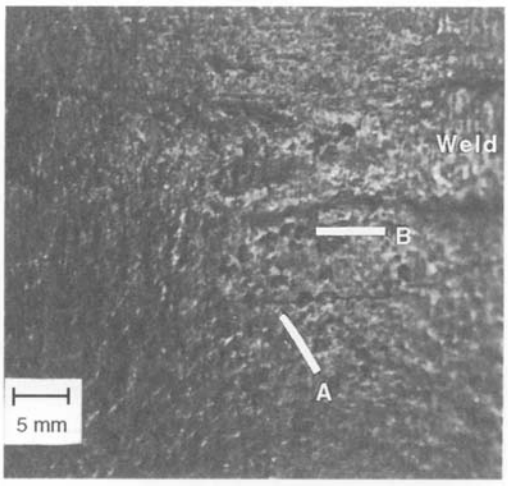

Fig. 7 Photograph of inside surface of a pipe showing 38 mm (1.5 in.) stress-corrosion crack (A) next to and parallel to a circumferential weld. Also shown are shallow corrosion pits (B). Source: Ref 20

It is interesting to note that other researchers also have metallographically examined numerous samples of similar cracks; their results can be summarized as follows:

- Cracks were essentially intergranular and were filled with gray oxide scale.

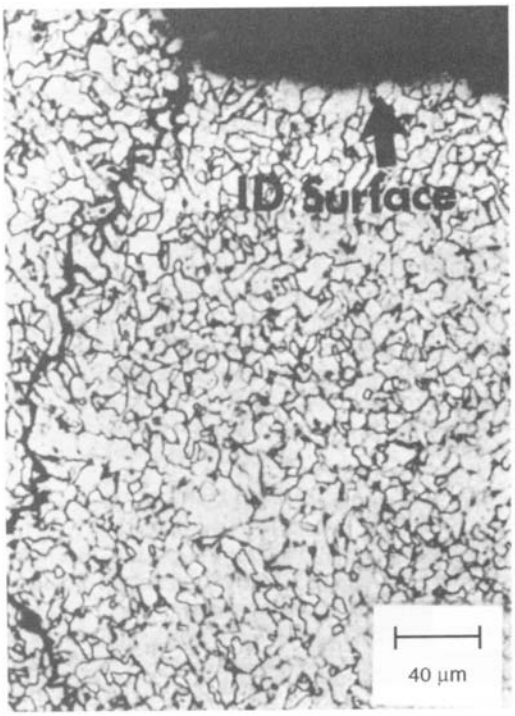

Fig. 8 Micrograph showing tight intergranular SCC originating at the inside surface of a pipe. ID, inside diameter. Source: Ref 20

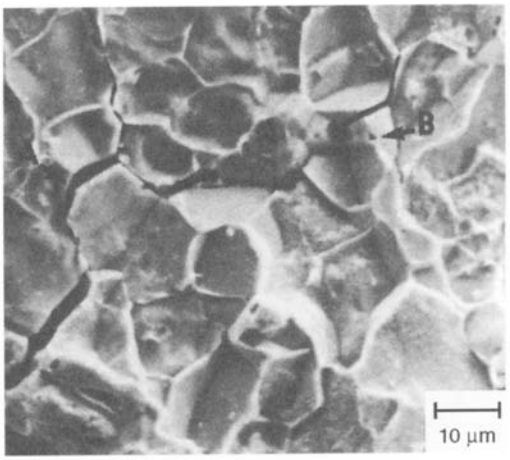

Fig. 9 Scanning electron micrograph showing inter-granular stress-corrosion cracking (A) and initiation sites for pitting (B) on the inside surface of a pipe. Source: Ref 20

- Hardness of welds and HAZs was less than 200 HB.
- Cause of fracture was believed to be a form of caustic SCC.
- Cracking occurs whether or not MEA solutions contain corrosion inhibitors.

Preventive Measures. As a result of this particular investigation and others, all welds in equipment in MEA service are being inspected. Wet fluorescent magnetic-particle inspection after sandblasting to remove oxides and scale appears to be the most effective technique. Shear-wave ultrasonic (SWU) inspection has also been used for piping, but it does not always distinguish SCC and other defect indications, such as shrinkage cracks, slag inclusions, lack of fusion, or fatigue cracks. Nevertheless, SWU is considered helpful, because these other types of defects also can pose a threat to the structural integrity of the system in question. Inspection frequency is dependent on the critical nature of the particular equipment in question, and, most important, all welds in these systems are now being post-weld stress relieved.

Corrosion of Welds in Carbon Steel Deaerator Tanks. Deaerator tanks, the vessels that control free oxygen and other dissolved gases to acceptable levels in boiler feedwater, are subject to a great deal of corrosion and cracking. Several years ago, there were numerous incidences of deaerator tank failures that resulted in injury to personnel and property damage losses. Since that time, organizations such as the National Board of Boiler and Pressure Vessel Inspectors and the Technical Association of the Pulp and Paper Industry have issued warnings to plant operators, and these warnings have resulted in the formation of inspection programs for evaluating the integrity of deaerator tanks. As a result, many operators have discovered serious cracking. The following example illustrates the problem (Ref 21).

Weld Cracking in Oil Refinery Deaerator Vessels. Two deaerator vessels with associated boiler feedwater storage tanks operated in similar service at a refinery. The vertical deaerator vessels were constructed of carbon steel (shell and dished heads), with trays, spray nozzles, and other internal components fabricated of type 410 stainless steel. Boiler feedwater was treated by sand filtration using pressure filters, followed by ion-exchange water softening. Hardness was controlled at less than 0.5 ppm calcium carbonate ($CaCO_3$). A strong cationic

primary coagulant (amine) was used to aid the filtering of colloidal material. Treated water was blended with condensate containing 5 ppm of a filming amine corrosion inhibitor. Final chemistry of the feedwater was controlled to the concentration limits given in Table 12. Oxygen scavenging was ensured by the addition of catalyzed sodium bisulfite ($NaHSO_3$) to the storage tanks. Treated water entered the top of the tray section of the deaerators through five or six spray nozzles and was stored in the horizontal tanks below the deaerators.

Inspection Results. Deaerator vessel and storage tank A were inspected. All tray sections were removed from the deaerator. With the exception of the top head-to-shell weld in the deaerator, all internal welds were ground smooth and magnetic particle inspected. No cracks were found. Corrosion damage was limited to minor pitting of the bottom head in the deaerator vessel.

Inspection of deaerator vessel B revealed cracking at one weld. Tray sections were removed from the deaerator vessel, and shell welds were gritblasted. Except for the top head-to-shell weld in the deaerator, all internal welds in both B units were then ground smooth and magnetic particle inspected. Three transverse cracks were found at the bottom circumferential weld in the deaerator vessel. These were removed by grinding to a depth of 1.5 mm (0.06 in.).

Inspection of storage tank B revealed numerous cracks transverse to welds. With the shell constructed from three rings of plate, the longitudinal ring welds were located just below the water level. These longitudinal welds exhibited no detectable cracking. One circumferential crack was found above the working water level in the vessel. The remaining cracks were located at circumferential welds below the working water level. Numerous cracks transverse to circumferential welds were detected, but only one longitudinal crack was detected. All cracks were removed by grinding to a depth of 2 mm (0.08 in.).

Unlike deaerator vessel A, it was noted that none of the spray nozzles in deaerator vessel B was operational at the time of inspection. In addition, two valves had fallen to the bottom of the deaerator vessel. The bottom section of trays in deaerator vessel B had fallen to the bottom of the storage vessel. Corrosion damage in deaerator vessel B was limited to underdeposit pitting attack at circumferential welds in the bottom.

Metallurgical Analysis. A section was cut from a circumferential weld region in storage tank B. As shown in Fig. 10, the cracking was predominantly transverse to the weld. Chemical analysis was performed on samples cut from weld metal and base metal; the results are given in Table 13. The results show that the steel plate was not aluminum-or silicon-killed but was

Table 12 Concentration limits on deaerator feedwater

Control parameter	Concentration limit
Total hardness	<0.5 ppm as $CaCO_3$
Phenolphthalein alkalinity	Trace (max)
Methyl orange alkalinity	14–18 ppm as $CaCO_3$
Chloride	7.6–8.8 ppm
Total dissolved solids	70–125 ppm

Source: Ref 21

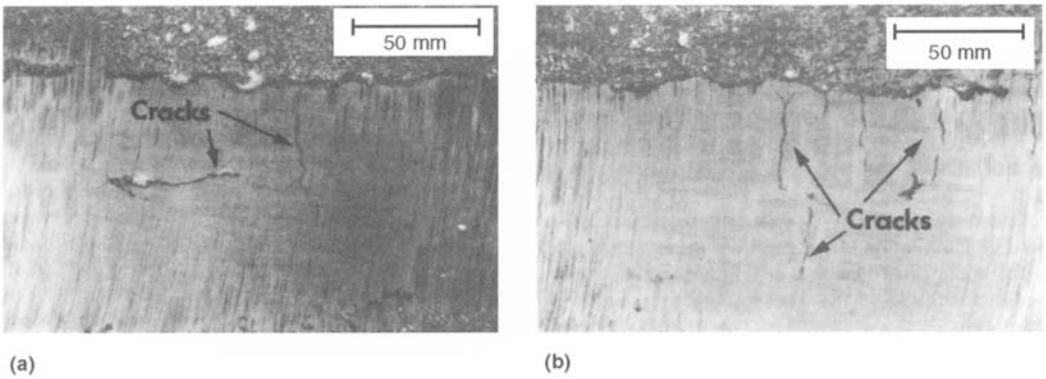

Fig. 10 Transverse and longitudinal cracks on as-ground weld areas on the inside surface of storage vessel B. (a) Transverse and longitudinal cracks. (b) Transverse cracks. Source: Ref 21

most likely a rimmed grade. Cross sections were cut perpendicular to both transverse and longitudinal cracks and were examined metallographically.

As shown in Fig. 11, metallographic examination of the base metal structures revealed ferrite and lamellar pearlite phases with a nearly equiaxed grain structure. The approximate grain size was ASTM 6 to 7. Figure 12 shows a longitudinal crack in a weld HAZ, with associated grain refinement. Cracking initiated from the bottom of a pit. The oxide associated with the major crack was extensive and contained numerous secondary cracks. Analysis of the oxide deposit within the crack by wavelength-dispersive spectroscopy revealed slightly less oxygen than an Fe_2O_3 standard. Therefore, it was assumed that the oxide deposit was a mixture of Fe_3O_4 and Fe_2O_3.

Figure 13 shows a crack extending into the base metal, transverse to the weld, with secondary cracking to the periphery of the oxidized region. It was clear that the oxide exhibited extensive internal cracking. Figure 13 also shows the entrainment of lamellar pearlite phase (dark) within the oxide corrosion product. In addition, the crack tips are blunt.

Discussion. The cracks described in this example are very similar to those found in many other investigations, despite a variety of deaerator vessel designs and operating conditions. Cracks typically display the following characteristics:

- Cracks occur most often in welds and HAZs but can also occur in the base metal.
- Cracks are generally transverse to the weld HAZ and occur both parallel and perpendicular to the hoop stress direction.
- The worst cracks appear to be located in circumferential and head-to-shell welds in horizontal vessel designs.
- Cracks are concentrated at, but not solely located within, the working water level in the vessel.
- Cracks are perpendicular to the vessel plate surface.
- Cracks are predominantly transgranular, with minor amounts of branching.
- Cracks are filled with iron oxide. Cracking of the oxide corrosion product is followed by progressive corrosion. The ferrite phase is selectively attacked, with retention of the pearlite phase within the oxide corrosion product.
- Cracks initiate from corrosion pits. Weld defects, however, can also become active sites for crack initiation.
- Crack tips are blunt.

Conclusions. These findings suggest that the failure mechanism is a combination of low-cycle corrosion fatigue and stress-induced corrosion. Extensive oxide formation relative to the depth of cracking is a key feature. The formation of oxide was associated with corrosion attack of the ferrite phase. The lamellar pearlite phase remained relatively intact and was contained within the oxide product. The oxide itself exhibited numerous cracks, allowing aqueous corrosion of fresh metal to occur at the oxide-metal interface. Mechanical or thermal stresses are most likely responsible for this network of cracks within the oxide product. The mechanism appears to be stress-assisted localized corrosion. Sharp, tight cracks were not found in fresh metal beyond the periphery of the oxide corrosion product. It therefore appears reasonable that cracking could have occurred subsequent to corrosion and within the brittle oxide.

Cracking at welds and HAZs suggests that residual weld shrinkage stresses play a major role. Welds in deaerator vessels typically have not been postweld stress relieved. It is not

Table 13 Chemical analyses of steels and weld deposit

	Analysis, wt%									
Sample	C	Mn	Si	P	S	Ni	Cr	Mo	Al	Fe
Plate 1	0.25	0.88	<0.05	0.029	0.036	<0.05	<0.05	<0.03	<0.01	bal
Plate 2	0.21	0.83	<0.05	0.03	0.024	<0.05	<0.05	<0.03	<0.01	bal
Weld deposit	0.14	0.53	0.14	0.035	0.031	<0.05	<0.05	<0.03	<0.01	bal

Source: Ref 21

unusual to find residual welding stresses of yield strength magnitude. This problem can be aggravated by vessel design (high localized bending stresses around saddle supports that fluctuate with water level and are accelerated by operational upsets).

No fault was found with the steel plate chemical composition or with welding consumables. There was no evidence of embrittlement or caustic SCC (that is, no branched intergranular cracks).

Recommendations. All welds in deaerator vessels should be postweld stress relieved. Operational upsets should be avoided, and water chemistry must be maintained within acceptable limits. This is especially true with regard to water oxygen levels, which should be kept low to minimize pitting corrosion. Detailed assessment of the influence of welding on the occurrence of such cracking and mitigation methods is provided in Ref 10.

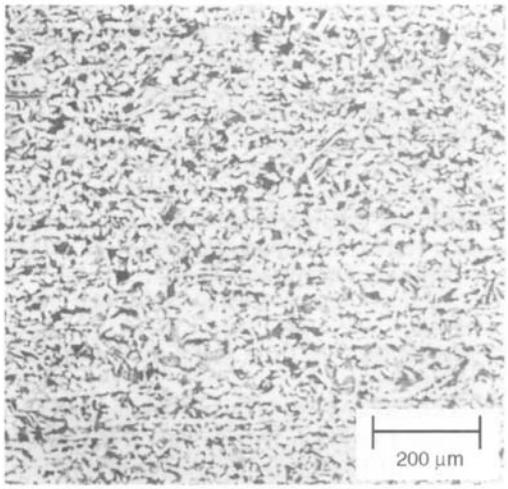

Fig. 11 Micrograph of the typical base metal microstructure of storage vessel B. Etching with nital revealed ferrite (light) and lamellar pearlite (dark). Source: Ref 21

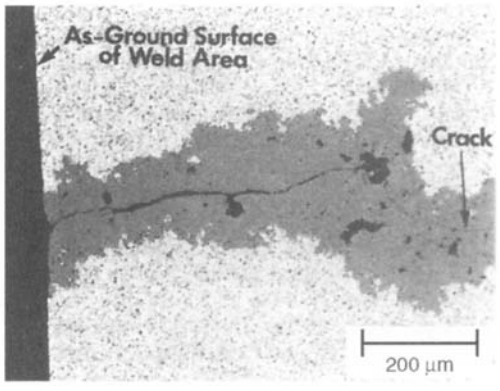

Fig. 12 Micrograph of a longitudinal crack in the HAZ of a weld from storage vessel B. Etched with nital. Source: Ref 21

Hydrogen-Induced Cracking (Ref 22, 23)

Hydrogen-induced cracking (HIC), which is also referred to as hydrogen-assisted cracking, cold cracking, delayed cracking, or underbead cracking, is a phenomenon associated with welds in hardenable carbon and low-alloy steels. This type of cracking results from the combined effects of four factors:

- A susceptible ("brittle") microstructure
- The presence of hydrogen in the weld metal
- Tensile stresses in the weld area
- A specific temperature range, –100 to 200 °C (–150 to 390 °F)

Hydrogen-induced cracking occurs after weld cooling (hence the term cold cracking) and is often delayed for many hours while atomic hydrogen diffuses to areas of high tensile stress. At microstructural flaws in a tensile stress field, the hydrogen changes to its molecular form, causing cracking. Cracking may occur in the HAZ or weld metal, and it may be longitudinal or transverse (Fig. 14). For carbon steels, cracking is more likely to occur in the HAZ because carbon steel electrodes are usually low in carbon and the weld metal is generally not hardenable. Exceptions would be if a highly alloyed electrode were being used, if the weld metal were made more hardenable by dilution of carbon from the base material, or in certain submerged arc welds where the use of excessive arc voltage and active fluxes results in high manganese and/or silicon pickup from the flux.

Cracks in the HAZ are most often longitudinal. Underbead cracks lie more or less parallel to the fusion line (Fig. 15). They do not normally extend to the surface and may therefore be difficult to detect. Underbead cracks will form at relatively low stress levels in martensite when high levels of hydrogen are present.

Toe cracks (Fig. 16) and root cracks start in areas of high stress concentration. Cracking may therefore occur in less susceptible microstructures or at relatively low hydrogen levels. This type of cracking is often delayed while the necessary hydrogen diffuses to the area.

Transverse cracking in the HAZ is less common. It will occur in high-carbon martensite under conditions of high longitudinal stresses (for example, outside fillet welds on heavy plate).

Weld metal cracks may be longitudinal or transverse. Longitudinal cracks start due to stress concentrations at the root of the weld. Transverse cracking starts at hydrogen-containing defects subject to longitudinal stresses. Weld metal cracks do not always extend to the surface. In submerged arc weld metal made with damp fluxes, a unique crack morphology known as chevron cracking can occur. Here the cracks lie at 45° to the weld axis.

One of the serious problems with hydrogen-induced cracking is the difficulty in detecting the presence of a crack. The delayed nature of some of the cracks demands that inspection not be carried out too soon, especially in welds that will have external stresses applied when put in service. Because some of the cracks do not extend to the surface, they are not detectable by visual inspection methods (for example, liquid penetrant, or magnetic particle inspection, which requires the defect to be near the surface). Radiography is most sensitive to volumetric flaws, and it may not detect cracks that are too fine or of the wrong orientation. Ultrasonic inspection is capable of detecting the crack if the operator knows where to look. Given the difficulty in detecting HIC and the possibility of this cracking leading to in-service failure, it is prudent to observe the precautions necessary to avoid cracking in the first place.

Prevention of HIC. The major preventative measures to avoid cold cracking are:

- Preheat, including maintenance of proper interpass temperature
- Heat input control
- Postweld heat treatment
- Bead tempering
- Use of low-hydrogen processes and consumables
- Use of alternate filler materials (for example, austenitic electrodes)

Detailed information on these preventative measures can be found in the article "Arc Welding of Carbon Steels" in Volume 6, *Welding, Brazing, and Soldering,* of the *ASM Handbook.*

The relative susceptibility of steels to HIC can be predicted by use of the Graville diagram, which suggests that the susceptibility can be evaluated by calculating the carbon equivalent and comparing it to the carbon content (Ref 24). An example of the Graville diagram for various classes of carbon and low-alloy steels is shown in Fig. 17. As indicated in this figure, zone I steels have low carbon and low hardenability and are not very susceptible to cracking. Zone III steels have both high carbon and high hardenability, and all welding conditions will produce crack-sensitive microstructures. Therefore, to avoid hydrogen-induced cold cracking in zone III steels, the user must apply low-hydrogen procedures, including preheat and PWHT. Zone II steels have higher carbon levels with lower hardenability. It is possible to avoid crack-sensitive microstructures in zone II steels by restricting

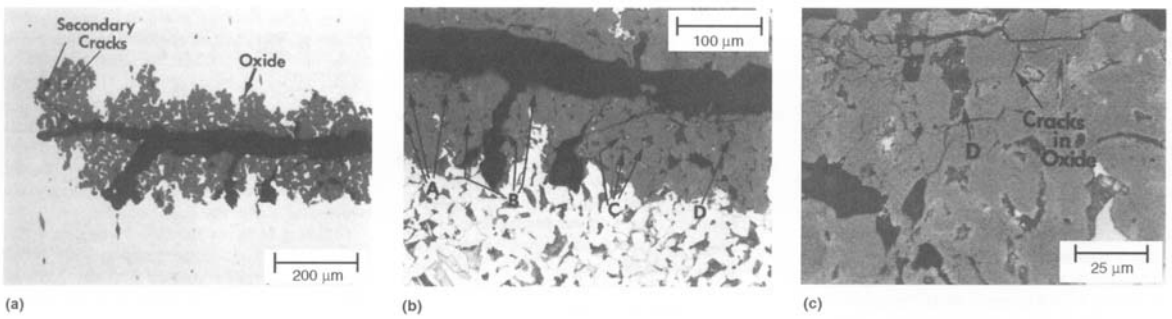

Fig. 13 Micrographs of a transverse crack in storage vessel B. (a) Crack extending into base metal. As-polished. (b) Lamellar pearlite phase (dark) entrained in the oxide corrosion product. (c) Microcracks and entrained pearlite phase in the oxide corrosion product. (b) and (c) Etched with nital. Source: Ref 21

HAZ cooling rates through control of heat input and, to a minor extent, with preheat.

Figure 17 also shows that HTLA steels, squarely in Zone III, require special considerations for welding. Chromium-molybdenum steels and quenched and tempered steels also require some attention, as do some HSLA steels. Low-carbon steels are readily welded except in thick sections, for which some precautions may be necessary. The TMCP steels have been specifically developed to lie in zone I, and so their weldability and resistance to cold cracking is excellent.

Effect of Welding Practice on Weldment Corrosion

As was discussed in Chapter 1, "Basic Understanding of Weld Corrosion," proper welding practices can minimize or eliminate corrosion problems. In the following example, poor weld quality led to the failure of a carbon steel piping cross-tee assembly used to convey H_2S process gas. This failure could have been prevented by a careful visual inspection of the weld and possible ultrasonic thickness measurements of the weld thickness at the time of fabrication.

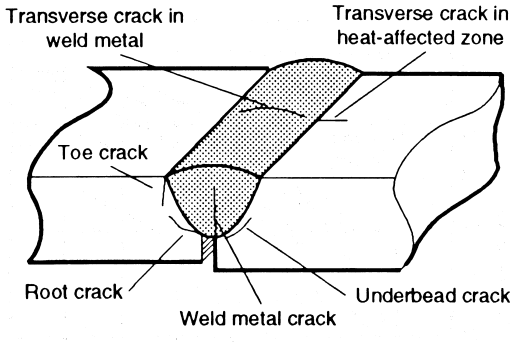

Fig. 14 Schematic showing location of hydrogen-induced cracks in carbon steel weldments. Source: Ref 23

Corrosion Failure of a Chemical Process Piping Cross-Tee Assembly (Ref 25). This cross-tee was located in piping which conveyed concentrated H_2S gas at 150 to 275 °C (300 to 525 °F) with a maximum allowable operating pressure (MAOP) of 3 MPa (450 psig). The H_2S gas was not dry. Three legs of the cross-tee were connected by elbows to long, straight vertical runs of pipe. The fourth leg was a blind stub. The cross-tee with its elbows is shown in Fig. 18. The cross-tee was subject to both frequent thermal and pressure cycling as a result of system operation.

The component had operated in the manner described for several years when the cross-tee ruptured at the toe of one of the welds. There were no known abnormal process occurrences immediately prior to the rupture. No other related components in the system had suffered failure.

The cross-tee was created by welding two 2 inch pipes* 180° apart to a run of 3 in. pipe. One 2 in. leg was welded directly to the 3 in. pipe, while the other was joined through a reduction socket fitting. The design of the cross-tee specified ASTM A-53 Grade B Schedule 80 steel pipe and ASTM A-105 and ASTM A-234 Grade WPB forged steel fittings.

Investigation. Figure 18 shows the failed cross-tee assembly. The C-D run of the cross-tee was 3 in. pipe, while the A and B legs were 2 in. pipe. Leg B was joined directly to the C-D run by a weld, while Leg A was joined to the C-D run through a forged reduction socket (see Fig. 19).

*The designation 2 in. and 3 in. are nominal pipe sizes and do not relate precisely to either interior or exterior dimensions; therefore, no metric equivalents are offered.

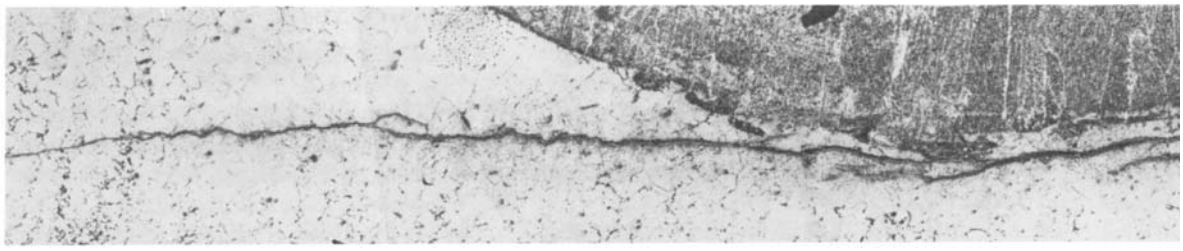

Fig. 15 Underbead crack, the result of hydrogen-induced cold cracking, in the HAZ of a shielded-metal arc weld in AISI 1045 steel. Etched with 2% nital. 30×

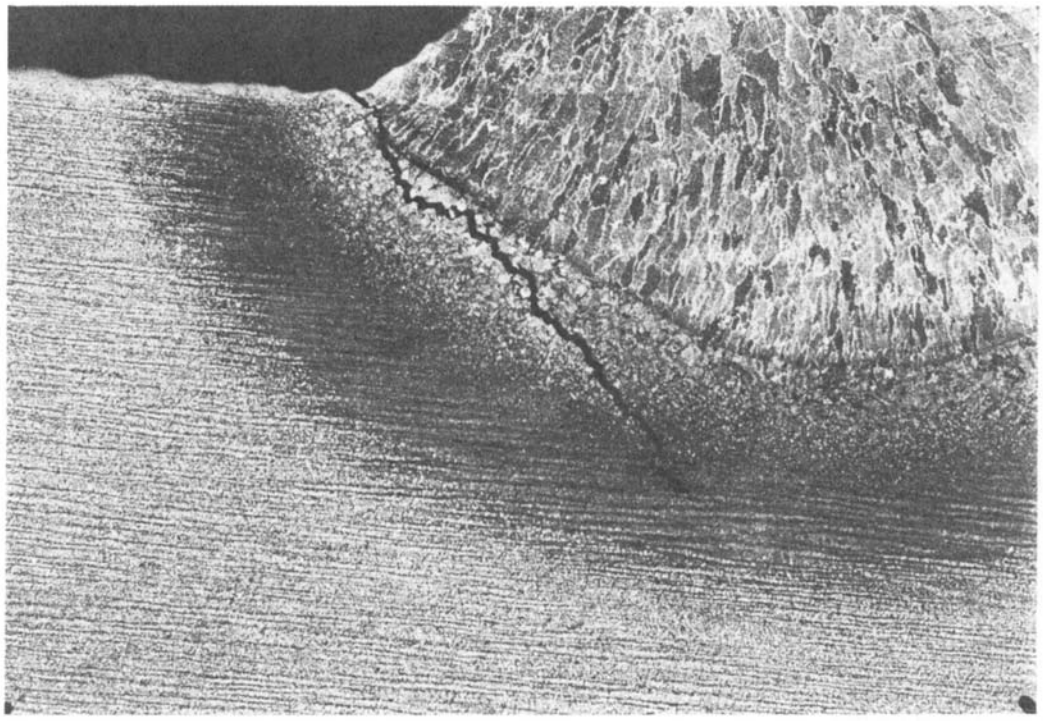

Fig. 16 Hydrogen-induced toe cracking in the HAZ of a shielded metal-arc weld in low-carbon steel. Etched with 2% nital. 18× Courtesy of The Welding Institute

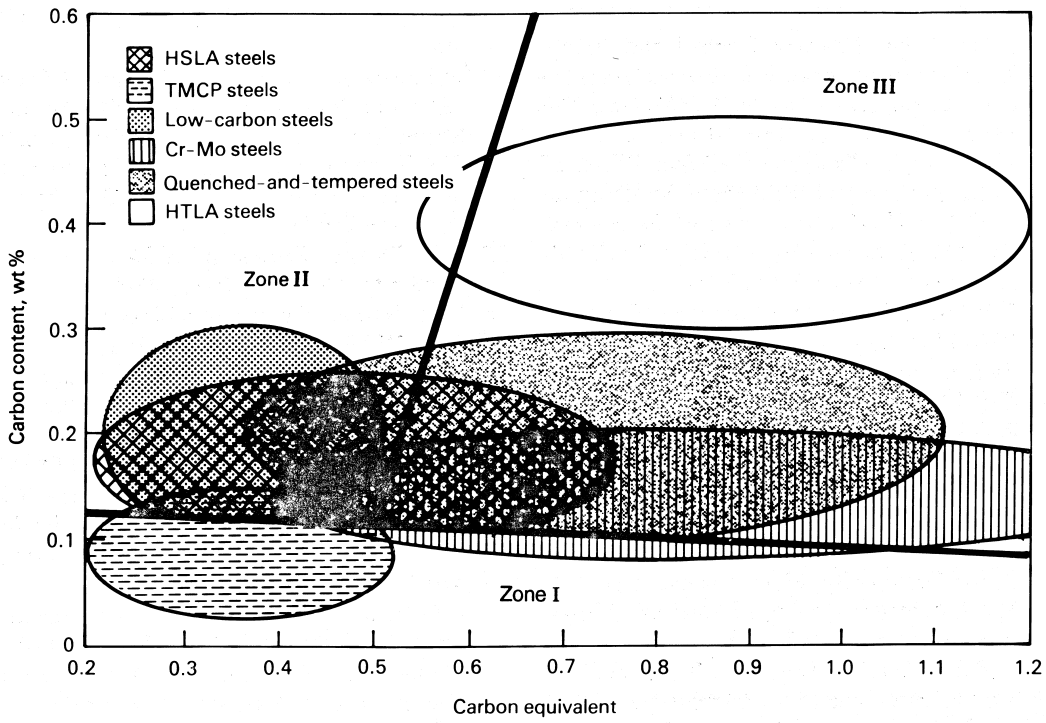

Fig. 17 Graville diagram showing susceptibility of steels to hydrogen-induced cold cracking relative to carbon content and carbon equivalent (CE), where CE = %C + (%Mn + %Si)/6 (%Ni + %Cu)/15 + (%Cr + %Mo + %V)/5. Susceptibility to cold cracking progressively increases as steels migrate from zones I to II to III. See text for details. HSLA, high-strength low-alloy; TMCP, thermomechanically controlled processed; HTLA, heat-treatable low-alloy. Source: Ref 24.

The arrow in Fig. 19 shows the location of the rupture at the toe of the weld joining the reduction socket to the 3 in. C-D run. The weld bead showed quite noticeable external lack of weld bead buildup at this location. The weld was visibly starved of filler metal at this location.

The internal surfaces of the piping were found to be coated with columnar crystalline deposits up to approximately 6 mm (0.25 in.) thick, deposited in concentric layers or rings.

The cross-tee was sectioned through the plane of the legs. When the internal deposits were removed, the surface was found to be covered with a reticulated pattern suggestive of thermal fatigue (Fig. 20).

Close visual examination of the rupture showed that the lips of the rupture were extremely thin with no obvious fracture faces.

A total of nine wall thickness measurements were made on the 2 in. pipe (remote from the cross-tee welds, using a ball micrometer, while 18 comparable measurements were made on the 3 in. pipe. The approximate locations of these measurements are shown in Fig. 21. The observed values were compared with both the nominal wall thicknesses for the pipe specifications, and with the ASTM A-53 minimum allowable wall thicknesses. The average wall thickness of the 2 in. pipe was 3.4 ± 0.178 mm (0.135 ± 0.007 in.) at the 95% confidence level, while the nominal wall thickness for Schedule 80, 50 mm (2 in.) pipe was 5.54 mm (0.218 in.), and the minimum allowable thickness under ASTM A-53 was 4.85 mm (0.191 in.). The average remaining wall thickness of the 3 in. pipe was 4.95 ± 0.305 mm (0.195 ± 0.012 in.), while the nominal wall thickness was 7.62 mm (0.300 in.) and the minimum allowable thickness under ASTM A-53 was 6.655 mm (0.262 in.).

Thus, the average metal loss for the 2 in. pipe was 2.108 ± 0.178 mm (0.083 ± 0.007 in.) based on the nominal wall thickness, or 1.42 ± 0.178 mm (0.056 ± 0.007 in.) based on the minimum allowable wall thickness. For the 3 in. pipe, the average metal loss was 2.667 ± 0.305 mm (0.105 ± 0.012 in.) based on the nominal wall

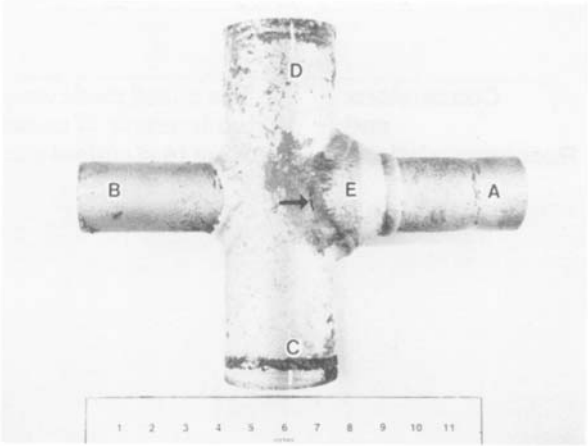

Fig. 19 Construction of the cross-tee, showing the 2 in. Schedule 80 pipe (A), joined to the 3 in. Schedule 80 pipe (C-D) by a reduction socket (E). The remaining arm of the cross (B) was a flanged nipple welded to the 3 in. pipe. The rupture is at the toe of the weld between the 3 in. pipe and the reduction socket (arrow).

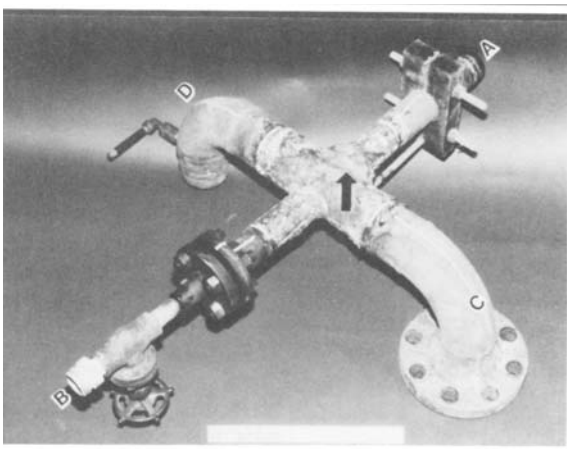

Fig. 18 The cross-tee assembly as received, showing the underside. The letters A through D identify the legs of the cross assembly. Arrow indicates the location of the rupture.

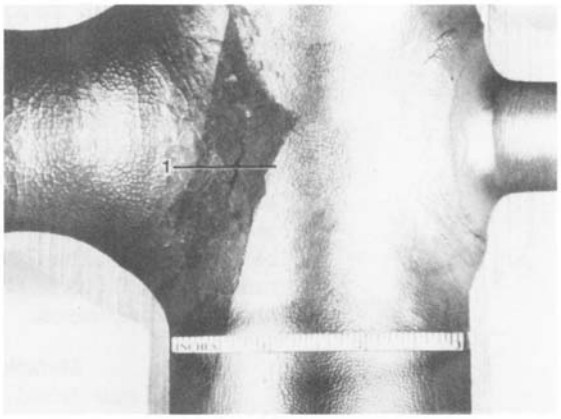

Fig. 20 The interior of the cross-tee showing the location of Weld Section 1 through the rupture at the toe of the weld joining the 3 in. pipe and the reduction socket. Note the reticulated pattern on the interior surfaces of the cross-tee, suggestive of thermal fatigue.

thickness or 1.70 ± 0.305 mm (0.067 ± 0.012 in.) based on the minimum allowable wall thickness. A composite analysis of all of the thickness data yielded an average metal loss of 2.49 ± 0.203 mm (0.098 ± 0.008 in.) based on nominal wall thicknesses or 1.626 ± 0.203 mm (0.064 ± 0.008 in.) based on minimum allowable wall thicknesses.

Polished and etched cross sections remote from the welds showed that the pipe and forged fitting microstructures consisted of pearlite in a ferrite matrix, typical of low to medium carbon steels.

A metallographic section was prepared through the weld between the 3 in. pipe and the reduction fitting at location 1 in Fig. 20, intersecting the rupture. Figure 22 shows the microstructure of Weld Section 1. Lip B consists entirely of weld metal. Lip A consists of altered pearlite in a ferrite matrix HAZ, transitioning into the normal pearlite in ferrite matrix of the carbon steel. There was no discernible weld metal at the tip of Lip A.

From Fig. 22 it is apparent that there was no distinct crack or fracture at the toe of the weld, but rather that internal thinning had simply progressed until the toe of the weld was penetrated. Because of the extreme thinness of the lips of the rupture, fractographic examination was not possible.

Figure 23 shows a comparable cross section through the same weld approximately 180° away from the center of the rupture. This figure demonstrates clearly that there was no preferential corrosion of the weld metal or HAZs.

Figure 24, a photomicrograph of the microstructure at the root of one of the reticular grooves in the 3 in. pipe, shows clearly that these grooves resulted from corrosion rather than thermal fatigue. There was no evidence of any wear or erosion morphology.

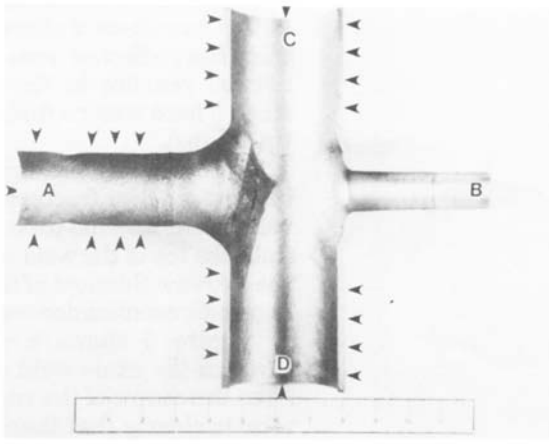

Fig. 21 Plane section of the cross-tee assembly showing the approximate locations of the wall thickness measurements

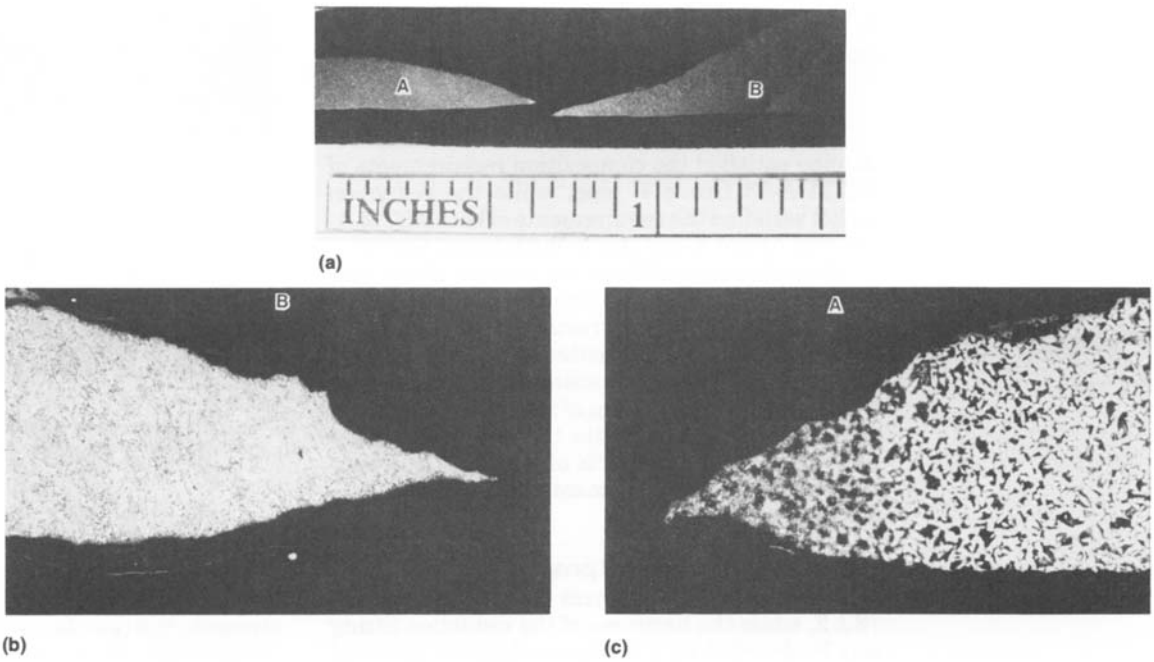

Fig. 22 The weld between the 3 in. pipe and the reduction socket at the rupture. The lower images are reversed relative to the upper image. The OD surfaces face upward in each image.

Chemical analysis showed that the 2 and 3 in. pipe satisfied the composition requirements of ASTM A-53 Grade B pipe, while the reduction socket satisfied the requirements of both ASTM A-105 and ASTM A-243 Grade WPB forged fittings.

Deposit material from the interior of the pipe was analyzed by energy dispersive x-ray spectros-copy (EDS) and x-ray diffraction (XRD).

The deposits which coated the entire interior surface of the piping consisted almost entirely of iron and sulfur in the form of two iron sulfides, pyrite (FeS_2 and pyrohotite ($Fe_{(1-x)}S$). Both are common corrosion products of steel in a hydrogen sulfide environment. Elemental sulfur was not detected.

Mechanical Properties. The Rockwell B hardness of the 3 in. pipe was 73 ± 2, while the hardness of the reduction fitting was Rockwell B 82 ± 2. The hardness of the weld metal remote from the rupture was Rockwell B 85 ± 2.

Based on the ASTM A-370 approximate correlation between Rockwell B hardness and tensile strength, the tensile strength of the 3 in. pipe was on the order of 434 to 455 MPa (63 to 66 ksi), while the tensile strength of the reduction fitting was on the order of 503 to 538 MPa (73 to 78 ksi). Within the uncertainty of the conversion, these values agree with the ASTM A-53 requirement of a minimum tensile strength of 414 MPa (60 ksi) for Grade B steel. These hardnesses are also far below the NACE Rockwell C 22 maximum hardness limitation for steel pipe in H_2S service. Together, these data show that the components satisfied the mechanical property requirements of their respective specifications and were suitable under NACE specifications for H_2S service.

Discussion. The exterior surfaces of the cross-tee showed no evidence of significant corrosion beyond slight atmospheric rusting. Visual examination of the exterior surfaces of the welds showed clearly that the weld at the location of the rupture was much thinner than elsewhere around its circumference. The appearance was consistent with failure to complete one or more weld passes at this location on the toe of the weld.

Both the visual inspection and metallographic cross sections showed clearly that appreciable corrosion had occurred over the entire interior surface of the cross-tee assembly and as much of the associated piping as was available for examination. This corrosion was essentially uniform except for the very shallow reticulated surface pattern. There was no evi-

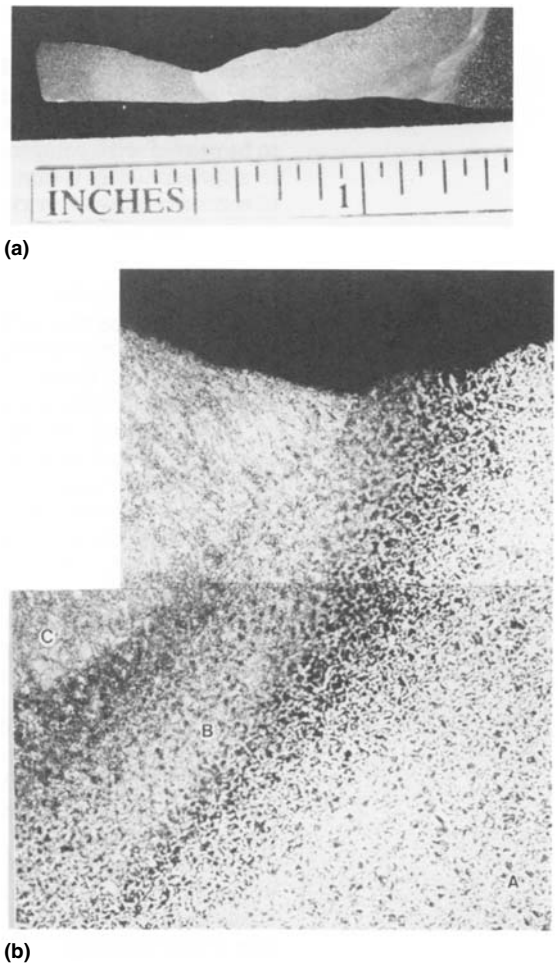

Fig. 23 The weld between the 3 in. pipe and the reduction socket 180° away from the rupture. The lower image is reversed relative to the upper image. The OD surface faces upward in each image.

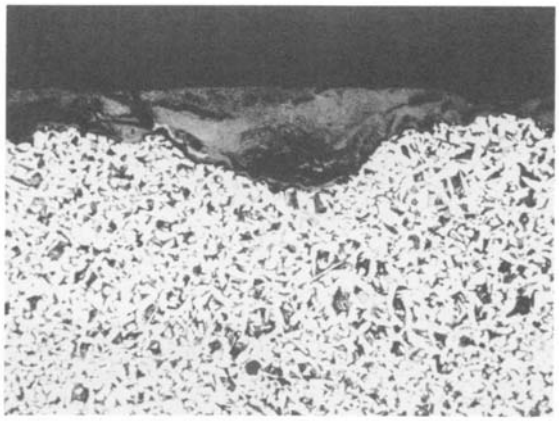

Fig. 24 Microstructure at the root of one of the reticulated grooves on the interior of the pipe

dence of preferential corrosion of any of the welds or HAZs.

Based upon numorous measurements of the thicknesses of the 2 and 3 in. piping remote from the welds, the interior surfaces of the cross-tee and associated piping had lost a minimum of approximately 1.588 mm (0.0625 in.) due to corrosion, and the actual amount was more likely in excess of 3.175 mm (0.125 in.).

The wastage from the interior surfaces of the cross assembly and piping resulted from corrosion by the H_2S gas rather than erosion. This conclusion is supported by two observations. First, the entire interior surface was coated with a relatively thick, multilayered, and somewhat friable columnar iron sulfide corrosion product deposit. If the metal loss were the result of erosive wear, the metal surfaces at the wasted locations would have been devoid of deposits. Second, the micro-morphology of the interior surfaces of the cross assembly is completely inconsistent with erosion.

Once the cross-tee was placed in service, corrosion thinned the walls of the assembly until the remaining thickness at the toe of the weld between the 3 in. pipe, and the reduction fitting could not contain the pressurized gas, resulting in a rupture. While cyclic pressure or thermal stresses may have had some secondary contributory role in the rupture mechanism, there was no evidence of a distinct cracking mechanism other than stress overload as the remaining material at the toe of the weld became too thin to contain the pressurized gas.

Reticulated corrosion patterns similar to those observed in this investigation have been observed beneath columnar deposits under service conditions in which thermal fatigue could not have occurred because there was no thermal cycling. It is probable that such reticulated corrosion patterns are produced when a somewhat protective deposit fractures by thermal contraction or structural shrinkage. The resulting fissures then allow increased mass transport of corrosive species to the metal surface at the tips of the fissures. Transport of reaction products from these sites is also facilitated. Under many circumstances, the corrosion rate of steel is mass-transport (or diffusion) controlled. The slightly enhanced mass transport results in slightly more rapid metal loss at the tips of the fissures in the deposit, producing grooves at these locations. The physical structure of the deposits in this equipment included a reticulated pattern of intercolumnar fissures, leading to the reticulated corrosion pattern on the metal surface.

Conclusions and Recommendations. The proximate cause of the rupture was internal corrosion thinning of the pipe and cross-tee walls until the remaining thickness at the toe of the weld between the 3 in. pipe and the reduction fitting could not sustain the internal pressure.

The root cause of the rupture was the very thinly fabricated weld bead at the toe of the weld between the 3 in. pipe and the reduction fitting. If the weld had been fabricated with the same original thickness as at the remaining points around its circumference, no failure would have occurred because the metal thickness would have provided a more than adequate corrosion allowance.

It was recommended that the cross-tee be replaced with a like component, with more careful attention to weld quality.

ACKNOWLEDGMENTS

Portions of this chapter were adapted from:

- S. Bond, Corrosion of Carbon Steel Weldments, *Corrosion: Fundamentals, Testing, and Protection,* Vol 13A, *ASM Handbook,* ASM International, 2003, p 294–300
- C.C. Chen and A. Pollack, Influence of Welding on Steel Weldment Properties, *Welding, Brazing, and Soldering,* Vol 6, *ASM Handbook,* ASM International, p 416–428
- R.B. Smith, Arc Welding of Carbon Steels, *Welding, Brazing, and Soldering,* Vol 6, *ASM Handbook,* ASM International, p 641–661
- B.R. Somers, Introduction to the Selection of Carbon and Low-Alloy Steels, *Welding, Brazing, and Soldering,* Vol 6, *ASM Handbook,* ASM International, p 405–407
- F.J. Winsor, Welding of Low-Alloy Steels, *Welding, Brazing, and Soldering,* Vol 6, *ASM Handbook,* ASM International, p 662–676

REFERENCES

1. *Welding Handbook,* Vol 4, 7th ed., American Welding Society, 1982, p 9
2. G. Linnert, *Welding Metallurgy,* Vol 1, 3rd ed., American Welding Society, p 45
3. S. Kalpakjian, *Manufacturing Processes for Engineering Materials,* Addison-Wesley, 1984, p 146

4. *Properties and Selection: Irons, Steels, and High-Performance Alloys,* Vol 1, *ASM Handbook,* ASM International, 1990, p 147–148, 390
5. C.D. Lundin, R. Menon, J.A. Henning, and M.W. Richey, Hydrogen-Assisted Cracking Sensitivity of Cr-Mo Steels During Welding, *Advances in Welding Science and Technology,* May 18–22, 1986 (Gatlinburg, Tennessee), ASM International, 1986, p 585–595
6. R.D. Stout and W.D. Doty, *Weldability of Steels,* 3rd ed., S. Epstein and R. E. Somers, Ed., Welding Research Council, New York, 1978
7. C-M Lee, S. Bond, and P. Woollin, "Preferential Weld Corrosion: Effects of Weldment Microstructure and Composition," Paper 05277, presented at *Corrosion 2005,* NACE International, 2005, 16 pages
8. T.G. Gooch, "The Effect of Welding on Material Corrosion Behaviour," NACE International Process Industries Corrosion Seminar, (Houston, TX) Oct. 13–16 1986
9. J.S. Smart, Weld Corrosion in Lines Deserves Closer Attention, *Pipeline Gas Ind.,* Vol 79 (No. 6), June 1996, p 33–35
10. T.G. Gooch and P.H.M. Hart, "Review of Welding Practices for Carbon Steel Deaerator Vessels," Paper 303, presented at *Corrosion/86*, (Houston, TX), National Association of Corrosion Engineers, March 1986
11. J.L. Robinson, Preferential Corrosion of Welds, *The Welding Institute Research Bulletin,* Vol 20, Jan and Feb 1979
12. "Preferential Corrosion of Carbon Steel Weldments in Oil and Gas Production Systems," Joint Industry Project 5563/28/89, TWI and CAPCIS, 1989
13. R.W. Revie, Ed., *Uhlig's Corrosion Handbook,* 2nd ed., John Wiley & Sons, 2000, p 542
14. M.B. Kermani and L.M. Smith, Ed., *CO_2 Corrosion Control in Oil and Gas Production,* European Federation of Corrosion Publication 23, The Institute of Materials, London, 1997
15. C.G. Arnold, "Galvanic Corrosion Measurement of Weldments," Paper 71, presented at *Corrosion/80*, (Chicago, IL), National Association of Corrosion Engineers, March 1980
16. R.J. Brigham et al., Evaluation of Weld-Zone Corrosion of Shipbuilding Steel Plates for Use in the Arctic Environment, *Can. Metall. Q.,* Vol 27 (No. 4), 1988, p 311–321
17. T. Taira et al., "Sulfide Corrosion Cracking of Girth-Welded Joint of Line Pipe for Sour Gas Service," Corrosion '79, T-1F Symposium (Atlanta, GA), NACE, March 1979
18. M. Itoh et al., "Hydrogen Sulfide Corrosion Cracking of Large Diameter Line Pipe Up to Grade X-65," Middle East Corrosion Conference (Bahrain), NACE, April 1979
19. S.K. Chauhan, Stress-Corrosion Cracking of C-Mn Steel in a CO_2 Absorber in a Chemical Plant, *Handbook of Case Histories in Failure Analysis,* Vol 1, K.A. Esaklul, Ed., ASM International, 1992, p 191–193
20. J. Gutzeit and J.M. Johnson, "Stress-Corrosion Cracking of Carbon Steel Welds in Amine Service," Paper 206, presented at *Corrosion/86*, (Houston, TX), National Association of Corrosion Engineers, March 1986
21. G.E. Kerns, "Deaerator Cracking—A Case History," Paper 310, presented at *Corrosion/86*, (Houston, TX), National Association of Corrosion Engineers, March 1986
22. B.A. Graville, *The Principles of Cold Cracking Control in Welds,* Dominion Bridge Company, 1975
23. H. Granjon, *Fundamentals of Welding Metallurgy,* Abington Publishing, 1991, p 156–177
24. B.A. Graville, Cold Cracking in Welds in HSLA Steels, *Welding of HSLA (Microalloyed) Structural Steels,* Proc. Int. Conf., American Society for Metals, Nov 1976
25. P.F. Ellis II, Corrosion Failure of a Chemical Process Piping Cross-Tee Assembly, *Handbook of Case Histories in Failure Analysis,* Vol 2, ASM International, 1993, p 156–159

Corrosion of Weldments
J.R. Davis, editor, p 43-75
DOI:10.1361/corw2006p043

CHAPTER 3

Corrosion of Austenitic Stainless Steel Weldments

AUSTENITIC STAINLESS STEELS exhibit a single-phase, face-centered cubic (fcc) structure that is maintained over a wide range of temperatures. This structure results from a balance of alloying additions that stabilize the austenite phase from elevated to cryogenic temperatures. Because these alloys are predominantly single phase, they can only be strengthened by solid-solution alloying or by work hardening.

The austenitic stainless steels were developed for use in both mild and severe corrosive conditions. They are also used at temperatures that range from cryogenic temperatures, where they exhibit high toughness, to elevated temperatures of nearly 600 °C (1110 °F), where they exhibit good oxidation resistance. Because the austenitic materials are nonmagnetic, they are sometimes used in applications where magnetic materials are not acceptable.

Grade Designations

Austenitic stainless steels can be divided into standard SAE grades and nonstandard grades. Most of the nonstandard grades have been given UNS designations, as have all of the standard grades. Tables 1 and 2 list the compositions of standard and representative nonstandard grades.

Standard Grades

The standard grades can be further subdivided into 300-series and 200-series stainless steels. The 300-series alloys are Fe-Cr-Ni austenitic grades containing 16 to 26% Cr and 6 to 22% Ni. Molybdenum, copper, silicon, aluminum, titanium, niobium/tantalum, and nitrogen can be added to confer certain characteristics such as improved resistance to pitting and crevice corrosion, intergranular corrosion caused by sensitization, stress-corrosion cracking (SCC), and attack by high-temperature gases. Figure 1 shows the effects of various alloying additions on the properties of austenitic stainless steels as well as ferritic, martensitic, and duplex stainless steels which are discussed in subsequent chapters.

The 200-series alloys are Fe-Cr-Mn-Ni-N austenitic grades containing 16 to 19% Cr, 5.5 to 15.5% Mn, 1 to 6% Ni, and up to 0.4% N. These alloys became popular in the 1950s during the Korean War when nickel was in short supply.

Nonstandard Grades

The nonstandard grades of austenitic stainless steels include modified versions of the 300-series and 200-series standard grades and more highly alloyed austenitics. It is important to describe some of the more highly alloyed austenitic stainless steel grades that contain less than 50% iron. Although many high-alloy stainless steel grades are classified as nickel-base alloys by the UNS designation system, their largest constituent is iron (hence, they are more accurately described as stainless steels), and they are produced and marketed through stainless steel manufacturers and distribution channels.

The high-alloy stainless steels were developed for applications where corrosive conditions are too severe for the standard or modified 300-series austenitic grades. A good example of

a high-alloy stainless steel is 20Cb-3 (N08020), which was designed for improved resistance to sulfuric acid. This alloy has been used in many applications in a wide variety of chemical and allied industry environments. The presence of niobium in the alloy minimizes weld sensitization (intergranular corrosion), and the higher nickel content (32.5 to 35%) confers resistance to chloride SCC. The molybdenum content (2 to 3%) increases resistance to pitting and crevice corrosion, and copper (3 to 4%) provides resistance to sulfuric acid. Other examples of high-alloy steels that exhibit a high degree of resistance to chloride SCC, pitting, and crevice corrosion are 904L (N08904), JS700 (N08700), Sanicro 28 (N08028), and 20Mo-4 (N08024). Such alloys are used in production of phosphoric acids (Sanicro 28 was specifically developed for phosphoric acid service), for handling sulfuric acid and many other acids, oil and gas production in sour wells, equipment for sea water, fluoride-bearing media, and equipment in sodium hydroxide plants.

Superaustenitic Stainless Steels. High-alloy steels containing 6% Mo are commonly referred to as superaustenitics. The first commercially successful superaustenitic alloy containing 6% Mo was Al-6X (N08366) produced in 1969. It was developed to provide sufficient pitting and crevice corrosion resistance for handling seawater. It was later replaced by the nitrogen-bearing AL-6XN (N08367). Nitrogen is an austenite stabilizer, retards the formation of the embrittling sigma phase and other intermetallic phases, increases strength, and adds to the pitting and crevice corrosion resistance. Other examples of superaustenitic grades include 254 SMO (S31254), 654 SMO (S32654), 20Mo-6 (N08026), and 1925 HMo (N08925). Such alloys are used in a wide variety of sea water applications (they are highly resistant to chloride SCC), the pulp and paper industry, and the chemical processing industry. Among the process industry environments to which the superaustenitics are resistant are phosphoric acid, sulfuric acid, hydrochloric acid, hydrofluoric acid, nitric acid,

Table 1 Chemical compositions of standard austenitic stainless steels

		Composition(a), %							
UNS No.	Type/designation	C	Mn	Si	Cr	Ni	P	S	Other
S20100	201	0.15	5.5–7.5	1.00	16.0–18.0	3.5–5.5	0.06	0.03	0.25 N
S20200	202	0.15	7.5–10.0	1.00	17.0–19.0	4.0–6.0	0.06	0.03	0.25 N
S20500	205	0.12–0.25	14.0–15.5	1.00	16.5–18.0	1.0–1.75	0.06	0.03	0.32–0.40 N
S30100	301	0.15	2.0	1.00	16.0–18.0	6.0–8.0	0.045	0.03	. . .
S30200	302	0.15	2.0	1.00	17.0–19.0	8.0–10.0	0.045	0.03	. . .
S30215	302B	0.15	2.0	2.0–3.0	17.0–19.0	8.0–10.0	0.045	0.03	. . .
S30300	303	0.15	2.0	1.00	17.0–19.0	8.0–10.0	0.20	0.15 min	0.6 Mo(b)
S30323	303Se	0.15	2.0	1.00	17.0–19.0	8.0–10.0	0.20	0.06	0.15 min Se
S30400	304	0.08	2.0	1.00	18.0–20.0	8.0–10.5	0.045	0.03	. . .
S30403	304L	0.03	2.0	1.00	18.0–20.0	8.0–12.0	0.045	0.03	. . .
S30451	304N	0.08	2.0	1.00	18.0–20.0	8.0–10.5	0.045	0.03	0.10–0.16 N
S30500	305	0.12	2.0	1.00	17.0–19.0	10.5–13.0	0.045	0.03	. . .
S30800	308	0.08	2.0	1.00	19.0–21.0	10.0–12.0	0.045	0.03	. . .
S30900	309	0.20	2.0	1.00	22.0–24.0	12.0–15.0	0.045	0.03	. . .
S30908	309S	0.08	2.0	1.00	22.0–24.0	12.0–15.0	0.045	0.03	. . .
S31000	310	0.25	2.0	1.50	24.0–26.0	19.0–22.0	0.045	0.03	. . .
S31008	310S	0.08	2.0	1.50	24.0–26.0	19.0–22.0	0.045	0.03	. . .
S31400	314	0.25	2.0	1.5–3.0	23.0–26.0	19.0–22.0	0.045	0.03	. . .
S31600	316	0.08	2.0	1.00	16.0–18.0	10.0–14.0	0.045	0.03	2.0–3.0 Mo
S31620	316F	0.08	2.0	1.00	16.0–18.0	10.0–14.0	0.20	0.10 min	1.75–2.5 Mo
S31603	316L	0.03	2.0	1.00	16.0–18.0	10.0–14.0	0.045	0.03	2.00–3.0 Mo
S31651	316N	0.08	2.0	1.00	16.0–18.0	10.0–14.0	0.045	0.03	2.0–3.0 Mo; 0.10–0.16 N
S31700	317	0.08	2.0	1.00	18.0–20.0	11.0–15.0	0.045	0.03	3.0–4.0 Mo
S31703	317L	0.03	2.0	1.00	18.0–20.0	11.0–15.0	0.045	0.03	3.0–4.0 Mo
S32100	321	0.08	2.0	1.00	17.0–19.0	9.0–12.0	0.045	0.03	5 × %C min Ti
S34700	347	0.08	2.0	1.00	17.0.–19.0	9.0–13.0	0.045	0.03	10 × %C min Nb
S34800	348	0.08	2.0	1.00	17.0–19.0	9.0–13.0	0.045	0.03	0.2 Co; 10 × %C min Nb; 0.10 Ta
S38400	384	0.08	2.0	1.00	15.0–17.0	17.0–19.0	0.045	0.03	. . .

(a) Single values are maximum values unless otherwise indicated. (b) Optional

Table 2 Chemical compositions of nonstandard austenitic stainless steels

UNS No.	Type/designation	Composition(a), %							
		C	Mn	Si	Cr	Ni	P	S	Other
S20103	201L	0.03	5.5–7.5	0.75	16.0–18.0	3.5–5.5.5	0.045	0.030	0.25N
S20161	Gall-Tough	0.15	4.00–6.00	3.00–4.00	15.0–18.0	4.00–6.00	0.040	0.040	0.08–0.02N
S20300	203 EZ (XM-1)	0.08	5.0–6.5	1.00	16.0–18.0	5.0–6.5	0.040	0.18–0.35	0.5 Mo; 1.75–2.25Cu
S20400	Nitronic 30	0.03	7.0–9.0	1.00	15.0–17.0	1.5–3.0	0.04	0.03	0.15–0.30N
S20430	204Cu	0.15	6.5–9.0	1.00	15.5–17.5	1.5–3.5	0.060	0.030	2.00–4.00Cu; 0.05–0.25N
S20910	Nitronic 50 (XM-19)	0.06	4.0–6.0	1.00	20.5–23.5	11.5–13.5	0.040	0.030	1.5–3.0Mo; 0.2–0.4N; 0.1–0.3Nb; 0.1–0.3V
S21300	15-5LC	0.25	15.0–18.0	1.00	16.0–21.0	3.00	0.05	0.05	0.50–3.00Mo; 0.50–2.00Cu
S21400	Tenelon (XM-31)	0.12	14.5–16.0	0.3–1.0	17.0–18.5	0.75	0.045	0.030	0.35N
S21460	Cryogenic Tenelon (XM-14)	0.12	14.0–16.0	1.00	17.0–19.0	5.0–6.0	0.060	0.030	0.35–0.50N
S21500	Esshete 1250	0.15	5.5–7.0	1.20	14.0–16.0	9.0–11.0	0.040	0.030	0.003–0.009B; 0.75–1.25 Nb; 0.15–0.40V
S21600	Type 216 (XM-17)	0.08	7.5–9.0	1.00	17.5–22.0	5.0–7.0	0.045	0.030	2.0–3.0Mo; 0.25–0.50N
S21603	Type 216L (XM-18)	0.03	7.5.–9.0	1.00	17.5–22.0	7.5–9.0	0.045	0.030	2.0–3.0Mo; 0.25–0.50N
S21800	Nitronic 60	0.10	7.0–9.0	3.5–4.5	16.0–18.0	8.0–9.0	0.040	0.030	0.08–0.18N
S21900	Nitronic 40 (XM-10)	0.08	8.0–10.0	1.00	19.0–21.5	5.5–7.5	0.060	0.030	0.15–0.40N
S21904	21-6-9 LC	0.04	8.00–10.00	1.00	19.00–21.50	5.50–7.50	0.060	0.030	0.15–0.40N
S24000	Nitronic 33 (18-3 Mn)	0.08	11.50–14.50	1.00	17.0–19.00	2.50–3.75	0.060	0.030	0.20–0.40N
S24100	Nitronic 32 (18-2 Mn)	0.15	11.00–14.00	1.00	16.50–19.50	0.50–2.50	0.060	0.030	0.20–0.40N
S28200	18-18 Plus	0.15	17.0–19.0	1.00	17.5–19.5	. . .	0.045	0.030	0.5–1.5Mo; 0.5–1.5Cu; 0.4–0.6N
S30310	303 Plus X (XM-5)	0.15	2.5–4.5	1.00	17.0–19.0	7.0–10.0	0.020	0.25 min	0.6Mo
S30409	Type 304H	0.04–0.10	2.00	1.00	18.0–20.0	8.0–11.0	0.04	0.03	. . .
S30415	153 MA(b)	0.05	0.60	1.30	18.5	9.50	. . .	. . .	0.15N; 0.04Ce
S30430	18-9 LW	0.10	2.00	1.00	17.0–19.0	8.0–10.0	0.045	0.03	3.00–4.00Cu
S30452	304HN (XM-21)	0.04–0.10	2.00	1.00	18.0–20.0	8.0–10.5	0.045	0.030	0.16–0.30N
S30453	Type 304LN	0.03	2.00	1.00	18.0–20.0	8.0–12.0	0.045	0.03	0.10–0.16N
S30454	Type 304L(Hi)N	0.03	2.00	1.00	18.0–20.0	8.0–12.0	0.045	0.03	0.16–0.03N
S30460	Type 304B	0.08	2.00	0.75	18.0–20.0	12.0–15.0	0.045	0.03	0.20–0.29B; 0.10 max N
S30461	Type 304B1	0.08	2.00	0.75	18.0–20.0	12.0–15.0	0.045	0.03	0.30–0.49B; 0.10 max N
S30462	Type 304B2	0.08	2.00	0.75	18.0–20.0	12.0–15.0	0.045	0.03	0.50–0.74B; 0.10 max N
S30463	Type 304B3	0.08	2.00	0.75	18.0–20.0	12.0–15.0	0.045	0.03	0.75–0.99B; 0.10 max N
S30464	Type 304B4	0.08	2.00	0.75	18.0–20.0	12.0–15.0	0.045	0.03	1.00–1.24B; 0.10 max N
S30465	Type 304B5	0.08	2.00	0.75	18.0–20.0	12.0–15.0	0.045	0.03	1.25–1.49B; 0.10 max N
S30466	Type 304B6	0.08	2.00	0.75	18.0–20.0	12.0–15.0	0.045	0.03	1.50–1.74B; 0.10 max N
S30467	Type 304B7	0.08	2.00	0.75	18.0–20.0	12.01–15.0	0.045	0.03	1.75–2.25B; 0.10 max N
S30600	Cronifer 1815 LCSi	0.018	2.00	3.37–4.3	17.0–18.5	14.0–15.5	0.020	0.020	0.2Mo
S30615	RA85H(b)	0.20	0.80	3.50	18.5	14.50	. . .	. . .	1.0Al
S30815	253 MA	0.05–0.10	0.80	1.4–2.0	20.0–22.0	10.0–12.0	0.040	0.030	0.14–0.20N; 0.03–0.08Ce; 1.0Al
S30909	Type 309H	0.04–0.10	2.00	0.75	22.0–24.0	12.0–16.0	0.04	0.03	. . .
S30940	Type 309Cb	0.08	2.00	1.00	22.0–24.0	12.0–15.0	0.045	0.030	10 × %C min to 1.00 max Nb
S30941	Type 309HCb	0.04–0.10	2.00	0.75	22.0–24.0	12.0–16.0	0.04	0.03	10C × min to 1.10 max Nb + Ta; 0.75Cu; 0.75Mo
S31002	2RE10	0.015	2.00	0.15	24.0–26.0	19.0–22.0	0.02	0.015	0.10Mo; 0.10N
S31009	Type 310H	0.04–0.10	2.00	0.75	24.0–26.0	19.0–22.0	0.04	0.03	. . .
S31040	Type 310Cb	0.08	2.00	1.50	24.0–26.0	19.0–22.0	0.045	0.030	10 × %C min to 1.10 max Nb + Ta
S31041	Type 310HCb	0.04–0.10	2.00	0.75	24.0–26.0	19.0–22.0	0.045	0.03	10 × C min Nb + Ta; 0.75Cu

(continued)

Table 2 (continued)

UNS No.	Type/designation	Composition(a), %							
		C	Mn	Si	Cr	Ni	P	S	Other
S31050	2RE69	0.03	2.00	0.4	24.0–26.0	20.5–23.5	0.02	0.15	0.09–0.16N
S31254	254 SMO	0.20	1.00	0.80	19.50–20.50	17.50–18.50	0.030	0.010	6.00–6.50Mo; 0.50–1.00Cu; 0.18–0.220N
S31266	Uranus B66	0.03	2.0–4.0	1.00	23.0–25.0	21.0–24.0	0.035	0.02	0.50–3.00Cu; 5.0–7.0Mo; 0.35–0.60N; 1.00–3.00W
S31609	Type 316H	0.04–0.10	2.00	1.00	16.0–18.0	10.0–14.0	0.04	0.03	2.00–3.00Mo
S31635	Type 316Ti	0.08	2.00	1.00	16.0–18.0	10.0–14.0	0.045	0.030	5 × %(C + N) min to 0.70 max Ti; 2.0–3.0Mo; 0.10N
S31640	Type 316Cb	0.08	2.00	1.00	16.0–18.0	10.0–14.0	0.045	0.030	10 × %C min to 1.10 max Nb + Ta; 2.0–3.0 Mo; 0.10N
S31653	Type 316LN	0.03	2.00	1.00	16.0–18.0	10.0–14.0	0.045	0.03	2.00–3.00Mo; 0.10–0.16N
. . .	Type 316HQ	0.030	2.00	1.00	16.00–18.25	10.00–14.00	0.030	0.015	3.00–4.00Cu; 2.00–3.00Mo
S31725	Type 317LM	0.03	2.00	1.00	18.0–20.0	13.5–17.5	0.045	0.030	4.0–5.0Mo; 0.10N
S31726	Type 317LMN	0.03	2.00	0.75	17.0–20.0	13.5–17.5	0.045	0.030	4.0–5.0Mo; 0.10–0.20N
S31753	Type 317LN	0.03	2.00	1.00	18.0–21.0	11.0–15.0	0.030	0.030	0.10–0.22N
S32109	Type 321H	0.04–0.10	2.00	1.00	17.0–20.0	9.0–12.0	0.04	0.03	4 × C-0.60Ti
S32654	654 SMO	0.02	2.0–4.0	0.50	24.0–25.0	21.0–23.0	0.03	0.005	7.00–8.00Mo; 0.30–0.60Cu; 0.45–0.55N
S33228	Nicrofer 3228 NbCe	0.04–0.08	1.0	0.30	26.0–28.0	31.0–33.0	0.02	0.15	0.6–1.0Nb; 0.05–0.10Ce; 0.025Al
S34709	Type 347H	0.04–0.10	2.00	1.00	17.0–20.0	9.0–13.0	0.04	0.03	8 × C–1.00Nb
S34710	Type 347HFG	0.06–0.10	2.00	0.75	17.0–20.0	9.0–13.0	0.04	0.03	8 × C–1.0Nb
S34720	. . .	0.08	2.00	1.00	17.0–19.0	9.0–12.0	0.04	0.18–0.35	10 × C–1.10Nb
S34723	. . .	0.08	2.00	1.00	17.0–19.0	9.0–12.0	0.11–0.17	0.03	10 × C–1.010Nb; 0.15–0.35Se
S34751	Type 347LN	0.005–0.02	2.00	0.75	17.0–19.0	9.0–13.0	0.04	0.03	0.2–0.5Nb + Ta; 0.06–0.10N
S34809	Type 348H	0.04–0.10	2.00	1.00	17.0–20.0	9.0–13.0	0.045	0.03	8 × C–1.00Nb; 0.20Co; 0.10Ta
S35315	353MA	0.04–0.08	2.00	1.2–2.0	24.0–26.0	34.0–36.0	0.04	0.03	0.12–0.18N; 0.03–0.08Ce
S37000	Type 370	0.03–0.05	1.65–2.35	0.5–1.0	12.5–14.5	14.5–16.5	0.040	0.010	1.5–2.5Mo; 0.1–0.4Ti; 0.005N; 0.05Co
S38100	18-18-2 (XM-15)	0.08	2.00	1.5–2.5	17.0–19.0	17.5–18.5	0.030	0.030	. . .
S63008	21-4N	0.48–0.58	8.00–10.00	0.25	20.0–22.0	3.25–4.50	0.030	0.04–0.09	0.28–0.50N
S63012	21-2N	0.50–0.60	7.0–9.50	0.25	19.25–21.50	1.50–2.75	0.050	0.04–0.09	0.20–0.40N
S36017	21-12N	0.15–0.25	1.00–1.50	0.70–1.25	20.0–22.0	10.50–12.50	0.03	0.03	0.15–0.25N
S36018	23-8N	0.28–0.38	1.50–3.50	0.60–0.90	22.0–24.0	7.0–9.0	0.04	0.015	0.28–0.35N; 0.50Co
S63198	19-9DL	0.28–0.35	0.75–1.50	0.03–0.8	18.0–21.0	8.0–11.0	0.040	0.030	1.0–1.75Mo; 0.1–0.35Ti; 1.0–1.75W; 0.25–0.60Nb
S70003	Nicrofer 2509 Si7	0.02	2.00	6.5–8.0	8.0–11.0	22.0–25.0	0.025	0.01	0.50Mo; 0.50Al
N08020	20Cb–3	0.07	2.00	1.00	19.0–21.0	32.0–38.0	0.045	0.035	2.0–3.0Mo; 3.0–4.0Cu; 8 × %C min to 1.00 max Nb
N08024	20Mo-4	0.03	1.00	0.50	22.5–25.0	35.0–40.0	0.035	0.035	3.50–5.00Mo; 0.05–1.50Cu; 0.15–035Nb
N08026	20Mo-6	0.03	1.00	0.50	22.0–26.00	33.0–37.20	0.03	0.03	5.00–6.70Mo; 2.00–4.00Cu
N08028	Sanicro 28	0.02	2.00	1.00	26.0–28.0	29.5–32.5	0.020	0.015	3.0–4.0Mo; 0.6–1.4Cu
N08330	RA-330	0.08	2.00	0.75–1.50	17.0–20.0	34.0–37.0	0.03	0.03	0.025Sn; 0.005Pb
N08332	RA 330TX	0.05–0.10	2.00	0.75–1.50	17.0–20.0	34.0–37.0	0.03	0.03	0.10–0.50Al; 1.00Cu; 0.005Pb; 0.025Sn; 0.20–0.60Ti
N08366	Al-6X	0.035	2.00	1.00	20.0–22.0	23.5–25.5	0.030	0.030	6.0–7.0Mo
N08367	Al-6XN	0.030	2.00	1.00	20.0–22.0	23.50–25.50	0.040	0.030	6.0–7.0Mo; 0.18–0.25N
N08700	JS-700	0.04	2.00	1.00	19.0–23.0	24.0–26.0	0.040	0.030	4.3–5.0Mo; 8 × %C min to 0.5 max Nb; 0.5Cu; 0.005Pb; 0.035S
N08904	904L	0.02	2.00	1.00	19.0–23.0	23.0–28.0	0.045	0.035	4.0–5.0Mo; 1.0.–2.0Cu
N08925	Cronifer 1925 hMo	0.02	1.00	0.50	24.0–26.0	19.0–21.0	0.045	0.030	6.0–7.0Mo; 0.8–1.5Cu; 0.10–0.20N
. . .	Cronifer 2328	0.04	0.75	0.75	22.0–24.0	26.0–28.0	0.030	0.015	2.5–3.5Cu; 0.4–0.7Ti; 2.5–3.0Mo

(a) Single values are maximum values unless otherwise indicated. (b) Nominal compositions

and organic acids, particularly acetic acid. The superaustenitics are also used in equipment for urea synthesis and sour gas environments. Equipment fabricated from 6% Mo superaustenitics has included crystallizers, mixing vessels, pressure vessels, tanks, columns, evaporators, heat exchangers, piping, pumps and valves, seawater-cooled condensers, water piping for nuclear power plants, and flue gas desulfurization components.

Properties

Mechanical Properties. The yield strengths of chromium-nickel austenitic stainless steels are rather modest and are comparable to those of mild steels. Typical minimum mechanical properties of annealed 300-series steels are yield strengths of 205 to 275 MPa (30 to 40 ksi), ultimate tensile strengths of 520 to 760 MPa (75 to 110 ksi), and elongations of 40 to 60%. Some nitrogen-strengthened superaustenitics have slightly higher yield strength values (up to about 310 MPa, or 45 ksi). Annealed 200-series alloys have still higher yield strengths ranging from 345 to 480 MPa (50 to 70 ksi). Higher strengths are possible in cold-worked forms, especially in drawn wire, in which a tensile strength of 1200 MPa (175 ksi) or higher is possible.

Corrosion Resistance. Even the leanest austenitic stainless steels (e.g., types 302 and 304) offer general corrosion resistance in the atmosphere, in many aqueous media, in the presence of foods, and in oxidizing acids such as nitric acid. The material selection process for service in corrosive environments often begins with type 304 or one of its variants (e.g., 304L). For industrial processes that require a higher level of resistance to corrosion than type 304 can offer, a molybdenum-bearing grade like type 316 can be selected. By virtue of the molybdenum addition (2 to 3%), type 316 can withstand corrosive attack by sodium and calcium brines, hypochlorite solutions, phosphoric acid, and the sulfite liquors and sulfurous acid used in the pulp and paper industry. This alloy, therefore, is specified for industrial equipment that handles the corrosive process chemicals used to produce inks, rayons, photographic chemicals, paper, textiles, bleaches, and rubber.

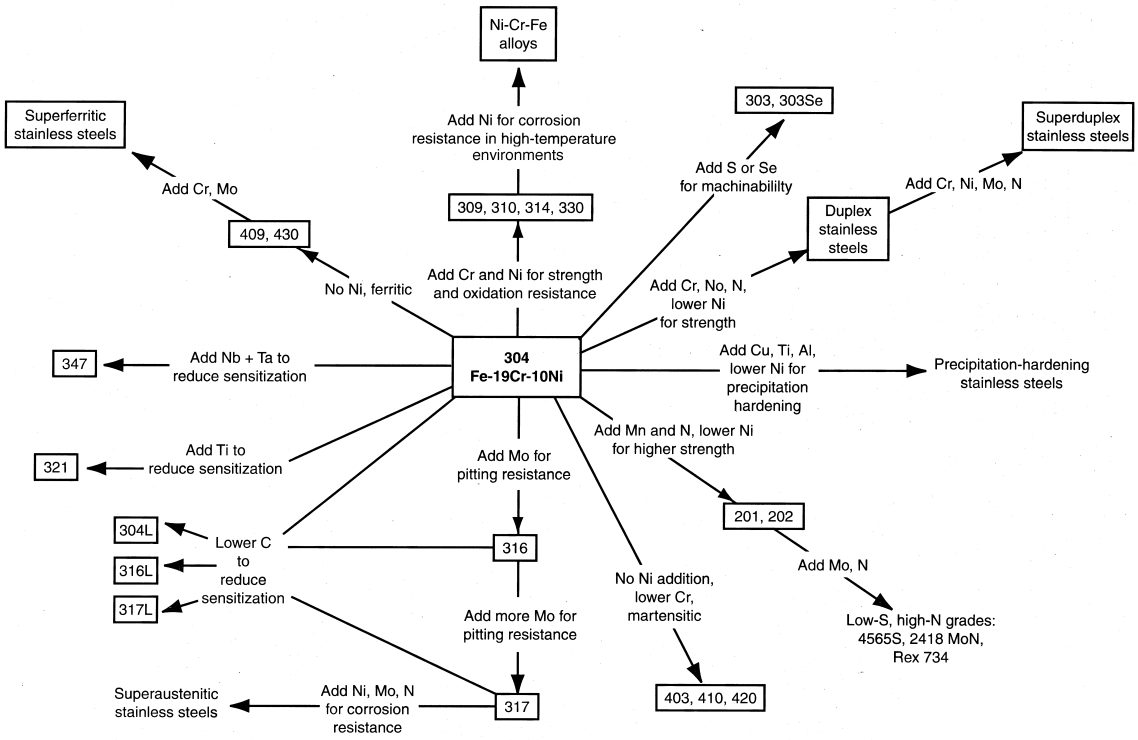

Fig. 1 Compositional and property linkages for stainless steels

High-purity versions of type 316 are also used for surgical implants within the hostile environment of the body. For those severe environments where type 316 is inadequate, high-nickel stainless grades should be used. These alloys offer superior resistance to hundreds of common industrial and process corrodents, including inorganic acids, acetate solvents, cadmium sulfate, trichlorethylene, ferrous sulfate, boric acid, and zinc chloride.

General Welding Considerations

Depending on alloy composition, the austenitic stainless steels may solidify with a microstructure containing some retained ferrite at room temperature, as a result of welding. Weld cracking, of which the most common form is solidification cracking, can be another consequence of welding. Cracks can occur in various regions of the weld with different orientations, such as centerline cracks, transverse cracks, and microcracks in the underlying weld metal or adjacent heat affected zone (HAZ). These cracks are due, primarily, to low-melting liquid phases, which allow boundaries to separate under the thermal and shrinkage stresses resulting from weld solidification and cooling. Other possible metallurgical consequences of welding are:

- The precipitation of intergranular, chromium-rich $M_{23}C_6$ chromium carbides in the weld HAZ, which can leave these regions sensitive to corrosion
- The transformation of weld ferrite to σ phase during elevated-temperature service, which can reduce ductility and toughness

These phenomena can be either minimized or eliminated through alloy selection, process optimization, or postweld heat treatment (PWHT).

The austenitic stainless steels are generally considered the most weldable of the stainless steels. Because of their physical properties, their welding behavior may be considerably different than those of the ferritic, martensitic, and duplex stainless steels. For example, the thermal conductivity of typical austenitic alloys is only approximately half that of the ferritic steels. Therefore, the weld heat input that is required to achieve the same penetration is considerably reduced. In contrast, the coefficient of thermal expansion (CTE) of austenite is 30 to 40% greater than that of ferrite, which can result in increases in both distortion and residual stress, because of welding. The molten weld pool of the austenitic stainless steels also tends to be more viscous, or "sluggish," than ferritic and martensitic grades. This impedes the metal flow and wettability of welds in these materials, which may promote lack-of-fusion defects.

A major concern, when welding the austenitic stainless steels, is the susceptibility to solidification and liquation cracking. These materials can be very resistant to these forms of high-temperature cracking, if the material is compositionally balanced such that the solidification behavior and microstructure is controlled to ensure that the weld metal contains more than 3 vol% ferrite.

In cases where fully austenitic welds are required, such as when the weld must be nonmagnetic or when it is placed in corrosive environments that selectively attack the ferrite phase, the welds will solidify as austenite and the propensity for weld cracking will increase. In some alloys, such as type 310 and the superaustenitic grades, all the allowable compositions within the specification range solidify as austenite when welded. To minimize cracking in these welds, it is generally advisable to weld with low heat input and under low constraint conditions.

Welds that are made at slower speeds and produce elliptical-, rather than teardrop-, shaped pools are also generally less susceptible to cracking. This effect is particularly pronounced when welding thin sheet, as in the production of thin-walled tubing. Residual elements, which form low-melting liquid phases that promote cracking, should be kept to a minimum. These elements include phosphorus, sulfur, boron, selenium, niobium, silicon, and titanium. Small additions of oxygen and nitrogen are somewhat beneficial and are thought to affect the wetting characteristics of the liquid phases. However, high concentrations of these elements may promote porosity. Manganese also can reduce cracking susceptibility, primarily by tying up sulfur and silicon that would otherwise be available to form low-melting phases.

Corrosion Behavior

Austenitic stainless steel weldments are often subject to corrosive attack. The nature of this attack is a function of weld thermal history, ser-

vice temperature and environment, and stress level (both residual and applied). Five general types of corrosive attack have been reported:

- Intergranular corrosion
- Preferential attack associated with weld metal precipitates
- Pitting and crevice corrosion
- Stress-corrosion cracking
- Microbiologically influenced corrosion

Each phenomena and its effect on service integrity is discussed below.

Intergranular Corrosion

The best known weld-related corrosion problem in austenitic stainless steels is sensitization (weld decay) caused by carbide precipitation in the weld HAZ. Sensitized structures are susceptible in intergranular corrosion.

Mechanism. At temperatures above approximately 1035 °C (1900 °F), chromium carbides are completely dissolved in austenitic stainless steels. However, when these steels are slowly cooled from these high temperatures or reheated into the range of 425 to 815 °C (800 to 1500 °F), chromium carbides are precipitated at the grain boundaries. These carbides contain more chromium than the matrix does.

The precipitation of the carbides depletes the matrix of chromium adjacent to the grain boundary. The diffusion rate of chromium in austenite is slow at the precipitation temperatures; therefore, the depleted zone persists, and the alloy is sensitized to intergranular corrosion. This sensitization occurs because the depleted zones have higher corrosion rates than the matrix in many environments. Figure 2 illustrates how the chromium content influences the corrosion rate of iron-chromium alloys in boiling 50% H_2SO_4 containing ferric sulfate, $Fe_2(SO_4)_3$. In all cases, the alloys are in the passive state. The wide differences in the corrosion rate are the result of the differences in the chromium content. With the lower-chromium-bearing stainless steels, the passive film is more soluble in the acid, and therefore, more metal must dissolve to repair the film.

If the austenitic stainless steels are cooled rapidly to below approximately 425 °C (800 °F), the carbides do not precipitate, and the steels are immune to intergranular corrosion. Reheating the alloys to 425 to 815 °C (800 to 1500 °F), as for stress relief, causes carbide precipitation and sensitivity to intergranular corrosion. The maximum rate of carbide precipitation occurs at approximately 675 °C (1250 °F). Because this is a common temperature for the stress relief of carbon and low-alloy steels, care must be exercised in selecting stainless steels to be used in dissimilar-metal joints that are to be stress relieved.

Welding is the common cause of the sensitization of stainless steels to intergranular corrosion. Although the cooling rates in the weld itself and the base metal immediately adjacent to it are sufficiently high to avoid carbide precipitation, the weld thermal cycle brings part of the HAZ into the precipitation temperature range. Carbides can precipitate, and a zone somewhat removed from the weld becomes susceptible to intergranular corrosion (Fig. 3). Welding does not always sensitize austenitic stainless steels. In thin sections, the thermal cycle may be such that no part of the HAZ is at sensitizing temperatures long enough to cause carbide precipitation. Once the precipitation has

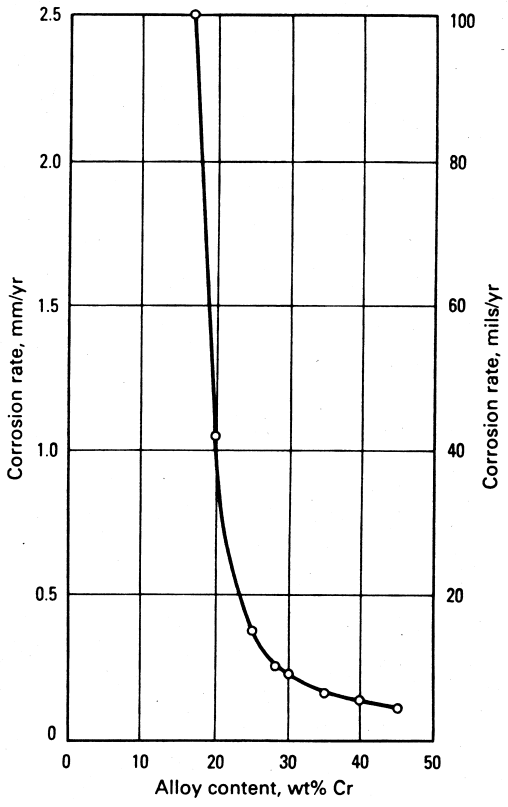

Fig. 2 The effect of chromium content on the corrosion behavior of iron-chromium alloys in boiling 50% H_2SO_4 with $Fe_2(SO_4)_3$. Source: Ref 1

occurred, it can be removed by reheating the alloy to above 1035 °C (1895 °F) and cooling it rapidly. This thermal treatment dissolves the chromium carbide precipitates and restores the chromium-depleted zone. This practice is commonly termed solution anneal.

Avoiding Intergranular Corrosion. Susceptibility to intergranular corrosion in austenitic stainless steels can be avoided by limiting their carbon contents or by adding elements whose carbides are more stable than those of chromium. For most austenitic stainless steels, restricting their carbon contents to 0.03% or less ("L-grade" alloys) prevents sensitization during welding and most heat treatment. This method is not effective for eliminating sensitization that would result from long-term service exposure at 425 to 815 °C (800 to 1500 °F).

At temperatures above 815 °C (1500 °F), titanium and niobium form more stable carbides than chromium and are added to stainless steels to form these stable carbides, which remove carbon from solid solution and prevent precipitation of chromium carbides. The most common of these stabilized grades are types 321 and 347. Type 321 contains minimum titanium content of 5 × (C% + N%), and type 347 a minimum niobium content of 8 × C%. Nitrogen must be considered when titanium is used as a stabilizer, not because the precipitation of chromium nitride is a problem in austenitic steels, but because titanium nitride is very stable. Titanium combines with any available nitrogen; therefore, this reaction must be considered when determining the total amount of titanium required to combine with the carbon.

The stabilized grades are more resistant to sensitization by long-term exposure at 425 to 815 °C (800 to 1500 °F) than the low-carbon grades are, and the stabilized grades are the preferred materials when service involves exposure at these temperatures. For maximum resistance to intergranular corrosion, these grades are given a stabilizing heat treatment at approximately 900 °C (1650 °F). The purpose of the treatment is to remove carbon from solution at temperatures where titanium and niobium carbides are stable, but chromium carbides are not. Such treatments prevent the formation of chromium carbide when the steel is exposed to lower temperatures.

Figure 4 illustrates how both carbon control and stabilization can eliminate intergranular corrosion in as-welded austenitic stainless steels. It also shows that the sensitized zone in these steels is somewhat removed from the weld metal.

Additional methods for minimizing or eliminating intergranular corrosion in austenitic stainless steel weldments include:

- Anneal the material prior to welding to remove any prior cold work (cold work accelerates carbide precipitation).
- Use low weld heat inputs and low interpass temperatures to increase weld cooling rates, thereby minimizing the time in the sensitization temperature range.
- In pipe welding, water cool the inside diameter after the root pass, which will eliminate sensitization of the inside diameter caused by subsequent passes.
- Solution heat treat after welding. Heating the structure into the temperature range from 900 to 1100 °C (1650 to 2010 °F) dissolves any carbides that may have formed along grain boundaries in the HAZ. For large structures, this approach is usually impractical.

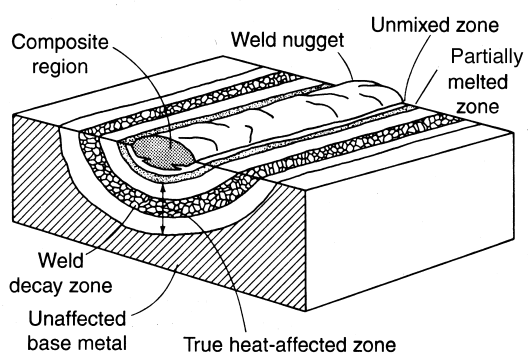

Fig. 3 Schematic diagram of the regions of a weld in austenitic stainless steel. Source: Ref 2

Sensitized HAZs in Type 304 and 316 Stainless Steels. Thiosulfate ($S_2O_3^{2-}$) pitting corrosion will readily occur in sensitized HAZs of type 304 weldments in paper machine whitewater service (Fig. 5). This form of attack can be controlled by limiting sources of $S_2O_3^{2-}$ contamination; the principal one is the brightening agent sodium hyposulfite ($Na_2S_2O_4$). However, nonsensitized type 304 will also be attacked. Consequently, type 316L is the preferred grade of stainless steel that should be specified for paper machine service.

At higher solution temperatures, sensitized type 304 and type 316 are particularly susceptible to SCC, whether caused by chlorides, sulfur compounds, or caustic. For example, type 304

or 316 kraft black liquor evaporators and white liquor tubing are subject to SCC in sensitized HAZs. In many cases cracking occurs after HCl acid cleaning. Although the initial crack path may be intergranular, subsequent propagation can have the characteristic branched appearance of transgranular chloride SCC. Intergranular SCC caused by sulfur compounds can also occur during the acid cleaning of sensitized stainless steels in kraft liquor systems.

Low-Temperature Sensitization. The intergranular corrosion of the weld HAZ has also been observed at service temperatures well below the classic sensitization temperature range. This behavior, often called low-temperature sensitization (LTS), typically occurs after years of service exposure at temperatures below 400 °C (750 °F), even in low-carbon grades. Mechanistically, it is proposed (Ref 5) that carbide embryos form along grain boundaries in the weld HAZ and then grow to form chromium-rich carbides in service. Corrosive attack occurs via the chromium-depletion mechanism described previously. In order to combat LTS, either stabilized alloys or alloys containing higher nitrogen contents (such as type 316LN) are substituted for conventional or L-grade materials.

Knife-Line Attack. Stabilized austenitic stainless steels may become susceptible to a localized form of intergranular corrosion known as knife-line attack or knife-line corrosion. During welding, the base metal immediately adjacent to the fusion line is heated to temperatures high enough to dissolve the stabilizing carbides, but the cooling rate is rapid enough to prevent carbide precipitation. If weldments in stabilized grades are then heated into the sensitizing temperature range of 425 to 815 °C (800 to 1500 °F), for example, during stress-relieving treatments, high-temperature service, or subsequent weld passes, chromium carbide can precipitate. The precipitation of chromium carbide leaves the narrow band

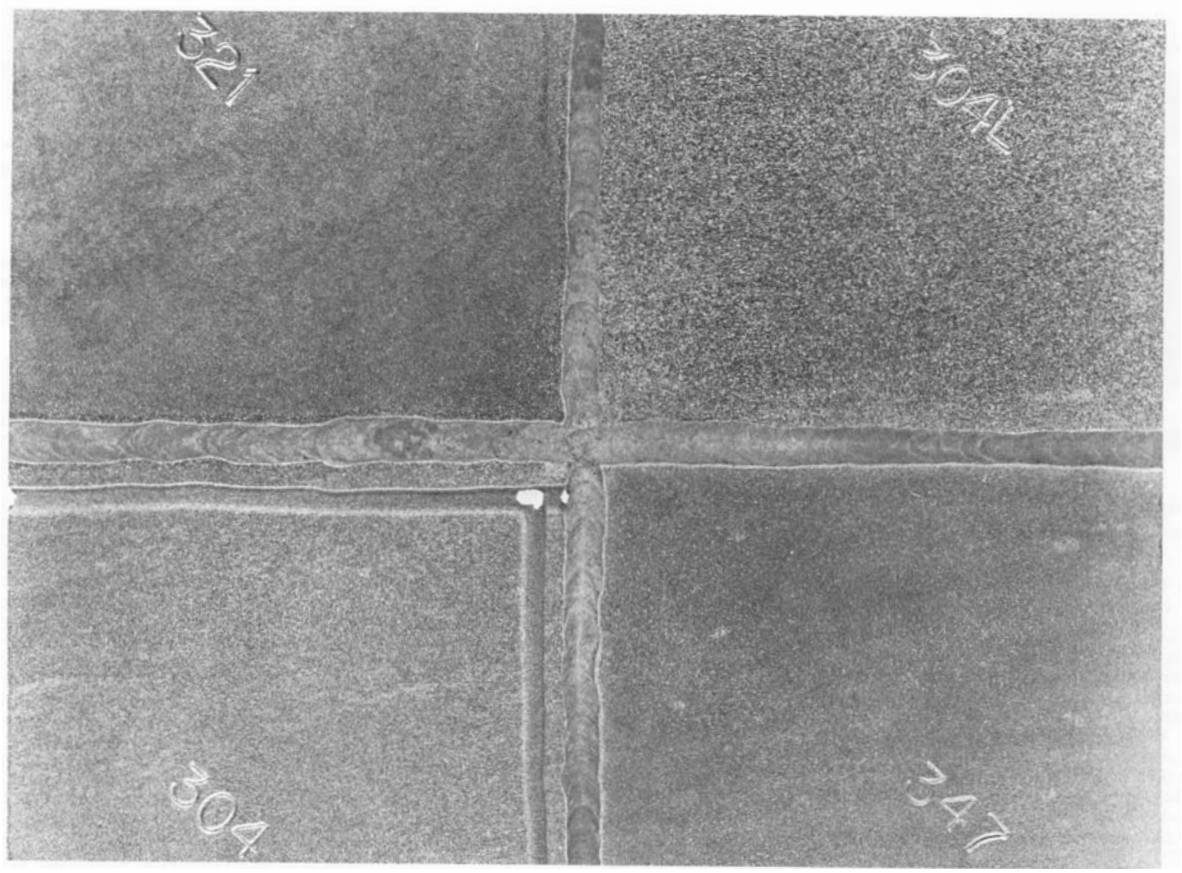

Fig. 4 Weld decay (sensitization) in austenitic stainless steel and methods for its prevention. Panels of four different 300-series stainless steels were joined by welding and exposed to hot HNO_3 + HF solution. The weld decay evident in the type 304 panel was prevented in the other panels by reduction in carbon content (type 304L) or by addition of carbide-stabilizing elements (titanium in type 321, and niobium in type 347). Source: Ref 3

adjacent to the fusion line susceptible to intergranular corrosion.

Knife-line attack can be avoided by the proper choice of welding variables and by the use of stabilizing heat treatments.

Intergranular SCC. Austenitic stainless steels that are susceptible to intergranular corrosion are also subject to intergranular SCC. The problem of the intergranular SCC of sensitized austenitic stainless steels in boiling high-purity water containing oxygen has received a great deal of study. This seemingly benign environment has led to cracking of sensitized stainless steels in many boiling water nuclear reactors. This subject is addressed in Chapter 10, "Weld Corrosion in Specific Industries and Environments."

Sensitized stainless alloys of all types crack very rapidly in the polythionic acid that forms during the shutdown of desulfurization units in petroleum refineries (Ref 6, 7). Because this service involves long-term exposure of sensitizing temperatures, the stabilized grades should be used.

Preferential Attack Associated with Weld Metal Precipitates

In austenitic stainless steels, the principal weld metal precipitates are δ-ferrite, σ-phase, and $M_{23}C_6$ carbides. Small amounts of M_6C carbide may also be present. Sigma phase is often used to describe a range of chromium- and molybdenum-rich precipitates, including χ and laves (η) phases. These phases may precipitate directly from weld metal, but they are most readily formed from weld metal δ-ferrite in molybdenum-containing austenitic stainless steels.

The δ-ferrite transforms into brittle intermetallic phases, such as σ and χ, at temperatures ranging from 500 to 850 °C (930 to 1560 °F) for σ and 650 to 950 °C (1200 to 1740 °F) for χ. The precipitation rate for σ and χ phases increases with the chromium and molybdenum contents. Continuous intergranular networks of a phase reduce the toughness, ductility, and corrosion resistance of austenitic stainless steels.

It is extremely difficult to discriminate between fine particles of σ and χ phases by using conventional optical metallographic techniques; hence the designation σ/χ phase. The use of more sophisticated analytical techniques to identify either phase conclusively is usually not justified when assessing corrosion properties, because the precipitation of either phase depletes the surrounding matrix of crucial alloying elements. Grain-boundary regions that are depleted in chromium and/or molybdenum are likely sites for attack in oxidizing and chlorine-bearing solutions. The damage caused by preferential-corrosion of alloy-depleted regions ranges from the loss of entire grains (grain dropping) to shallow pitting at localized sites, depending on the distribution and morphology of the intermetallic precipitate particles at grain boundaries. Figure 6 shows two views of an austenitic stainless steel exhibiting intergranular corrosion. Figure 6(a) shows the surface of the sample. The grain structure is visible due to the attack, and some grains have fallen out (grain dropping). The cross-sectional view (Fig. 6b) shows the depth of penetration of the attack along the grain boundaries.

Because these precipitates are usually chromium- and molybdenum-rich, they are generally more corrosion resistant than the surrounding austenite. However, there are some exceptions to this rule.

Preferential attack associated with δ-ferrite and σ-phase can be a problem when a weldment is being used close to the limit of corrosion resistance in environments represented by three types of acidic media:

- Mildly reducing (e.g., hydrochloric acid, HCl)
- Borderline active-passive (e.g., sulfuric acid, H_2SO_4)

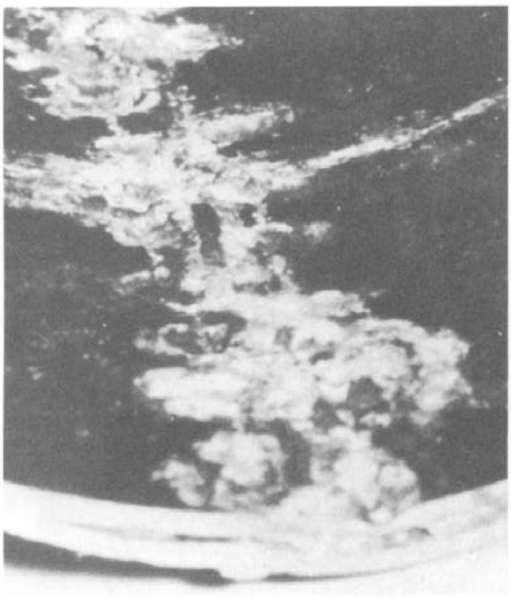

Fig. 5 Thiosulfate pitting in the HAZ of a type 304 stainless steel welded pipe after paper machine white-water service. Source: Ref 4

- Highly oxidizing (e.g., nitric acid, HNO_3)

Acid cleaning of type 304 and 316 stainless steel black liquor evaporators in the pulp and paper industry with poorly inhibited HCl can lead to weld metal δ-ferrite attack (Fig. 7, 8). Attack is avoided by adequate inhibition (short cleaning times with sufficient inhibitor at low enough temperature) and by specification of full-finished welded tubing (in which the δ-ferrite networks within the weld metal structure are altered by cold work and a recrystallizing anneal). The latter condition can easily be verified with laboratory HCl testing, and such a test can be specified when ordering welded tubular products.

Sulfuric acid attack of a phase or of chromium- and molybdenum-depleted regions next to σ-phase precipitates is commonly reported. However, it is difficult to predict because the strong influence of tramp oxidizing agents, such as ferric (Fe^{3+}) or cupric (Cu^{2+}) ions, can inhibit preferential attack. Type 316L weld filler metal has been formulated with higher chromium and lower molybdenum to minimize σ-phase formation, and filler metals for more highly alloyed materials such as 904L (Fe-22Cr-26Ni-4.5Mo) are balanced to avoid δ-ferrite precipitation and thus minimize σ-phase.

Highly oxidizing environments such as those found in bleach plants could conceivably attack δ-ferrite networks and σ-phase. However, this mode of attack is not often a cause of failure, probably because free-corrosion potentials are generally lower (less oxidizing) than that required to initiate attack. Preferential attack of δ-ferrite in type 316L weld metal is most often reported after prolonged HNO_3 exposure, as in nuclear-fuel reprocessing or urea production. For these applications, a low corrosion rate in the Huey test (ASTM A 262, practice C) is specified (Ref 4).

Pitting and Crevice Corrosion

Localized attack in the weld metal and HAZ may occur in the form of pitting and crevice corrosion, particularly in aqueous, chloride-bearing environments.

Pitting Corrosion. Under moderately oxidizing conditions, such as a pulp and paper bleach plant, weld metal austenite may suffer preferential pitting in alloy-depleted regions. This attack is independent of any weld metal precipitation and is a consequence of microsegregation or coring in weld metal dendrites. Preferential pitting is more likely:

- In autogenous (no filler) gas-tungsten arc (GTA) welds (Fig. 9)
- In 4 to 6% Mo alloys (Table 3)
- When the recommended filler metal has the same composition as the base metal (Fig. 10)
- When higher-heat-input welding leaves a coarse microstructure with surface-lying dendrites. (Fig. 11). Such a microstructure is

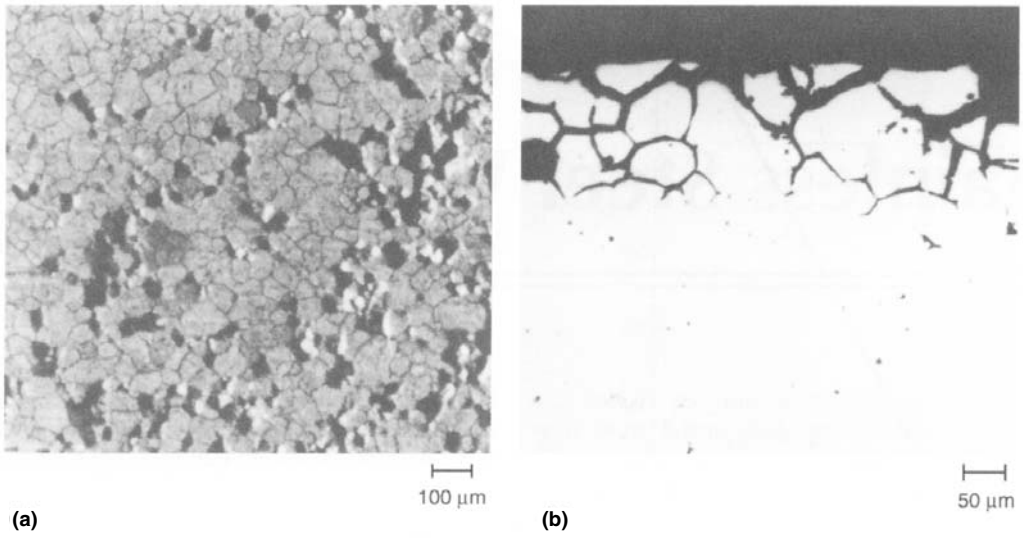

Fig. 6 (a) Planar and (b) cross-sectional views of intergranular corrosion (grain dropping) in a sensitized austenitic stainless steel. As-polished. (a) 50×. (b) 100×. Courtesy of G.F. Vander Voort, Carpenter Technology Corporation

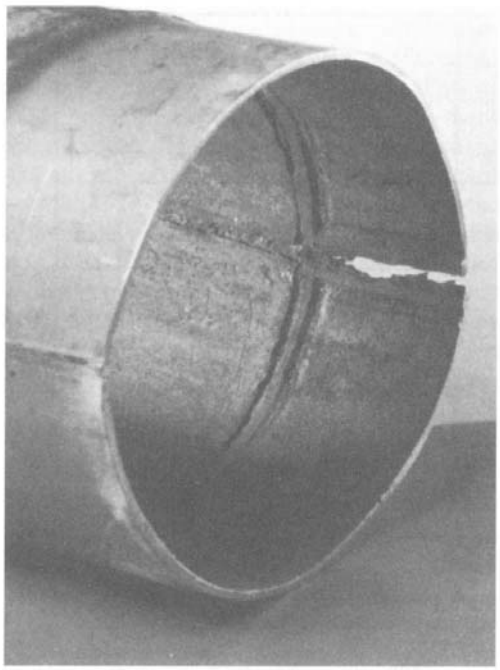

Fig. 7 Corroded type 316 stainless steel pipe from a black liquor evaporator. Two forms of attack are evident: preferential attack of the weld metal ferrite, suffered during HCl acid cleaning, and less severe attack in the sensitized HAZ center. Source: Ref 4

Fig. 8 Preferential corrosion of the vermicular ferrite phase in austenitic stainless steel weld metal. Discrete ferrite pools that are intact can be seen in the lower right; black areas in the upper left are voids where ferrite has been attacked. Electrolytically etched with 10% ammonium persulfate. 500×. Source: Ref 8

avoided by use of a suitably alloyed filler metal (Fig. 10).

Filler metals with pitting resistance close to or better than that of corresponding base metals include:

Base metal	Filler metals
Type 316L	316L, 317L, 309MoL
Type 317	317L, 309MoL
Alloy 904	Sandvik 27.31.4.LCuR, Thermanit 30/40 E, Nicro 31/27, Fox CN 20 25 M, IN-112, Avesta P12, Hastelloy alloy C276
Avesta 254 SMO	Avesta P12, IN-112, Hastelloy alloy C-276

Even when suitable fillers are used, preferential pitting attack can still occur in an unmixed zone of weld metal. High-heat-input welding can leave bands of melted base metal close to the fusion line. The effect of these bands on cor-

Table 3 Amounts of principal alloying elements in stainless steels tested for pitting resistance

Test results are shown in Fig. 9 and 10

	Composition, %			
Alloy	Cr	Ni	Mo	N
Base metals				
Type 316L	16	13	2.8	. . .
Type 317L	18	14	3.2	. . .
34L	17	15	4.3	. . .
34LN	18	14	4.7	. . .
1.4439	18	14	4.3	0.13
Nitronic 50	21	14	2.2	0.20
20Cb-3	20	33	2.4	. . .
Alloy 904L	20	25	4.2	. . .
2RK65	20	25	4.5	. . .
JS700	21	25	4.5	. . .
19/25LC	20	25	4.8	. . .
AL-6X	20	24	6.6	. . .
254SMO	20	18	6.1	0.20
19/25HMO	21	25	5.9	0.15
Filler metals				
Type 316L	19	12	2.3	. . .
Type 317L	19	13	3.8	. . .
309MoL	23	14	2.5	. . .
Batox Cu	19	24	4.6	. . .
254SLX	20	24	5.0	. . .
SP-281	20	25	4.6	. . .
Jungo 4500	20	26	4.4	. . .
Nicro 31/27	28	30	3.5	. . .
Thermanit 30/40E	28	35	3.4	. . .
SAN 27.31.4.LCuR	27	31	3.5	. . .
Incoloy alloy 135	27	31	3.5	. . .
Hastelloy alloy G	22	38	3.7	. . .
P 12	21	61	8.6	. . .
Inconel alloy 112	21	61	8.7	. . .
Hastelloy alloy C-276	15	58	15.4	. . .

Source: Ref 4

rosion resistance can be minimized by welding techniques that bury unmixed zones beneath the surface of the weldment.

When the wrong filler metal is used, pitting corrosion can readily occur in some environments. In the example shown in Fig. 12, the type 316L base metal was welded with a lower-alloy filler metal (type 308L). Tap water was the major environmental constituent contributing to crust formation on the weld joint. The type 316L base metal on either side of the joint was not affected.

Crevice Corrosion. Defects such as residual welding flux and microfissures create weld metal crevices that are easily corroded, particularly in chloride-containing environments. Some flux formulations on coated shielded metal arc electrodes produce easily detached

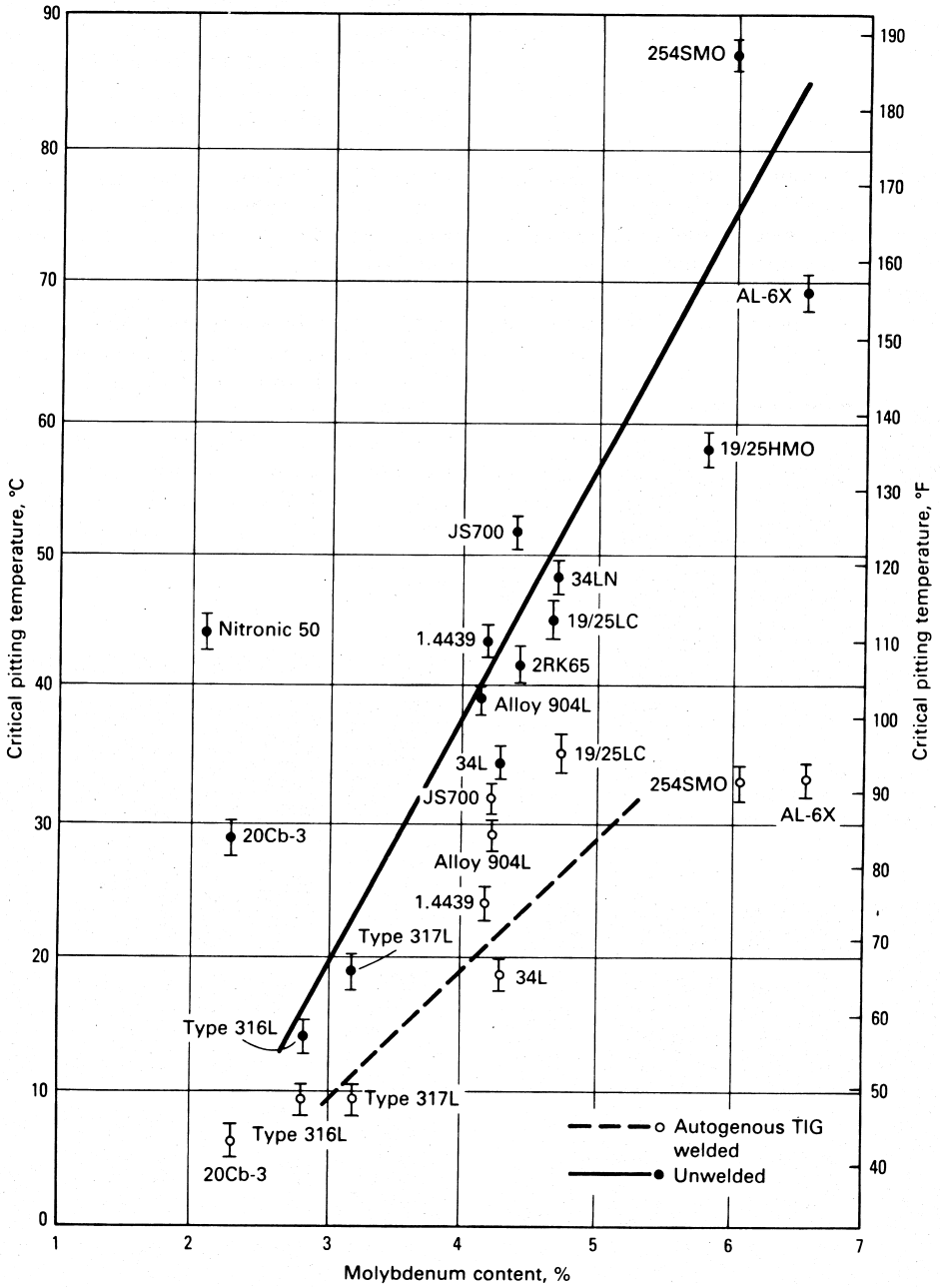

Fig. 9 Critical pitting temperature versus molybdenum content for commercial austenitic stainless steels tested in 10% $FeCl_3$. Resistance to pitting, as measured by the critical pitting temperature, increases with molybdenum content and decreases after autogenous tungsten inert gas welding. Source: Ref 4

slags, and others give slags that are difficult to remove completely, even after grit blasting. Slags from rutile (titania-base) coatings are easily detached and give good bead shape. In contrast, slags from the basic-coated electrodes for out-of-position welding can be difficult to remove; small particles of slag may remain on the surface, providing an easy initiation site for crevice attack (Fig. 13).

Microfissures or their larger counterparts, hot cracks, also provide easy initiation sites for crevice attack, which will drastically reduce the corrosion resistance of a weldment in the bleach plant. Microfissures are caused by thermal contraction stresses during weld solidification and are a problem that plagues austenitic stainless steel fabrications. These weld metal cracks are more likely to form when phosphorus and sulfur levels are higher (i.e., >0.015% P and >0.015% S), with high-heat-input welding, and in austenitic weld metal in which the δ-ferrite content is low (<3%).

Small-scale microfissures are often invisible to the naked eye, and their existence can readily explain the unexpectedly poor pitting performance of one of a group of weldments made with filler metals of apparently similar general composition. The microfissure provides a crevice, which is easily corroded because stainless alloys are more susceptible to crevice corrosion than to pitting. However, microfissure-crevice corrosion is often mistakenly interpreted as self-initiated pitting (Fig. 14, 15).

Crevice corrosion sites can also occur at the beginning or end of weld passes, between weld passes, or under weld spatter areas. Weld spatter is most troublesome when it is loose or poorly adherent. A good example of this type of crevice condition is the type 304 stainless system shown in Fig. 16.

Microfissure corrosion in austenitic stainless steel weldments containing 4 to 6% Mo is best avoided with the nickel-base Inconel 625, Inconel 112, or Avesta P12 filler metals, which are very resistant to crevice attack. Some stainless electrodes are suitable for welding 4% Mo steels, but they should be selected with low phosphorus and sulfur to avoid microfissure problems.

Hot tap water is not thought to be particularly aggressive; however, Fig. 17 shows what can happen to a weld that contains a lack-of-fusion defect in the presence of chlorides. In this case, the base metal is type 304 stainless steel, and the weld metal is type 308.

Crater Corrosion. Type 347 stainless steel is sometimes subject to a type of crevice corrosion known as crater corrosion, which occurs at the stop point of a weld. The failure is related to microsegregation of certain constituents in the pool of molten metal that is the last to solidify on a weld. In a manner similar to zone-melting

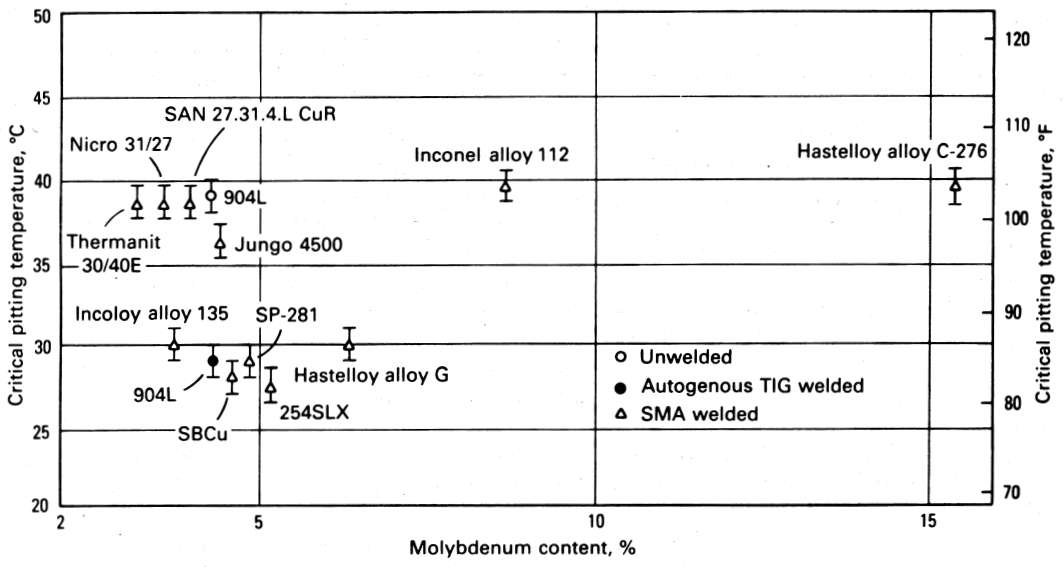

Fig. 10 Effects of various welding techniques and filler metals on the critical pitting temperature of alloy 904L. Data for an unwelded specimen are included for comparison. Source: Ref 4

refinement, the moving weld pool continuously sweeps selected constituents ahead of it, and the concentration of these selected constituents in the pool increases continuously until the welding is stopped and the pool solidifies. The center of the stop point is attacked rapidly in oxidizing acids, such as nitric acid, in a form of self-accelerating crevice corrosion. The final solidification pool need not extend through the thickness of the part for full perforation to occur, as described in the following example.

Example 1: Weld Craters in Stainless Steel Heat Exchanger Tubes. Beveled weld-joint V-sections were fabricated to connect inlet and outlet sections of tubes in a type 347 stainless steel heat exchanger for a nitric acid concentrator. Each V-section was permanently marked with the tube numbers by a small electric-arc pencil.

After one to two years of service, multiple leaks were observed in the heat-exchanger

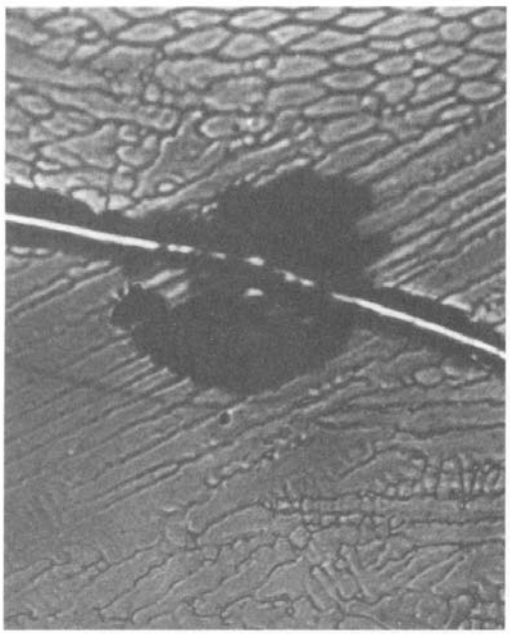

Fig. 11 A scratch-initiated pit formed in type 317L weld metal at 190 mV versus SCE in 0.6 *N* NaCl (pH 3) at 50 °C (120 °F). Pitting occurred at a grain with primary dendrites lying parallel to the surface rather than in grains with dendrites oriented at an angle to the surface.

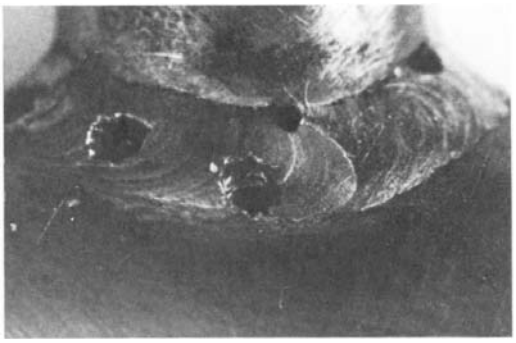

Fig. 12 Pitting of underalloyed (relative to base metal) type 308L weld metal. The type 316L stainless steel base metal is unaffected. About 2.5×

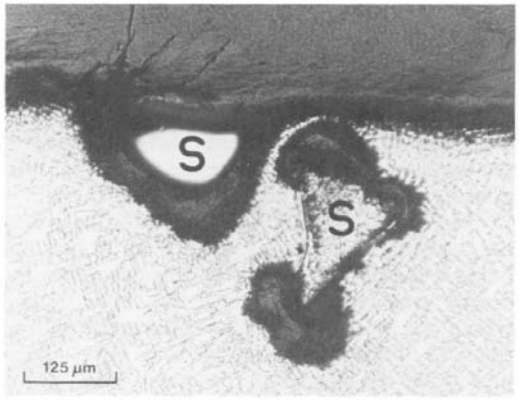

Fig. 13 Crevice corrosion under residual slag (S) in IN-135 weld metal after bleach plant exposure. Etched with glycergia. Source: Ref 4

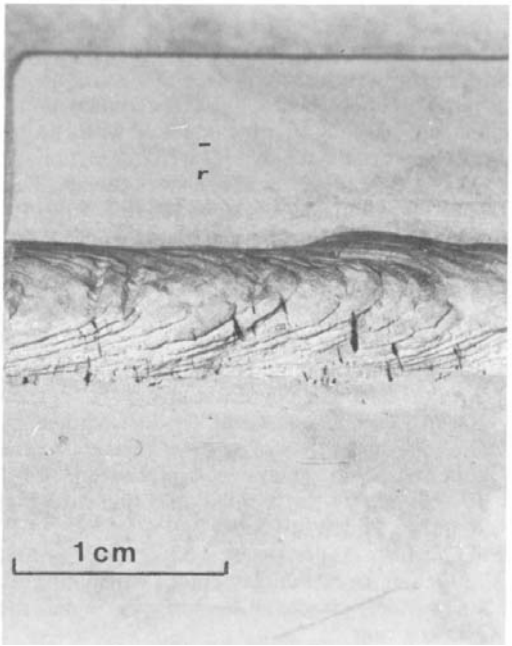

Fig. 14 Microfissure corrosion on IN-135 weld metal on an alloy 904L test coupon after bleach plant exposure. See also Fig. 15. Source: Ref 4

tubes. When the tubes were removed and examined, it was found that the general corrosion rate was normal for service of heat-exchanger tubes in a nitric acid concentrator, but that crater corrosion had perforated the tubes.

The crater corrosion occurred at two general locations. One location was at the stop point of the welds used to connect the inlet and outlet legs of the heat exchanger. The other location was at the stop points on the identifying numerals. The material was changed to type 304L stainless steel, in which the zone-melting concentration does not take place.

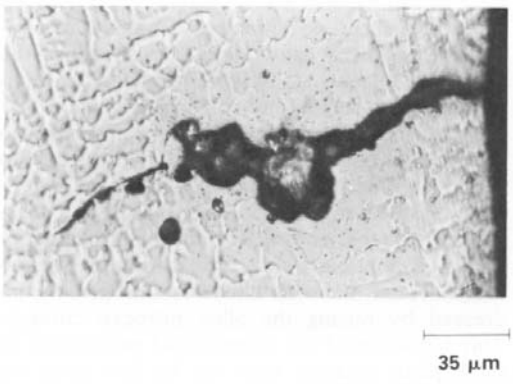

Fig. 15 Section from the bleach plant test coupon in Fig. 14 showing crevice corrosion that has almost obliterated evidence of a microfissure. This form of attack is often mistakenly interpreted as self-initiating pitting: more often, crevice corrosion originates at a microfissure. Etched with glycergia. Source: Ref 4

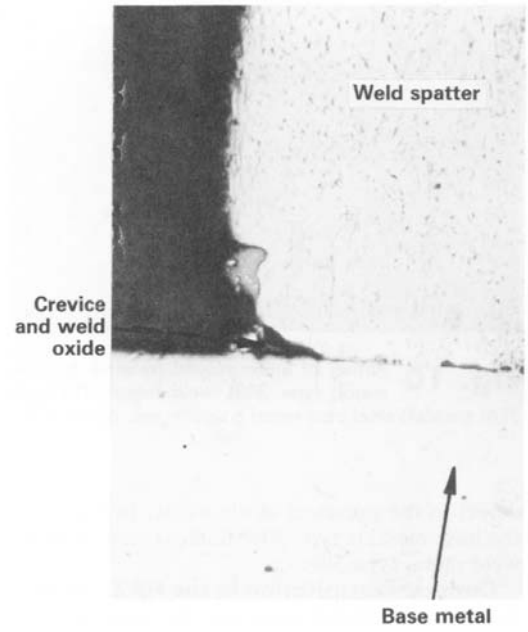

Fig. 16 Cross section of a weldment showing crevice corrosion under weld spatter. Oxides (light gray) have formed on the spatter and in the crevice between spatter and base metal.

Stress-Corrosion Cracking

The stress-corrosion cracking of austenitic stainless steels may occur when an alloy is subjected simultaneously to a tensile stress and a specific corrosive medium. The important variables affecting SCC are temperature, environment, material composition, stress level, and microstructure. Crack propagation may be either transgranular or intergranular, depending on the interaction of these variables. Intergranular stress-corrosion cracking (IGSCC) can occur even though the alloy is insensitive to intergranular corrosion. The presence of residual tensile stresses in the HAZ may accelerate corrosion attack and cracking, particularly along sensitized grain boundaries.

Transgranular SCC is also observed in austenitic stainless steels. This form of cracking is usually indigenous to chloride environments (seawater), but may also occur in caustic media. The ions of the halogen family (fluorine, chlorine, bromine, and iodine) are largely responsible for promoting transgranular SCC. Of the halides, the chloride ion causes the greatest number of failures. Figure 18 shows an example of transgranular SCC in type 316 stainless steel. Note that cracking has initiated at the toe of the weld, probably because of the high residual stress level at that location.

Chloride SCC. Welds in the 300-series austenitic stainless steels, with the exception of types 310 and 310Mo, contain a small amount of δ-ferrite (usually less than 10%) to prevent hot cracking during weld solidification. In hot, aqueous chloride environments, these duplex weldments generally show a marked resistance to cracking, while their counterparts crack readily (Fig. 19). The generally accepted explanation for this behavior is that the ferrite phase is resistant to chloride SCC and impedes crack propagation through the austenite phase. Electrochemical effects may also play a part; however, under sufficient tensile stress, temperature, and chloride concentration, these duplex weldments will readily crack. An example is shown in Fig. 20.

Caustic Embrittlement (Caustic SCC). Susceptibility of austenitic stainless steels to

this form of corrosion usually becomes a problem when the caustic concentration exceeds approximately 25% and temperatures are above 100 °C (212 °F). Because welding is involved in most fabrications, the weld joint becomes the focus of attention because of potential stress-raiser effects and because of high residual shrinkage stresses. Cracking occurs most often in the weld HAZ.

In one case, a type 316L reactor vessel failed repeatedly by caustic SCC in which the process fluids contained 50% sodium hydroxide (NaOH) at 105 °C (220 °F). Failure was restricted to the weld HAZ adjacent to bracket attachment welds used to hold a steam coil. The stresses caused by the thermal expansion of the Nickel 200 steam coil at 1034 kPa (150 psig) aggravated the problem. Figure 21 shows the cracks in the weld HAZ to be branching and intergranular. Because it was not practical to reduce the operating temperature below the threshold temperature at which caustic SCC occurs, it was recommended that the vessel be weld overlayed with nickel or that the existing vessel be scrapped and a replacement fabricated from Nickel 200.

Methods for controlling SCC include:

- A stress-relieving or annealing heat treatment to reduce weld residual stresses
- Substitution of more-resistant high-nickel alloys, high-chromium ferritic stainless steels, or duplex stainless steels, the latter of which have been designed specifically to minimize SCC
- Reduction of chloride and oxygen contents from the environment, because these two elements, in combination, are responsible for most SCC failures in austenitic stainless steels

Example 2: SCC of a Type 304 Stainless Steel Pipe Caused by Residual Welding Stresses. A 150 mm (6 in.) schedule 80S type 304 stainless steel pipe (11 mm, or 0.432 in., wall thickness), which had served as an equalizer line in the primary loop of a pressurized-water reactor, was found to contain several circumferential cracks 50 to 100 mm (2 to 4 in.) long. Two of these cracks, which had penetrated the pipe wall, were responsible for leaks detected in a hydrostatic test performed during a general inspection after 7 years of service.

Investigation. The general on-site inspection had included careful scrutiny of all pipe welds by both visual and ultrasonic examination. Following discovery of the two leaks, the entire line of 150 mm (6 in.) pipe, which contained 16 welds, was carefully scanned. Five additional defects were discovered, all circumferential and all in HAZs adjacent to welds. In contrast, scans of larger-diameter pipes in the system (up to 560 mm, or 22 in., in diameter) disclosed no such defects.

Samples of the 150 mm (6 in.) pipe were submitted to three laboratories for independent examination. Inspection in all three laboratories disclosed that all the defects were circumferential intergranular cracks that had originated at

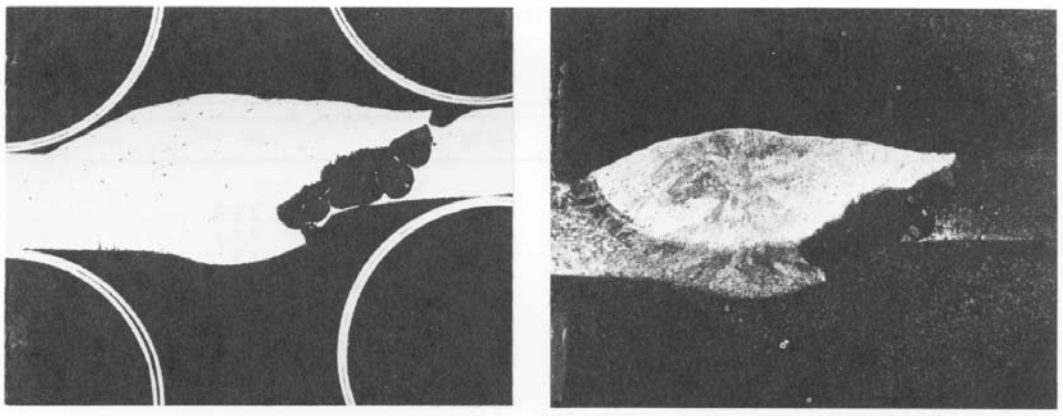

(a) (b)

Fig. 17 (a) Unetched and (b) etched cross sections of a type 304 stainless steel weldment showing chloride pitting attack along a crevice by a lack-of-fusion defect. Service environment: hot tap water

the inside surface of the pipe and that were typical of stress-corrosion attack. A majority of the cracks had occurred in HAZs adjacent to circumferential welds. Some cracks had penetrated the entire pipe wall; others had reached a depth of two-thirds of the wall thickness. In general, the cracks were 50 to 100 mm (2 to 4 in.) long. Branches of the cracks that had approached weld deposits had halted without invading the structure (austenite plus δ-ferrite) of the type 308 stainless steel welds. All HAZs examined contained networks of precipitated carbides at the grain boundaries, which revealed that welding had sensitized the 304 stainless steel in those local areas.

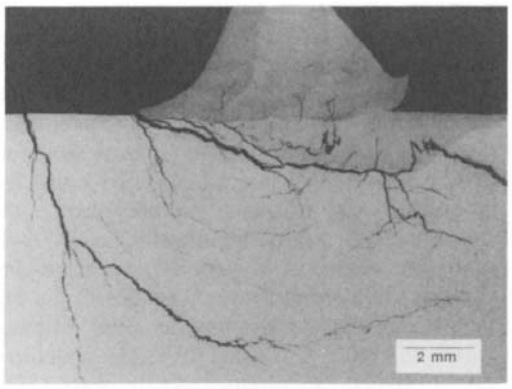

Fig. 18 Transgranular SCC that has initiated near the toe of a weld in type 316L alloy

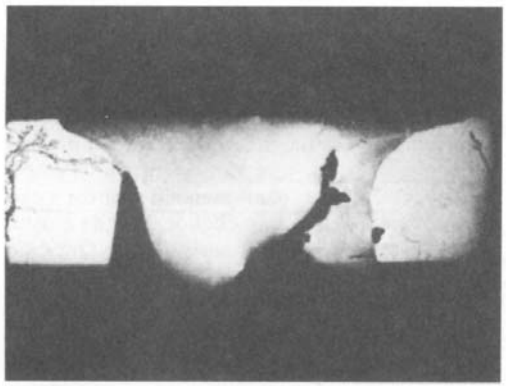

Fig. 19 Selective attack of a type 317L stainless steel weldment and chloride SCC of the adjacent 317L base metal. The environment was a bleaching solution (7 g/L Cl_2) at 70 °C (160 °F).

Additional cracks, also intergranular and circumferential and originating at the inner surface of the pipe, were discovered at locations remote from any welds. These cracks penetrated to a depth of only one-sixth to one-fourth of the wall thickness through a solution-annealed structure, showing evidence of some cold work at the inner surface.

The water in this heat exchanger was of sufficient purity that corrosion had not been anticipated. The water conditions were:

- Temperature: 285 °C (545 °F)
- Pressure: 7 MPa (1000 psi)
- pH: 6.5 to 7.5
- Chloride content: <0.1 ppm
- Oxygen content: 0.2 to 0.3 ppm
- Electrical conductivity: <0.4 mS/cm

Analysis of the pipe showed the chemical composition to be entirely normal for type 304 stainless steel. The material was certified by the producer as conforming to ASME SA-376, grade TP304. All available data indicated that the as-supplied pipe had been of acceptable quality.

Several types of stress-corrosion tests were conducted. In one group of tests, samples of 150 mm (6 in.) type 304 stainless steel pipe were welded together using type 308 stainless steel filler metal. Two different welding procedures were used—one consisting of three passes with a high heat input and the other consisting of ten passes with a low heat input. The welded samples were stressed and exposed to water containing 100 ppm dissolved oxygen at 285 °C (545 °F) and 7 MPa (1000 psi). Samples that were welded with the high heat input procedure, which promotes carbide precipitation and residual stress, cracked after 168 h of exposure, whereas samples that were welded with the low heat input procedure remained crack free. These results were considered significant because service reports indicated that the cracked pipe had been welded using a high heat input and a small number of passes and that the larger-diameter piping in the primary loop, which did not crack in service, had been welded with the use of a low heat input, multiple-pass procedure.

Conclusions. The intergranular SCC of the 150 mm (6 in.) schedule 80S type 304 stainless steel pipe exposed to high-temperature, high-pressure, high-purity water in 7 years of heat

exchanger service was believed to have been caused by:

- *Stress:* The welding procedure, which employed few passes and high heat input, undoubtedly generated unacceptably high levels of residual stress in the HAZs. The cold working of the internal surface in a sizing operation also set up residual stresses in areas apart from the welds. Both conditions were conducive to SCC.
- *Sensitization:* The high heat input welding caused precipitation of chromium carbides at the grain boundaries in the HAZs. This rendered the steel sensitive to intergranular attack, which, combined with the residual stress, afforded a completely normal setting for SCC.
- *Environment:* Although the level of dissolved oxygen in the water was quite low, it was considered possible that, on the basis of prolonged exposure, oxygen in the range of 0.2 to 1.0 ppm could have provided the necessary ion concentration.

Corrective Measures. All replacement pipe sections were installed using low-heat-input, multiple-pass welding procedures. When stress corrosion is identified as the mechanism of a failure, the proper corrective action can be either a reduction in stress (or stress concentration) or an alteration of the environment. When the cause of failure is inadvertent concentration of a corrodent or inadvertent exposure of the part to a corrosive foreign substance, such as

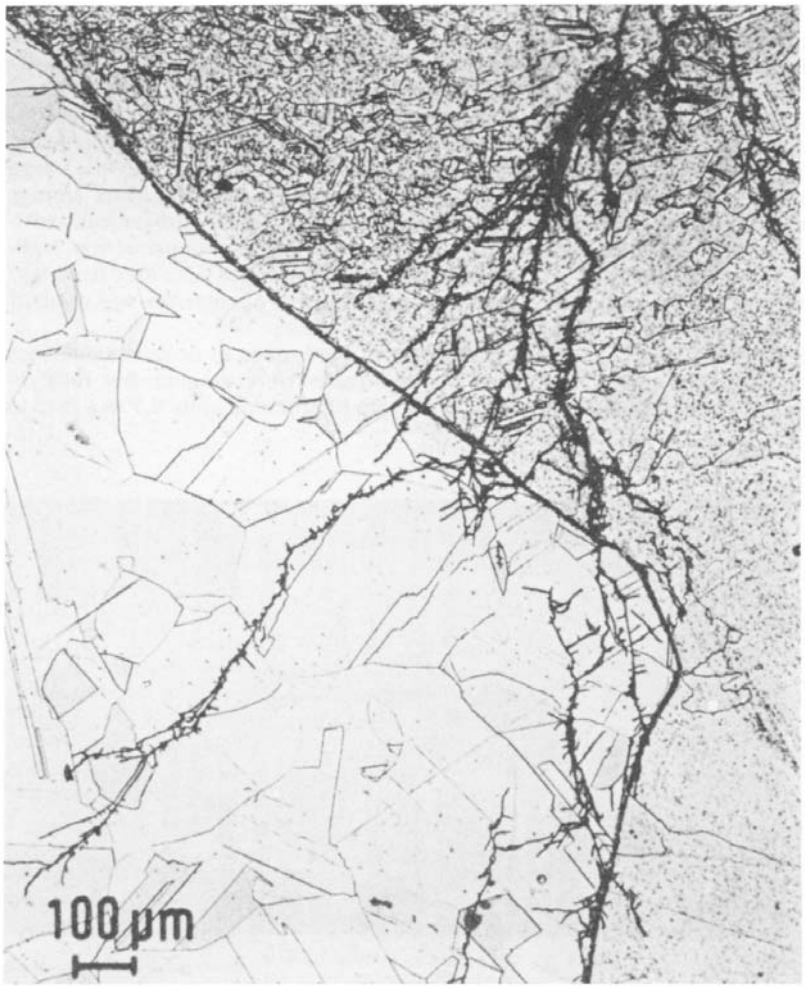

Fig. 20 Chloride SCC of type 304 stainless steel base metal and type 308 weld metal in an aqueous chloride environment at 95 °C (200 °F). Cracks are branching and transgranular.

use of a steam line to feed concentrated caustic during chemical cleaning, the preventive measure may be no more complicated than exclusion of the corrodent from that region of the system. In many instances, however, reduction of the level of residual stress is the most effective means of minimizing or preventing SCC.

Microbiologically Induced Corrosion (MIC)

Microbiologically induced corrosion on austenitic stainless steel leads mostly to pitting or crevice corrosion. Most failures are associated with welds, because areas of joining tend to be inherently more susceptible to corrosion attack than the base metal. Studies have shown that heat-tinted zones are especially vulnerable. As described later in this chapter, these zones are created in a welding process where material above the scaling temperature is contacted by air. The result is a migration of chromium into the surface scale, leaving underlying material depleted and susceptible to corrosion. Removing the heat-tinted scale and underlying surface by pickling, electrochemical cleaning, or mechanical grinding prevents corrosion damage with or without bacteria for 304L, 308L, or 316L material. It has been suggested that pickling is the most effective approach. Heat tinting can be avoided by use of an effective inert gas blanket in the welding procedure.

Fig. 21 Caustic SCC in the HAZ of a type 316L stainless steel NaOH reactor vessel. Cracks are branching and intergranular.

Microbiologically induced corrosion is perhaps the only mechanism that can perforate stainless steel piping in neutral aqueous service, such as river water cooling, in a matter of months. It is suggested that this may be due to the ratio of cathodic to anodic areas, where a single phase, for example, ferrite, is preferentially attacked relative to a large area of less susceptible material. Penetration rates of 17 mm/year (0.7 in./year) in type 308 welds have been reported. Perforation of 316L stainless steel weldments in piping with 5.5 mm (0.2 in.) wall thickness in industrial water systems under intermittent flow in four months has been described (Ref 9).

Preferential attack of some sort is a common feature of MIC case studies. Corrosion is often focused on the weld material or at the fusion line for the weld (Fig. 22). Pit surfaces are often described as dendritic, consistent with preferential corrosion, but the preferential attack of a single phase need not be a feature of MIC. From detailed study of type 308 weld specimens, it has been concluded that either ferrite or austenite can be preferentially attacked, or they may corrode together, depending on a number of possible conditions (Ref 9). Abiotic attack by $FeCl_3$ solutions has been found to give similar effects to MIC, based on comparison of chemically degraded specimens with samples from identified MIC sites (Ref 9, 10). Preferential attack can also occur in a single phase, due to cold work effects on microstructure (Ref 9, 10).

Microbiologically induced intergranular pitting and IGSCC can occur in sensitized stainless steels, where low chromium content at grain boundaries allows preferential dissolution. However, it has been found that transgranular pitting due to MIC in the heat-affected zone in socket-welded specimens of 304 stainless steel exposed to flowing lakewater (500 to 600 ppm chloride) over 6 to 18 months was not focused in sensitized areas (Ref 10). Instead, pitting occurred along deformation lines left by cold working of the metal during manufacturing. Annealing the material at 1150 °C (2100 °F) was suggested as a way to remove these features

and increase resistance of the material to MIC. No pitting was seen in the base metal for either furnace-sensitized or girth-welded specimens of 304 or 316 stainless steel after similar exposure (Ref 10).

A number of trends seem apparent, based on past failure analyses:

- Microbiologically induced corrosion is often associated with stagnant, untreated water being left in piping over extended periods. It has been suggested that intermittent flow or low flow rates are most damaging.
- Damage often occurs at many welds in an affected section of piping. In one power plant cooling system using lake water, radiography indicated that 50% of the welds in 316L piping showed indications of deep MIC pitting.
- Pitting seems more prevalent in the bottom third of the pipe.
- Low pH or high chloride concentrations in the pit environment enhance attack.

It has been noted that higher alloying in weld combinations seems to improve resistance to MIC (Ref 11). This observation is supported by a systematic laboratory study of stainless steel (304, 316L, and 317L) and Ni-Cr-Mo (alloy 625) alloy weldments cleaned of surface thermal oxides (Ref 12); however, later work on as-received welds showed that thermal oxides produced during the welding process can obscure this dependence. In all cases, exposure of specimens to lake water augmented by active sulfate-reducing bacteria (SRB) reduced the polarization resistance of the alloys relative to sterile controls. This was true even for alloys with 9% Mo content; however, no documented corrosion failures due to MIC in alloys with 6% Mo or more could be found to support the idea that elevated molybdenum content can provide added resistance to corrosion damage.

It was recommended that failure analysis for stainless steel cooling systems include biological analysis of associated water and deposits, chemical analysis of water, and radiography of welds. Microbially induced corrosion in pitting at weldments in stainless steel was identified by Ref 10.

- The combination of bacteria present and morphology of pits

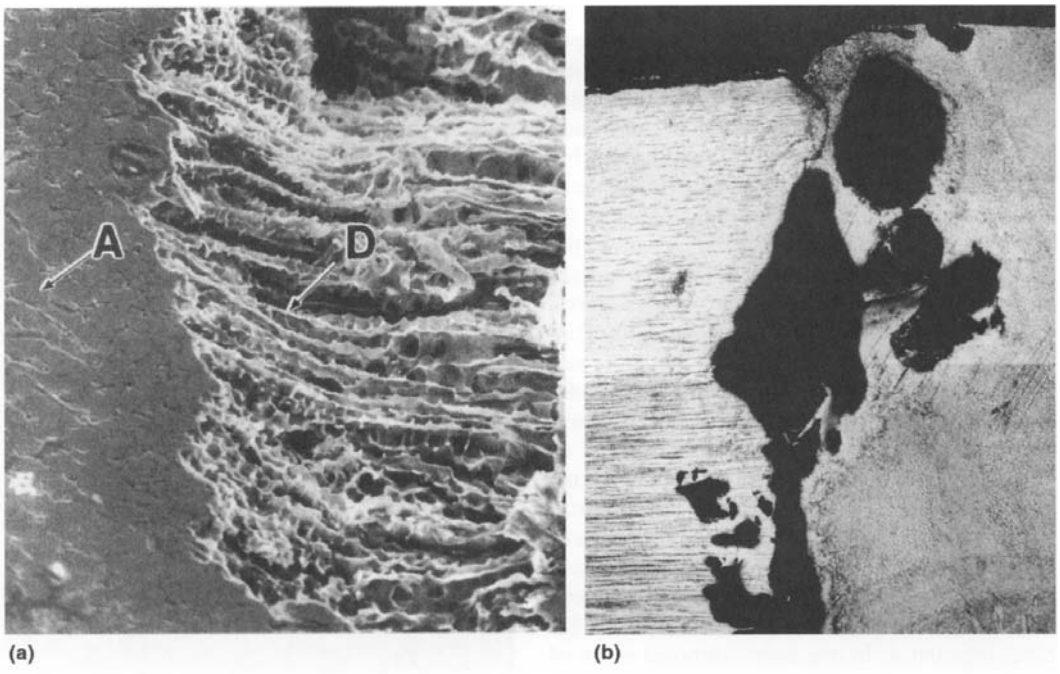

Fig. 22 MIC of stainless steel weldments. (a) MIC showing a surface view of interdendritic attack at the fusion line of a stainless steel weldment. "A," nondendritic; "D," dendrite. (b) Cross section of MIC at a stainless steel weldment showing extensive corrosion of weld metal and fusion line, with a relatively small opening at the bold surface. Source: Ref 17

- Corrosion features with small surface openings leading to bulbous cavities in the steel matrix at welds
- The absence of other agents that could account for the attack

While SRB in mixed populations are a favorite for laboratory studies, and sulfides are often found in associated deposits on affected metal surfaces in the field, the microbiology found in case studies tends to be complex. A wide range of organisms can be present, especially in cooling systems drawing on natural waters. All sorts of bacteria were found to be present in once-through cooling systems using untreated river water, including sulfur oxidizers, iron oxidizers, iron reducers, SRB, nitrogen oxidizers, and denitrifiers (Ref 13). Aerobes, anaerobes, SRB, and acid producing bacteria (APB) were reported to be present in slimes and nodules on the metal surface (Ref 10). The presence of iron oxidizers and slimers for MIC problems in type 308 stainless steel welds has been cited (Ref 14), while *Gallionella* in characteristic MIC pits has been specifically identified (Ref 15). Enhanced numbers of manganese-oxidizing bacteria have been noted in deposits formed on corroded welds in 304L stainless steel specimens exposed to Lake of Constance water in lab studies (Ref 16).

Surface deposits in nine case studies (Ref 13, 15, and 17) contained iron, silicon, and sulfur in >75% of the samples analyzed (Fig. 23). Manganese, chromium, and aluminum were also frequently found (>50% of samples), but more soluble ions, such as chloride and potassium, were detected in less than half the samples.

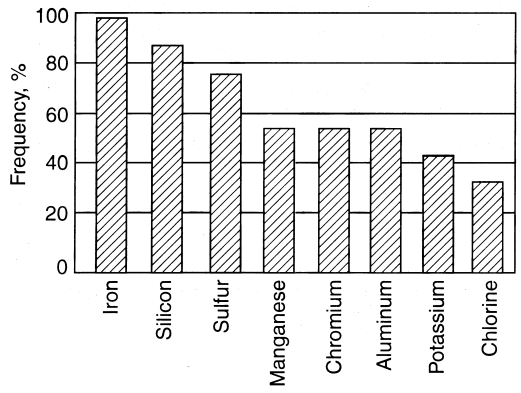

Fig. 23 Most commonly found elements in nine deposits from MIC sites in stainless steel cooling water systems (expressed as percent of deposits showing element). Source: Ref 13, 15, 17

At least two sorts of surface deposits were reported. Most of the surface of service water piping receiving lake water was covered by a tightly packed, black, slimy deposit that had a high content of manganese and iron, with trace sulfide, silicon, and aluminum present. No corrosion was reported under these deposits. Rust-colored deposits found in a small area (6.5 cm^2) at the weld were rich in chromium and iron, with sulfur, chlorine, aluminum, and silicon in smaller concentrations. This rust-colored deposit covered the opening of an extensive corrosion cavity in the underlying metal (Fig. 22). This is a unique form of pitting associated with MIC in weldments in stainless steel. The cavity openings are often associated with rust-colored stains on the surface metal or with rust-colored deposits rich in iron and manganese (Ref 13, 15).

Radiography or destructive testing of field specimens reveals the large cavities to be a series of pits branching off one another to give a bulbous and irregular void volume sometimes associated with tunneling in the direction of rolling along stringers of ferrite or austenite (Ref 10, 15). This form of pitting is focused on weld metal or the fusion line, with wall perforation occurring through a second small opening on the opposite metal surface. The frequent observation of sulfide in associated surface deposits (Fig. 23) implies that SRB are commonly involved at some stage, but iron-oxidizing bacteria, particularly *Gallionella,* found in the pits have come to be associated with this corrosion morphology. *Gallionella* oxidize Fe^{2+} to Fe^{3+} in their metabolism, leading to the formation of characteristic rust-colored deposits. The acidity of the hydrated ferric ion produced decreases the pH of the local environment. Whether *Gallionella* initiate pitting or are attracted to the anodic area by the release of ferrous ions through a previously existing anaerobic corrosion process is not clear. The latter seems more likely. Once iron-oxidizing organisms are established, reduction in the pH of the corrosion pit and concentration cells established by the buildup of iron (III) oxide deposits help to drive the corrosion process.

Literature reports identify several possible MIC scenarios on stainless steel weldments. Table 4 summarizes the organisms and features that may be useful in failure analysis.

Example 3: Microbiological Corrosion of Butt Welds in Water Tanks (Ref 18). New production facilities at one plant site required austenitic stainless steels, primarily types 304L and 316L, for resistance to HNO_3 and organic acids and for maintaining product purity. The piping was shop fabricated, field erected, and then hydrostatically tested. All of the large (>190,000 L or 25,000 gal) flat-bottom storage tanks were field erected and hydrostatically tested. During the early stages of construction, sodium-softened plant well water (also used for drinking) containing 200 ppm of chlorides was used for testing.

No attempts were made to drain the pipelines after testing. Tanks were drained, but then refilled to a depth of approximately 0.5 to 1 m (2 to 3 ft) for ballast because of a hurricane threat. The water was left in the tanks to evaporate.

The problem became evident when water was found dripping from butt welds in type 304L and 316L piping (nominal wall thickness 3.2 mm or 1/8 in.) approximately 1 and 4 months, respectively, after the hydrotest. Internal inspection showed pits in and adjacent to welds under reddish brown deposits. Tank manways were uncovered, and similar conditions were found. As shown in Fig. 24, moundlike deposits were strung out along weld seams in the tank bottoms.

Figure 25 shows a closeup view of a typical deposit still wet with test water. The brilliantly colored deposit was slimy and gelatinous in appearance and to the touch, and it measured 75 to 100 mm (3 to 4 in.) in width. At one point during the investigation, a similar deposit on a weld that was covered with about 150 mm (6 in.) of water was thoroughly dispersed by hand. Twenty-four hours later, the deposit had returned in somewhat diminished form at exactly the same location.

Figure 26 shows a nearly dry deposit. After wiping the deposit clean, a dark ring-shape stain outlining the deposit over the weld was noted (Fig. 27). There was, however, no evidence of pitting or other corrosion, even after light sanding with emery. Finally, probing with an icepick revealed a large, deep pit at the edge of the weld as shown in Fig. 28. Figure 29, a radiograph of this weld seam, shows the large pit that nearly consumed the entire width of the weld bead, as well as several smaller pits. A cross section through a large pit in a 9.5 mm (3/8 in.) thick type 304L tank bottom is shown in Fig. 30.

The characteristics of this mode of corrosion were a tiny mouth at the surface and a thin shell of metal covering a bottle-shape pit that had consumed both weld and base metal. There was no evidence of intergranular or interdendritic attack of base or weld metal. However, pitted welds in a type 316L tank showed preferential attack of the δ-ferrite stringers (Fig. 31)

This type 316L tank was left full of hydrotest water for 1 month before draining. The bottom showed severe pitting under the typical reddish-brown deposits along welds. In addition, vertical rust-colored streaks (Fig. 32) were found above and below the sidewall horizontal welds, with deep pits at the edges of the welds associated with each streak (Fig. 33)

Analyses of the well water and the deposits showed high counts of iron bacteria (*Gallionella*) and iron-manganese bacteria (*Siderocapsa*). Both sulfate-reducing and sulfur-

Table 4 MIC scenarios that may play a role in the corrosion of weldments in stainless steel

MIC by	Mechanism	Indicators
Manganese oxidizers	Ennoblement of stainless steel potential due to MnO_2	Elevated manganese-oxidizing organisms, manganese, and possibly chloride in deposits
SRB primary	Sulfides, SRB facilitate chloride attack in anaerobic systems	Dark-colored corrosion products with iron sulfide, chloride, and a high ratio of Fe^{2+}/Fe^{3+}; near-neutral pH
SRB secondary oxidation	Pitting stabilized by thiosulfate formed by oxidation of sulfides	Cyclic anaerobic, aerobic conditions; surface of corrosion products in pit oxidized red, orange, or brown
Iron-oxidizing bacteria	Decrease of pH by oxidation of Fe^{2+} to Fe^{3+} in pits	Red/orange corrosion products rich in Fe^{3+}; iron-oxidizing organisms such as *Gallionella;* pH acidic

Source: Ref 15–17

oxidizing bacteria were absent. The deposits also contained large amounts (thousands of parts per million) of iron, manganese, and chlorides.

As indicated, nearly all biodeposits and pits were found at the edges of, or very close to, weld seams. It is possible that the bacteria in stagnant well water were attracted by an electrochemical phenomenon or surface imperfections (oxide or slag inclusions, porosity, ripples, and so on) typically associated with welds. A sequence of events for the corrosion mechanism in this case might be:

1. Attraction and colonization of iron and iron-manganese bacteria at welds
2. Microbiological concentration of iron and manganese compounds, primarily chlorides, because Cl^- was the predominant anion in the well water
3. Microbiological oxidation to the corresponding ferric and manganic chlorides, which either singly or in combination are severe pitting corrodents of austenitic stainless steel
4. Penetration of the protective oxide films on the stainless steel surfaces that were already weakened by oxygen depletion under the biodeposits.

All affected piping was replaced before the new facilities were placed in service. The tanks were repaired by sandblasting to uncover all pits, grinding out each pit to sound metal, and then welding with the appropriate stainless steel filler metal. Piping and tanks subsequently placed in corrosive service suffered very few leaks, indicating that the inspection, replacement, and repair program was effective.

Other Factors Influencing Corrosion of Weldments

Sigma Precipitation in HAZs. When the higher molybdenum alloys such as 904L, AL-6XN, and 254SMO were first developed, one of the anticipated corrosion problems was attack of single-phase precipitates in weld HAZs. This form of attack has subsequently proved to be either superficial or nonexistent in most applications, probably because the compositions of the

Fig. 24 Moundlike microbiological deposits along a weld seam in the bottom of a type 304L stainless steel tank after several months of exposure to well water at ambient temperature. Source: Ref 18

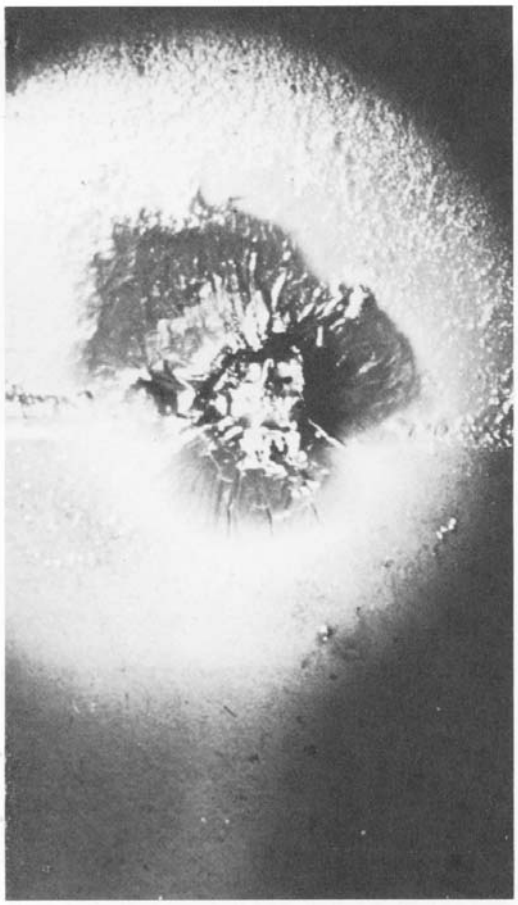

Fig. 25 Close-up of a wet deposit as shown in Fig. 24. Source: Ref 18

alloys have been skillfully formulated to minimize phase-related hot-rolling problems.

More recently, nitrogen has been added to molybdenum-bearing austenitic stainless steels to retard the precipitation of chromium- and molybdenum-rich intermetallic compounds (σ or χ phases). The incubation time for intermetallic precipitation reactions in Fe-Cr-Ni-Mo stainless alloys is significantly increased by raising the alloy nitrogen content. This has allowed the commercial production of thick plate sections that can be fabricated by multipass welding operations. In addition to suppressing the formation of deleterious phases, nitrogen, in cooperation with chromium and molybdenum, has a beneficial effect on localized corrosion resistance in oxidising acid-chloride solutions.

Corrosion Associated with Postweld Cleaning. Postweld cleaning is often specified to remove the heat-tinted metal formed during welding. Recent work has shown that cleaning

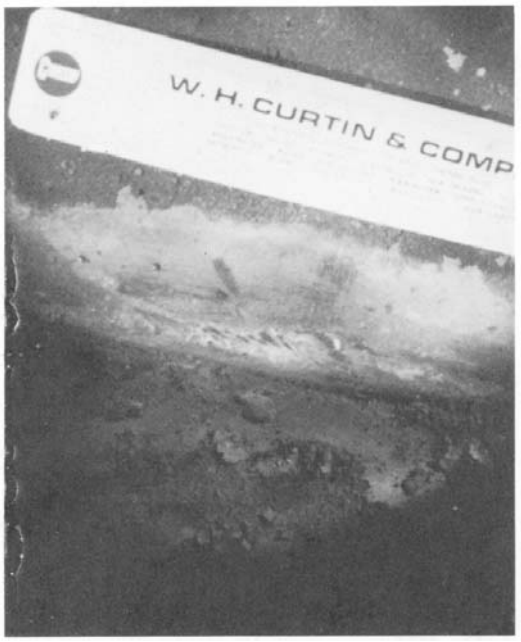

Fig. 27 Ring-shape stain left around a weld after removal of the type of deposit shown in Fig. 24 to 26. Source: Ref 18

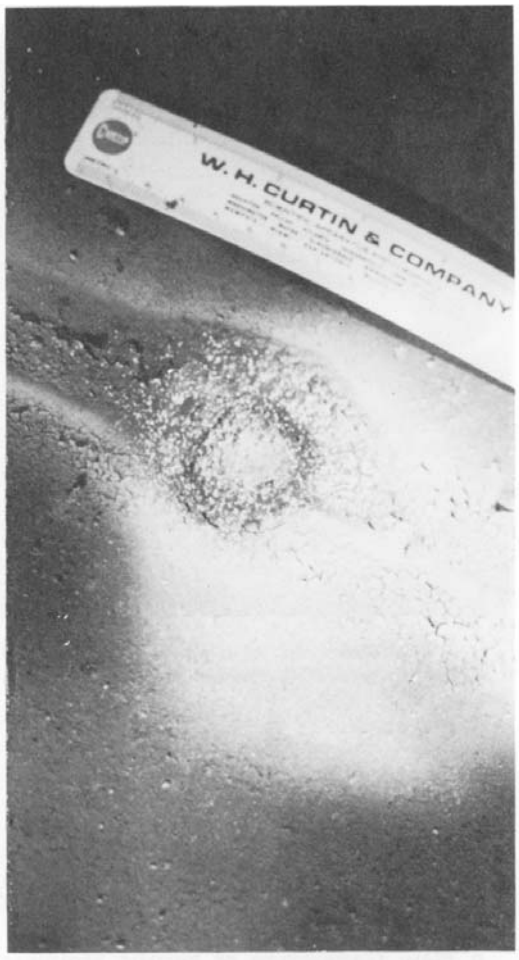

Fig. 26 Close-up of a dry deposit. See also Fig. 24 and 25. Source: Ref 18

Fig. 28 Large pit (center) at the edge of the weld shown in Fig. 27. The pit was revealed by probing with an ice pick. Source: Ref 18

by stainless steel wire brushing can lower the corrosion resistance of a stainless steel weldment (Fig. 34). This is a particular problem in applications in which the base metal has marginal corrosion resistance. The effect may be caused by inadequate heat-tint removal, by the use of lower-alloy stainless steel brushes such as type 410 or 304, or by the redeposition of abraded metal or oxides.

Any cleaning method may be impaired by contamination or by lack of control. Results of a study in bleach plants suggest that pickling and glass bead blasting can be more effective than

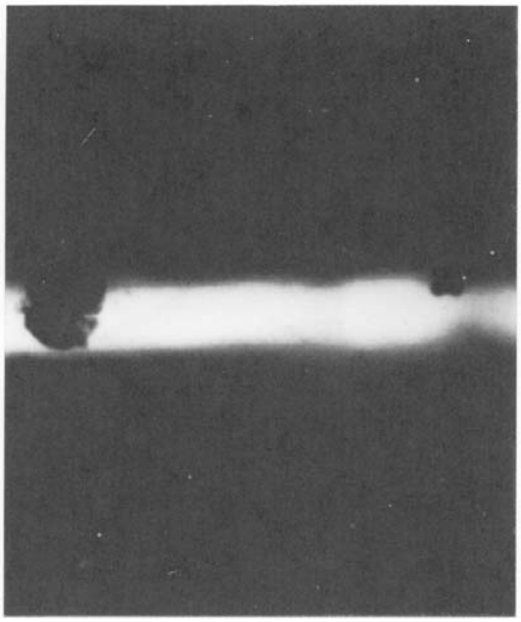

Fig. 29 Radiograph of a pitted weld seam in a type 304L stainless steel tank bottom. Source: Ref 18

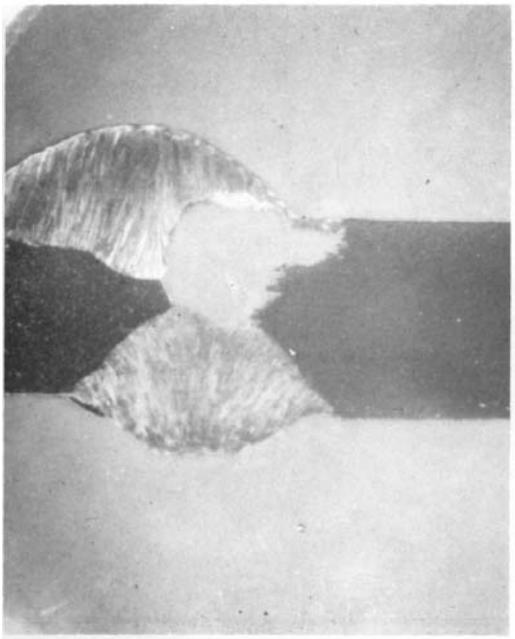

Fig. 30 Cross section through a pitted weld seam from a type 304L tank showing a typical subsurface cavity. Source: Ref 18

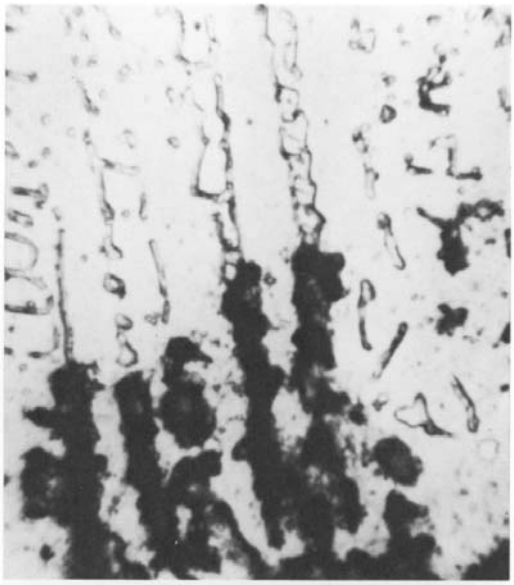

Fig. 31 Micrograph showing preferential attack of δ-ferrite stringers in type 316L stainless steel weld metal. 250×. Source: Ref 18

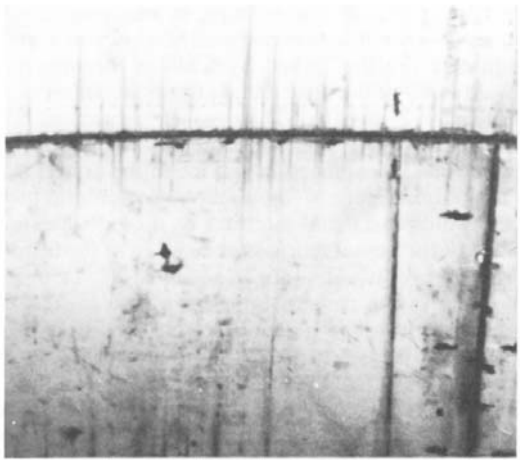

Fig. 32 Rust-colored streaks transverse to horizontal weld seams in the sidewall of a type 316L stainless steel tank. Source: Ref 18

stainless wire brushing and that brushing is more difficult to perform effectively in this case.

Corrosion Associated with Weld Backing Rings. Backing rings are sometimes used when welding pipe. In corrosion applications, it is important that the backing ring insert be consumed during the welding process to avoid a crevice. In the example shown in Fig. 35 the wrong type of backing ring was used, which left a crevice after welding. The sample was taken from a leaking brine cooling coil used in the production of nitroglycerin. The cooling coils contained calcium chloride ($CaCl_2$) brine inhibited with chromates. Coils were made by butt welding sections of seamless type 304L stainless steel tubing. This failure was unusual because several forms of corrosion had been observed.

A metallographic examination of a small trepanned sample revealed:

- *Microstructure:* The base metal and weld metal microstructures appeared satisfactory.
- *Pitting:* Irregular corrosion pits were seen on the inside tube surface at crevices formed by the tube and the backing ring adjacent to the tube butt weld. The deepest pits extended 0.1 to 0.2 mm (4 to 8 mils) into the 1.65 mm (0.065 in.) thick tube wall.
- *Cracking:* There were numerous brittle, branching transgranular cracks originating on the inside surface at the crevice under the backing ring.
- *Preferential weld corrosion:* Extensive preferential corrosion of the ferrite phase (vermicular morphology) in the tube weld had occurred and penetrated almost completely through the tube wall. Corrosion originated on the outside surface of the tube.

It was concluded that the preferential weld corrosion from the process side was the most probable cause of the actual leak in the nitrator coil. The preferential corrosion of ferrite in nitrating

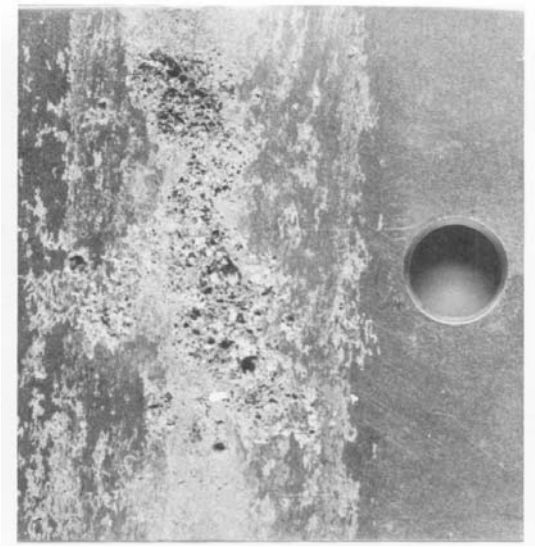

Fig. 34 Pitting corrosion associated with stainless steel wire brush cleaning on the back of a type 316L stainless steel test coupon after bleach plant exposure. Source: Ref 4

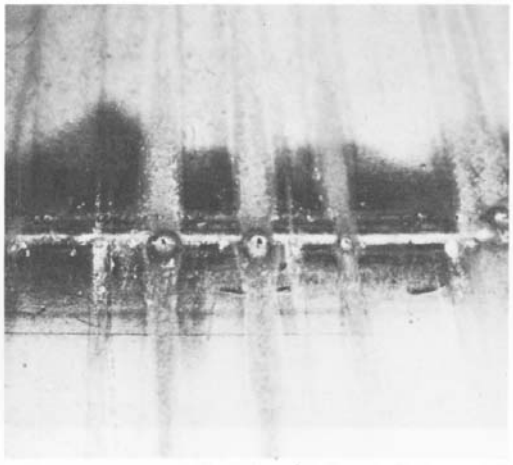

Fig. 33 Close-up of the rust-colored streaks shown in Fig. 32. Source: Ref 18

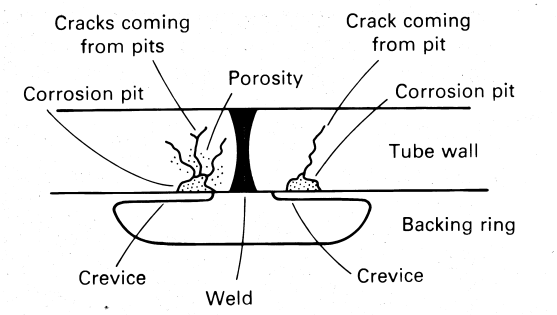

Fig. 35 Stainless steel nitrator cooling coil weld joint. Failure was caused by improper design of a backing ring that was not consumed during welding and left a crevice. Source: Ref 19

mixtures of HNO_3 and H_2SO_4 is well known. Whether this corrosion causes a serious problem depends on the amount of ferrite present in the weld. If the amount of ferrite is small and the particles are not interconnected, the overall corrosion rate is not much higher than that of a completely austenitic material. If the particles are interconnected, as in this case, there is a path for fairly rapid corrosion through the weld, causing failure to occur.

To minimize this problem, two possible solutions were considered. The first was to weld the coils with a filler metal that produces a fully austenitic deposit, and the second was to solution anneal at 1065 °C (1950 °F) after welding to dissolve most of the ferrite. It would also help to select stainless steel base metal by composition (e.g., high nickel, low chromium content) to minimize the production of ferrite during welding. Welding with a fully austenitic filler metal was considered to be the best approach.

Cracking on the brine side was caused by chloride SCC. The cracking probably did not happen during operation at 15 °C (60 °F) or lower. It is thought that the cracking most likely occurred while the coil was being decontaminated at 205 to 260 °C (400 to 500 °F) in preparation for weld repairing of the leak. Brine trapped in the crevice between the tube wall and the backing ring was boiled to dryness. Under these conditions, SCC would occur in a short time.

There probably were stress cracks behind all of the backing rings. Because the future life of this coil was questionable, a new coil was recommended.

The pitting corrosion caused by the brine was not considered to be as serious as it first appeared. If this had been the only corrosion (and the sample had been representative of the coil), the coil would not have failed for a considerable length of time. The decontamination process, which evaporated the trapped brine, produced some of the observed corrosion and made the pitting appear worse than it was before decontamination.

Because chromates are anodic inhibitors, they can also greatly increase the corrosion (usually by pitting) in the system if insufficient quantities are used. This might have occurred in the crevices in the nitrator coil butt welds, regardless of the bulk solution concentration. The best solution to this problem was to eliminate the crevices, that is, not to use backing rings.

Effects of GTA Weld Shielding Gas Composition. The chromium in a stainless steel has a strong chemical affinity for oxygen and carbon. Weld pools formed by electric arc processes must be shielded from the atmosphere to prevent slag formation and oxidation (Fig. 36), to maintain a stable arc, and to reduce contamination of the molten metal by the weld environment. Argon or argon plus helium gas

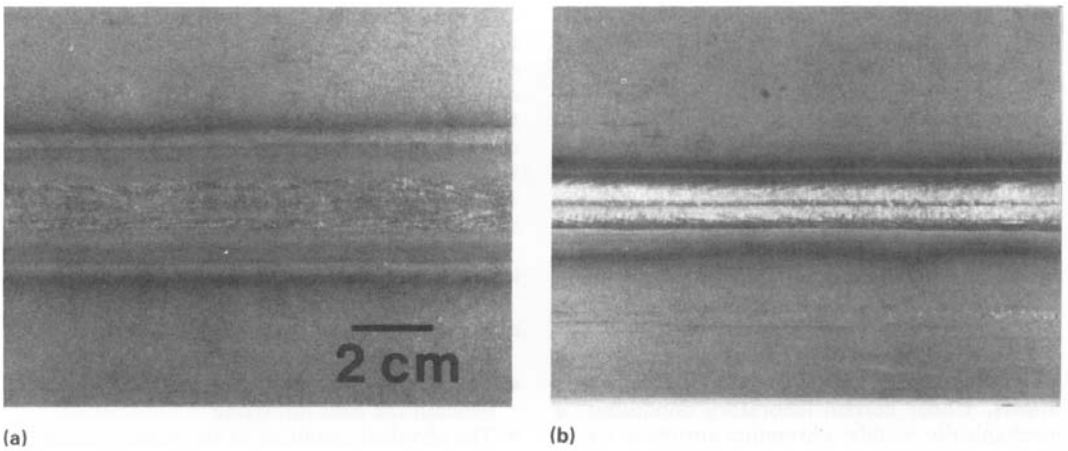

Fig. 36 Examples of (a) properly shielded and (b) poorly shielded autogenous gas tungsten arc welds in type 304 stainless steel strip. Source: Ref 19

mixtures are commonly used in GTA welding processes to create a barrier between the solidifying weld and the atmosphere. In other cases, nitrogen is commonly used as a backing gas to protect the backside of the root pass.

The composition of a shielding gas can be modified to improve the microstructure and properties of GTA welds in austenitic stainless steels. More specifically, the use of argon mixed with small volumes of nitrogen (10 vol% N_2 or less) in a GTA welding process enhances the corrosion resistance of Fe-Cr-Ni-Mo-N stainless alloys in oxidizing acid chloride solutions (Fig. 37). In certain nonoxidizing solutions, argon-nitrogen shielding gas reduces the δ-ferrite content of weld metal and influences weld metal solidification behavior.

The nitrogen content of weld metal increases with the partial pressure of nitrogen in the GTA weld shielding gas. The increase in weld metal nitrogen content is greater when nitrogen is mixed with an oxidizing gas, such as carbon dioxide (CO_2), than with either a reducing (hydrogen) or a neutral (argon) gas. Porosity and concavity are observed in austenitic stainless steel weld metals when more than 10 vol% N is added to an argon shielding gas. Although solid-solution additions of nitrogen are not detrimental to the SCC resistance of unwelded molybdenum containing austenitic stainless steels, an increased weld metal nitrogen content tends to increase susceptibility to SCC.

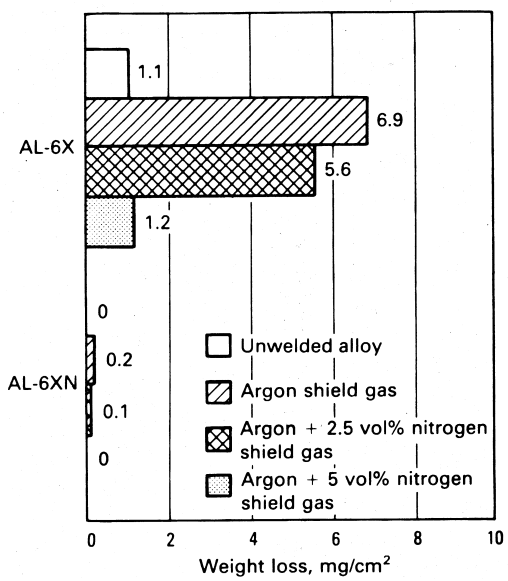

Fig. 37 Effect of gas tungsten arc weld shielding gas composition on the corrosion resistance of two austenitic stainless steels. Welded strip samples were tested according to ASTM G 48; test temperature was 35 °C (95 °F). Source: Ref 19

Effects of Heat-Tint Oxides on Corrosion-Resistance. Under certain laboratory conditions, a mechanically stable chromium-enriched oxide layer can be formed on a stainless steel surface that enhances corrosion resistance. In contrast, the conditions created by arc-welding operations produce a scale composed of elements that have been selectively oxidized from the base metal. The region near the surface of an oxidized stainless steel is depleted of one or more of the elements that have reacted with the surrounding atmosphere to form the scale. The rate of oxidation for a stainless steel, and consequently the degree of depletion in the base metal, are independent of the alloy composition. They are controlled by diffusion through the oxide.

The oxidized, or heat-tinted, surface of a welded stainless steel consists of a heterogeneous oxide composed primarily of iron and chromium above a chromium-depleted layer of base metal. The properties of such a surface depend on:

- The time and temperature of the thermal exposure
- The composition of the atmosphere in contact with the hot metal surface
- The chemical composition of the base metal beneath the heat-tint oxide
- The physical condition of the surface (contamination, roughness, thermomechanical history) prior to heat tinting
- The adherence of the heat-tint oxide to the base metal

The defects, internal stresses, and composition of the heat-tint oxide make it a poor barrier to any corrosive media that might initiate localized corrosion in the chromium-depleted layer of base metal.

The severity of localized corrosion at heat-tinted regions exposed to oxidizing chloride solutions is directly related to the temperature of the hot metal surface during welding. A heat-tint oxide on an austenitic stainless steel exposed in air first becomes obvious at approximately 400 °C (750 °F). As the surface temper-

ature is increased, differently colored oxides develop that appear to be superimposed on the oxides formed at lower temperatures. Table 5 shows the relationship between welding conditions and heat-tint color (Ref 20). Dark blue heat-tint oxides are the most susceptible to localized corrosion. Gas-shielded surfaces do not form the same distinctly colored oxides as surfaces exposed to air during welding, but gas-shielded surfaces can also be susceptible to preferential corrosion.

Whether a weld heat tint should be removed prior to service depends on the corrosion behavior of the given alloy when exposed to the particular environment in question. Preferential corrosion at heat-tinted regions is most likely to occur on an alloy that performs near the limit of its corrosion resistance in service, but certain solutions do not affect heat-tinted regions. Even when heat-tinted regions are suspected of being susceptible to accelerated corrosion in a particular environment, the following factors should be considered:

- The rate at which pits, once initiated in the chromium-depleted surface layer, will propagate through sound base metal
- The hazards associated with the penetration of a process unit due to localized corrosion
- The cost and effectiveness of an operation intended to repair a heat-tinted stainless steel surface

The corrosion resistance of heat-tinted regions can be restored in three stages. First, the heat-tint oxide and chromium-depleted layer are removed by grinding or wire brushing. Second, the abraded surface is cleaned with an acid solution or a pickling paste (a mixture of HNO_3 and HF suspended in an inert paste or gel) to remove any surface contamination and to promote the reformation of a passive film. Third, after a sufficient contact time, the acid cleaning solution or pickling paste is thoroughly rinsed with water, preferably demineralized or with a low chloride ion (Cl^-) content.

Grinding or wire brushing might not be sufficient to repair a heat-tinted region. Such abrading operations may only smear the heat-tint oxide and embed the residual scale into the surface, expose the chromium-depleted layer beneath the heat-tint oxide, and contaminate the surface with ferrous particles that were picked up by the grinding wheel or wire brush. A stainless steel surface should never be abraded with a wheel or brush that has been used on a carbon or low-alloy steel; wire brushes with bristles that are not made of a stainless steel of similar composition should also be avoided. Conversely, attempting to repair a heat-tinted region with only a pickling paste or acid solution can stain or even corrode the base metal if the solution is overly aggressive or is allowed to contact the surface for an extended time. If the acid is too weak, a chromium-depleted scale residue could remain on a surface, even if the chromium-depleted layer were completely removed by a grinding operation. Mechanically ground surfaces generally have inferior corrosion resistance compared to properly acid-pickled surfaces.

Laboratory investigations using polarization techniques have shown that the base metal is passive and resistant to corrosion when clean and free of heat tint-scale, as is the normal behavior for austenitic stainless steels (Fig. 38).

Table 5 Welding conditions and corrosion resistance of heat-tinted UNS S31726 stainless steel plate

Welding conditions(a)				Corrosion test results(b)		
Heat input				Maximum pit depth		
kJ/mm	kJ/in.	Welding current, A	Centerline heat-tint color	mm	mils	Number of pits on heat-tinted surface
0.3	7.525	50	None	0.1	4	2
0.59	15.050	100	Straw	0.7	28	10
0.89	22.576	150	Rose	0.8	31	50
1.19	30.101	200	Blue	0.7	28	>70
1.48	37.626	250	White	0.9	35	>70

(a) Single-pass autogenous bead-on-plate GTA welds were made to heat tint the root surface of 6.4 mm ($^1/_4$ in.) thick plate samples. (b) Duplicate coupons, each with one 25 × 51 mm (1 × 2 in.) heat-tinted surface, were exposed to 10% $FeCl_3$ solutions at 50 °C (120 °F). The weld face and edges of each coupon were covered with a protective coating.

The vertical section of the dashed curve in Fig. 38 shows the normal passive range typical of stainless steels. The solid curve for the HAZ as-welded (i.e., with the heat-tint scale intact and a chromium-reduced layer just underneath) has no significant vertical section, or no significant passive range.

Unmixed Zones. All methods of welding stainless steel with a filler metal produce a weld fusion boundary consisting of base metal that has been melted but not mechanically mixed with filler metal and a partially melted zone in the base metal. The weld fusion boundary lies between a weld composite consisting of filler metal diluted by base metal and an HAZ in the base metal (see Fig. 1 in Chapter 1). The width of the unmixed zone depends on the local thermal conditions along the weld fusion line. For a GTA welding process, the zone is narrowest at the weld face and widest near the middle of the weld thickness.

An unmixed zone has the composition of base metal but the microstructure of an autogenous weld. The microsegregation and precipitation phenomena characteristic of autogenous weldments decrease the corrosion resistance of an unmixed zone relative to the parent metal. Unmixed zones bordering welds made from overalloyed filler metals can be preferentially attacked when exposed on the weldment surface (Fig. 39) The potential for preferential attack of unmixed zones can be reduced by minimizing the heat input to the weld and/or by flowing molten filler metal over the surface of the unmixed zone to form a barrier to the service environment. Care must be taken in this latter operation to avoid cold laps and lack-of-fusion defects. In both cases, preferential attack is avoided as long as the surface of the unmixed zone lies beneath the exposed surface of the weldment.

Molybdenum Segregation. The segregation of molybdenum in 6% Mo superaustenitic alloys during weld solidification has been reported to reduce corrosion resistance (Ref 22), particularly in severe pitting environments. The cell or dendrite cores in these alloys may exhibit

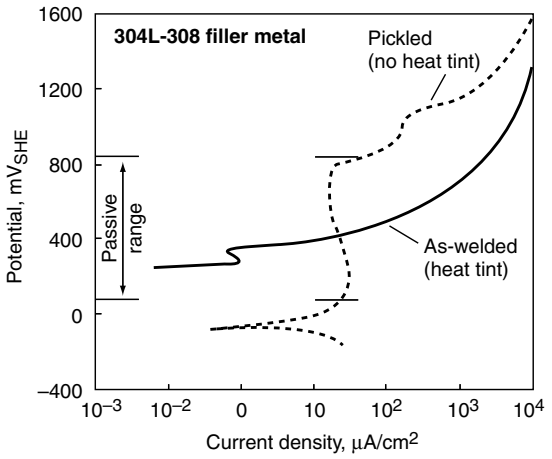

Fig. 38 Polarization curves for type 304L in the as-welded and pickled conditions. Source: Ref 21

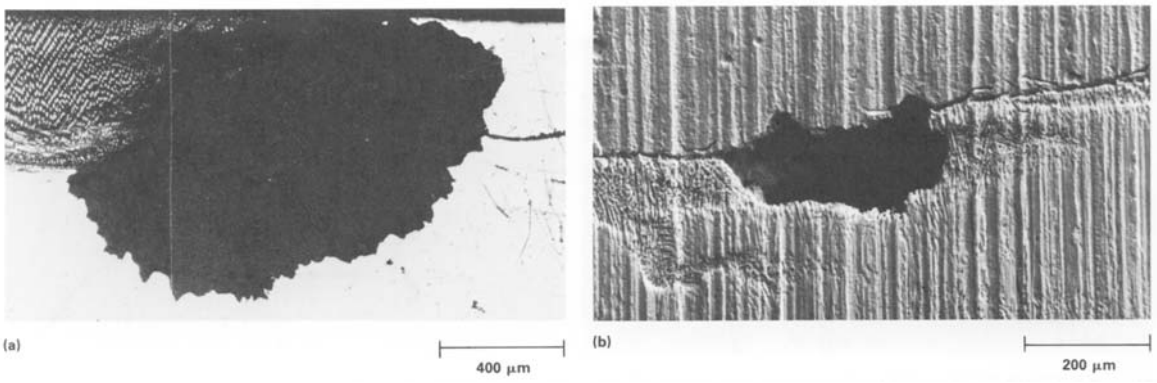

Fig. 39 (a) Optical and (b) scanning electron micrographs of pitting in the unmixed zone of Fe-Cr-Ni-Mo stainless steel plates that were gas tungsten arc welded with an overalloyed filler metal. The unmixed zones were preferentially attacked in an oxidizing acid chloride solution at elevated temperatures.

molybdenum contents as low as 4.2 wt%, resulting in localized pitting attack at these sites (Fig. 40). As a result, autogenous welding or the use of matching filler materials is normally avoided when severe service environments are anticipated. The use of molybdenum-containing, nickel-base filler materials, such as alloy 625 (AWS ERNi-CrMo-3), alloy C-276 (AWS ER NiCrMo-4), or alloy C-22 (AWS ERNiCrMo-10), is often recommended in order to avoid pitting. As discussed in the previous section, precautions must be taken to prevent the formation of an unmixed zone adjacent to these overalloyed weld metals (Fig. 41) because this region may have the same susceptibility to corrosive attack as autogenous weld metal does.

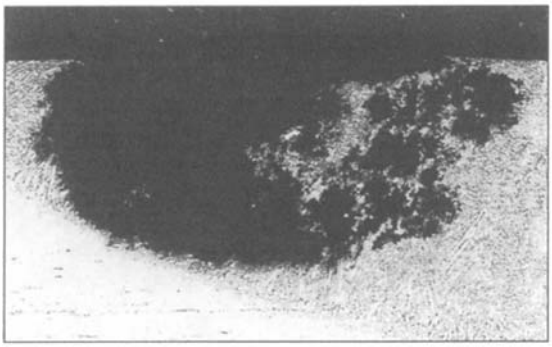

Fig. 40 Pitting of a superaustenitic stainless steel weld metal associated with molybdenum depletion during solidification. Source: Ref 23

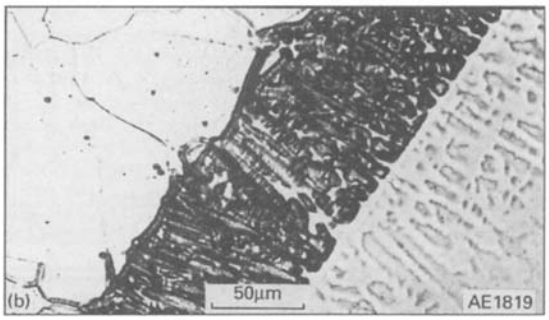

Fig. 41 Unmixed zone that formed at the fusion boundary between a superaustenitic stainless steel welded with a nickel-base filler metal. Source: Ref 23

ACKNOWLEDGMENTS

This chapter was adapted from:

- J.A. Brooks and J.C. Lippold, Selection of Wrought Austenitic Stainless Steels, *Welding, Brazing, and Soldering,* Vol 6, *ASM Handbook,* 1993, p 456–470
- Corrosion of Stainless Steel Weldments, *Corrosion: Fundamentals, Testing, and Protection,* Vol 13A, *ASM Handbook,* ASM International, 2003, p 301–316
- J.D. Fritz, Effect of Metallurgical Variables on the Corrosion of Stainless Steels, *Corrosion: Fundamentals Testing, and Protection,* Vol 13A, *ASM Handbook,* ASM International, 2003, p 266–274
- T.R. Jack, Biological Corrosion Failures, *Failure Analysis and Prevention,* Vol 11, *ASM Handbook,* ASM International, 2002, p 881–898

REFERENCES

1. R.F. Steigerwald, *Metall. Trans.,* Vol 5, 1974, p 2265–2269
2. W.F. Savage, *Weld. Des. Eng.,* Dec 1969
3. M.A. Streicher, Theory and Application of Evaluation Tests For Detecting Susceptibility to Intergranular Attack in Stainless Steels and Related Alloys—Problems and Opportunities, in *Intergranular Corrosion of Stainless Alloys,* STP 656, American Society for Testing and Materials, 1978, p 70
4. A. Garner, How Stainless Steel Welds Corrode, *Met, Prog.,* Vol 127 (No 5), April 1985, p 31
5. M.C. Juhas and B.E. Wilde, *Corrosion,* Vol 46, 1990, p 812–822
6. A. Dravnieks and C.H. Samans, *Proc. API,* Vol 37 (No. 3), 1957, p 100
7. R.C. Scarberry, S.C. Pearman, and J.R. Crum, *Corrosion,* Vol 32, 1976, p 401-406
8. K.F. Krysiak, "Cause and Prevention of Unusual Failures of Materials," Paper 19, presented at Corrosion/83, Anaheim, CA, National Association of Corrosion Engineers, April 1983
9. Y. Chung, H.J. Mantle, and G.E. Lakso, *Proc. 1995 Int. Conf., on Microbially*

Influenced Corrosion, P. Angell, S.W. Boronstein, R.A. Buchanan, S.C. Dexter, N.J.E. Dowling, B.J. Little, C.D. Lundin, M.B. McNeil, D.H. Pope, R.E. Tatnall, D.C. White, and H.G. Ziegenfuss, Ed., May 8–10, 1995 (New Orleans), National Association of Corrosion Engineers International, 1995, p 13-1–13-13

10. A.A. Stein, "Metallurgical Factors Affecting the Resistance of 300 Series Stainless Steels to Microbiologically Influenced Corrosion," Paper 107, presented at Corrosion '91, National Association of Corrosion Engineers, 1991
11. N.J.E. Dowling, C. Lundin, D. Sachs, J.A. Bullen, and D.C. White, Principles of the Selection of Effective and Economic Corrosion-Resistant Alloys in Contact with Biologically Active Environments, *Proc. Mat. Res. Soc. Symp.,* Vol 294, Materials Research Society, 1993, P 361–367
12. T.A. Petersen and S.R. Taylor, The Effects of Sulfate Reducing Bacteria on Stainless Steel and Ni-Cr-Mo Alloy Weldments, *Proc. 1995 Int. Conf. on Microbially Influenced Corrosion,* P. Angell, S.W. Boronstein, R.A. Buchanan, S.C. Dexter, N.J.E. Dowling, B.J. Little, C.D. Lundin, M.B. McNeil, D.H. Pope, R.E. Tatnall, D.C. White, and H.G. Ziegenfuss, Ed., May 8–10, 1995 (New Orleans), National Association of Corrosion Engineers, 1995, p 56/1–56/20
13. M.H.W. Renner, "Corrosion Engineering Aspects Regarding MIC Related Failures on Stainless Steel," Paper 285, presented at Corrosion '98, National Association of Corrosion Engineers International, 1998
14. P. Gümpel, K. Neumann, T. Volimer, and W. Racky, Effect of Surface Conditions on Microbially Influenced Corrosion of Stainless Steels, *Proc. 1995 Int. Conf. on Microbially Influenced Corrosion,* P. Angell, S. W. Boronstein, R.A. Buchanan, S.C. Dexter, N.J.E. Dowling, B.J. Little, C.D. Lundin, M.B. McNeil, D.H. Pope, R.E. Tatnall, D.C White, and H.G. Ziegenfuss, Ed., May 8–10, 1995 (New Orleans), National Association of Corrosion Engineers International, 1995, p 26/1–26/10
15. S.W. Boronstein and P.B. Lindsay, "Planning and Conducting Microbiologically Influenced Corrosion Failure Analysis," Paper 381, presented at Corrosion '87, National Association of Corrosion Engineers, 1987
16. C. Zhigang, P. Gumpel, and M. Kaesser, Microbiologically Influenced Corrosion of Weld on Stainless Steel 304L, *Chin. J. Mech. Eng. (Engl. Ed),* Vol 11 (No. 2) 1998, p 159–164
17. F. Kajiyama, Role of Sulfate-Reducing Bacteria in Corrosion of Type 316 Stainless Steel, *Corros. Eng.,* Vol 46, 1997, p 377–387
18. G. Kobrin, Corrosion by Microbiological Organisms in Natural Waters, *Mater. Perform.,* Vol 15 (No. 7), 1976
19. J.R. Kearns and H.E. Deverell, "The Use of Nitrogen to Improve Fe-Cr-Ni-Mo Alloys for the Chemical Process Industries," Paper 188, presented at Corrosion 86, Houston, TX, National Association of Corrosion Engineers, March 1986
20. J.R. Kearns, "The Corrosion of Heat Tinted Austenitic Stainless Alloys," Paper 50, presented at Corrosion/85, Boston, MA, National Association of Corrosion Engineers, March 1985
21. A.H. Tuthill and R.E. Avery, Heat Tints on Stainless Steels Can Cause Corrosion Problems, Nickel Development Institute Reprint Series No. 14 050 (reprinted from *Materials Performance,* February 1999)
22. T. G. Gooch, *Proc. Corrosion '92* (Nashville), Paper 296, NACE, 1992
23. J.C. Lippold, Recent Developments in the Understanding of Stainless Steel Welding Metallurgy, *Sixth International Trends in Welding Research Conf. Proc.,* April 15–19, 2002, Pine Mountain, GA, ASM International, 2003, p 1–10

Corrosion of Weldments
J.R. Davis, editor, p 77-97
DOI:10.1361/corw2006p077

CHAPTER 4

Corrosion of Ferritic Stainless Steel Weldments

FERRITIC STAINLESS STEELS are essentially iron-chromium alloys with body-centered cubic (bcc) crystal structures. Chromium content is usually in the range of 11 to 30%. Some grades may contain molybdenum, nickel, aluminum, titanium, and niobium to confer particular characteristics. For example, type 405, containing nominally 12% Cr, is made with lower carbon and a small aluminum addition of 0.20% to restrict the formation of austenite at high temperature so that hardening is reduced during welding. In addition, sulfur or selenium are added to some alloys to improve machinability.

The ferritic alloys are ferromagnetic. They have good ductility and formability, but high-temperature strengths are relatively poor compared to those of the austenitic grades. Toughness may be somewhat limited at low temperatures and in heavy sections. Unlike the martensitic stainless steels, the ferritic stainless steels cannot be strengthened by heat treatment. Also, because the strain-hardening rates of ferrite are relatively low and cold work significantly lowers the ductility, the ferritic stainless steels are not often strengthened by cold work.

The primary advantage of the ferritic stainless steels, and in particular the high-chromium, high-molybdenum grades, is their excellent stress-corrosion cracking (SCC) resistance and good resistance to pitting and crevice corrosion in chloride environments. Additional information on corrosion resistance can be found in the section "Properties" later in this chapter.

Grade Classifications

The ferritic stainless steels can be classified in three groups. These include Group I (first generation) alloys, which are comprised of standard SAE ferritic grades; Group II (second generation) alloys, which are modified versions of Group I alloys; and Group III alloys, which contain very low interstitial element contents or stabilizing elements for improved corrosion resistance and weldability. Tables 1 through 4 list the compositions of ferritic stainless steels. Figure 1 shows the relationships among the various standard grades.

Group I Alloys. Ferritic stainless steels of the 400-series Group I variety listed in Table 1 have been available for many years and are used primarily for their resistance to corrosion and scaling at elevated temperatures. As indicated in Fig. 1, the general-purpose alloy in this group is type 430 (UNS S43000). Free-machining variations of this grade containing phosphorus, sulfur, or selenium are also available.

While Group I ferritics have useful properties in the wrought condition, welding is known to reduce toughness, ductility, and corrosion resistance because of grain coarsening and formation of martensite (the exception is the lower carbon content type 405). For these reasons, the application of the 400-series Group I ferritic stainless steels is not as extensive as it might otherwise be, compared with the 300-series austenitic stainless steels.

Group II Alloys. To overcome some of the difficulties and to improve weldability, several of the standard Group I ferritics have been modified. These Group II ferritic stainless steels contain lower levels of carbon and chromium, along with additions of ferrite stabilizers (see Table 2). Applications of these alloys involve exposure to high temperatures, such as for quenching tanks and annealing boxes, and also tanks for agriculture sprays, transformer cases, and automotive applications.

The prototype of the Group II alloys is type 409 (UNS S40900), which typically contains 0.04% C, 11% Cr, and 0.5% Ti. Largely because of its consumption in the automotive industry, the current production of type 409 in

Table 1 Nominal chemical composition of representative Group I standard-grade 400-series ferritic stainless steels

UNS No.	Type	Composition(a), wt%			
		C	Cr	Mo	Other
S40500(b)	405(b)	0.08	11.5–14.5	. . .	0.10-0.30Al
S42900	429	0.12	14.0–16.0	. . .	. . .
S43000	430	0.12	16.0–18.0	. . .	. . .
S43020	430F	0.12	16.0–18.0	0.6	0.06 P; 0.15 min S
S43023	430FSe	0.12	16.0–18.0	. . .	0.15 min Se
S43400	434	0.12	16.0–18.0	0.75–1.25	. . .
S43600	436	0.12	16.0–18.0	0.75–1.25	Nb+Ta = 5 x %C min
S44200	442	0.20	18.0–23.0	. . .	. . .
S44600	446	0.20	23.0–27.0	. . .	. . .

(a) Single values are maximum values unless otherwise indicated. (b) Although originally classified as a standard SAE-AISI grade (see Fig. 1), type 405 can also be classified as a Group II alloy due to its lower carbon content

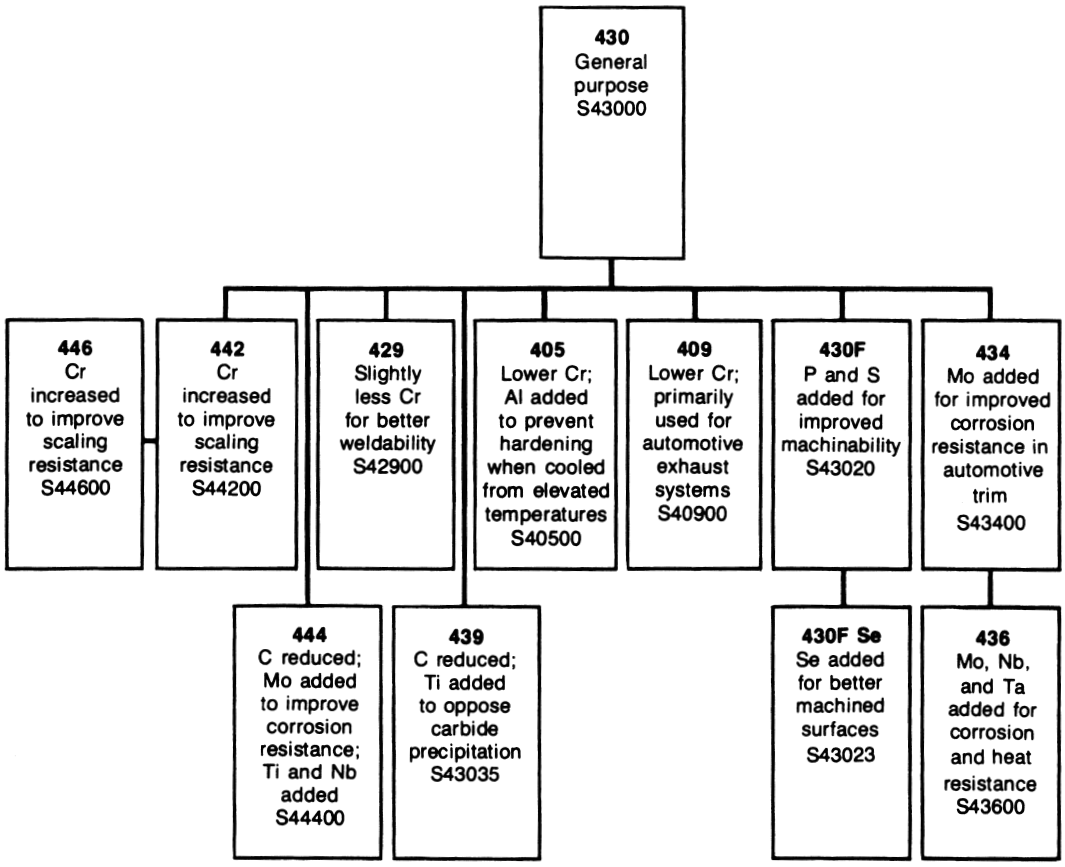

Fig. 1 Family relationships for standard SAE ferritic stainless steels

the United States almost equals the tonnage of the most popular stainless steel, the austenitic type 304 (UNS S30400).

Group III Alloys. In the late 1960s and early 1970s, researchers recognized that highly alloyed (higher chromium and molybdenum content) ferritic stainless steels possessed a desirable combination of resistance to general corrosion, pitting, and SCC. These properties made the third-generation "superferritic" alloys attractive alternatives to the 300-series austenitics that are commonly plagued by failure as a result of chloride SCC. It was found that by controlling the interstitial element content (carbon, oxygen, and nitrogen) of these alloys by either ultrahigh purity processing or by stabilization, the formation of martensite could be eliminated and welds would be corrosion resistant, tough, and ductile in the as-welded condition. To achieve these results, electron-beam vacuum refining, argon oxygen decarburization (AOD), vacuum oxygen decarburization (VOD), and vacuum induction melting (VIM) steelmaking processes were used.

The Group III alloys can be further divided into intermediate-purity alloys (Table 3) and ultrahigh-purity alloys (Table 4). When the (C + N) interstitial element content exceeds 150 ppm (but is less than 800 ppm), ferritic alloys are considered to be of intermediate purity. These alloys, which are produced by AOD processing and the addition of stabilizers (titanium and/or niobium), are limited in metal thickness to a maximum of about 3 mm (1/8 in.) where toughness is adequate. Because these steels have higher carbon and nitrogen contents, their ductility and toughness are inferior to those of the ultrahigh-purity alloys. The ultrahigh-purity Group III ferritics have an interstitial element (C + N) content of less than 150 ppm. The VIM grades exhibit carbon levels in the 30 to 50 ppm range. Plate is available up to 13 mm (1/2 in.) in thickness.

Properties

Mechanical Properties. Unlike the martensitic stainless steels, the ferritic stainless steels cannot be strengthened by heat treatment. Also,

Table 2 Chemical compositions of Group II ferritic stainless steels

UNS No.	Alloy designation	Composition(a), wt%				
		C	Cr	Mo	Ni	Other
S40900	409	0.08	10.5–11.75	. . .	0.5	Ti = 6 × C min to 0.75 max
S40945	409Cb	0.02(b)	12.5(b)	. . .	0.2(b)	0.4 Nb(b)
S40975	409Ni	0.02(b)	11.0(b)	. . .	0.85(b)	0.20 Ti(b)
. . .	11Cr-Cb	0.01(b)	11.35(b)	. . .	0.2(b)	0.35 Nb(b), 0.35 Al(b), 0.2 Ti(b)
S41050	E-4	0.04(b)	11.5(b)	. . .	0.85(b)	. . .
S44100	441	0.02(b)	18.0(b)	. . .	0.3(b)	0.7 Nb(b), 0.3 Ti(b)
S44500	AL433	0.02(b)	19.0(b)	. . .	0.3(b)	0.4 Nb(b), 0.5 Si(b), 0.4 Cu(b)
S40930	AL446	0.01(b)	11.5(b)	. . .	0.2(b)	0.2 Nb(b), 0.1 Ti(b)
S46800	AL468	0.01(b)	18.2(b)	. . .	0.2(b)	0.2 Nb(b), 0.1 Ti(b)
. . .	YUS436S	0.01(b)	17.4(b)	1.2(b)	. . .	0.2 Ti(b)
S43035	439	0.07	17.00–19.00	. . .	0.5	Ti = 0.20 + 4(C + N) min to 1.0 max
. . .	12SR	0.2	12.0	. . .	. . .	1.2 Al, 0.3 Ti
. . .	18SR	0.04	18.0	. . .	. . .	2.0 Al, 0.4 Ti
K41970	406	0.06	12.0–14.0	. . .	0.5	2.75–4.25 Al, 0.6 Ti

(a) Single values are maximum values unless otherwise indicated. (b) Typical value

Table 3 Nominal chemical compositions of Group III intermediate-purity ferritic stainless steels

UNS No.	Alloy designation	Composition(a), wt%					
		C	N	Cr	Mo	Ni	Ti
S44626	26-1 Ti	0.02(b)	0.025(b)	26(b)	1(b)	0.25(b)	0.5(b)
S44400	AISI 444	0.02(b)	0.02(b)	18(b)	2(b)	0.4(b)	0.5(b)
S44660	Sea-Cure	0.025	0.035	25–27	2.5–3.5	1.5–3.5	[0.20 + 4 (C + N)] ≤ (Nb + Ti) ≤ 0.80
S44635	Monit	0.025	0.035	24.5–26	3.5–4.5	3.5–4.5	[0.20 + 4 (C + N)] ≤ (Nb + Ti) ≤ 0.80
S44735	AL29-4C	0.030	0.045	28–30	3.6–4.2	1.0	6(C + N) ≤ (Nb + Ti) ≤ 1.0

(a) Single values are maximum values unless otherwise stated. (b) Typical value

because the strain-hardening rates of ferrite are relatively low and cold work significantly lowers ductility, the ferritic stainless steels are not often strengthened by cold work. Typical annealed yield and tensile strengths for ferritic stainless steels are 240 to 380 MPa (35 to 55 ksi) and 415 to 585 MPa (60 to 85 ksi), respectively. Ductilities tend to range between 20 and 35%. Higher strengths, up to 515 MPa (75 ksi) for yield strength and 655 MPa (95 ksi) for tensile strength, are obtained in the more highly alloyed superferritic steels.

Corrosion Resistance. Whereas the martensitic stainless steels offer only moderate corrosion resistance, that of ferritic stainless steels can range from moderate for the low-to-medium chromium content alloys to outstanding for the superferritics, such as Sea-Cure (UNS S44660), Monit (S44635), 29-4C (S44735), and 29-4-2 (S44800). The low-chromium (10 to 14% Cr) alloys, such as types 405 and 409, have fair corrosion and oxidation resistance and good fabricability at low cost. Type 409, the most widely used ferritic stainless steel, has gained wide acceptance for use in automotive exhaust systems. The intermediate chromium (16 to 18% Cr) alloys include type 430, which resists mild oxidizing acids and organic acids and is used in food-handling equipment. The high-chromium (19 to 30% Cr) alloys, which include Group I grades 442 and 446 as well as the superferritics, are used for applications that require a high level of corrosion and oxidation resistance. By controlling interstitial element content via AOD or vacuum processing, it is possible to produce grades with unusually high chromium and molybdenum (4% Mo) contents and very low carbon contents (as low as 0.005% C). Such highly alloyed superferritics offer exceptional resistance to localized corrosion induced by exposure to aqueous chlorides. Localized corrosion, such as pitting, crevice corrosion, and SCC are problems that affect many austenitic stainless steels. Therefore, the superferritics are often used in heat exchangers and piping systems for chloride-bearing aqueous solutions and seawater. The superferritics are also used in the chemical processing industry for handling caustics, sulfuric acid, nitric acid, organic acids, and amines.

General Welding Considerations

The ferritic stainless steels are generally less weldable than the austenitic stainless steel and produce welded joints having lower toughness because of grain coarsening that occurs at the high welding temperatures. Group I alloys (Table 1) exhibit the poorest weldability. These alloys require both preheating and postweld heat treatments (PWHTs). Group II alloys (Table 2) are more easily welded, but still require preheating and post heating. The Group III superferritics contain much lower carbon than do the other ferritic grades and exhibit improved weldability. The superferritics do not require preheating or PWHTs (more detailed information on the weldability of ferritic stainless steels can be found in the following section).

Welds in ferritic stainless steel base metals can be produced in several ways: (a) autogenously (i.e., without the addition of filler metal), (b) with a matching filler metal, (c) with an austenitic stainless steel filler metal, or (d) using a high-nickel filler alloy. Table 5 lists some base metal-filler metal combinations for selected ferritic stainless steels.

The most commonly used welding processes to join ferritic stainless are the arc welding processes—namely gas-tungsten arc welding (GTAW), gas-metal arc welding (GMAW), shielded-metal arc welding, and plasma arc welding. Other welding processes occasionally

Table 4 Nominal chemical compositions of Group III ultrahigh-purity ferritic stainless steel

		Composition(a), wt%						
UNS No.	Alloy designation	C	N	Cr	Mo	Ni	Nb	Other
S44726	E-Brite 26-1 (XM-27)	0.010	0.015	25–27	0.75–1.5	0.30	0.05–0.20	0.4 Mn
S44800	AL 29-4-2	0.010	0.020	28–30	3.5–4.2	2.0–2.5	. . .	. . .
S44700	AL 29-4	0.010	0.020	28–30	3.5–4.2	0.15	. . .	0.3 Mn
. . .	SHOMAC 30-2	0.003(b)	0.007(b)	30(b)	2(b)	0.2(b)	. . .	0.3 Mn
S44400	YUS 190L	0.004(b)	0.0085(b)	18(b)	2(b)	0.4(b)	. . .	. . .

(a) Single values are maximum values unless otherwise stated. (b) Typical value

used include resistance welding, electron beam welding, laser welding, and friction welding. Submerged arc welding is not suitable for most of the ferritic alloy grades.

Weldability. The term "weldability" is defined here as meaning the ease with which sound welds can be made and the suitability of these welds to perform satisfactorily in service. It is necessary, therefore, that weldability include both the mechanical aspects, such as strength, ductility, and Charpy V-notch (CVN) impact toughness, and the corrosion aspects, such as resistance to intergranular attack (IGA), SCC, and general overall corrosion resistance.

Over the years, two schools of thought have existed on how to weld the Group III ferritic stainless steels. One school recommends welding these alloys as one would the austenitics (this is not acceptable), and the other endorses using extra care and special techniques somewhat like those used to weld titanium. Extra care and special techniques are mandatory for Group III alloys. While the Group I alloys also require care, the welding of the Group II alloys is rather routine.

During the early to mid-1970s, a reluctance developed on the part of many users and fabricators to follow recommended procedures (Ref 1). As a result, many welds were produced that had inferior corrosion resistance, ductility, and impact toughness. Because of these problems, the weldability of the new ferritics was explored by many (Ref 2–8).

The unique as-welded properties of the Group III ferritics have been made possible by obtaining either very low levels of impurities, including carbon, nitrogen, and oxygen (ultrahigh-purity Grade III alloys), and a careful balance of niobium and/or titanium to match the carbon, nitrogen, and oxygen contents (intermediate-purity Group III alloys). For these reasons, every precaution must be taken and welding procedures must be selected that optimize gas shielding and cleanliness to avoid pickup of carbon, nitrogen, oxygen, and hydrogen.

Autogenous welds in ferritic stainless steels exhibit relatively simple microstructures. The grain size gradually increases from the edge of the heat-affected zone (HAZ) to the fusion boundary. In unstabilized or niobium-stabilized welds, columnar grains extend from the fusion boundary to meet at a well-defined centerline (Fig. 2). In titanium-stabilized or dual-stabilized welds (niobium and titanium), there is typically a transition from columnar grains near the fusion boundary to equiaxed grains near the weld centerline (Ref 11, 12). The former structure shows a greater tendency for hot cracking (Ref 13).

With lower chromium or high-carbon-content ferritic stainless alloys, such as types 409, 430, 434, 442, and 446, martensite formation during welding can occur as illustrated in Fig. 3 This leads to increased susceptibility to weld cracking. Caution is advised when making welds under high restraint or in heavier section sizes. Preheat can be used under these conditions to slow the cooling rate and minimize stresses that can lead to cracking.

A further word of caution is advised regarding selection of preheat and welding parameters. One must not forget that while higher heat

Table 5 Typical ferritic base metal-filler metal combinations

Base metal	Covered electrode, bare rod, or fuller wire	Application
405	405 Nb	As-welded
	430	Annealed
	308(L), 309(L), 310 (ELC)	As-welded
409	430	Annealed
	308(L), 409, 409Nb, 309LSi	As-welded
429	208(L), 309(L), 310(ELC)	As-welded
430	430	Annealed
	308(L), 309(L), 310(ELC)	Annealed or as-welded
439	430, 430Ti	Annealed or as-welded
442	442	Annealed
	308(L), 309(L), 310(ELC)	As-welded
446	446	Annealed
	308(L), 309(L), 310(ELC)	As-welded
E-Brite 26-1	ER26-1	As-welded
	Inconel 112, Hastelloy C-276, or Hastelloy C-22	As-welded
AL 29-4C	AL 29-4-2	As welded
AL 29-4	AL 29-4-2	As welded
AL 29-4-2	AL 29-4-2	As welded

inputs and preheats can reduce weld cracking in some ferritic stainless steels, grain growth in the weld HAZ can occur. Figure 4 shows grain growth in an ultrahigh-purity Fe-28Cr-2Mo alloy in the base metal and HAZ. Excessive grain growth can produce loss in fracture toughness, ductility, and corrosion resistance.

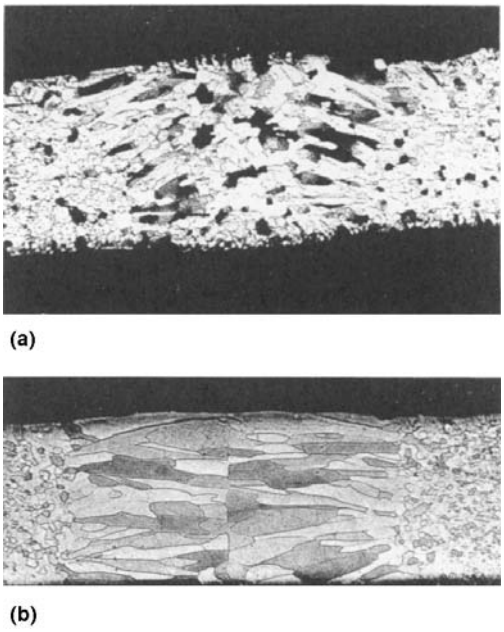

Fig. 2 Photomicrograph showing cross sections of welds in 1.4 mm (0.06 in.) sheet. (a) 18Cr-2Mo-Ti steel. (b) 18Cr-2Mo-Nb steel. Etchant used was X20 (hydrochloric-nitric-glycerol solution). Source: Ref 9, 10

Under some conditions, annealing after welding can be performed to eliminate martensite, however the ferrite grains that have coarsened may grow even more. Generally, annealing after welding is costly, can cause distortion, and usually is not practical in the field. Annealing of tubular products at the steel mill is the exception and is performed as standard procedure. This tube annealing is performed at high rates and is followed by quenching.

Regardless of which welding process is used, joint preparation and thorough solvent degreasing (using a solvent that does not leave a residue) on both sides of the joint (inside and outside) are of paramount importance.

Corrosion Behavior

Intergranular corrosion is the most common cause of failure in ferritic stainless steel weldments and will be the emphasis of this section. Both examples (case histories) that are presented at the conclusion of this chapter also describe failures due to intergranular corrosion. A brief discussion of hydrogen embrittlement is also included.

Hydrogen Embrittlement

Like other ferritic materials, the ferritic stainless steels are susceptible to hydrogen embrittlement. For this reason, the use of hydrogen-

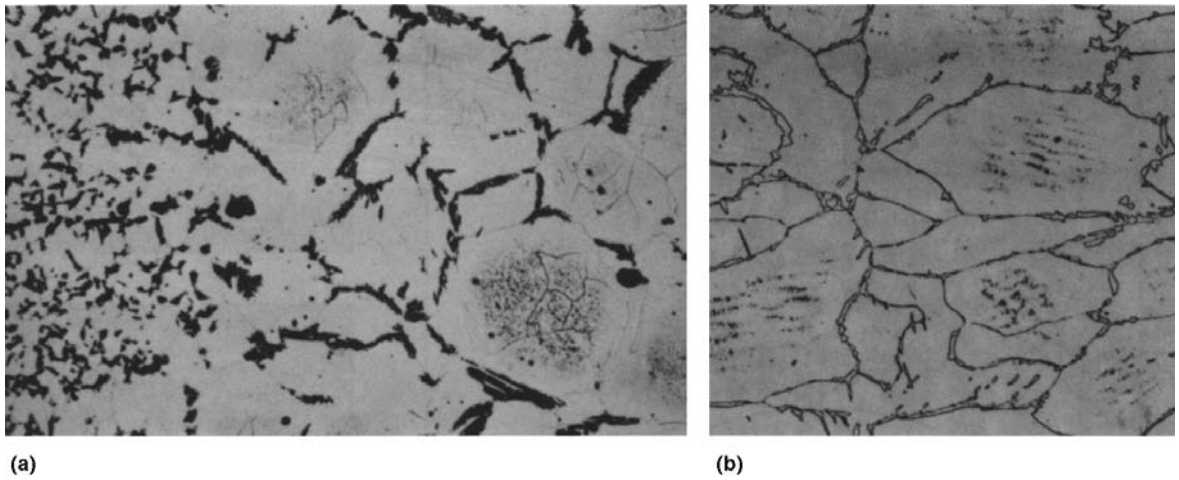

Fig. 3 Grain boundary martensite formation in a type 430 ferritic stainless steel gas-tungsten arc weld. (a) Fusion zone. 100×. (b) Heat-affected zone. 150×. Source: Ref 13, 14

containing shielding gas should be avoided. Hydrogen can also be created from water, water vapor, or oils, and these should be rigorously excluded from the weld region. The presence of hydrogen in the weld can lead to cracking of the weld bead shortly after welding. It can also reduce ductility in uncracked welds. Hydrogen is often spontaneously outgassed from these alloys at room temperature and is readily lost during low-temperature (90 to 200 °C, or 200 to 400 °F) heat treatments. Hydrogen outgassing at room temperature, if it will occur, requires a few days to a few weeks. Surface films of oxides and/or nitrides can inhibit hydrogen outgassing, and it may be necessary to remove such films to facilitate hydrogen outgassing and restoration of ductility. Sensitivity to hydrogen is a function of alloy composition, microstructure, and strength. In general, the stabilized, high-chromium plus molybdenum materials, such as AL 29-4C alloy, are more sensitive than the high-purity, lower-chromium plus molybdenum materials, such as the E-Brite alloy.

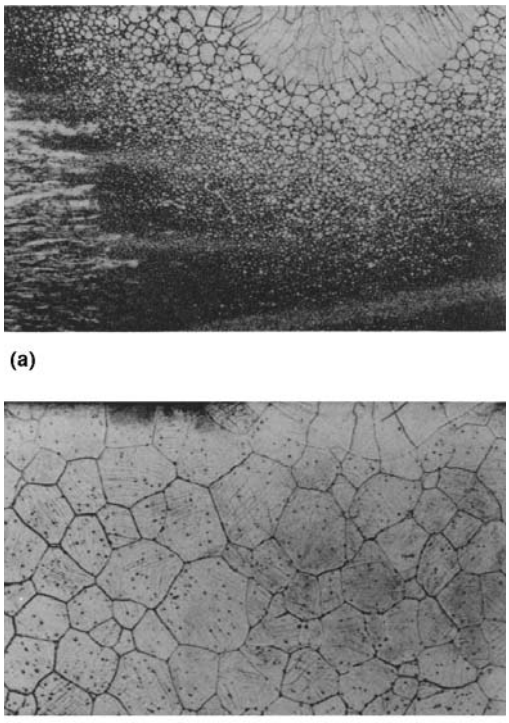

Fig. 4 Cross sections of partial penetration gas-tungsten arc welds in high-purity Fe-28Cr-2Mo ferritic stainless steel. (a) Weld in warm-rolled sheet. (b) Weld in sheet which was preweld annealed at 1040 °C (1900 °F) for 60 min. Etched in 40% nitric acid electroetch. 11×

Intergranular Corrosion

The mechanism for intergranular corrosion in ferritic stainless steels is largely accepted as being the same as that in austenitic stainless steels (see Chapter 3 for a discussion of intergranular corrosion in austenitic grades). Chromium compounds precipitate at grain boundaries, and this causes chromium depletion in the grains immediately adjacent to the boundaries (Ref 15, 16). This lowering of the chromium content leads to increased corrosion rates in the oxidizing solutions usually used to evaluate intergranular corrosion.

There are several differences between the sensitization of ferritic and austenitic stainless steels to intergranular corrosion. The first is that the solubility of nitrogen in austenite is great enough that chromium nitride precipitation is not a significant cause of intergranular corrosion in austenitic steels. It is, however, a significant cause in ferritic stainless steels. The second is the temperature at which sensitization occurs. Sensitization in austenitic steels is produced by heating between 425 and 815 °C (800 and 1500 °F). In conventional ferritic alloys, sensitization is caused by heating above 925 °C (1700 °F). This difference is the result of the relative solubility of carbon and nitrogen in ferrite and austenite. Because the sensitization temperatures are different for austenitic and ferritic steels, it is not surprising that the welding of susceptible steels produces different zones of intergranular corrosion. In austenitic steels, intergranular corrosion occurs at some distance from the weld, where the peak temperature reached during welding is approximately 675 °C (1250 °F). Because the sensitization of ferritic stainless steels occurs at higher temperatures, the fusion zone and the weld itself are the most likely areas for intergranular corrosion.

The mere presence of chromium carbides and nitrides in ferritic stainless steels does not ensure that they will be subject to intergranular corrosion. On the contrary, the usual annealing treatment for conventional ferritic stainless steels is one that precipitates the carbides and nitrides at temperatures (700 to 925 °C, or 1300 to 1700 °F) at which the chromium can diffuse back into the depleted zones. These same treatments would, of course, sensitize austenitic

stainless steels because of the much slower rate of diffusion of chromium in austenite.

Avoiding Intergranular Corrosion

Lower Interstitial Levels. Clearly, the most straightforward method of preventing intergranular attack in ferritic stainless steels is to restrict their interstitial contents. The results shown in Table 6 give an indication of the levels of carbon and nitrogen required to avoid intergranular corrosion of Fe-Cr-Mo alloys in boiling 16% H_2SO_4-copper-copper sulfate ($CuSO_4$) solutions. Evaluation was by bending. The samples that passed had no cracks after bending.

For 18Cr-2Mo alloys to be immune to intergranular corrosion, it appears that the maximum level of carbon plus nitrogen is 60 to 80 ppm; for 26Cr-1Mo steels, this level rises to approximately 150 ppm. The notation of partial failure for the 26Cr-1Mo steel containing 0.004% C and 0.010% N indicates that only a few grain boundaries opened on bending and that it probably represents the limiting composition. Using the 50% H_2SO_4-$Fe_2(SO_4)_3$ test, it was determined that the interstitial limits for the 29Cr-4Mo steel were 0.010% C (max) and 0.020% N (max), with the additional restriction that the combined total not exceed 250 ppm (Ref 16). As their alloy contents increase, the Fe-Cr-Mo steels seem to grow more tolerant of interstitials with regard to intergranular corrosion.

The levels of carbon and nitrogen that are needed to keep 18Cr-Mo alloys free of intergranular corrosion are such that very low interstitial versions of 18% Cr alloys have received little commercial attention: The 26Cr-1Mo and 29Cr-4Mo steels have been made in considerable quantity with very low interstitials, for example, 20 ppm C and 100 ppm N.

Figure 5 shows the relationship of chromium content and interstitial (C + N) content on the combined properties of as-welded corrosion resistance and ductility. Table 7 lists this relationship separately for each property. As chromium content increases, the amount of (C + N) that can be tolerated for intergranular corrosion resistance increases. Conversely, for as-welded ductility, the amount of tolerable (C + N) is drastically reduced. Thus, at low chromium levels, as-welded corrosion resistance is the controlling factor, at high chromium levels, as-welded ductility is the factor that limits the use of high-chromium stainless steels.

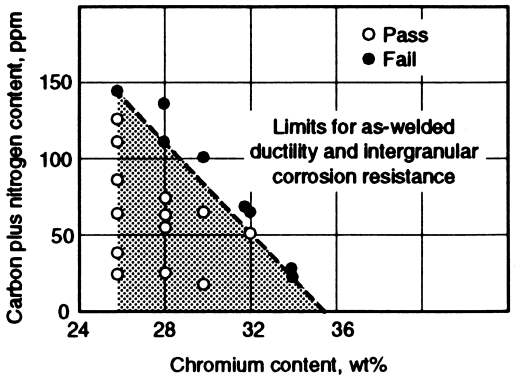

Fig. 5 The effect of interstitial levels and chromium content on as-welded ductility and intergranular corrosion resistance. Source: Ref 18.

Table 6 Results of ASTM A 763, practice Z, on representative as-welded ferritic stainless steels

Welds were made using the gas tungsten arc welding technique with no filler metal added.

Alloy	Interstitial content, wt%		Result
	C	N	
18Cr-2Mo	0.002	0.004	Pass
	0.010	0.004	Fail
	0.002	0.009	Fail
26Cr-1Mo	0.002	0.005	Pass
	0.004	0.010	Partial failure
	0.003	0.016	Fail
	0.013	0.006	Fail

Source: Ref 17

Table 7 Limits of interstitial element (C + N) content for acceptable as-welded intergranular corrosion resistance and as-welded ductility

Sample thickness: 2.5 mm (0.1 in.)

Chromium content, wt%	Intergranular corrosion resistance(a), ppm (C + N)	Ductility(b) ppm (C + N)
19	60–80	>700
26	100–130	200–500
30	130–200	80–100
35	<250	<20

(a) Intergranular corrosion resistance in boiling 50% ferric sulfate-50% sulfuric acid solution. (b) No cracking as determined by slow bending around a 5 mm (0.2 in.) mandrel

The low-interstitial ferritic stainless steels respond to heat treatment in a manner somewhat similar to that of austenitic stainless steels. Rapid cooling from high temperature preserves resistance to intergranular corrosion. However, depending on alloy content and interstitial levels, these alloys may be sensitive to a cooling rate from temperatures above approximately 600 °C (1110 °F) (Ref 19, 20). Less pure Fe-Cr-Mo alloys can also be affected by a cooling rate from approximately 800 °C (1470 °F), but at higher temperatures, it is impossible to quench them fast enough to avoid intergranular attack.

Stabilization of Carbon and Nitrogen. The very low levels of interstitials needed to ensure that ferritic stainless steels are immune to intergranular corrosion suggest that stabilizing elements might offer a means of preventing this type of corrosion without such restrictive limits on the carbon and nitrogen. Both titanium and niobium can be used, and each has its advantages (Ref 21). In general, weld ductility is somewhat better in the titanium-containing alloys, but the toughness of the niobium steels is better. Titanium-stabilized alloys are not recommended for service in HNO_3, but the niobium-containing steels can be used in this environment.

Table 8 shows the results of Cu-$CuSO_4$-16% H_2SO_4 tests on 26Cr-1Mo and 18Cr-2Mo steels with additions of either titanium and/or niobium. Inspection of the data suggests that the required amount of titanium cannot be described by a simple ratio as it is in austenitic steels. The amount of titanium or niobium required for ferritic stainless steels to be immune to intergranular corrosion in the $CuSO_4$-16% H_2SO_4 test has been investigated (Ref 22). It has been determined that for 26Cr-1Mo and 18Cr-2Mo alloys, the minimum stabilizer concentration is given by:

$$Ti + Nb = 0.2 + 4(C + N) \quad \text{(Eq 1)}$$

According to Ref 22, this minimum combination is valid for combined carbon and nitrogen contents in the range of 0.02 to 0.05%. It should be emphasized that the limits set in Eq 1 are truly minimal and are needed in the final product if intergranular attack is to be avoided.

This guideline is empirical and cannot be explained on the basis of stoichiometry. The alloys in the study (Ref 22) were fully deoxidized with aluminum before the stabilizing additions were made. Therefore, it is unlikely that excess stabilizer is required for the purpose of reacting with oxygen.

Proper Welding and PWHT Procedures. It should be pointed out that weldment corrosion resistance can be improved by following proper welding procedures and recommendations. This is particularly true when welding the Group III superferritic stainless steels. As discussed earlier in this chapter, the unique as-welded properties of these steels have been made possible by obtaining very low levels of impurities, including carbon, nitrogen, hydrogen, and oxygen in the case of the alloys described as ultrahigh purity and by obtaining a careful balance of niobium and/or titanium to

Table 8 Results of ASTM A 763, practice Z, tests on as-welded ferritic stainless steels with titanium or niobium

Welds were made using gas tungsten arc welding with no filler metal added.

Alloy	(C + N), wt%	Tl, wt%	Nb, wt%	Tl or Nb/(C + N), %	Result
18Cr-2Mo	0.022	0.16	. . .	7.3	Fail
	0.028	0.19	. . .	6.8	Fail
	0.027	0.23	. . .	8.5	Pass
	0.057	0.37	. . .	6.5	Pass
	0.079	0.47	. . .	5.9	Pass
18Cr-2Mo	0.067	. . .	0.32	4.8	Fail
	0.067	. . .	0.61	9.1	Pass
	0.030	. . .	0.19	6.3	Pass
26Cr-1Mo	0.026	0.17	. . .	6.5	Fail
	0.026	0.22	. . .	8.5	Fail
	0.026	0.26	. . .	10.0	Pass
26Cr-1Mo	0.026	. . .	0.17	6.5	Fail
	0.025	. . .	0.33	13.2	Pass

Source: Ref 17

match the carbon content in the case of the intermediate purity alloys. For these reasons, every precaution must be taken, and welding procedures that optimize gas shielding and cleanliness must be selected to avoid pickup of carbon, nitrogen, hydrogen, and oxygen.

To achieve maximum corrosion resistance, as well as maximum toughness and ductility, the GTAW process with a matching filler metal is usually specified; however, dissimilar high-alloy weld metals have also been successfully used (refer to Table 5). In this case, the choice of dissimilar filler metal must ensure the integrity of the ferritic metal system. Regardless of which of the Group III ferritic stainless steels is to be welded, the following precautions are considered essential.

First, the joint groove and adjacent surfaces must be thoroughly degreased with a solvent, such as acetone, that does not leave a residue. This will prevent pickup of impurities, especially carbon, before welding. The filler metal must also be handled carefully to prevent it from picking up impurities. Solvent cleaning is also recommended. *Caution:* Under certain conditions, when using solvents, a fire hazard or health hazard may exist.

Second, a welding torch with a large nozzle inside diameter, such as 19 mm (3/4 in.), and a gas lens (inert gas calming screen) is necessary. Pure, welding grade argon with a flow rate of 28 L/min (60 ft^3/h) is required for this size nozzle. In addition, the use of a trailing gas shield is beneficial, especially when welding heavy-gage materials. Use of these devices will drastically limit the pickup of nitrogen and oxygen during welding. Back gas shielding with argon is also essential. *Caution:* Procedures for welding austenitic stainless steels often recommend the use of nitrogen backing gas. Nitrogen must not be used when welding ferritic stainless steels. Standard GTAW procedures used to weld stainless steels are inadequate and therefore must be avoided.

Third, overheating and embrittlement by excessive grain growth in the weld and HAZ should be avoided by minimizing heat input. In multipass welds, overheating and embrittlement should be avoided by keeping the interpass temperature below 95 °C (200 °F).

Lastly, to avoid embrittlement further, preheating (except to remove moisture) or postweld heat treating should not be performed. Postweld heat treatment is used only with the conventional ferritic stainless alloys. Example 1 which follows illustrates the results of not following proper procedures.

Postweld heat treatment is another critical element in the welding process. As discussed earlier, both Group I and II alloys must undergo PWHTs. Proper postweld annealing can restore weldment ductility and corrosion resistance. For example, Fig. 6 shows an example of a saturator tank used to manufacture carbonated water at room temperature that failed by leakage through the weld HAZ of the type 430 base metal after being in service for only two months. This vessel, fabricated by welding with a type 308 stainless steel welding electrode, was placed in service in the as welded condition. Figure 7 shows a photomicrograph of the weld/base metal interface at the outside surface of the vessel; corrosion initiated at the inside surface. Postweld annealing—at 785 °C (1450 °F) for 4 h in the case of type 430 stainless steel—restored weld area ductility and

Fig. 6 As-welded type 430 stainless steel saturator tank used in the manufacture of carbonated water that failed after 2 months of service. The tank was shielded metal arc welded using type E308 filler metal. Source: Ref 23

resistance to corrosion equal to that of the unwelded base metal.

Improper PWHT can, however, lead to corrosion failures. Example 2 describes failure of type 430 tube-to-header welds that failed in a heat recovery steam generator because of problems associated with PWHT.

Example 1: Leaking Welds in a Ferritic Stainless Steel Wastewater Vaporizer

Background. A nozzle in a wastewater vaporizer began leaking after approximately three years of service with acetic and formic organic acid wastewaters at 105 °C (225 °F) and 414 kPa (60 psig).

Investigation. The shell of the vessel was weld fabricated from 6.4 mm (1/4 in.) E-Brite stainless steel plate. The shell measured 1.5 m (58 in.) in diameter and 8.5 m (28 ft) in length. Nondestructive examination included 100% radiography, dye-penetrant inspection, and hydro-static testing of all E-Brite welds.

An internal inspection of the vessel revealed that portions of the circumferential and longitudinal seam welds, in addition to the leaking nozzle weld, displayed intergranular corrosion. At the point of leakage, there was a small intergranular crack. Figure 8 shows a typical example of a corroded weld. A transverse cross section through this weld will characteristically display intergranular corrosion with grains dropping out (Fig. 9). It was also noted that the HAZ next to the weld fusion line also experienced intergranular corrosion a couple of grains deep as result of sensitization (Fig. 10).

The evidence indicated weldment contamination; therefore, effort was directed at finding the levels of carbon, nitrogen, and oxygen in the various components present before and after welding. The averaged results were as follows:

E-Brite

Base plate

C = 6 ppm
N = 108 ppm (C + N = 114 ppm)
O = 57 ppm

Corroded longitudinal weld

C = 133 ppm
N = 328 ppm (C + N = 461 ppm)
O = 262 ppm

Corroded circumferential weld

C = 34 ppm
N = 169 ppm (C + N = 203 ppm)
O = 225 ppm

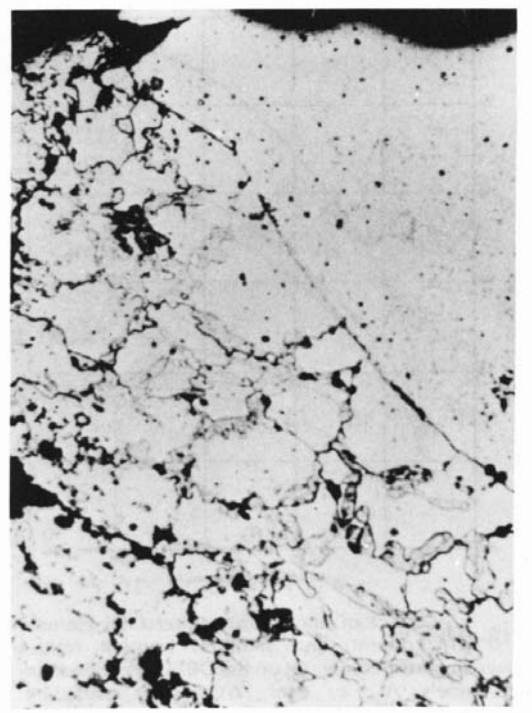

Fig. 7 Photomicrograph of the outside surface of the saturator tank shown in Fig. 6 showing corrosion at the fusion line. Source: Ref 23

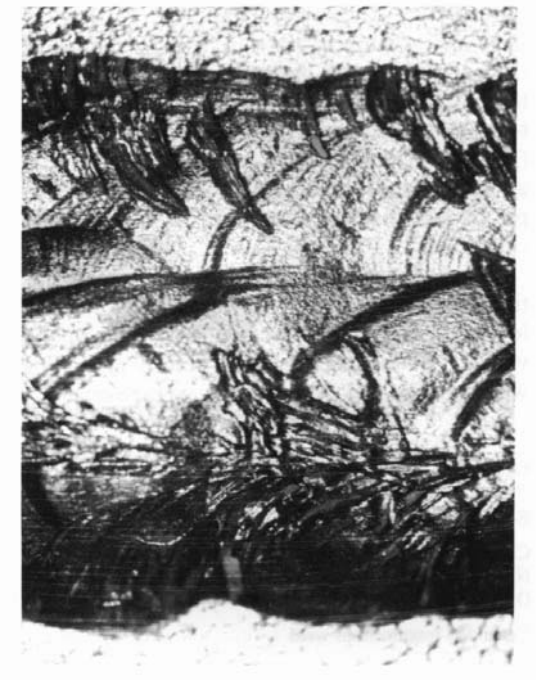

Fig. 8 Top view of a longitudinal weld in 6 mm (1/4 in.) thick E-Brite stainless steel plate showing intergranular corrosion. The weld was made with matching filler metal. About 4×.

E-Brite

Weld wire

C = 3 ppm
N = 53 ppm (C + N = 56 ppm)
O = 55 ppm

Sound longitudinal weld

C = 10 ppm
N = 124 ppm (C + N = 134 ppm)
O = 188 ppm

Sound circumferential weld

C = 20 ppm
N = 106 ppm (C + N = 126 ppm)
O = 85 ppm

These results confirmed suspicions that failure was due to excessive amounts of nitrogen, carbon, and oxygen. To characterize the condition of the vessel further, CVN impact tests were run on the unaffected base metal, the HAZ, and the uncorroded (sound) weld metal. These tests showed the following ductile-to-brittle transition temperatures:

	Ductile-to-brittle transition temperature	
Specimen	**°C**	**°F**
Base metal	40 ± 3	105 ± 5
HAZ	85 ± 3	180 ± 5
Weld	5 ± 3	40 ± 5

Comparison of the interstitial levels of the corroded welds, sound welds, base metal, and filler wire suggested that insufficient joint preparation (carbon pickup) and faulty gas shielding were probably the main contributing factors that caused this weld corrosion failure. Discussions with the vendor uncovered two discrepancies First, the welder was using a large, 19 mm (3/4 in.) inside diameter ceramic nozzle with a gas lens, but was flowing only 19 L/min (40 ft^3/h) of argon; this was the flow rate previously used with a 13 mm (1/2 in.) inside diameter gas lens nozzle. Second, a manifold system was used to distribute pure argon welding gas from a large liquid argon tank to various satellite welding stations in the welding shop. The exact cause for the carbon pickup was not determined.

Conclusion. Failure of the nozzle weld was the result of intergranular corrosion caused by the pickup of interstitial elements and subsequent precipitation of chromium carbides and

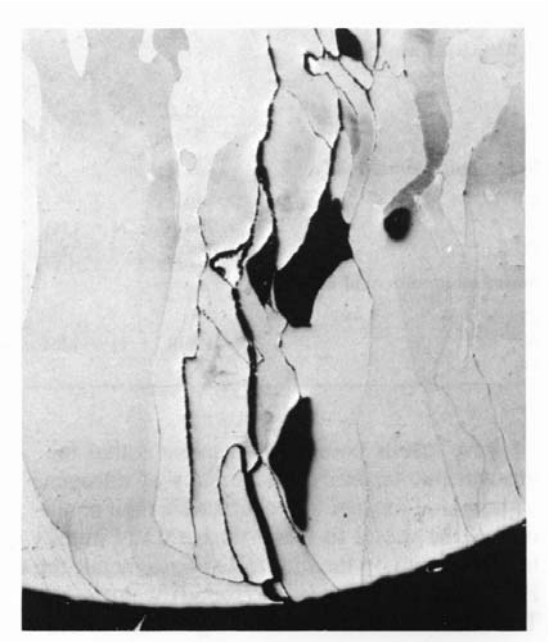

Fig. 9 Intergranular corrosion of a contaminated E-Brite stainless steel weld. Electrolytically etched with 10% oxalic acid. 200×.

Fig. 10 Intergranular corrosion of the inside surface HAZ of E-Brite stainless steel adjacent to the weld fusion line. Electrolytically etched with 10% oxalic acid. 100×

nitrides. Carbon pickup was believed to have been caused by inadequate joint cleaning prior to welding. The increase in the weld nitrogen level was a direct result of inadequate argon gas shielding of the molten weld puddle. Two areas of inadequate shielding were identified:

- Improper gas flow rate for a 19 mm (3/4 in.) diameter gas lens nozzle
- Contamination of the manifold gas system

In order to preserve the structural integrity and corrosion performance of the new generation of ferritic stainless steels, it is important to avoid the pickup of the interstitial elements carbon, nitrogen, oxygen, and hydrogen. In this particular case, the vendor used a flow rate intended for a smaller welding torch nozzle. The metal supplier recommended a flow rate of 23 to 28 L/min (50 to 60 ft^3/min) of argon for a 19 mm (3/4 in.) gas lens nozzle. The gas lens collect body is an important and necessary part of the torch used to weld these alloys. Failure to use a gas lens will result in a flow condition that is turbulent enough to aspirate air into the gas stream, thus contaminating the weld and destroying its mechanical and corrosion properties.

The manifold gas system also contributed to this failure. When this system is first used, it is necessary to purge the contents of the manifold of any air to avoid oxidation and contamination. When that is done, the system functions satisfactorily; however, when it is shut down overnight or for repairs, air infiltrates back in, and a source of contamination is reestablished. Manifold systems are never fully purged, and leaks are common.

The contaminated welds were removed, and the vessels were rewelded and put back into service. Some rework involved the use of covered electrodes of dissimilar composition. Leak problems were eliminated using proper welding and cleaning procedures.

Recommendations. First, to ensure proper joint cleaning, solvent washing and wiping with a clean lint-free cloth should be performed immediately before welding. The filler wire should be wiped with a clean cloth just prior to welding. Also, a word of caution: Solvents are generally flammable and can be toxic. Ventilation should be adequate. Cleaning should continue until cloths are free of any residues.

Second, when GTAW, a 19 mm (3/4 in.) diameter ceramic nozzle with gas lens collect body is recommended. An argon gas flow rate of 28 L/min (60 ft^3/min) is optimum. Smaller nozzles are not recommended. Argon back gas shielding is mandatory at a slight positive pressure to avoid disrupting the flow of the welding torch.

Third, the tip of the filler wire should be kept within the torch shielding gas envelope to avoid contamination and pickup of nitrogen and oxygen (they embrittle the weld). If the tip becomes contaminated, welding should be stopped, the contaminated weld area ground out, and the tip of the filler wire that has been oxidized should be snipped off before proceeding with welding.

Fourth, a manifold gas system should not be used to supply shielding and backing gas. Individual argon gas cylinders have been found to provide optimum performance. A weld button spot test should be performed to confirm the integrity of the argon cylinder and all hose connections. In this test, the weld button sample should be absolutely bright and shiny. Any cloudiness is an indication of contamination. It is necessary to check for leaks or to replace the cylinder.

Fifth, it is important to remember that corrosion resistance is not the only criterion when evaluating these new ferritic stainless steels. Welds must also be tough and ductile, and these factors must be considered when fabricating welds.

Lastly, dissimilar weld filler metals can be successfully used. To avoid premature failure, the dissimilar combination should be corrosion tested to ensure suitability for the intended service.

Example 2: Weld Failure Due to Intergranular Corrosion and Cracking in a Heat-Recovery Steam Generator

Background. Type 430 ferritic stainless steel tube-to-header welds failed in a heat recovery steam generator (HRSG) within one year of commissioning. The HRSG was a combined cycle, gas-fired, combustion turbine electric power plant. Type 430, a 17% Cr ferritic stainless steel, was selected because of its resistance to chloride and sulfuric acid dewpoint corrosion under conditions potentially present in the HRSG low-pressure feedwater economizer.

Heat-Recovery Steam Generator Design. An HRSG generates steam from the heat of exhaust gases from a combustion turbine (CT). The steam produced in the HRSG is sent either to a steam turbine (ST) to produce electricity and/or to be used in another process. Natural gas is normally used for fuel, although some CTs

are fired with oil or are designed for both natural gas and oil fuels. Supplemental duct firing with a variety of fuels can also be used. Combined cycle power plants provide a major source of electricity. The heat-transfer surface in the HRSG consists of finned tubes connected to upper and lower headers (Fig. 11). The headers carry water or steam that is heated by the CT exhaust gas flowing over the finned tube harp assemblies (Fig. 12).

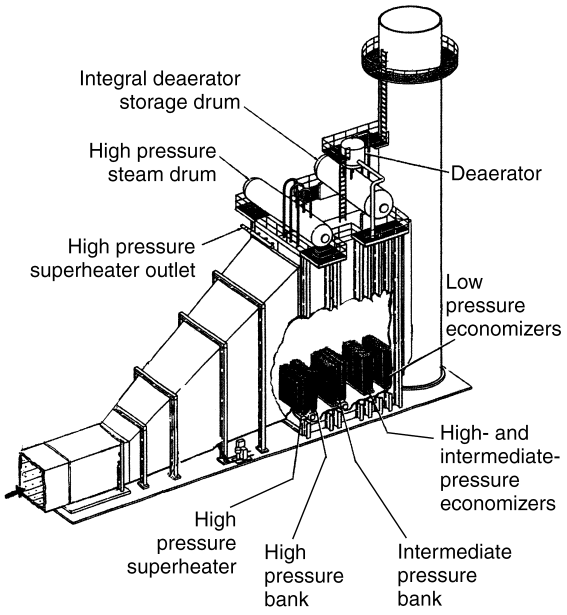

Fig. 11 Heat-recovery steam generator

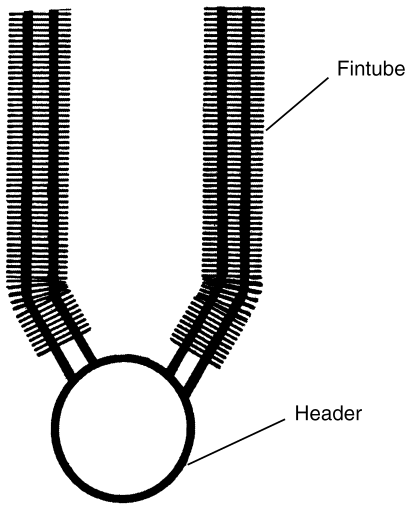

Fig. 12 Feedwater economizer, finned tube harp assembly

Economizers, evaporators, superheaters, and reheaters are specific heat transfer sections within the HRSG. Economizers heat the incoming boiler feedwater to just below the saturation temperature and supply water to the steam drum. Evaporators draw water from the steam drum and heat the water to saturation temperature, producing a steam-water mixture that is separated in the steam drum. Evaporators can have either natural or forced circulation.

Superheaters heat saturated steam from the steam drum to the main steam conditions (superheated steam). Reheaters heat superheated steam, which cooled when it partially expanded in an ST, back to the main steam operating temperature.

Multiple pressure levels of steam (low, intermediate, and high) are typically produced in an HRSG, and each pressure level has its dedicated economizer, evaporator, and superheater. Typical pressure levels are 5 bar (75 psi), 30 bar (450 psi), and 125 bar (1800 psi), respectively. The heating surface, in the direction of CT exhaust flow, is arranged in the following order: high-pressure (HP) superheater, reheater, low-pressure (LP) evaporator, and feedwater economizer. The superheater and reheater see the highest gas temperatures, and the feedwater economizer sees the lowest gas temperatures.

Type T91, T22, and T11 alloy steel tube materials are typically used in HP superheaters and reheaters. Carbon steel is used for intermediate and LP superheaters and also in evaporators and economizers. The feedwater economizers operate at 45 to 150 °C (110 to 300 °F) and are located immediately before the exhaust stack. Economizers generally receive special attention in the materials selection processes, due to the potential of acid dew-point corrosion under normal operating conditions. Some HRSG units use stainless steel alloys 430, 439, or 2205 in this location to avoid dew-point corrosion, while others simply use carbon steel.

The feedwater economizer service life can be extended with either a bypass system or a recirculation system that partially redirects water from its outlet back to its inlet. This helps maintain the CT exhaust gas temperature flowing over the harps and maintains temperatures above the acid dew-point temperature. The addition of a recirculation system causes a minor reduction in overall plant performance when the recirculation system is in service.

Ferritic Stainless Steel Metallurgy. Standard grades of ferritic stainless steels have nom-

inal chromium contents of 12, 17, and 27% corresponding to alloys 405, 430, and 446, respectively (Table 1 and Fig. 13). The carbon content is 0.12% maximum for type 430. This steel is normally supplied in the annealed condition and, with the exception of the rapid cooling such as may occur after welding, type 430 is considered a nonhardenable material. By comparison, martensitic alloy 410 with 12% Cr and 0.12% C is fully air hardenable, while 12% Cr ferritic alloy 405 with 0.08% C is not (Ref 24).

Similar to standard 18Cr-8Ni austenitic stainless steels, chromium and carbon in these chromium-iron ferritic alloys react to form chromium carbide precipitates when heated to 315 to 925 °C (600 to 1700 °F). Precipitates form both at grain boundaries and within the grains. Sensitization develops as chromium is depleted from the areas surrounding the precipitates (Ref 24). Toughness is also reduced by carbide precipitation. Between 370 and 480 °C (700 and 900 °F), precipitation of α prime, a bcc, chromium-rich phase, also occurs and reduces overall toughness. The time required for precipitation of α prime is much longer than the time required for sensitization; therefore, α-prime precipitation is generally associated with in-service exposure, while sensitization may develop during short-term exposure, such as welding. The combined effect of these precipitates results in 475 °C (885 °F) embrittlement (Ref 25).

Sensitization makes ferritic chromium alloys susceptible to intergranular corrosion and SCC. This effect is similar to what occurs in standard 18Cr-8Ni grades of austenitic, face-centered cubic stainless steel. However, carbide precipitation occurs much faster in ferritic stainless steel, due to the higher carbon contents and much lower solubility of carbon in its bcc atomic structure.

Unlike austenitic alloys, type 430 can be annealed at temperatures within its sensitization range to restore its corrosion resistance. Heating at 760 to 815 °C (1400 to 1500 °F) for 4 h allows diffusion of chromium from the remainder of the matrix to replenish the chromium depleted zones surrounding chromium carbide precipitates. This increases the resistance to intergranular attack and to chloride-induced stress-corrosion cracking. (Ref 24). The annealing also removes the embrittling effects of α prime. Solution annealing, as in austenitic alloys, requires heating above 980 °C (1800 °F), high enough to dissolve chromium-rich precipitates.

Type 430 has limited hardenability when rapidly cooled from above its lower critical transformation temperature of 845 °C (1550 °F). Quenching from temperatures above 845 °C (1550 °F) can induce a martensitic transformation (Fig. 14); thus, welds and weld HAZs may partially transform. Nickel is not intentionally added to type 430, but its presence is somewhat normal. A higher nickel content increases the

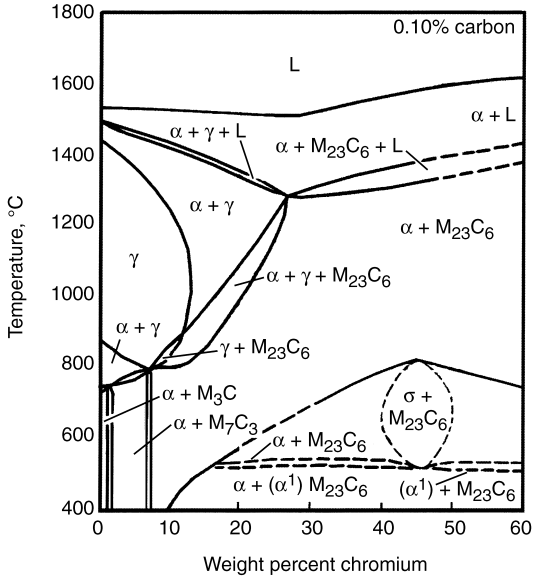

Fig. 13 The iron-chromium (Fe-Cr) alloy phase diagram.

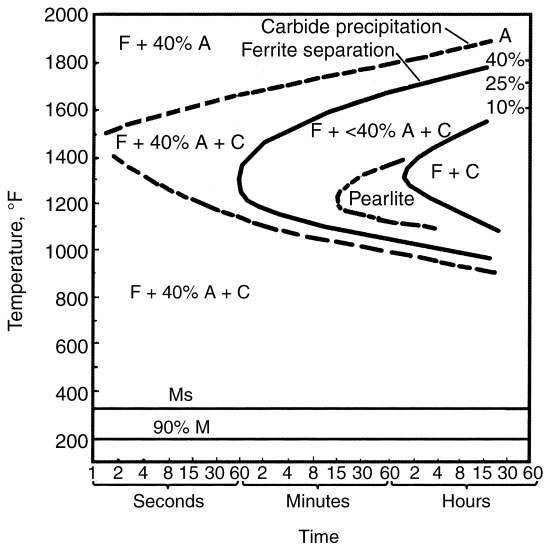

Fig. 14 Time-temperature transformation diagram for type 430 ferritic stainless steel

amount of martensite transformation on rapid cooling or quenching. The martensitic phase contains less chromium than ferrite and therefore corrodes more rapidly.

Partially transformed steels are also very susceptible to intergranular corrosion in the untempered condition. Because of this, type 430 used in the as-welded condition generally has a greatly reduced corrosion resistance, even in warm tap water (Ref 24, 26). Tempering of type 430 proceeds in a comparable manner to tempering in fully martensitic 12% Cr type 410 stainless steel (Fig. 15).

Postweld heat treatment of type 430 at 760 °C (1400 °F) tempers martensite and replenishes chromium to depleted areas surrounding chromium carbide precipitates in the weld and HAZ. Softening takes place relatively quickly, while annealing at this temperature to restore corrosion resistance takes up to 4 h, depending on the specific composition of the alloy and its thermomechanical processing history.

When type 430 is only partially annealed during PWHT, slow furnace cooling of the weld and HAZ from above 650 °C (1200 °F) allows agglomerated carbides and pearlite to form. Rapid cooling from 650 °C (1200 °F) prevents renewed 475 °C (885 °F) embrittlement due to chromium carbide precipitation (Ref. 25). Base metal away from the HAZ, which has been fully mill annealed at 760 °C (1400 °F) during manufacture, does not sensitize during PWHT. Mill annealing effectively precipitates any available carbon and prevents sensitization at and below the mill annealing temperature range (Ref 24).

Precipitation of the iron-chromium nonmagnetic σ phase in type 430 takes tens to thousands of hours at 650 to 760 °C (1200 to 1400 °F) and does not noticeably develop during PWHT. Precipitation of the α-prime phase at 425 to 540 °C (800 to 1000 °F) requires a few hours or more and also does not pose a problem during cooling following PWHT (Ref 27).

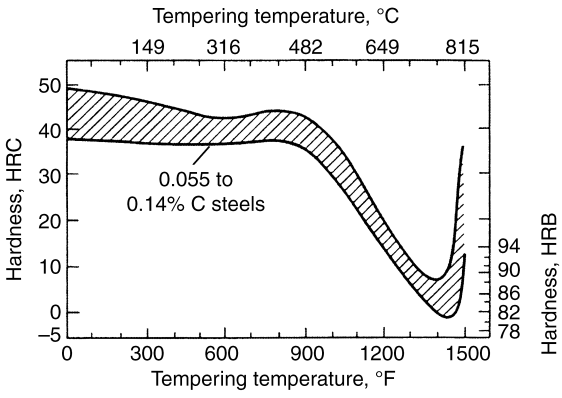

Fig. 15 Effect of tempering temperature on the hardness of type 410 martensitic stainless steel

Corrosion testing in a copper-copper sulfate-16% boiling sulfuric acid solution can be used to confirm that mill annealing and PWHTs have been effectively performed (Ref 28).

Feedwater Economizer Design and Fabrication. The natural-gas-fired combined cycle plant in this study has two separate power trains—units A and B—each having a CT and HRSG. The HRSGs were manufactured in modules with up to 10 harp assemblies each. The modules were assembled in the field, three across and five deep in the direction of gas flow. The last modules contained the feedwater economizer that included one in-line type 430 harp assembly in each of the three-abreast modules. These harps were positioned immediately before the exhaust stack.

Each feedwater economizer harp assembly consisted of an upper and lower header made of 200 mm (8 in.) outside diameter (OD), 8.1 mm (0.322 in.) thick, 4.6 m (15 ft) long pipe connecting two staggered rows of 30 finned tubes each, which were 50 mm (2 in.) OD, 3.0 mm (0.120 in.) thick, and 18.3 m (60 ft) long. A flow-separating partition plate was positioned at the midlength of the lower headers. The tubes were arc welded to the header using a single 45° bevel, partial penetration, joint design machined into the header and a reinforcing fillet weld. The completed tube-to-header welds received a PWHT and were then hydrotested.

The type 430 harps were fabricated in accordance with American Society of Mechanical Engineers (ASME) Boiler and Pressure Vessel (B&PV) Code Section I for Power Boilers (Ref 29). Autogenously seamwelded tubes were manufactured to SA-268, Grade 430, Unified Numbering System (UNS) S43000, with a mill heat treatment of 650 °C (1200 °F) minimum and a maximum hardness of 90 HRB (Ref 27). Tube-to-header welds were made with type 430 weld filler metal. A PWHT temperature of 730 °C (1350 °F) minimum and a holding time of 1 h/25 mm, 15 min minimum, were required by the code for the ASME P-No. 7, group No. 2 tube-to-header welds.

Postweld heat treatment was performed in the shop using a clamshell-type furnace that encased the tube-to-header welds and a portion

of the finned tubes. In the field, joints were wrapped with electrical resistance strip heaters and insulation. Temperature monitoring and control was by direct attachment of thermocouples and multiple channel controllers and chart recorders. The extra heat sink caused by the tube fins and the internal venting of heat due to chimney effects increased the difficulty of performing PWHT. The fins increased the weight of the 50 mm (2 in.) OD tubes to an equivalent wall thickness of 13.7 mm (0.54 in.), more than four times their nominal wall thickness and effectively 70% thicker than the 8.1 mm (0.32 in.) wall thickness of the header pipe.

Feedwater Economizer Performance. One of the harp assemblies leaked during hydrostatic testing. The design required a 15° bend to form a dogleg between the riser and the headers. No heat was applied for bending. Brittle cracking originated in the weld seams, partially because the welds had been positioned on the outside of the bend. The welds had a coarse-grained microstructure that was indicative of brittleness and an elevation in the nil ductility transition temperature (Fig. 16). Repositioning the weld seams to the neutral axis of the bend prevented further problems.

A leak was found in a tube-to-lower-header weld joint within seven months of initial operation. However, the unit was returned to service without repair, because the leak was small, and PWHT of type 430 welds would be required if repairs were made.

The unit was reinspected five months later during a scheduled outage, and the leak had increased in size. In addition, other tube-to-lower-header welds on this harp had pitting, weld toe cracking, and many other liquid penetrant test (PT) indications. A second harp on this unit had pitting on the inlet side of its lower header. The remaining harp had no indications. The two corroded harps were bypassed, with their feedwater flow redirected to the carbon steel LP evaporator. The other unit in the plant was inspected during a later outage after two years of operation, and no PT indications were found on its feedwater economizer lower headers. The inlet halves of its lower headers had a dark and wet deposit, which was apparently a hygroscopic acidic condensate.

Test Results and Metallographic Examination. Hardness testing was performed on a tube sample in the as-received condition. The bulk hardness obtained by the Vickers 500 g test method averaged the coarse-grained, dual-phase, microhardness of the autogeneous seam weld (Fig. 16). Vickers 50 g microhardness testing differentiated between the two phases in the weld fusion zone; the ferrite phase was 175 HV50 (88 HRB), and the martensite phase was 251 HV50 (23 HRC). The tube base metal hardness met the 90 HRB maximum requirement of ASME SA-268. Hardness testing required by this standard is performed away from the weld seam, in accordance with SA-450, paragraph 21.7 (Ref 31). Table 9 lists hardness values for the tube-to-header welds.

A corroded tube-to-header weld sample removed from the leaking header after seven months of service was also hardness tested. Its weld and HAZs, particularly the tube HAZ,

(a)

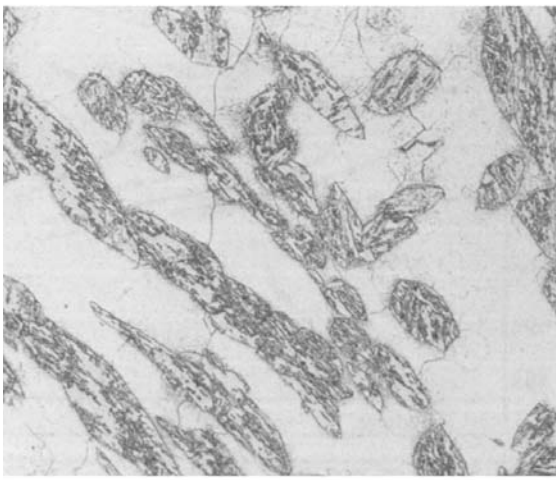

(b)

Fig. 16 Autogenous weld microstructure of ASTM A-268, Grade 430 tubing. Light phase—ferrite, dark phase—martensite. Vilella's etch. (a) 50× and (b) 500×. Source: Ref 30

showed high-average and localized microhardness results.

Metallography performed on the corroded sample confirmed intergranular corrosion and cracking in the type 430 weld metal and in the HAZ on the tube side of the joint (Fig. 17 and 18). Corrosion proceeded preferentially at the lower-Cr-content martensitic phase that formed preferentially along the grain boundaries. The Rockwell hardness values shown in Fig. 17 were converted from Knoop HK 500 g measurements. Vilella's reagent was used for etching to distinguish any martensite phase. There were no signs of fatigue cracking.

Discussion. The HRSG incorporates either an ASME B&PV Code Section I or Section VIII design for LP feedwater economizers. (Ref 28, 29) ASME Section I requires PWHT for P-No. 7, 17% Cr ferritic stainless steel welds. While this is necessary to restore ductility and corrosion resistance in type 430 welds, it is not necessary for titanium-stabilized type 439 (UNS S43035). Electric-resistance-welded P-No. 7 finned tubes are exempt from PWHT under the conditions of Code Case 2215 (Ref 33). Section VIII does not require PWHT for type 439 tubing manufactured to SA/A-268, grade XM8, UNS S43035. Section VIII also permits the use of P-No. 10H duplex stainless steels, such as 22Cr-5Ni alloy 2205, UNS S31803. Numerous HRSG economizers have seen satisfactory service with these two alloys.

SA-268 type 430 seam-welded tubes are required to be heat treated at 650 °C (1200 °F) minimum. The minimum holding temperature partially tempers the weld and HAZ. While this may be suitable when using this alloy for elevated-temperature oxidizing service, the PWHT can leave a sensitized microstructure reducing the resistance of the alloy to acid dew-point corrosion and SCC.

Optimal resistance to SCC requires mill annealing at 760 °C (1400 °F) for sufficient time to allow chromium replenishment in the sensitized regions of the microstructure (Ref 24).

Type 439 seam-welded tubes manufactured to SA-803 are supplied in the solution-annealed condition (Ref 34). Modified type 439 compositions with low carbon contents (0.030% max) are available that have improved formability and corrosion resistance. The use of AOD steel-refining practices makes low-carbon-content type 439 readily available. Welding is generally performed with a matching type 430 titanium weld filler or austenitic stainless steel alloy type 309.

Postweld heat treatment of the HRSG economizer harp assemblies requires close control of resistance heater, insulation, and thermocouple placement. To ensure an adequately wide heated band around each tube-to-header weld, thermocouples are required on both sides of the joints and at each end of the headers. Special precautions arc necessary to minimize chimney effects in the tubes. ASME Sections I and VIII require the PWHT soak time to be 1 h/25 mm and 15 min minimum. Additional time is required to replenish chromium to areas surrounding chromium carbide and nitride precipitates, eliminating sensitization in type 430. Cooling from the PWHT holding temperature is 55 °C (100 °F)/h maximum to 650 °C (1200 °F), then sufficiently rapid to prevent 475 °C (885 °F) embrittlement. Because titanium stabilized type 439 does not require PWHT, it is preferable to type 430 for most welded applications.

Standard metallographic examination and corrosion test methods may be used to evaluate the effectiveness of annealing heat treatments for ferritic stainless steels. Electrolytic oxalic acid etching is used as a screening test for sensitization in type 439. However, it has limited usefulness with type 430, because it does not reveal incomplete chromium replenishment to areas surrounding precipitates. Electrolytic sulfuric acid etching procedures should be used to detect sensitization for this alloy instead (Ref 24).

Martensite is readily detected in type 430 stainless steels with Vilella's etchant. Tempering of martensite in weld and HAZ grain boundaries is detectable with microhardness test

Table 9 Average microhardness results with equivalent Rockwell Hardness for tube-to-header weld joints

Tube			Tube-to-Header Joint			Header
Base Metal	Seam Weld	Weld HAZ	Tube HAZ	Weld Metal	Header HAZ	Base Metal
178 HK500 85 HRB	202 HV500 93 HRB	199 HV500 93 HRB	317–350 HK500 31–35 HRC	218 HK500 93 HRB	238 HK500 97 HRB	210 HK500 92 HRB

methods and, to a limited extent, with the Rockwell B and C macrohardness test methods. Corrosion testing may be performed to ASTM A 763, practice Z, by immersing samples in boiling copper-copper sulfate-16% sulfuric acid solutions for 24 h for both type 430 and type 439 (Ref 28). The absence of intergranular fissuring in bend specimens indicates a sensitization-free microstructure.

Conclusions. Type 430 stainless steel tube-to-header welds failed in an HRSG feedwater economizer within one year of commissioning in a combined cycle, gas-fired, combustion turbine electric power plant. Intergranular corrosion and cracking were found in weld metal and HAZs with hardness up to 35 HRC. Metallographic examination revealed that these areas contained undertempered martensite. Fully tem-

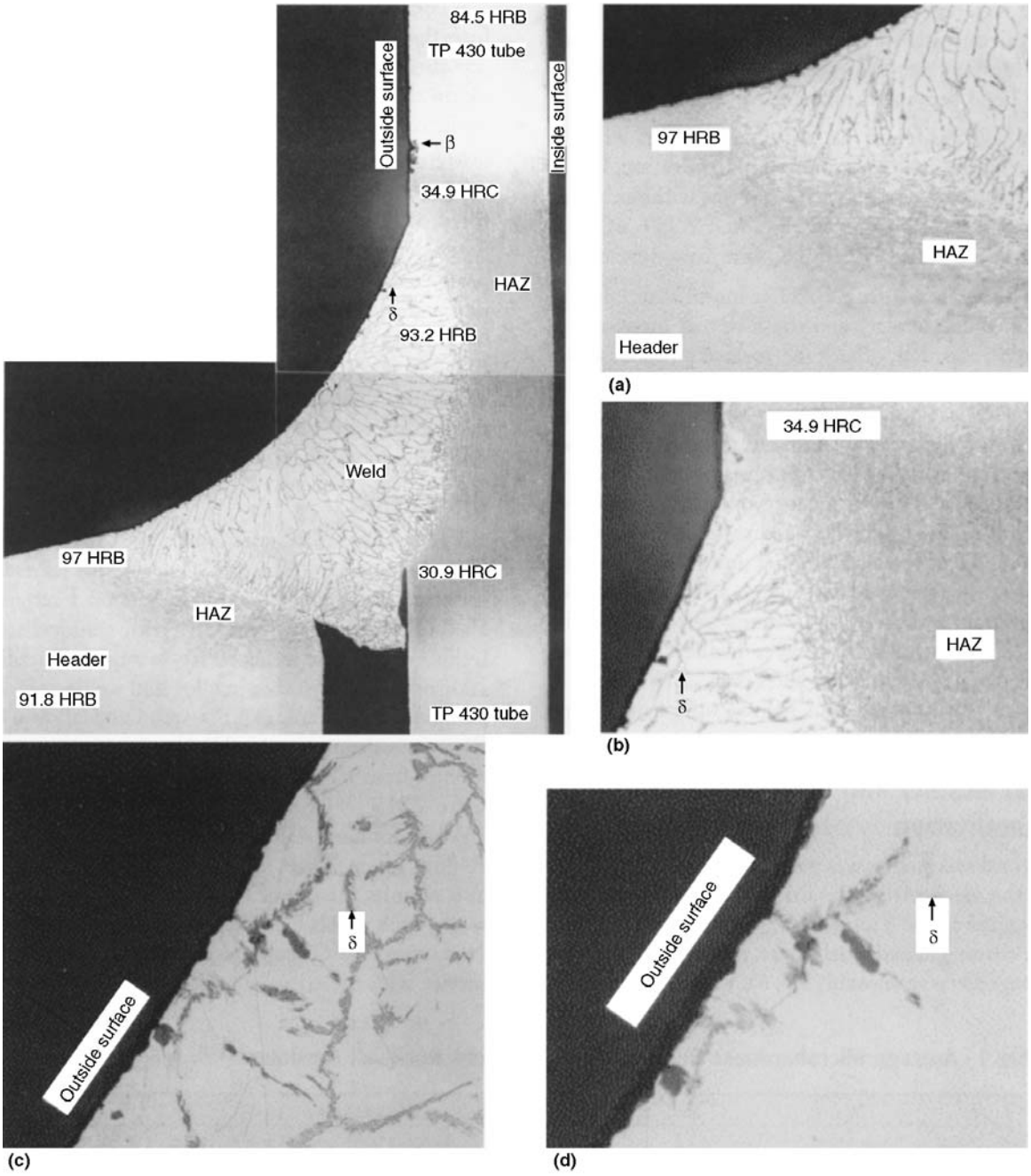

Fig. 17 Tube-to-header weld, axial section, Vilella's etch, 12.8×. (a) Header-weld HAZ; (b) Tube-weld HAZ; (c) Etched 100×; (d) As polished 100×. Source: Ref 32

pered weld areas with a maximum hardness of 93 HRB were not attacked. No evidence of corrosion fatigue was found. Uneven temperature control during PWHT of the feedwater economizer harp sections resulted in incomplete annealing and chromium-carbide-induced grain-boundary sensitization. Intergranular corrosion and cracking occurred as a result of the acid dew-point operating conditions. Titanium stabilized ferritic type 439 and duplex alloy 2205 stainless steels resist sensitization due to welding and are fabricated without PWHT. These alloys have been used successfully in HRSG economizer applications and are acceptable alternatives to type 430.

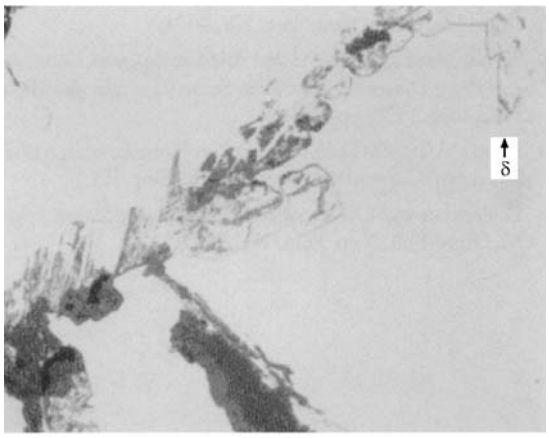

(a)

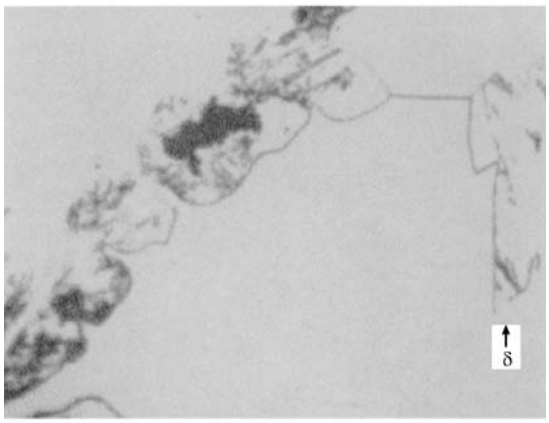

(b)

Fig. 18 Tube-to-header weld, axial section (from Fig. 17 at arrow δ). (a) As-polished, 500×. (b) As-polished 1000×. Source: Ref 32

ACKNOWLEDGMENTS

This chapter was adapted from:

- K. F. Krysiak, J. F. Grubb, B. Pollard, and R. D. Campbell, Selection of Wrought Ferritic Stainless Steels, *Welding, Brazing, and Soldering,* Vol 6, *ASM Handbook,* ASM International, 1993, p 441–455
- J. D. Fritz, Effects of Metallurgical Variables on the Corrosion of Stainless Steels, *Corrosion: Fundamentals, Testing, and Protection,* Vol 13A, *ASM Handbook,* ASM International, 2003, p 266–274
- K. F. Krysiak, et al., Corrosion of Weldments, *Corrosion,* Vol 13, 9th ed., *Metals Handbook,* ASM International, 1987, p 344–368

In addition, Example 2 was adapted from H. Krafft, Alloy 430 Ferritic Stainless Steels Welds Fail due to Stress-Corrosion Cracking in Heat-Recovery Steam Generator, *Practical Failure Analysis,* Vol 2 (No. 4), August 2002, p 39–46

REFERENCES

1. G. Rothschild, "Welding of E-Brite 26-1 Procedure No. W-2," Welding Seminar held in Houston, Texas, Sept 13, 1973
2. K. E. Dorschu, Weldability of a New Ferritic Stainless Steel, *Weld. J.,* Sept 1971
3. R. N. Wright, "The Toughness of Ferritic Stainless Steels," Materials Engineering Department, Rensselaer Polytechnic Institute, Troy, NY, 1979
4. D. H. Kah and D. W. Dickinson, Weldability of Ferritic Stainless Steels, *Weld. J.,* Aug 1981, p 135s–142s
5. K. F. Krysiak, "Weldability of the New Generation of Ferritic Stainless Steels—Part I," Paper No. 92, presented at the National Association of Corrosion Engineers Conference (Toronto, Canada), April 14–18, 1975
6. K. F. Krysiak, "Weldability of the New Generation of Ferritic Stainless Steels—Update," *Symposium on Ferritic Stainless Steels* (San Francisco, CA), May 23–24, 1979
7. R. Lowrie, Welding E-Brite 26-1 to Other Alloys, *Weld. J.,* Nov 1973, p 500s–506s
8. Y. Okazaki, R. Todoroki, T. Sakamoto, and T. Zaizen, "On the Properties of

High-Purity 19 Cr-2 Mo Ferritic Stainless Steel Welds," Paper No. 118, presented at The National Association of Corrosion Engineers Conference (Toronto, Canada) April 6–10, 1981
9. J. M. Sawhill, Jr. and A. P. Bond, Ductility and Toughness of Stainless Steel Welds, *Weld. J.,* Vol 55 (No. 10), 1976, p 33s–41s
10. J. F. Grubb and S. D. Washko, The Effect of Niobium and Titanium Dual Stabilization on the Weldability of 11% Chromiun Ferritic Stainless Steels, *Proc. Int. Conf. Stainless Steels* (Chiba, Japan), ISIJ, June 10–13, 1991, p 1062–1068
11. J. C. Villafuerte and H. W. Kerr, Electromagnetic Stirring and Grain Refinement in Stainless Steel GTA Welds, *Weld. J.,* Vol 69 (No. 1), 1990, p 1s–13s
12. J. C. Villafuerte, E. Pardo, and H. W. Kerr, The Effect of Alloy Composition and Welding Compositions on Columnar-Equiaxed-Transitions in Ferritic Stainless Steel Gas-Tungsten Arc Welds, *Metall. Trans. A,* Vol 21 (No. 7), July 1990, p 2009–2019
13. *Corrosion,* Vol 13, *Metals Handbook,* 9th ed., ASM International, 1987, p 355–358
14. J. F. Grubb, Ph.D. thesis, Rensselaer Polytechnic Institute, Troy, NY, May 1982
15. A. P. Bond, *Trans. Metall. Soc. AIME,* Vol 245, 1969, p 2127–2134
16. M. A. Streicher, *Corrosion,* Vol 29, 1973, p 337–360
17. R. F. Steigerwald, *Metalloved. Term. Obrab. Met.,* No. 7, 1973, p 16–20
18. J. J. Demo, *Metall. Trans.,* Vol 5 (No. 11), Nov 1974, p 2253
19. D. Van Rooyen, *Corrosion,* Vol 27, 1971, p 327–337
20. R. J. Hodges, *Corrosion,* Vol 27, 1971, p 119–127, 164–167
21. A. P. Bond and E. A. Lizlovs, *J. Electrochem. Soc.,* Vol 116, 1969, p 1306–1311
22. H. J. Dundas and A. P. Bond, in "Intergranular Corrosion of Stainless Alloys," STP 656, R. F. Steigerwald, Ed., American Society for Testing and Materials, 1978, p 154–178
23. R. H. Espy, "How Corrosion and Welding Conditions Affect Corrosion Resistance of Weldments in Type 430 Stainless Steel," Paper No. 22, presented at *Corrosion 68* (Houston, Tx), National Association of Corrosion Engineers, 1968
24. M. A. Streicher, The Role of Carbon, Nitrogen, and Heat Treatment in the Dissolution of Iron-Chromium Alloys in Acids, *Corrosion,* 1973, Vol 29, (No. 9), p 337–60
25. P. J. Grobner, The 885 °F (475 °C) Embrittlement of Ferritic Stainless Steels, *Metall, Trans. A,* 1973, Vol 4, p 251
26. R. H. Espy, How Composition and Welding Conditions Affect Corrosion Resistance of Type 430 Stainless Steel, Preprint 22, National Association of Corrosion Engineers (Cleveland, OH), 1968
27. "Specification for Seamless and Welded Ferritic and Martensitic Stainless Steel Tubing for General Service," *ASME SA-268* American Society of Mechanical Engineers, 2001
28. "Standard Practices for Detecting Susceptibility to Intergranular Attack in Ferritic Stainless Steels" in *Annual Book of ASTM Standards*, ASTM, *ASTM A 763* 2001
29. "ASME Boiler & Pressure Vessel (B&PV) Code Section I, Rules for Construction of Power Boilers," American Society of Mechanical Engineers, 2001
30. M. P. Borden, ABB Alstrom Power Corp., private communication, Windsor, CT, 1999
31. "General Requirements for Carbon, Ferritic Alloy, and Austenitic Alloy Steel Welded Ferritic Stainless Steel Feedwater Heater Tubes," *ASME SA-450*, American Society of Mechanical Engineers, 2001
32. Y. Chung, "Metallographic Evaluation of Type 430 Stainless Steel Economizer Tube/Header Weld Samples, Lab Test Report, FTI Anamet Inc., Hayward, CA, 2000
33. "ASME B&PV Code Section VIII, Division 1, Rules for Construction of Pressure Vessels," American Society of Mechanical Engineers, 2001
34. "Specification for Welded Ferritic Stainless Steel Feedwater Heater Tubes," *ASME, SA-803* American Society of Mechanical Engineers, 2001

Corrosion of Weldments
J.R. Davis, editor, p 99-114
DOI:10.1361/corw2006p099

CHAPTER 5

Corrosion of Duplex Stainless Steel Weldments

DUPLEX STAINLESS STEELS are two-phase alloys based on the Fe-Cr-Ni system. These materials typically comprise approximately equal amounts of body-centered cubic (bcc) ferrite and face-centered cubic (fcc) austenite in their microstructures and are characterized by their low carbon content (<0.03 wt%) and additions of molybdenum, nitrogen, copper, and/or tungsten. Typical chromium and nickel contents are about 20 to 30% and 4 to 8%, respectively.

Duplex stainless steels offer several advantages over the common austenitic stainless steels. The duplex grades are highly resistant to chloride stress-corrosion cracking (Cl SCC); have excellent resistance to pitting and crevice corrosion; are about twice as strong as the common austenitics; and, with only about half of the nickel content of the common austenitics, are less sensitive to fluctuation in nickel prices. Although there are some problems with welding duplex alloys, considerable progress has been made in defining the correct parameters and chemistry modifications for achieving sound welds.

Duplex Stainless Steel Development and Grade Designations (Ref 1)

The original alloy in the duplex stainless steel family was S32900 (type 329), which contains nominally 25% Cr, 3 to 4% Ni, and 1.5% Mo. This alloy, which was introduced in the 1930s, has good localized corrosion resistance because of its high chromium and molybdenum contents. When welded, however, this grade loses the optimal balance of austenite and ferrite, and, consequently, corrosion resistance and toughness are reduced. While these properties can be restored by a postweld heat treatment (PWHT), most of the applications of S32900 and other early developed duplex grades used fully annealed material without further welding.

In the 1970s, this problem was made manageable through the use of nitrogen as an alloy addition. The introduction of argon-oxygen decarburization (AOD) technology permitted the precise and economical control of nitrogen in stainless steel. Although nitrogen was first used because it was an inexpensive austenite former, replacing some nickel, it was quickly found that nitrogen has other benefits. These include improved tensile properties and pitting, and crevice corrosion resistance.

Nitrogen also causes austenite to form from the ferrite at a higher temperature, allowing for restoration of an acceptable balance of austenite and ferrite after a rapid thermal cycle in the heat-affected zone (HAZ) after welding. This nitrogen advantage enables the use of duplex grades in the as-welded condition and has created a new generation of duplex stainless steels.

Table 1 covers the duplex stainless steels covered by the Unified Numbering System (UNS). There are three basic categories of duplex stainless steels—low-alloy, intermediate alloy, and highly alloyed- (or "superduplex") grades—grouped according to their pitting resistance equivalent number with nitrogen (PREN), which is derived from:

$$\text{PREN} = \%\text{Cr} + 3.3 \times (\%\text{Mo}) + 16 \times (\%\text{N})$$

When tungsten is introduced into duplex grades, a modified form of the PREN relationship has been proposed, namely:

$$PREN_w = \%Cr + 3.3 \times (\%Mo + 0.5 \times \%W) + 16 \times (\%N)$$

Low-alloy duplex grades have PRENs of <32, intermediate alloy grades have PRENs between 32 and 39. Superduplex grades have PRENs ≥40.

Of the duplex stainless steels listed in Table 1, by far the most widely used is alloy 2205, which is available from a wide variety of stainless steel producers. It is classified under two UNS numbers, the older S31803 and the more alloy-content-restrictive S32205, which keeps the nitrogen content toward the upper end of the range.

The superduplex grades, which were developed during the 1980s and 1990s, contain approximately 25% Cr, 6 to 7% Ni, 3 to 4% Mo, 0.2 to 0.3% N, 0 to 2% Cu, and 0 to 2% W. As stated previously, these grades have PRENs equal to or greater than 40. Figure 1 charts the development of duplex stainless steel grades with regard to nitrogen, chromium, and molybdenum contents.

Microstructure and Properties

Microstructure. Duplex stainless steels have approximately equal proportions of austenite and ferrite, with the matrix comprising ferrite. The base metal microstructure in Fig. 2 exhibits a ferritic matrix with austenite islands of various morphologies. The wrought structure in Fig. 2(a) parallel to the rolling direction has a pronounced orientation. The transverse view in Fig. 2(b) shows the austenite islands "end-on." The plan view in Fig. 2(c) also has some directionality, but it is not as pronounced as in Fig. 2(a).

The solidification morphologies of weldments in the as-welded and solution-annealed conditions are shown in Fig. 3. Figure 3(a) and Fig. 3(d) show the alloy 2205 base metal microstructure in the as-welded and the solution-annealed conditions, respectively. Figure 3(b) and Fig. 3(e) show the composite region microstructures of the as-welded and the solution-annealed weldments, respectively. Figure 3(c) and Fig. 3(f)

Table 1 Composition and pitting resistance equivalent numbers (PREN) of wrought duplex stainless steels covered by UNS designations

		Composition(a), wt%											
UNS No.	Common designation	C	Mn	S	P	Si	Cr	Ni	Mo	Cu	W	N_2	PREN
Low-alloy grades (PREN <32)													
S31500	3RE60	0.03	1.2–2.0	0.03	0.03	1.4–2.0	18.0–19.0	4.25–5.25	2.5–3.0	. . .	. . .	0.05–0.10	28
S32001	19D	0.03	4.0–6.0	0.03	0.04	1.00	19.5–21.5	1.0–3.0	0.60	1.00	. . .	0.05–0.17	23.6
S32304	2304	0.03	2.5	0.04	0.04	1.00	21.5–24.5	3.0–5.5	0.05–0.60	0.05–0.060	. . .	0.05–0.20	25
S32404	UR50	0.04	2.0	0.010	0.30	1.00	20.5–22.5	5.5–8.5	2.0–3.0	1.0–2.0	. . .	0.20	31
Intermediate-alloy grades (PREN 32–39)													
S31200	44LN	0.03	2.00	0.03	0.045	1.00	24.0–26.0	5.5–6.5	1.2–2.0	. . .	. . .	0.14–2.0	33
S31260	DP3	0.03	1.00	0.030	0.030	0.75	24.0–26.0	5.5–7.5	2.5–3.5	0.20–0.80	0.10–0.50	0.10–0.30	38
S31803	2205	0.03	2.00	0.02	0.03	1.00	21.0–23.0	4.5–6.5	2.5–3.5	. . .	. . .	0.08–0.20	34
S32205	2205+	0.03	2.00	0.02	0.030	1.00	22.0–23.0	4.5–6.5	3.0–3.5	. . .	. . .	0.14–0.20	35–36
S32550	255	0.03	1.5	0.03	0.04	1.00	24.0–27.0	4.5–6.5	2.9–3.9	1.5–2.5	. . .	0.10–0.25	38
S32900	10RE51	0.06	1.00	0.03	0.04	0.75	23.0–28.0	2.5–5.0	1.0–2.0	. . .	. . .	. . .	33
S32950	7-Mo Plus	0.03	2.00	0.01	0.035	0.60	26.0–29.0	3.5–5.20	1.0–2.5	. . .	. . .	0.15–0.35	35
Superduplex grades (PREN ≥40)													
S32520	UR52N+	0.03	1.5	0.020	0.035	0.80	24.0–26.0	5.5–8.0	3.0–5.0	0.50–3.00	. . .	0.20–0.35	41
S32750	2507	0.03	1.2	0.02	0.035	1.00	24.0–26.0	6.0–8.0	3.0–5.0	0.5	. . .	0.24–0.32	≥41
S32760	Zeron 100	0.03	1.0	0.01	0.03	1.00	24.0–26.0	6.0–8.0	3.0–4.0	0.5–1.0	0.5–1.0	0.30	≥40
S32906	Safurex	0.030	0.80–1.50	0.03	0.03	0.50	28.0–30.0	5.8–7.5	1.50–2.60	0.80	. . .	0.30–0.40	≥41
S39274	DP3W	0.030	1.0	0.020	0.030	0.80	24.0–26.0	6.0–8.0	2.50–3.50	0.20–0.80	1.50–2.50	0.24–0.32	42(b)
S39277	AF 918	0.025	. . .	0.002	0.025	0.80	24.0–26.0	4.5–6.5	3.0–4.0	1.2–2.0	0.80–1.20	0.23–0.33	≥41

(a) Single values are maximum (b) $PREN_W$ value. Source: Ref 1

show a typical microstructure representing the weld metal in the as-welded and the solution-annealed conditions. The darker areas, as for example in Fig. 3(d), represent the ferrite phase, while the lighter areas represent the austenite phase. The austenite islands are coarser in the solution-annealed microstructures as compared to the as-welded microstructures. The coarse grain HAZ of the as-welded condition was removed by solution-annealing heat-treatment, as shown in Fig. 3(b) and Fig. 3(e). Thus, solution-annealing has the beneficial effect of eliminating the coarse grain HAZ which is usually detrimental due to carbide precipitation. The weld metal microstructures (Fig. 3c and 3f) revealed coarser austenite regions in the solution-annealed weld metal as compared to the weld metal in the as-welded condition.

Mechanical and Physical Properties. Duplex stainless steels characteristically are stronger than either of their two phases considered separately. The duplex grades have yield strengths twice those of the common austenitic grades while retaining good ductility (Table 2). In the annealed condition, the duplex grades have outstanding toughness. With the more recently developed intermediate and high-alloy grades, it is possible to retain toughness and corrosion resistance after welding.

The coefficient of thermal expansion and the heat-transfer characteristics of the duplex stainless steels fall between those of the ferritic and the austenitic stainless steels.

When installing a duplex stainless-steel component in an existing austenitic stainless-steel structure, consideration should be given to the relative strengths and expansion coefficients of the materials. The high strength of the duplex grade and its relatively low expansion coefficient may impose high stresses on the transition welds or the host structure.

Elevated-Temperature Properties. The high alloy content and the presence of a ferritic matrix render duplex stainless steels susceptible to embrittlement and loss of mechanical properties, particularly toughness, through prolonged exposure to elevated temperatures. This is caused by the precipitation of intermetallic phases, most notably alpha prime (α') sigma (σ), chi (χ), and Laves (η) phases. For this reason, duplex stainless steels are generally not used at temperatures above 300 °C (570 °F). Figure 4 shows the phases that can be formed in duplex stainless steels over the temperature range of 300 to approximately 1000 °C (570–1830 °F).

Corrosion Resistance. Duplex stainless steels comprise a family of grades with a wide range of corrosion resistance. They are typically higher in chromium than the corrosion-resistant, austenitic stainless steels and have molybdenum contents as high as 4.0%. The higher chromium plus molybdenum combination is a cost-efficient way to achieve good chlo-

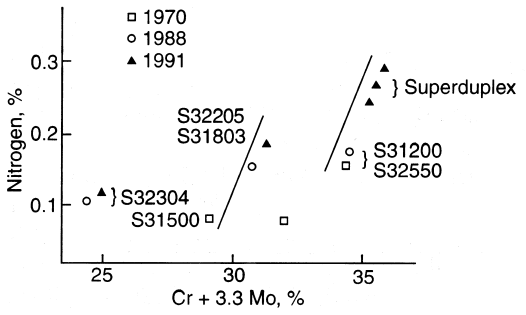

Fig. 1 The development of hot-rolled duplex stainless steels in terms of their nitrogen versus chromium plus molybdenum contents. Source: Ref 1

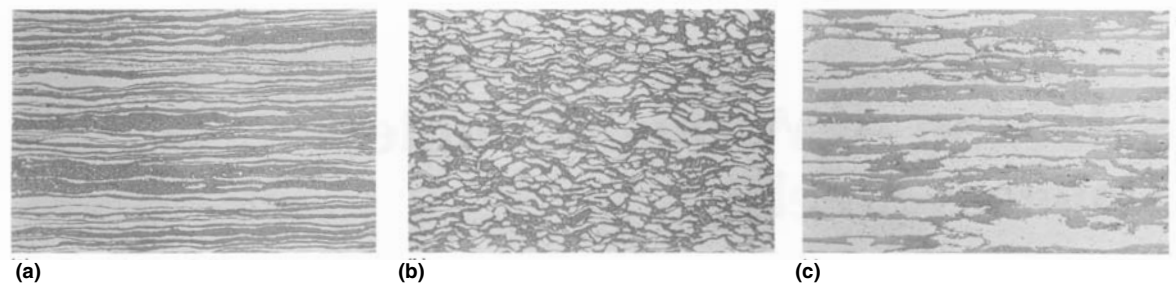

Fig. 2 Effect of orientation plane on the microstructure of Fe-22Cr-5.5Ni-3Mo-0.15N wrought duplex stainless steel base material electrolytically etched in 40% NaOH. (a) Parallel to rolling direction. (b) Transverse to rolling direction. (c) Plan view. 100×

ride pitting and crevice corrosion resistance. Many duplex stainless steels exceed the chloride resistance of the common austenitic stainless-steel grades and also alloy 904L (UNS N08904) (Table 3). SAF 2507 (UNS S32750) has chloride resistance comparable to the 6% molybdenum austenitic stainless steels.

The constraints of achieving the desired balance of phases define the amount of nickel in a duplex stainless steel. The resulting nickel contents, however, are sufficient to provide significant benefit in many chemical environments. As shown in Table 4, alloy 2205 and Ferralium 255 (UNS S32550) compare favorably with type 317L (UNS S31703) and alloy 20 (UNS N08020) in a variety of chemical environments.

One of the primary reasons for using duplex stainless steels is their excellent resistance to Cl SCC. Compared with conventional austenitics, they are clearly superior (Fig. 5). The more highly alloyed superduplex grades are more resistant to Cl SCC than those with lower alloying contents. The SCC resistance in the annealed condition of the superduplex grades is comparable to that observed with highly alloyed austenitic grades like 20Cb-3 (UNS N08020) and the 6% molybdenum superaustenitics like AL-6XN (UNS N08367).

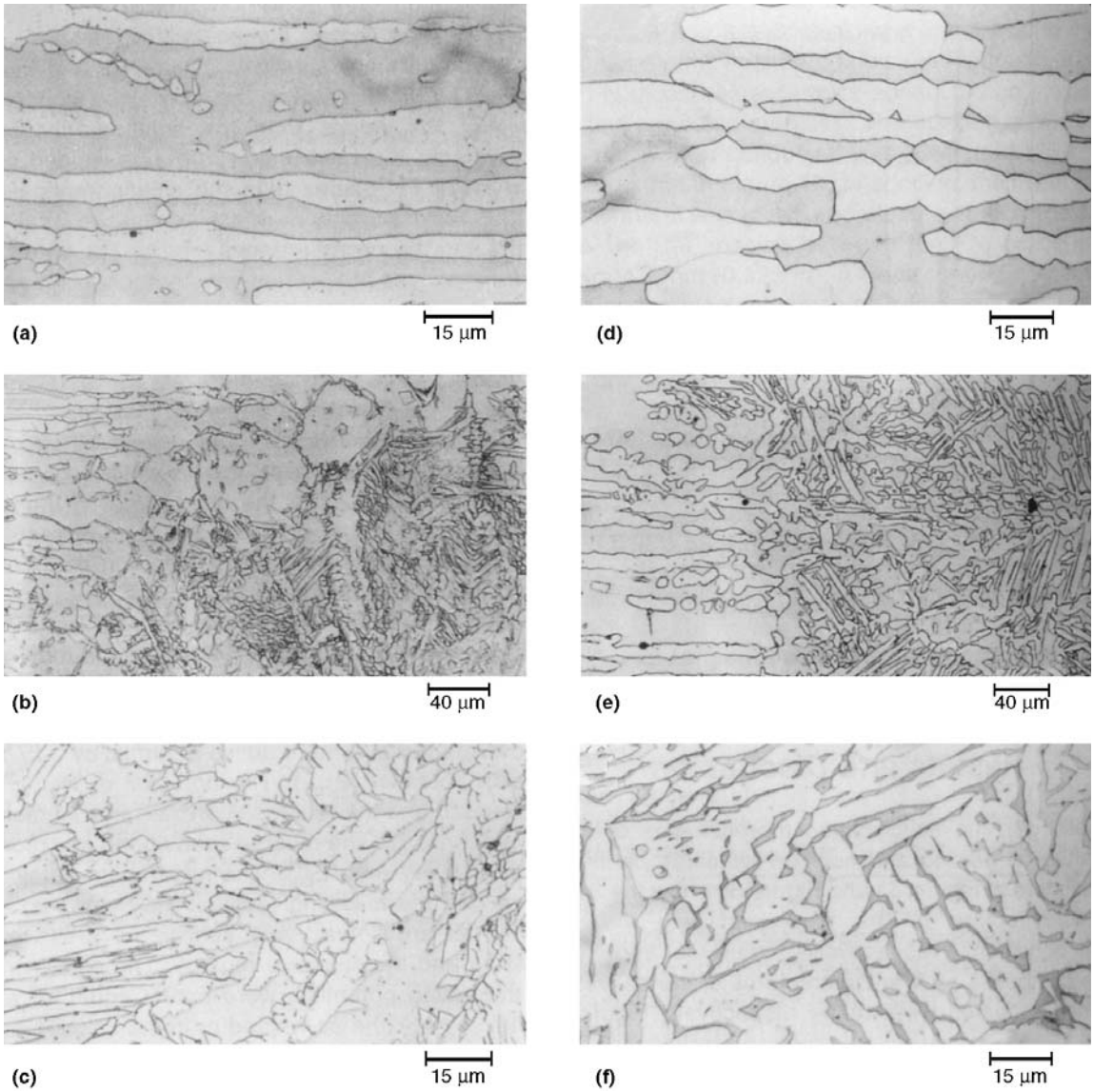

Fig. 3 Solidification morphologies of fusion welded alloy 2205. (a) As-welded base metal. (b) As-welded composite region. (c) As-welded weld metal. (d) Postweld heat treated solution-annealed base metal. (e) Solution annealed composite region. (f) Solution annealed weld metal. Source: Ref 2

General Welding Considerations

The performance of duplex stainless steels can be significantly affected by welding. Due to the importance of maintaining a balanced microstructure and avoiding the formation of undesirable metallurgical phases, the welding parameters and filler metals employed must be accurately specified and closely monitored. The balanced microstructure of the base material (that is, equal proportions of austenite and ferrite) will be affected by the welding thermal cycle. If the balance is significantly altered and the two phases are no longer in similar proportions, the loss of material properties can be acute. Because the steels derive properties from both austenitic and ferritic portions of the structure, many of the single-phase base material characteristics are also evident in duplex materials. Austenitic stainless steels have excellent weldability and low-temperature toughness, whereas their Cl SCC resistance and strength are comparatively poor. Ferritic stainless steels have high resistance to Cl SCC but have poor toughness, especially in the welded condition. A duplex microstructure with high ferrite content can therefore have poor low-temperature notch toughness, whereas a structure with high austenite content can possess low strength and reduced resistance to Cl SCC (Ref 3). The high alloy content of duplex stainless steels also renders them susceptible to formation of intermetallic phases from extended exposure to high temperatures. Extensive intermetallic precipitation may lead to a loss of corrosion resistance and sometimes to a loss of toughness (Ref 4).

Duplex stainless steels weldability is generally good, although they are not as forgiving as austenitic stainless steels or as prone to degradation of properties as fully ferritic stainless steels. The current commercial grades are low in carbon (less than 0.03 wt%), thereby essentially eliminating the risk of sensitization and intergranular corrosion from carbide precipitation. The base material and filler metals also have low sulfur and phosphorus levels (less than 0.03 wt%), which in combination with the ferritic solidification reduce the likelihood of solidification cracking (hot cracking). Hydrogen cracking (cold cracking) resistance is also good due to the high hydrogen solubility in the austenite and the high percentage of austenite in the matrix. Nevertheless, hydrogen cracking can occur in duplex alloys, and is discussed later in the section "Corrosion Behavior of Weldments."

Fusion Welding. Nearly all of the arc welding processes that are employed for other stainless steels can be used with duplex alloys, except where the process characteristic is to weld autogenously, such as electron-beam welding and laser-beam welding. In such circumstances a PWHT is nearly always necessary to restore the correct phase balance to the weld metal and remove any undesirable precipitates. There are few reported differences in corrosion resistance between welding processes, but the nonmetallic inclusion distribution would be anticipated to have an effect. In most instances of pipe welding where access is from one side only, gas-tungsten arc welding (GTAW) is almost exclusively employed for the root pass (Ref 5). This provides a controllable, high-

Table 2 Comparison of mechanical properties of commonly used stainless steels in the annealed condition

		Tensile strength		Yield strength(a)			
UNS No.	Common designation	MPa	ksi	MPa	ksi	Elongation, %	Hardness (max), HRB
Austenitic grades							
S30400	Type 304	515	75	205	30	40	88
N08020	20Cb-3	585	85	275	40	30	95
Duplex grades							
S31803	2205	620	90	450	65	25	30.5 HRC(b)
S32750	2507	800	116	550	80	15	32 HRC(b)
Ferritic grades							
S40900	Type 409	415	60	205	30	22(c)	80
S44625	E-Brite 26-1	450	65	275	40	22(c)	90

(a) At 0.2% offset. (b) Typical values. (c) 20% elongation for thicknesses of 1.3 mm (0.050 in.) or less. Source : Ref 1

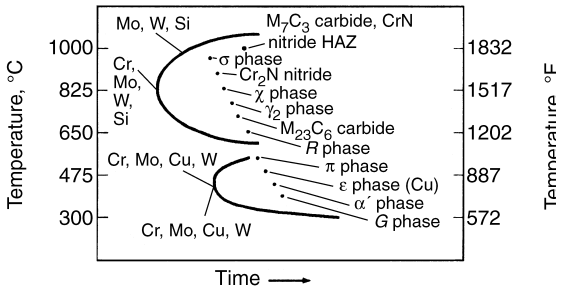

Fig. 4 Time-temperature-transformation (TTT) curve for alloy 2205 (UNS 31803) showing the effect of alloying elements on precipitation reactions. These phases can negatively affect the corrosion resistance and the ductility of the material and are the most serious threats to the successful applications of duplex grades. Source: Ref 4

Table 3 Critical crevice corrosion temperatures

UNS No.	Common name	Critical crevice temperature in 10% $FeCl_3 \cdot 6H_2O$; pH = 1;24 h exposure °C	°F
Duplex grades			
S32900	Type 329	5	41
S31200	44LN	5	41
S31260	DP-3	10	50
S32950	7-Mo PLUS	15	60
S31803	2205	17.5	63.5
S32250	Ferralium 255	22.5	72.5
Austenitic grades			
S30400	Type 304	<-2.5	<27.5
S31600	Type 316	-2.5	27.5
S31703	Type 317L	0	32
N08020	20Cb-3	0	32
N08904	904L	0	32
N08367	AL-6XN	32.5	90.5
S31254	254 SMO	32.5	90.5

Source: Ref 1

quality root bead that dictates the final corrosion performance of the weld. The inert gas on the backside of the weld can also be more closely controlled with this process. Aside from this preference, process selection will probably be dictated more by the availability of consumable form and economic and logistic considerations than by desired properties for the particular welding process. Welds in duplex stainless steels have been made by all the major fusion welding processes and have performed satisfactorily. However, in a very few cases, the final application may necessitate the stipulation of a particular welding process. Where exceptional low-temperature toughness is required, gas-shielded processes may be specified because they produce higher weld metal toughness properties than flux-shielded processes. Some consumable forms have not yet been fully developed for all grades of duplex stainless steels. Nevertheless, GTAW, shielded metal arc welding (SMAW), submerged arc welding (SAW), flux-cored arc welding, and gas metal arc welding (GMAW), are commonly used with success for most alloy classes.

Filler Metal Requirements. For most duplex stainless steels grades there are two types of filler metals:

- Matching composition filler metals
- Filler metals that are slightly overalloyed, principally with respect to nickel

The matching filler metal is used where a PWHT is performed, whereas welds made with the filler metal enriched with nickel are used in the as-welded condition. The weld metal microstructure from a composition exactly matching that of the parent steel will contain a high ferrite content. The increase in nickel is made to improve

Table 4 Corrosion rate in selected chemical environments

Solution temperature	Corrosion rate, mils per year: Type 304	Type 316	Type 317L	Alloy 20	Alloy 2205	Ferralium 255
1% hydrochloric, boiling	. . .	. . .	0.1	. . .	0.1	0.1
10% sulfuric, 150 °F (66 °C)	. . .	. . .	8.9	. . .	1.2	0.2
10% sulfuric, boiling	16,420	855	490	43	206	40
30% phosphoric, boiling	. . .	. . .	6.7	. . .	1.6	0.2
85% phosphoric, 150 ° F (66 °C)	. . .	. . .	0.2	. . .	0.4	0.1
65% nitric, boiling	8	11	21	8	21	5
10% acetic, boiling	. . .	. . .	0.2	. . .	0.1	0.2
20% acetic, boiling	300	2	. . .	2	0.1	. . .
20% formic, boiling	. . .	. . .	8.5	. . .	1.3	0.4
45% formic, boiling	1,715	520	. . .	7	4.9	. . .
3% sodium chloride, boiling	. . .	. . .	1	. . .	0.1	0.4

Source: Ref 1

the as-welded phase balance and increase austenite content. The ferrite content of a weld made with a nickel-enriched consumable would decrease significantly if it underwent a PWHT. It may suffer from slightly reduced weld metal strength and could also be more susceptible to σ phase formation during heat treatment (Ref 6). The nickel level in the enriched weld metal will be approximately 2.5 to 3.5% greater than in the base material (for example, for the Fe-22Cr-5.5Ni-3Mo-0.15N duplex stainless steel base material containing 5.5% Ni, the filler metal will comprise 8.0 to 9.0% Ni, depending on consumable manufacturer and form).

The higher alloy filler metals are sometimes used for welding a less alloyed base material (for example, a duplex stainless steel filler metal with 25% Cr could be used for the root run in a Fe-22Cr-5.5Ni-3Mo-0.15N base metal). This is usually done to improve root weld metal corrosion resistance and thereby pass the qualification test requirements. In most cases, this does not lead to loss of mechanical properties; indeed, the more highly alloyed filler metal in the case previously is likely to have greater strength.

To avoid all the requirements for weld metal phase balance and microstructural control necessary with duplex filler metals, nickel-base consumables (for example, AWS A 5.14 ERNiCrMo-3) have been used. The yield strength, however, is slightly below that of the more highly alloyed grades, and the lack of nitrogen and the presence of niobium in the filler metal may contribute to unfavorable metallurgical reactions and the formation of intermetallic precipitates and areas of high ferrite content in the HAZ (Ref 7, 8).

Preheat is generally not recommended for duplex stainless steels, but may sometimes be specified in low-nitrogen grades, because thick sections and low heat input welding processes may, in combination, develop highly ferritic HAZs (Ref 9). For the more highly alloyed duplex stainless steels, a preheat can be highly detrimental and reduce corrosion resistance and mechanical properties.

Postweld heat treatment is not commonly used except in autogenous welds or welds with a filler metal composition that exactly matches the base steel. Although not always necessary, particularly if a nickel-enriched filler metal is used, it is common to PWHT duplex stainless steel welded pipe after longitudinal seam welding. The PWHT will largely be for the purpose of restoring the correct phase balance and redissolving unwanted precipitates. Postweld heat treatment temperatures of approximately 1050 to 1100 °C (1920 to 2010 °F) are used, depending on grade, followed by the same heat treatment applied to the base material during solution annealing—usually water quenching. The heat treatments commonly used for structural steels (for example, 550 to 600 °C, or 1020 to 1110 °F) are totally inappropriate for duplex alloys and should never be considered.

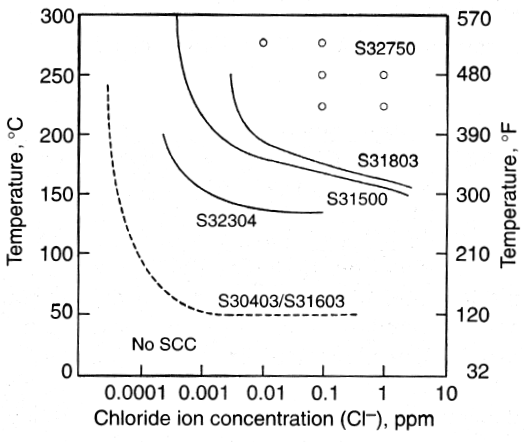

Fig. 5 Stress-corrosion cracking (SCC) resistance of selected duplex stainless steels (S31803, S32304, and S32750) relative to austenitic stainless steels (S30400, S30403, S31600, and S31603) as a function of temperature and chloride concentration in neutral O^2-bearing solutions (approximately 8 ppm). Test duration was 1000 h. Applied stress was equal to yield strength. Source: Ref 1

Corrosion Behavior of Weldments

Corrosion characteristics of duplex stainless steel weldments are complex. The HAZ suffers more corrosion attack than either the base metal or the weld metal because of the unbalance in austenite/ferrite fractions in the HAZ (Ref 2). Pitting corrosion resistance of wrought duplex stainless steels is superior to the cast version. Less austenite is typically present in the cast structure. Thus, the duplex stainless steel weld consumables are enriched with nickel to achieve higher levels of austenite in their as-welded microstructures, since the weld metal is essentially a cast material.

The welding heat input affects the pitting corrosion resistance of the duplex stainless steel weldments. As shown in Fig. 6, the best pitting corrosion resistance is achieved when the weld-

ing practice involves higher heat inputs (Ref 3). In addition, cooling rates also affect the pitting corrosion resistance. The slower the cooling rate, the better is the pitting corrosion resistance (Ref 2). Best corrosion resistance and mechanical properties are achieved when approximately equal amounts of austenite and ferrite are present in both the weld metal and the HAZ (Ref 2). A balanced austenite/ferrite content can be achieved by slowing the cooling rate, through high heat input, preheating in multipass welding operations, and controlled interpass temperatures. The interpass temperature is usually kept between 150 and 200 °C (300 and 400 °F).

Alloying elements in duplex stainless steels play a key role in determining the mechanical and corrosion properties. Due to the high chromium content, duplex stainless steels have excellent high-temperature oxidation resistance. However, they are prone to carbide precipitation and to σ phase and chromium nitride (e.g., CrN, Cr_2N) formation (Ref 2). The carbide precipitation and other problems related to the high chromium content can be resolved through solution annealing and controlled welding practices such as slower cooling rates and controlled-interpass temperatures (Ref 2). Nitrogen reduces the partitioning of chromium between the austenite and the ferrite phases. It also improves the pitting and crevice corrosion resistance of the duplex stainless steels (Ref 2). Very high nickel contents (e.g., 10 wt%) in duplex stainless steel weld metal degrades pitting corrosion resistance by diluting the nitrogen content in the austenite (Ref 2).

Influence of Ferrite-Austenite Balance on Corrosion Resistance. The distribution of austenite and ferrite in the weld and HAZ is known to affect the corrosion properties and the mechanical properties of duplex stainless steels. Figure 7 shows the effect of the ferrite-austenite balance on the pitting resistance of a duplex stainless steel. To achieve a satisfactory balance in properties, it is essential that both base metal and weld metal be of the proper composition. For example, without nickel enrichment in the filler rod, welds can be produced with ferrite levels in excess of 80%. Such microstructures have very poor ductility and inferior corrosion resistance. For this reason, autogenous welding (without the addition of filler metal) is not recommended unless postweld solution annealing is performed, which is not always practical. To achieve a balanced weld microstructure, a low carbon content (approximately 0.02%) and the addition of nitrogen (0.1 to 0.2%) should be specified for the base metal. Low carbon helps to minimize the effects of sensitization, and the nitrogen slows the precipitation kinetics associated with the segregation of chromium and molybdenum during the welding operation. Nitrogen also enhances the reformation of austenite in the HAZ and weld metal during cooling.

Because these duplex alloys have been used for many years, guidelines relating to austenite-ferrite phase distribution are available. It has been shown that to ensure resistance to Cl SCC,

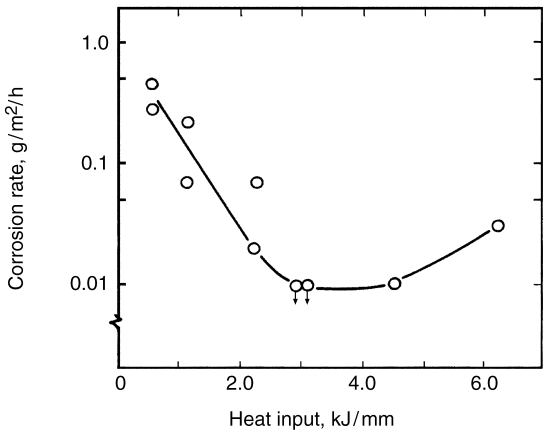

Fig. 6 Influence of heat input on corrosion of welded S31803 steel in ferric chloride. Source: Ref 3

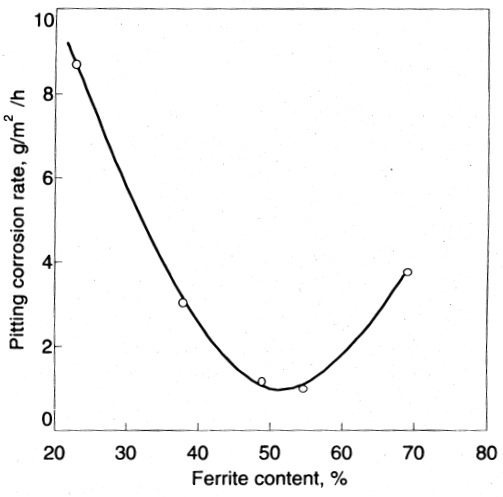

Fig. 7 Effect of ferrite-austenite balance on pitting resistance of Fe-22Cr-5.5Ni-3.0Mo-0.12N gas tungsten arc stainless steel welds. Source: Ref 3

welds should contain at least 25% ferrite. To maintain a good phase balance for corrosion resistance and mechanical properties (especially ductility and notch toughness) comparable to those of the base metal, the average ferrite content of the weld should not exceed 60%. This means using welding techniques that minimize weld dilution, especially in the root pass. Conditions that encourage mixing of the lower-nickel base metal with the weld metal reduce the overall nickel content. Weld metal with a lower nickel content will have a higher ferrite content, with reduced mechanical and corrosion properties. Once duplex base metal and welding consumables have been selected, it is then necessary to select joint designs and weld parameters that will produce welding heat inputs and cooling rates so as to produce a favorable balance of austenite and ferrite in the weld and HAZ.

Researchers have shown that the high-ferrite microstructures that develop during welding in lean (low-nickel) base metal and weld metal compositions can be altered by adjusting welding heat input and cooling rate. In these cases, a higher heat input that produces a slower cooling rate can be used to advantage by allowing more time for ferrite to transform to austenite. There are, however, some practical aspects to consider before applying higher heat inputs indiscriminately. For example, as heat input is increased, base metal dilution increases. As the amount of lower-nickel base metal in the weld increases, the overall nickel content of the deposit decreases. This increases the potential for more ferrite, with a resultant loss in impact toughness, ductility, and corrosion resistance. This would be another case for using an enriched filler metal containing more nickel than the base metal. Grain growth and the formation of embrittling phases are two other negative effects of high heat inputs. When there is uncertainty regarding the effect that welding conditions will have on corrosion performance and mechanical properties, a corrosion test is advisable.

Effect of Welding on Pitting and SCC Resistance. The weld is usually the part of a system with reduced corrosion resistance and low-temperature toughness, and therefore in many cases it is the limiting factor in material application. From a corrosion standpoint, welding primarily affects pitting corrosion and Cl SCC.

Pitting corrosion resistance can be affected by many features of the welding operation, including:

- Localized segregation of alloying elements to the different constituent phases in the microstructure, producing areas lean in molybdenum and chromium
- Incorrect ferrite/austenite phase balance
- Formation of nitrides or intermetallic phases
- Loss of nitrogen from the root pass
- Presence of an oxidized surface on the underside of the root bead

The extent to which the reduction of corrosion resistance occurs depends on which of these factors are active and to what degree. Partitioning of alloying elements between the austenite and ferrite occurs in the weld metal, with chromium, molybdenum, and silicon partitioning to the ferrite and carbon, nickel, and nitrogen to the austenite (Ref 10, 11). The effect is not so apparent in as-deposited weld metals, but it becomes more significant as a result of reheating a previously deposited weld pass.

Weld metal and HAZ microstructures with very high ferrite contents are also less resistant to pitting attack than are balanced structures. This is largely because predominantly ferritic structures are more prone to chromium nitride precipitation, which locally denudes the chromium concentration and lowers resistance to pitting attack.

Nitrogen loss in the root pass may reduce weld metal corrosion resistance. Up to 20% loss of nitrogen has been reported for GTA welds (Ref 12), and nitrogen-bearing backing gases have been explored and used in limited applications.

Cleanliness of the root side purge gas may also affect pitting resistance. Figure 8 shows the effect of reducing oxygen content in an otherwise pure argon purge gas and its beneficial effect on pitting resistance. Also shown is the apparent benefit of using a reducing gas (NH_{10}), which would significantly reduce the tendency

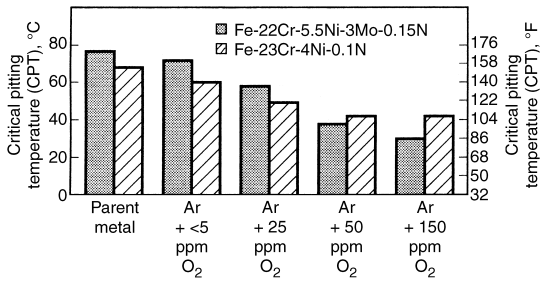

Fig. 8 Plot of pitting temperature versus oxygen content of backing gas for Fe-22Cr-5.5Ni-3Mo-0.15N and Fe-23Cr-4Ni-0.1N duplex stainless steels tested in 3% NaCl and 0.1% NaCl solutions, respectively, both at anodic potential of +300 mV. Source: Ref 13

for oxide formation and leave the underbead appearance very shiny (Ref 13).

The net effect on pitting corrosion resistance may be observed by applying the ASTM G 48 pitting corrosion test to welds and base material with the same PREN value, then assessing the reduction in critical pitting temperature (that is, the temperature at which pitting in the ferric chloride solution is first observed). The difference is approximately 20 °C (35 °F), as reported in Fig. 9, thereby quantifying the effect of reduced weld metal properties. Figure 9 also shows that the use of a superduplex stainless steel filler metal with a PREN value of about 40 on an Fe-22Cr-5.5Ni-3Mo-0.15N parent steel (which typically has a PREN value of about 33 to 35) will improve the weld metal pitting corrosion resistance, as assessed by the ASTM G 48 test, to approximately match that of the base material.

Resistance to Cl SCC does not appear to be affected significantly by welding per se (Ref 15). Nevertheless, welds are likely regions of attack for Cl SCC due to the presence of high stresses and the structural inhomogeneity present at the weld. If localized pitting is a necessary precursor for Cl SCC, the effects described above will also ultimately affect Cl SCC resistance. See also the discussion on SCC of alloy 2205 in the section "Corrosion Behavior of Alloy 2205 Weldments."

Hydrogen-Induced Cracking. Duplex stainless steels can suffer from weld metal hydrogen cracking, but HAZ cracking has not been reported in practice and is considered highly unlikely to develop. Hydrogen cracking from welding and in-service hydrogen pickup has been observed (Ref 16). The duplex microstructure provides a combination of a ferritic matrix, where hydrogen diffusion can be fairly rapid, with intergranular and intragranular austenite, where the hydrogen diffusion is significantly slower, thereby acting as a barrier to hydrogen diffusion. The net effect appears to be that hydrogen can be "trapped" within ferrite grains by the surrounding austenite, particularly where it decorates the prior ferrite grain boundaries. Due to these characteristics, low-temperature hydrogen release treatments are not effective, and the hydrogen is likely to remain in the structure for a long period (Ref 16). Whether cracking actually develops will depend upon a number of factors, including the total amount of trapped hydrogen, the applied strain, and the amount of ferrite and austenite in the structure. Weld metal hydrogen content from covered electrodes can be relatively high, and levels up to 25 ppm have been reported (Ref 17).

The problem of weld metal hydrogen cracking in practice must not be overstated. The reported incidences of hydrogen cracking in duplex stainless steels have been restricted to cases in which the alloy has been heavily cold worked or weld metals have seen high levels of restraint or possessed very high ferrite contents in combination with very high hydrogen levels as a result of poor control of covered electrodes or the use of hydrogen-containing shielding gas.

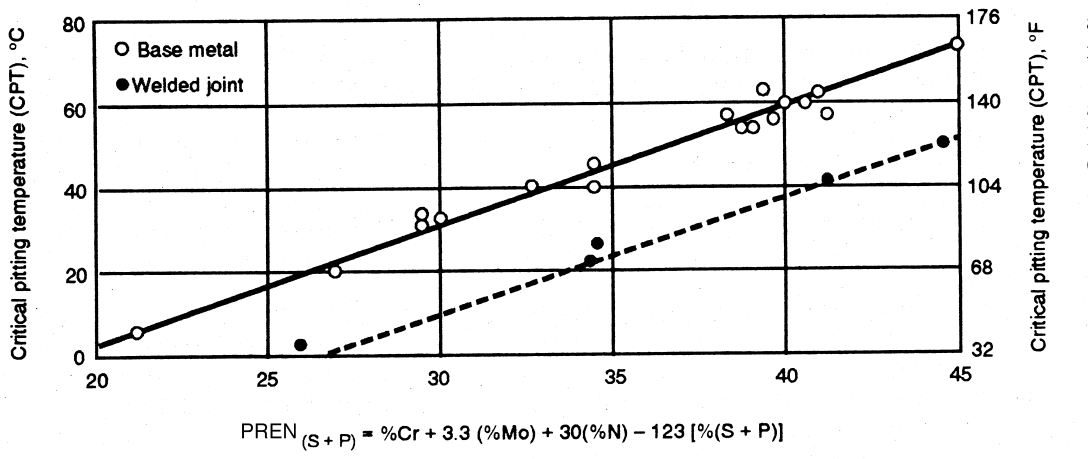

Fig. 9 Pitting corrosion resistance of base metal relative to weld metal placed in 6 wt % $FeCl_3$ solution for 24 h duration per ASTM 648 (method A). Source: Ref 14

Indeed, other studies have shown how resistant duplex stainless steel weld metals are to hydrogen cracking, even with consumables intentionally humidified (Ref 18), and that hydrogen-containing backing gases can be employed without producing cracking. There is no doubt an effect of hydrogen on the ductility of duplex stainless steel, and to avoid fabrication-related cracking problems, high-hydrogen-potential welding processes, such as SMAW, should be controlled by careful storage and use of electrodes, and by ensuring that the weld metal phase balance is within acceptable limits.

Corrosion Behavior of Alloy 2205 Weldments

The influence of different welding conditions on various material properties of alloy 2205 (UNS S31803, Fe-22Cr-5.5Ni-3.0Mo-0.15N) has been studied (Ref 19). Chemical compositions of test materials are given in Table 5, and the results of the investigation are detailed in the following sections.

Intergranular Corrosion. Despite the use of very high arc energies (0.5 to 6 kJ/mm, or 13 to 150 kJ/in.) in combination with multipass welding, the Strauss test (ASTM A 262, practice E) failed to uncover any signs of sensitization after bending through 180°. The results of Huey tests (ASTM A 262, practice C) on submerged-arc welds showed that the corrosion rate increased slightly with arc energy in the studied range of 0.5 to 6.0 kJ/mm (13 to 150 kJ/in.). For comparison, the corrosion rate for parent metal typically varies between 0.15 and 1.0 mm/yr (6 and 40 mils/yr), depending on surface finish and heat treatment cycle.

Similar results were obtained in Huey tests of specimens from bead-on-tube welds produced by GTAW welding. In this case, the corrosion rate had a tendency to increase slightly with arc energy up to 3 kJ/mm (75 kJ/in.).

Pitting tests were conducted in 10% ferric chloride ($FeCl_3$) at 25 and 30 °C (75 and 85 °F) in accordance with ASTM G 48. Results of tests on submerged-arc test welds did not indicate any significant change in pitting resistance when the arc energy was increased from 1.5 to 6 kJ/mm (38 to 150 kJ/in.). Pitting occurred along the boundary between two adjacent weld beads. Attack was caused by slag entrapment in the weld; therefore, removal of slag is important.

Gas tungsten arc weld test specimens (arc energies from 0.5 to 3 kJ/mm, or 13 to 75 kJ/in.) showed a marked improvement in pitting resistance with increasing arc energy. In order for duplicate specimens to pass the $FeCl_3$ test at 30 °C (85 °F), 3 kJ/mm (75 kJ/in.) of arc energy was required. At 25 °C (75 °F), at least 2 kJ/mm (50 kJ/in.) was required to achieve immunity. Welds made autogenously (no nickel enrichment) were somewhat inferior; improvements were achieved by using higher arc energies.

Table 5 Chemical compositions of alloy 2205 specimens tested and filler metals used in Ref 19

Specimen size and configuration	Element, %									
	C	Si	Mn	P	S	Cr	Ni	Mo	Cu	N
Parent metals										
48.1 mm (1.89 in.) OD, 3.8 mm (0.149 in.) wall tube	0.015	0.37	1.54	0.024	0.003	21.84	5.63	2.95	0.09	0.15
88.9 mm (3.5 in.) OD, 3.6 mm (0.142 in.) wall tube	0.017	0.28	1.51	0.025	0.003	21.90	5.17	2.97	0.09	0.15
110 mm (4.3 in.) OD, 8 mm (0.31 in.) wall tube	0.027	0.34	1.57	0.027	0.003	21.96	5.62	2.98	0.09	0.13
213 mm (8.4 in.) OD, 18 mm (0.7 in.) wall tube	0.017	0.28	1.50	0.026	0.003	21.85	5.77	2.98	0.10	0.15
20 mm (3/4 in.) plate	0.019	0.39	1.80	0.032	0.003	22.62	5.81	2.84	. . .	0.13
Filler metals										
1.2 mm (0.047 in.) diam wire	0.011	0.48	1.61	0.016	0.003	22.50	8.00	2.95	0.07	0.13
1.6 mm (0.063 in.) diam rod	0.011	0.48	1.61	0.016	0.003	22.50	8.00	2.95	0.07	0.13
3.2 mm (0.125 in.) diam wire	0.011	0.48	1.61	0.016	0.003	22.50	8.00	2.95	0.07	0.13
3.25 mm (0.127 in.) diam covered electrode	0.020	1.01	0.82	0.024	0.011	23.1	10.4	3.06	. . .	0.13
4.0 mm (0.16 in.) diam covered electrode	0.016	0.94	0.78	0.015	0.011	23.0	10.5	3.13	. . .	0.11

For comparison with a different alloy, Fig. 10 shows the effect of heat input on the corrosion resistance of Ferralium alloy 255 (UNS S32550, Fe-25.5Cr-5.5Ni-3.0Mo-0.17N) welds made autogenously and tested on $FeCl_3$ at 15 °C (60 °F). Preferential corrosion of the ferrite phase is shown in Fig. 11. In a different test, Ferralium alloy 255 was welded autogenously and tested in a neutral chloride solution according to ASTM D 1141 at 60 to 100 °C (140 to 212 °F). In this case, preferential attack of the austenite phase was observed. An example is shown in Fig. 12. Similar results would be expected for alloy 2205.

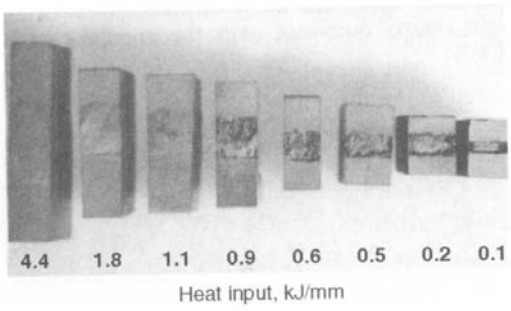

Fig. 10 Effect of welding heat input on the corrosion resistance of autogenous gas tungsten arc welds in Ferralium alloy 255 in 10% $FeCl_3$ at 10 °C (40 °F). The base metal was 25 mm (1 in.) thick. Source: Ref 20

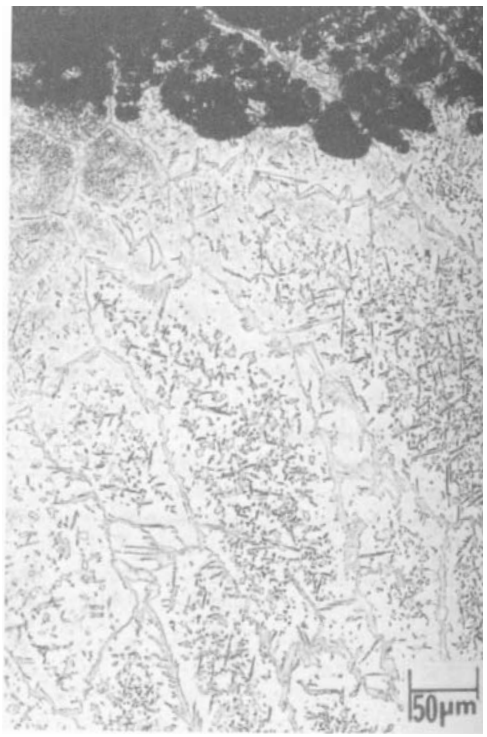

Fig. 11 Preferential corrosion of the ferrite phase in the weld metal of Ferralium alloy 255 gas tungsten arc welds in 10% $FeCl_3$ at room temperature. Base metal was 3.2 mm ($^1/_8$ in.) thick.

A study of the alloy 2205 weld microstructures (Ref 19) revealed why high arc energies were found to be beneficial to pitting resistance. Many investigations have indicated that the presence of chromium nitrides in the ferrite phase lowers the resistance to pitting of the weld metal and the HAZ in duplex stainless steels. In this study, both weld metal and HAZ produced by low arc energies contained an appreciable amount of chromium nitride (Cr_2N) (Fig. 13). The nitride precipitation vanished when an arc energy of 3 kJ/mm (75 kJ/in.) was used (Fig. 14).

The results of $FeCl_3$ tests on submerged-arc welds showed that all top weld surfaces passed the test at 30 °C (85 °F) without pitting attack, irrespective of arc energy in the range of 2 to 6 kJ/mm (50 to 150 kJ/in.). Surprisingly, the weld metal on the root side, which was the first to be deposited, did not pass the same test temperature.

The deteriorating effect of high arc energies on the pitting resistance of the weld metal on the root side was unexpected. Potentiostatic tests carried out in 3% sodium chloride (NaCl) at 400 mV versus saturated calomel electrode (SCE) confirmed these findings. Microexamination of the entire joint disclosed the presence of extremely fine austenite precipitates, particularly in the second weld bead (Fig. 15) but also

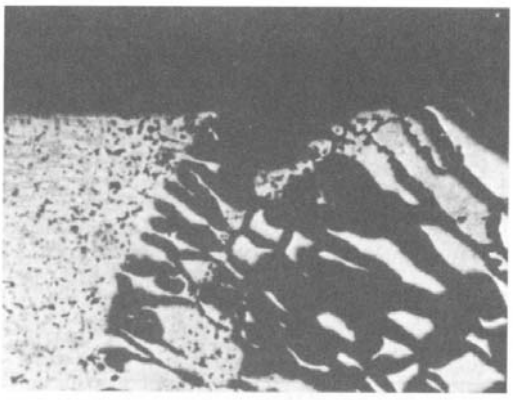

Fig. 12 Preferential attack of the continuous austenite phase in an autogenous gas tungsten arc weld in Ferralium alloy 255. Crevice corrosion test was performed in synthetic seawater according to ASTM D 1141 at 100 °C (212 °F). Etched with 50% HNO_3. 100×

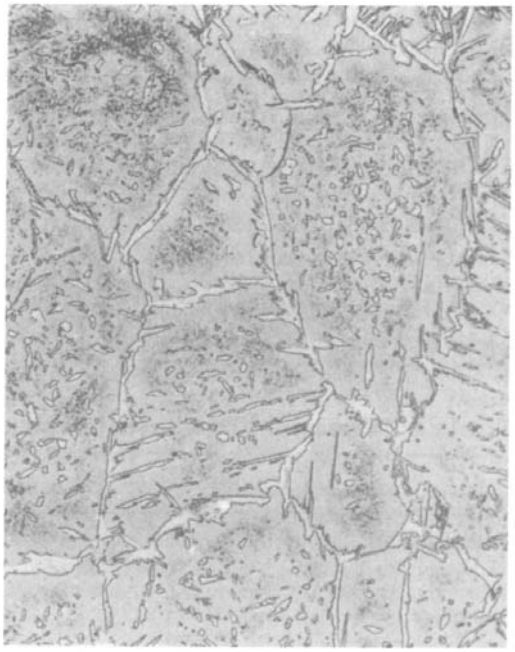

Fig. 13 Microstructure of bead-on-tube weld made by autogenous GTAW with an arc energy of 0.5 kJ/mm (13 kJ/in.). Note the abundance of chromium nitrides in the ferrite phase. See also Fig. 14. 200×. Source: Ref 19

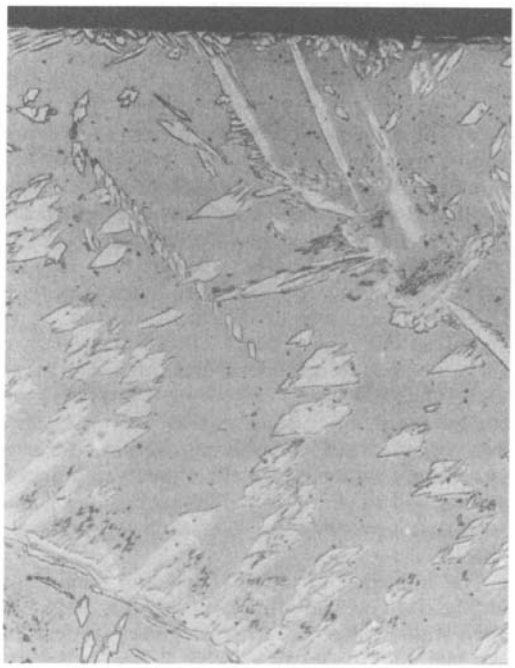

Fig. 14 Microstructure of bead-on-tube weld made by autogenous GTAW with an arc energy of 3 kJ/mm (76 kJ/in.). Virtually no chromium nitrides are present, which results in adequate pitting resistance. 200×. Source: Ref 19

in the first or root side bead. The higher the arc energy, the more austenite of this kind was present in the first two weld beads. Thus, nitrides give rise to negative effects on the pitting resistance, as do fine austenite precipitates that were presumably reformed at as low a temperature as approximately 800 °C (1470 °F).

Therefore, the resistance of alloy 2205 to pitting corrosion is dependent on several factors. First, Cr_2N precipitation in the coarse ferrite grains upon rapid cooling from temperatures above approximately 1200 °C (2190 °F) causes the most severe impairment to pitting resistance. This statement is supported by a great number of $FeCl_3$ tests as well as by potentiostatic pitting tests. Generally, it seems difficult to avoid Cr_2N precipitation in welded joints completely, particularly in the HAZ, the structure of which can be controlled only by the weld thermal cycle. From this point of view, it appears advisable to employ as high an arc energy as practical in each weld pass. In this way, the cooling rate will be slower (but not slow enough

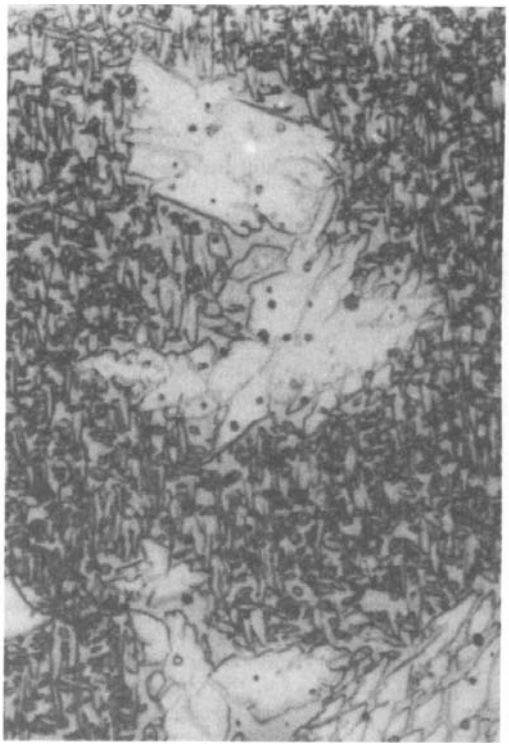

Fig. 15 Microstructure of the second weld bead of a submerged-arc weld joint in 200 mm (3/4 in.) duplex stainless steel plate. The extremely fine austenite precipitate was formed as a result of reheating from the subsequent weld pass, which used an arc energy of 6 kJ/mm (150 kJ/in.). 1000×. Source: Ref 19

to encounter 475 °C, or 885 °F, embrittlement), and the reformation of austenite will clearly dominate over the precipitation of Cr_2N.

In addition, if there were no restriction on maximum interpass temperature, the heat produced by previous weld passes could be used to decrease the cooling rate further in the critical temperature range above approximately 1000 °C (1830 °F). Preliminary tests with preheated workpieces have shown the significance of temperature in suppressing Cr_2N precipitation. Currently, the maximum recommended interpass temperature for alloy 2205 is 150 °C (300 °F). This temperature limit does not appear to be critical, and it is suggested that this limit could be increased to 300 °C (570 °F). The maximum recommended interpass temperature for Ferralium alloy 255 is 200 °C (390 °F). Excessive grain growth as a result of too much heat input must also be considered to avoid loss of ductility and impact toughness.

Second, the fine austenite precipitates found in the reheated ferrite when high arc energies and multipass welding were combined are commonly referred to as γ_2 the literature. The harmful influence of γ_2 on the pitting resistance has been noted with isothermally aged specimens, but as far as is known, it has never been observed in connection with welding. It is felt however, that γ_2 is less detrimental to pitting than Cr_2N. Moreover, γ_2 formation is believed to be beneficial to mechanical properties, such as impact strength and ductility.

A third factor that lowers pitting resistance is oxide scale. Where possible, all surface oxides should be removed by mechanical means or, preferably, by pickling. Root surfaces (in pipe), however, are generally inaccessible, and pitting resistance must rely on the protection from the backing gas during GTAW. It is therefore advisable to follow the current recommendation for stainless steels, which is a maximum of 25 ppm oxygen in the root backing gas.

Stress-Corrosion Cracking. The SCC resistance of alloy 2205 in aerated, concentrated chloride solutions is very good. The effect of welding on the SCC resistance is negligible from a practical point of view. The threshold stress for various welds, as well as for unwelded parent metal in the calcium chloride ($CaCl_2$) test, is as high as 90% of the tensile strength at the testing temperature. This is far above all conceivable design limits.

Also, in environments containing both hydrogen sulfide (H_2S) and chlorides, the resistance of welds is almost as high as for the parent metal. In this type of environment, however, it is important to avoid too high a ferrite content in weld metal and the HAZ. For normal welding of joints, the resulting ferrite- contents should not cause any problems. For weld repair situations, however, care should be taken so that extremely high ferrite contents (>75%) are avoided. To preserve the high degree of resistance to SCC, the ferrite content should not be less than 25%.

Another reason to avoid coarse weld microstructures (generated by excessive welding heat) is the resultant nonuniform plastic flow, which can locally increase stresses and induce preferential corrosion and cracking effects.

Use of High-Alloy Filler Metals. In critical pitting or crevice corrosion applications, the pitting resistance of the weld metal can be enhanced by the use of high Ni-Cr-Mo alloy filler metals. The corrosion resistance of such weldments in Ferralium alloy 255 is shown in Table 6. For the same weld technique, it can be seen that using high-alloy fillers does improve corrosion resistance. If high-alloy fillers are used, the weld metal will have better corrosion resistance

Table 6 Corrosion resistance of Ferralium alloy 255 weldments using various nickel-base alloy fillers and weld techniques

3.2 mm (0.125 in.) plates tested in 10% $FeCl_3$ for 120 h

	Critical pitting temperature					
	Gas tungsten arc		Gas metal arc		Submerged arc	
Filler metal	°C	°F	°C	°F	°C	°F
Hastelloy alloy G-3	30–35	85–95(a)	30	85(a)	30–35	85–95(b)
IN-112	30	85(a)	. . .	. . .	35–40	95–105(b)
Hastelloy alloy C-276	. . .	. . .	. . .	. . .	25–30	75–85(a)
Hastelloy alloy C-22	30	85(a)	. . .	. . .	35-40	95–105(a)

(a) Haz. (b) HAZ plus weld metal

than the HAZ and the fusion line. Therefore, again, proper selection of welding technique can improve the corrosion resistance of the weldments.

ACKNOWLEDGMENTS

Portions of this chapter were adapted from:

- D.N. Noble, Selection of Wrought Duplex Stainless Steels, *Welding, Brazing, and Soldering,* Vol 6, *ASM Handbook,* ASM International, 1993, p 471–481
- K. F. Krysiak, et al., Corrosion of Weldments, *Corrosion,* Vol 13, *Metals Handbook,* 9th ed., ASM International, 1987, p 344–368

REFERENCES

1. Wrought Duplex Stainless Steels, *Alloy Digest Source Book: Stainless Steels,* J.R. Davis, Ed., ASM International, 2000, p 317–356
2. D.K. Aldun, K.M. Makhamreh, and D.J. Morrison, Corrosion Resistance of Second-Generation Duplex Stainless Steel Weldments in NACE Solution, *International Trends in Welding Science and Technology,* Proc. 3rd Int. Conf. Trends in Welding Research, S.A. David and J.M. Vitek, Ed., ASM International, 1992, p 661–666
3. T.G. Gooch, Corrosion Resistance of Welds in Duplex Stainless Steels, *Duplex Stainless Steels '91*, Vol 1, J. Charles and S. Bernhardsson, Ed., Les Éditions de Physique, Oct 1991, p 325–346
4. J. Charles, Super Duplex Stainless Steels: Structure and Properties, *Duplex Stainless Steels '91*, Vol 1, J. Charles and S. Bernhardsson, Ed., Les Éditions de Physique, Oct 1991, p 151–168
5. J. Harston, E. Hutchins, and S. Sweeney, The Development and Construction of Duplex Stainless Steel Pipelines for Use Offshore in the Southern North Sea, *Proc. 3rd Int. Conf. Welding and Performance of Pipelines,* The Welding Institute, 1986
6. D.J. Kotecki, Heat Treatment of Duplex Stainless Steel Weld Metals, *Weld. J.,* Nov 1989, p 431s–441s
7. L. Odegarg and S.-A. Fager, Choice of Right Filler Metal for Joining Sandvik SAF 2507 to a Super Austenitic Stainless 6 Mo Steel, *ASM Materials Week '87,* ASM International, Oct 1987, p 441–449
8. R.N. Gunn, The Influence of Composition and Microstructure on the Corrosion Behaviour of Commercial Duplex Alloys, *Recent Developments in the Joining of Stainless Steels and High Alloys,* Edison Welding Institute, Columbus, Ohio, Oct 1992
9. "How to Weld 2205," Avesta Welding Trade Literature
10. T. Ogawa and T. Koseki, Effect of Composition Profiles on Metallurgy and Corrosion Behaviour of Duplex Stainless Steel Weld Metals, *Weld. J.,* Vol 88 (No. 5), May 1989, p 181s–191s
11. R.A. Walker and T.G. Gooch, Pitting Resistance of Weld Metal for 22Cr-5Ni Ferritic-Austenitic Stainless Steel, *Br. Corros. J.*, Vol 26 (No. 1), 1991, p 51–59
12. T.G. Gooch, Weldability of Duplex Ferritic-Austenitic Stainless Steels, *Duplex Stainless Steels,* R.A. Lula, Ed., American Society for Metals, 1983, p 573–602
13. L. Odegard and S.-A. Fager, "The Root Side Pitting Corrosion Resistance of Stainless Steel Welds," *Sandvik Steel Weld. Rep.,* No. 1, 1990
14. R. Dolling, V. Neubert, and P. Knoll, The Corrosion Behaviour of Super Duplex Steel Cast Alloys with a PREN>41, *Duplex Stainless Steels Conf. Proc.,* Vol 2, Les Éditions de Physique, Les Ulis Cedex, France, Oct 1991, p 1341–1351
15. T.G. Gooch, *Welding in the World,* Vol 24 (No. 7/8), 1986, p 148–167
16. P. Sentance, The Brae Field, *Stainl. Steel Eur.,* Vol 4 (No. 20), Sept 1992, p 38–41
17. C.D. Lundin, K. Kikuchi, and K. K. Kahn, "Measurement of Diffusible Hydrogen Content and Hydrogen Effects on the Cracking Potential of Duplex Stainless Steel Weldments," Phase 1 Report, The Welding Research Council, March 1991
18. R.A. Walker and T.G. Gooch, Hydrogen Cracking of Welds in Duplex Stainless Steel, *Corrosion,* Vol 47 (No. 8), Sept 1991, p 1053–1063
19. B. Lundquist, P. Norberg, and K. Olsson, "Influence of Different Welding Conditions on Mechanical Properties and Corrosion Resistance of Sandvik SAF 2205 (UNS S31803)," Paper 10, presented at the Duplex Stainless Steels '86 Conference, the Hague, Netherlands, Oct 1986

20. N. Sridhar, L.H. Flasche, and J. Kolts, Effect of Welding Parameters on Localized Corrosion of a Duplex Stainless Steel, *Mater. Perform.,* Dec 1984, p 52– 55

SELECTED REFERENCES

- R. Bradshaw, R.A. Cottis, and M.J. Schofield, Stress Corrosion Cracking of Duplex Stainless Steel Weldments in Sour Conditions, *Mater. Perform.,* April 1996, p 65–70
- R.M. Davison and J.D. Redmond, Practical Guide to Using Duplex Stainless Steels, *Mater. Perform.,* Jan 1990, p 57–62
- B. Gissler and B. Bouldin, Corrosion Performance of Welded Super Duplex Stainless Steel with Multiple Re-weld/Re-work Weld Repairs in Aqueous H_2S and $FeCl_3$ Environments, Paper No. 04143, presented at Corrosion 2004, NACE International
- H. Inoue, T. Ogawa, and R. Matsuhashi, Corrosion Behavior of Duplex Stainless Steel Welds in Highly Concentrated Sulfuric Acid, *International Trends in Welding Science and Technology, Proc. 3rd Int. Conf.* Trends in Welding Research, S.A. David and J.M. Vitek, Ed., ASM International, 1992, p 667–671

Corrosion of Weldments
J.R. Davis, editor, p 115-124
DOI:10.1361/corw2006p115

CHAPTER 6

Corrosion of Martensitic Stainless Steel Weldments

MARTENSITIC STAINLESS STEELS are essentially Fe-Cr-C alloys that possess a body-centered tetragonal (bct) crystal structure (martensitic) in the hardened condition. They are ferromagnetic and generally resistant to corrosion only in relatively mild environments. Martensitic stainless steels are similar to plain carbon or low-alloy steels that are austenitized, hardened by quenching, and then tempered for increased ductility and toughness. Chromium content is generally in the range of 10.5 to 18%, and carbon content can exceed 1.2%. The chromium and carbon contents are balanced to ensure a martensitic structure. Elements such as niobium, silicon, tungsten, and vanadium can be added to modify the tempering response after hardening. Small amounts of nickel and molybdenum can be added to improve corrosion and toughness. However, the addition of these elements is somewhat restricted, because higher amounts result in a microstructure that is not fully martensitic. Sulfur or selenium is added to some grades to improve machinability. Martensitic stainless steels are specified when the application requires a good combination of tensile strength, creep, and fatigue strength properties in combination with moderate corrosion resistance and heat resistance up to approximately 650 °C (1200 °F).

Grade Designations

Martensitic stainless steels can be divided into standard SAE grades and nonstandard grades. Most of the nonstandard grades have been given UNS designations. Table 1 lists the compositions of both standard and representative nonstandard grades. Figure 1 shows the relationships among the various standard grades.

Standard Grades

The standard grades can be further subdivided into low-carbon, nickel-free martensitic stainless steels; low-carbon, nickel-containing martensitic stainless steels; and the high-carbon, high-chromium martensitic stainless steels.

The low-carbon, nickel-free martensitic grades include types 403, 410, 416, 416Se, 420, and 420F. As shown in Fig. 1, the general-purpose alloy of this group, and indeed the most commonly used, is type 410, which contains approximately 12 wt% Cr and 0.1% C to provide strength. A free-machining version of type 410 is type 416, which contains higher amounts of sulfur (about 0.15 to 0.30% S). Type 416Se is the free-machining variant containing selenium. Type 403 contains less silicon than type 410 and is used in the form of forgings for turbine parts. Type 420, which has a higher carbon content than type 410, is the original cutlery grade, while the sulfur-containing, free-machining grade is type 420F.

The low-carbon, nickel-containing martensitic grades include type 414, 422, and 431. Type 414 is a modified version of type 410 to which 2% Ni has been added to improve the corrosion resistance, particularly to salt spray and to mild reducing acids. Type 422 contains nickel for corrosion resistance as well as molybdenum, vanadium, and tungsten to improve elevated-temperature mechanical properties and/or corrosion resistance. Type 431 has quite good corrosion resistance as a result of its higher chromium content plus the 2% Ni. It has the highest total alloy content of the standard hardenable chro-

mium grades and for that reason is the most corrosion resistant of any of these steels.

High-carbon high-chromium martensitic grades include types 440A, 440B, and 440C which contain from 16 to 18% Cr and a minimum of 0.75% Mo. The carbon level, and consequently strength and hardness increase in the 440A (0.60% C, 51 HRC), 440B (0.80% C, 55 HRC), and 440C (1.0% C, 60 HRC) series. The high-carbon, high-chromium grades are used for applications such as bearings, where high hardness and wear resistance are required. Nonstandard free-machining varieties of higher carbon grades are also available (see alloys 440F and 440FSe in Table 1).

Nonstandard Grades

Examples of martensitic grades not covered by SAE designations include:

- Modified versions of type 422, for example, Lapelloy (UNS S42300), Moly Ascoloy (UNS S41500), Greek Ascoloy (UNS S41800), HT9 (DIN 1.4935), and 248 SV (DIN 1.4418) used for elevated-temperature applications such as steam turbines, jet en-

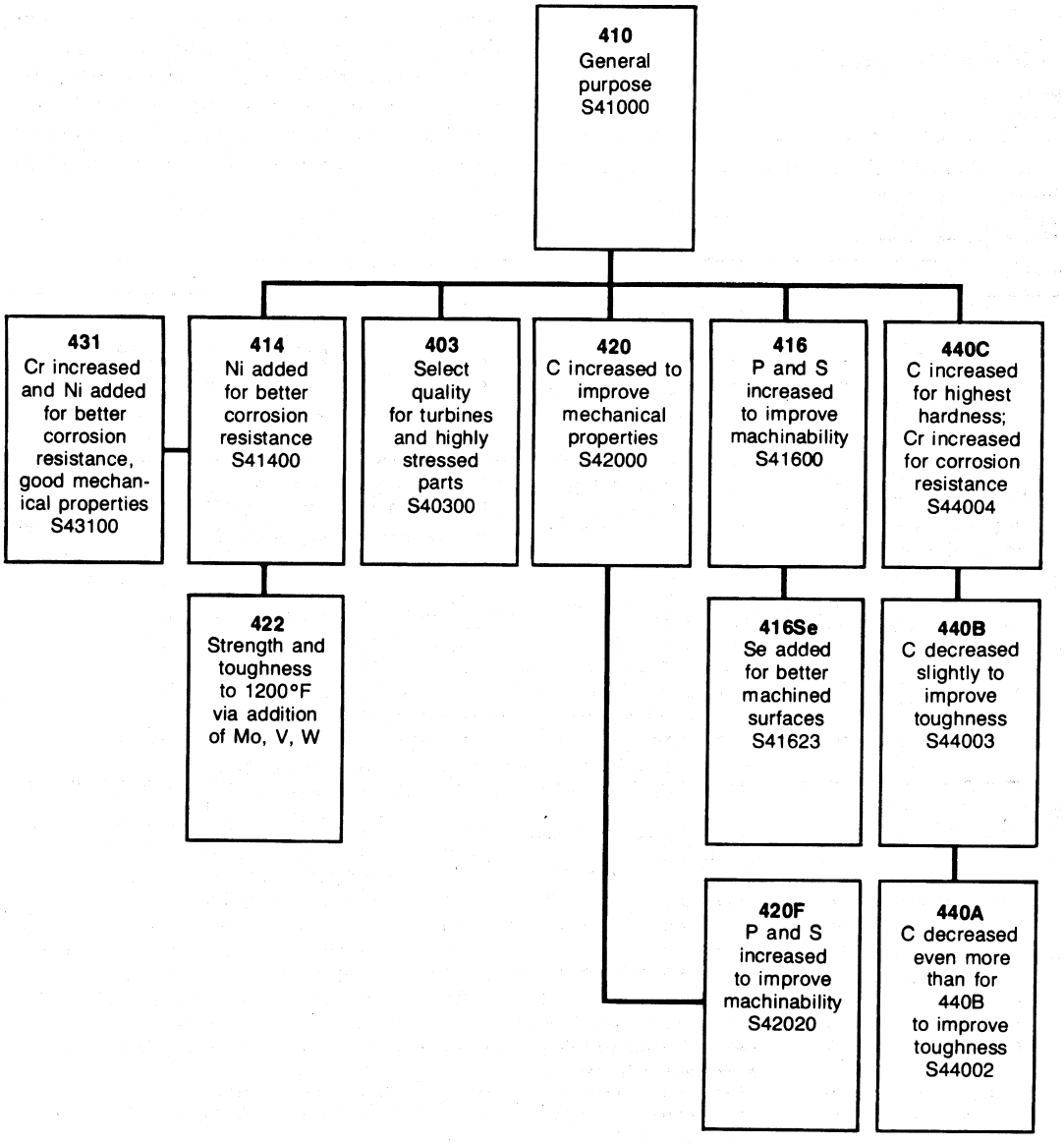

Fig. 1 Family relationships for standard martensitic stainless steels

gines, gas turbines, and pressure-containment applications including steam piping and steam generator reheater and super-heater tubing used in fossil fuel power plants
- Modified versions of type 410, for example, type 410S (UNS S41008) and 410 Cb (XM-30 or UNS S41040)
- Free-machining versions of type 440, for example, type 440F (UNS S44020) and type 440FSe (UNS S44023)
- Corrosion-resistant, wear-resistant grades used for bearing and gearing applications, for example, CRB-7 (a modified version of type 440C), BG42 (UNS S42700), and Pyrowear 675 (UNS S42670)
- Recently developed "supermartensitic" grades used for oil and gas pipelines. These alloys contain nominally 11 to 13% Cr, 2 to 6% Ni, 1 to 3% Mo, and 0.01 to 0.03 % C. Additional information on these grades can be found in the section "Corrosion Behavior" later in this chapter.

Table 1 lists the compositions of nonstandard grades.

Properties

Mechanical Properties. In the annealed condition, martensitic stainless steels have a ten-

Table 1 Chemical compositions of martensitic stainless steels

UNS No.	Type/designation	Composition(a), %							
		C	Mn	Si	Cr	Ni	P	S	Other
Standard (SAE) grades									
S40300	403	0.15	1.00	0.50	11.5–13.0	. . .	0.04	0.03	. . .
S41000	410	0.15	1.00	1.00	11.5–13.5	. . .	0.04	0.03	. . .
S41400	414	0.15	1.00	1.00	11.5–13.5	1.25–2.50	0.04	0.03	. . .
S41600	416	0.15	1.25	1.00	12.0–14.0	. . .	0.06	0.15 min	0.6 Mo(b)
S41623	416Se	0.15	1.25	1.00	12.0–14.0	. . .	0.06	0.06	0.15 min Se
S42000	420	0.15 min	1.00	1.00	12.0–14.0	. . .	0.04	0.03	. . .
S42020	420F	0.15 min	1.25	1.00	12.0–14.0	. . .	0.06	0.15 min	0.6 Mo(b)
S42200	422	0.20–0.25	1.00	0.75	11.5–13.5	0.5–1.0	0.04	0.03	0.75–1.25 Mo; 0.75-1.25 W; 0.15–0.3 V
S43100	431	0.20	1.00	1.00	15.0–17.0	1.25–2.50	0.04	0.03	. . .
S44002	440A	0.60–0.75	1.00	1.00	16.0–18.0	. . .	0.04	0.03	0.75 Mo
S44003	440B	0.75–0.95	1.00	1.00	16.0–18.0	. . .	0.04	0.03	0.75 Mo
S44004	440C	0.95–1.20	1.00	1.00	16.0–18.0	. . .	0.04	0.03	0.75 Mo
Nonstandard grades									
S41008	Type 410S	0.08	1.00	1.00	11.5–13.5	0.60	0.040	0.030	. . .
S41040	Type 410Cb (XM-30	0.15	1.00	1.00	11.5–13.5	. . .	0.040	0.030	0.05–0.20 Nb
DIN 1.4935(c)	HT9	0.17–0.23	0.30–0.80	0.10–0.50	11.0–12.5	0.30–0.80	0.035	0.035	0.80–1.20 Mo; 0.25–0.35 V; 0.50–1.00 Mo
S41500	Moly Ascology	0.05	0.50–1.00	0.60	11.5–14.0	3.50–5.50	0.030	0.030	
$41610	416 Plus X (XM-6)	0.15	1.5–2.5	1.00	12.0–14.0	. . .	0.060	0.15 min	0.6 Mo
S41800	Greek Ascoloy	0.15–0.20	0.50	0.50	12.0–14.0	1.8–2.2	0.040	0.030	2.5–3.5 W
S42010	TrimRite	0.15–0.30	1.00	1.00	13.5–15.0	0.25–1.00	0.040	0.030	0.40–1.00 Mo
S42023	Type 429 F Se	0.3–0.04	1.25	1.00	12.0–14.0	. . .	0.060	0.060	0.15 min Se; 0.06 Zr; 0.6 Cu
S42300	Lapelloy	0.27–0.32	0.95–1.35	0.50	11.0–12.0	0.50	0.05	0.025	2.5–3.0 Mo; 0.2–0.3 V
S42670	Pyrowear 675	0.05–0.09	0.50–1.00	0.10–0.70	12.0–14.0	2.00–3.00	0.015	0.010	4.00–7.00 Co; 1.50–2.50 Mo; 0.40– 0.80 V
S42700	BG42	1.10–1.20	0.30–0.60	0.20–0.40	14.0–15.0	0.40	0.015	0.010	3.75–4.25 Mo; 0.35 Cu; 1.10–1.30 V
S44020	Type 440F	0.95–1.20	1.25	1.00	16.0–18.0	0.75	0.040	0.10–0.35	0.08 N
S44023	Type 440F Se	0.95–1.20	1.25	1.00	16.0–18.0	0.75	0.040	0.030	0.15 min Se; 0.60 Mo

See Table 5 for compositions of supermartensitic stainless steels. (a) Single values are maximum values unless otherwise indicated. (b) Optional. (c) German (DIN) specification

sile yield strength of approximately 275 MPa (40 ksi) and can be moderately hardened by cold working. However, martensitic alloys are typically heat treated by both hardening and tempering to yield strength levels up 1900 MPa (275 ksi), depending on the carbon level. These alloys have good ductility and toughness properties, which decrease as strength increases. Depending on the heat treatment, hardness values range from approximately 150 HB (80 HRB) for materials in the annealed condition to levels greater than 600 HB (60 HRC) for fully hardened materials.

Corrosion resistance and oxidation resistance are described for both standard and nonstandard martensitic stainless steels in Table 2. Typical applications for martensitic grades are also listed.

General Welding Considerations

Martensitic stainless steels are considered the most difficult to weld of the five families of stainless steels because they are chemically balanced to become harder, stronger, and less ductile through hardening. The thermal cycle of heating and rapid cooling, which occurs within the confined heat-affected zone (HAZ) during welding, is equivalent to a quenching cycle. The high-carbon martensitic structure that is produced is extremely brittle, regardless of the prior condition of the metal (annealed, hardened, or hardened and tempered). Cracking can occur when the heated weldment and the surrounding martensitic HAZ are unable to contract to the same degree and at the same rate as the weld metal. Preheat and postweld cooling rates are important vehicles for controlling these shrinkage stresses.

Increasing carbon content in martensitic stainless steels generally results in increased hardness and reduced ductility. Thus, the three type 440 stainless steels are seldom considered for applications that require welding, and filler metals of the type 440 compositions are not readily available.

Both preheating and postweld heat treatment (PWHT) are critical to successful welds. The usual preheating temperature range of martensitic steels is 200 to 300 °C (400 to 600 °F). The temperature varies according to the material composition (particularly the carbon content) and the material thickness. The function of the PWHT is to temper the martensite in the weld metal and HAZ, in order to increase the toughness and decrease residual stresses associated with welding.

The following correlations of preheating and PWHT practice with carbon contents and welding characteristics of martensitic stainless steels can be used:

- *Carbon content below 0.10%:* Neither preheating nor PWHT is required except for very heavy sections; martensitic stainless steels with carbon contents this low are not standard.
- *Carbon content 0.10 to 0.20%:* Preheat to 260 °C (500 °F). Weld at this temperature, and slow cool below 65 °C (150 °F). Temper.
- *Carbon content 0.20 to 0.50%:* Preheat to 260 °C (500 °F), and weld at this temperature. Slow cool below 65 °C (150 °F). Austenitize and temper.
- *Carbon content over 0.50%:* Preheat to 260 °C (500 °F), and weld with high heat input. Anneal without letting the weldment cool below 260 °C (500 °F). Then, austenitize and temper.

Both austenitic and martensitic filler metals are used for welding martensitic stainless steels. The use of austenitic filler metal (AWS E/ER 308, 309, and 310) is preferable to the use of martensitic consumables of matching composition when weld metal cracking must be avoided. Matching filler metals are used when the strength of the weld metal must be similar to that of the base metal or when maximum weld toughness is specified. Only AWS E410 and E410NiMo type are available in covered form. These compositions, as well as AWS ER420, are available in solid wires.

Corrosion Behavior

Hydrogen-Induced Cracking. Weld-area cracking in martensitic stainless steels is primarily due to the presence of hydrogen in the hardened structure (Ref 1). Hydrogen-induced cold cracks form in welds when the weldment is at or near room temperature (typically, less than 150 °C, or 300 °F). Cracking may occur almost immediately or hours after cooling. In steel, cold cracks depend on the presence of a tensile stress, a susceptible microstructure, and suffi-

Table 2 Corrosion/oxidation resistance and typical applications of martensitic stainless steels

UNS No.	Corrosion resistance	Oxidation resistance	Typical applications
S40300	S40300 is resistant to the corrosive action of the atmosphere, fresh water, and various alkalis and mild acids but is not recommended where resistance to severe corrodents is a prime factor. S40300 does not possess the superior corrosion resistance of the austenitic chromium-nickel stainless steels. It exhibits best corrosion resistance in the hardened and stress relieved condition. Tempering between approximately 400–570 °C (750–1050 °F) lowers its resistance in some media.	This grade has good oxidation resistance up to 680 °C (1250 °F) in continuous service. Scaling becomes excessive above approximately 760 °C (1400 °F) in intermittent service.	Turbine blades and highly stressed sections in gas turbines, furnace parts, and burners operating below 650 °C (1200 °F), valve parts, cutlery, fasteners, hardware, oil refinery equipment, mining machinery, screens, pump parts, fingernail files, sporting goods such as fishing poles, and rifle barrels
S41000	S41000 is resistant to the corrosive action of the atmosphere, fresh water, and various alkalis and mild acids but is not recommended where resistance to severe corrodents is a prime factor. S41000 does not possess the superior corrosion resistance of the austenitic chromium-nickel stainless steels. It exhibits best corrosion resistance in the hardened and stress relieved condition. Tempering between approximately 400–570 °C (750–1050 °F) lowers its resistance in some media.	This grade has good oxidation resistance up to 680 °C(1250 °F) in continuous service. Scaling becomes excessive above approximately 760 °C (1400 °F) in intermittent service.	Turbine blades and highly stressed sections in gas turbines, furnace parts, and burners operating below 650 °C (1200 °F), valve parts, cutlery, fasteners, hardware, oil refinery equipment, mining machinery, screens, pump parts, fingernail files, sporting goods such as fishing poles, and rifle barrels
S41040	S41040 is resistant to the corrosive action of the atmosphere, fresh water, and various alkalis and mild acids but is not recommended where resistance to severe corrodents is a prime factor. S41040 does not possess the superior corrosion resistance of the austenitic chromium-nickel stainless steels. It exhibits best corrosion resistance in the hardened and stress relieved condition. Tempering between approximately 400–570 °C (750–1050 °F) lowers its resistance in some media.	This grade has good oxidation resistance up to 680 °C (1250 °F) in continuous service. Scaling becomes excessive above approximately 760 °C (1400 °F) in intermittent service.	Aircraft and missile components, steam turbine blades, valve parts, and fasteners
S41400	S41400 is resistant to the corrosive action of the atmosphere, fresh water, and various alkalis and mild acids to a slightly greater extent than S41000. It exhibits best corrosion resistance in the hardened and tempered condition. Tempering between approximately 400–570 °C (750–1050 °F) lowers its resistance in some media.	This grade has good oxidation resistance up to approximately 680 °C (1250 °F) in continuous service. Scaling becomes excessive above 760 °C (1400 °F).	Beater bars, fasteners, gage parts, mild springs, mining equipment, scissors, scraper knives, shafts, spindles, and valve seats
S41500	S41500 is resistant to the corrosive action of the atmosphere, fresh water, and various alkalis and mild acids but is not recommended where resistance to severe corrodents is a prime factor. S41500 does not possess the superior corrosion resistance of the austenitic chromium-nickel stainless steels. It exhibits best corrosion resistance in the hardened and stress relieved condition. Tempering between approximately 400–570 °C (750–1050 °F) lowers its resistance in some media.	This grade has good oxidation resistance up to 680 °C (1250 °F) in continuous service. Scaling becomes excessive above approximately 760 °C (1400 °F) in intermittent service.	Parts with improved weldability over S41000
S41600	S41600 is resistant to the corrosive action of the atmosphere, fresh water, various alkalis, and mild acids. The fine finish obtainable on this grade enhances corrosion resistance.	This grade has good oxidation resistance up to 650 °C (1200 °F) in continuous service. Scaling becomes excessive above 760 °C (1400 °F in intermittent service.	Nongalling and nonseizing corrosion resistant parts machined on automatic screw machines. Various valve parts such as bodies, stems and trim, many types of threaded fasterners, shafts, and pump components are among the applications served by this free machining stainless steel.
S41623	S41623 is resistant to the corrosive action of the atmosphere, fresh water, various alkalis, and mild acids. The fine finish obtainable on this grade enhances corrosion resistance.	This grade has good oxidation resistance up to 650 °C (1200 °F) in continuous service. Scaling becomes excessive above 760 °C (1400 °F) in intermittent service.	Improved surface finish over that of S41600
S42000	S42000 attains its full corrosion resistance in the hardened and polished condition. Much lower resistance is shown by annealed material and material having its surface contaminated by foreign particles. For this reason, it is advisable to passivate final parts. For most applications, S42000 exhibits corrosion resistance about the same as that of S41000. S42000 is melted to slightly higher chromium than S41000 in order to offset the detrimental effect of higher carbon.	This grade has good oxidation resistance up to approximately 650 °C (1200 °F) in continuous service. Scaling becomes excessive above 760 °C (1400 °F).	Cutlery, hand tools, dental and surgical instruments, valve trim and parts, shafts, and plastic mold steel

(continued)

Table 2 (continued)

UNS No.	Corrosion resistance	Oxidation resistance	Typical applications
S42010	S42010 attains its full corrosion resistance in the hardened and polished condition. Much lower resistance is shown by annealed material and material with a surface contaminated by foreign particles. For this reason, it is advisable to passivate final parts. For most applications, S42010 exhibits corrosion resistance about the same as that of S41000. S42010 is melted to slightly higher chromium than S41000 in order to offset the detrimental effect of higher carbon.	This grade has good oxidation resistance up to approximately 650 °C (1200 °F) in continuous service. Scaling becomes excessive above 760 °C (1400 °F).	Fasteners, cutlery, valves, gages, and guides
S42020	S42020 attains its full corrosion resistance in the hardened and polished condition. Much lower resistance is shown by annealed material and material having surfaces contaminated by foreign particles. For this reason, it is advisable to passivate final parts. For most applications, S42020 exhibits corrosion resistance about the same as that of S41000. S42020 is melted to slightly higher chromium than S41000 in order to offset the detrimental effect of higher carbon.	This grade has good oxidation resistance up to approximately 650 °C (1200 °F) in continuous service. Scaling becomes excessive above 760 °C (1400 °F).	Fasteners, cutlery, valves, gages, and guides
S42200	S42200 is resistant to the corrosive action of the atmosphere, fresh water, various alkalis, and mild acids but is not recommended where resistance to severe corrodents is a prime factor. S42200 does not possess the superior corrosion resistance of the austenitic chromium-nickel stainless steels. It exhibits best corrosion resistance in the hardened and stress relieved condition. Tempering between approximately 400–570 °C (750–1050 °F) lowers its resistance in some media.	This grade has good oxidation resistance up to 680 °C (1250 °F) in continuous service. Scaling becomes excessive above approximately 760 °C (1400 °F) in intermittent service.	Turbine blades and highly stressed sections in gas turbines, furnace parts, and burners operating below 650 °C (1200 °F), valve parts, cutlery, fasteners, hardware, oil refinery equipment, mining machinery, screens, pump parts, fingernail files, sporting goods such as fishing poles, and rifle barrels
S43100	S43100 is resistant to the corrosive action of the atmosphere, various alkalis, and mild acids. It has better resistance to corrosion from marine atmosphere and is considered to have better resistance to stress corrosion than the other martensitic stainless steels.	This grade has good oxidation resistance up to approximately 820 °C (1500 °F), in continuous service. Scaling becomes excessive above approximately 870 °C (1600 °F).	Aircraft fittings, beater bars, fasteners, conveyor parts, valve parts, pump shafts, and marine hardware
S44002	S44002 attains its full corrosion resistance in the hardened and polished condition. Much lower resistance is shown by annealed material and material having surfaces contaminated by foreign particles. For this reason, it is advisable to passivate final parts. The grade is resistant to the corrosive action of the atmosphere, fresh water, perspiration, mild acids, fruit and vegetable juices, foodstuffs, etc.	This alloy is not normally used for elevated temperature service since its resistance to corrosion as well as its hardness and strength are lowered by exposure above approximately 430 °C (800 °F). The grade scales appreciably at temperatures above approximately 760 °C (1400 °F).	Cutlery, bearings, valves, seaming rolls, and surgical and dental instruments
S44003	S44003 attains its best corrosion resistance in the hardened and polished condition. Much lower resistance to certain media is shown by annealed material or material having surfaces contaminated by foreign particles. For this reason it is advisable to passivate final parts. The grade is resistant to the corrosive action of the atmosphere, fresh water, perspiration, mild acids, fruit and vegetable juices, foodstuffs, etc.	This alloy is not normally used for elevated temperature service since its resistance to corrosion is lowered by exposure above 430 °C (800 °F). The grade scales appreciably at temperatures above approximately 760 °C (1400 °F).	Bearings, cutlery, spatula blades, and food processing knives
S44004	S44004 attains its full corrosion resistance in the hardened and polished condition. Much lower resistance to certain media is shown by annealed material or material having surfaces contaminated by foreign particles. For this reason it is advisable to passivate final parts. The grade is resistant to the corrosive action of the atmosphere, fresh water, perspiration, mild acids, fruit and vegetable juices, foodstuffs, etc.	This alloy is not normally used for elevated temperature service, since its resistance to corrosion is lowered by exposure above 430 °C (800 °F). The grade scales appreciably at temperatures above approximately 760 °C (1400 °F).	Cutlery, bearings, nozzles, valve parts, pivot pins, and balls and seats for oil well pumps
S44020	S44020 attains its full corrosion resistance in the hardened and polished condition. Much lower resistance to certain media is shown by annealed material or material having surfaces contaminated by foreign particles. For this reason it is advisable to passivate final parts. The grade is resistant to the corrosive action of the atmosphere, fresh water, perspiration, mild acids, fruit and vegetable juices, foodstuffs, etc.	This alloy is not normally used for elevated temperature service, since its resistance to corrosion is lowered by exposure above 430 °C (800 °F). The grade scales appreciably at temperatures above approximately 760 °C (1400 °F).	Cutlery, bearings, nozzles, valve parts, pivot pins, and balls and seats for oil well pumps

cient hydrogen in the weld. Elimination of one or more of these factors greatly reduces crack susceptibility. The stress may arise from restraint by other components of a weldment or from the simple thermal stresses created by welding in a butt, groove, or "T" joint.

The susceptibility of the microstructure to cold cracking relates to the solubility of hydrogen and the possibility of supersaturation. Austenite, in which hydrogen is highly soluble, is least susceptible to cold cracking, and martensite, in which the solubility is lower, is most susceptible, because the rapid cooling necessary for the austenite-to-martensite transformation traps the hydrogen in a state of supersaturation in the martensite. Because the solubility of hydrogen in body-centered crystal martensite is low and diffusivity is high, austenitic filler metals are often selected to weld martensitic stainless steels. Refer to the discussion on filler metals in the section "General Welding Considerations" for additional information.

The presence of hydrogen in a weld is generally due to moisture that is introduced in the shielding gas (or the electrode coating or flux), dissociated by the arc to form elemental hydrogen, and dissolved by the molten weld pool and by the adjacent region in the HAZ. In the supersaturated state, the hydrogen diffuses to regions of high stress, where it can initiate a crack. Continued diffusion of the hydrogen to the region of stress concentration at the crack tip extends the crack. This behavior means that hydrogen-induced cold cracking is time dependent—that is, time is needed for hydrogen diffusion—and the appearance of detectable cracks can be delayed until long after the weld has passed inspection. Additional information on the mechanisms of hydrogen cracking of weldments can be found in Ref 2 and 3.

For most commercial steels, the avoidance of hydrogen-induced cold cracking is based on the control of hydrogen (Ref 1). The sources of hydrogen (water, oils, greases, waxes, and rust that contains hydrogen or hydrates) should be eliminated. The hydrogen potential also can be minimized by using low-hydrogen, inert-gas welding processes, such as gas-tungsten arc welding (GTAW) or gas-metal arc welding (GMAW), or by paying stringent attention to consumable drying and baking for flux-shielded welding processes, such as shielded metal arc welding (SMAW) or flux-cored arc welding (FCAW). In addition, preheating must be applied to slow the rate of cooling. This allows more time for hydrogen to diffuse away from the weld area during cooling within the austenite range and, especially, following transformation to martensite.

Preheating is generally carried out in the temperature range from 200 to 300 °C (400 to 600 °F). In multipass welds, interpass temperatures must be maintained at the same level, and it is frequently beneficial to hold this temperature for some time after arc extinction to permit further hydrogen diffusion out of the joint. Postweld tempering is carried out to improve weld-area toughness. For higher-carbon steels (>0.2 wt% C), this process should be applied as soon as possible after welding to avoid the possibility of hydrogen-induced cracking from atmospheric corrosion. The weld must be cooled to a sufficiently low temperature to induce the austenite-to-martensite transformation (in principle, below the martensite completion point, M_f prior to PWHT.

Sulfide Stress Corrosion (SSC) Resistance of Type 410 Weldments. A study was carried out to determine the effect of various heat treatments on the SSC resistance of type 410 weldments in sour service conditions. (Ref 4). One 12.5 mm (½ in.) thick plate was used for all 410 stainless steel testing. The welding process was multipass, manual, GTAW welding with matching filler metal ER410.

Base metal heat treating was done in accordance with the requirements of NACE Standard MR0175 for sour gas service. Samples were austenitized at 900°C or 982°C (1652 °F or 1800 °F), quenched and double tempered prior to welding. After welding the samples were subjected to:

- Austenitize at 900°C or 982°C (1652 °F or 1800 °F) and double temper
- Stress relieve at 662°C and 649°C (1224 °F and 1200 °F) or 676 °C and 649 °C (1248 °F and 1200 °F)
- Stress relieve at 649°C (1200 °F)

Heat treat conditions and mechanical properties are listed in Table 3.

The SSC testing was done in accordance with the requirements of NACE Standard MR0175 for sour gas service. The results of the SSC tests are shown in Table 4. The threshold stress included in Table 4 is defined as the maximum stress at which a specimen completes a 720 h exposure without rupture.

Comparing the results of base metal with a 900 °C (1652 °F) austenitizing cycle, specimen A1, (threshold 65% of yield strength) and weldments with only stress relief treatments after welding, specimens A3 and A4, (threshold 10% and 15% of yield strength), there is a significant decrease in the SSC resistance of the weldments. A reheat treatment after welding consisting of austenitizing at 900 °C (1652 °F) and double tempering, specimen A2, increases the SSC threshold to 45% of yield strength.

Similar results occur with the 982 °C (1800 °F) austenitizing cycle material. Base metal SSC resistance, specimen B1 (threshold 40% of yield strength), is greater than that of weldments with only stress relieving after welding, specimens B3 and B4 (threshold 20% of yield strength). Austenitizing and double tempering subsequent to welding, specimen B2, increases the SSC threshold to 40% of yield strength, matching the base metal.

Austenitizing at 900 °C (1652 °F), specimen A1, yields a higher base metal SSC threshold (65% of yield strength) than austenitizing at 982 °C (1800 °F), specimen B1 (40% of yield strength). Weldments with the respective austenitizing temperatures, specimens A2 and B2, show a slight increase in SSC threshold for the 900 °C (1652 °F) treatment, 45% of yield strength compared to 40% of yield strength.

Based on these results, the following conclusions were drawn:

- The SSC resistance of 410 stainless steel weldments subjected to only stress relieving after welding is much less than the base metal.
- An austenitizing heat treatment subsequent to welding is required for 410 stainless steel to achieve weldment SSC resistance approaching that of base metal.
- 410 stainless steel base metal austenitized at 900 °C (1652 °F) has a significantly higher SSC resistance than that austenitized at 982 °C (1800 °F), when subjected to the same tempering treatment.
- 410 stainless steel weldments austenitized at 900 °C (1652 °F) have a slightly higher SSC resistance than weldments austenitized at 982 °C (1800 °F) when subjected to the same tempering treatment.

Supermartensitic stainless steels are a family of steels that are normally divided into three types:

- Low alloyed grades (11Cr-2Ni with molybdenum below 1 wt%) used for sweet service
- Medium alloyed grades (13Cr-4.5Ni-1.5Mo) used for intermediate sour service applications
- Highly alloyed grades (12Cr-6Ni-2.5Mo) for applications involving increasing hydrogen sulfide (H_2S) and decreasing pH

Carbon contents for all three grades range from about 0.01 to 0.03. Compositions of selected supermartensitic stainless grades are given in Table 5.

The low carbon content improves weldability by ensuring resistance against hydrogen-induced cracking. Nickel is added to compensate for the low carbon content and prevent high levels of ferrite. Molybdenum improves corrosion resistance (Ref 5). Some alloys may contain additions of titanium and copper to promote some precipitation strengthening. Yield strengths in the range of 620 to 760 MPa (90 to 110 ksi) can be achieved with ductility from 20 to 25%. These alloys have been used for oil and gas pipeline applications. The combination of strength and corrosion resistance has lead to their use as replacement alloys for duplex stainless steels.

Table 3 Heat treat cycles and mechanical properties for type 410 stainless steel

Specimen identification	Heat treat prior to welding, °C	Heat treat after welding, °C	Tensile strength, MPa (ksi)	Yield strength, MPa (ksi)	Elongation, %
A1 (base metal)	900, 676, 649	. . .	716 (104)	572 (83)	25
A2 (weldment)	900, 676, 649	900, 676, 649	702 (102)	565 (82)	21
A3 (weldment)	900, 676, 649	662, 649	716, (104)	572 (83)	27
A4 (weldment)	900, 676, 649	649	702 (102)	558 (81)	20
B1 (base metal)	982, 676, 649	. . .	710 (103)	585 (85)	22
B2 (weldment)	982, 676, 649	982, 676, 649	730 (106)	592 (86)	23
B3 (weldment)	982, 676, 649	662, 649	689 (100)	544 (79)	26
B4 (weldment)	982, 676, 649	649	689 (100)	751 (76)	23

Source: Ref 4

The low carbon content must be offset by high nickel contents in order to prevent excessive ferrite formation in the weld metal and HAZ. The addition of such high levels of nickel to compensate for low carbon significantly reduces the temperature at which austenite forms upon reheating (A_{Cl}). This can present problems during PWHT, since austenite may reform at the PWHT temperature. Upon subsequent cooling, this austenite will transform to untempered martensite resulting in reduced toughness and ductility. The following relationship has been proposed to determine the A_{Cl} for these alloys (Ref 6):

$$A_{Cl}\ (°C) = 850–1500\ (C+N) – 50\ Ni – 25\ Mn + 25Si + 25Mo + 20(Cr-10)$$

Despite the low carbon levels, a PWHT is normally recommended to optimize ductility, toughness, and corrosion resistance. For pipeline materials for oil and gas production, short term PWHTs in the range of 5 to 10 min at temperatures between 600 and 700 °C (1110 and 1290 °F) are carried out.

The supermartensitic stainless steels are most frequently welded by GTAW and GMAW. Traditionally, these metals have been welded with duplex or superduplex stainless steel filler metals, which has caused a strength undermatch of the weld metal compared to the base metal and its HAZ. Matching filler metals have thus been developed and undergone extensive testing (Ref 7, 8)). Much lower stresses and strains are produced during welding and cooling with the use of supermartensitic stainless steels filler metals instead of duplex filler metals (Ref 8). In addition, complex tri-phase microstructures in the HAZ can be eliminated resulting in improved resistance to stress corrosion cracking in supermartensitic weldments.

These alloys are resistant to weld solidification and liquation cracking, and are inherently resistant to hydrogen-induced cracking due to the low carbon levels. The most critical issues regarding the use of these alloys are (1) control of ferrite content in the weld metal and HAZ, and (2) PWHT procedures that avoid untempered martensite and optimize mechanical and corrosion properties.

Table 4 Sulfide stress corrosion results for type 410 stainless steel

Specimen identification	Yield strength, MPa (ksi)	Threshold stress, MPa (ksi)	Threshold, % yield strength
A1 (base metal)	572 (83)	371 (53.4)	65
A2 (weldment)	565 (82)	257 (37.4)	45(a)
A3 (weldment)	572 (83)	57 (8.3)	10
A4(weldment)	558 (81)	83 (12)	15
B1 (base metal)	585 (85)	234 (34)	40
B2 (weldment)	592 (86)	238 (34.6)	40
B3 (weldment)	544 (79)	109 (15.8)	20
B4 (weldment)	751 (76)	105 (15.2)	20

(a) A single specimen stressed at 50% of yield strength failed in 687 hours with the gage section greatly reduced due to corrosion. Source: Ref 4

REFERENCES

1. R.A. Walker and T.G. Gooch, Arc Weldability of Stainless Steels, *Met. Mater.,* Vol 2 (No. 1), 1986, p 18–24
2. J.H. Devletian and W.E. Wood, Principles of Joining Metallurgy, *Metals Handbook,* 9th ed., Vol 6, American Society for Metals, 1983, p 21–49
3. R.D. Stout et al., *Weldability of Steels,* 3rd ed., Welding Research Council, 1978
4. D.D. Vitale, "Sulfide Stress Corrosion Resistance of Stainless Steel Weldments," Paper No. 00161, presented at *Corrosion 2000,* NACE International, 2000
5. J.C. Lippold, " Recent Developments in the Understanding of Stainless Steel Welding Metallurgy," presented at *Sixth International Trends in Welding Research Conf.,* April 2000, Pine Mountain, GA, ASM International, 2003

Table 5 Chemical compositions of selected supermartensitic stainless steels

Steel	C	Si	Mn	P	S	Cu	Ni	Cr	Mo	Al	N
A	0.020	0.28	0.18	0.015	0.0006	0.09	4.70	13.62	1.66	0.016	0.077
B	0.020	0.22	1.51	0.013	0.002	0.49	0.80	10.94	. . .	0.023	0.0092
C	0.028	0.30	0.49	0.012	0.001	1.43	3.76	11.16	1.17	0.020	0.0082
D	0.010	0.30	0.44	0.016	0.001	. . .	6.11	11.99	2.47	. . .	. . .

6. T.G. Gooch, P. Woolin, and A.G. Haynes, Welding Metallurgy of Low Carbon 13% Chromium Steels, *Proc. Supermartensitic Stainless Steels 1999,* Belgian Welding Institute, 1999, p 188–195
7. S. Olsen, L. Borvik, and G. Rorvik, "Corrosion Testing of Supermartensitic Weldments with Matching Consumables," Paper No. 00129, presented at *Corrosion 2000,* NACE International, 2000
8. Th. Boellinghaus, Th. Kannengiesser, C. Jochum, and I. Stiebe-Springer, "Effect of Filler Metal Material Selection on Stress Strain Build Up and Stress Corrosion Cracking Resistance of Welded Supermartenstic Stainless Steel Pipes," Paper No. 02061, presented at *Corrosion 2002,* NACE International, 2002

SELECTED REFERENCES

- P.E. Kvaale and S. Olsen, Experience with Supermartensitic Stainless Steels in Flowline Applications, *Stainless Steel World 99 Conf.*, KCL Publishing BV, 1999, p 19–26
- S. Hashizume and T. Ono, "Effect of PWHT Temperature on SCC Behavior of Low C-13% CR Steels Weld Joints in Hot Acidic Production Environments," Paper No. 05094, presented at *Corrosion 2005,* NACE International, 2005

Corrosion of Weldments
J.R. Davis, editor, p 125-142
DOI:10.1361/corw2006p125

CHAPTER 7

Corrosion of High-Nickel Alloy Weldments

NICKEL-BASE ALLOYS are solid solutions based in the element nickel. Even though nickel-base alloys, in general, contain a large proportion of other alloying elements, these alloys maintain the face-centered cubic (fcc) structure from the nickel-base element. As a consequence of the fcc structure, nickel-base alloys have excellent ductility, malleability, and formability. Nickel alloys are also readily weldable.

There are two basic groups of the commercial nickel-base alloys. One group was designed to withstand high-temperature and dry or gaseous corrosion, while the other is mainly dedicated to withstanding low-temperature aqueous corrosion. Nickel-base alloys used for low-temperature aqueous corrosion are commonly referred to as corrosion-resistant alloys (CRAs), and nickel alloys used for high-temperature applications are known as heat-resistant alloys (HRAs), high-temperature alloys (HTAs), or superalloys. The practical industrial boundary between high- and low-temperature is approximately 500 °C (or near 1000 °F). Most of the nickel alloys have a clear use as CRAs or HRAs; however, a few alloys can be used for both applications (e.g., alloy 625, or Unified Numbering System, or UNS, N06625).

The emphasis in this chapter is on the CRAs and in particular Ni-Cr-Mo alloys. These are the most versatile nickel alloys, because they contain molybdenum, which protects against corrosion under reducing conditions, and chromium, which protects against corrosion under oxidizing conditions. Information on alloys used for high-temperature service can be found in Ref 1 to 3.

Types of Corrosion-Resistant Alloys (CRAs)

The nickel alloys designed to resist aqueous corrosion can be categorized according to their major alloying elements, In addition to pure nickel, which possesses high resistance to caustic soda and caustic potash, there are six important nickel alloy families:

- Nickel-copper (Ni-Cu)
- Nickel-molybdenum (Ni-Mo)
- Nickel-chromium (Ni-Cr)
- Nickel-chromium-molybdenum (Ni-Cr-Mo)
- Nickel-chromium-iron (Ni-Cr-Fe)
- Nickel-iron-chromium (Ni-Fe-Cr)

As shown in Fig. 1, alloying of nickel with other elements (e.g., chromium, molybdenum, and copper) broadens its use in corrosion-resistant applications.

Many of the current wrought alloys are descended from casting materials developed during the early part of the 20th century. Some of these early casting materials are still in general use for pump and valve components and other intricate parts.

A listing of popular wrought and cast nickel alloys resistant to aqueous corrosion is provided in Table 1. The basic structure of these alloys, like that of nickel itself, is fcc. However, most are alloyed beyond the solubility limits to maximize corrosion resistance and require an annealing treatment (usually followed by water quenching) to minimize deleterious second phases. Such second phases can occur during reheating, as in weld

heat-affected zones (HAZs), typically as grain-boundary precipitates. Modern wrought alloys, with their very low carbon and silicon contents, are quite stable and can be used in the as-welded condition with only a low risk of intergranular attack. Older cast alloys with higher carbon and silicon contents, however, are more prone to grain-boundary precipitation during welding and generally require postweld annealing.

The roles of the various elements in the nickel alloys are discussed for each alloy category, but a synopsis for the key elements follows:

- *Nickel:* This element is an ideal base because it not only possesses moderate corrosion resistance by itself, but it also can be alloyed with significant quantities of copper, molybdenum, chromium, iron, and tungsten, while retaining its ductile fcc structure. Some inherent properties imparted by nickel to its alloys are resistance to stress-corrosion cracking (SCC), resistance to caustic compounds, and resistance to hydrofluoric acid.
- *Copper:* The addition of copper to nickel enhances its resistance to reducing-acid media, in particular, hydrofluoric acid. Copper, even at levels as low as 1.5 to 2 wt%, is also very beneficial in sulfuric acid.
- *Chromium:* The role of chromium in the nickel alloys is the same as that in the stainless steels, that is, to participate in the formation of passive films. These films provide protection in a wide range of oxygen-bearing environments. A secondary role of chromium is to provide some strengthening of the solid solution.
- *Molybdenum:* The addition of molybdenum to nickel greatly enhances its nobility under active corrosion conditions. In particular, it provides high resistance to reducing chemicals, such as hydrochloric acid. In combination with chromium, it produces alloys that are extremely versatile (resistant to both oxidizing and reducing chemicals) and that can withstand chloride-induced pitting and crevice corrosion. Molybdenum also greatly increases the strength of the nickel-rich solid solution, by virtue of its large atomic size.
- *Tungsten:* This element behaves in the same way as molybdenum and is often used in combination with molybdenum. It is an even more effective solid-solution strengthener.

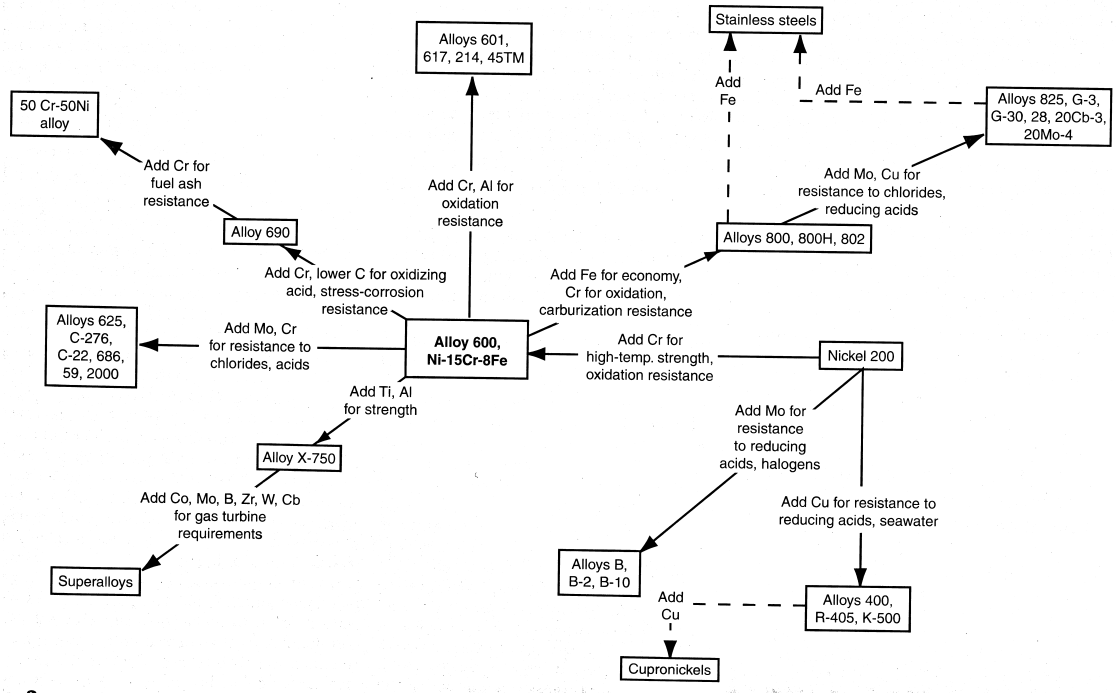

Fig. 1 Compositional and property linkages for nickel-base alloys

Table 1 Nominal compositions of nickel alloys resistant to aqueous corrosion

Family	Common name	UNS No.	Form	Composition, wt %											
				Ni	Cu	Mo	Cr	Fe	W	Mn	Si	C	Al	Ti	Other
Ni	200	N02200	Wrought	99.5	0.1	...	...	0.2	...	0.2	0.2	0.08	...	...	...
	201	N02201	Wrought	99.5	0.1	...	...	0.2	...	0.2	0.2	0.01	...	...	...
	301	N03301	Wrought (age hardenable)	96.5	0.1	...	...	0.3	...	0.2	0.5	0.2	4.4	0.6	...
Ni-Cu	400	N04400	Wrought	66.5	31.5	...	...	1.2	...	1	0.2	0.2	...	...	...
	K-500	N05500	Wrought (age hardenable)	66.5	29.5	...	...	1	...	0.8	0.2	0.1	2.7	0.6	...
	M-35-1	N24135	Cast	bal	29.5	...	...	3.5(a)	...	1.5(a)	1.25(a)	0.35(a)	...	...	Nb 0.5(a)
Ni-Mo	B	N10001	Wrought	bal	...	29.5	1.00(a)	6.00(a)	...	1.00	1.00	0.12(a)	...	...	Co 2.5(a)
	B-2	N10665	Wrought	69	0.5(a)	28	1(a)	2(a)	0.5(a)	1(a)	0.1(a)	0.01(a)	...	...	...
	B-3	N10675	Wrought	65(b)	0.2(a)	28.5	1.5	1.5	3(a)	3(a)	0.1(a)	0.01(a)	0.5(a)	...	...
	N-7M	N30007	Cast	bal	...	31.5	1(a)	3(a)	...	1(a)	1(a)	0.07(a)	...	...	...
Ni-Cr	600	N06600	Wrought	76	0.2	...	15.5	8	...	0.5	0.2	0.08	...	...	...
	625	N06625	Wrought	61	...	9	21.5	2.5	...	0.2	0.2	0.05	0.2	0.2	Nb + Ta 3.6
	690	N06690	Wrought	58(b)	0.5(a)	...	29	9	...	0.5(a)	0.5(a)	0.05(a)	...	...	...
	725	N07725	Wrought (age hardenable)	57	...	8	21	7.5	...	0.35(a)	0.2(a)	0.03(a)	0.35(a)	1.5	Nb 3.5
	FM 72	N06072	Filler Metal	bal	0.5(a)	...	44	0.5(a)	...	0.2(a)	0.2(a)	0.1(a)	...	0.7	...
	G-35	N06035	Wrought	58	0.3(a)	8.1	33.2	2(a)	0.6(a)	0.5(a)	0.6(a)	0.05(a)	0.4(a)	...	...
	Allcorr	N06110	Wrought	bal	...	10	31	...	2	...	...	0.02	0.25	0.25	Nb 0.4
Ni-Cr-Mo	C-4	N06455	Wrought	65	0.5(a)	16	16	3(a)	...	1(a)	0.08(a)	0.01(a)	...	0.7(a)	...
	C-22	N06022	Wrought	56	0.5(a)	13	22	3	3	0.5(a)	0.08(a)	0.01(a)	...	...	V 0.35(a)
	C-22HS	...	Wrought (age hardenable)	61	0.5(a)	17	21	2(a)	1(a)	0.8(a)	0.08(a)	0.01(a)	0.5(a)	...	...
	C-276	N10276	Wrought	57	0.5(a)	16	16	5	4	1(a)	0.08(a)	0.01(a)	...	...	V 0.35(a)
	C-2000	N06200	Wrought	59	1.6	16	23	3(a)	...	0.5(a)	0.08(a)	0.01(a)	0.5(a)	...	...
	59	N06059	Wrought	bal	...	16	23	1.5(a)	...	0.5(a)	0.1(a)	0.01(a)	0.25	...	...
	686	N06686	Wrought	bal	...	16	21	5(a)	3.7	0.75(a)	0.08(a)	0.01(a)	...	0.15	...
	CW-2M	N26455	Cast	bal	...	16.25	16.25	2(a)	1(a)	1(a)	0.8(a)	0.02(a)	...	...	...
	CW-6M	N30107	Cast	bal	...	18.5	18.5	3(a)	...	1(a)	1(a)	0.07(a)	...	...	...
	CW-12MW	N30002	Cast	bal	...	17	16.5	6	4.5	1(a)	1(a)	0.12(a)	...	...	V 0.3
Ni-Cr-Fe	G-3	N06985	Wrought	44	2	7	22	19.5	1.5(a)	1(a)	1(a)	0.015(a)	...	...	Nb 0.5(a) Co 5(a)
	G-30	N06030	Wrought	43	2	5.5	30	15	2.5	1.5(a)	0.8(a)	0.03(a)	...	...	Nb 0.8 Co 5(a)
	G-50	N06950	Wrought	50(b)	0.5(a)	9	20	17	1(a)	1(a)	1(a)	0.015(a)	0.4(a)	...	Co 2.5(a), Nb 0.5(a)
	718	N07718	Wrought (age hardenable)	52.5	0.2	3	19	18.5	...	0.2	0.2	0.04	0.5	0.9	Nb + Ta 5.1
Ni-Fe-Cr	825	N08825	Wrought	42	2.2	3	21.5	30	...	0.5	0.2	0.03	0.1	0.9	...

(a) Maximum. (b) Minimum

- *Iron:* The chief purpose of adding iron to the nickel alloys is to reduce their cost. However, it does provide benefits in concentrated sulfuric acid and in nitric acid, probably by contributing to the formation of passive films.

Commercially Pure Nickel. Commercially pure wrought nickel has good corrosion resistance and mechanical properties. A combination of good ductility and malleability, low hardness, a low work-hardening rate, and good weldability make the metal highly fabricable. Good low-temperature ductility and impact strength make it a useful material at cryogenic temperatures. Nickel is also noted for very good resistance to aqueous corrosion in certain environments. The most common product is nickel 200 (N02200). It contains 99.6% Ni with small amounts of iron, copper, manganese, silicon, and carbon. It has found a wide variety of applications involving caustic soda, water, nonoxidizing acids, alkaline salt solutions, chlorine, hydrogen chloride, fluorine, and molten salts. Nickel has relatively high electrical and thermal conductivity as well as a high Curie temperature and good magnetostrictive properties. This leads to use in many electrical and electronic applications. Minor variations of residual elements allow use in other specific applications, such as automotive spark plugs.

The low-carbon grade 201 (N02201) is used at elevated temperatures, at or above 315 °C (600 °F), where graphitization can occur in the higher-carbon material. As is the case with nickel-copper and other nickel alloys, commercially pure nickel can be age hardened by the addition of aluminum and titanium to form gamma prime (γ'), an fcc compound $Ni_3(Al,Ti)$. Age-hardened nickel 301 (N03301) has high strength in addition to the corrosion resistance and electrical and magnetic properties of pure nickel. This material is often used in extrusion dies for plastics and magnetostrictive units under stress.

Nickel-Copper Alloys. Nickel and copper form a continuous solid solution in all proportions, making a variety of nickel-copper and copper-nickel alloys possible. These alloys, which are commonly referred to as Monels, are characterized by good strength, good ductility and weldability, and resistance to aqueous corrosion and SCC in a variety of environments and applications. Nickel-copper alloys also have good electrical and thermal conductivity and have a Curie temperature in the ambient range. Specialized electrical and magnetic properties allow use in critical electrical, electronic, and other applications.

The first commercial and most common nickel-copper alloy in use was alloy 400 (N04400). This alloy was developed in 1905 and is still used in a wide variety of applications, such as seawater, nonoxidizing acids, hydrocarbon processing, water-fed heat exchangers, neutral and alkaline salts and alkali process equipment, industrial plumbing and valves, marine fixtures, petrochemical equipment, and pickling equipment. Small additions of aluminum and titanium to N04400 allow age hardening through the precipitation of fine particles of γ'. This age-hardenable material, N05500 (alloy K-500), is used for pump shafts and impellers, valves, oil well drill parts, springs, and fasteners.

Nickel-molybdenum alloys, or B-type alloys, are known for their excellent resistance to nonoxidizing (reducing) media, such as hydrochloric and sulfuric acids. The original B alloy (N10001) was invented in the 1920s, and it had a nominal composition of Ni-28Mo-5Fe-0.3V, with a maximum carbon content of 0.05 wt% and a maximum silicon content of 1 wt%. The alloy was used successfully for many years, but it suffered an important drawback in that fabricated components required a solution heat treatment in order to avoid corrosion attack in the weld HAZs. Experimental work from 1958 to 1960 indicated that the corrosion resistance of the alloy could be significantly improved by reducing the carbon, iron, and silicon levels (Ref 4, 5). However, the achievement of very low carbon levels on a production scale did not occur until the invention of the argon-oxygen decarburization (AOD) melting process (Ref 6). This enabled the commercialization of an improved nickel-molybdenum material, B-2 alloy (N10665), in the early 1970s (Ref 7).

The new alloy lived up to expectations in terms of corrosion resistance, but it soon became apparent that the reductions in the residual alloying elements, especially iron, had adversely impacted its thermal stability. That is, the alloy became very susceptible to the Ni_4Mo transformation when it was exposed to the 650 to 750 °C (1200 to 1380 °F) temperature range. As a result of this embrittling transformation, cracking was encountered during some of the alloy manufacturing operations as well as during customer fabrication of components. In addition a number of in-service cases of environmental cracking were observed. These were usually associated with weld HAZs.

In order to solve the embrittlement problems of B-2 alloy, without sacrificing its excellent corrosion resistance, a research program was undertaken that led to the development of B-3 alloy (N10675) (Ref 8). By carefully controlling additions of iron, chromium, and manganese, the equilibrium structure of the alloy was redirected toward the Ni_3Mo transformation, which is more sluggish than the Ni_4Mo transformation. This provides more time to effect a heat treatment without the risk of cracking. The new alloy is also more resistant to SCC (Ref 9).

Additions of molybdenum to nickel impart a pseudopassive behavior to the resulting alloy in nonoxidizing acids, which gives it good resistance to corrosion (Ref 10). However, contamination of the environment with oxidizing ions such as Fe^{3+} or Cu^{2+} destroys this behavior and dramatically increases the corrosion rate. Consequently, the nickel-molybdenum alloys should never be used where oxidizing conditions are known to exist.

Nickel-Chromium Alloys. Many materials within this category are useful not only to resist aqueous corrosion but also at high temperatures, where their chromium additions encourage the growth of protective oxide scales. A prime example is alloy 625 (N06625), which is used in many aggressive chemicals and hot, gaseous environments. While it is not quite as resistant to reducing acids as the Ni-Cr-Mo alloys, because of its lower molybdenum content, it is better than stainless steels in this respect. It also exhibits moderately high resistance to chloride-induced phenomena, such as pitting, crevice corrosion, and SCC.

Alloy 600 (N06600) is used as an alternate to alloy 200 (N02200) in caustic environments, when the latter is not of sufficient strength. Alloy 600 was also used extensively in nuclear steam generators, until superseded by alloy 690 (N06690), which was found to be considerably more resistant to SCC in pure water, at high temperatures.

Those nickel-chromium materials with very high chromium contents, such as N06072 (filler metal 72 with 44 wt% Cr), N06035 (G-35 alloy with 33.2 wt% Cr), and N06690 (alloy 690 with 29 wt% Cr), possess outstanding resistance to oxidizing aqueous environments, such as nitric acid and nitric-hydrofluoric acid mixtures.

The nickel-chromium-molybdenum alloys, which are commonly referred to as C-type alloys, are the most versatile of the nickel alloys designed to resist aqueous corrosion and are consequently the most widely used within the chemical process industries. They exhibit good resistance to both oxidizing and reducing media and possess exceptional resistance to chloride-induced pitting, crevice attack, and SCC. They are also easily formed and welded into complex components.

The chromium contents of the Ni-Cr-Mo alloys range from approximately 15 to 25 wt%, while their molybdenum contents range from approximately 12 to 17 wt%. The primary function of chromium is to provide passivity in oxidizing acid solutions; this is also its main function in the stainless steels. Molybdenum greatly enhances the resistance of nickel to reducing acids, in particular hydrochloric, and increases the resistance to localized attack (pitting and crevice corrosion), perhaps because these forms of attack involve the local formation of hydrochloric acid. Molybdenum provides considerable strength to the fcc solid solution because of its atomic size.

Optional minor element additions include iron, tungsten, and copper. The primary purpose of including iron is to lessen the cost of furnace charge materials during melting. Interestingly, in the most recently developed Ni-Cr-Mo alloys, iron has been relegated to the role of an impurity, to increase the solubility of other more useful elements. Tungsten is sometimes used as a partial replacement for molybdenum. In fact, a specific tungsten-to-molybdenum ratio was shown to provide increased resistance to localized attack during the development of C-22 alloy (N06022).

Copper, which has so far been added to only one of the Ni-Cr-Mo alloys, is known to enhance resistance to both sulfuric and hydrofluoric acids. The mechanisms are poorly understood, but even at the 1.6 wt% level in C-2000 alloy (N06200), copper plating of samples has been observed in sulfuric acid. The mechanism in hydrofluoric acid may be one of augmentation of the fluoride films that are known to form on nickel alloys in this environment (Ref 11).

To maximize their corrosion resistance, the amounts of chromium, molybdenum, or other element added to the C-type alloys exceed their solubility limits at room temperature. In fact, the alloys are metastable below their solution-annealing temperatures of approximately 1050 to 1150 °C (1920 to 2100 °F). The extent of alloying is actually governed by the kinetics of second-phase precipitation, the design principle being that the alloys should retain their solution-

annealed structures when water quenched and should not suffer continuous grain-boundary precipitation of deleterious second phases in weld HAZs.

As to the types of second-phase precipitate normally found in the C-type alloys, Ref 12 describes those observed in C-276 alloy (N10276), as follows:

- At temperatures between 300 and 650 °C (570 and 1200 °F), an ordered phase of the type A_2B, or, in this case, $Ni_2(Cr,Mo)$, occurs by long-range ordering. The precipitation reaction is described as being homogeneous, with no preferential precipitation at the grain boundaries or twin boundaries. The reaction is slow at lower temperatures within this range; it has been established, for example, that it takes in excess of 38,000 h for A_2B to form in C-276 alloy (N10276) at 425 °C (800 °F).
- At temperatures above 650 °C (1200 °F), three precipitate phases can nucleate heterogeneously at grain boundaries and twin boundaries. These are μ phase, M_6C carbide, and *P* phase. The μ phase is described as having a hexagonal crystal structure and an A_7B_6 stoichiometry. M_6C has a diamond cubic crystal structure, and *P* phase has a tetragonal structure. Reference 13 indicates that μ phase precipitates in C-276 alloy within the temperature range 760 to 1093 °C (1400 to 2000 °F), whereas M_6C carbide precipitates at temperatures between 650 and 1038 °C (1200 and 1900 °F). The same reference indicates that the kinetics of carbide formation are faster than those of μ phase.

To reduce the susceptibility of the alloys to the precipitation of M_6C, μ phase, and *P* phase, steps are taken during melting to minimize their carbon and silicon contents, silicon being a known promoter of intermetallic phases, such as μ. As to the effects of these second-phase precipitates on the properties of the C-type alloys, it is well known that the heterogeneous precipitates that occur at temperatures in excess of 650 °C (1200 °F) are detrimental to both corrosion resistance and material ductility. On the other hand, the homogeneous precipitation reaction that occurs at lower temperatures can be used to strengthen the C-type alloys while maintaining good ductility (Ref 14). Indeed, a Ni-Cr-Mo composition (C-22HS alloy) that can be strengthened by this mechanism in a short period of time (48 h) has been developed.

Nickel-chromium-iron alloys comprise a large number of industrially important materials. Most of these alloys fall within the broad austenitic, γ phase field of the ternary Ni-Cr-Fe phase diagram, and they are noted for good elevated-temperature strength, good workability, and resistance to corrosion and oxidation. Many of these alloys serve equally well in a wide range of both high-temperature and aqueous corrosion applications. The high nickel content provides metallurgical stability and corrosion resistance in reducing environments, while the chromium addition contributes to strength, oxidation resistance, and aqueous corrosion resistance in oxidizing environments.

Among the Ni-Cr-Fe alloys designed purely for resistance to aqueous corrosion are G-3 (N06985), G-30 (N06030), and G-50 (N06950) alloys. G-3 and G-50 alloys are popular for downhole tubulars in the oil and gas industries, while G-30 alloy was designed specifically for use in tubular form, in wet process phosphoric acid evaporators in the agrichemical industry.

Nickel-Iron-Chromium Alloys. These materials bridge the gap between the high-nickel austenitic stainless steels and the Ni-Cr-Fe alloys. Their main advantage over the stainless steels is enhanced resistance to environmental cracking. One of the most commonly used Ni-Fe-Cr materials is alloy 825 (N08825), which contains 2.2 wt% Cu to improve its resistance to sulfuric acid. This alloy is used in sulfuric acid, phosphoric acid, seawater, and in downhole oilfield environments.

General Welding Considerations

As nickel replaces iron in alloys, the weld pool becomes less fluid, and weld penetration is reduced. Special attention is required to avoid lack of penetration and lack of fusion defects. It is always good practice to develop a qualified welding procedure, whether or not it is required by a code.

In comparison to welding steels and stainless steels, joints must be more open when welding nickel-base alloys, to compensate for reduced penetration and fluidity. V-groove included angles of approximately 70° are recommended. Root openings should be slightly greater, and land thickness should be less than for steels.

Nickel alloys are more susceptible than stainless steels to cracking caused by contamination

with compounds of sulfur, phosphorus, or with low-melting-point metals. Standard preparation of new material involves removing any grease or oils by wiping with a solvent, then removing the as-received surface with an abrasive. If material is known to have been exposed to sulfur compounds or low-melting-point metals, chemical cleaning methods may be required to remove the contamination, because grinding may smear contaminants into the surface. Thermal cutting methods, such as plasma arc, laser beam, or air carbon arc, may be used to prepare bevels, but the cut surfaces should be ground to bright metal prior to welding. Oxyfuel cutting is not effective on nickel alloys.

High-current and heat-input welding conditions increase the likelihood of problems such as sensitization and solidification cracking; therefore, the heat input should be kept at low to moderate levels. A maximum heat-input recommendation would be alloy and service-environment specific; thus, some engineering judgment is required. The same concerns that lead to the requirement of relatively low heat input also necessitate maintenance of relatively low interpass temperatures. Maximum interpass temperature recommendations vary between alloys and manufacturers, but maximum temperatures are usually between 90 and 200 °C (195 and 390 °F). The low fluidity of nickel-base filler metals may require manipulation or slight weaving to avoid steep toe angles that can lead to lack of fusion defects. Excessive weaving with a low travel speed produces high heat input and should be avoided. The low-carbon, low-silicon nickel-base alloys generally have good resistance to solidification cracking. The likelihood of solidification cracking can be minimized by favoring a convex weld bead crown and low-to-moderate current and travel speed.

Postweld heat treatment (PWHT) is usually not required for modern wrought nickel alloys with low carbon and silicon contents. Cast alloys, however, are more prone to precipitation in the HAZ, due to their higher carbon and silicon contents; thus, PWHT may be required. A postweld solution anneal, if practical, may have the beneficial effect of relieving residual stress and providing some homogenization of the weld metal. Stress-relief heat treatments below the solution-annealing temperature, at temperatures that are commonly used for steels, should not be used on nickel alloys, because grain-boundary precipitation can lead to sensitization or loss of ductility.

Passivation treatments used on some stainless steels are not usually required for nickel alloys. Slag, undercut, and other potential crevices should be removed, to avoid crevice corrosion. Grinding and polishing are sometimes used where low process contamination is needed, as in pharmaceutical or fine chemical production, but must welds are placed in service in the as-welded condition. Heat tint oxidation is not as harmful to nickel alloys as it is to stainless steels but can be removed by grinding or pickling.

Welding Processes. The highest-quality weld joints, with the best mechanical properties and corrosion resistance, can be achieved by using the inert gas welding processes. The maximum recommended welding current (nonpulsing) for gas tungsten arc welding (GTAW) is approximately 200 A. The maximum recommended welding current (nonpulsing) for gas metal arc welding (GMAW) is approximately 250 A. Both processes use bare wire welding consumables, which are covered by the American Welding Society (AWS) A5.14 specification (Ref 15).

The use of flux-bearing welding processes can offer improved deposition rates and bead profiles compared to the inert gas processes. The tensile strength of weld metal is usually not affected by use of a flux-bearing process, but impact toughness and ductility are somewhat reduced, in comparison to inert gas weldments, by the oxide inclusions that are inherent in flux-deposited weld metal. The corrosion resistance of flux-deposited weld metal is usually not degraded, assuming that the weld metal composition falls within the specified limits for the alloy. Some pickup of silicon from the flux is unavoidable and is allowed for in specifications such as AWS A5.11 (Ref 16)

Coated electrodes for shielded metal arc welding (SMAW) are covered by the AWS A5.11 specification. The maximum recommended welding current is approximately 180 A, with electrodes of diameter 4.8 mm (0.19 in.). Flux-cored arc welding (FCAW) is occasionally used to join corrosion-resistant nickel-base alloys. The compositional ranges and properties in the AWS A5.11 specification are sometimes referenced when purchasing these welding consumables.

Submerged arc welding (SAW) has been successfully used to join corrosion-resistant nickel-base alloys; however, this process should be used with caution, particularly with the highly alloyed Ni-Cr-Mo and Ni-Mo alloys. Potential

problems include solidification cracking, microfissuring, modification of the weld metal composition, and sensitization. High welding currents will exacerbate all of these problems, so currents should be limited to approximately 250 A maximum. Low arc voltages will help to prevent pickup of silicon and loss of chromium, due to reaction with the flux; the recommended voltage is therefore approximately 26 to 28 V. Proper flux selection is critical to success. A highly basic, nonalloying flux is recommended. A procedure qualification that involves chemical analysis or corrosion testing of the weld metal, in addition to mechanical testing, should always be conducted when using SAW.

Filler-Metal Selection. Matching composition filler metals are available for most alloys and are selected in the majority of applications. Segregation of alloying elements occurs during the solidification of the weld metal. Dendrite cores are depleted in elements such as molybdenum and tungsten, while interdendritic areas are consequently enriched. The resulting nonuniform composition usually causes the weld metal to have higher uniform corrosion rates and less pitting resistance than matching-composition wrought alloys.

Excessive corrosion of the weld metal is usually only a problem when the selected alloy is subjected to an environment that is near the limit of the alloy useful range. Overalloyed filler metals may be selected in special cases, but the filler metal must be matched with the anticipated corrosive environment. For example, C-22 alloy (N06022) is sometimes used as an overalloyed filler metal for C-276 alloy (N10276) in hot chlorine bleach (an oxidizing environment where high chromium is beneficial), but C-22 alloy filler metal would suffer higher corrosion rates than matching C-276 alloy in pure hydrochloric acid (HCl) (a reducing environment where high molybdenum in beneficial). Another common application of over-alloyed filler metals is the use of 625 or C-22 alloy filler metals to join 6% Mo superaustenitic stainless steels in environments where pitting corrosion is a concern. However, there is no single, overalloyed filler metal that will provide the best performance under all conditions. Even when overalloyed filler metals are selected, localized corrosion of the unmixed zone is possible. Therefore, overalloyed filler metals are only selected in special cases where the combination is known to be effective.

Nickel alloys can be readily joined to steels and stainless steels by welding. The filler metal matching the nickel-base side of the joint is often a good choice for dissimilar metal welds. Alloy manufacturers should be contacted for specific recommendations.

Welding Metallurgy of CRAs Containing Molybdenum

Heat-Affected Zone. The phenomenon of HAZ grain boundary sensitization is addressed in Chapter 3, "Corrosion of Austenitic Stainless Steel Weldments." However, it should be noted here that the solid solubility of carbon is considerably lower in nickel-base alloys than in stainless steels. The net effect is that during the welding of low-carbon nickel-molybdenum and nickel-chromium-molybdenum CRAs, HAZ grain boundary precipitation is still a potential reality, despite the relatively low carbon content of these alloys. The amount and severity of precipitation will depend on the cooling rate through the intermediate temperature range from 1000 to 600 °C (1830 to 1110 °F). Some heat-to-heat variations in grain boundary precipitation have also been observed during simulated HAZ studies in alloy B-2 (Ref 17). The adverse effects of minor grain boundary precipitation depend on the severity of the corrosive environment. From example, the maximum corrosion penetration after testing in boiling 10% hydrochloric acid (HCl) varied little for simulated HAZs in alloy B-2. However, when harsher autoclave testing environments were used (20% HCl at 150 °C, or 300 °F), penetration by corrosion increased as the simulated HAZ cooling rate decreased from 20 to 120 s through the critical intermediate temperature range (Ref 17). Despite these laboratory findings, most low-carbon nickel-molybdenum and nickel-chromium-molybdenum alloys have been put into corrosion service in the as-welded condition with good results. Only occasionally are poor results encountered. Metallographic examination of the corroded part will usually reveal evidence of grain boundary precipitation in the HAZ (Fig. 2).

Aside from the possibility of grain growth, few other metallurgical HAZ problems have been reported for these alloys. HAZ hot cracking, especially of the type created by constitutional liquation of primary carbide particles, is not a problem with these alloys.

Fusion zone welding metallurgy of the nickel-molybdenum and nickel-chromium

molybdenum alloy family is important, because base materials are usually welded with filler metals of matching composition and because these alloys can be welded autogeneously (no filler added), as in the case of welded tubular products.

From a corrosion standpoint, the primary issue that should be considered in terms of the fusion zone is the effect of weld metal segregation on corrosion resistance. Because of the segregation of solute elements upon solidification (principally molybdenum, which segregates to the cellular dendritic boundaries of the fusion zone), it is generally accepted that the corrosion resistance of the weld metal will be marginally less than that of the more homogeneous wrought base material. Differences in corrosion performance, however, depend heavily on the severity of the corrosion environment. In mild corrosion environments, little difference is observed. In severe environments, the fusion zone may be preferentially attacked, as illustrated in Fig. 3, a cross section of an as-welded alloy B-2 coupon exposed for about 1 year in a chemical plant process stream. Figure 4(a) is a high-magnification view of the surface attack on alloy B-2 weld metal when tested for 96 h in 20% HCl at 150 °C (300 °F) in an autoclave. Under these conditions, corrosion attack appears to be the most aggressive at the dendrite cores (molybdenum lean). Figure 4(b) shows the lack of corrosion attack on weld meal from a specially devised overalloyed B-type filler material (Ref 18). This alloy consists of 42% Mo, rather than the nominal 28% Mo. The higher-molybdenum nickel alloy solidifies as a nonequilibrium hypoeutectic structure consisting of a metastable α phase, with Ni_3Mo and NiMo in the interdendritic regions. In this case, despite solidification segregation, the dendrite core regions are sufficiently saturated with molybdenum to resist preferential fusion zone attack.

It should be noted that although the microstructure of the Ni-42Mo material in Fig. 4(b) offers high corrosion resistance, the alloy is characterized by limited weld ductility (Ref 19). However, the use of overalloyed filler metals as a solution to preferential weld metal corrosion attack has been demonstrated elsewhere. For example, alloy C-22 (22% Cr) has been used

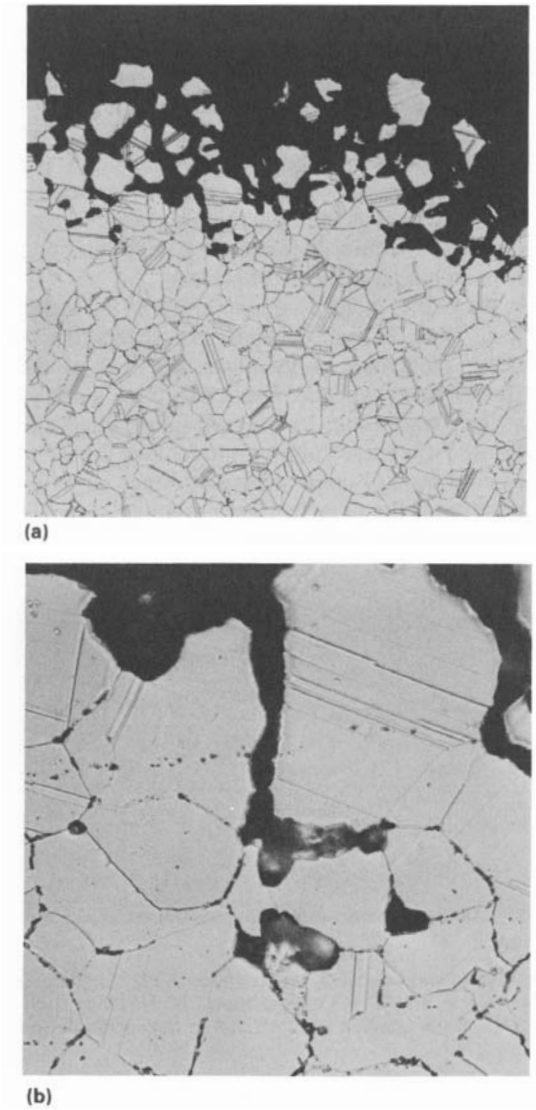

Fig. 2 Photomicrographs showing corrosion attack in alloy C-276 (UNS N10276) caused by grain boundary precipitation in the HAZ of the weld. The sample was taken from a pipe removed after 18 months of service in a hydrochloric acid vapor environment in a chemical plant. Sample was etched in HCl and oxalic acid. (a) 75×. (b) 375×

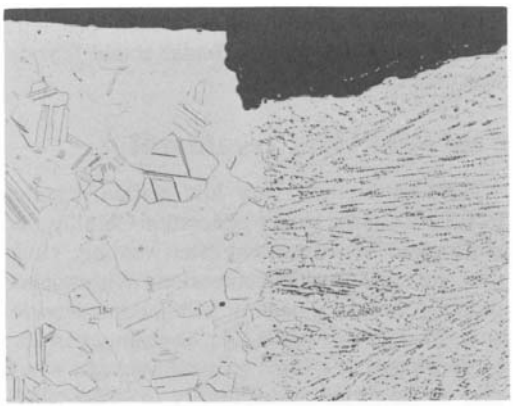

Fig. 3 Metallographic cross section showing preferential fusion zone attack in alloy B-2 (UNS N10665). Sample was a welded coupon placed in a chemical plant process stream for approximately 1 year. Hydrochloric and chromic acid etch. 75×

successfully to refurbish corroded welds in an alloy C-276 (16% Cr) pulp and paper mill bleach-mixing device. Alloy G-30 (30% Cr) is also a logical choice as an overalloyed filler for certain alloy G-3 components.

Welding Metallurgy of Ni-Cu, Ni-Cr, and Ni-Cr-Fe CRAs

As with the nickel alloys containing molybdenum, the factors influencing corrosion of Ni-Cu, Ni-Cr, and Ni-Cr-Fe alloy weldments include grain boundary precipitation in the HAZ and segregation in the fusion zone.

Grain Boundary Precipitation in the HAZ. Grain boundaries are the weak link in a microstructure that is exposed to elevated temperature, whether that exposure occurs during service or, in the case of welding, during the thermal cycles that are part of the welding operation. Precipitates that form in the grain boundaries can vary in size and composition and can be either harmful or beneficial. Intermetallic compounds, such as carbides, act as barriers to grain growth and can be very beneficial. Intergranular carbides in alloys 600 and 690 can also deter SCC during high-purity water exposure in nuclear reactor steam generator primary side environments (Ref 20).

Microsegregation in the Fusion Zone of Autogenous Welds. When a weld solidifies, an inhomogeneous dendritic structure forms. Solidification begins with the highest-melting-point liquid and continues until the whole structure is solid. A condition called microsegregation, or coring, occurs during this solidification process, and areas of the solidified microstructure can have great differences in composition. This becomes a problem in corrosion situations where an alloy was chosen for its particular resistance to corrosion. For example, because the dendritic weld material can have vastly different chromium and molybdenum levels, preferential corrosion may initiate and propagate at those areas of the microstructure that are lean in the element responsible for providing the corrosion resistance.

Microsegregation cannot be eliminated in a weld, but it can be minimized by judicious selection of welding parameters, such as the control of heat input. High-temperature heat treatments for several hours can partially equalize the composition gradients by diffusion. Cold working the weld structure, followed by annealing, can also break down this microsegregation, if the component lends itself to this type of treatment. In addition to improving the corrosion resistance of the welds, cold working and annealing the weld area also increases weld ductility.

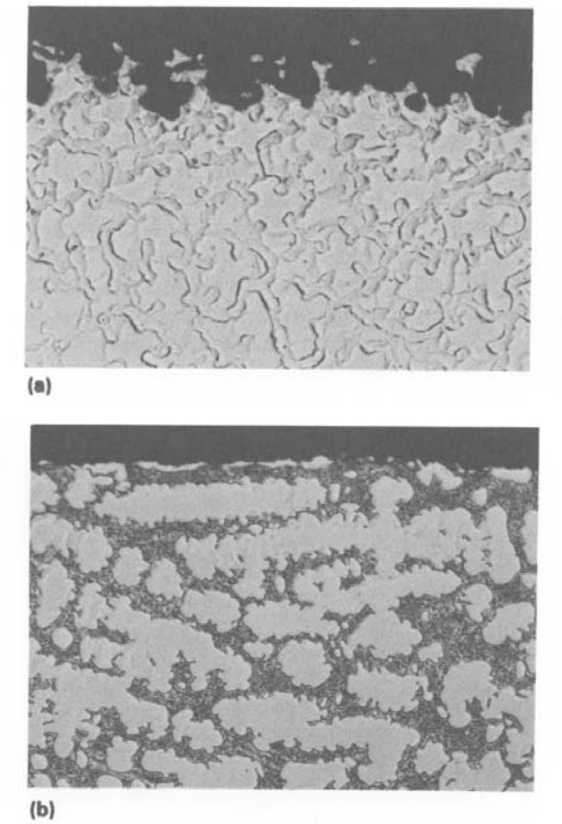

Fig. 4 Metallographic cross sections of the corroded surface of weld deposits on alloy B-2 (UNS N10665) after testing in an autoclave at 150 °C (300 °F) for 96 h in a 20% HCl environment. (a) Ni-28Mo (UNS N10665) alloy filler metal. 375× (b) Ni-42Mo filler metal. 375×. Both samples were etched in hydrochloric and chromic acid. See text for explanation.

Corrosion Behavior

The corrosion of metal and alloys depends on internal and external factors. Internal factors include chemical composition and microstructure of the alloy, and external factors include electrolyte composition, temperature, and electrode potential. In general, the use of nickel-base alloys in corrosive applications is based on their chemical composition. For example, a nickel-base alloy such as N06030 (Table 1) could be used under highly oxidizing acidic conditions, because it contains a large amount of chromium. Other alloys, such as B-3 (Table

1) are recommended for highly reducing acidic conditions, because they contain a large amount of molybdenum. However, for each alloy of unique chemical composition, the corrosion behavior also depends on the particular microstructural or metallurgical condition of its matrix. A typical example of this is the behavior of autogenously welded pipes in industrial corrosive applications. Both the weld seam and the wrought matrix from which the weld seam was derived have essentially the same overall chemical composition. However, it is commonly observed in specimen returned from the field that the weld seam and the immediately adjacent matrix have lower corrosion resistance than the contiguous unaffected wrought matrix. This dissimilar corrosion behavior is not due to a different chemical composition but to a different microstructure or metallurgical condition of the alloy. The weld seam would have a cast microstructure, which is generally anisotropic, with areas of high concentration of alloying elements, while other areas are impoverished in these same elements. The matrix area immediately adjacent to the weld is called the HAZ. The area of the HAZ still retains the overall wrought isotropic structure of the matrix; however, it can suffer solid-state transformations (intergranular precipitation) due to the higher temperature excursion during welding. The area immediately next to the HAZ has the isotropic fcc microstructure of a wrought matrix with equiaxed grains. Therefore, in a narrow region near the weld, there are three areas of equivalent chemical composition but of differentmicrostructure. Each of these areas responds differently to the external corrosive environment.

Nickel-Molybdenum Alloys. As discussed earlier in this chapter, alloy B has been used since the 1920s and has suffered from one significant limitation: weld decay. The welded structure has shown high susceptibility to knife-line attack adjacent to the weld metal and to HAZ attack at some distance from the weld. The former has been attributed to the precipitation of molybdenum carbide (Mo_2C); the latter, to the formation of M_6C-type carbides. This necessitated postweld annealing, a serious shortcoming when large structures are involved. The knife-line attack on as alloy B weldment is shown in Fig. 5. Many approaches to this problem were attempted, including the addition of carbide-stabilizing elements, such as vanadium, titanium, zirconium, and tantalum, as well as the lowering of carbon.

The addition of 1% V to an alloy B-type composition was first patented in 1959. The resultant commercial alloys—Corronel 220 and Hastelloy alloy B-282—were found to be superior to alloy B in resisting knife-line attack but were not immune to it. In fact, it was demonstrated that the addition of 2% V decreased the corrosion resistance of the base metal in HCl solutions. During this time, improvements in melting techniques led to the development of a low-carbon low-iron version of alloy B called alloy B-2. This alloy did not exhibit any propensity to knife-line attack (Fig. 6).

Segregation of molybdenum in weld metal can be detrimental to corrosion resistance in some environments. In the case of boiling hydrochloric acid solutions, the weld metal does not corrode preferentially. However, in sulfuric + hydrochloric and sulfuric + phosphoric acid mixtures, preferential corrosion of as-welded alloy B-2 has been observed (Fig. 7). No knife-line or HAZ attack was noted in these tests. During solidifica-

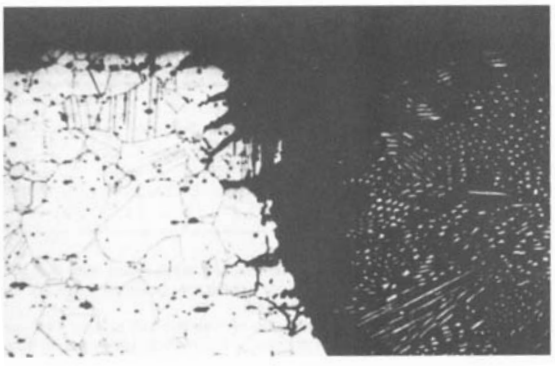

Fig. 5 Cross section of an alloy B weldment corroded after 16 days of exposure in boiling 20% HCl. 80×. Source: Ref 21

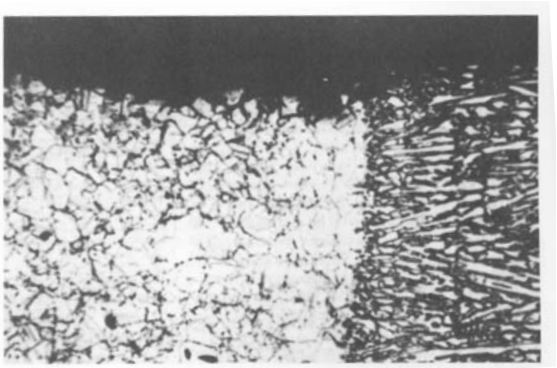

Fig. 6 Cross section of an alloy B-2 weldment after 16 days of exposure to boiling 20% HCl. 80×. Source: Ref 21

tion, the initial solid is poorer in molybdenum and therefore can corrode preferentially. This is shown in Fig. 7 for an autogenous GTA weld in alloy B-2. In such cases, postweld annealing at 1120 °C (2050 °F) is beneficial.

The nickel-chromium-molybdenum alloys represented by the C-type family of alloys have also undergone evolution because of the need to improve the corrosion resistance of weldments. Alloy C (UNS N10002), containing nominally 16% Cr, 16% Mo, 4% W, 0.04% C, and 0.5% Si, had been in use for some time but had required the use of postweld annealing to prevent preferential weld and HAZ attack. Many investigations ware carried out on the nature of precipitates formed in alloy C, and two main types of precipitates were identified. The first is a Ni_7Mo_6 intermetallic phase called μ, and the second consists of carbides of the Mo_6 type. Other carbides of the $M_{23}C_6$ and M_2C were also reported. Another type, an ordered Ni_2Cr-type precipitate, occurs mainly at lower temperatures and after a long aging time: it is not of great concern from a welding viewpoint.

Both the intermetallic phases and the carbides are rich in molybdenum, tungsten, and chromium and therefore create adjacent areas of alloy depletion that can be selectively attacked. Carbide precipitation can be retarded considerably by lowering carbon and silicon; this is the principle behind alloy C-276. The time-temperature behaviors of alloys C and C-276 are compared in Fig. 8, which shows much slower precipitation kinetics in alloy C-276. Therefore, the evolution of alloy C-276 from alloy C enabled the use of this alloy system in the as-welded condition. However, because only carbon and silicon were controlled in C-276, there remained the problem of intermetallic μ-phase precipitation, which occurred at longer times of aging. Alloy C-4 was developed with lower iron, cobalt, and tungsten levels to prevent precipitation of μ phases.

The effect of aging on sensitization of alloys C, C-276, and C-4 is shown in Fig. 9. For alloy C, sensitization occurs in two temperature ranges (700 to 800 °C, or 1290 to 1470 °F, and 900 to 1100 °C, or 1650 to 2010 °F) corresponding to carbide and μ-phase precipitation, respectively. For alloy C-276, sensitization occurs essentially in the higher temperature region because of μ-phase precipitation. Also, the μ-phase precipitation kinetics in alloy C-276 are slow enough not to cause sensitization problems in many high-heat-input weldments; however, precipitation can occur in the HAZ of alloy C-276 welds (Fig. 10). Because C-4 has lower tungsten than C-276, it has lower pitting and crevice corrosion resistance, for which tungsten is beneficial. Therefore, an alternate solution to alloy C-4 was needed in which both corrosion resistance and thermal stability are preserved. Alloy C-22 has demonstrated improved corrosion resistance and thermal stability.

Because of the low carbon content of alloy C-22, the precipitation kinetics of carbides were

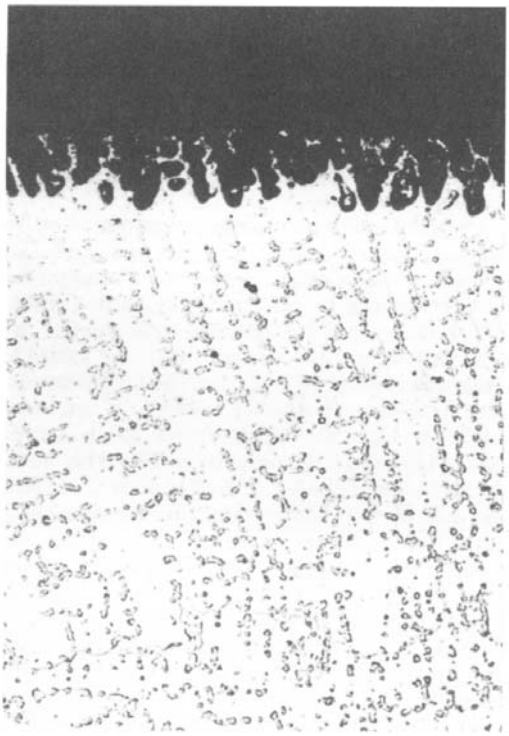

Fig. 7 Preferential corrosion of autogenous gas tungsten arc weld in alloy B-2 exposed to boiling 60% H_2SO_4 +8% HCl

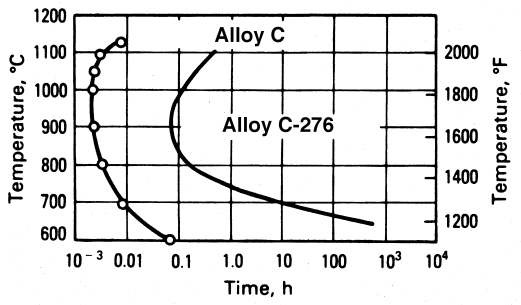

Fig. 8 Time-temperature transformation curves for alloys C and C-276. Intermetallics and carbide phases precipitate in the regions to the right of the curves. Source: Ref 22

slowed. Because alloy C-22 has lower molybdenum and tungsten levels than alloy C-276, μ-phase precipitation was also retarded.

From a weld HAZ point of view, this difference is reflected in lower grain-boundary precipitation even in a high-heat-input weld (Fig. 11). The HAZ microstructure of alloy C-4 was similar to this. This difference in the sensitization of the HAZ is also illustrated in Fig. 12, which shows that the HAZ and weld metal of alloy C-276 are attacked to a considerable extent in an oxidizing mixture of sulfuric acid (H_2SO_4) plus ferric sulfate ($Fe_2(SO_4)_3$), and other chemicals.

Phase Stability of Nickel-Base Alloys and Corrosion Behavior

Second-Phase Precipitation. In general Ni-Cr-Mo and Ni-Cr-Fe alloys (Table 1) contain a large amount of alloying elements, which determine their specific corrosion resistance and therefore field applicability. These elements are dissolved into the liquid metal at high temperature, and they remain in solid solution when the final product is cooled. At ambient temperatures, these alloys remain a single-phase fcc microstructure indefinitely. However, if most of these nickel-base alloys are exposed to temperatures above 500 °C (930 °F) for varying periods of time, they may develop second-phase precipitates, which in turn change the mechanical properties and corrosion resistance of these alloys. In general, the larger the amount of alloying elements, the more unstable the fcc microstructure of the alloy. Currently, there are several commercial Ni-Cr-Mo alloys (Table 1) that are highly alloyed to increase their corro-

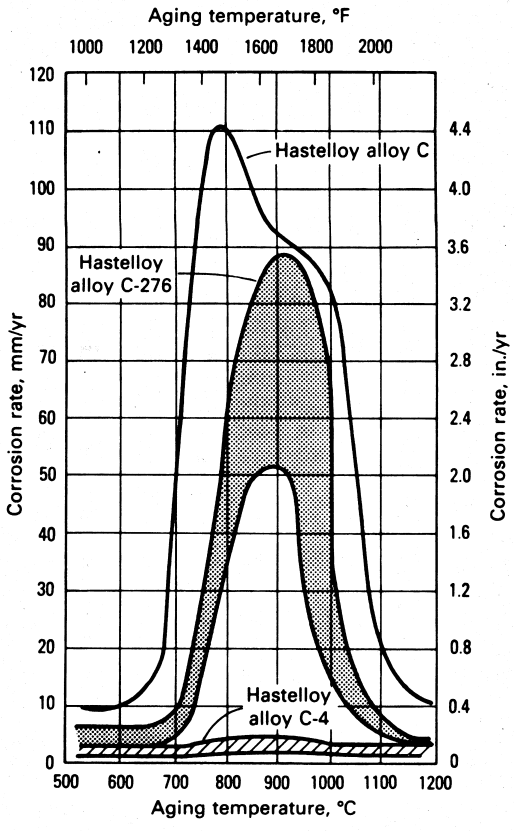

Fig. 9 Effect of 1 h aging treatment on corrosion resistance of three alloys in 50% H_2SO_4 + 42 g/L $Fe_2(SO_4)_3$. Source: Ref 23

Fig. 10 Typical microstructure of the HAZ of a multipass submerged arc weld in alloy C-276. Source: Ref 24

sion resistance; however, this overalloying may adversely impact their phase stability. The effects on corrosion behavior of second-phase formation due to thermal instability is discussed in detail for alloy C-22 (N06022), but similar behavior may happen in alloys C-276, C-4, 686, and 59.

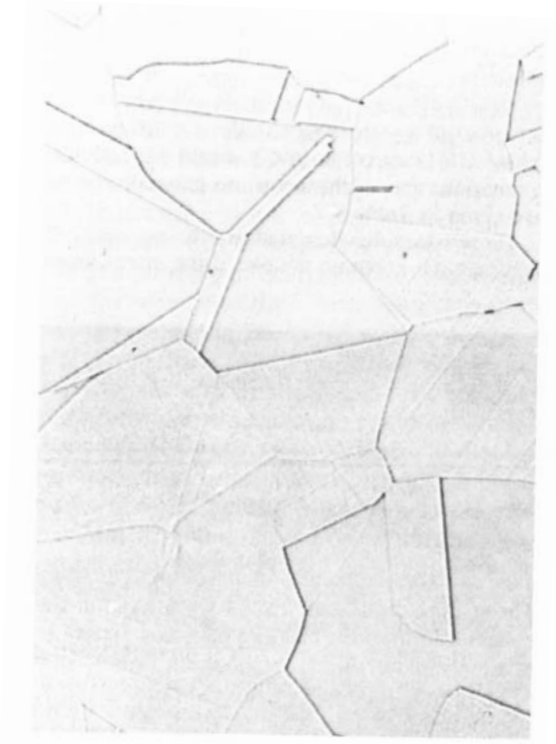

Fig. 11 Typical microstructure of the HAZ of a multipass submerged arc weld in alloy C-22. Matching filler metal was used. Source: Ref 24

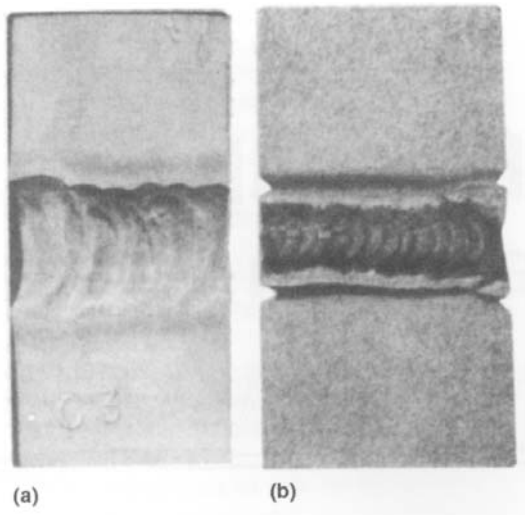

Fig. 12 Corrosion of the weld metal and the HAZ in alloys (a) C-22 and (b) C-276 in an aerated mixture of 6 vol% H_2SO_4 + 3.9% $Fe_2(SO_4)_3$ + other chemicals at 150 °C (300 °F.) Source: Ref 24

Effect of Intermetallic Phases. Alloy C-22 (N06022) is a Ni-Cr-Mo alloy (Table 1) that contains approximately 22% Cr, 13% Mo, 3% W, and 3% Fe. Due to its high chromium content, this alloy remains passive in most industrial applications and therefore has a very low general corrosion rate. The combination of the alloying elements chromium, molybdenum, and tungsten imparts the alloy with an excellent resistance to pitting corrosion, crevice corrosion, and SCC, especially in halide-containing environments (Ref 25–32).

Due to its overall resistance to corrosion, this alloy is a candidate material to fabricate the external layer of the high-level nuclear waste containers for the potential repository site that the Department of Energy is characterizing in Yucca Mountain, Nevada. As a result of the heat generated by the radioactive decay of the waste, the containers might experience temperatures as high as 160 °C (320 °F) during their first 1000 years of emplacement. The lifetime design of the containers is 10,000 years, and their maximum allowed temperature is 350 °C (660 °F). Because of concerns that alloy N06022 may suffer phase instability during the long predicted time of emplacement, systematic studies are being carried out to fully characterize the ranges of time and temperature at which the alloy might undergo solid-state phase transformation.

Haynes International started low-temperature aging studies of alloy N06022 and other alloys in 1989. The most recent results were obtained from samples removed after 40,000 h of aging. Laboratory studies of these aged samples have shown that the mechanical and corrosion properties of the alloy did not change after it was aged for up to 40,000 h at 427, 343 or 260 °C (800, 650, or 500 °F) (Ref 26, 27). The next test on these aged samples occurs for a total aging time of 100,000 h (approximately 12 years).

It is known that precipitation of detrimental second phases occurs when alloy N06022 is aged at temperatures above 600 °C (1110 °F) for much shorter periods of time. Therefore, several studies have been carried out to fully characterize the second-phase precipitation in the alloy for shorter periods of time at higher temperatures (Ref 33–37). The precipitation of these secondary phases affects the corrosion resistance in aggressive acidic solutions and the mechanical properties of wrought and welded alloy N06022 (Ref 38–42). In the fully annealed

condition, alloy N06022 is a metastable fcc solid solution. When the alloy is aged at intermediate temperatures (600 °C, or 1110 °F), it can precipitate several intermetallic phases (Ref 37). Two of the most common phases are μ phase and *P* phase, which are similar both chemically and crystallographically. Precipitation of the intermetallic detrimental phases, in general, begins at the grain boundaries, and for longer aging times, the precipitation starts growing at twin boundaries and later, inside the grains (Ref 37). Temperature-time-transformation diagrams and micrographs for alloy N06022 have been published (Ref 34, 37, 39). These intermetallic secondary phases tend to be rich in either chromium or molybdenum, which are the elements that give the alloy its excellent corrosion resistance. Therefore, it can be suggested that the formation of the intermetallic phases may leave a narrow adjacent area of the matrix depleted in these beneficial elements (chromium and molybdenum), causing an increase in the corrosion rate of the alloy in aggressive acidic solutions. On the other hand, the corrosion behavior of the aged alloy N06022 microstructure in multiionic underground water was the same as the corrosion behavior of the unaged microstructure (Ref 42). Similarly, the corrosion rate of aged alloy N06022 was the same as the corrosion rate of an unaged alloy when tested in boiling 10% NaOH (caustic solution) (Ref 38).

Changes in the Corrosion Rate of Alloy N06022 as a Consequence of Second-Phase Precipitation. Figures 13(a) and (b) show the corrosion rate of wrought and GTA welded

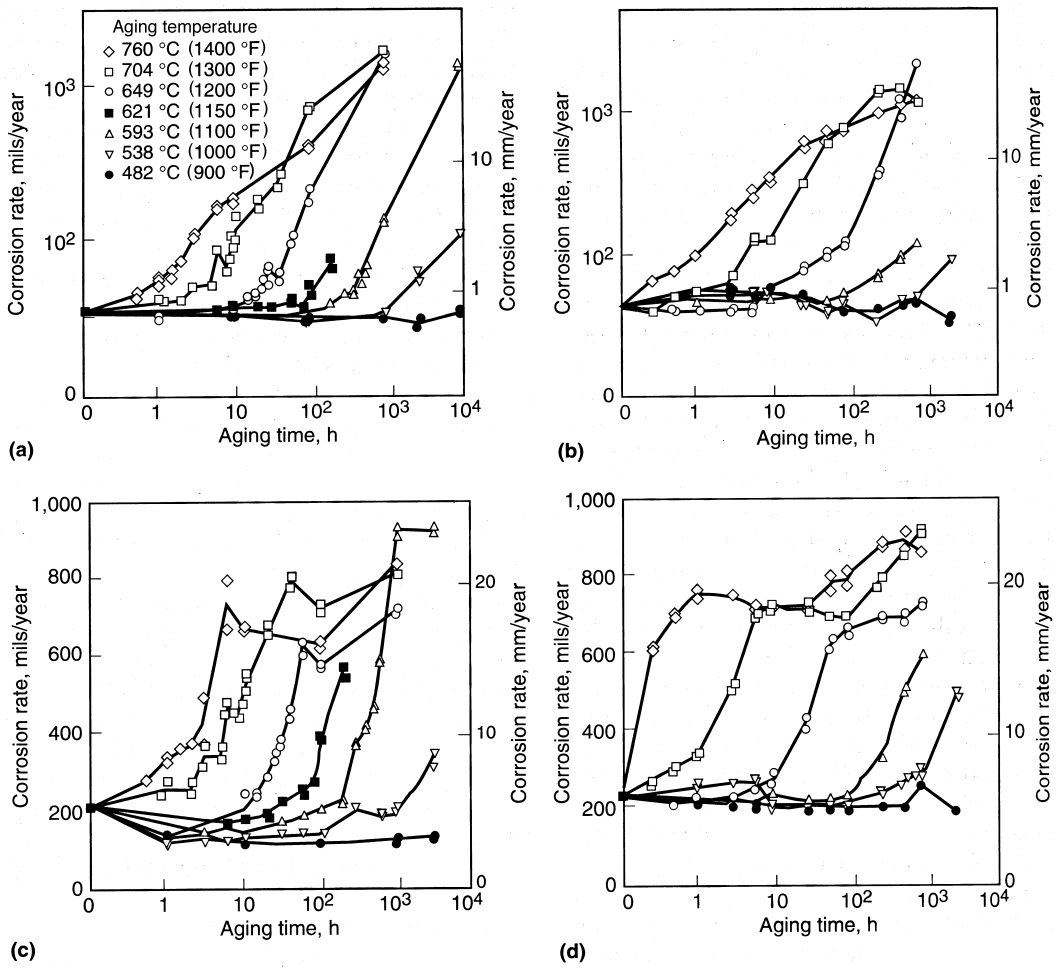

Fig. 13 Corrosion rate as a function of aging time and temperature for alloy C-22 (UNS N06022). (a) Aged wrought alloy in boiling sulfuric acid/ferric sulfate (ASTM G 28 Method A). (b) Gas tungsten arc welded (GTAW) alloy in boiling sulfuric acid/ferric sulfate (ASTM G 28 Method A). (c) Aged wrought alloy in boiling 2.5% HCl. (d) GTAW alloy in boiling 2.5% HCl. Source: Ref 43

alloy N06022, respectively, in ASTM G 28 Method A solution for seven aging temperatures and thirteen different aging times (Ref 43). The ASTM G 28 Method A test involves the immersion of the testing coupon in an oxidizing acidic solution consisting of boiling 50% sulfuric acid plus 42 g/L of ferric sulfate for 24 h. Details about testing coupon configuration, aging procedures, and corrosion testing are published elsewhere (Ref 43).

The corrosion rate of aged alloy N06022 in this oxidizing solution increases gradually as the aging time and the aging temperature *(T)* increase, for $T \geq 538$ °C (1000 °F). For samples aged at 482 °C (900 °F) the corrosion rate remains the same, even after aging for 10,000 h (Fig. 13). Coupons that were aged, for example, at 704 and 760 °C (1300 and 1400 °F) for times longer than 3 h show preferential corrosion at the grain boundaries. At higher aging times, deeper grain-boundary attack is observed, and in certain testing conditions, some grains fell away, because they became completely detached from the samples. Aging increases the susceptibility of attack of the HAZ in ASTM G 28 Method A solution. Figures 13(c) and (d) show the corrosion rate of wrought and GTA welded alloy N06022, respectively, in boiling 2.5% HCl solution (Ref 43). For both types of coupons, the corrosion rate increases approximately 3 times after a certain threshold aging time at each temperature. The threshold time increases as the temperature decreases. Figure 13(c) shows that for the wrought coupons, the corrosion rate initially decreases slightly with the aging time. This behavior seems to suggest that a small amount of aging would be beneficial for corrosion resistance under reducing conditions (Ref 43). The reason for this behavior is still not fully understood. For the higher aging temperatures, 760, 704, and 649 °C (1400, 1300, and 1200 °F), the corrosion rate seems to reach a plateau for an intermediate aging time. This behavior is more noticeable for the GTA welded coupons (Fig. 13d). For both types of the samples aged at 482 °C (900 °F), the corrosion rate remains the same, even after aging for 3000 h. Observation of the tested coupons in boiling 2.5% HCl solution shows preferential intergranular attack that becomes deeper and wider as the aging time increases. At aging times of 1000 h and higher, preferential corrosion attack at twins inside the grains is observed. For the shorter aging times, there is preferential attack at the HAZ; however, for the longer aging times, the attack becomes more uniform across the testing coupon.

Figure 14 shows the effect of welding on the corrosion rate of alloy N06022. Figure 14(a) shows the corrosion rate in ASTM G 28 Method A for wrought and as-welded coupons at two aging temperatures, 760 and 538 °C (1400 and 1000 °F), as a function of aging time. For all aging times, the corrosion rate of welded coupons is always higher than the corrosion rate of wrought coupons. At the aging temperature

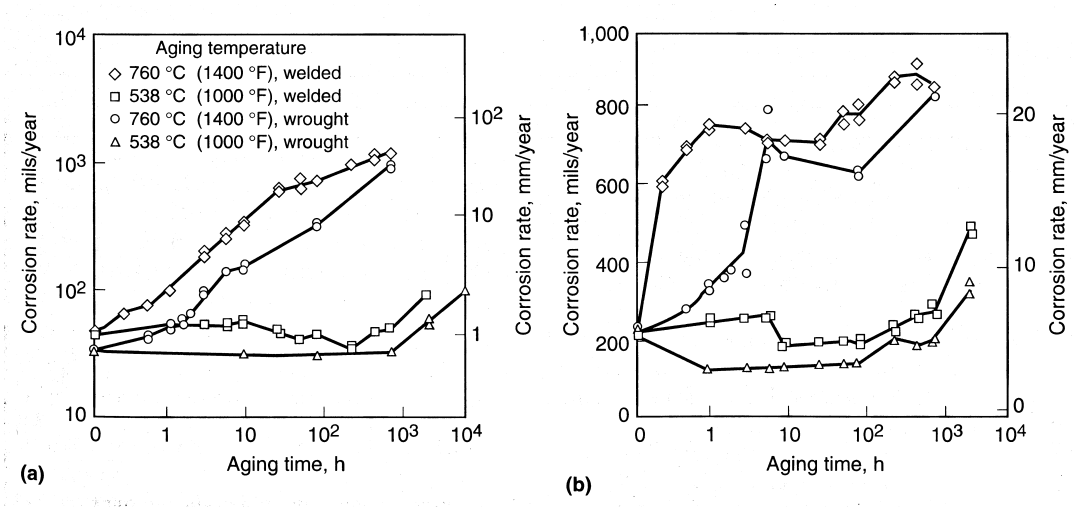

Fig. 14 Corrosion rates for wrought and for gas tungsten arc welded (GTAW) alloy C-22 (UNS N06022). (a) In boiling sulfuric acid/ferric sulfate (ASTM G 28 Method A). (b) In boiling 2.5% HCl solution. Source: Ref 42

of 760 °C (1400 °F) and at the aging time of 10 h, the corrosion rate of the welded coupons is approximately 2 times the corrosion rate of the wrought coupons. Figure 14(b) shows the corrosion rate in boiling 2.5% HCl solution for wrought and as-welded coupons at two aging temperatures, 760 and 538 °C (1400 and 1000 °F), as a function of aging time. For the shorter aging times (up to 3 to 6 h), the corrosion rate of the welded coupons is approximately 3 times the corrosion rate of the wrought coupons; however, for aging times of 6 h and longer, the difference in the corrosion rate is smaller.

The increase in the corrosion rate of high-temperature aged alloy N06022 is pronounced in highly reducing conditions (boiling pure HCl solutions) and highly oxidizing solutions (boiling 50% H_2SO_4 plus 42 g/L $Fe_2(SO_4)_3$. However, at intermediate oxidizing potentials, the aged alloy is still able to maintain passivity. This was corroborated through potentiodynamic anodic polarization (Ref 40) and through corrosion immersion tests in boiling HCl solutions contaminated with different levels of ferric ions (Ref 38).

ACKNOWLEDGMENTS

This chapter was adapted from:

- P. Crook et al., Corrosion of Nickel and Nickel-Base Alloys, *Corrosion: Materials,* Vol 13B, *ASM Handbook,* ASM International, 2005, p 228–251
- K.F. Krysiak et al., Corrosion of Weldments, *Corrosion,* Vol 13, *Metals Handbook,* 9th ed., ASM International, 1987, p 344–368
- S.J. Matthews, Selection of Nickel-Base Corrosion-Resistant Alloys Containing Molybdenum, *Welding, Brazing, and Soldering,* Vol 6, *ASM Handbook,* ASM International, 1993, p 593–597
- R.B. Rebak, Effects of Metallurgical Variables on the Corrosion of High-Nickel Alloys, *Corrosion: Fundamentals, Testing, and Protection,* Vol 13A, *ASM Handbook,* ASM International, 2003, p 279–286
- A.J. Sedriks, Corrosion Resistance of Stainless Steels and Nickel Alloys, *Corrosion; Fundamentals, Testing, and Protection,* Vol 13A *ASM Handbook,* ASM International, 2003, p 697–702
- D.J. Tillack, Selection of Nickel, Nickel-Copper, Nickel-Chromium, and, Nickel-Chromium-Iron Alloys, *Welding, Brazing, and Soldering,* Vol 6, *ASM Handbook,* ASM International, 1993, p 586–592

REFERENCES

1. M.J. Donachie and S.J. Donachie, Superalloys, *Metals Handbook Desk Edition,* 2nd ed., ASM International, 1998, p 394–414
2. M.J. Donachie and S.J. Donachie, *Superalloys: A Technical Guide,* 2nd ed., ASM International, 2002
3. G.Y. Lai, *High-Temperature Corrosion of Engineering Alloys,* ASM International, 1990
4. G.N. Flint, *J. Inst. Met.,* Vol 87, 1959, p 303–310
5. G.N. Flint *Metallurgia,* Vol 62, 1960, p 195–200
6. W.A. Krivsky, U.S. Patent 3,252,790, May 1966
7. F.G. Hodge and R.W. Kirchner, *Mater. Perform.,* Vol 15 (No. 8), 1976, p 40–45
8. D.L. Klarstrom, A New Ni-Mo Alloy with Improved Thermal Stability, *Pro. 12th Intl. Corrosion Congress,* Sept 1993 (Houston, TX), NACE International, 1993
9. M.M. James, D.L. Klarstrom, and B. Saldanha, Stress-Corrosion Cracking of Nickel-Molybdenum Alloys, Paper 432, *Pro. Corrosion 96,* March 1996 (Houston, TX), NACE International, 1996
10. C.R. Brooks, J.E. Spruiell, and E.E. Standsbury, *Int. Met. Rev.,* Vol 29 (No. 3), 1984, p 210–248
11. S.J. Pawel, *Corrosion,* Vol 50 (No. 12), 1994, p 963–971
12. M. Raghavan, B.J. Berkowitz, and J.C. Scanlon, *Metall. Trans. A,* Vol 13, 1982, p 979–984
13. F.G. Hodge, *Corrosion,* Vol 29 (No. 10), 1973, p 375–383
14. L.M. Pike, D.L. Klarstrom, and M.F. Rothman, U.S. Patent 6,544,362, April 2003
15. "Specification for Nickel and Nickel Alloy Bare Welding Electrodes and Rods," A5.14, American Welding Society, 1997
16. "Specification for Nickel and Nickel Alloy Welding Electrodes for Shielded Metal Arc Welding," A5.11, American Welding Society, 1997
17. S.J. Matthews, Simulated Heat-Affected Zone Studies of Hastelloy Alloy B-2 *Weld. J. Res. Suppl.,* March 1979

18. A.I. Asphahani and S.J. Matthews, High Molybdenum Nickel-Base Alloy, U.S. Patent 4,846,885, July 11, 1989
19 E.M. Horn, P. Mattern, H. Schlecke, J. Korkhaus, A.I. Asphahani, and S.J. Matthews, Hastelloy Alloy B-42 Weld Overlay Welding, *Werkst. Korros.,* Vol 43, 1992, p 396–401
20. J.M. Sarver, J.R. Crum, and W.L. Mankins, "Carbide Precipitation and the Effect on Thermal Treatments on the Stress Corrosion Cracking Behaviour of Inconel Alloy 690," paper presented at Corrosion '87, NACE, 1987
21. F.G. Hodge and R.W. Kirchner, Paper 60, presented at Corrosion/75 (Toronto, Canada), National Association of Corrosion Engineers, April 1975
22. R.B. Leonard, *Corrosion,* Vol 25 (No. 5), 1969, p 222—228
23. F.G. Hodge and R.W. Kirchner, paper presented at the Fifth European Congress on Corrosion (Paris), Sept 1973
24. P.E. Manning and J.D. Schöbel, paper presented at ACHEMA '85 (Frankfurt, West Germany), 1985
25. P.E. Manning and J.D. Schöbel, *Werkst. Korros.,* Vol 37 1986, p 137
26. R.B. Rebak, in *Proc. Symposium on Passivity and Its Breakdown,* Vol 97-26, The Electrochemical Society, 1998, p 1001
27. R.B. Rebak and N.E. Koon, Paper 153, Corrosion/98, NACE International, 1998
28. K.A. Gruss, G.A. Cragnolino, D.S. Dunn, and N. Sridhar, Paper 149, Corrosion/98, NACE International, 1998
29. R.B. Rebak and P. Crook, in *Critical Factors in Localized Corrosion III,* Vol PV 98-17, The Electrochemical Society, 1999, p 289
30. R.B. Rebak, N.E. Koon, J.P. Cotner, and P. Crook, in *Passivity and Localized Corrosion,* Vol PV 99-27, The Electrochemical Society, 1999, p 473
31. D.S. Dunn, G.A. Cragnolino, and N. Sridhar, in *Scientific Basis for Nuclear Waste Management XXII,* Vol 556, Materials Research Society, 1998, p 879
32. B.A. Kehler, G.O. Ilevbare, and J.R. Scully, Paper 182, Corrosion 2000, NACE International, 2000
33. S.J. Matthews, *Proc. Third International Conf. on Superalloys,* Claitor's Publishing Division, 1976, p 215
34. U.L. Heubner, E. Altpeter, M.B. Rockel, and E. Wallis, *Corrosion* Vol 45, 1989, p 249
35. H.M. Tawancy, *J. Mater, Sci.,* Vol 31, 1996, p 3929
36. T.S. Edgecumbe Summers, M.A. Wall, M. Kumar, S.J. Matthews, and R.B. Rebak, in *Scientific Basis for Nuclear Waste Management XXII,* Vol 556, Materials Research Society, 1999, p 919
37. T.S. Edgecumbe Summers, T. Shen, and R.B. Rebak, in *Aging Studies and Lifetime Extension of Materials,* Kluwer Academic/Plenum Publisher, 2001, p 507
38. R.B. Rebak, N.E. Koon, J.R. Dillman, P. Crook, and T.S. Edgecumbe Summers, Paper 181, Corrosion/2000, NACE International, 2000
39. R.B. Rebak, T.S. Edgecumbe Summers, and R.M. Carranza, in *Scientific Basis for Nuclear Waste Management XXIII,* Vol 608, Materials Research society, 2000, p 109
40. R.B. Rebak, N.E. Koon, and P. Crook, in *Electrochemical Approach to Selected Corrosion and Corrosion Control Studies,* No. 28, the Institute of Materials, 2000, p 245
41. T.S. Edgecumbe Summers, R.B. Rebak, T.A. Palmer, and P. Crook, in *Scientific Basis for Nuclear Waste Management XXV,* Materials Research Society, 2002
42. R.B. Rebak, T.S. Edgecumbe Summers, T. Lian, R. M. Carranza, J. R. Dillman, T. Corbin, and P. Crook, Paper 542, Corrosion/2002, NACE International, 2002
43. R.B. Rebak and P. Crook, Transportation, Storage and Disposal of Radioactive Materials *ASME Pressure Vessel and Piping Conf.,* Aug 4–8, 2002 (Vancouver, Canada), American Society of Mechanical Engineers, p 111

Corrosion of Weldments
J.R. Davis, editor, p 143-168
DOI:10.1361/corw2006p143

CHAPTER 8

Corrosion of Nonferrous Alloy Weldments

THE NONFERROUS ALLOYS described in this chapter include aluminum and aluminum alloys, copper and copper alloys, titanium and titanium alloys, zirconium and zirconium alloys, and tantalum and tantalum alloys (corrosion of nickel-base alloy weldments is discussed in Chapter 7). Some of the factors that affect the corrosion performance of welded nonferrous assemblies include galvanic effects, crevices, assembly stresses in products susceptible to stress-corrosion cracking (SCC), and hydrogen pickup and subsequent cracking.

Aluminum and Aluminum Alloys

The unique combinations of properties provided by aluminum and its alloys make aluminum one of the most versatile, economical, and attractive metallic materials for a broad range of uses—from soft, highly ductile wrapping foil to the most demanding engineering applications. Aluminum alloys are second only to steels in use as structural metals.

Aluminum has a density of only 2.7 g/cm^3, approximately one third as much as steel (7.83 g/cm^3). One ft^3 of steel weighs about 490 lb; a cubic foot of aluminum, approximately 170 lb. Such light weight, coupled with the high strength of some aluminum alloys (exceeding that of structural steel), permits design and construction of strong, lightweight structures that are particularly advantageous for anything that moves—space vehicles and aircraft as well as all types of land- and water-borne vehicles.

Aluminum resists the kind of progressive oxidization that causes steel to rust away. The exposed surface of aluminum combines with oxygen to form an inert aluminum oxide film only a few ten-millionths of an inch thick, which blocks further oxidation. And, unlike iron rust, the aluminum oxide film does not flake off to expose a fresh surface to further oxidation. If the protective layer of aluminum is scratched, it will instantly reseal itself.

The thin oxide layer itself clings tightly to the metal and is colorless and transparent—invisible to the naked eye. The discoloration and flaking of iron and steel rust do not occur on aluminum.

Appropriately alloyed and treated, aluminum can resist corrosion by water, salt, and other environmental factors, and by a wide range of other chemical and physical agents. The corrosion characteristics of aluminum alloys are examined in the article "Corrosion of Aluminum and Aluminum Alloys" in Volume 13B of the *ASM Handbook* and in Ref 1.

General Welding Considerations

Aluminum and its alloys can be joined by as many or more methods as any other metal. The primary welding methods used are the gas-shielded arc welding processes, that is, gas metal arc welding (GMAW) and gas tungsten arc welding (GTAW). These methods eliminate the potential hazard of flux removal inherent with oxyfuel gas welding and shielded metal arc welding (SMAW). Flux residues, of course, are corrosive. If the welding method requires flux, the joint must permit thorough flux removal.

Factors that affect the welding of aluminum include:

- Aluminum oxide coating
- Thermal conductivity

- Thermal expansion coefficient
- Melting characteristics
- Electrical conductivity

Aluminum oxide immediately forms on aluminum surfaces exposed to air. Before aluminum can be welded by fusion methods, the oxide layer must be removed mechanically by machining, filing, wire brushing, scraping, or chemical cleaning. If oxides are not removed, oxide fragments may be entrapped in the weld and will cause a reduction in ductility, a lack of fusion, and possibly weld cracking. During welding, the oxide must be prevented from reforming by shielding the joint area with a nonoxidizing gas such as argon, helium, or hydrogen, or chemically by use of fluxes.

Thermal conductivity is a property that most affects weldability. The thermal conductivity of aluminum alloys is about one-half that of copper and four times that of low-carbon steel. This means that heat must be supplied four times as fast to aluminum alloys as to steel to raise the temperature locally by the same amount. However, the high thermal conductivity of aluminum alloys helps to solidify the molten weld pool of aluminum and, consequently, facilitates out-of-position welding.

The coefficient of linear expansion which is a measure of the change in length of a material with a change in its temperature, is another physical property of importance when considering weldability. The coefficient of linear thermal expansion for aluminum is twice that for steel. This means that extra care must be taken in welding aluminum to ensure that the joint space remains uniform. This may necessitate preliminary joining of the parts of the assembly by tack welding prior to the main welding operation.

The combination of high coefficient of thermal expansion and high thermal conductivity would cause considerable distortion of aluminum during welding were it not for the high welding speed possible.

Melt Characteristics. The melting ranges for aluminum alloys are considerably lower than those for copper or steel. Melting temperatures and the volumetric specific heats and heats of fusion of aluminum alloys determine that the amount of heat required to enter the welding temperature range is much lower for aluminum alloys.

Electrical conductivity has little influence on fusion welding but is a very important property for materials that are to be resistance welded. In resistance welding, resistance of the metal to the flow of welding current produces heat that causes the portion of the metal through which the current flows to approach or reach its melting point. Aluminum has higher conductivity than steel, which means that much higher currents are required to produce the same heating effect. Consequently, resistance welding machines for aluminum must have much higher output capabilities than those normally used for steel, for welding comparable sections.

More detailed information on the welding characteristics of both wrought- and cast-aluminum alloys can be found in the article "Welding of Aluminum Alloys" in Volume 6 of the *ASM Handbook.*

Corrosion Behavior of Aluminum Alloy Weldments

Galvanic Effects. The resistance to corrosion of weldments in aluminum alloys is affected by the alloy being welded and by the filler alloy and welding process used. Galvanic cells that cause corrosion can be created because of corrosion potential differences among the base (parent) metal, the filler metal, and the heat-affected regions where microstructural changes have been produced.

Corrosion Resistance. Wrought aluminum alloys can be classified as either non-heat treatable alloys or heat treatable alloys (Table 1). The corrosion resistance of the non-heat treatable alloys is not altered significantly by the

Table 1 Classification of wrought aluminum alloys according to their strengthening mechanism

Alloy system	Aluminum series
Non-heat-treatable (work-hardenable) alloys	
Pure Al	1*xxx*
Al-Mn	3*xxx*
Al-Si	4*xxx*
Al-Mg	5*xxx*
Al-Fe	8*xxx*
Al-Fe-Ni	8*xxx*
Heat treatable (precipitation-hardenable) alloys	
Al-Cu	2*xxx*
Al-Cu-Mg	2*xxx*
Al-Cu-Li	2*xxx*
Al-Mg-Si	6*xxx*
Al-Zn	7*xxx*
Al-Zn-Mg	7*xxx*
Al-Zn-Mg-Cu	7*xxx*
Al-Li-Cu-Mg	8*xxx*

heat of welding. The Al-Mg-Si heat treatable alloys, such as 6061 and 6063, also have high corrosion resistance in the welded condition. The 2*xxx* and 7*xxx* series heat treatable alloys, which contain substantial amounts of copper and zinc, respectively, can have their resistance to corrosion altered by the heat of welding. For example, in the aluminum-copper alloys, the heat-affected zone (HAZ) becomes cathodic, whereas in the aluminum-zinc alloys, it becomes anodic to the remainder of the weldment in the presence of water or other electrolytes (Ref 2). The corrosion (or solution) potentials across the weld zone for a 5*xxx,* 2*xxx,* and 7*xxx* series weldment are shown in Fig. 1. These differences in potential can lead to localized corrosion, as demonstrated by the corrosion of the HAZ of an as-welded structure of alloy 7005 shown in Fig. 2. In general, the welding procedure that puts the least amount of heat into the metal has the least influence on microstructure and the least chance of reducing the corrosion behavior of aluminum weldments.

Different aluminum alloys compositions produce slightly different electrode potentials in the presence of various solutions. Selective corrosion can result in immersed service, where the base alloy and weld metal possess significant differences in potential. Table 2 lists the solution potentials for common aluminum alloys in a salt solution.

The alloy with the more negative potential in the weldment will attempt to protect the other part. Thus, if the weld metal is anodic to the base metal (as is a 5356 weld in 6061-T6), the small weld can be attacked preferentially to protect the larger surface area of the base metal. The greater the area to be protected and the greater the difference in electrode potential, the more rapidly will corrosive action occur.

Optimum corrosion resistance is obtained when the solution potential of the filler is the same as that of the base alloy, as shown in Table 2 for 4043 for filler alloy and 6061-T6. If this is not practical, then a preferred arrangement is to have the larger base alloy surface area be anodic to the weld metal, such as 7005-T6 welded with 5356 filler.

For the welds shown in Fig. 1, the HAZ in the 5*xxx* alloy is mildly cathodic, whereas the 2*xxx* alloy exhibits a greater cathodic differential. The 7*xxx* series HAZ is anodic to the unaffected material and would be of greatest concern. Fabrications in the 7*xxx* alloys are usually painted to avoid galvanic corrosion. However, as an additional safety precaution in some cases, the weld area is metallized with another aluminum alloy to prevent galvanic corrosion if a void occurs in the paint coating. Most unprotected aluminum-base filler alloy combinations are very satisfactory for general atmospheric conditions.

In some cases, an alloy constituent can be formed by alloying components of the base and filler alloys to produce an anodic zone at the

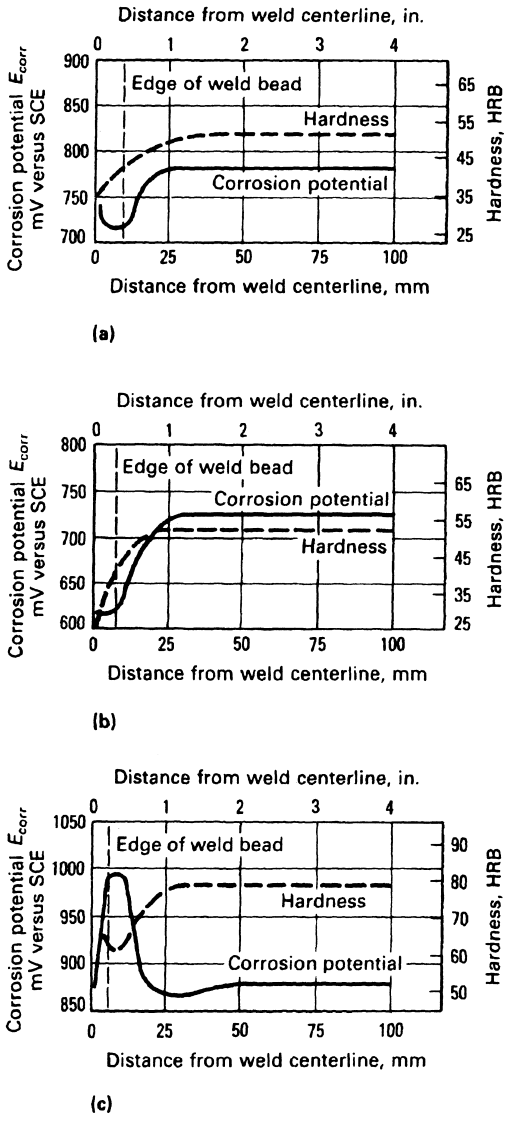

Fig. 1 Effect of the heat of welding on microstructure, hardness, and corrosion potential of welded assemblies of three aluminum alloys. The differences in corrosion potential versus saturated calomel electrode (SCE) between the heat-affected zone (HAZ) and the base metal can lead to selective corrosion. (a) Alloy 5456-H321 base metal with alloy 5556 filler; three-pass metal inert gas weld. (b) Alloy 2219-T87 base metal with alloy 2319 filler; two-pass tungsten inert gas weld. (c) Alloy 7039–T651 base metal with alloy 5183 filler; two-pass tungsten inert gas weld

transition of the weld and base metal. If a 5*xxx* alloy is welded with an aluminum-silicon filler, or vice versa, then a magnesium silicide constituent can be formed. For certain immersed conditions, such as a mild acid condition, the magnesium silicide can be highly anodic to all other parts of the weldment (Ref 3, 4). A very selective knife-line corrosive attack can result from this immersed service.

A study involving corrosion potential measurements taken across weldments (through base metal, HAZ, and weld metal) has identified certain aluminum-lithium alloy compositions as being susceptible to galvanic attack in a saline environment (Ref 5). In particular, two experimental alloys with high lithium content (2.9 wt% Li and 3.0 wt% Cu), welded with either 2319 or 4043 fillers, displayed a narrow region within the HAZ that was highly anodic to both base metal and weld metal. This behavior was attributed to the formation of the equilibrium δ (AlLi) phase and resulted in severe pitting in the HAZ. In contrast, a 2090-type alloy containing approximately 2.3 wt% Li and 2.7 wt% Cu showed a continuously increasing (cathodic) potential when going from base metal to weld metal and was resistant to pitting attack. This behavior was attributed to the absence of the δ phase due to a higher copper-lithium ratio.

Filler Alloy Selection. Although aluminum alloys can be welded autogenously (without the addition of a filler metal), the use of a filler metal is preferred to avoid weld cracking during welding and to optimize corrosion resistance. Table 3 summarizes filler alloy selection recommended for welding various combinations of base metal alloys to obtain maximum properties, including corrosion resistance. Table 4 lists the chemical composition and melting range of standard aluminum filler alloys.

The corrosion data in Table 3 are based on performance in fresh or salt water and do not necessarily apply to other exposure conditions. Therefore, care must be taken not to extrapolate the corrosion performance ratings indiscriminately. Corrosion behavior ratings generally pertain only to the particular environment tested, usually rated in continuous or alternate immersion in fresh or salt water. For example, the highest corrosion rating (A) is listed for use

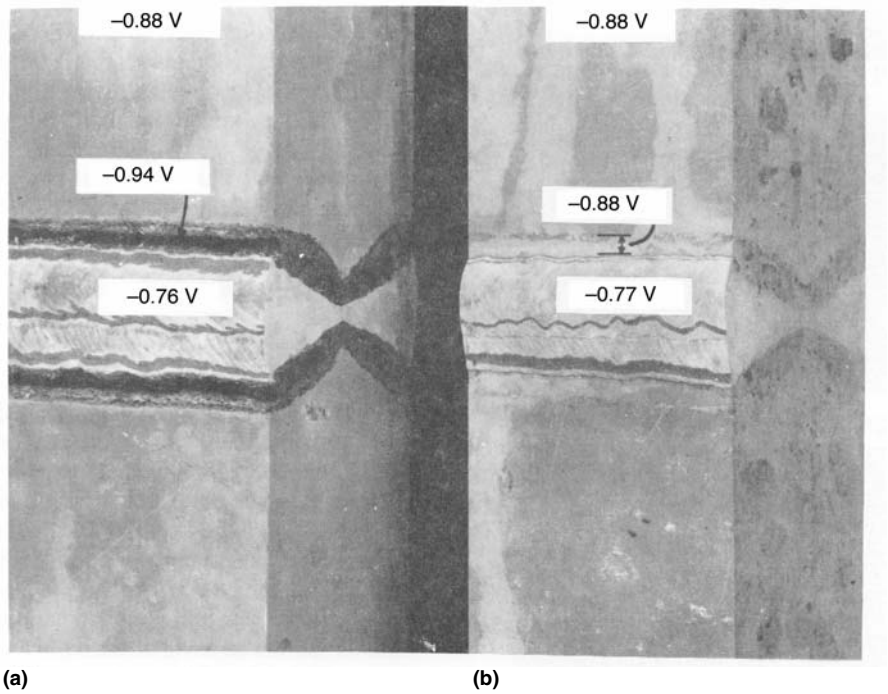

Fig. 2 Welded assemblies of aluminum alloy 7005 with alloy 5356 filler metal after a one-year exposure to seawater. (a) As-welded assembly shows severe localized corrosion in the HAZ. (b) Specimen showing the beneficial effects of postweld aging. Corrosion potentials of different areas of the weldments are shown where they were measured. Electrochemical measurements performed in 53 g/L NaCl plus 3 g/L H_2O_2 versus a 0.1 *N* calomel reference electrode and recalculated to a saturated calomel electrode (SCE)

of filler alloy 4043 to join 3003 alloy to 6061 alloy. In strong (99%) nitric acid (HNO_3) service, however, a weldment made with 4043 filler alloy would experience more rapid attack than a weldment made using 5556 filler metal. With certain alloys, particularly those of the heat treatable 7*xxx* series, thermal treatment after welding is sometimes used to obtain maximum corrosion resistance (Fig. 2) (Ref 6–8). When postweld solution heat treating and aging is carried out on 7*xxx* base metals, aluminum-magnesium filler alloys containing more than 3.5% magnesium should not be used because the fusion zone can be sensitized to SCC.

Effect of Chemistry Control. Some chemical exposures or special circumstances can require special controls within the elements of an alloy. In the case of hydrogen peroxide exposure, the manganese and copper impurities have been controlled to low limits in 5652 and 5254 base alloys, as well as in 5654 filler alloy. In some cases, a high-purity aluminum alloy is chosen for special exposure. A filler alloy of equal or higher purity to that of the base alloy is generally acceptable in these cases, and filler alloy 1188 would meet most of these requirements.

Crevice Corrosion. As with many other alloy systems, attention must be given to the threat of crevice corrosion under certain conditions. Strong (99%) HNO_3 is particularly aggressive toward weldments that are not made with full weld penetration. Although all of the welds shown in Fig. 3 appear to be in excellent condition when viewed from the outside surface, the first two welds (Fig. 3a and b), viewed from the inside, are severely corroded. The weld made using standard GTAW practices with full weld penetration (Fig. 3c) is in good condition after two years of continuous service.

Table 2 Electrode potential of aluminum alloys in NaCl—H_2O_2 solution

Aluminum alloy(a)	Potential volts 0.1 *N* calomel scale(b)	Filler alloy
A712.0	–0.99	. . .
Alclad 3003, alclad 6061, 7072	–0.96	. . .
7005-T6, 7039-T6	–0.93 to –0.96	. . .
5083, 5456, 514.0	–0.87	5183, 5356, 5556
5154, 5254, 5454, 5086	–0.86	5554, 5654
5052	–0.85	. . .
1350, 3004, 5050, 7075-T73	–0.84	1188
1100, 3003, 5005, 6061-T6, 6063, Alclad 2014, Alclad 2024, 413.0, A443.0	–0.82 to –0.83	1100, 4043, 4047
6061-T4, 7075-T6, 356.0-T6, 360.0	–0.80 to –0.81	. . .
2219-T6 and -T8	–0.79 to –0.82	2319
2014-T6, 355.0-T6	–0.78 to –0.79	. . .
380.0, 319.0, 333.0	–0.75	4145
2014-T4, 2024-T3 and -T4	–0.68 to –0.70(c)	. . .
2219-T3 and -T4	–0.63 to –0.65(c)	. . .

(a) Potential of all tempers is the same unless a specific temper is designated. (b) Measured in an aqueous solution of 53 g NaCl + 3 g H_2O_2 per liter at 25 °C (77 °F). (c) Potential varies with quenching rate during fabrication.

Knife-Line Attack. Researchers have shown that aluminum alloys, both welded and unwelded, have good resistance to uninhibited HNO_3 (both red and white) up to 50 °C (120 °F). Above this temperature, most aluminum alloys exhibit knife-line attack (a very thin region of corrosion) adjacent to the welds. Above 50 °C (120 °F), the depth of knife-line attack increases markedly with temperature. One exception was found in the case of a fusion-welded 1060 alloy in which no knife-line attack was observed even at temperatures as high as 70 °C (160°F). In inhibited fuming HNO_3 containing at least 0.1% hydrofluoric acid (HF), no knife-line attack was observed for any commercial aluminum alloy or weldment even at 70 °C (160 °F).

Avoiding SCC. Wrought alloys usually have greater resistance to SCC in the longitudinal orientation (direction of working) than in the transverse orientation or in the short-transverse orientation (through the thickness) (Ref 9). Because of this, welding of the 7*xxx* series alloys near a base-metal edge can result in a tensile stress in the short-transverse direction sufficient to cause SCC in the exposed edge. "Buttering" the edge with weld metal provides compressive stress at the edge and overcomes the SCC problem.

Resistance spot-welding has been used in aircraft and other applications (Ref 10), including (more recently) the automotive industry (Ref 11). Generally, the resistance to corrosion of resistance spot-welded aluminum is high, but in the case of high-strength 2*xxx* and 7*xxx* alloys, selective attack of the welds can develop in corrosive service, as a result of changes in microstructure that occur during welding. Protection to alloys of this type should be provided when they are used under severe environmental conditions.

Crevice corrosion can occur in spot-welded assemblies. One approach used to solve this problem is a procedure called weld bond (Ref 12–14) that combines adhesive bonding with

Table 3 Relative rating of selected aluminum filler alloys used to fillet weld or butt weld two component base alloys

Data are for welded assembles that were not heat treated after welding. Alloys 1 and 2 are base alloys to be joined. See Table 4 for filler alloy compositions.

Alloy 1	Alloy 2	Filler alloys	Filler alloy characteristic(a) W	S	D	C	T	M
319.0, 333.0, 354.0, 355.0 C355.0, 380.0	1060, 1350	4043	B	A	A	A	A	A
		4145	A	A	B	A	A	A
	1100	4043	B	A	A	A	A	A
		4145	A	A	B	A	A	A
	2014, 2036	2319	B	A	A	A	A	A
		4043	C	C	B	C	A	A
		4145	A	B	C	B	A	A
	2219	2319	B	A	A	A	A	A
		4043	C	C	B	C	A	A
		4145	A	B	C	B	A	A
	3003, Alclad 3003	4043	B	B	A	A	A	A
		4145	A	A	B	A	A	A
	3004	4043	B	B	A	A	A	A
		4145	A	A	B	A	A	A
	Alclad 3004	4043	B	B	A	A	A	A
		4145	A	A	B	A	A	A
	5005, 5050	4043	B	B	A	A	A	A
		4145	A	A	B	A	A	A
	5052, 5652	4043	A	A	A	A	A	A
	5083, 5456	4043	A	A	A	A	…	A
	5086, 5356	4043	A	A	A	A	…	A
	514.0, A514.0 B514.0, F514.0, 5154, 5254	4043	A	A	A	A	…	A
	5454	4043	A	A	A	A	A	A
	6005, 6063, 6101, 6151, 6201, 6351, 6951	4043	B	B	A	A	A	A
		4145	A	A	B	A	A	A
	6061, 6070	4043	B	B	A	A	A	A
		4145	A	A	B	A	A	A
	7005, 7021, 7039, 7046, 7146, A712.0, C712.0	4043	B	B	A	A	A	A
		4145	A	A	B	A	A	A
	413.0, 443.0, 444.0, 356.0, A356.0, A357.0, 359.0	4043	B	B	A	A	A	A
		4145	A	A	B	A	A	A
	319.0, 333.0, 354.0, 355.0 C355.0, 380.0	2319	B	A	A	A	A	A
		4145	A	B	B	B	A	A
413.0, 443.0, 444.0, 356.0, A356.0, A357.0, 359.0	1060, 1350	4043	A	A	A	A	A	A
		4145	A	A	B	B	A	…
	1100	4043	A	A	A	A	A	A
		4145	A	A	B	B	A	…
	2014, 2036	4043	B	B	A	A	A	A
		4145	A	A	B	A	A	…
	2219	4043	B	B	A	A	A	A
		4145	A	A	B	A	A	…
	3003, Alclad 3003	4043	A	A	A	A	A	A
		4145	A	A	B	B	A	…
	3004	4043	A	A	A	A	A	A
	Alclad 3004	4043	A	A	A	A	A	A
	5005, 5050	4043	A	A	A	A	A	A
	5052, 5652	4043	A	B	A	A	A	A
		5356	B	A	B	B	…	A
	5083, 5456	4043	A	B	B	A	…	A
		5356	A	A	A	A	…	A
	514.0, A514.0, B514.0, F514.0, 5154, 5254	4043	A	B	B	A	…	A
		5356	A	A	A	B	…	A
	5454	4043	A	B	B	A	A	A
		5356	A	A	A	B	…	A
	6005, 6063, 6101, 6151, 6201, 6351, 6951	4043	A	B	A	A	A	A
		4145	A	A	B	B	A	…
	6061, 6070	4043	A	B	A	A	A	A
		4145	A	A	B	A	A	A
	7005, 7021, 7039, 7046, 7146, A712.0, C712.0	4043	A	B	B	A	A	A
		4145	A	A	B	B	A	…
		5356	A	A	A	B	…	A
	413.0, 443.0, 444.0, 356.0, A356.0, A357.0, 359.0	4043	A	B	B	A	A	A
		4145	A	A	B	B	A	…
		5356	A	A	A	B	…	A
	319.0, 333.0, 354.0, 355.0 C355.0, 380.0	2319	A	B	B	B	A	A
		4043	A	B	B	B	A	A
		4145	A	A	B	B	A	…
		5356	A	A	A	B	…	A
7005, 7021, 7039, 7046, 7146, A712.0, C712.0	1060, 1350	4043	A	A	C	A	A	…
		5183	B	A	B	A	…	A
		5356	B	A	A	A	…	A
		5556	B	A	B	A	…	A
	1100	4043	A	A	C	A	A	…
		5183	B	A	B	A	…	A
		5356	B	A	A	A	…	A
		5556	…	A	B	A	…	A
	2014, 2036	4043	B	B	A	A	A	…
		4145	A	A	B	A	A	…
	2219	4043	B	B	A	A	A	…
		4145	A	A	B	A	A	…
	3003, Alclad 3003	4043	A	B	C	A	A	…
		5183	B	A	B	A	…	A
		5356	B	A	A	A	…	A
		5556	B	A	B	A	…	A
	3004	4043	A	D	C	B	A	…
		5183	B	A	B	A	…	A
		5356	B	B	A	A	…	A
		5554	C	C	A	A	A	A
		5556	B	A	B	A	…	A
		5654	C	C	A	A	…	B
	Alclad 3004	4043	A	D	C	B	A	…
		5183	B	A	B	A	…	A
		5356	B	B	A	A	…	A
		5554	C	C	A	A	A	A
		5556	B	A	B	A	…	A
		5654	C	C	A	A	…	B
	5005, 5050	4043	A	B	C	B	A	…
		5183	B	A	B	A	…	A
		5356	B	A	A	A	…	A
		5554	C	A	A	A	A	A
		5556	B	A	B	A	…	A
		5654	C	A	A	A	…	A
	5052, 5652	4043	B	D	C	B	A	…
		5183	A	A	B	A	…	A
		5356	A	B	A	A	…	A
		5554	B	C	A	A	A	A
		5556	A	A	B	A	…	A
		5654	B	C	A	A	…	A
	5083, 5456	5183	A	A	B	A	…	A
		5356	A	B	A	A	…	A
		5556	A	A	B	A	…	A
	5086, 5356	5183	A	A	B	A	...	A
		5356	A	B	A	A	...	A
		5556	A	A	B	A	...	A
	514.0, A514.0, B514.0, F514.0, 5154, 5254	5183	A	A	B	A	…	A
		5356	A	B	A	A	…	A
		5554	B	C	A	A	…	A
		5556	A	A	B	A	…	A
		5654	B	C	A	A	…	A
	5454	5183	A	A	B	A	…	A
		6151, 6201, 6351, 6951	4145	A	A	B	B	A	…
	6061, 6070	4043	A	B	A	A	A	A
		4145	A	A	B	B	A	…
	7005, 7021, 7039, 7046, 7146, A712.0, C712.0	4043	A	B	B	A	A	A
		4145	A	A	B	B	A	…
		5356	A	A	A	A	…	B
	413.0, 443.0, 444.0, 356.0, A356.0, A357.0, 359.0	4043	A	B	A	A	A	A
		4145	A	A	B	B	A	…
		5356	A	A	A	A	…	A

(continued)

(a) A, B, C, and D represent relative ratings (where A is best and D is worst) of the performance of the two component base alloys combined with each group of selected filler alloys. W, ease of welding (relative freedom from weld cracking); S, strength of welded joint in as-welded condition (rating applies specifically to fillet welds, but all rods and electrodes rated will develop presently specific minimum strengths for butt welds); D, ductility (rating based on free bend elongation of the weld); C, corrosion resistance in continuous or alternate immersion of fresh or salt water, T, performance in service at sustained temperatures >65 °C (>150 °F); M, color match after anodizing. (b) No filler suitable. *Note:* Combinations having no ratings are not recommended. Source: Aluminum Company of America

Table 3 (continued)

Alloy 1	Alloy 2	Filler alloys	Filler alloy characteristic(a) W	S	D	C	T	M
7005, 7021, 7039, 7046, 7146, A712.0, C712.0 (continued)	5454 (continued)	5356	A	B	A	A	…	A
		5554	B	C	A	A	A	A
		5556	A	A	B	A	…	A
		5654	B	C	A	A	…	A
	6005, 6063, 6101, 6151, 6201 6351, 6951	4043	A	D	C	B	A	…
		5183	A	A	B	A	…	A
		5356	A	B	A	A	…	A
		5554	B	C	A	A	A	A
		5556	A	A	B	A	…	A
		5654	B	C	A	A	…	A
	6061, 6070	4043	A	D	C	B	A	…
		5183	A	A	B	A	…	A
		5356	A	B	A	A	…	A
		5554	B	C	A	A	A	A
		5556	A	A	B	A	…	A
		5654	B	C	A	A	…	A
	7005, 7021, 7039, 7046, 7146, A712.0, C712.0	4043	B	D	C	B	A	…
		5183	A	A	B	A	…	A
		5356	A	B	A	A	A	A
		5554	B	C	A	A	…	A
		5556	A	A	B	A	…	A
		5654	B	C	A	A	…	A
6061, 6070	1060, 1350	4043	A	A	C	A	A	…
		4145	A	A	D	B	A	…
		5183	B	A	B	…	…	A
		5356	B	A	A	…	…	A
		5556	B	A	B	…	…	A
	1100	4043	A	A	C	A	A	…
		4145	A	A	D	B	A	…
		5183	B	A	B	…	…	A
		5356	B	A	A	…	…	A
		5556	B	A	B	…	…	A
	2014, 2036	4043	B	B	A	A	A	…
		4145	A	A	B	A	A	…
	2219	4043	B	B	A	A	A	…
		4145	A	A	B	A	A	…
	3003, Alclad 3003	4043	A	B	C	A	A	…
		4145	A	A	D	B	A	…
		5183	B	A	B	…	…	A
		5356	B	A	A	…	…	A
		5556	B	A	B	…	…	A
	3004	4043	A	D	C	A	A	…
		4145	B	C	D	B	A	…
		5183	B	A	B	…	…	A
		5356	B	B	A	…	…	A
		5556	B	A	B	…	…	A
	Alclad 3004	4043	A	D	C	A	A	…
		4145	B	C	D	B	A	…
		5183	B	A	B	…	…	A
		5356	B	B	A	…	…	A
		5556	B	A	B	…	…	A
	5005, 5050	4043	A	B	C	A	A	…
		4145	A	B	D	B	A	…
		5183	B	A	B	…	…	A
		5356	B	A	A	…	…	A
		5556	B	A	B	…	…	A
	5052, 5652	4043	A	D	C	A	A	…
		5183	B	A	B	C	…	B
		5356	B	B	A	C	…	A
		5554	C	C	A	B	A	B
		5556	B	A	B	C	…	B
		5654	C	C	A	B	…	A
	5083, 5456	4043	A	D	C	A	…	…
		5183	A	A	B	A	…	A
		5356	A	B	A	A	…	A
		5554	B	C	A	A	…	A
		5556	A	A	B	A	…	A
		5654	B	C	A	A	…	A
	5086, 5356	4043	A	D	C	A	…	…
		5183	A	A	B	A	…	A
		5356	A	B	A	A	…	A
		5554	B	C	A	A	…	A
		5556	A	A	B	A	…	A
		5654	B	C	A	A	…	B
	514.0, A514.0, B514.0, F514.0, 5154, 5254	4043	A	D	C	A	…	…
		5183	B	A	B	C	…	B
		5356	B	B	A	C	…	A
		5554	C	C	A	B	…	B
		5556	B	A	B	C	…	B
		5654	C	C	A	B	…	A
	5454	4043	A	D	C	B	A	…
		5183	B	A	B	C	…	A
		5356	B	B	A	C	…	A
		5554	C	C	A	A	A	A
		5556	B	A	B	C	…	A
		5654	C	C	A	B	…	B
	6005, 6063, 6101, 6151, 6201, 6351, 6951	4043	A	C	B	A	A	…
		5183	B	A	A	C	…	A
		5356	B	A	A	C	…	A
		5554	C	B	A	B	B	A
		5556	B	A	A	C	…	A
		5654	C	B	A	B	…	B
	6061, 6070	4043	A	C	B	A	A	…
		5183	B	A	A	C	…	B
		5356	B	B	A	C	…	A
		5554	C	B	A	B	B	B
		5556	B	A	A	C	…	B
		5654	C	B	A	B	…	B
6005, 6063, 6101, 6151, 6201, 6351, 6951	1060, 1350	4043	A	A	C	A	A	…
		4145	A	A	D	B	A	…
		5183	B	A	B	…	…	A
		5356	B	A	A	…	…	A
		5556	B	A	B	…	…	A
	1100	4043	A	A	C	A	A	…
		4145	A	A	D	B	A	…
		5183	B	A	B	…	…	A
		5356	B	A	A	…	…	A
		5556	B	A	B	…	…	A
	2014, 2036	4043	B	B	A	A	A	…
		4145	A	A	B	A	A	…
	2219	4043	B	B	A	A	A	…
		4145	A	A	B	A	A	…
	3003, Alclad 3003	4043	A	B	C	A	A	…
		4145	A	A	D	B	A	…
		5183	B	A	B	…	…	A
		5356	B	A	A	…	…	A
		5556	B	A	B	…	…	A
	3004	4043	A	D	C	A	A	…
		4145	B	C	D	B	A	…
		5183	B	A	B	…	…	A
		5356	B	B	A	…	…	A
		5556	B	A	B	…	…	A
	Alclad 3004	4043	A	D	C	A	A	…
		4145	B	C	D	B	A	…
		5183	B	A	B	…	…	A
		5356	B	B	A	…	…	A
		5556	B	A	B	…	…	A
	5005, 5050	4043	A	B	C	A	A	…
		4145	A	B	D	B	A	…
		5183	B	A	B	…	…	A

(continued)

(a) A, B, C, and D represent relative ratings (where A is best and D is worst) of the performance of the two component base alloys combined with each group of selected filler alloys. W, ease of welding (relative freedom from weld cracking); S, strength of welded joint in as-welded condition (rating applies specifically to fillet welds, but all rods and electrodes rated will develop presently specific minimum strengths for butt welds); D, ductility (rating based on free bend elongation of the weld); C, corrosion resistance in continuous or alternate immersion of fresh or salt water, T, performance in service at sustained temperatures >65 °C (>150 °F); M, color match after anodizing. (b) No filler suitable. *Note:* Combinations having no ratings are not recommended. Source: Aluminum Company of America

Table 3 (continued)

Alloy 1	Alloy 2	Filler alloys	Filler alloy characteristic(a) W	S	D	C	T	M
6005, 6063, 6101 6151, 6201, 6351, 6951 (continued)	5005, 5050 (continued)	5356	B	A	A	…	…	A
		5556	B	A	B	…	…	A
	5052, 5652	4043	A	D	C	A	A	…
		5183	B	A	B	C	…	B
		5356	B	B	A	C	…	A
		5554	C	C	A	B	A	B
		5556	B	A	B	C	…	B
		5654	C	C	A	B	…	A
	5083, 5456	4043	A	B	C	A	…	…
		5183	A	A	B	A	…	A
		5354	A	A	A	A	…	A
		5556	B	A	A	A	…	A
		5556	A	A	B	A	…	A
		5654	B	A	A	A	…	B
	5086, 5356	4043	A	B	C	A	…	…
		5183	A	A	B	A	…	A
		5356	A	A	A	A	…	A
		5554	B	A	A	A	…	A
		5556	A	A	B	A	…	A
		5654	B	A	A	A	…	B
	514.0, A514.0, B514.0, F514.0, 5154, 5254	4043	A	B	C	A	…	…
		5183	B	A	B	C	…	A
		5356	B	A	A	C	…	A
		5554	C	A	A	B	…	A
		5556	B	A	B	C	…	A
		5654	C	A	A	B	…	B
	5454	4043	A	B	C	B	A	…
		5183	B	A	B	C	…	A
		5356	B	A	A	C	…	A
		5554	C	A	A	A	A	A
		5556	B	A	B	C	…	A
		5654	C	A	A	B	…	B
	6005, 6063, 6101, 6151, 6201, 6351, 6951	4043	A	C	B	A	A	…
		5183	B	A	A	C	…	A
		5356	B	A	A	C	…	A
		5554	C	B	A	B	B	A
		5556	B	A	A	C	…	A
		5654	C	B	A	B	…	B
5454	1060, 1350	4043	A	B	C	C	A	…
		5183	B	A	B	B	…	A
		5356	B	A	A	B	…	A
		5554	C	A	A	A	A	A
		5556	B	A	B	B	…	A
	1100	4043	A	B	C	C	A	…
		5183	B	A	B	B	…	A
		5356	B	A	A	B	…	A
		5554	C	A	A	A	A	A
		5556	B	A	B	B	…	A
	2041, 2036	(b)	…	…	…	…	…	…
	2219	4043	A	A	A	A	A	…
	3003, Alclad 3003	4043	A	B	C	C	A	…
		5183	B	A	B	B	…	A
		5356	B	A	A	B	…	A
		5554	C	A	A	A	A	A
		5556	B	A	B	B	…	A
	3004	4043	A	D	C	C	A	…
		5183	B	A	B	B	…	A
		5356	B	B	A	B	…	A
		5554	C	C	A	A	A	A
		5556	B	A	B	B	…	A
	Alclad 3004	4043	A	D	C	C	A	…
		5183	B	A	B	B	…	A
		5356	B	B	A	B	…	A
		5554	C	C	A	A	A	A
		5556	B	A	B	B	…	A
	5005, 5050	4043	A	B	C	C	A	…
		5183	B	A	B	B	…	A
		5556	B	A	B	B	…	A
	5052, 5652	4043	A	D	C	C	A	…
		5183	A	A	A	B	…	A
		5356	A	B	A	B	…	A
		5554	C	C	A	A	A	A
		5556	A	A	B	B	…	A
		5654	B	C	A	B	…	B
	5083, 5456	5183	A	A	B	B	…	A
		5356	A	B	A	B	…	A
		5554	B	C	A	A	…	A
		5556	A	A	B	B	…	A
	5086, 5356	5183	A	A	B	B	…	A
		5356	A	B	A	B	…	A
		5554	B	C	A	A	…	A
		5556	A	A	B	B	…	A
	514.0, A514.0, B514.0, F514.0, 5154, 5254	5183	A	A	B	B	…	A
		5356	A	B	A	B	…	A
		5554	B	C	A	A	…	A
		5556	A	A	B	B	…	A
		5654	B	C	A	A	…	B
	5454	5183	A	A	B	B	…	A
		5356	A	B	A	B	…	A
		5554	B	C	A	A	A	A
		5556	A	A	B	B	…	A
		5654	B	C	A	B	…	B
514.0, A514.0, B514.0, F514.0, 5514, 5254	1060, 1350	4043	A	B	C	C	…	…
		5183	B	A	B	B	…	A
		5356	B	A	A	B	…	A
		5554	C	A	A	A	…	A
		5556	B	A	B	B	…	A
		5654	C	A	A	A	…	B
	1100	4043	A	B	C	C	…	…
		5183	B	A	B	B	…	A
		5356	B	A	A	B	…	A
		5554	C	A	A	A	…	A
		5556	B	A	B	B	…	A
		5654	C	A	A	A	…	B
	2014, 2036	(b)	…	…	…	…	…	…
	2219	4043	A	A	A	A	…	…
	3003, Alclad 3003	4043	A	B	C	C	…	…
		5183	B	A	B	B	…	A
		5356	B	A	A	B	…	A
		5554	C	A	A	A	…	A
		5556	B	A	B	B	…	A
		5654	C	C	A	A	…	B
	3004	4043	A	D	C	C	…	…
		5183	B	A	B	B	…	A
		5356	B	B	A	B	…	A
		5554	C	C	A	A	…	A
		5556	B	A	B	B	…	A
	Alclad 3004	4043	A	D	C	C	…	…
		5183	B	A	B	B	…	A
		5356	B	B	A	B	…	A
		5554	C	C	A	A	…	A
		5556	B	A	B	B	…	A
		5654	C	C	A	A	…	B
	5005, 5050	4043	A	B	C	C	…	…
		5183	B	A	B	B	…	A

(continued)

(a) A, B, C, and D represent relative ratings (where A is best and D is worst) of the performance of the two component base alloys combined with each group of selected filler alloys. W, ease of welding (relative freedom from weld cracking); S, strength of welded joint in as-welded condition (rating applies specifically to fillet welds, but all rods and electrodes rated will develop presently specific minimum strengths for butt welds); D, ductility (rating based on free bend elongation of the weld); C, corrosion resistance in continuous or alternate immersion of fresh or salt water, T, performance in service at sustained temperatures >65 °C (>150 °F); M, color match after anodizing. (b) No filler suitable. *Note:* Combinations having no ratings are not recommended. Source: Aluminum Company of America

Table 3 (continued)

Alloy 1	Alloy 2	Filler alloys	Filler alloy characteristic(a) W	S	D	C	T	M
514.0, A514.0, B514.0, F514.0, 5514, 5254 (continued)	5005, 5050 (continued)	5356	B	A	A	B	…	A
		5554	C	A	A	A	…	A
		5556	B	A	B	B	…	A
		5654	C	A	A	A	…	B
	5052, 5652	4043	A	D	C	C	…	…
		5183	A	A	B	B	…	B
		5356	A	B	A	B	…	A
		5554	C	C	A	A	…	B
		5556	A	A	B	B	…	B
		5654	B	C	A	A	…	A
	5083, 5456	5183	A	A	B	A	…	A
		5356	A	B	A	A	…	A
		5554	B	C	A	A	…	A
		5556	A	A	B	A	…	A
		5654	B	C	A	A	…	B
	5086, 5356	5183	A	A	B	A	…	A
		5356	A	B	A	A	…	A
		5554	B	C	A	A	…	A
		5556	A	A	B	A	…	A
		5654	B	C	A	A	…	B
	514.0, A514.0, B514.0, F514.0, 5154, 5254	5183	A	A	B	B	…	B
		5356	A	B	A	B	…	A
		5554	B	C	A	A	…	B
		5556	A	A	B	B	…	B
		5654	B	C	A	A	…	A
5086, 5356	1060, 1350	4043	A	B	C	B	…	…
		5183	A	A	B	A	…	A
		5356	A	A	A	A	…	A
		5556	A	A	B	A	…	A
	1100	4043	A	B	C	B	…	…
		5183	A	A	B	A	…	A
		5356	A	A	A	A	…	A
		5556	A	A	B	A	…	A
	2014, 2036	(b)	…	…	…	…	…	…
	2219	4043	A	A	A	A	…	…
	3003, Alclad 3003	4043	A	B	C	B	…	…
		5183	A	A	B	A	…	A
		5356	A	A	A	A	…	A
		5556	A	A	B	A	…	A
	3004	4043	A	C	C	B	…	…
		5183	A	A	B	A	…	A
		5356	A	B	A	A	…	A
		5556	A	A	B	A	…	A
	Alclad 3004	4043	A	C	C	B	…	…
		5183	A	A	B	A	…	A
		5356	A	B	A	A	…	A
		5556	A	A	B	A	…	A
	5005, 5050	4043	A	B	C	B	…	…
		5183	A	A	B	A	…	A
		5356	A	A	A	A	…	A
		5556	A	A	B	A	…	A
	5052, 5652	5183	A	A	B	A	…	A
		5356	A	B	A	A	…	A
		5554	C	C	A	A	…	A
		5556	A	A	B	A	…	A
		5654	B	C	A	A	…	B
	5083, 5456	5183	A	A	B	A	…	A
		5356	A	B	A	A	…	A
		5556	A	A	B	A	…	A
	5086, 5356	5183	A	A	B	A	…	A
		5356	A	B	A	A	…	A
		5556	A	A	B	A	…	A
5083, 5456	1060, 1350	4043	A	B	C	B	…	…
		5183	A	A	B	A	…	A
		5356	A	A	A	A	…	A
		5556	A	A	B	A	…	A
	1100	4043	A	B	C	B	…	…
		5183	A	A	B	A	…	A
		5356	A	A	A	A	…	A
		5556	A	A	B	A	…	A
	2014, 2036	(b)	…	…	…	…	…	…
	2219	4043	A	A	A	A	…	…
	3003, Alclad 3003	4043	A	B	C	B	…	…
		5183	A	A	B	A	…	A
		5356	A	A	A	A	…	A
		5556	A	A	B	A	…	A
	3004	4043	A	C	C	B	…	…
		5183	A	A	B	A	…	A
		5356	A	B	A	A	…	A
		5556	A	A	B	A	…	A
	Alclad 3004	4043	A	C	C	B	…	…
		5183	A	A	B	A	…	A
		5356	A	B	A	A	…	A
		5556	A	A	B	A	…	A
	5005, 5050	4043	A	B	C	B	…	…
		5183	A	A	B	A	…	A
		5356	A	A	A	A	…	A
		5556	A	A	B	A	…	A
	5052, 5652	4043	A	D	C	B	A	…
		5183	A	A	B	C	…	B
		5356	A	B	A	C	…	A
		5554	C	C	A	A	A	B
		5556	A	A	B	C	…	B
		5654	B	C	A	B	…	A
5005, 5050	1060, 1350	1100	C	B	A	A	A	A
		5556	A	A	B	A	…	A
	1100	4043	A	B	C	B	…	…
		5183	A	A	B	A	…	A
		5356	A	A	A	A	…	A
		5556	A	A	B	A	…	A
	2014, 2036	(b)	…	…	…	…	…	…
	2219	4043	A	A	A	A	…	…
	3003, Alclad 3003	4043	A	B	C	B	…	…
		5183	A	A	B	A	…	A
		5356	A	A	A	A	…	A
		5556	A	A	B	A	…	A
	3004	4043	A	C	C	B	…	…
		5183	A	A	B	A	…	A
		5356	A	B	A	A	…	A
		5556	A	A	B	A	…	A
	Alclad 3004	4043	A	C	C	B	…	…
		5183	A	A	B	A	…	A
		5356	A	B	A	A	…	A
		5556	A	A	B	A	…	A
	5005, 5050	4043	A	B	C	B	…	…
		5183	A	A	B	A	…	A
		5356	A	A	A	A	…	A
		5556	A	A	B	A	…	A
	5052, 5652	4043	A	D	C	B	A	…
		5183	A	A	B	C	…	B
		5356	A	B	A	C	…	A
		5554	C	C	A	A	A	B
		5556	A	A	B	C	…	B
		5654	B	C	A	B	…	A
5052, 5652	1060, 1350	4043	A	B	C	A	A	…
		5183	B	A	B	…	…	A
		5356	B	A	A	…	…	A
		5556	B	A	B	…	…	A
	1100	4043	A	B	C	A	A	…
		5183	B	A	B	…	…	A
		5356	B	A	A	…	…	A
		5556	B	A	B	…	…	A
	2014, 2036	4043	A	A	A	A	A	…
	2219	4043	A	A	A	A	A	…
	3003, Alclad 3003	4043	A	B	C	A	A	…
		5183	B	A	B	…	…	A
		5356	B	A	A	…	…	A
		5556	B	A	B	…	…	A
	3004	4043	A	C	C	A	A	…
		5183	B	A	B	…	…	A
		5356	B	B	A	…	…	A
		5556	B	A	B	…	…	A
	Alclad 3004	4043	A	C	C	A	A	…
		5183	B	A	B	…	…	A
		5356	B	B	A	…	…	A
		5556	B	A	B	…	…	A
	5005, 5050	4043	A	B	C	A	A	…
		5183	B	A	B	…	…	A
		5356	B	A	A	…	…	A
		5556	B	A	B	…	…	A
	5052, 5652	4043	A	D	C	B	A	…
		5183	A	A	B	C	…	B
		5356	A	B	A	C	…	A
		5554	C	C	A	A	A	B
		5556	A	A	B	C	…	B
		5654	B	C	A	B	…	A
5005, 5050	1060, 1350	1100	C	B	A	A	A	A

(continued)

(a) A, B, C, and D represent relative ratings (where A is best and D is worst) of the performance of the two component base alloys combined with each group of selected filler alloys. W, ease of welding (relative freedom from weld cracking); S, strength of welded joint in as-welded condition (rating applies specifically to fillet welds, but all rods and electrodes rated will develop presently specific minimum strengths for butt welds); D, ductility (rating based on free bend elongation of the weld); C, corrosion resistance in continuous or alternate immersion of fresh or salt water, T, performance in service at sustained temperatures >65 °C (>150 °F); M, color match after anodizing. (b) No filler suitable. *Note:* Combinations having no ratings are not recommended. Source: Aluminum Company of America

Table 3 (continued)

Alloy 1	Alloy 2	Filler alloys	Filler alloy characteristic(a) W	S	D	C	T	M
5005, 5050 (continued)	1060, 1350 (continued)	4043	A	A	C	A	A	…
		4145	B	A	D	B	A	…
		5183	C	A	B	…	…	B
		5356	C	A	B	…	…	B
		5556	C	A	B	…	…	B
	1100	1100	C	B	A	A	A	A
		4043	A	A	C	A	A	…
		4145	B	A	D	B	A	…
		5183	C	A	B	…	…	B
		5356	C	A	B	…	…	B
		5556	C	A	B	…	…	B
	2014, 2036	4043	B	B	A	A	A	…
		4145	A	A	B	A	A	…
	2219	4043	B	B	A	A	A	…
		4145	A	A	B	A	A	…
	3003, Alclad 3003	1100	C	C	A	A	A	A
		4043	A	B	C	A	A	…
		4145	B	B	D	B	A	…
		5183	C	A	B	C	…	B
		5356	C	A	B	C	…	B
		5556	C	A	B	C	…	B
	3004	4043	A	B	C	A	A	…
		5183	B	A	B	…	…	A
		5356	B	A	A	…	…	A
		5556	B	A	B	…	…	A
	Alclad 3004	4043	A	B	C	A	A	…
		5183	B	A	B	B	…	A
		5356	B	A	A	B	…	A
		5556	B	A	B	B	…	A
	5005, 5050	1100	B	…	A	A	A	A
		4043	A	B	D	A	A	…
		5183	B	A	C	…	…	B
		5356	B	A	B	…	…	B
		5556	B	A	C	…	…	B
Alclad 3004	1060, 1350	1100	D	B	A	A	A	A
		4043	A	A	C	A	A	…
		4145	B	A	D	B	A	…
		5183	C	A	B	C	…	B
		5356	C	A	B	C	…	B
		5556	C	A	B	C	…	B
	1100	1100	D	B	A	A	A	A
		4043	A	A	C	A	A	…
		4145	B	A	D	B	A	…
		5183	C	A	B	C	…	B
		5356	C	A	B	C	…	B
		5556	C	A	B	C	…	B
	2014, 2036	4043	B	B	A	A	A	…
		4145	A	A	B	A	A	…
	2219	4043	B	B	A	A	A	…
		4145	A	A	B	A	A	…
	3003, Alclad 3003	1100	C	C	A	A	A	A
		4043	A	B	C	A	A	…
		4145	B	B	D	B	A	…
		5183	C	A	B	C	…	B
		5356	C	A	B	C	…	B
		5556	C	A	B	C	…	B
	3004	4043	A	D	D	A	A	…
		5183	B	A	C	C	…	A
		5356	B	B	B	C	…	A
		5554	C	C	A	B	A	A
		5556	B	A	C	C	…	A
	Alclad 3004	4043	A	D	D	A	A	…
		5183	B	A	C	C	…	A
		5356	B	B	B	C	…	A
		5554	C	C	A	B	A	A
		5556	B	A	C	C	…	A
3004	1060, 1350	1100	D	B	A	A	A	A
		4043	A	A	C	A	A	…
		4145	B	A	D	B	A	…
		5183	C	A	B	…	…	B
		5356	C	A	B	…	…	B
		5556	C	A	B	…	…	B
	1100	1100	D	B	A	A	A	A
		4043	A	A	C	A	A	…
		4145	B	A	D	B	A	…
		5183	C	A	B	…	…	B
		5356	C	A	B	…	…	B
		5556	C	A	B	…	…	B
	2014, 2036	4043	B	B	A	A	A	…
		4145	A	A	B	A	A	…
	2219	4043	B	B	A	A	A	…
		4145	A	A	B	A	A	…
	3003, Alclad 3003	1100	C	C	A	A	A	A
		4043	A	B	C	A	A	…
		4145	B	B	D	B	A	…
		5183	C	A	B	C	…	A
		5356	C	A	B	C	…	A
		5556	C	A	B	C	…	A
	3004	4043	A	B	D	A	A	…
		5183	B	A	C	C	…	A
		5356	B	B	B	C	…	A
		5554	C	C	A	B	A	A
		5556	B	A	C	C	…	A
	Alclad 3004	5554	C	C	A	B	A	A
		5556	B	A	C	C	…	A
3003, Alclad 3003	1060, 1350	1100	B	B	A	A	A	A
		4043	A	A	B	A	A	…
		4145	A	A	C	B	A	…
	1100	1100	B	B	A	A	A	A
		4043	A	A	B	A	A	…
		4145	A	A	C	B	A	…
	2014, 2036	4043	B	A	A	A	A	…
		4145	A	A	B	A	A	…
	2219	4043	B	A	A	A	A	…
		4145	A	A	B	A	A	…
	3003, Alclad 3003	1100	B	B	A	A	A	A
		4043	A	A	B	A	A	…
		4145	A	A	C	B	A	…
2219	1060, 1350	4043	B	A	A	A	A	…
		4145	A	A	B	A	A	…
	1100	4043	B	A	A	A	A	…
		4145	A	A	B	A	A	…
	2014, 2036	2319	B	A	A	A	A	A
		4043	B	C	B	C	A	…
		4145	A	B	C	B	A	…
	2219	2319	A	A	A	A	A	A
		4043	B	C	B	C	A	…
		4145	A	B	C	B	A	…
2014, 2036	1060, 1350	4043	B	A	A	A	A	…
		4145	A	A	B	A	A	…
	1100	4043	B	A	A	A	A	…
		4145	A	A	B	A	A	…
	2014, 2036	2319	C	A	A	A	A	A
		4043	B	C	B	C	A	…
		4145	A	B	C	B	A	…
1100	1060, 1350	1100	B	B	A	A	A	A
		4043	A	A	B	A	A	…
	1100	1100	B	B	A	A	A	…
		4043	A	A	B	A	A	…
1060, 1350	1060, 1350	1100	B	B	A	A	A	B
		1188	C	C	A	A	A	A
		4043	A	A	B	A	A	…
		5554	C	C	A	B	A	A
		5556	B	A	C	C	…	A

(a) A, B, C, and D represent relative ratings (where A is best and D is worst) of the performance of the two component base alloys combined with each group of selected filler alloys. W, ease of welding (relative freedom from weld cracking); S, strength of welded joint in as-welded condition (rating applies specifically to fillet welds, but all rods and electrodes rated will develop presently specific minimum strengths for butt welds); D, ductility (rating based on free bend elongation of the weld); C, corrosion resistance in continuous or alternate immersion of fresh or salt water, T, performance in service at sustained temperatures >65 °C (>150 °F); M, color match after anodizing. (b) No filler suitable. *Note:* Combinations having no ratings are not recommended. Source: Aluminum Company of America

resistance spot welding. Usually, the pieces to be joined are first bonded by adhesives that seal the crevices, followed by resistance spot welding.

A more recent development in resistance spot welding involves joining aluminum to dissimilar metals by the use of transition joints. In this case, aluminum is first spot welded to a compatible metal that in turn is joined to the dissimilar metal. This procedure improves resistance to galvanic corrosion by minimizing dissimilar metal contact and also eliminates brittle intermetallic compounds that form at the joint interface (Ref 15, 16). In the automotive industry, the dissimilar metals of interest are principally aluminum and steel. The aluminum/steel transition sheet is typically made by rolling sheets of the two metals together under high roll forces such that when the sheets elongate, the oxides on their contacting surfaces are disrupted, exposing bare clean metal. A metallurgical bond results. There is no crevice; that is, potential galvanic corrosion will be confined to the sheet edges, which can be painted or sealed to prevent corrosion. The direct aluminum-to-steel metallurgically bonded joint has high mechanical integrity. Outside the transition joint, the aluminum side is joined to an aluminum automotive component, and the steel side is joined to a steel component. Figure 4 shows the principle of a clad transition metal. Spot welded assemblies made using transition materials include (Ref 15, 16):

- Lap joints of 1008 low-carbon steel to 7046 aluminum that is spot welded with a low-carbon steel-clad 7046 aluminum (40-to-60 ratio) transition
- Lap joints of 1006 low-carbon steel to 6111 aluminum that is spot welded with a low-carbon steel-clad 5052 aluminum (60-to-40 ratio) transition
- Lap joints of electrogalvanized 1006 low-carbon steel to 6111 aluminum that is spot welded with electrogalvanized 1006 steel-clad 5052 aluminum (60-to-40 ratio) transition.

Friction stir welding (FSW) is a solid-state process invented at The Welding Institute (TWI) in 1991. A schematic of the FSW process is shown in Fig. 5. The FSW process uses a nonconsumable pin (or probe) made from a high-strength material that extends from a cylindrical shoulder. The shoulder and the pin rotate at several hundred revolutions per minute. The workpieces that are to be joined are firmly clamped to the work table, and the pin is plunged into the workpieces where the weld bond line is desired. The height of the pin is slightly smaller than the thickness of the alloy plates that are being joined, so the penetration of the pin into the workpieces stops as soon as the shoulder of the cylinder makes contact with the surface of the workpiece. The rotating pin (extending from the cylindrical shoulder) produces the stirring ac-

Table 4 Nominal composition and melting range of standard aluminum filler alloys

	Nominal composition, wt %								Approximate melting range	
Aluminum alloys	Si	Cu	Mn	Mg	Cr	Ti	Al	Others	°C	°F
1100	...	0.12	...	...	...	...	≥99.00	...	643–657	1190–1215
1188	...	...	...	...	...	...	≥99.88	...	657–660	1215–1220
2319	...	6.3	0.30	...	...	0.15	bal	0.18 Zr, 0.10 V	543–643	1010–1190
4009(a)	5.0	1.25	...	0.50	...	...	bal	...	546–621	1015–1150
4010(b)	7.0	...	...	0.35	...	...	bal	...	557–613	1035–1135
4011(c)	7.0	...	...	0.58	...	0.12	bal	0.55 Be	557–613	1035–1135
4043	5.25	...	...	...	...	...	bal	...	574–632	1065–1170
4047	12.0	...	...	...	...	...	bal	...	577–582	1070–1080
4145	10.0	4.0	...	...	...	...	bal	...	521–585	970–1085
4643	4.1	...	...	0.20	...	...	bal	...	574–635	1065–1175
5183	...	...	0.75	4.75	0.15	...	bal	...	579–638	1075–1180
5356	...	...	0.12	5.0	0.12	0.13	bal	...	571–635	1060–1175
5554	...	...	0.75	2.7	0.12	0.12	bal	...	602–646	1115–1195
5556	...	...	0.75	5.1	0.12	0.12	bal	...	568–635	1055–1175
5654	...	...	...	3.5	0.25	0.10	bal	...	593–643	1100–1190
C355.0	5.0	1.25	...	0.50	...	...	bal	...	546–621	1015–1150
A356.0	7.0	...	...	0.35	...	...	bal	...	557–613	1035–1135
A357.0	7.0	...	...	0.58	...	0.12	bal	0.55 Be	557–613	1035–1135

(a) Wrought alloy with composition identical to cast alloy C355.0 (b) Wrought alloy with composition identical to cast alloy A356.0 (c) Wrought alloy with composition identitical to cast alloy A357.0

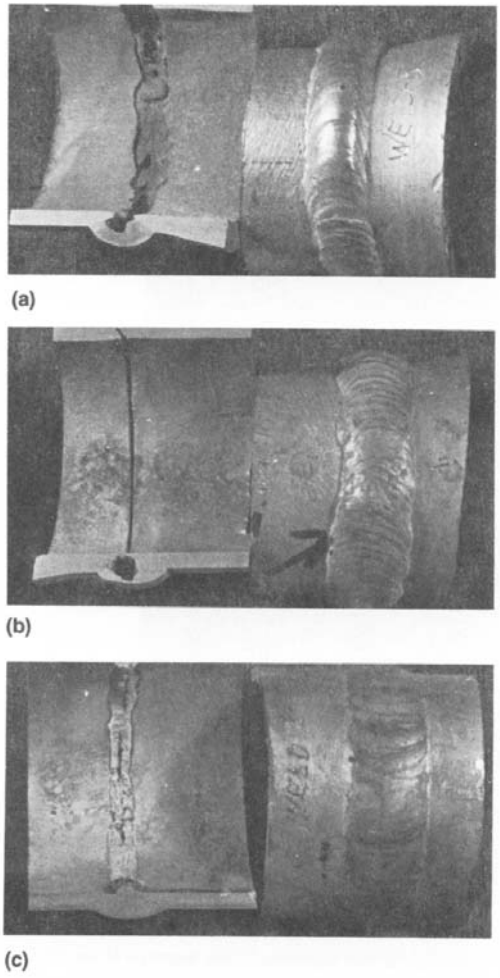

Fig. 3 Corrosion of three aluminum weldments in HNO_3 service. (a) and (b) Gas tungsten arc (GTA) and oxyacetylene welds, respectively, showing crevice corrosion on the inside surface. (c) Standard GTA weld with full penetration is resistant to crevice corrosion.

tion in the material along the bond line and produces the required thermomechanical deformation. Frictional heating is produced from the interaction of the cylinder shoulder with the workpiece and the downward applied forging pressure. To produce a longitudinal weld, the workpiece assembly is translated relative to the shoulder and pin assembly. To produce an ideal defect-free weld, the revolutions per minute of the cylinder shoulder-pin assembly, travel speed, downward forging force, and pin tool design have to be optimized.

Due to absence of parent metal melting, the FSW process offers several advantages over fusion welding. The benefits that stand out most are welding difficult-to-weld aluminum alloys such as the 7*xxx* series, better retention of baseline material properties, fewer weld defects, low residual stresses, and better dimensional stability of the welded structure.

Although melting does not generally occur during FSW, temperatures are sufficiently high enough to cause dissolution, nucleation, and/or coarsening of strengthening precipitates in some heat-treatable alloys, most notably 7*xxx* series alloys such as 7050 and 7075. The altered microstructure in the weld zone leads to sensitization in the as-welded condition and studies have shown that the weld zone is more susceptible to pitting, intergranular corrosion, and SCC than the parent metal (Ref 17, 18). Corrective measures that have been investigated to either produce less sensitization or restore corrosion resistance following FSW include (Ref 19):

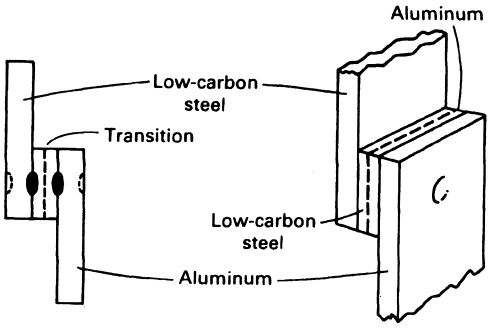

Fig. 4 Illustration of a steel-clad aluminum transition material insert used for joining aluminum to carbon steel

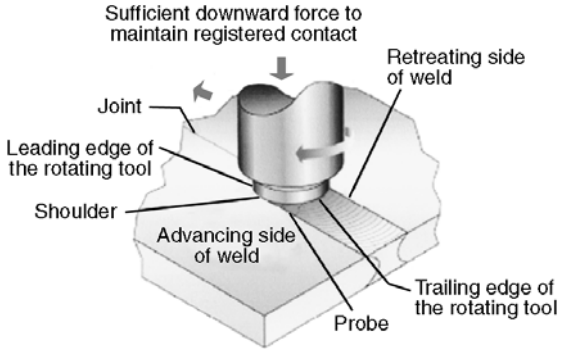

Fig. 5 Schematic illustration of the friction stir welding process

- Active cooling during FSW, where cold water is circulated through the anvil and a mist of water is sprayed on the tool. This is a process change which lowers the maximum temperature and decreases time at elevated temperature.
- Laser surface melting where surface melting and rapid quenching alters the microstructure
- Low plasticity burnishing, where a tool puts compressive stresses in a surface layer
- Pre- and post-weld heat treatments which homogenize the grain boundary chemistry
- Change in tool design which alters the temperature/time profile and microstructure during FSW

Other studies on aluminum alloys have, however, shown different results. For example, FSW samples of aluminum alloy 5454 exhibited superior resistance to pitting corrosion compared to the parent metal and arc-welded samples (Ref 20). Favorable results have also been achieved in FSW of 2*xxx* and 6*xxx* alloys (Ref 21, 22).

Copper and Copper Alloys

Copper and copper alloys offer a unique combination of material properties that makes them advantageous for many manufacturing environments. They are widely used because of their excellent electrical and thermal conductivities, outstanding resistance to corrosion, ease of fabrication, and good strength and fatigue resistance. Other useful characteristics include spark resistance, metal-to-metal wear resistance, low-permeability properties, and distinctive color.

Copper and copper alloys find their greatest use as electrical conductors and in the manufacture of electrical components. In its pure form, copper has a face-centered cubic crystal structure and a density of 8.968 g/cm^3, that is about three times the density of aluminum. The electrical conductivity of copper is only slightly lower than that of silver, but it exceeds the electrical and thermal conductivity of aluminum by more than 60%. The electrical conductivity reference standard of engineering materials is copper with a rating of 100% IACS (International Annealed Copper Standard). All other materials are compared on a conductivity basis to the IACS standard. Special processing of copper can produce some forms which reach 102% IACS.

Their excellent resistance to fresh water, salt water, and alkaline solutions makes copper alloys ideally suited for fabrication of tubing, valve fittings, heat exchangers, and chemical equipment. Copper reacts with sulfur and ammonia compounds. Ammonium hydroxide solutions will rapidly attack copper and its alloys, causing severe corrosion.

General Welding Considerations

In manufacturing, copper is often joined by welding. The arc welding processes are of prime concern. Arc welding can be performed using SMAW, GTAW, GMAW, plasma arc welding (PAW), and submerged arc welding (SAW).

The weldability varies among the different alloys for a variety of reasons, including the occurrence of hot cracking in the free-machining alloys and unsound welds in alloys containing copper oxide. Both tin and zinc reduce the weldability of copper alloys. In addition, zinc has a low boiling temperature, which results in the production of toxic vapors when welding copper-zinc (brass) alloys. The presence in an alloy of residual phosphorus is beneficial to weldability, because it combines with absorbed oxygen, thereby preventing the formation of copper oxide in the weld.

Besides the effects of alloying elements on weldability, several other factors affect weldability. These factors are thermal conductivity of the alloy being welded, the shielding gas, the type of current used during welding, the joint design, the welding position, and the surface condition and cleanliness.

More detailed information on copper welding metallurgy and the factors that influence weldability can be found in the article "Welding of Copper Alloys" in Volume 6 of the *ASM Handbook.*

Corrosion Behavior of Copper Weldments

The corrosion behavior of copper weldments is very similar to the parent (base) metal (see the article "Corrosion of Copper and Copper Alloys" in Volume 13B of the *ASM Handbook*). For example, virtually all copper alloys, including their weldments, are highly susceptible to SCC in aqueous ammonia environments. The most susceptible alloys are the brasses containing more than 15% Zn, such as admiralty brass (UNS C44300, 28% Zn), yellow brass (UNS C27000, 34% Zn), and Muntz metal (UNS C28000, 40%

Zn), followed by red brass (UNS C23000, 15% Zn) and several bronzes. The least susceptible alloys are 90Cu-10Ni (UNS C70600), 70Cu-30Ni (UNS C71500), and unalloyed copper.

The conditions that are conducive to SCC by aqueous ammonia are water, ammonia, air or oxygen, and tensile stress in the metal. Cracking is always intergraular, requires only trace quantities of ammonia in many cases, and occurs at ambient temperature. For example, U-bends in admiralty brass condenser tubes cracked in warm water from a cooling tower that contained 15 to 25 ppm ammonia because of close proximity to an ammonia plant. Other sources of ammonia include the decomposition of amines and the microbiological breakdown of organic matter.

Thermal stress relief is generally not one of the better preventive measures, because ammoniacal SCC occurs at relatively low stress levels. In fairly mild ammoniacal environments, such as the cooling tower water system mentioned previously, the copper-nickel alloys, particularly 90Cu-10Ni, give good service.

Recently there has been a great deal of research into containment materials for radioactive waste isolation. Radioactive materials are extensively used in a variety of applications such as medical, weapons, and power generation. Once these materials lose their commercial value they are considered radioactive waste. Broadly, the wastes can be separated into defense (weapons) and civilian (power, medical).

The safe disposal of radioactive waste requires that the waste be isolated from the environment until radioactive decay has reduced its toxicity to innocuous levels for plants, animals, and humans. Many different types of radioactive waste are produced during commercial and defense nuclear fuel cycles. One type of waste, denoted high-level waste (HLW), contains the highest concentration of radiotoxic and heat-generating species. Because of this factor, the most stringent standards for disposing of radioactive wastes are being placed worldwide on HLW, and the majority of the radioactive-waste management effort is being directed toward the HLW problem. One of the most common types of HLW is the spent nuclear fuel (SNF) from commercial nuclear reactors for power generation.

The proposed design for a final repository for SNF and other long-lived residues in Sweden is based on the multi-barrier principle. The waste will be encapsulated in sealed cylindrical containers which will then be placed in granite bedrock and surrounded by compacted bentonite clay. The canister design is based on a thick cast iron container fitted inside a corrosion-resistant pure copper canister.

One of the concerns using this design was the possibility of grain boundary corrosion of the copper canister weld material which seals the bottom and lid portions of the canister. During weld fabrication of the outer copper canisters there will be some unavoidable grain growth in the welded areas. As grains grow, they will tend to concentrate impurities within the copper at the new grain boundaries.

A comprehensive study was undertaken to determine if grain boundary corrosion of copper weld material would adversely affect the canisters under the conditions of the repository (Ref 23). Electron beam welded (EBW) copper specimens cut from welds of actual copper canisters were exposed to aerated 1% ammonium hydroxide solution for a period of 14 days at 80 °C (175 °F) and 10 bar pressure. The samples were investigated prior to exposure using the scanning Kelvin probe technique to characterize anodic and cathodic areas on the samples. The degree of corrosion was determined by optical microscopy. No grain boundary corrosion could be observed in the experiments, however, a higher rate of general corrosion was observed for the weld material compared to the base material.

Titanium and Titanium Alloys

Titanium-base alloys were originally developed in the early 1950s for aerospace applications, where their high strength-to-density ratios were especially attractive (titanium has a density of approximately 4.5 g/cm^3 which is approximately 60% of the density of iron). Although titanium alloys are still vital to the aerospace industry, recognition of the excellent resistance of titanium to many highly corrosive environments, particularly oxidizing and chloride-containing process streams has led to widespread nonaerospace applications such as tanks, heat exchangers, or reactor vessels for chemical-processing, desalination, or power-generation plants. Because of the decreasing cost and increasing availability of titanium alloy products, many titanium alloys have become standard engineering materials for a host of common industrial applications.

The designations and nominal compositions of several commercial titanium-base alloys are

listed in Table 5. These titanium alloys are commonly used in industrial applications where corrosion resistance is of primary concern. With the exception of the Ti-6Al-4V alloy, these alloys consist of single α-phase (hexagonal close-packed crystal structure) or near-α alloys containing relatively small amounts of β-phase (body-centered cubic crystal structure) in an α matrix. Other titanium alloys have been developed for aerospace purposes. In such alloys, significantly increased strengths are achieved by solid-solution alloying and stabilization of two-phase structures.

The excellent corrosion resistance of titanium-base alloys results from the formation of very stable, continuous, highly adherent, and protective oxide films on metal surfaces. Because titanium metal itself is highly reactive and has an extremely high affinity for oxygen, these beneficial surface oxide films form spontaneously when fresh metal surfaces are exposed to air and/or moisture. In fact, a damaged oxide film can generally reheal itself instantaneously if at least traces (parts per million) of oxygen or water (moisture) are present in the environment. However, anhydrous conditions in the absence of an oxygen source may result in titanium corrosion, because the protective film may not be regenerated if damaged.

The nature, composition, and thickness of the protective surface oxides that form on titanium alloys depend on environmental conditions. Although these naturally formed films are typically less than 10 nm (100 Å) thick and are invisible to the eye, titanium dioxide (TiO_2) is highly chemically resistant and is attacked by very few substances. Solutions that attack titanium include hot, concentrated hydrochloric acid (HCl), sulfuric acid (H_2SO_4), sodium hydroxide (NaOH) and (most notably) hydrofluoric acid (HF). The potential-pH diagram for the titanium-water system of 25 °C (75 °F) is shown in Fig. 6 and depicts the wide region over which the passive TiO_2 film is predicted to be stable, based on thermodynamic (free energy) considerations. Oxide stability over the full pH scale is indicated over a wide range of highly oxidizing to mildly reducing potentials, whereas oxide film breakdown and the resultant corrosion of titanium occur under reducing acidic conditions. Under strongly reducing (cathodic) conditions, titanium hydride formation is predicted.

Thus, successful use of titanium alloys can be expected in mildly reducing to highly oxidizing environments in which protective TiO_2 and Ti_2O_3 films form spontaneously and remain stable. On the other hand, uninhibited, strongly reducing acidic environments may attack titanium, particularly as temperature increases.

Table 5 Designations and nominal compositions of several titanium-base alloys

Common alloy designation	UNS No.	Nominal composition, %	ASTM grade	Alloy type
Grade 1	R50250	Unalloyed titanium	1	α
Grade 2	R50400	Unalloyed titanium	2	α
Grade 3	R50550	Unalloyed titanium	3	α
Grade 4	R50700	Unalloyed titanium	4	α
Ti-Pd	R52400/R52250	Ti-0.15Pd	7–11	α
Grade 12	R53400	Ti-0.3Mo-0.8Ni	12	Near-α
Ti-3-2.5	. . .	Ti–3Al-2.5V	9	Near-α
Ti-6-4	R56400	Ti–6Al-4V	5	α-β

General Welding Considerations (Ref 24)

As stated in the previous section, titanium has a strong chemical affinity for oxygen, and a stable, tenacious oxide layer forms rapidly on a clean surface, even at room temperature. This behavior leads to a natural passivity that provides a high degree of corrosion resistance. The strong affinity of titanium for oxygen increases with temperature and the surface oxide layer increases in thickness at elevated temperatures. At temperatures exceeding 500 °C (930 °F), its oxidation resistance decreases rapidly, and the metal becomes highly susceptible to embrittlement by oxygen, nitrogen, and hydrogen, which dissolve interstitially in titanium. Therefore, the melting,

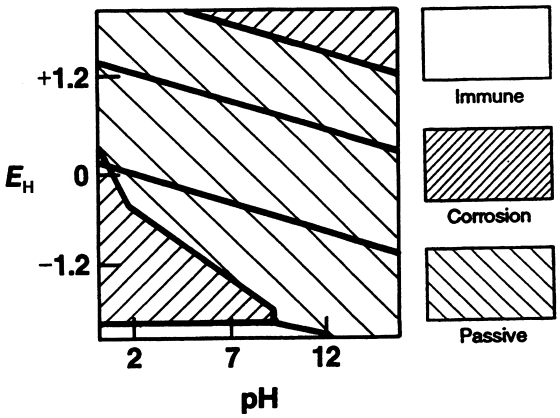

Fig. 6 Potential-pH diagram for titanium

solidification, and solid-state cooling associated with fusion welding must be conducted in completely inert or vacuum environments. The fusion welding processes most widely used for joining titanium are GTAW, GMAW, PAW, EBW, and laser beam welding (LBW). With the arc and laser welding processes, protection of the weld zone can be provided by localized inert-gas shielding. Complete enclosure in a protective chamber of the high vacuum environment associated with the electron-beam welding process inherently provides better atmospheric protection. In addition to proper shielding, welded component cleanliness (including filler metals) is necessary to avoid weld contamination.

The welding of thin-to-moderate section thicknesses in titanium alloys can be accomplished using all of the aforementioned processes. The GTAW process offers the greatest flexibility for both manual and automatic application at minimum capital investment. If production volume is large, the high capital investment required for LBW and EBW systems can be acceptable, based on higher welding rates and improved productivity. For titanium plate thickness exceeding about 5 mm (0.20 in.), the high-energy density processes are the most efficient. Plasma arc welding, for producing welds up to about 15 mm (0.6 in.) thick, and EBW, which can readily generate single-pass welds in plates over 50 mm (2 in.) thick, are used in current aerospace practice. In addition to thickness requirements, complex geometries may require manual welding or the use of extensive fixturing. The automatic welding of extremely large components may also prove difficult, particularly with the EBW process.

Residual stresses in titanium welds can greatly influence the performance of a fabricated component by degrading fatigue properties, while distortion can cause difficulties in the final assembly and operation of high-tolerance systems. Thus, the use of high-energy-density welding processes to produce full-penetration, single-pass autogenous welds, rather than multipass conventional arc welding is desirable to minimize these difficulties.

Several important and interrelated aspects of welding phenomena contribute to the overall understanding of titanium alloy welding metallurgy. These factors include melting and solidification effects on weld microstructure, post-weld heat treatment effects, and structure/mechanical property fracture relationships. Each of these are described in the article "Selection and Weldability of Conventional Titanium Alloys" in Volume 6 of the *ASM Handbook.*

Corrosion Behavior of Titanium and Titanium Alloy Weldments

In unalloyed titanium and many titanium alloys, weld zones are just as resistant to corrosion as the base metal. Other fabrication processes (such as bending or machining) also appear to have no influence on basic corrosion resistance.

Weldments and castings of unalloyed grades and α-β alloys such as Ti-6Al-4V generally exhibit corrosion resistance similar to that of their unwelded, wrought counterparts. These titanium alloys contain so little alloy content and second phase that metallurgical instability and thermal response are not significant. Therefore, titanium weldments and associated HAZs generally do not experience corrosion limitations in welded components when normal passive conditions prevail for the base metal. However, under marginal or active conditions, for corrosion rates greater than or equal to 100 μm/year, weldments can experience accelerated corrosion attack relative to the base metal, depending on alloy composition. The increasing impurity (e.g., iron, sulfur, oxygen) content associated with the coarse, transformed β microstructure of weldments appears to be a factor. Few published data are available concerning the corrosion resistance of titanium alloy weldments and castings other than Ti-6Al-4V, and limited information on other product forms has been reported.

Hydrogen Embrittlement. When titanium is exposed to air, moisture, or hydrocarbons at temperatures exceeding 500 °C (930 °F), it will readily pick up oxygen, nitrogen, carbon, and hydrogen. These small atoms of the interstitial elements will enter the crystal lattice in monatomic form and will migrate to interstitial sites (sites located between titanium atoms). The presence of these interstitial elements serves to inhibit plastic deformation and increase strength, but with a substantial loss in ductility. If contamination levels exceed a certain amount, cracking may ensue from the stresses generated during welding.

While hydrogen can play a role in contamination cracking, it can also lead to hydrogen embrittlement, or hydrogen delayed cracking. One mechanism proposed for this problem involves the precipitation of titanium hydrides

in the vicinity of cracks (Ref 25). If it is assumed that a microcrack is present in the weldment, it follows that hydrogen atoms will diffuse to the crack tip, where a triaxial stress state produces large interstitial sites (holes) in the lattice. These large interstitial sites can more easily accommodate the hydrogen atoms.

Once a critical concentration of hydrogen is reached, titanium hydrides will precipitate ahead of the crack tip (Fig. 7). Hydrogen may also diffuse to the crack to form diatomic gas, increasing pressure within the crack and increasing the load at the crack tip. Eventually the hydrides will rupture, allowing the crack to advance. Upon rupture, the hydrides will redissolve and hydrogen will diffuse to the new crack tip, thus reinitiating the sequence. This cycle may repeat many times, each cycle resulting in a small advancement of the crack.

Because the hydrogen embrittlement sequence requires diffusion of hydrogen, the rate of crack advancement depends on time and temperature. Hours, days, or months may pass following welding before significant cracking is observed. This problem can be avoided by minimizing exposure of the weld to hydrogen (hydrocarbons and moisture). Hydrogen concentrations on the order of 200 ppm are known to cause cracking problems, although the combined presence of other interstitials (for example, oxygen or nitrogen) may lower this tolerance limit. The inert shielding gas should have a dew point of at least –50 °C (–60 °F) (34 ppm H_2O). Welding-grade argon or helium gas (grade 4.5 with 50 ppm impurities) may not always satisfy this requirement. Also, the use of postweld heat treatment is beneficial because it relieves residual stress, thus reducing the driving force for crack advancement.

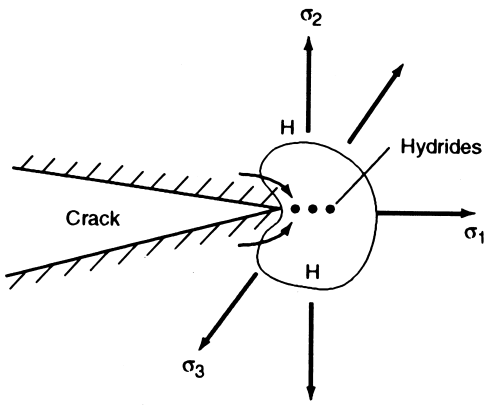

Fig. 7 Schematic diagram showing how hydrogen atoms may diffuse to a crack tip in a titanium weldment to form titanium hydrides

Example 1: Failure of Pressure Vessel Welds due to Hydrogen Embrittlement. During the Apollo space program, pressure vessels made of Ti-6A1-4V, an α-β alloy, were welded with either Ti-6A1-4V wire or commercially pure titanium wire. The commercially pure wire was softer and more easily handled. One aerospace supplier reported that an explosion occurred in a Ti-6Al-4V helium pressure vessel and that the explosion resulted in the failure of other helium pressure vessels in the vicinity. The failed pressure vessels used multipass welding and commercially pure wire to join thick weld joints (>25 mm, or 1 in.).

Examination of the failed weld showed excessive hydride needle formation following the contour of the molten weld metal, essentially perpendicular to the transverse loading across the bead. Failure occurred because of the brittle hydride needles (Fig. 8). It was postulated that the high solubility for hydrogen of Ti-6A1-4V alloy compared to that of commercially pure titanium was the source of the hydrogen and that repeated weld cycles allowed diffusion of hydrogen to pure titanium followed by precipitation at the pure metal Ti-6A1-4V interface. Theories of strain aging were also advanced, suggesting that hydrogen migrated lo the highest strain areas.

All of the solution-treated and aged Ti-6A1-4V pressure vessels on the Apollo command and service modules were welded with Ti-6A1-4V wire except for the final pass on the service propulsion system (SPS) fuel and oxidizer tanks. In this case, the root side of weld was back chipped, and a filler pass was made with commercially pure wire.

Specimens from SPS qualification tanks were examined and, in some cases, cycle tested. Hydride formation, although limited in nature, did follow the inside diameter bead contour. Because the pass was wide and shallow, the hydride path changed from perpendicular to the weld to a plane parallel to the surface. This undoubtedly explained why no problem had occurred with these pressure vessels. Existing SPS vessels were considered safe based on proof pressure, x-ray. and penetrant inspection.

In future programs, commercially pure titanium wire was not permitted for welding α-β titanium alloys. This experience pointed out that

the migration and precipitation of hydrogen must be considered in α-rich titanium structural members that undergo thermal cycles.

Zirconium and Zirconium Alloys

There are two major categories for zirconium and its alloys: nuclear and nonnuclear, as listed in Table 6. They all have low alloy contents. They are based on the α structure, that is, the hexagonal close-packed lattice, with dilute additions of solid-solution strengthening and α stabilizing elements such as oxygen and tin. However, in niobium-containing alloys, there is the presence of some niobium-rich β particles of the body-centered cubic lattice.

One of the major differences between nuclear and nonnuclear zirconium alloys is the hafnium content. Nuclear grades of zirconium alloys are virtually free of hafnium (not greater than 100 ppm). Nonnuclear grades of zirconium alloys

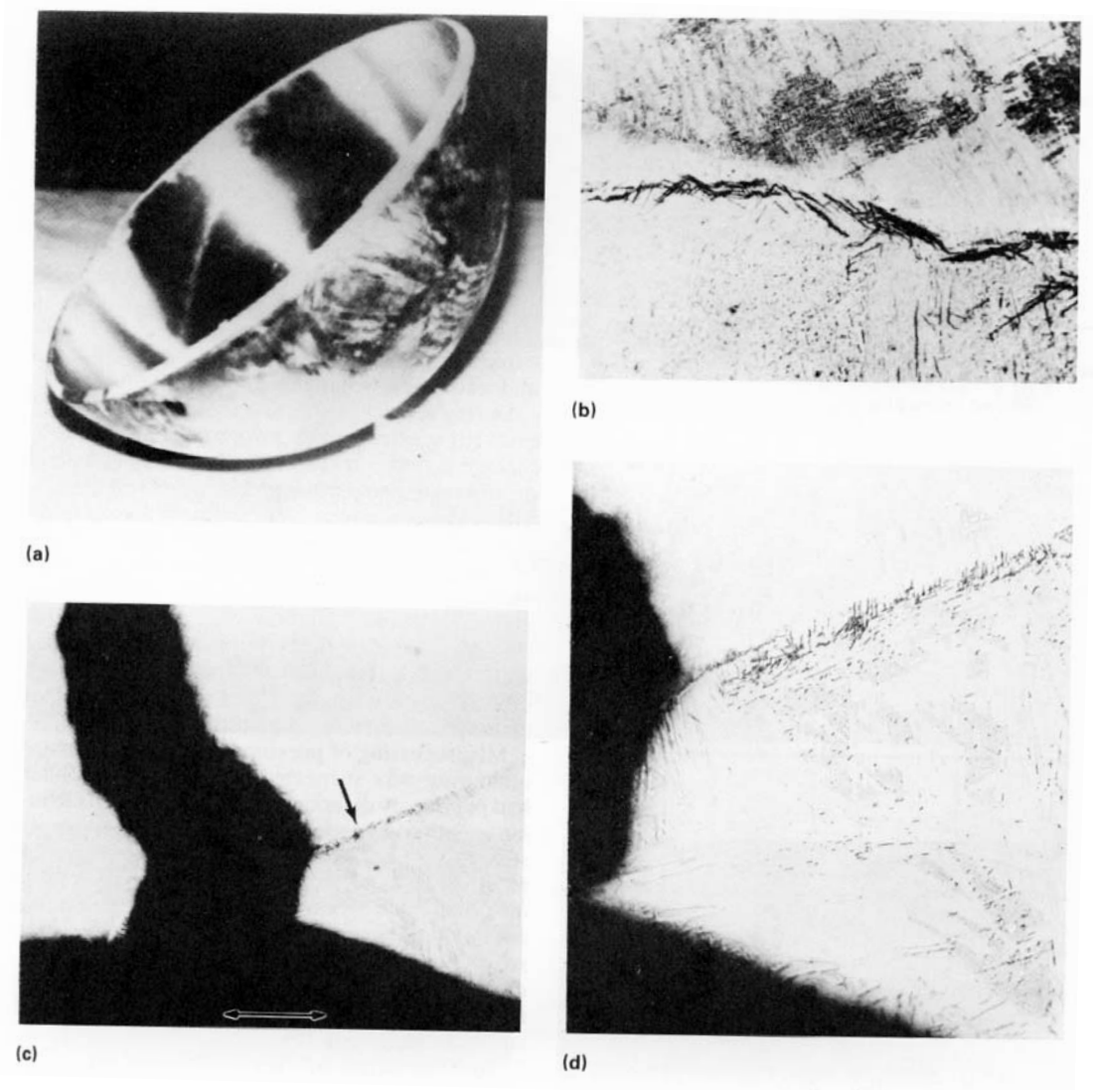

Fig. 8 Hydrogen embrittlement failure of a Ti-6Al-4V helium pressure vessel used on the Saturn IV B. Similar hydriding occurred in Apollo SPS pressure vessels. (a) Failed pressure vessel due to brittle hydride formation along weld bead made with commercially pure titanium. (b) Hydride at edge of pure metal weld bead in Ti-6Al-4V vessel shown in (a); 620×. (c) Section through a Ti-6Al-4V Apollo SPS pressure vessel welded with pure titanium on the root side. Coupon was stress cycled 200 times, then tested in tension to failure (lower arrow indicates direction of test loading). Hydride needles adjacent to the weld bead are shown; 45×. (d) Path of hydride needles changes direction and becomes parallel to load across weld; 70×

are permitted to have 4.5% Hf but normally have less. Hafnium has an enormous effect on absorbing thermal neutrons and is suitable for nuclear reactor control rods. It has a minor effect on zirconium mechanical and chemical properties.

The major use of nuclear-grade zirconium tubing is for nuclear fuel rod cladding, guide tubes, pressure tubes, and ferrule spacer grids. Flat materials, such as sheets and plates, are used for spacer grids, water channels, and channel boxes for nuclear fuel bundles. Bars are used for nuclear fuel rod end plugs.

For nonnuclear applications, product forms include ingots, forgings, pipes, tubes, plates, sheets, foils, bars, wires, castings, and clad materials. They are used to construct corrosion resistant equipment such as heat exchangers, condensers, vaporizers, reactors, columns, piping systems, pumps, valves, and packing for industries, including chemical processing, petrochemical, food, pharmaceutical, and waste management.

Zirconium is a reactive metal and depends on a passive film for corrosion resistance. Zirconium is very resistant to corrosive attack in most mineral and organic acids, strong alkalis, saline solutions, and some molten salts. It is not attacked by oxidizing media unless halides are present. Zirconium is not resistant to HF, ferric chloride ($FeCl_3$), cupric chloride ($CuCl_2$), aqua regia, concentrated H_2SO_4, and wet chloride gas.

The most prevalent use of zirconium, zirconium-hafnium alloys, and Zr-Hf-Nb alloys has been in the chemical processing industry for handling hot H_2SO_4. Zirconium and its alloys have excellent resistance to H_2SO_4 up to 50% concentration at temperatures to boiling and above. From 50 to 65% concentration, resistance is generally excellent at elevated temperatures, but the passive film is a less effective barrier. Experience has shown that oxidizing species in more than 50% H_2SO_4 can encourage selective attack. In concentrated H_2SO_4 above 70%, the corrosion rate of zirconium increases rapidly with increasing concentration. See the article "Corrosion of Zirconium and Zirconium Alloys" in Volume 13B of the *ASM Handbook* for more detailed information.

General Welding Considerations

Zirconium and zirconium alloys have weldability characteristics similar to those of titanium. They readily react with oxygen and form very stable oxides. Like titanium, they have high solubilities for oxygen, nitrogen, and hydrogen at elevated temperatures. Small amounts of dissolved oxygen and nitrogen significantly increase the hardness of the metal, whereas dissolved hydrogen reduces toughness and reduces notch sensitivity. Therefore, zirconium and zirconium alloys must be welded in a shield of high-purity inert gas or in a vacuum. Furthermore, zirconium should be free of oil, grease, and dirt to avoid the dissolving of carbon- and oxygen-containing materials, which can embrittle the metal or create porosity and

Table 6 Nuclear and nonnuclear grades of zirconium alloys

		Composition, wt%									
Alloy design	UNS No.	Zr+Hf(a)	Hf(b)	Sn	Nb	Fe	Cr	Ni	Fe+Cr	Fe+Cr+Ni	O(b)
Nuclear grades											
Zircaloy-2	R60802	...	0.01	1.20-1.70	...	0.07-0.2	0.05-0.15	0.03-0.08	...	0.18-0.38	...
Zircaloy-4	R60804	...	0.01	1.20-1.70	...	0.18-0.24	0.07-0.13	...	0.28-0.37	...	...
Zr-2.5Nb	R60901	...	0.01	...	2.40-2.80	...	...	...	...	...	...
Nonnuclear wrought grades											
Zr700	R60700	99.2	4.5	...	...	...	...	...	0.2(b)	...	0.10
Zr702	R60702	99.2	4.5	...	...	...	...	...	0.2(b)	...	0.16
Zr704	R60704	97.5	4.5	1.0-2.0	...	...	...	...	0.2-0.4	...	0.18
Zr705	R60705	95.5	4.5	...	2.0-3.0	...	...	...	0.2(b)	...	0.18
Zr706	R60706	95.5	4.5	...	2.0-3.0	...	...	...	0.2(b)	...	0.16
Nonnuclear casting grades											
Zr702C	...	98.8	4.5	...	...	...	...	...	0.3(b)	...	0.25
Zr704C	...	97.1	4.5	1.0-2.0	...	...	...	...	0.3(b)	...	0.3
Zr705C	...	95.1	4.5	...	2.0-3.0	...	...	...	0.3(b)	...	0.3

(a) Minimum. (b) Maximum

may reduce the corrosion-resistant properties of the metal.

Zirconium can only be welded to itself or to other reactive metal alloys, such as titanium, niobium, or tantalum. When welded to nonreactive metals, intermetallics that embrittle the weld metal are formed.

Although the GTAW process is the most common method for welding zirconium, other welding can be used. These include GMAW, PAW, EBW, LBW, resistance welding, and friction welding. The selection of a welding process depends on several factors: weld joint, tensile and corrosion-resistant property requirements, cost, and design configurations. See the article "Welding of Zirconium Alloys" in Volume 6 of the *ASM Handbook* for details.

Corrosion Behavior of Zirconium and Zirconium Alloy Weldments

Generally, zirconium welds exhibit similar corrosion resistance to nonwelded areas, except when used at the higher concentrations of sulfuric acid. Improper welding processes; however, can affect the mechanical and corrosion properties of zirconium. Interstitial element pickup, such as hydrogen, nitrogen, oxygen, and carbon in welds, will generally not increase the corrosion rate of zirconium. These interstitials may, however, reduce the ductility of the metal and cause premature mechanical failures. Nitrogen contamination caused by plasma cutting with nitrogen gas may increase the corrosion rate of zirconium in nitric acid environments. If any type of cutting operation is performed (oxyacetylene, plasma, or laser), the HAZ should be removed by grinding or machining prior to welding. Waterjet cutting should be used for the cutting of zirconium, where possible, to avoid the potential for contamination caused by the heat input. The waterjet cut should also be conditioned, because this process uses an abrasive (such as garnet) that will embed into the zirconium surface.

Delayed Hydride Cracking (DHC). Certain metals, such as titanium and zirconium, that form brittle hydrides can fail by two embrittlement processes. One process is a reduction in the fracture toughness of the metal due to the presence of a high concentration of hydride platelets that have their in-plane dimensions in the crack growth direction. The second process is DHC, which is the result of a mechanism of crack initiation and slow propagation.

In DHC, hydrogen diffusion in the metal is required. Gradients of concentration (C_x,) temperature (T), and stress (σ) are all important factors in controlling diffusivity, as given in the general diffusion equation:

$$J = \frac{DC_x}{RT}\left[RT\frac{d\ln C_x}{dx} + \frac{Q^*}{T}\frac{dT}{dx} - \frac{V^*}{3} - \frac{d\sigma}{dx}\right]$$

where J is hydrogen flux, D is diffusivity of hydrogen at any point x, R is the gas constant, Q^* is the heat of transport of hydrogen in metal, V^* is the volume of transport of hydrogen in metal and σ is positive for tensile stress and negative if compressive.

That is, hydrogen is driven by three forces to an area of lower concentration, colder temperature, and higher tensile stresses. Because DHC may occur at low temperatures in a matrix of uniformly distributed hydrogen, its mechanism is believed to be as follows: Stress gradients at stress concentration sites attract hydrogen, resulting in local hydride precipitation, growth, and reorientation. When the growing hydride reaches some critical size, the hydride either cleaves, or the hydride-matrix interface opens up to nucleate a crack. Once a crack has nucleated, propagation occurs by repeating the same process at the crack tip and, as such, is a discontinuous process. It should be noted that the formation of hydrides is not a necessary requirement for this mechanism to operate, as is the case in delayed hydrogen embrittlement in high-strength steels.

Stress and stress gradient are two necessary requirements for DHC to occur, and, fortunately, they are controllable. High stresses without gradients will not induce DHC. Hydrogen cannot move when high stresses are uniformly distributed in the structure. High-stress gradients are needed to move hydrogen but cannot be created without high stresses. High stresses are also required in fracturing hydrides.

It is estimated that hydrogen can hardly move from stress gradients generated by stressing up to 240 MPa (35 ksi). The common ASME requirement for unfired pressure vessels is to set the maximum allowable stresses at one-fourth the tensile strength at the operating temperature. As indicated in Table 7, the maximum allowable design stresses for zirconium alloys 702 and 705 are much lower than 200 MPa (29 ksi). Consequently, DHC should not occur when ASME requirements are met.

Table 7 ASME mechanical requirements for Zr702 and Zr705 used for unfired pressure vessels

Material form and condition	ASME specification number	Alloy grade	Tensile strength		Minimum yield strength		Maximum allowable stress in tension for metal temperature not exceeding °C (°F)													
							–4 to 40 (25 to 100)		95 (200)		150 (300)		205 (400)		260 (500)		315 (600)		370 (700)	
			MPa	ksi	MPa	ksi	MPa	ksi	MPa	ksi	MPa	ksi	MPa	ksi	MPa	ksi	MPa	ksi	MPa	ksi
Plate, sheet, strip	SB 551	702	359	52	207	30	108	16	84.3	12.2	70.1	10.2	62.4	9.0	47.9	6.9	40.3	5.8	35.5	5.1
		705	552	80	379	55	158	23	128	19	111	16	98.2	14.2	88.6	12.8	81.2	11.8	77.6	11.3
Seamless tubing	SB 523	702	359	52	207	30	108	16	84.3	12.2	70.1	10.2	62.4	9.0	47.9	6.9	40.3	5.8	35.5	5.1
		705	552	80	379	55	158	23	128	19	111	16	98.2	14.2	88.6	12.8	81.2	11.8	77.6	11.3
Welded tubing(a)	SB 523	702	359	52	207	30	92.1	13.4	76.9	11.2	63.7	9.2	52.9	7.7	43.3	6.3	35	5	30.9	4.5
		705	552	80	379	55	134	19	111	16	94.7	13.7	83.8	12.2	75.5	10.9	69.4	10.1	66	9.6
Forgings	SB 493	702	359	52	207	30	108	16	84.3	12.2	77	11	62.4	9.0	47.9	6.9	40.3	5.8	35.5	5.1
		705	552	80	379	55	158	23	128	19	111	16	98.2	14.2	88.6	12.8	69.4	10.1	77.6	11.3
Bar	SB 550	702	359	52	207	30	108	16	84.3	12.2	77.2	11.2	62.4	9.0	47.9	6.9	40.3	5.8	35.5	5.1
		705	552	80	379	55	158	23	128	19	111	16	98.2	14.2	88.6	12.8	81.2	11.8	77.6	11.3
Seamless pipe	SB 658	702	359	52	207	30	108	16	84.3	12.2	76.9	11.2	62.4	9.0	47.9	6.9	40.3	5.8	35.5	5.1
		705	552	80	379	55	158	23	128	19	111	16	98.2	14.2	88.6	12.8	81.2	11.8	77.6	16.3
Welded pipe(a)	SB 658	702	359	52	207	30	92.1	13.4	76.9	11.2	63.7	9.2	52.9	7.7	43.3	6.3	35	5	30.9	4.3
		705	552	80	379	55	134	19	111	16	94.7	13.7	83.5	12.1	75.5	10.9	69.4	10.1	66	9.6

(a) 0.85 factor used for welded product

Due to its low coefficient of thermal expansion, residual stresses from welding are typically below the yield points. Nevertheless, residual stresses greater than 240 MPa (35 ksi) are possible. Minimum ASTM International yield requirements, however, for Zr702, Zr704, and Zr705 at room temperature are 210, 240, and 380 MPa (30, 35, and 55 ksi), respectively. This implies that only Zr705 is likely to retain high enough stresses from welding to become susceptible to DHC. Practically, this has been the case.

Stress-relieving treatment is one of the most effective measures in preventing DHC, a time-dependent process. It takes considerable time for hydrogen to reach the highly stressed area and to precipitate out as hydride platelets. The platelets must grow large enough for cracking to occur Depending on many factors, it sometimes takes two years for DHC to happen, but five week after welding is the shortest known period for Zr705 to suffer DHC at room temperature. This provides a base for the *Boiler and Pressure Vessel Code of the ASME* (Ref 26):

> "Within 14 days after welding, all products of zirconium Grade R60705 shall be heat-treated at 1000 °F–1100 °F (538 °C–593 °C) for a minimum of 1 hr for thicknesses up to 1 in. (25.4 mm) plus ½ hr for each additional inch of thickness. Above 800 °F (427 °C), cooling shall be done in a closed furnace or cooling chamber at a rate not greater than 500 °F/hr (260 °C/hr) divided by the maximum metal thickness of the shell or head plate in inches but in no case more than 500 °F/hr. From 800 °F, the vessel may be cooled in still air."

Tantalum and Tantalum Alloys

Tantalum is a very dense (over 3.5 times the density of titanium) corrosion resistant material. It is an inherently soft, fabricable metal that has a very high melting temperature, approximately 3000 °C (5400 °F). It has a body-centered cubic crystal structure, with no allotropic transformation at elevated temperature. Unlike many bcc metals, tantalum retains good ductility to very low temperatures, and exhibits a ductile-to-brittle transition temperature (DBTT) of approximately –250 °C (–420 °F).

Tantalum and its alloys have excellent corrosion resistance to a wide variety of acids, alcohols, chlorides, sulfates, and other chemicals. For this reason, they are widely used for chemical equipment that operates at ambient temperatures.

Tantalum oxidizes in air above approximately 300 °C (570 °F) and is attacked by hydrofluoric, phosphoric, and sulfuric acids, and by chlorine and fluorine gases at temperatures above 150 °C (300 °F). Tantalum also reacts with carbon, hydrogen, and nitrogen at elevated temperatures. Because of the high per unit weight cost of tantalum and its high density, the cost effectiveness of this material has been increased by using clad, explosion clad, or resistance-welded clad products.

General Welding Considerations

Tantalum and its alloys can be welded by GTAW (the most common welding method), solid-state diffusion bonding, friction welding, resistance welding, and explosive bonding. Welding of tantalum is similar to welding of titanium and zirconium with respect to equipment and technology.

Tantalum and its alloys have good weldability, provided the welds and the heated base metal are free from contamination. Contamination by oxygen, nitrogen, hydrogen, and carbon should be avoided to prevent embrittlement of the weld. If required, fixturing devices should not come in close contact with the weld joint. Tantalum melts at 3000 °C (5430 °F); consequently, fixture materials may melt and alloy with tantalum to produce brittle welds. Graphite should not be used as a fixturing material, because it reacts with hot tantalum to form carbides, which also cause brittleness.

Tantalum cannot be arc welded to common structural metals because they form brittle intermetallic compounds, which in turn embrittle the welds. Tantalum can be welded to other reactive metals, with which it forms solid-solution alloys that are harder than tantalum but have usable ductility.

Corrosion Behavior of Tantalum and Tantalum Alloy Weldments

Examination of equipment fabricated from tantalum that has been used in a wide variety of service conditions and environments generally shows that the weld, HAZ, and base metal display equal resistance to corrosion. This same resistance has also been demonstrated in laboratory corrosion tests conducted in a number of different acids and other environments. How-

ever, in applications for tantalum-lined equipment, contamination of the tantalum with iron from underlying backing material, usually carbon steel, can severely impair the corrosion resistance of tantalum. About the only known reagents that rapidly attack tantalum are fluorine; HF and acidic solutions containing fluoride; H_2SO_4 (oleum), which contains free sulfur trioxide (SO_3); and alkaline solutions.

An exception to the generalization that base metal and weldments in tantalum show the same corrosion resistance under aggressive media is discussed in the following example. Because tantalum is a reactive metal, the pickup of interstitial elements, such as oxygen, nitrogen, hydrogen, and carbon, during welding can have a damaging effect on a refractory metal such as tantalum.

Example 2: Preferential Pitting of a Tantalum Alloy Weldment in H_2SO_4 Service. A 76 mm (3-in). diameter tantalum alloy tee removed from the bottom of an H_2SO_4 absorber that visually showed areas of severe etching attack was examined. The absorber had operated over a period of several months, during which time about 11,400 kg (25,000 lb) of H_2SO_4 was handled. The absorber was operated at 60 °C (140 °F) with nominally 98% H_2SO_4. There was a possibility that some of the H_2SO_4 fed into the process stream may have been essentially anhydrous or even in the oleum range. Oleum is known to attack tantalum very rapidly at temperatures only slightly higher than 60 °C (140 °F). In addition, the H_2SO_4 effluent was found to contain up to 5 ppm of fluoride.

Investigation. The materials in both the flange and the corrugated portion of the tee were verified by x-ray fluorescence to be Tantaloy 63 (Ta-2.5W-0.15Nb). Corrosive attack was visible to the unaided eye on the radius of the flange, on the first corrugation of the part and in two bands—one on each side of the GTA weld about 13 mm (0.5 in.) from the weld centerline and running the full length of the piece. Other areas of the part, such as the lip weld joining the corrugated tube section to the flange, other areas of the base metal away from the weld, and even the weld metal itself (including the adjacent HAZ), appeared on a cursory visual basis to be free from significant attack.

Stereo microexamination showed that the corrosive attack took the form of pitting. The areas of most severe attack that were observed were parallel to the longitudinal weld, circumferentially around the first corrugation of the part, and on the radius of the flange. Corrosion was characterized by a large number of closely occurring pits. What appeared to be markings resembling lines or scratches during an examination with the unaided eye were actually found at magnifications up to 30 × to be rows of corrosion pits aligned in the longitudinal direction and parallel to the weld. However, fewer somewhat shallower pits were found generally over the entire part.

In some locations, the pitting was extensive in the weld metal, in the HAZ, and even in the base metal 180° away from the weld. The extent of pitting appeared to be most severe on the inside diameter at sites that had been abraded by the tool used in forming the corrugations and in some areas containing scratches. There was no noticeable corrosion anywhere on the outside of the part.

Metallographic examination showed classical corrosion pits that were nearly spherical in shape. The maximum pit depth observed was 0.06 mm (2.5 mils). Pits did not appear to be typical of erosion or impingement-type attack, because the pits did not show the typical undercutting or undermining. Pitting did not follow the grain boundaries. No cracks were found propagating from the base of the pits in any of the samples; therefore, there was no evidence of corrosion fatigue or SCC.

A transverse section taken from another area of severe attack 13 mm (0.5 in.) from the weld metal was bent in the transverse direction with the inside diameter of the sample in tension. The sample was fully ductile; it was cold flattened 180° on itself with a sharp bend radius.

Conclusions. The corrosion on the tee was pitting that occurred generally over the entire part. Pitting was more severely concentrated parallel to the weld metal at a distance of 13 mm (0.5 in.) from the centerline of the weld (which was well outside the HAZ of the weld), on the radius of the flange, and on the first corrugation at the inlet. There was no evidence that the attack was due to cavitation erosion, corrosion fatigue, or SCC. The attack did not reduce the ductility of the material. All areas of the part were fully ductile, as evidenced by the soft, ductile nature of the part during sawing and cutting and by bend tests in the area of most severe attack.

The specific corrosion agents responsible were believed to be H_2SO_4 in the oleum concentration range in the presence of some fluoride ion (F^-). Corrosion tests and years of indus-

trial experience with equipment indicate that in the absence of F^- (or free fluorine) and in H_2SO_4 concentrations of 98% and below such pitting attack does not occur on tantalum or Tantaloy 63 metal at 60 °C (140 °F).

Related Laboratory Experiments. Some laboratory experiments were performed on weldments of tantalum and Tantaloy 63 that may relate to and suggest why preferential corrosion attack was observed parallel to the longitudinal weld of the tee in Example 2 at locations considerably beyond the weld HAZ.

Gas tungsten arc butt welds were made in specimens of Tantaloy 63 and tantalum in a copper welding fixture operated in open air with an argon-flooded torch and trailing shield and with an argon flood on the backside of the root of the weld. Both materials showed surface oxidation parallel to the weld at about the location of the hold-down clamps of the welding fixture. The presence of this oxide film or heat-tint was revealed by electrolytically anodizing the samples in a dilute phosphoric acid (H_3PO_4) solution at 325 V. This film has been arbitrarily designated as a heat-tint oxide. The zone of oxidation could have occurred either by air leaking past the hold-down clamps and reacting with the hot tantalum at this location or by oxygen that may have been present in the welding atmosphere at this location. Heat-tint oxides were not noted on the weld metal or the HAZ. This is perhaps because these regions of the weld reached a much higher temperature—sufficiently high to volatilize oxygen from the tantalum weld metal and HAZ as tantalum suboxide (TaO).

The heat-tint oxide layer was removed from the welded specimens by swabbing with a strong pickling solution of nitric acid (HNO_3), HF, and H_2SO_4 before the samples were anodized. The heat-tint oxide layer, as well as the clean base metal, was found to be unaffected by aqua regia (3 parts concentrated HCl and 1 part concentrated HNO_3 by volume) after 6 h of exposure at 80 °C (175 °F).

During pickling in the HNO_3-HF-H_2SO_4 mixture, it was noted that the heat-tint oxide was attacked more rapidly than the weld metal, the HAZ, or the base metal outside of the thermally oxidized region. Such heat-tint oxide was often barely visible on the as-welded samples, appearing only as a slight yellowish tinge on the surface in many cases. However, minimal immersion (a few seconds) in the acid pickle revealed the heat-tinted area as whitish or grayish, hazy or smoky bands parallel to the weld. After the oxide was completely removed by pickling, either by swab pickling or by completely immersing the sample in an HF-containing medium, all parts of the sample appeared to corrode at approximately the same rate.

Therefore, the pitting observed at certain regions parallel to the welds was believed to be associated with the initial removal of the heat-tint oxide. Once the heat-tint oxide was removed, this selective attack no longer occurred. and corrosion was uniform.

Oxygen Tolerance of Tantalum Weldments. Tantalum reacts with oxygen, nitrogen, and hydrogen at elevated temperatures. The absorption of these interstitial elements, often called a gettering reaction, produces a sharp reduction in ductility and can cause embrittlement. This impairment in ductility (and also in notch toughness, as manifested by an increase in ductile-to-brittle transition temperature) can be considered a form of corrosion. The other Group Va refractory metals (niobium and vanadium) and the Group IVa reactive metals (titanium, zirconium, and hafnium) can also suffer similar attack.

An investigation was conducted to determine the approximate tolerances of tantalum and Tantaloy 63 weldments for oxygen contamination that may be permitted during fabrication or subsequent service. Weldments of the materials were doped with various amounts of oxygen added, either by anodizing or by oxidation in air. This was followed by vacuum annealing treatments to diffuse the oxygen through the sample cross section. The oxygen concentration was monitored principally by hardness tests. Hardness is generally believed to be a better indicator of the extent of interstitial contamination than chemical analysis, which is subject to scatter and inaccuracy because of sampling difficulty. Bend tests (at room and liquid argon temperatures) and room-temperature Olsen cup formability tests were conducted to determine the hardness levels at which the materials embrittled.

The results showed that weldments of both materials remain ductile when hardened by interstitial contamination by oxygen up to a Rockwell 30T hardness in the low 80s. Above this hardness, embrittlement may be expected. The hardness level at which embrittlement occurs is substantially above the typical maximum allowable hardness of 65 HR30T specified for Tantaloy 63 or the 50 HR30T for tantalum

flat mill products. Thus, if the extent of interstitial contamination by oxygen (and/or nitrogen) is controlled so that these maximum allowable hardness limits are not exceeded, embrittlement of weldments should not occur.

On the basis of chemical composition, the maximum oxygen tolerance for tantalum weldments appears to be approximately 400 to 550 ppm: for Tantaloy 63 weldments, it is approximately 350 to 500 ppm. Although commercially pure tantalum exhibits a somewhat higher tolerance for oxygen (and total interstitial contamination) than Tantaloy 63, the latter material appears to have somewhat better resistance to oxidation: this tends to offset the advantage tantalum has of a higher allowable oxygen pickup before embrittlement occurs. It should be further emphasized that the results are based on the assumption that oxygen was believed to be distributed relatively uniformly throughout the cross section in all parts of the weldment. A locally high concentration, such as a high surface contamination of oxygen or nitrogen, could result in a severe loss in ductility and could possibly even produce embrittlement. Therefore, all handling, cleaning, and fabrication practices on tantalum and its alloys should avoid producing such surface contamination as well as gross contamination. The article "Corrosion of Tantalum and Tantalum Alloys" in Volume 13 B of the *ASM Handbook* gives more detailed information on the corrosion of tantalum and tantalum alloys.

REFERENCES

1. J.R. Davis, Ed., *Corrosion of Aluminum and Aluminum Alloys,* ASM International, 1999
2. M. B. Shumaker, R. A Kelsey, D.O. Sprowls, and J.G. Williamson, "Evaluation of Various Techniques for Stress-Corrosion Testing Welded Aluminum Alloys," presented at ASTM Stress-Corrosion Testing Symposium, June 1966
3. S. L Wöhler and O. Schliephake, Über einem Gers., durh Potentialmessunger das Aufgregen der Verb. Mg_2Si zu Bestätigen. *Z. Anorg. Chem.,* 1962, p 151
4. G.W. Akimow and A.S. Oleschko, *Gmelins Handbuch der anorganischen Chemie* (No. 8), Auflage, 1942, p 393
5. G. Beverini, "Investigations of the Corrosion Characteristics of Al-Li and Al-Li-Cu Weldments in a 3.5% NaCl Solution," master's thesis T-3508, Colorado School of Mines, 1988
6. *Welding Aluminum,* American Welding Society—The Aluminum Association, 1972
7. J.G. Young, BWRA Experience in the Welding of Aluminum-Zinc-Magnesium Alloys, *Weld. Res. Suppl.,* Oct 1968
8. "Alcoa Aluminum Alloy 7005," *Alcoa Green Letter,* Aluminum Company of America, Sept 1974
9. Environmentally Assisted Cracking, *Corrosion of Aluminum and Aluminum Alloys,* J.R. Davis, Ed., ASM International, 1999, p 101–134
10. J.G. Young, BWRA Experience in the Welding of Aluminum-Zinc-Magnesium Alloys, *Weld. Res. Suppl.,* Oct 1968
11. Tentative Guide to Automotive Resistance Spot "Welding of Aluminum," T10, The Aluminum Association, Washington, DC, Oct 1973
12. "Weldbonding—An Alternate Joining Method for Aluminum Auto Body Alloys," T17, The Aluminum Association, Washington, DC, 1978
13. T.L. Wilkinson and W.H. Ailor, "Joining and Testing Bimetallic Automotive Panels," SAE Technical Paper, Series 78 0254, Society of Automotive Engineers, 1978
14. J.J. Bethke and S. J. Ketcham, Polysulfide Sealants for Corrosion Protection of Spot Welded Aluminum Joints, *Adhes. Age,* Nov 1979, p 17
15. G. Haynes and R. Baboian, Laboratory and Field Corrosion Test Results on Aluminum-Transition-Steel Systems on Automobiles, *Corrosion and Corrosion Control of Aluminum and Steel in Lightweight Automotive Applications,* E. N. Soepenberg, Ed., National Association of Corrosion Engineers, 1985, p 383-1 to 383-13
16. R. Baboian and G. Haynes, Corrosion Resistance of Aluminum-Transition-Steel Joints for Automobiles, Paper 268, presented at *Proc. Sixth Automotive Corrosion Prevention Conf.,* Society of Automotive Engineers, 1993
17. J.B. Lumsden, M.W. Mahoney, C.G. Rhodes, and G.A. Pollock, Corrosion Behavior of Friction-Stir-Welded AA7050-T7651, *Corrosion,* Vol 59 (No. 3), 2003, p 212–219

18. J.M. Lumsden, M.W. Mahoney, G. Pollock, and C.G. Rhodes, Intergranular Corrosion Following Friction Stir Welding of Aluminum Alloy 7075-T651, *Corrosion,* Vol 55 (No. 12), 1999, p 1127–1135
19. "Corrective Measures to Restore Corrosion Resistance Following Friction Stir Welding," Corporate Report, Rockwell Scientific Company, Thousand Oaks, CA, 2004, 21 pages
20. G.S. Frankel and Z. Xia, Localized Corrosion and Stress Corrosion Cracking Resistance of Friction Stir Welded Aluminum Alloy 5454, *Corrosion,* Vol 55 (No. 2), 1999, p 139–150
21. Z.X. Li, W.J. Arbegast, P.J. Hartley, and E.I. Meletis, Microstructure Characterization and Stress Corrosion Evaluation of Friction Stir Welded Al 2195 and Al 2219 Alloys, *Trends in Welding Research,* ASM International, 1998, p 568–573
22. N.R. Mandal, Friction Stir Welding, *Aluminum Welding,* 2nd ed., Narosa Publishing House and ASM International, 2005, p 149–163
23. R. Gubner, U. Andersson, M. Linder, A. Nazarov, and C. Taxén, "Grain Boundary Corrosion of Copper Canister Weld Material," Technical Report, TR-06-01, Svensk Kärnbränslehantering AB, Jan 2006
24. W.A. Baeslack III, D.W. Becker, and F.H. Froes, Advances in Titanium Alloy Welding Metallurgy, *J. Met.,* May 1984, p 46–58
25. N. E. Paton and J.C. Williams, The Effect of Hydrogen on Titanium and Its Alloys, *Hydrogen in Metals,* American Society for Metals, 1974, p 409–431
26. "Boiler and Pressure Vessel Code of the ASME," Section VIII, Division 1, Subsection C, UNF-56, (d), American Society of Mechanical Engineers, 1992, p 183

Corrosion of Weldments
J.R. Davis, editor, p 169-175
DOI:10.1361/corw2006p169

CHAPTER 9

Corrosion of Dissimilar Metal Weldments

VARIOUS PORTIONS of a process system operate at different service conditions, therefore, different structural alloys are used in the design, and hence, dissimilar-metal welded joints may be required. Many factors must be considered when welding dissimilar metals, and the development and qualification of adequate procedures for the various metals and sizes of interest for a specific application must be undertaken.

Most combinations of dissimilar metals can be joined by solid-state welding (diffusion welding, explosion welding, friction welding, or ultrasonic welding), brazing, or soldering where alloying between the metals is normally insignificant. In these cases, only the differences in the physical and mechanical properties of the base metals and their influence on the serviceability of the joint should be considered. When dissimilar metals are joined by arc (fusion) welding processes, alloying between the base metals and a filler metal; when used, becomes a major consideration. The resulting weld metal can behave much differently from one or both base metals during subsequent processing or in service. The most popular arc welding processes for joining dissimilar metals are shielded metal arc welding (SMAW), gas metal arc welding (GMAW), and gas tungsten arc welding (GTAW).

Factors Influencing Joint Integrity (Ref 1)

Dissimilar metal weldments are characterized by compositional gradients and microstructural changes which produce large variations in chemical, physical and mechanical properties across the weldment. Welding of dissimilar metals is therefore normally more complex than joining of similar metals. The difficulties encountered when joining dissimilar metals comprise problems experienced when welding each base metal individually, and problems unique to the range of compositions possible when combining the alloys in various proportions. Additional complexity arises with the addition of filler metal, which is common practice in dissimilar metal welding.

The principal factors that are responsible for failure (cracking) of dissimilar metal arc welds include:

- General alloying problems (brittle phase formation and limited mutual solubility) of the two metals
- Widely differing melting points
- Differences in coefficients of thermal expansion
- Differences in thermal conductivity
- Corrosion problems including galvanic corrosion, oxidation, hydrogen-induced cracking, and sensitization

Weld Metal. In the fusion welding of dissimilar-metal joints, the most important consideration is the weld metal composition and its properties. Its composition depends upon the compositions of the base metals; the filler metal, if used; and the relative dilutions of these. The weld metal composition is usually not uniform, particularly with multipass welds, and a composition gradient is likely to exist in the weld metal adjacent to each base metal.

These solidification characteristics of the weld metal are also influenced by the relative dilutions and the composition gradients near each base metal. These characteristics are important with respect to hot cracking of the weld metal during solidification.

The basic concepts of alloying, the metallurgical characteristics of the resultant alloy, and its mechanical and physical properties must be considered when designing a dissimilar-metal joint. For the fusion welding processes it is important to investigate the phase diagram of the two metals involved. If there is mutual solubility of the two metals, the joint can usually be made successfully. If there is little or no solubility between the two metals to be joined, the weld joint will not be successful. The intermetallic compounds that are formed between the dissimilar metals must be investigated to determine their crack sensitivity, ductility, susceptibility to corrosion, and so on. The microstructure of this intermetallic compound is extremely important. In some cases, it is necessary to use a third metal that is soluble with each metal in order to produce a successful joint (see the discussion "Buttering" later in this chapter).

Bimetallic Inserts. Very brittle intermetallic compounds are formed when metals such as steel, copper, magnesium, or titanium are fusion welded to aluminum. Bimetallic transition material inserts in sheet, plate, and tubular forms are commercially available in combinations of aluminum to such other metals as steel, stainless steel, and copper. These are made by rolling, explosion welding, friction welding, flash welding, or hot pressure welding and provide the easiest method for fusion welding aluminum to other metals. Conventional GTAW and GMAW methods, as well as resistance spot welding, are used to join the aluminum side of the transition piece to the intended component. The dissimilar metal is joined to the opposite side of the bimetallic transition. An example of a transition material insert to join aluminum to steel can be found in Fig. 4 in Chapter 8, "Corrosion of Nonferrous Alloy Weldments."

Dilution is the change in chemical composition of a welding filler metal caused by the admixture of the base metal or previously deposited weld metal in the deposited weld bead. It is normally measured by the percentage of base metal or previously deposited weld metal in the weld bead. Dilution control, which is of primary concern when joining dissimilar metal combinations, is described in detail in the article "Hardfacing, Weld Cladding, and Dissimilar Metal Joining" in Volume 6 of the *ASM Handbook*.

In dissimilar-metal welding, the filler metal must alloy readily with the base metals to produce a weld metal that has a continuous, ductile matrix phase. Specifically, the filler metal must be able to accept dilution (alloying) by the base metals without producing a crack-sensitive microstructure. The weld metal microstructure must also be stable under the expected service conditions. A successful weld between dissimilar metals is one that is as strong as the weaker of the two metals being joined, that is, possessing sufficient tensile strength and ductility so that the joint will not fail.

Melting Temperatures. The difference in melting temperatures of the two metals that are to be joined must also be considered. This is of primary interest when a fusion welding process utilizing considerable heat is involved, since one metal may be molten long before the other when subjected to the same heat source. Significant difference between the melting temperatures of the two base metals or between those of the weld metal and a base metal can result in rupture of the metal having the lower melting temperature. Solidification and contraction of the metal with the higher melting temperature will induce stresses in the other metal while it is in a weak, partially solidified condition.

Buttering. The problem of differences in melting temperature of two dissimilar metals may be solved by depositing one or more layers of a filler metal of intermediate temperature on the face of the base metal with the higher melting temperature. The procedure is known as "buttering." The weld is then made between the buttered face and the other base metal. The buttering layer should serve to reduce the melting temperature differential. Buttering may also be used to provide a transition between materials with substantially different coefficients of thermal expansion but which must endure cycling temperatures in service. Similarly, buttering may be used to provide a barrier layer that will slow the migration of undesirable elements from the base metal to the weld metal during postweld heat treatment or in service at elevated temperatures. The buttering technique is illustrated in Fig. 1.

Thermal Conductivity. Most metals and alloys are relatively good conductors of heat, but some are much better than others. Rapid conduction of heat from the molten weld pool

by an adjacent base metal may affect the energy input required to locally melt the base metal. When two dissimilar metals of significantly different thermal conductivities are welded together (for example, plain carbon steels and copper-base alloys), the welding procedure must provide for this difference. Often the welding heat source must be directed at the metal having the higher thermal conductivity to obtain the proper heat balance.

When welding dissimilar metals, heat loss to the base metals can be balanced somewhat by selectively preheating the metal having the higher thermal conductivity. Dilution is more uniform with balanced heating.

Preheating the base metal of higher thermal conductivity also reduces the cooling rate of the weld metal and the heat-affected zone (HAZ). The net effect of pre-heating is to reduce the heat needed to melt that base metal.

The coefficient of thermal expansion of the two dissimilar base metals is another important factor. Large differences in thermal expansion coefficients of adjacent metals during cooling will induce tensile stress in one metal and compressive stress in the other. The metal subject to tensile stress may hot crack during welding, or it may cold crack in service unless the stresses are relieved thermally or mechanically. This factor is particularly important in joints that will operate at elevated temperatures in a cyclic temperature mode. A common example of this is austenitic stainless steel/ferritic steel pipe butt joints used in energy conversion plants.

Ideally, the thermal expansion coefficient of the weld metal should be intermediate between those of the base metals, especially if the difference between those of the two base metals is large. If the difference is small, the weld metal may have an expansion coefficient equivalent to that of one of the base metals.

Selection of a suitable filler metal is an important factor in producing a dissimilar-metal joint that will perform well in service. One objective of dissimilar-metal welding is to minimize undesirable metallurgical interactions between the metals. The filler metal should be compatible with both base metals and be capable of being deposited with a minimum of dilution.

Two important criteria that should govern the selection of a proper filler metal for welding two dissimilar metals are as follows:

- The candidate filler metal must provide the joint design requirements, such as mechanical properties or corrosion resistance.

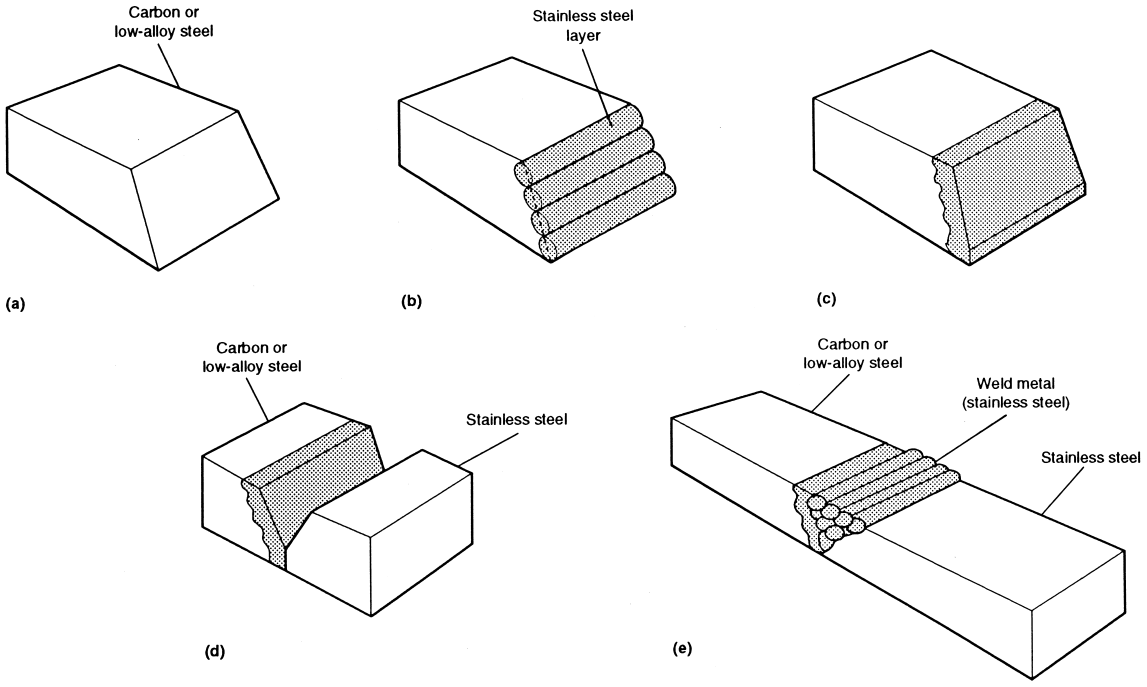

Fig. 1 Buttering technique used to assist welding stainless steel to carbon or low-alloy steel. (a) Edge prepared for buttering. (b) Face buttered with filler metal. (c) Buttered face prepared for welding. (d) Joint aligned for welding. (e) Joint welded with stainless steel filler metal. Source: Ref 1

- The candidate filler metal must fulfill the weldability criteria with respect to dilution, melting temperature, and other physical property requirements of the weldment.

The Schaeffler diagram is commonly used to predict weld metal microstructure and subsequent filler metal selection when joining a stainless steel to a carbon or low-alloy steel. Figure 2 illustrates the procedure with an example of a single-pass weld joining mild steel to type 304 stainless steel with ER309 stainless steel filler metal. First a connecting line is drawn between the two points representing the base metal compositions, based on their chromium and nickel equivalents. Point X, representing the relative dilutions contributed by each base metal is then located on this line. If the relative dilutions are equal, point X is at the midpoint of the line. A second line is drawn between point X and the point representing the ER309 filler metal composition. The composition of the weld pass lies somewhere on this line, the exact location depending upon the total dilution. With 30% dilution, the composition would be at point Y and would be considered acceptable. If a succeeding pass joins the first pass to mild steel, the dilution with the mild steel should be kept to a minimum, to avoid martensite formation in the weld metal.

Suggested filler metals for joining dissimilar metals are also published in various tables found in Volume 6 of the *ASM Handbook*. See, in particular, the following articles:

- "Dissimilar Welds With Stainless Steels"
- "Welding of Nickel Alloys"
- "Welding of Copper Alloys"
- "Hardfacing, Weld Cladding, and Dissimilar Metal Joining"

Property Considerations. A dissimilar metal joint normally contains weld metal having a composition different from that of one or both base metals. The properties of the weld metal depend on the filler metal composition, the welding procedures, and the relative dilution with each base metal. There are also two different HAZs, one in each base metal adjacent to the weld metal. The mechanical and physical properties of the weld metal, as well as those of the two HAZs, must be considered for the intended service.

Special considerations are generally given to dissimilar-metal joints intended for elevated-temperature service. A favorable situation exists when the joint will operate at constant temperatures. During elevated-temperature service, internal stresses can decrease by relaxation and reach an equilibrium. However, it is best to

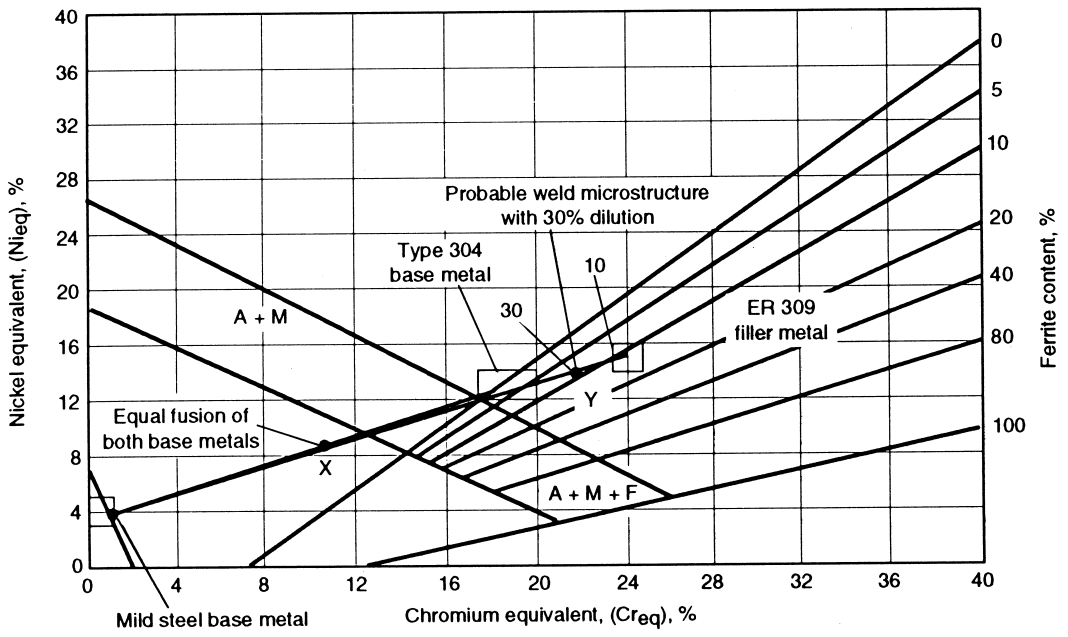

Fig. 2 Prediction of weld metal composition from the Schaeffler diagram. A, austenite; F, ferrite; M, martensite. See text for details. Source: Ref 1

reduce the effect of large differences in coefficients of thermal expansion when large temperature fluctuations cannot be avoided in service. The problem can be avoided by selecting base metals with similar thermal expansion characteristics.

Corrosion Behavior

Galvanic Corrosion and Oxidation Resistance. The weld metal and both base metals have specific corrosion behaviors that must be considered by the designer in the initial selection of materials. For example, with dissimilar metal weldments, the formation of galvanic cells can cause corrosion of the most anodic metal or phase in the joint. Also, the weld metal is usually composed of several microstructural phases, and very localized cells between phases can result in galvanic corrosion at the microstructural level. To minimize galvanic corrosion, the composition of the weld metal can be adjusted to provide cathodic protection to the base metal that is most susceptible to galvanic attack. However, other design requirements should not be seriously compromised to do this. Instead, some other form of protection should be used.

A galvanic cell associated with a high-strength steel may promote hydrogen embrittlement in the HAZ of that steel if it is the cathode of the cell. Hydrogen embrittlement must be considered if the service temperature of the weldment will be in the range of –40 to 95 °C (–40 to 200 °F), and the weld will be in a highly stressed area of the assembly. Residual stresses developed in the weld zone are often sufficient to promote hydrogen embrittlement and stress-corrosion cracking.

Chemical compositional differences in a dissimilar-metal weld can also cause high-temperature corrosion problems. Compositional variations at the interfaces between the different metals can result in selective oxidation when operating at high temperatures in air and formation of notches at these locations. Such notches are potential stress-raisers in the joint and can cause oxidation failure along the weld interface and cyclic thermal conditions.

Hydrogen-Induced Cracking (Ref 2). Dissimilar metal welds are used extensively in the power generation, oil and gas, chemical and petrochemical, and heavy fabrication industries. Numerous instances of cracking along the dissimilar metal fusion boundary have been reported, particularly in cladding applications where a corrosion-resistant austenitic alloy is applied to a ferritic structural steel. Often this cracking, or disbonding, has been associated with exposure during service, and, as a result, the mechanism has been described by various authors as a form of hydrogen-induced cracking.

This form of cracking has also occurred during fabrication, prior to exposure to a hydrogen environment. The fact that disbonding of clad steels can occur without prolonged exposure to hydrogen in service suggests that either hydrogen is not necessary for disbonding to occur, or hydrogen absorbed during the welding process can cause cracking near the dissimilar metal fusion boundary.

In order to determine the influence of hydrogen during welding, a series of experiments were conducted in which dissimilar metal welds were made using the GTAW process with pure argon shielding gas or Ar-6%H_2 shielding gas. Following welding, the weldments were inspected for cracking using side-bend tests, and by sectioning and metallography. The objective was to determine if cracking near the fusion boundary of dissimilar metal welds could be caused by hydrogen absorbed during welding and to characterize the microstructures in which cracking occurred.

The filler metals selected for this investigation, which are commonly used in industry for dissimilar metal welding, were ER308 and ER309LSi austenitic stainless steels and ERNiCr-3, a nickel-base filler metal. A36 structural steel was selected as the base metal. The chemical compositions of these materials are listed in Table 1.

Table 1 Chemical composition of base and filler metals, wt %

Element	A36 Steel	ER308	Er309LSi	ERNiCr-3
Fe	bal	bal	bal	1.33
Cr	0.09	20.51	23.16	19.32
Ni	0.13	9.69	13.77	73.23
Mn	0.71	1.86	1.75	2.90
Si	0.18	0.50	0.79	0.10
Mo	0.05	0.11	0.16	. . .
Cu	0.29	0:24	0.20	0.09
Ti	. . .	. . .	0.005	0.35
Nb+Ta	. . .	. . .	0.005	2.62
C	0.17	0.045	0.020	0.05
N	. . .	0.033	0.110	. . .
P	0.009	0.019	0.019	. . .
S	0.027	0.022	0.014	0.001
Cr_{eq}(a)	0.42	21.37	24.51	20.78
Ni_{eq}(a)	5.59	11.97	15.25	76.18

(a) Schaeffler equivalents See Fig. 3. Source: Ref 2

Cracking was observed in single-pass welds made with Ar-6%H_2 shielding gas using all three filler metals. Cracking was not observed in welds made with pure argon shielding gas; therefore it can be concluded that the cracking was hydrogen induced.

Cracking was always associated with regions of martensite near the fusion boundary. The ferrofluid color metallography technique revealed that the cracks occurred in regions containing a ferromagnetic constituent, which is consistent with the presence of martensite. Microhardness indentations revealed that the regions where cracking occurred had a hardness significantly higher than that of the austenitic weld metal, which is also consistent with the presence of martensite.

Welds made with ERNiCr-3 and ER309LSi filler metals exhibited less cracking than welds made with 308 filler metal. According to the Schaeffler diagram (Fig. 3), the minimum base metal dilution necessary to form martensite in these filler metals is 16% for ER308, 33% for ER309LSi and 78% for ErNiCr-3. For a given dilution, welds made with ER308 filler metal contained the most martensite and experienced the most severe cracking. Low dilution welds made with ER309LSi and ERNiCr-3 can only form crack-susceptible martensite in select locations near the fusion boundary where the local dilution is higher than that of the bulk weld metal.

The results of this study demonstrated that hydrogen introduced during welding can lead to hydrogen-induced cracking in dissimilar welds between austenitic filler metals and ferritic base metals. Hydrogen in the welding arc is detrimental in two ways:

- It increases dilution by the carbon steel base metal, increasing the amount of martensite formed
- It interacts with martensite under stress to cause cracking

The incidence of cracking was most pronounced in single-pass welds. This suggests that the use of multipass techniques or thermal treatments that allow for hydrogen diffusion will minimize cracking susceptibility. The use of low-hydrogen practice with dissimilar metal welds is also suggested.

Sensitization. Selection of an appropriate preheat or post-weld heat treatment (PWHT) for a welded joint can present a problem with some dissimilar-metal combinations. The appropriate heat treatment for one component of the weldment may be deleterious to the other component for the intended service conditions. For example, if an age-hardenable nickel-chromium alloy is welded to a nonstabilized austenitic stainless

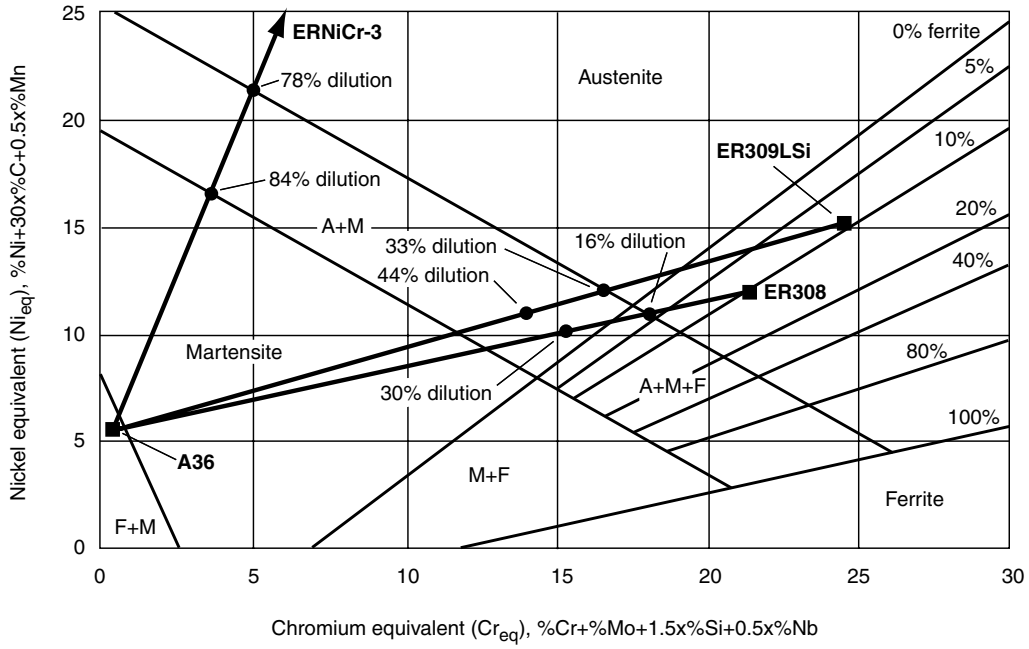

Fig. 3 Schaeffler diagram showing predicted microstructures and minimum dilutions necessary to form martensite for A36 base metal and three austenitic filler metals. Source: Ref 2

steel, exposure of the weldment to the aging treatment for the nickel-chromium alloy would sensitize the stainless steel and decrease its resistance to intergranular corrosion (weld decay).

One solution is to use a stabilized austenitic stainless steel if that is acceptable. Another solution might be to butter the face of the age-hardenable, nickel-chromium alloy component with a similar alloy that is not age-hardenable. This component is then heat-treated to obtain the desired properties. Finally, the buttered surface is welded to the stainless steel component.

Stainless steel cladding materials are also susceptible to sensitization. Sensitization can occur when unstabilized stainless steels are heated in the range of 430 to 820 °C (800 to 1500 °F) either during stress relief or in service. The best way to inhibit these problems is to use low-carbon grades (such as type 308L or 309L) or stabilized grades (such as type 347) of austenitic stainless steels that are not readily sensitized. Also, finer microstructures produced by the lower-heat-input processes improve corrosion resistance for all grades. Additional material on weld sensitization can be found in Chapter 3, "Corrosion of Austenitic Stainless Steel Weldments."

REFERENCES

1. Dissimilar Metals, *Welding Handbook: Metals and Their Weldability,* Vol 4, 7th ed., American Welding Society, 1982, p 514–547
2. M. D. Rowe, T. W. Nelson, and J. C. Lippold, Hydrogen-Induced Cracking Along the Fusion Boundary of Dissimilar Metal Welds, Welding Research Supplement to the *Weld. J.,* Feb 1999, p 31-s–37-s

SELECTED REFERENCES

- "Dissimilar Weld Failure Analysis and Development Program," Vol 1–4, Report CS-4252, Electric Power Research Institute, Palo Alto, CA
- A. L. Schaeffler, Constitution Diagram for Stainless Steel Weld Metal, *Met Prog.,* Vol 56 (No. 11), 1949, p 680–688

Corrosion of Weldments
J.R. Davis, editor, p 177-202
DOI:10.1361/corw2006p177

CHAPTER 10

Weld Corrosion in Specific Industries and Environments

WELD CORROSION in the three key application areas will be examined in this chapter:

- Petroleum refining and petrochemical operations
- Boiling water reactor (BWR) piping systems
- Components used in pulp and paper plants

In petroleum and petrochemical operations, hydrogen-induced cracking (HIC), particularly in the presence of wet hydrogen sulfide (H_2S), has been a major concern for carbon and low-alloy, steel weldments. In BWR piping systems, the primary concern has been intergranular stress-corrosion cracking (IGSCC). Corrosive environments are found in a number of process stages in the pulp and paper industry including pulp production, pulp processing and chemical recovery, pulp bleaching, and paper manufacturing.

Corrosion of Weldments in Petroleum Refining and Petrochemical Operations

For practical purposes, corrosion in refineries and petrochemical plants can be classified into two types of corrosion:

- Low-temperature (aqueous) corrosion occurring below approximately 260 °C (500 °F) in the presence of water
- High-temperature (nonaqueous) corrosion occurring above approximately 205 °C (400 °F) in the presence of liquid or gaseous hydrocarbons

In this section, emphasis is placed on low-temperature aqueous corrosion in H_2S-containing environments. Sour crude oils and gases that contain H_2S are handled by most refineries. Hydrogen sulfide is also present in some feedstocks handled by petrochemical plants.

Fabricability Considerations

With very few exceptions, process equipment and piping are fabricated by welding wrought steels. The shells of pressure vessels are usually made from rolled plate, while nozzles are forgings. This requires that the steels have sufficient ductility for forming and are readily weldable. Weldability of steels is important not only for initial fabrication but also for future field repairs or modifications. Weld repairs and postweld heat treatments (PWHT) can affect the mechanical properties of wrought components that have been processed by normalizing or quenching and tempering. This can leave the wrought material with a lower strength than expected, based solely on its mill processing and composition.

Welding may result in certain other problems. Hydrogen coming from moisture in certain weld consumables or during nonoptimal field welding conditions can become dissolved in liquid weld metal. This dissolved hydrogen can cause cracking during solidification, as well as embrittlement of the weld. Dissolved hydrogen in the material as a result of exposure to refinery wet H_2S service environments can also affect weldability and the subsequent performance of repair welds.

The risk of hydrogen cracking of weldments is reduced by the use of low-hydrogen electrodes, careful drying of electrodes, and close control of pre- and postweld heat treatments. Equipment exposed to wet H_2S service environments often needs to be baked prior to weld repairs to reduce

or remove the accumulated hydrogen that can lower weldability. In some severe cases, this can result in cracks being formed as a result of high-temperature hydrogen attack. Information on the effect of bake-out treatments and other wet H_2S repair techniques is presented later in the section "Wet H_2S Cracking."

Stress-relief or reheat cracking is intergranular cracking in the weld HAZ. The HAZ cracking occurs when weldments are heated during PWHT, or it occurs by subsequent exposure to elevated service temperatures. Low-alloy steels are especially susceptible to the aforementioned phenomena, but hydrogen cracking can occur with any of the ferritic steels if proper care is not taken.

Wet H_2S Cracking

Corrosion of carbon and low-alloy steels by aqueous H_2S solutions or sour waters (generically referred to as refinery wet H_2S environments) can result in one or more types of environmentally assisted cracking (EAC). These forms of EAC are related primarily to the damage caused by hydrogen that results from the production of hydrogen by the sulfide corrosion process in aqueous media. They include loss of ductility on slow application of strain (hydrogen embrittlement), formation and propagation of hydrogen-filled blisters or voids in the material (hydrogen blistering or HIC), and spontaneous cracking of high-strength or high-hardness steels (hydrogen embrittlement cracking, also known more familiarly as sulfide stress cracking, or SSC, when involving environments that include exposure to H_2S). A monograph of classic papers published on cracking of steels in petroleum upstream and downstream wet H_2S environments was published by NACE International and is given in Ref 1.

In wet H_2S refinery environments, atomic hydrogen (H^0) forms as part of the sulfide corrosion process. When steel corrodes in aqueous H_2S-containing environments, it forms a mostly insoluble FeS corrosion product and also liberates hydrogen atoms (also referred to as monatomic hydrogen). If these hydrogen atoms come in close proximity to each other, they can recombine to form molecular hydrogen (H_2). Once this recombination process takes place on the metal surface, molecular hydrogen is too large to enter the metal lattice. It is only the atomic form of hydrogen that can enter the material during aqueous corrosion and potentially lead to the aforementioned forms of EAC.

During these corrosion processes, hydrogen atoms formed from cathodic reactions first adsorb on the metal surface prior to recombination. It is at this point that the hydrogen atoms can recombine to form H_2 gas that is commonly seen bubbling off the corroding metal surfaces. However, in the presence of certain chemical species known as hydrogen recombination poisons, the formation of hydrogen molecules can be retarded. Sulfur (from H_2S), arsenic, phosphorus, tin, lead, and bismuth are commonly known hydrogen recombination poisons. Due to the retarding effect of sulfur species on the recombination process, the atomic hydrogen produced by the corrosion process is more likely to reside in the atomic form, become absorbed into the material, and permeate according to its diffusivity and solubility in the microstructure. Information on these processes and ways to measure hydrogen permeation are given in ASTM G 148 (Ref 2).

Sulfide Stress Cracking. While still in the atomic state, monatomic hydrogen can diffuse to and concentrate at sites of microstructural discontinuities, such as phase, precipitate or grain boundaries, dislocations, and sites of high stress and/or lattice distortion (strain), where they can interfere with the normal ductility processes of the material. The accumulation of atomic hydrogen in the locally distorted metal lattice is the direct result of the lattice dilation, which is better able to accommodate the presence of the interstitial hydrogen. At sufficiently high concentrations in the solid state, atomic hydrogen can also affect the bonding between atoms to promote decohesion, particularly along grain boundaries and other zones where the lattice has already been distorted by strain, cold working, or hardening. These are solid-state reactions between the atomic hydrogen and the metal lattice and its local defect structures. This is the basis for SSC of steels and most other engineering materials.

Sulfide stress cracking is normally associated with high-strength steels and alloys—yield strength greater than 550 MPa (80 ksi)—and with high-hardness (>22 HRC) structures in weld HAZs. Non-PWHT weldments are particularly problematic, because they often contain both high HAZ hardness and high residual tensile stresses that can initiate SSC and promote crack propagation. Resistance to SSC is usually improved through the use of PWHT and through

the use of lower-carbon-equivalent plate steels and quenched-and-tempered wrought steels.

Hydrogen-Induced Cracking. Once atomic hydrogen has diffused into the material, it can also recombine to form molecular hydrogen (H_2) within the metal at internal defects, inclusions, and pores. Sites for recombination are commonly observed to be weak internal interfaces such as those at manganese sulfide inclusions or metallurgical laminations. Ferrite-pearlite banding and related inclusions can also produce locally weak interfaces in the material that can result in small hydrogen-filled blisters being produced. Because hydrogen molecules are much larger than atomic hydrogen, once the hydrogen recombines to form hydrogen gas (H_2), it cannot readily diffuse out of these sites. This results in a buildup of pressure inside these blisters, which drives their growth, and eventually results in propagation and linkage of hydrogen-filled blister cracks in the material, commonly known as HIC and also referred to as stepwise cracking due to the visual appearance of these cracks stepping through the material (Fig. 1). This phenomenon usually is of concern in lower-strength plate steels—less than 550 MPa (80 ksi) and low hardness (<HRC 22)—used in rolled and longitudinally seam welded or electric resistance welded pipe, or plate steels used in the manufacturing of refinery vessels and tanks.

Refinery Experience with SSC. Sour water containing H_2S can cause spontaneous cracking of highly stressed, high-strength steel components, such as bolting and compressor rotors as a result of SSC (Ref 3). Cracking has also occurred in carbon steel components containing hard welds (Ref 4). Cracking can be transgranular, intergranular (with respect to prior-austenite grain boundaries), or mixed mode and will contain sulfide corrosion products, as shown in Fig. 2 and 3. Cracking of this type has become known as SSC and should not be confused with HIC presented previously in this section.

Sulfide stress cracking was first identified in the production of sour crude oils when high-strength steels used for well-head and downhole equipment cracked readily after contacting with produced water that contained H_2S. Sulfide stress cracking was not experienced by refineries and petrochemical plants until the introduction of high-pressure processes that required high-strength bolting and other high-strength components in gas compressors. With the increased use of submerged arc welding for pressure vessel construction, it was found that weld deposits significantly harder and stronger than the base metal could be produced. This led to transverse cracking in weld deposits with hardness greater than 200 HB (Ref 4).

The mechanism of SSC has been the subject of many investigations, most of which attempted to address the cracking seen in high-strength steels instead of the lower-strength steels used in refinery and petrochemical plant equipment. In general terms, SSC occurs in the same corrosive environments that lead to the other forms of refinery wet H_2S cracking. Hydrogen sulfide affects the corrosion rate and the relative amount of hydrogen absorption but

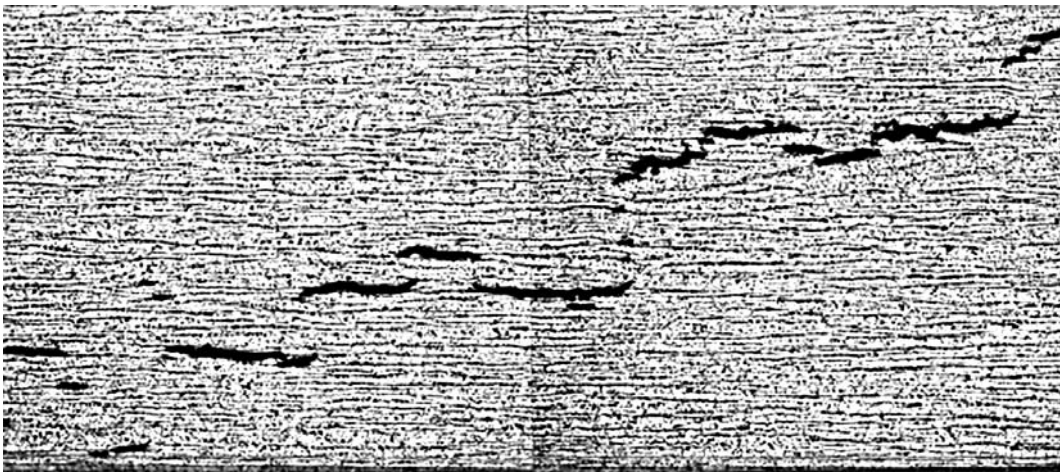

Fig. 1 Hydrogen-induced cracking, which is also referred to as stepwise cracking

otherwise does not appear to be directly involved in the cracking mechanism. As a general rule of thumb, SSC can be expected to occur in process streams containing in excess of 50 ppm H_2S in the gas phase (not dissolved in solution). However, SSC susceptibility is actually related to the partial pressure of H_2S in the service environment, and this H_2S limit may vary with total pressure. Therefore, there can be SSC occurring at lower H_2S concentrations.

There is also a direct relationship between H_2S concentration and the allowable maximum hardness value of the HAZ on one hand and cracking threshold stress on the other. Typically, the allowable maximum hardness value decreases 30 HB, and the allowable threshold stress decreases by 50% for a tenfold increase in H_2S concentration (Ref 5). Also, SSC occurs most readily at or near ambient temperature, with susceptibility decreasing with increasing service temperature. As in the case of hydrogen embrittlement and hydrogen blistering, SSC of steel in refineries and petrochemical plants often requires the presence of cyanides.

The most effective way of preventing SSC is to ensure that the steel is in the proper metallurgical condition. This usually means that weld hardness is limited to 200 HB (Ref 6). Because hard zones can also form in the HAZs of welds and shell plates from hot forming, the same hardness limitation should be applied in these areas. Guidelines for dealing with the SSC that occurs in refineries and petrochemical plants are given in API RP 942 (Ref 7) and NACE RP0472 (Ref 8). The most comprehensive guidelines for materials selection for resistance to SSC in refinery operations are now provided in NACE MR0103 (Ref 9).

Postweld heat treatment of fabricated equipment will greatly reduce the occurrence of SSC. The effect is twofold: first, there is the tempering effect of heating to 620 °C (1150 °F) on most hard microstructures (the possible exception being highly microalloyed steels), and second, the residual stresses from welding or forming are reduced. The residual tensile stresses typically represent a much larger effect on the equipment than the internal pressure or other mechanical stresses.

A large number of the ferrous alloys, including stainless steels, as well as certain nonferrous alloys, are susceptible to SSC. Cracking may be

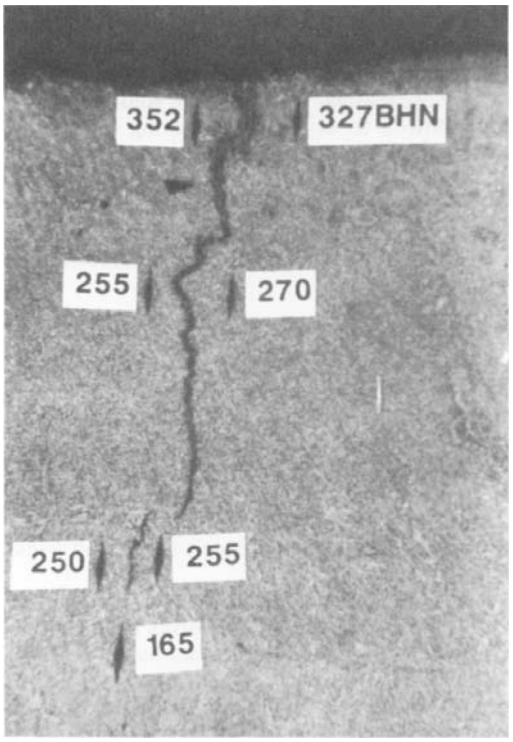

Fig. 2 Sulfide stress cracking of a hard weld of a carbon steel vessel in sour water service. BHN, Brinell hardness. 40×

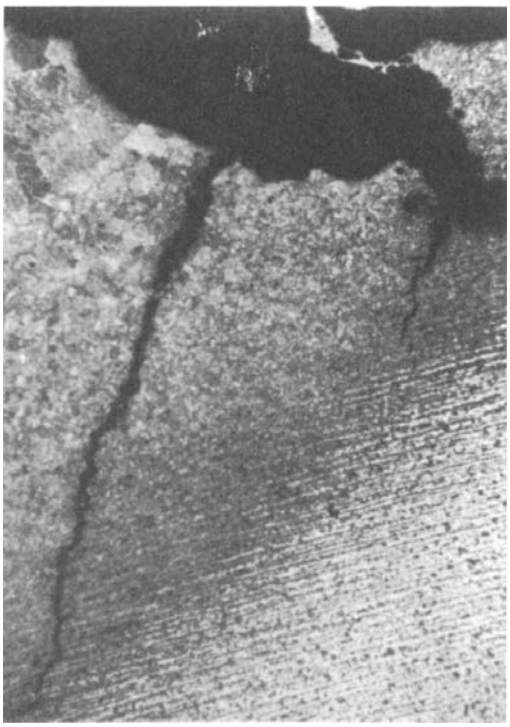

Fig. 3 Sulfide stress cracking of hard HAZ next to weld in A516-70 pressure vessel steel after exposure to sour water. 35×

expected to occur with carbon and low-alloy steels when the tensile strength exceeds 550 MPa (80 ksi). Because there is a relationship between hardness and strength in steels, the aforementioned strength level approximates the 200 HB hardness limit. For ferrous and nonferrous alloys used primarily in upstream oil field equipment, limits on hardness and/or heat treatment have been established in NACE MR0175/ISO 15156 (Ref 10). In the past, versions of this standard have also been used for petroleum refinery service. However, due to their acidic nature and high levels of chloride, many oil field environments can be generally more corrosive than those encountered during many refining operations (the exception being refinery environments with cyanide). It is now recommended that the MR0175 standard not be used for selection of materials for petroleum refining service. The use of the newer NACE MR0103 standard for refinery operations is preferred (Ref 9).

The oil and gas industries have increasing need for the use of high-strength low-alloy (HSLA) steels such as API 5L X70 and X80 due to the cost savings they afford, especially in long piping systems that transport crude oil or natural gas. Transport conditions, however, are becoming increasingly sour (higher H_2S concentrations) and the use of higher strength HSLA grades is prevented where NACE MR0175 is employed as a governmental regulation. Of particular importance is the performance of pipeline girth welds used to connect pipe segments in the field. Circumferential girth welds are typically multipass welds, in which subsequent welds temper underlying hard HAZ regions, leaving the hardest HAZ regions in the final untempered cap passes. The cap passes are on the exterior of the pipeline girth weld and thus are exposed to lower hydrogen concentrations than weld regions in contact with the sour environment within the pipe. Because SSC is a hydrogen embrittlement mechanism, higher hardness values (exceeding HRC 22) should be tolerable in hard weld cap regions, which are exposed to relatively low hydrogen concentrations. Testing performed at The Welding Institute (TWI) showed that, in fact, hard external weld regions exceeding a Vickers hardness (HV) of 300 (248 HV = HRC 22) were resistant to SSC in a stresses pipe containing the NACE test solution (Ref 11). This investigation was aimed at assessing the conservatism of the NACE requirements for HSLA weldments, with focus on weld hardness requirements and extrapolation to service conditions. Many of the corrosion and embrittlement aspects of this work are described in Ref 12 and 13.

Hydrogen-Induced Disbonding

A form of damage potentially resulting from refinery high-temperature hydrogen service is hydrogen-induced disbonding (HID) of stainless steel clad or weld overlaid steel plates used in hydroprocessing equipment (Fig. 4). This form of attack usually results in the formation of blisters at or near the bond/fusion line between the steel and stainless alloys. Hydrogen-induced disbonding occurs with increasing frequency at high hydrogen pressures and service temperatures and with increased rapid cooling as a result of process changes and shutdown, start-up cycles (Ref 14). It has also been found that the process of cladding or weld overlaying can also affect susceptibility to HID. A laboratory test procedure involving exposure of bimetallic samples to high-temperature hydrogen environments has been developed and standardized in ASTM G 146 (Ref 15). These procedures can be tailored to specific service applications (temperature, hydrogen partial pressure, and cooling rates) for purposes of qualification of particular fabrication and welding techniques used in vessel construction.

Liquid Metal Embrittlement

Although liquid metal embrittlement has been recognized for at least 60 years, it has received far less attention than the more commonly encountered hydrogen damage or SCC. This is due in part to the fact that the probability of liquid metal

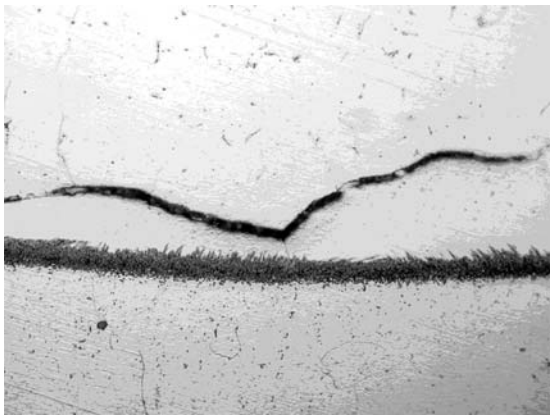

Fig. 4 Hydrogen-induced disbonding of stainless steel clad plate steel produced in a laboratory test in accordance with ASTM G 146 in high-pressure hydrogen. The crack is in the stainless steel cladding shown at the top of the micrograph. 200×

contact occurring in refineries and petrochemical plants is normally rather small. In situations in which liquid metal embrittlement has occurred, it has been mainly due to the zinc embrittlement of austenitic stainless steels. Isolated failures have been attributed to welding in the presence of residues of zinc-rich paint or to the heat treating of welded pipe components that carried splatter of zinc-rich paint. However, most of the reported failures due to zinc embrittlement have involved welding or fire exposure of austenitic stainless steel in contact with galvanized steel components.

For example, in one case, severe and extensive cracking in the weld HAZ of process piping made from austenitic stainless steel occurred in a petrochemical plant during the final stages of construction. Much of the piping had become splattered with zinc-rich paint. Although the welders had been instructed to clean piping prior to welding, no cleaning and only limited grinding were performed. After welding, dye-penetrant inspection revealed many thin, branched cracks in the HAZ of welds, as shown in Fig. 5.

In many cases, through-wall cracks cause leaks during hydrotesting. Typically, zinc embrittlement cracks contain zinc-rich precipitates on fracture surfaces and at the very end of the crack tip. Cracking is invariably intergranular in nature (Ref 16).

Fig. 5 Intergranular cracking in HAZ of stringer bead weld on type 304 (S30400) stainless steel pipe due to zinc embrittlement. Weld area had been covered with zinc-rich paint.

Several different models for the zinc embrittlement of austenitic stainless steel have been proposed. The most accepted model involves the reduction in atomic bond strength at a surface imperfection, grain boundary, or crack tip by chemisorbed zinc metal. Zinc embrittlement is commonly a relatively slow process that is controlled by the rate of zinc diffusion along austenitic grain boundaries. Zinc combines with nickel, and this results in nickel-depleted zones adjacent to the grain boundaries. The resulting transformation of face-centered cubic austenite (γ) to body-centered cubic ferrite (α) in this region is thought to produce not only a suitable diffusion path for zinc but also the necessary stresses for initiating intergranular cracking. Externally applied stresses accelerate cracking by opening prior cracks to liquid metal.

Although the melting point of zinc is 420 °C (788 °F), no zinc embrittlement has been observed at temperatures below 750 °C (1380 °F), probably because of phase transformation and/or diffusion limitations. There is no evidence that an upper temperature limit above which zinc embrittlement does not occur exists. In the case of zinc-rich paints, only those having metallic zinc powder as a principal component can cause zinc embrittlement of austenitic stainless steels. Paints containing zinc oxide or zinc chromates are known not to cause embrittlement.

Prevention of Zinc Embrittlement. Obviously, the best approach to prevent zinc embrittlement is to avoid or minimize zinc contamination of austenitic stainless steel components in the first place. In practice, this means limiting the use of galvanized structural steel, such as railings, ladders, walkways, or corrugated sheet metal, at locations where molten zinc is likely to drop on stainless steel components if a fire occurs. If zinc-rich paints will be used on structural steel components, shop priming is preferred. Field application of zinc-rich paints should be done after all welding of stainless steel components has been completed and after insulation has been applied. Otherwise, stainless steel components should be temporarily covered with plastic sheathing to prevent deposition of overspray and splatter.

If stainless steel components have become contaminated despite these precautionary measures, proper cleaning procedures must be im-

plemented. Visible paint overspray should be removed by sandblasting, wire brushing, or grinding. These operations should be followed by acid pickling and water rinsing. Acid pickling will remove any traces of zinc that may have been smeared into the stainless steel surface by mechanical cleaning operations. Suitable acid pickling solutions include 5 to 10% nitric acid, phosphoric acid, or weak sulfuric acid. Hydrochloric acid should not be used in order to avoid pitting and intergranular attack of sensitized weldments, or stress-corrosion cracking (SCC) problems. After removal of all traces of acid by water rinsing, final cleaning with a nonchlorinated solvent should be performed immediately before welding.

Stress-Corrosion Cracking of Weldments in BWR Service

For more than three decades, BWR piping systems fabricated from austenitic stainless steel have suffered from SCC. This has resulted in loss of plant availability, increased cost of electrical energy, and increased exposure to radiation of skilled personnel involved in inspection and repair operations (Ref 17). This section will review the phenomenon of SCC in welded BWR pipe and present methods for its mitigation.

BWR Piping Systems

There are differences in specific design details between the various BWR reactor manufacturers. The model described in this section is a General Electric design. Regardless of the BWR model, their piping systems are essentially the same, fabricated of types 304 (S30400), 309 (S30900), or 316 austenitic stainless steel (most plants use type 304).

Boiling water reactor pipes are produced either by extrusion or by plate rolling and seam welding. Pipes of 304 mm (12 in.) diameter or less are generally extruded, while larger pipes are plate rolled and welded. Extruded pipe is usually delivered in the mill-annealed condition, which varies from one pipe fabricator to another. As a result, some pipes are delivered in the "sensitized" condition (for a discussion of sensitization of stainless steels, see Chapter 3, "Corrosion of Austenitic Stainless Steel Weldments" in this book). For plate-rolled and seam-welded pipes, solution heat treatment following welding removes the weld sensitization, including any residual sensitization in the base material and weld residual stresses.

Incidents of SCC have been reported in BWR weldments of austenitic stainless steel pipe ranging from 76 to 710 mm (3 to 28 in.) in diameter. Most of the cracking has occurred in the recirculation piping system, but systems involving the core spray, reactor water cleanup, residual heat removal, control-rod return lines, and isolation condenser lines have also been affected. A schematic of a recirculation piping system representative of one BWR model is shown in Fig. 6. Piping systems in a typical BWR may have 150 to 200 welded joints, depending on the model.

Stress-Corrosion Cracking of Pipe Weldments

Cracking in types 304 and 316 stainless steel pipe weldments has been confined largely to the HAZ. The cracking morphology is intergranular, following the sensitized grain boundaries in the HAZ. In some of the pipe weldments, IGSCC penetrates the weld metal, but there have been no reported weld failures. In general, IGSCC propagation in the weld is very limited because of the weld microstructure and mechanical properties

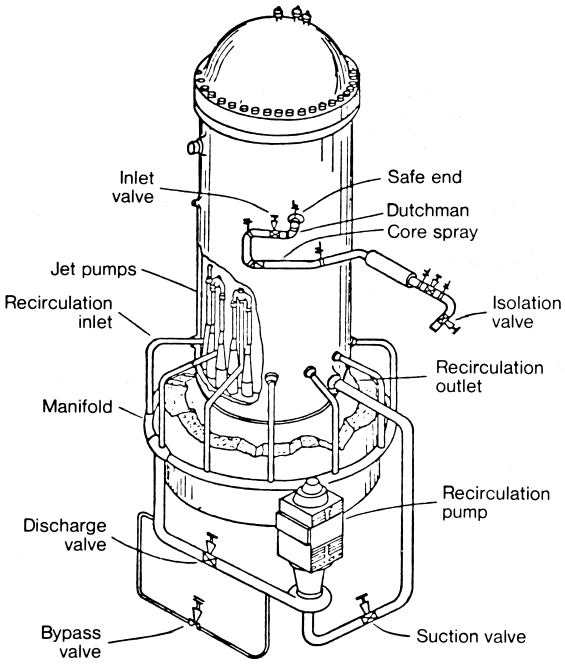

Fig. 6 Schematic of BWR recirculation piping system

of the weld. The technical basis for this will be discussed in a later section. Intergranular SCC is predominantly oriented along the circumference of the girth or butt weld in the HAZ. Axial stresses are responsible for this crack orientation. Although there have been a few observations of axially oriented IGSCC, these are rare and result from pipe hoop stresses. Axially oriented cracks are also confined to the HAZ because of the barriers on each side of it—namely, the weld metal and the base material, both of which resist IGSCC. Intergranular SCC in a type 304 pipe weldment is shown in Fig. 7 and 8. Cracking is in the HAZ and originates on the internal diameter of the pipe.

Intergranular SCC initiates on the inside of the pipe, where the three key conditions necessary for its promotion exist: tensile stresses, sensitization in the HAZ, and an aqueous environment provided by the BWR coolant water. Once IGSCC is initiated, the crack will continue to propagate, provided sufficient tensile stresses are present. Initiation may occur in several locations in the HAZ, depending on the local conditions that promote IGSCC. Both initiation and propagation are highly variable processes that depend on the level of sensitization, the chemistry of the BWR coolant, and the state of stress.

Model for IGSCC

The phenomenon of IGSCC in welded austenitic stainless steel pipes has been the subject of much research and development (Ref 18, 19), and a model for the mechanism of IGSCC has been developed (Ref 20). The basis for this

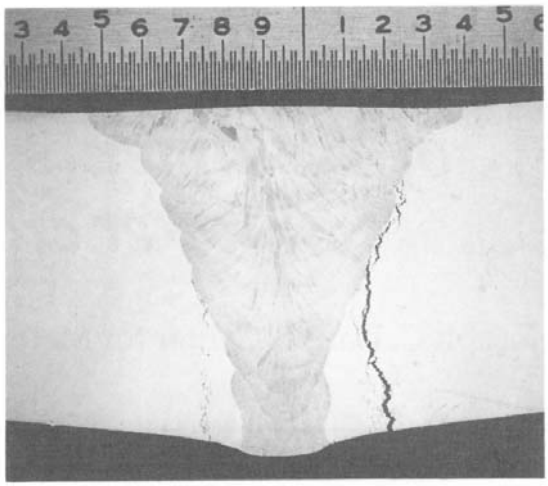

Fig. 7 Photomacrograph of IGSCC in a type 304 stainless steel pipe weldment

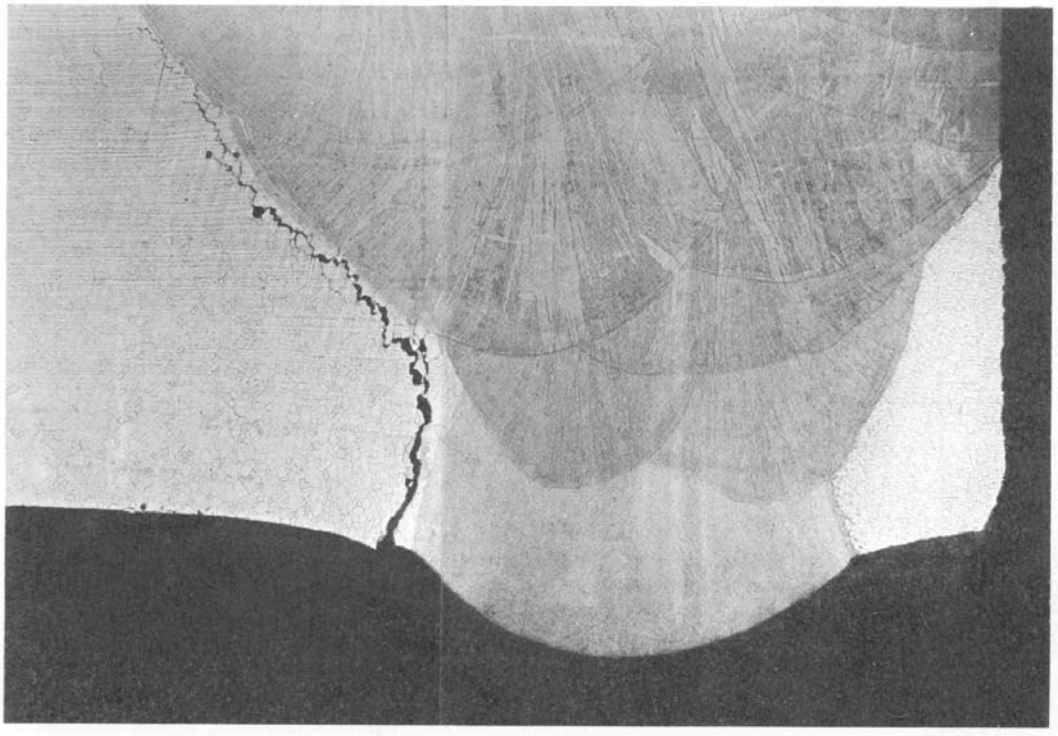

Fig. 8 Pipe test results showing IGSCC in a 400 mm (16 in.) type 304 stainless steel pipe HAZ. 13×

model is the coexistence of three major contributors in the weldment: (1) tensile stresses above the yield stress of the base material, (2) a sensitized microstructure, and (3) the BWR water coolant.

Applied tensile stresses acting on the pipe weldment at or above the yield stress of the base material are needed for the initiation and propagation of IGSCC. These tensile stresses include stresses generated by plant operation and residual stresses from welding, pipe installation, and pipe fabrication.

Sensitization is defined as a metallurgical condition of chromium depletion in the austenite grain boundaries that results when chromium-rich carbides ($Cr_{23}C_6$) precipitate during the thermal cycles of the welding process. When the chromium content in the austenite grain boundaries is reduced from the bulk concentration of 18 wt% to 12 wt% or less, passivation or resistance to corrosion is lost. This leads to initiation sites for IGSCC, and crack propagation follows the grain boundary.

The BWR coolant is high-purity water with a neutral pH. At the BWR operating temperature of 288 °C (550 °F), the water contains small amounts of impurities and 100 to 300 ppb of dissolved oxygen resulting from radiolytic dissociation of the water. In this environment, the electrochemical potential (ECP) of welded types 304 and 316 stainless steel is in the range for IGSCC (Ref 21).

A schematic representation of the three key factors contributing to intergranular SCC is shown in Fig. 9. The degree to which any given factor must be present for IGSCC to occur depends on the level of intensity and overlap with the other two factors. For example, with a high level of sensitization and high tensile stresses, a relatively unaggressive BWR environment is necessary for IGSCC initiation and propagation. On the other hand, elimination of one of the factors will suppress cracking. Thus, the model provides three direct technical solutions for the mitigation of IGSCC in BWR weldments. These solutions include improved materials, tensile stress reductions, and environmental control (see the section "Mitigation of IGSCC in Boiling Water Reactors").

Weld Residual Stresses

Residual stresses can be produced from pipe fabrication, fit-up, and welding. Of these various stresses, those from welding are a major contributor to the total stresses acting on pipe weldments.

Weld residual stresses, both surface and through-wall, were measured in a variety of type 304 stainless steel pipe sizes using strain-gage and x-ray methods. Pipe girth welds were prepared using field welding procedures. A plot of peak axial stresses for welded pipes with diameters of 100, 254, and 660 mm (4, 10, and 26 in.) is shown in Fig. 10. Axial stresses are responsible for the initiation of IGSCC of circumferential orientation. As shown in Fig. 10, very high tensile surface residual stresses exist in the sensitized HAZ. Clearly, these residual

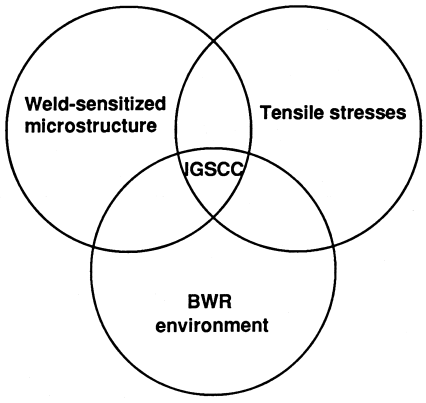

Fig. 9 Three key contributors necessary for IGSCC in welded types 304 and 316 stainless steel pipes

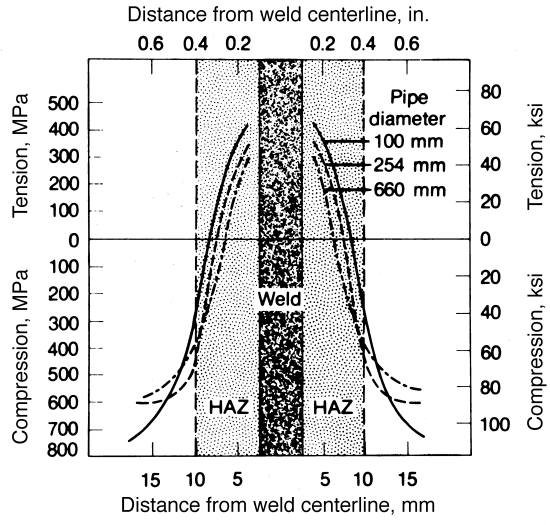

Fig. 10 Peak axial residual stresses on the inside surface of welded type 304 stainless steel pipes. Source: Ref 19

stresses are a major contributor to the overall tensile stresses acting on the pipe weldments.

Measurements of through-wall residual stresses on the same three pipes showed tensile stresses at the inside surface and partial through-wall for the 100 and 254 mm (4 and 10 in.) diameter pipes. However, the 660 mm (26 in.) pipe showed compressive residual stresses just beneath the surface that extended well into the pipe wall (Fig. 11).

These residual stress patterns help explain the IGSCC behavior of the BWR pipe welds. When these stresses are added to operating stresses, the yield stress of the pipe material is likely exceeded. The high peak surface axial tensile residual stresses are a major contributor to the initiation of IGSCC. The through-wall axial tensile residual stresses contribute to crack propagation. This view is consistent with actual plant incidents. The propensity for IGSCC is greater for the 100 mm (4 in.) pipes and decreases with increasing pipe diameter. In large-diameter pipes of 660 mm (26 in.), the lower surface tensile residual stresses increase initiation time while the subsurface compressive stresses decrease the rate of crack propagation. Hence, much longer plant operating times are needed for IGSCC in large-diameter pipes.

To complete this discussion of the role of residual stresses in IGSCC, three other important factors must be considered: the permanence of the weld residual stresses, the mechanical properties of the weldment, and the effect of the pipe weld preparation method.

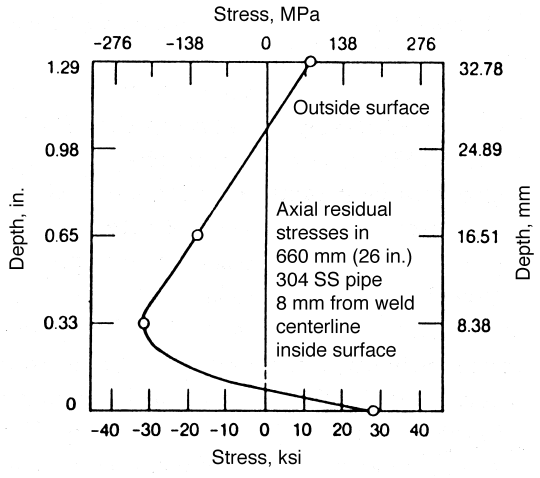

Fig. 11 Through-wall distribution of weld residual stresses in a 660 mm (26 in.) diam type 304 stainless steel pipe. Source: Ref 22

Permanence of Weld Residual Stresses. The high residual stresses in austenitic stainless steel weldments were considered to lessen during plant operation at 288 °C (550 °F). For this reason, weld residual stresses were not considered in code piping analysis. However, this theory was dispelled when residual stress measurements were made on a 610 mm (24 in.) type 304 pipe weldment removed from a BWR after 10 years of service (Ref 23). Residual stress patterns were obtained that were quite similar to those measured in as-welded 660 mm (26 in.) type 304 pipe (Fig. 11). Subsequently, other pipes removed from operating plants showed similar permanence of the weld residual stresses. These results support the position that weld residual stresses need to be factored into the pipe system design stress analysis.

Mechanical properties of weldments depend on a number of factors. Only the more important ones will be considered here. The chemistry of the weld filler material and the cooling rate during welding determine the ratio of austenite to ferrite in the weld metal. Ferrite is much stronger than austenite; as the ferrite level increases, so does the strength of the weld. Toughness, on the other hand, decreases with increasing ferrite level. The morphology and fineness of the microstructure also affect mechanical properties. A filler material of 308 composition is normally used for type 304 stainless steel. A minimum of 5% ferrite in the as-deposited condition is specified to avoid hot cracking of the weld (Ref 24). The presence of the ferrite at this level also increases resistance to IGSCC.

The welding process affects the final weld microstructure and thus mechanical properties. For shop welds, submerged arc welding (SAW) is generally used, depending on the pipe joining configuration. Field welding may use shielded metal arc welding (SMAW) and gas tungsten arc welding (GTAW). Typically, manual GTAW is used for the root pass, followed by either SMAW or automated GTAW. The best balance of mechanical properties is produced by GTAW followed by SMAW. The SAW method produces an acceptable but less desirable balance of strength and toughness (Ref 25).

The mechanical properties of a weldment will vary from the weld centerline to the base material. Microtensile samples removed from the weldment of a 660 mm (26 in.) type 304 stainless steel pipe were used to measure tensile properties. A plot of the yield strength across the weld-

ment at 288 °C (550 °F) is shown in Fig. 12. The highest yield strength is in the weld metal, with a continuous drop in yield strength occurring as the base material is reached. The reason for this variation is the presence of δ-ferrite in the weld and the warm working in the HAZ that results from the shrinkage of the weld metal during solidification. A greater warm-working strain occurs near the weld fusion line and decreases as the base material is approached.

Two very significant pieces of technical information emerge from these results. One is the high yield strength of the weldment at the BWR operating temperature of 288 °C (550 °F). This explains why the residual stresses are above the yield strength of the type 304 base material at room temperature and at the BWR operating temperature. The second relates to the region of IGSCC in the pipe weldments. From a yield-strength basis, the weakest region in the weldment is the base material. However, this region is not susceptible to IGSCC because it is not sensitized. The presence of δ-ferrite in the weld metal provides additional resistance to IGSCC. Therefore, the HAZ is the area with a susceptible microstructure and a yield stress less than the weld metal. Initiations sites for IGSCC in the HAZ depend on the intensity and overlap of tensile stress and degree of sensitization (assuming the environmental factor is constant across the weldment).

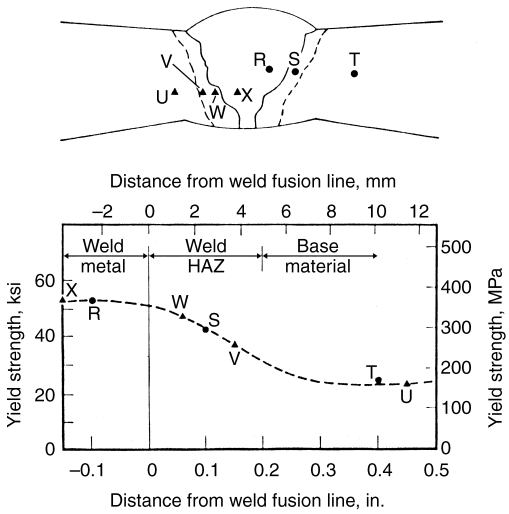

Fig. 12 Yield strength profile at 288 °C (550 °F) across a 660 mm (26 in.) diam type 304 stainless steel pipe weldment. Source: Ref 19

Effect of Weld Preparation Method. In preparing a pipe for welding, the inside surface of the pipe is machined or ground to match the two pipe pieces. Depending on the pipe diameter, postweld grinding may also be used to clean up the weld for inspection. The method of surface preparation will affect the surface residual stresses. Heavy machining and grinding will result in cold working, high residual stresses, and areas of stress intensification. These cold-worked areas will also result in surface recrystallization during welding. All of these changes enhance the initiation process of IGSCC.

Surface residual stresses caused by surface preparation methods are presented in Table 1. These data show significant tensile residual stresses associated with machining and grinding. These stresses, added to the weld residual stresses, contribute to the initiation of IGSCC. The high surface residual stresses of weld preparation also contribute significantly to recrystallization during welding. This process exacerbates IGSCC initiation.

Mitigation of IGSCC in Boiling Water Reactors

The following discussion presents several IGSCC mitigation techniques for BWR components. The mitigation methods are presented under general categories of material solutions, stress solutions, and environmental solutions. A

Table 1 Maximum tensile surface residual stresses caused by surface treatments of type 304 stainless steel

Sample	Surface preparation	Maximum tensile surface residual stress(a), MPa (ksi)	
		Parallel to lay	Perpendicular to lay
Pipe, inside surface	Machined	550(80)T	70(10)T
Pipe, inside surface	Light grind (hand grinder)	550(80)T	0(0)
Flat coupon, inside surface	Heavy grind (hand grinder)	550(80)T	120(17)T
Flat coupon, inside surface	Ground (hand grinder)	760(110)T	275(40)T

(a) T, tension; C, compression

few of the remedies address two of the three necessary conjoint factors illustrated in Fig. 9.

Materials Solutions

The materials solutions to the piping IGSCC concern in the United States consist primarily of replacing the susceptible types 304 and 316 stainless steels with more sensitization-resistant materials, such as types 316 and 304 nuclear grades (NG), redissolving the chromium carbides by solution heat treatment, and cladding with crack-resistant weld metal. Other materials, such as type 347NG, have been used successfully in Europe.

Nuclear-Grade Stainless Steels. The replacement of current piping materials with materials more resistant to sensitization is a straightforward approach to mitigating IGSCC. It is well documented that decreasing the carbon content and increasing the molybdenum content of stainless steel will reduce the kinetics of sensitization (Ref 26–29). However, type 316NG and type 304NG (with no added molybdenum) stainless steels take this theme a step further. Instead of the nominal 0.03% C maximum of the L-grade stainless steels, the nuclear grades are characterized by a maximum carbon content of 0.020%. The second important composition characteristic of type 304NG and type 316NG is the specification of 0.060 to 0.100% N. This modification is designed to recover the decrease in alloy strength due to the reduction of the carbon content Another successful approach that has been used in Germany is the use of low-carbon niobium-stabilized type 347 stainless steel.

For the nuclear-grade materials, full-size pipe tests have shown that factors of improvement over reference type 304 stainless steel performance can be expected to be at least 50 to 100 times in normal BWR operation (Ref 27). The necessary factors for improvement for the current 40-year service life are approximately 20. Therefore, the replacement of type 304 stainless steel piping with type 316NG, type 304NG, or type 347NG provides substantial resistance to IGSCC. It is important to note that materials-based resolutions can be rendered insufficient if there are other secondary aggravating effects; for instance, creviced design or the introduction of cold-worked microstructures through various fabrication practices. For example, a data-based life-prediction analysis at one Swedish nuclear plant determined that nearly 50% of failures were attributable to cold work fabrication practices (Ref 30). Normally resistant stainless steels can also suffer IGSCC if good-quality water chemistry in the BWR is not maintained.

Solution Heat Treatment. Immunity against IGSCC of type 304 stainless steel can be provided by eliminating weld-sensitized regions. This can be accomplished by solution heat treatment to redissolve the chromium carbides and eliminate chromium depletion around previously sensitized grain boundaries. Moreover, solution heat treatment will eliminate detrimental cold work and weld residual stress in the pipe. Following a butt-welding operation, the entire pipe segment is solution annealed at 1040 to 1150 °C (1900 to 2100 °F) for 15 min per 25 mm (1.0 in.) of thickness but not less than 15 min or more than 1 h, regardless of thickness. The pipe segment is then quenched in circulating water to a temperature below 205 °C (400 °F). Solution heat treatment is generally limited to those weld joints made in the shop where heat treatment facilities are available, because of dimensional tolerance consideration, size constraints of the vendor facilities (furnace and quench tank), and cooling rate requirements (dead end legs).

Corrosion-resistant cladding achieves its resistance to IGSCC by using the IGSCC resistance inherent in duplex austenitic-ferritic weld metals (Ref 27). Although the carbide precipitation observed in the HAZ inside surface is also present in the weld metal, the nature of the duplex structure of the weld metal provides resistance to IGSCC in the BWR. ln fact, IGSCC propagating from the weld HAZ is generally blunted when it reaches the weld metal if sufficient ferrite is present. As shown in Fig. 7 and 8, the cracking will actually curve away from the weld metal. Field experience has indicated that in the as-welded condition very little ferrite is required to prevent IGSCC. These results and numerous laboratory data generated on welded and furnace-sensitized type 308 and type 308L weld metal prompted the conclusion that a minimum amount of ferrite (8%) must be present to provide a high degree of resistance to IGSCC in BWR environments. As with type 304 stainless steel, reducing the carbon level is also beneficial.

In the corrosion-resistant cladding technique, type 308L weld metal is applied using controlled heat input process to the inside surface of the pipe at the pipe weld ends before making the final field weld. This duplex weld metal covers the region that will become sensitized during the final weld process, thus providing IGSCC resistance by maintaining low carbon and a suf-

ficient ferrite level in the region that would normally be sensitized.

Weld overlay repair is similar to corrosion-resistant cladding in that it uses layers of IGSCC resistant duplex weld metal (Ref 28). For cases where alloy 182 is to be overlaid, alloy 82 or 52 weld metal is used. The most significant difference is that the layer of weld metal is placed on the outside surface of the pipe while the pipe is being cooled internally with water and is used to prevent an existing crack from penetrating through the wall. The weld overlay is also applied as a structural reinforcement to restore the original piping safety margins (Fig. 13). An equally important effect of the weld overlay is that it produces a favorable (compressive) residual stress pattern that can retard or arrest crack growth.

The weld overlay technique has the potential for being the most cost-effective method as compared to other repair techniques (pipe replacement, solution heat treatment, corrosion-resistant cladding), which require draining of the system.

Tensile Stress Reduction Solutions

The tensile stress solutions primarily affect the weld residual stress profile by placing the inner surface weld residual stress in compression. These solutions, which are discussed in this chapter, include heat sink welding, induction heating stress improvement, and last-pass heat sink welding.

Heat Sink Welding. If a pipe can be welded without producing a sensitized structure and high residual tensile stresses in the weld HAZ, the resultant component will be resistant to IGSCC in the BWR environment. The heat sink welding program developed procedures that reduce the sensitization produced on the inside surface of welded pipe and, more important, change the state of surface residual welding stresses from tension to compression. This approach can be used in shop or field applications. Heat sink welding involves water cooling the inside surface of the pipe during all weld passes subsequent to the root pass or first two layers. Water cooling can be applied by using flowing or turbulent water, by spray cooling through a sparger placed inside the pipe, or, in a vertical run, by still water. Laboratory type 304 stainless steel butt welds have been produced to evaluate the inside surface heat sink welding techniques (Ref 29). Residual stresses were measured with strain gages. It was found that in a variety of pipe sizes the inside surface tensile residual stress is reduced substantially or changed from tension to compression as a result of this approach. Heat sink welding, as mentioned previously, has a secondary benefit in that it reduces the time at temperature for sensitization due to the presence of the cooling water heat sink.

Induction Heating Stress Improvement. This technique changes the normally high tensile stress present on the pipe inside surface of weld HAZs to a benign compressive stress (Ref 31, 32). This process involves induction heating of the outer pipe surface of completed girth welds to approximately 400 °C (750 °F) while simultaneously cooling the inside surface, preferably with flowing water (Fig. 14). Thermal expansion caused by the induction heating plastically yields the outside surface in compression, while the cool inside surface plastically yields in tension. After cool down, contraction of the pipe outside surface causes the stress state to reverse, leaving the inner surface in compression and the outside surface in tension (Fig. 15).

Qualification of the effectiveness of induction heating stress improvement has been accomplished by establishing (Ref 28, 32):

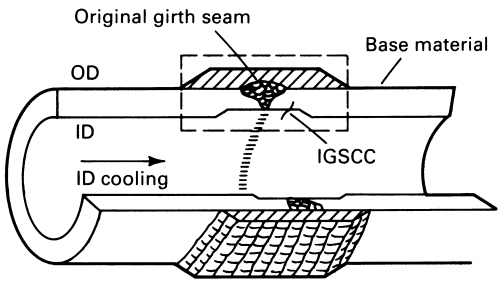

Fig. 13 Weld overlay IGSCC mitigation technique. ID, inside diameter; OD, outside diameter

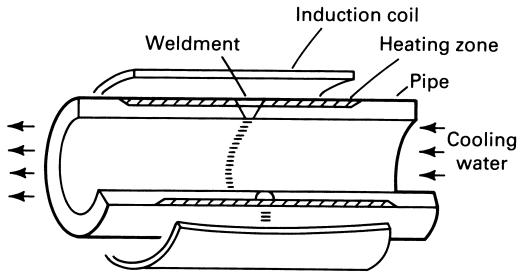

Fig. 14 Heating and cooling process for induction heating stress improvement

- Induction heating stress improvement treatment reliably reduces normally high tensile inside surface residual stresses to a zero compressive state.
- Full-size environmental pipe testing and residual stress tests have demonstrated that these beneficial residual stresses result in a large improvement in IGSCC resistance.
- Metallurgical investigations have shown that an induction heating stress improvement treatment produces no adverse effects. No increase in sensitization is found, and no significant variation in mechanical properties occurs.
- A minimum life of 12 fuel cycles (approximately 216 months) has been measured on induction heated stress improved precracked pipes in the laboratory if the initial cracking does not exceed about 20% of wall thickness.

Last-Pass Heat Sink Welding. As discussed in the previous section, induction heating stress improvement is an IGSCC mitigation technique that favorably alters the weld residual stress pattern. The welding torch is the heat source that initially produces the undesirable residual stress that induction heating stress improvement counterbalances. Analysis was able to establish that this residual stress state could be made compressive by the introduction of inside surface water cooling during the welding operation. Cooling during the entire welding process (heat sink welding) or just during the last pass could be effective in reversing the residual stresses analogous to the induction heating stress improvement process. Qualification of the last-pass heat sink welding process consisted of magnesium chloride ($MgCl_2$) residual stress tests, which verified that the last-pass heat sink welding process does produce compressive residual stresses uniformly around the pipe circumference (Ref 33). Stress-relief strain-gage measurements quantified the compressive axial stress and revealed that the stresses were compressive up to about 50% through-wall.

Finally, IGSCC improvement was evaluated by using pipe tests performed at applied stresses above yield in a high-oxygen (8 ppm) high-temperature (288 °C, or 550 °F) water environment. As shown in Fig 16, at the end of the program period, the pipes had been on test for more than 5500 h, demonstrating a factor of more than 5.5 and more than 6.5 improvement, respectively, at the two test stresses of 193.7 and 211 MPa (28.1 and 30.6 ksi), respectively. This factor of improvement approaches that determined for induction heating stress improvement.

Environmental Solutions

At normal operating conditions, the BWR recirculation coolant, a high-purity neutral-pH water, contains 100 to 300 ppb of dissolved

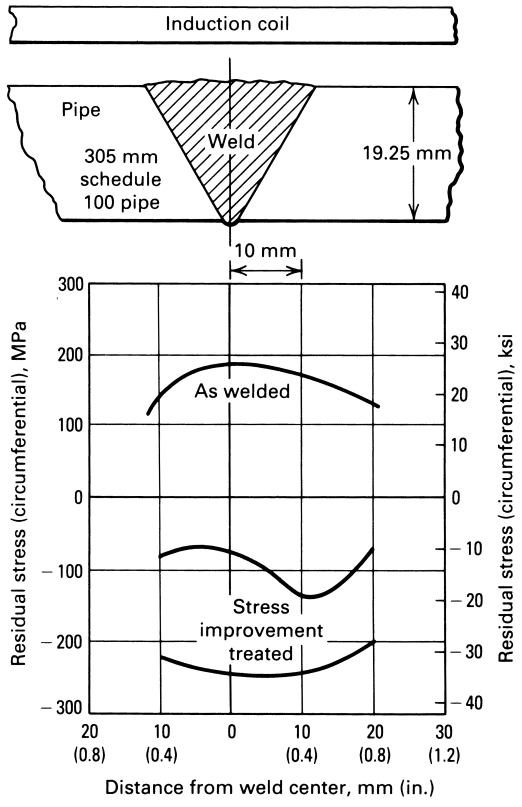

Fig. 15 Residual stress comparison for induction heating stress improvement

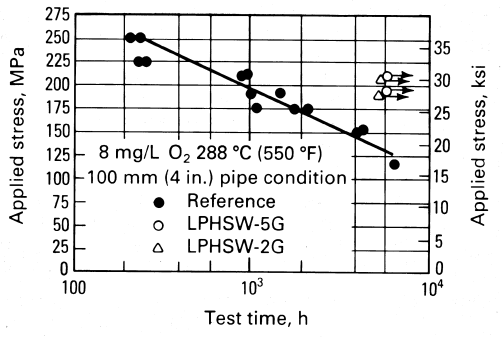

Fig. 16 Comparison of last-pass heat sink welding pipe tests with reference pipe tests

oxygen. The source of this oxygen is the radiolytic decomposition of the water, which also contains 20 ppb of dissolved hydrogen. At a level of 100 to 300 ppb of dissolved oxygen, IGSCC will occur in the sensitized HAZ of types 304 and 316 stainless steel (Ref 34). If the oxygen content is reduced to levels below 20 ppb, IGSCC is extremely difficult to initiate. This reduction can be accomplished by hydrogen water chemistry, which controls the oxygen level in the entire coolant system through additions of hydrogen to the feed water. Laboratory and in-reactor experiments have revealed that the conductivity of the water (the content of ionic impurities) must be closely controlled to a level of 03 μS/cm or less to suppress IGSCC in sensitized types 304 and 316 components and pipe welds (Ref 35). The electrochemical potential, a measure of the dissolved oxygen level, must be less than –230mV (SHE). More detailed information on water purity control and hydrogen water chemistry can be found in the article "Corrosion in Boiling Water Reactors" in Volume 13C of the *ASM Handbook.*

Corrosion in the Pulp and Paper Industry

Corrosive environments are found in a number of process stages in the pulp and paper industry including:

- Pulp production
- Pulp processing and chemical recovery
- Pulp bleaching
- Paper manufacturing

Each manufacturing step has its own corrosion problems related to the size and quality of the wood fibers, the amount of and temperature of the process water, the concentration of the treatment chemicals, and the materials used for machinery construction. In terms of weldment corrosion, the two most common problems are corrosion of welds by kraft pulping liquids and corrosion of welds in bleach plants.

Pulp Production

The kraft process is the predominant pulping process used in North America to extract fibers from wood for use in the manufacture of paper, tissue, and board. The term *kraft* is derived from the German word for strong, which reflects the high strength of paper products derived from kraft pulp. This high strength, together with effective methods of recovering pulping chemicals, explains the popularity of kraft pulping. Approximately 80% of pulp is produced by the kraft process.

In the kraft process, hot alkaline sulfide liquor is used to dissolve the lignin from wood chips and to separate individual wood fibers for use in papermaking. Wood chips are exposed to cooking liquors for several hours at elevated temperature and pressure in a process called digestion. Digestion may occur by repetitive batch processes in small batch digesters, or the process may occur continuously in larger continuous digesters. The contents of the digester are then discharged under pressure into a receiver called a blow tank. Finally, the fibers are separated from the spent liquor in a series of washing stages. Pulping chemicals are then recovered from the spent liquor by a series of chemical recovery steps. More detailed information on pulp and paper processing can be found in the article "Corrosion in the Pulp and Paper Industry" in Volume 13C of the *ASM Handbook.*

Corrosion of Digester Welds. Although welds are often sites of preferential attack in batch digesters, including accelerated corrosion and occasional episodes of SCC, most problems with weldment corrosion have been associated with continuous digesters. The most serious corrosion problem with carbon steel continuous digesters has been caustic SCC of unstress-relieved seam welds in the impregnation zone or in the impregnation vessel for two-vessel systems (Ref 36–46). The ASME Boiler and Pressure Vessel Code (Ref 47) does not require post-weld stress relief treatment for wall thicknesses less than 32 mm (1.25 in.), which often is the case at the top of continuous digesters. In 1980 there was catastrophic caustic SCC failure of an unstress-relieved top section of a continuous digester. The combination of high tensile stress (from residual welding stresses) and corrosion potential in a critical range is a prerequisite for caustic SCC. Since the early 1980s most if not all continuous digesters have been fully post-weld heat treated, even though stress relief was not mandated by the ASME Code for wall thicknesses less than 32 mm (1.25 in.). Carbon steel welds and weld buildup made in the impregnation zone of digester vessels and not subsequently stress relieved are susceptible to caustic SCC. Below the cooking screens, caustic SCC has not been reported.

Following the 1980 failure described previously, subsequent inspection of similar digesters revealed that more than half of the 140 continuous digesters operating in North America exhibited cracking in structural welds (Ref 48). Cracking has been found in girth and vertical shell welds, attachment welds inside the digester, and nozzle welds. Both longitudinal and transverse cracking have been observed, but the deepest cracking has been found in longitudinal cracks in the weld HAZ. Examples of cracking in actual digester welds are shown in Fig. 17.

An extensive survey of digester cracking statistics failed to reveal differences in digester design or operation that would account for differences in cracking susceptibility (Ref 48). As shown in Fig. 18, PWHT significantly reduced, but did not eliminate, susceptibility to severe cracking.

Cracking similar to digester cracking was reproduced in the laboratory by using accelerated slow strain rate and fracture mechanics tests (Ref 49). These tests indicated that the caustic concentration in cooking liquors at the impregnation zone was sufficient for caustic cracking of pressure vessel weldments. Furthermore, caustic cracking occurred only when the potential of the digester steel was within a 100 mV range centered close to digester potentials. Figure 19 shows the dependence of cracking susceptibility on potential as determined in slow strain rate tests performed on welded specimens in simulated impregnation zone liquor (Ref 50). Potential measurements made on an operating digester indicated that the digester rest potential remained above the cracking range, except for a few days following an upset in operating routine (Ref 51).

Preferential weld corrosion is often observed in continuous digesters and is the result of the poorer corrosion resistance of weld metal (which has a coarse-grain structure similar to a casting), compared with the parent metal plate (which is typically lower in silicon content). The common practice of restoring corroded weld seams without subsequent stress relief results in welds with high residual stresses that may make the digester more susceptible to caustic SCC.

Stainless steels in digester vessels can experience corrosion as a result of hydrochloric acid (HCl) cleaning, which preferentially attacks the ferrite phase in welds, but can also cause widespread pitting if the temperature is high enough. Attack of circumferential welds in type 304L central pipes has resulted in central pipe failures. The welds often have incomplete penetration, which contributes to failure. Stainless steel top and bottom dome liners may experience SCC or intergranular attack (IGA) if they are heat treated with the digester. This practice can result in sensitization through chromium carbide precipitation at the grain boundaries. Continuous digester vessels constructed from roll-clad austenitic stainless steel can also undergo IGA if they become sensitized during PWHT, which is mandatory for the carbon steel digester shell (Ref 52).

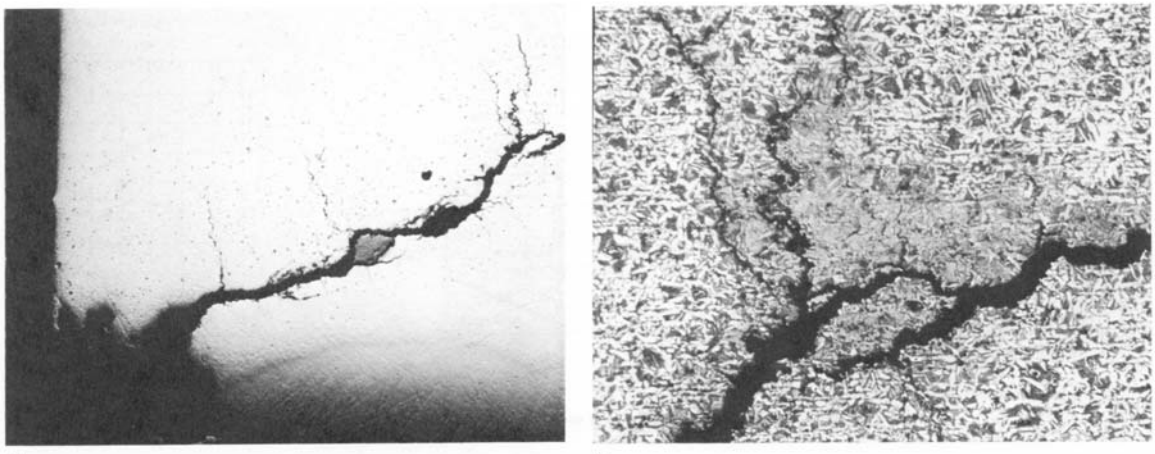

(a) (b)

Fig. 17 Examples of digester weld cracking. (a) Macrograph showing cracking in a sample taken from a continuous digester weld. 10×. (b) Photomicrograph showing branched, intergranular nature of cracking in an actual continuous digester weld. 40×

Prevention of Digester Weld Cracking. Two measures have been successful in controlling digester weld cracking: high alloy barrier coatings placed over susceptible welds and anodic protection. Other remedial measures, such as shot peening, temper-bead weld repair in situ stress relief, and unsealed thermal spray coatings, have not been uniformly successful in preventing recracking.

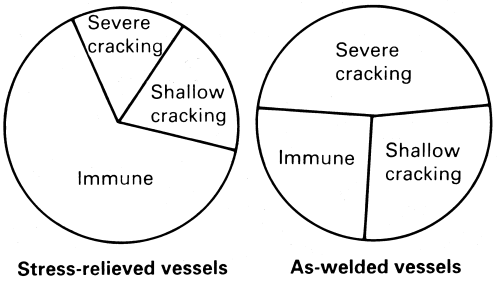

Fig. 18 Effect of stress relief on SCC susceptibility of continuous digester

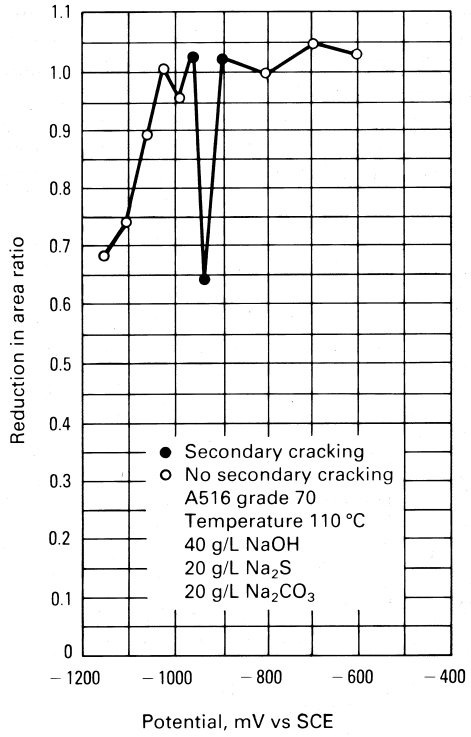

Fig. 19 Plot showing the effect of potential on cracking severity in controlled-potential slow strain rate testing of digester steels exposed to a simulated impregnation zone liquor. SCE, saturated calomel electrode

Weld overlays and thermal sprayed coatings have both been successfully used to control cracking. Weld overlays—primarily alloy 82 (AWS ERNiCr3), alloy 625 (AWS ERNiCrMo3), and type 309 stainless steel—have been applied in bands over structural welds to isolate them from contact with cooking liquor. The overlay bands are themselves resistant to corrosion damage, but there have been cases of cracking of the carbon steel substrate in the HAZ at the edge of the overlay band. Both batch and continuous digesters have been protected from corrosion by the application of thermal spray coatings. Most coating alloys are alloy 625 (N06625) or a similar alloy. Both the twin-wire arc spray and high-velocity oxygen fuel processes have been employed.

Anodic protection has been effective in controlling both corrosion and caustic cracking in a number of continuous digesters (Ref 53). Protection is achieved by passing a controlled direct current (dc) through an electrolytic cell consisting of the digester wall, the cooking liquor, and a special cathode installed inside the digester. Currents as high as 1000 A (at 12 V dc) may be required to passivate the vessel initially, but only a few hundred watts of electrical power is required to maintain anodic protection. The digester potential is maintained approximately 100 mV above the upper limit of the potential range required for cracking. Anodic protection has suppressed further cracking in several digesters previously susceptible to severe and chronic cracking.

Example 1: Intergranular SCC of Carbon Steel Pipe Welds in a Kamyr Continuous Digester Equalizer Line (Ref 54). Schedule 80 low-carbon steel pipes used to transfer kraft liquor in a Kamyr continuous pulp digester failed within 18 months after installation.

The Kamyr continuous digester equalizer line consisted of several hundred feet of Schedule 80 low-carbon steel pipes with a nominal diameter of 75 to 125 mm (3 to 5 in.). The pipe joints were field welded using E6010 for the root passes and E7018 for the cover passes. The equalizer line had been in service for 18 months and was used to transfer alkaline kraft liquor at approximately 175 °C (350 °F).

Several cracks in and next to the pipe welds leaked within 18 months of service. No abnormal digester operating conditions were reported during that time.

Investigation. Visual and magnetic particle inspections of the equalizer line indicated that

the cracks were in and next to the field-welded pipe joints. The cracks were both longitudinal and transverse in the welds and in the HAZs (Fig. 20).

Cracked pipe sections were removed for laboratory examination, which revealed that the cracks initiated on the internal surfaces and propagated through the welds and HAZs (Fig. 21). The internal surfaces were covered with a thin, tightly adherent layer of iron oxides. No general corrosion or pitting corrosion were found. The quality of the field welds was poor, with defects such as lack of penetration, weld undercut, improper weld profile, and excessive burn-through.

The fracture/crack morphology was brittle and primarily intergranular (Fig. 22). Scanning electron microscopy/energy dispersive spectroscopy (SEM/EDS) analysis of the deposits at the crack tips indicated that they were primarily iron oxides with significant amounts of sodium compounds. The laboratory-induced fracture surface consisted of dimples, characteristic of microvoid coalescence—a high-energy, ductile form of fracture (Fig. 23).

Metallographic examination of the cracked pipe welds indicated that the cracks initiated on the internal surfaces. The microstructure of the welds and base metal was primarily ferrite, with

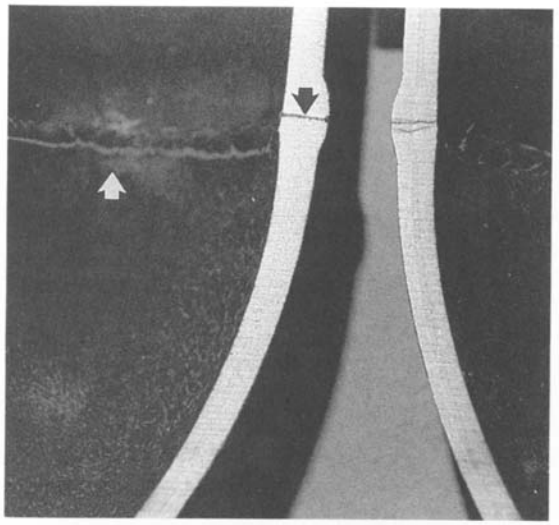

Fig. 20 Magnetic particle enhancement of cracks in the weld of an equalizer line elbow section. Cracks were localized in the weld and HAZs.

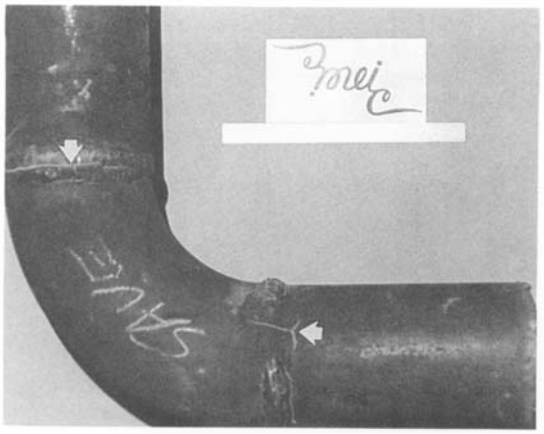

Fig. 21 The internal surface of this pipe section was free of general and pitting corrosion and was covered with a thin, adherent oxide layer. Cracks had initiated in the weld and HAZ.

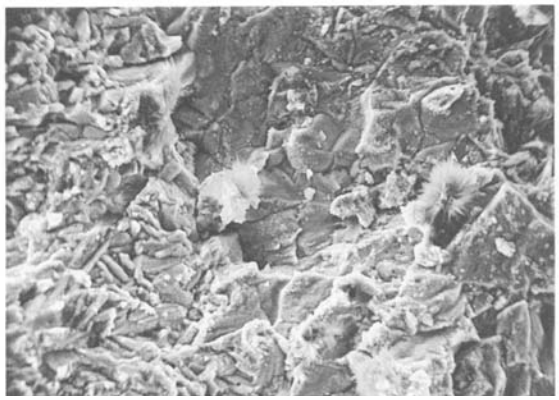

Fig. 22 The fracture surface was primarily intergranular and was covered with a thin oxide layer. The crack tip had significant sodium compound deposits.

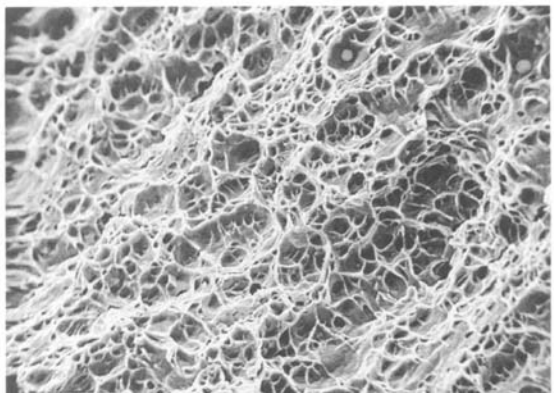

Fig. 23 Scanning electron micrograph of the laboratory-induced fracture. Dimples are characteristic of microvoid coalescence, a ductile form of fracture.

some pearlite, characteristic of low-carbon steels. The hardnesses were 73 to 93 HRB. No significant hardness gradient or undesirable microstructural constituents were found.

The cracks had originated on the internal surfaces of the welds and in the HAZs and had propagated along the intergranular grain boundaries in a multiple branching mode. The crack walls were covered primarily with iron oxides, with some sodium-bearing compounds (Fig. 24–26).

Discussion. Visual and metallographic examinations clearly established that the cracking initiated on the internal surfaces of the equalizer pipes in the welds and HAZs. Lack of corrosion-related deterioration, that is, general corrosion or corrosion pitting on the internal surfaces, indicates that the pipe material was suitable for the intended service, provided the conditions that led to the IGSCC were eliminated.

The primary factor leading to IGSCC was probably high residual tensile stresses in the welds and HAZs. The field welding of the pipe joints had apparently been done under highly constrained conditions, using inadequate welding procedures. Although carbon steels are acceptable for corrosion service in alkaline kraft pulping, highly stressed areas, particularly non-stress-relieved welds, are known to be susceptible to IGSCC (caustic embrittlement). The alkaline caustic kraft liquor provided the necessary aggressive environment for IGSCC at the highly stressed weld joints. No material-related deficiencies, such as hardness gradient or unacceptable microstructure, were found.

Conclusions and Recommendations. The most probable cause for the failure was high residual tensile stresses in the welds and HAZs of the pipe joints. The highly alkaline kraft liquor provided the necessary aggressive environment for IGSCC.

The failure of the pipe welds could have been prevented if the residual stress conditions of the joints had been kept below the threshold levels for SCC. The minimize the residual stresses, it was recommended that the welding procedures include appropriate preweld and interpass temperatures. Postweld stress-relief heat treatment at 650 °C (1200 °F) was recommended for the weld joints.

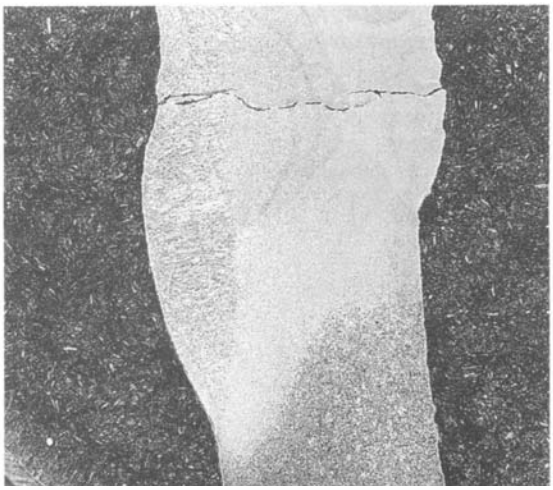

Fig. 24 Cracks initiated on the inside surface and propagated through the weld in a multiple branching mode.

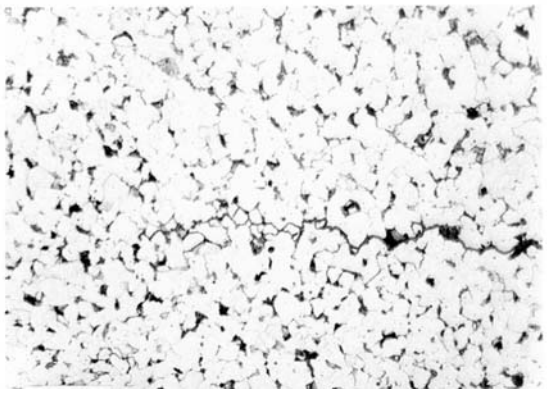

Fig. 25 Tip of an intergranular stress crack that partially penetrated the weld. The crack was covered with oxides.

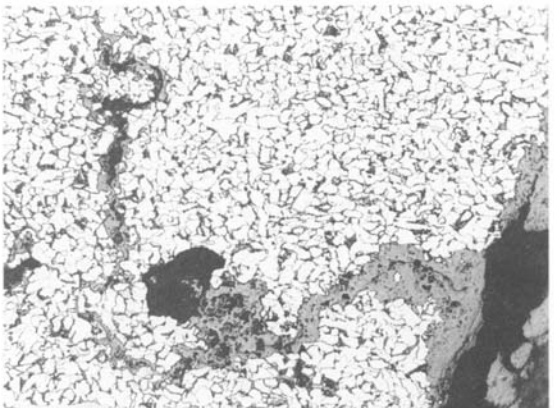

Fig. 26 Crack morphology in the weld HAZ of the base metal. Note the IGSCC, followed by lateral oxidation.

Corrosion of Weldments in Pulp Bleach Plants

Stainless steel bleached pulp washers and other related equipment often fail by corrosion associated with welds. To investigate this problem, a number of studies have been carried out by the Technical Association of the Pulp and Paper Industry (TAPPI) (Ref 55 and 56). Some of the findings from these studies are summarized below.

Corrosion of Washers. Stainless steel washers fail occasionally because of weld-related corrosion. The principal causes of weld-related corrosion are detailed in Table 2 and outlined in Ref 57.

Welding without filler metal creates a preferential attack site on austenitic stainless steel and should be avoided in washer construction. It is important not to select a filler metal that gives a deposit that is less corrosion resistant than the base metal. For type 316L, the American Welding Society standard filler is adequate (Ref 13). However, for type 317L and the more highly alloyed materials, recent field and laboratory tests have shown that a filler metal with a composition similar to that of the base metal can have much lower pitting resistance (Ref 58, 59).

There are a number of weld filler metals that are suitable for welding 4.5 to 6% Mo austentic stainless steels used for washers used in chlorine and chlorine dioxide bleaching. They include:

- Alloy 112 (AWS ENiCrMo-3)
- Alloy 625 (AWS ERNiCrMo-3)
- Avesta P12R (AWS ENiCrMo-12)
- Alloy G-30 (AWS ERNiCrMo-11)

These filler metals are good choices because:

- They are metallurgically compatible with all austenitic stainless steels
- They are highly resistant to pitting and crevice corrosion in the as-welded condition
- There is not significant galvanic effect between these filler metals and austenitic stainless steels in bleach plant liquors
- If microfissures or hot cracks occur in the weld metal, they will not be preferentially attacked by crevice corrosion. This is a particular problem for most ferrite-free stainless steel fillers

Microfissuring or hot cracking is a phenomenon associated with thermal stresses during welding. These stresses usually cause small cracks to form in the weld metal or HAZ of a stainless steel or nickel-base alloy weldment. Higher nickel content alloys, which have a greater coefficient of thermal expansion, are more susceptible to hot cracking. Cracking is more likely to occur because of higher phosphorus (>0.015% P) and sulfur (>0.015% S) in the alloy or contamination of the weld area. It is most commonly seen in the HAZ in the previous pass of a multiple-pass weld. Hot cracking rarely has a detrimental effect on the mechanical properties or structural integrity of a fabrication. However, it can be very detrimental to the corrosion properties of a weldment. Microfissures form crevice corrosion sites that are readily attacked.

Table 2 Principal causes of corrosion of austenitic stainless steel weldments

Attack site and mode	Reason for attack	When is it a problem?	How to avoid
Weld metal pitting	Welding with no filler	All molybdenum-containing austenitics(a)	Use appropriate filler
	Welding with underalloyed filler	3 to 6% Mo austenitics(a)	Use appropriate filler, for example, alloy 112
Crevice corrosion	Microfissures in weld metal create sites for crevice corrosion (looks like pitting)	In ferrite-free stainless steel weld metal, for example, fillers commonly recommended for 904L(a)	Use alloy 112, 625, or G-30 electrodes for 3 to 6% Mo austenitics
	Lack of penetration	In one-side or stitched butt-weld joints	Ensure full penetration, and do not use stichwelds on process side
	Entrapped welding flux	Shielded metal arc welded joints	Use electrode with good flux detachment
Heat-affected zone	Precipitation of carbides during welding	When steel has over 0.03% C	Use steel with 0.03% C max
Fusion line	Unmixed zone formed at fusion line	With high-alloy steels close to their corrosion limits	Use lower heat input on final pass
	Precipitation of carbides at fusion line (knife-line attack)	In niobium- or titanium-stabilized steels	A very rare problem. Niobium- and titanium-stabilized steels not common

(a) Particularly after high heat input welding

Recent laboratory tests have shown that some nickel-base filler metals normally used for fabrication, such as alloys C-276 (AWS ERNiCrMo-4) and C-22 (AWS ERNiCrMo-10), are subject to what has been termed transpassive corrosion in near-neutral chlorine dioxide environments. These filler metals undergo molybdenum dissolution, which renders them unsuitable for the near-neutral chlorine dioxide environment. After some investigation, it was found that alloy G-30 (AWS ERNiCrMo-11) with higher chromium and lower molybdenum had much better corrosion resistance in the near-neutral chlorine dioxide environment while still maintaining good resistance to acid chloride environments. Alloy G-30 has become the preferred filler metal for fabricating 6% Mo stainless steel washers for near-neutral chlorine dioxide stage service.

Another common problem with stainless steel weldments—sensitization in the HAZ—is avoided in bleach plants by the use of low-carbon steels (0.03% C max for austenitics). Similarly, fusion-line attack (sometimes called knife-line attack) due to precipitation of carbides at the fusion line in niobium- and titanium-stabilized austenitic steels is rarely seen, because these steels have been made obsolescent by new steelmaking technology.

However, attack at the fusion line is possible when overalloyed fillers such as alloy 112 are used with high heat input welding. Such welding can create zones consisting of melted base metal that is not mixed with weld filler—called unmixed zones—at the fusion line. Cases of unmixed zone corrosion have occasionally been observed in the bleach plant. In practice, this can be minimized by the use of lower heat input on the final weld passes.

Example 2: Intergranular Corrosion/Cracking of a Stainless Steel Pipe Reducer Section in Bleached Pulp Stock Service (Ref 60). A type 316 stainless steel pipe reducer section failed in service of bleached pulp stock transfer within 2 years in a pulp and paper mill. The reducer section fractured in the HAZ of the flange-to-pipe weld on the flange side.

The pipe reducer consisted of 250 and 200 mm (10 and 8 in.) diameter flanges, welded to a tapered pipe section. The tapered pipe section was 3.3 mm (0.13 in.) thick type 316 stainless steel sheet, and the flanges were 5 mm (0.2 in.) thick CF8M (type 316) stainless steel castings. The assembly was fabricated using type 316 stainless steel weld metal. The pipe reducer section was used to transfer bleach pulp stock at about 43 °C (110 °F). Chemistry of the bleach stock solution was not available; however, in general, the solutions are pH 4, with traces of free chlorine and several hundred ppm of chlorides.

The failure occurred within 2 years of service because of a circumferential fracture in the 250 mm (10 in.) diameter flange next to the weld (Fig. 27).

Investigation. Visual examination of the pipe reducer section revealed several smaller secondary cracks in the flange fillet area, in addition to the fracture next to the weld (Fig. 27). The external surface of the flange had patches of reddish brown corrosion products. The weld had no corrosion, and the tapered pipe section had no corrosion on either its internal or external surfaces. A few secondary cracks had penetrated the flange thickness and were present on the internal surface (Fig. 28).

The fracture was brittle, with no significant necking or deformation next to it. The fracture morphology was primarily intergranular, with secondary cracks enveloping grain boundaries (Fig 29 and 30). Scanning electron microscopy/energy dispersive spectroscopy (SEM/EDS) analyses of the fracture surface deposits indicated that, in addition to corrosion oxides of

Fig. 27 Fracture in the cast CF8M stainless steel flange next to the weld. Note fine SCC in the flange fillet. 1.5×

type 316 stainless steel, calcium, sulfur, chlorine, magnesium, and sodium were also present. The deposits were a mixture of corrosion products and bleach stock filtrate solids.

Metallographic examination of a flange/pipe cross section from the vicinity of the weld and the flange fillet was performed (Fig. 31 and 32). The microstructure of the flange casting was a mixture of equiaxed and dendritic grains. The exterior surface of the flange exhibited severe intergranular corrosion and grain spalling (Fig. 33). The interior surfaces of the flange, weld, and pipe section exhibited no significant corrosion.

Intergranular corrosion had developed into IGSCC, which propagated through the flange wall in the weld, HAZ, and upper toe of the flange fillet, and partially penetrated the lower toe of the fillet (Fig. 31 and 32). The cracks initiated at the intergranular corrosion of the flange external surface and propagated as IGSCC through the flange thickness.

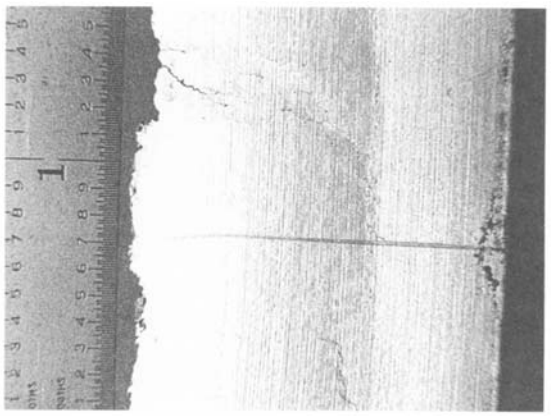

Fig. 28 Internal surface of the flange was free of corrosion. Several secondary stress-corrosion cracks penetrated the flange thickness. 1.5×

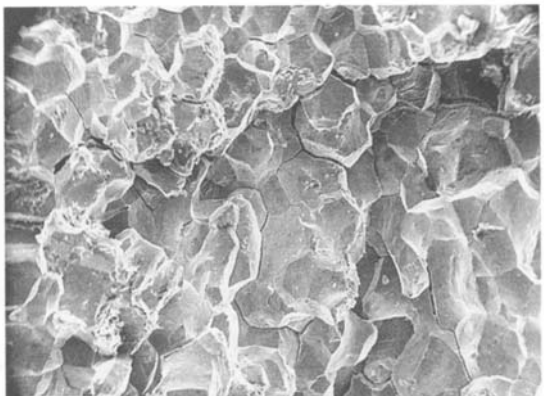

Fig. 29 Scanning electron micrograph showing primarily intergranular fracture morphology. 75×

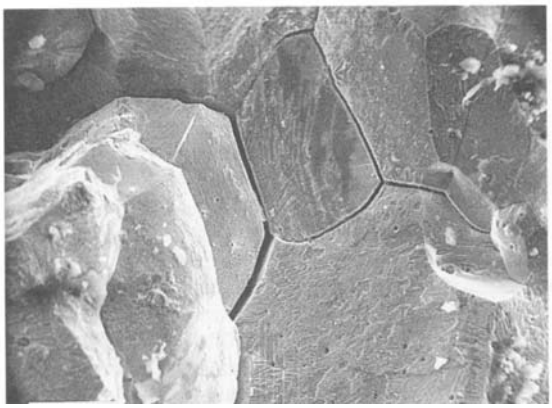

Fig. 30 Scanning electron micrograph showing secondary intergranular cracks propagating from the primary fracture. 375×

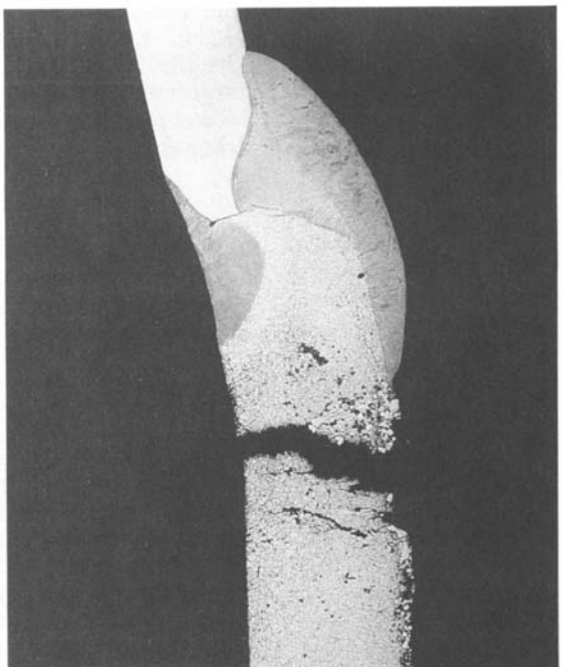

Fig. 31 Intergranular corrosion on the external surface of the flange and IGSCC in the weld HAZ. Note that the type 316 weld and the wrought stainless steel pipe section were unaffected by corrosion. 5×

Chemical analysis of the flange, weld, and tapered section showed that they were within the compositional limits for type 316 stainless steel. Susceptibility to intergranular corrosion tests (sensitization) per ASTM A 262, Practice A, indicated an unacceptable ditch structure of the flange material (Fig. 34), while the weld and the tapered section showed acceptable structures.

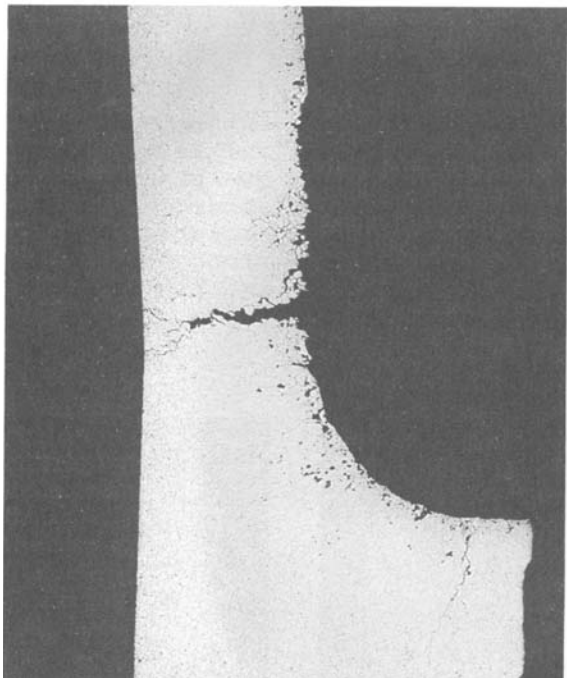

Fig. 32 Intergranular corrosion at the external surface of the flange and IGSCC next to the flange fillet. 5×

Discussion. Visual and metallographic examinations clearly established that the corrosion and cracking initiated at the external surface of the 250 mm (10 in.) diameter stainless steel flange. Lack of corrosion-related deterioration on the inside surfaces of the flange, weld, and tapered pipe section indicated that the assembly was suitable for the intended service in bleach stock transfer.

Factors leading to corrosion of the flange included exposure to the aggressive environment of the bleach plant. Evaporative concentrations of bleach stock solution on the flange can enhance the concentration of aggressive ions, such as chlorides. The flange was a CF8M (type 316) stainless steel casting, exhibiting sensitization (chromium carbide precipitation at the grain boundaries) and susceptibility to intergranular corrosion.

The sensitization of the stainless steel casting was probably the consequence of slow cooling after the casting process and thus longer dwell time at the chromium carbide precipitation temperatures of 480 to 820 °C (900 to 1500 °F). The heat of welding added to the sensitization of the flange casting. The tapered pipe and the weld, which were not sensitized, were resistant to the aggressive environment of the bleach plant.

Intergranular corrosion at the external surface of the flange had propagated through the flange thickness as multiple, branching IGSCC. Ser-

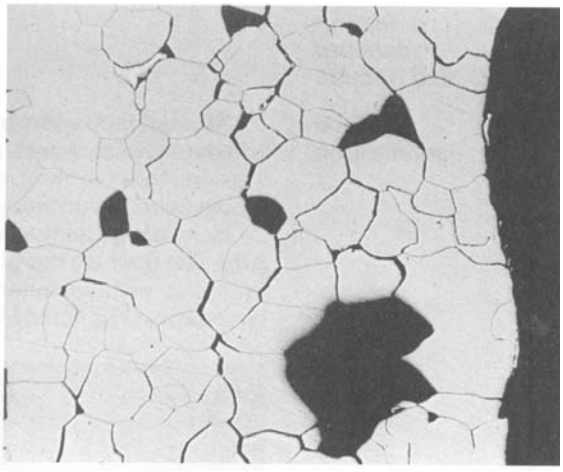

Fig. 33 Intergranular corrosion at the external surface of the flange. The voids are the locations of the spalled grains. 50×

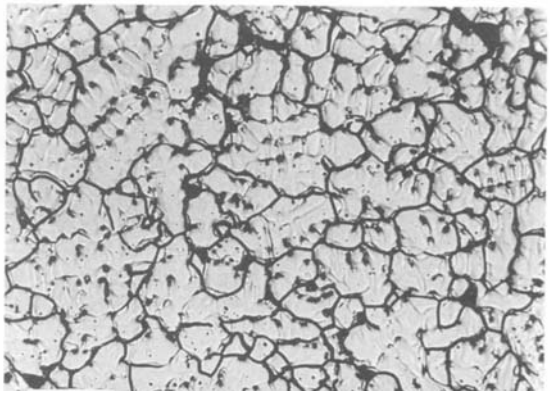

Fig. 34 Microstructure of the CF8M flange casting after testing per ASTM A 262, Practice A, to determine susceptibility to intergranular corrosion. The etching resulted in ditches surrounding each grain, which was unacceptable. 75×

vice, plus residual tensile stresses in the flange, apparently contributed to the IGSCC growth.

Conclusions and Recommendations. The probable cause of the failure was the sensitized condition of the stainless steel casting, which had rendered the flange vulnerable to IGSCC in an aggressive environment. Secondary factors included the aggressive environment of the bleach plant and residual tensile stresses from casting/welding processes.

The failure of the pipe reducer section was a consequence of the sensitized condition of the CF8M stainless steel flange casting. The failure could have been prevented if the flange casting had been subjected to a solutionizing anneal at 1040 to 1205 °C (1900 to 2200 °F), followed by rapid cooling by water quenching. This procedure inhibits chromium carbide precipitation and thus susceptibility to intergranular corrosion. It was recommended that the replacement flange be made of CF3M (type 316L), which is a low-carbon version of CF8M, and that the flange casting be solution annealed and water quenched.

ACKNOWLEDGMENTS

Portions of this chapter were adapted from:

- J.C. Danko, Stress-Corrosion Cracking of Weldments in Boiling Water Reactor Service, *Stress-Corrosion Cracking: Materials Performance and Evaluation,* R.H. Jones, Ed., ASM International, 1992, p 345–354
- F.P. Ford, B.M. Gordon, and R.M. Horn, Corrosion in Boiling Water Reactors, *Corrosion: Environments and Industries,* Vol 13C, *ASM Handbook,* ASM International, 2006, p 341–361
- R.D. Kane, Corrosion in Petroleum Refining and Petrochemical Operations, *Corrosion: Environments and Industries,* Vol 13C, *ASM Handbook,* ASM International, 2006, p 967–1014

REFERENCES

1. R.D. Kane, R.J. Horvath, and M.S. Cayard, *Wet H_2S Cracking of Carbon Steels and Weldments*, NACE International, 1996
2. "Standard Practice for Evaluation of Hydrogen Uptake, Permeation, and Transport in Metals by an Electrochemical Technique," G 148, ASTM International
3. G.B. Kohut and W.J. McGuire, Sulfide Stress Cracking Causes Failure of Compressor Components in Refinery Service, *Mater. Prot.,* Vol 7 (No. 6), 1968, p 17–21
4. E.L. Hildebrand, Aqueous Phase H_2S Cracking of Hard Carbon Steel Weldments—A Case History, *Proc. API,* Vol 50 (III), 1970, p 593–613
5. T.G. Gooch, Hardness and Stress Corrosion Cracking of Ferritic Steel, *Weld. Inst. Res. Bull.,* Vol 23 (No. 8), 1982, p 241–246
6. D.J. Kotecki and D.G. Howden, Wet Sulfide Cracking of Submerged Arc Weldments, *Proc. API,* Vol 52 (III), 1972, p 631–653
7. "Controlling Weld Hardness of Carbon Steel Refinery Equipment to Prevent Environmental Cracking," RP 942, American Petroleum Institute
8. "Methods and Controls to Prevent In-service Environmental Cracking of Carbon Steel Weldments Corrosive Petroleum Refining Environments," RP0472, NACE International, 1972
9. "Materials Resistant to Sulfide Stress Cracking in Corrosive Petroleum Refining Environments," MR0103, NACE International, 2003
10. "Petroleum and Natural Gas Industries—Materials for Use in H_2S-Containing Environments in Oil and Gas Production—Parts 1, 2 and 3," MR0175/ISO 15156, NACE International
11. R.A. Walker, "The Significance of Local Hard Zones on the Outside of Pipeline Girth Welds," Final Contract Report, PR-164-804, The Welding Institute, Cambridge, U.K., 1989
12. G.M. Omweg, G.S. Frankel, W.A. Bruce, J.E. Ramirez, and G. Koch, Effect of Welding Parameters and H_2S Partial Pressure on the Susceptibility of Welded HSLA Steels to Sulfide Stress Cracking, Welding Research Supplement, *Welding Journal,* June 2003, p 136S–144S
13. G.M. Omweg, G.S. Frankel, W.A. Bruce, J.E. Ramirez, and G. Koch, Performance of Welded High-Strength Low-Alloy Steels in Sour Environments, *Corrosion,* Vol 59 (No. 7), July 2003, p 640–653
14. R.D. Kane, "ASTM G 146—Standard Practice for Evaluation of Disbonding of Bimetallic Stainless Alloy/Steel Plate for Use in High Pressure, High Temperature

Refinery Hydrogen Service," API Meeting (San Diego, CA), April 1997
15. "Standard Practice for Evaluation of Disbonding of Bimetallic Stainless Alloy/Steel Plate for Use in High-Pressure, High-Temperature Refinery Hydrogen Service," G 146, ASTM International
16. J.M. Johnson and J. Gutzeit, Embrittlement of Stainless Steel Welds by Contamination with Zinc-Rich Paint, *Proc. API,* Vol 63 (III), 1984, p 65–72
17. R.E. Smith, Progress in Reducing Stress Corrosion Cracking in BWR Piping, in *American Power Conf. Proc.,* Vol 39, 1977, p 232–240
18. H.H. Klepfer et al., Investigation of Causes of the Cracking in Austenitic Stainless Steel Piping, in *NEDO 21000,* Vol 1 and 2, General Electric Co., July 1975
19. "Studies on AISI Type 304 Stainless Steel Piping Weldments for Use in BWR Applications," EPRI NP-944 Final Report on Project RP-449-2, Electric Power Research Institute, Dec 1979
20. R.E. Hanneman, "Model for Intergranular Stress Corrosion Cracking of Welded Type 304 Stainless Steel Piping in BWRs," EPRI WS-74-174, Vol 1, Electric Power Research Institute, May 1980
21. J. C. Danko and M.E. Indig, In-Reactor and Ex-Reactor Electrochemical Methods for Corrosion and Stress Corrosion Cracking Testing, in *Predictive Methods for Assessing Corrosion Damage to BWR Piping and PWR Steam Generator Proceedings,* National Association of Corrosion Engineers, 1982
22. "Measurement of Residual Stresses in Type-304 Stainless Steel Piping Butt Weldments," EPRI NP-1413, Electric Power Research Institute, 1980
23. H. Flache and R. Ettemeyer, Piping Repair Case Study at KRB Unit A, *Trans. Am. Nucl. Soc.,* Vol 35, 1980, p 487
24. F.C. Hull, Effect of Delta Ferrite on the Hot Cracking of Stainless Steel, *Weld. J.,* Vol 46 (No. 91), 1967, p 3995–4095
25. "Toughness of Austenitic Stainless Steel Pipe Welds," EPRI NP-4768 on Project 1238-2, Electric Power Research Institute, Oct 1986
26. C. Strawstrom and M. Hillert, *J. Iron Steel Inst.,* Vol 207, 1969, p. 77
27. J. Alexander, "Alternative Alloys for BWR Pipe Applications," NP-2671-LD, Electric Power Research Institute, Oct 1982
28. A.E. Pickett, Assessment of Remedies for Degraded Piping, *Seminar on Countermeasures for Pipe Cracking in BWRs,* Electric Power Research Institute, Nov 1986
29. N.R. Hughes, "Evaluation of Near-Term BWR Piping Remedies," NP-1222, Electric Power Research Institute, May 1980
30. K. Gott, Cracking Data Base as a Basis for Risk Informed Inspection, *Proc. Tenth Int. Conf. Environmental Degradation in Nuclear Power Systems—Water Reactors* (Lake Tahoe, NV), Aug 5–9, 2001, F.P. Ford and G. Was, Ed., NACE International
31. Fukushima Daiichi Nuclear Power Station Unit 3, "Primary Loop Recirculation System Work Report for Pipe Branches Replacement," paper presented at BWR Operating Plant Technical Conference No. 8 (Monterey, CA), General Electric Co., Feb 1983
32. H.P. Offer, "Induction Heating Stress Improvement," NP-3375, Electric Power Research Institute, Nov 1983
33. R.M. Horn, "Last Pass Heat Sink Welding" NP-3479-LD, Electric Power Research Institute, March 1984
34. B.M. Gordon and G.M. Gordon, Corrosion in Boiling Water Reactors, in *Metals Handbook,* 9th ed., Vol. 13, *Corrosion,* ASM International, 1987, p 929–937
35. R.L. Jones, Prevention of Stress Corrosion Cracking in Boiling Water Reactors, *Mater. Perform.* Feb. 1991, p 70–73
36. D. Singbeil and D. Tromans, Stress Corrosion Cracking of Mild Steel in Alkaline Sulfide Solutions, *Proc. Third Int. Symp. Corrosion in the Pulp and Paper Industry,* National Association of Corrosion Engineers, 1980, p 40–46
37. D.C. Bennett, Cracking in Continuous Digesters, *TAPPI J.,* Vol 65 (No. 12), 1982, p 43–45
38. R. Yeske, "Stress Corrosion Cracking of Continuous Digesters for Kraft Pulping—Final Report to the Digester Cracking Research Committee," Project 3544, Institute of Paper Chemistry, 1983
39. D.C. Bennett, Cracking of Continuous Digesters—Review of History, Corrosion Engineering, Aspects and Factors Affecting Cracking, *Proc. Fourth Int. Symp.*

Corrosion in the Pulp and Paper Industry (Stockholm, Sweden), National Association of Corrosion Engineers, 1983, p 2–7
40. O. Pichler, Stress Corrosion in the Pre-Impregnation Vessel of a Continuous Kraft Digester, *Proc. Fourth Int. Symp. Corrosion in the Pulp and Paper Industry* (Stockholm, Sweden), National Association of Corrosion Engineers, 1983, p 15–20
41. N.J. Olson, R.H. Kilgore, M.J. Danielson and K.H. Pool, Continuous Digester Stress Corrosion Cracking Results from a Two-Vessel Kraft System, *Proc. Fourth Int. Symp. Corrosion in the Pulp and Paper Industry* (Stockholm, Sweden), National Association of Corrosion Engineers, 1983, p 21–26
42. P.E. Thomas and D.M. Whyte, Stress Corrosion Cracking in a Kraft Continuous Digester, *Appita,* Vol 37 (No. 9), 1984, p 748–752
43. D. Singbeil, Kraft Continuous Digester Cracking: Causes and Prevention, *Pulp Paper Can.,* Vol 87 (No. 3), 1986, p T93–T97
44. D. Singbeil, Kraft Continuous Digester Cracking: A Critical Review, *Proc. Fifth Int. Symp. Corrosion in the Pulp and Paper Industry* (Vancouver, B.C., Canada), Canadian Pulp and Paper Association, June 1986, p 267–271
45. R. Yeske, In-Situ Studies of Stress Corrosion Cracking in Continuous Digesters, *TAPPI J.,* Vol 69 (No. 5), 1986, p 104–108
46. D. Crowe, Stress Corrosion Cracking of Carbon Steel in Kraft Digester Liquors, *Proc. Sixth Int. Symp. Corrosion in the Pulp and Paper Industry* (Helsinki, Finland), 1989, p 35–47
47. Pressure Vessels, *American Society of Mechanical Engineers (ASME) Boiler and Pressure Vessel Code,* Section VIII, Division 1
48. R. Yeske, *Pulp Paper,* Vol 57 (No. 10), 1983, p 75
49. D. Singbeil and A. Garner, in *Proceedings of the Fifth International Symposium on Corrosion in the Pulp and Paper Industry,* National Association of Corrosion Engineers, 1986, p 267–271
50. D. Singbeil and A. Garner, "Second Semi-Annual Progress Report on the Research Program to Investigate Cracking of Continuous Digesters," Pulp and Paper Research Institute of Canada, 1984
51. R. Yeske and C. Guzi, *TAPPI J.,* Vol 69 (No. 5), 1986, p. 104–108
52. A. Wensley, Intergranular Attack of Stainless Steels in Kraft Digester Liquors, paper No. 465, *Corrosion 96 Conf.,* NACE International, 1996
53. I. Munro, in *Proceedings of the 1985 TAPPI Engineering Conference,* Technical Association of the Pulp and Paper Industry, 1985, p 37
54. D.G. Chakrapani, Intergranular Stress-Corrosion Cracking of Carbon Steel Pipe Welds in a Kamyr Continuous Digester Equalizer Line, *Handbook of Case Histories in Failure Analysis,* Vol 1, ASM International, 1992, p 168–170
55. A Garner, Corrosion of Weldments in Pulp Bleach Plants, *Welding Journal,* Sept 1986, p 39–44
56. E.L. Hibner, E.B. Hinshaw, and S. Lamb, Weld Fabrication of a 6% Molybdenum Alloy to Avoid Corrosion in Bleach Plant Service, Nickel Development Institute Reprint Series No. 14 020, 1992
57. A. Garner, How Stainless Steel Welds Corrode, *Met. Prog.,* Vol 127 (No. 5), April 1985, p 31
58. A. Garner, *Pulp Paper Can.,* Vol 82 (No. 12), 1981, p T414
59. A. Garner, *Weld. J.,* Vol 62 (No. 1), 1983, p 27
60. D.G. Chakrapani, Intergranular Corrosion/Cracking of a Stainless Steel Pipe Reducer Section in Bleached Pulp Stock Service, *Handbook of Case Histories in Failure Analysis,* Vol 1, ASM International, 1992, p 164–167

Corrosion of Weldments
J.R. Davis, editor, p 203-216
DOI:10.1361/corw2006p203

CHAPTER 11

Monitoring and Testing of Weld Corrosion

MONITORING is an essential part of any corrosion mitigation system. No corrosion prevention system is completely reliable, and in many cases failure can be catastrophic, both from a personal safety perspective and from an environmental and/or economic perspective. There are a wide variety of monitoring inspection techniques. Direct testing of coupons is used frequently to monitor in-service corrosion because of the simplicity and accuracy of the technique. Electrochemical techniques such as linear polarization resistance and electrochemical noise have moved from the laboratory to the processing plant and beyond to help with the detection of general and localized corrosion. Nondestructive testing techniques, such as ultrasonic thickness measurements, work from outside the vessel or piping.

Properly conducted corrosion tests can mean the savings of millions of dollars. They are a means of avoiding the use of a metal under unsuitable conditions or of using a more expensive material than is required. Corrosion tests also help in the development of new alloys that perform more inexpensively, more efficiently, longer, or more safely than the alloys currently in use. Corrosion testing programs can be simple ones that are completed in a few minutes or hours, or they can be complex, requiring the combined work of a number of investigators over a period of years. Immersion testing is the more frequently conducted procedure for evaluating corrosion resistance. However, when more information than corrosion rate is needed, electrochemical techniques are often considered.

Corrosion Monitoring

Three categories of corrosion monitoring will be addressed in this section. They include:

- Direct testing of coupons
- Electrochemical techniques
- Nondestructive testing techniques

Direct Testing of Coupons

A simple and inexpensive method of corrosion monitoring involves the exposure and subsequent evaluation of actual metal specimens or "coupons." Small specimens are exposed to the environment of interest for a specific period of time and subsequently removed for weight-loss measurement and more detailed examination. ASTM G 4 (Ref 1) was designed to provide guidance for this type of testing.

Although they are not intended to replace laboratory tests, plant coupon tests usually are designed to monitor the damage rate occurring on existing equipment, to evaluate alternative materials of construction, and sometimes to determine the effects of process conditions that cannot be reproduced in the laboratory.

Advantages of Coupon Testing (Ref 2). Plant coupon testing provides several specific advantages over laboratory coupon testing. A large number of materials can be exposed simultaneously and can be ranked in actual process streams with actual process conditions. Testing can be used to monitor the corrosivity of process streams. The coupons can be designed for spe-

cific forms of corrosion, but the exposure time is usually determined by the plant operation.

Large Number of Coupons. Because many coupons can be exposed simultaneously, they can be tested in duplicate or triplicate (to measure scatter), and they can be fabricated to simulate such conditions as welding, residual stresses, or crevices. These variations can provide the engineer with increased confidence in selecting materials for new equipment, maintenance, or repair.

Actual process streams reveal the synergistic effects of combinations of chemicals or contaminants. In addition, the possibility is remote that the corrosion of specific coupons contaminates the process and affects the corrosion resistance of other coupons. However, one potential source of error that must be checked is contamination of the process stream by the corrosion of the existing equipment.

Monitoring of Inhibitor Programs. Coupons often are used to monitor inhibitor programs in, for example, water treatment or refinery overhead streams. With retractable coupon holders, the coupons can be extracted from the process without having to shut down in order to determine the corrosion rate.

Long Exposure Times. Some forms of localized corrosion, such as crevice corrosion, pitting, and stress-corrosion cracking (SCC), require time to initiate. To increase confidence in the test results, coupons can be exposed for as long as necessary to ensure that the initiation time has been exceeded.

Coupon design can be selected to test for specific forms of corrosion. Coupons can be designed to detect such phenomena as crevice corrosion, pitting corrosion, and SCC. For example, some pulp mill bleach plant washer drums are protected electrochemically to mitigate crevice corrosion. Specifically designed crevice-corrosion test coupons are used to monitor the effectiveness of the electrochemical protection program. These coupons are removed periodically from the equipment and examined for evidence of crevice corrosion.

Disadvantages of Coupon Testing (Ref 2). Coupon testing has four main limitations:

- Coupon testing cannot be used to detect rapid changes in the corrosivity of a process.
- Localized corrosion cannot be guaranteed to initiate before the coupons are removed—even with extended test durations.
- Corrosion rate calculated from coupons may not reflect the corrosion of the plant equipment because of factors such as multiphase flow, where the aqueous phase is much more corrosive than the organic or vapor phase, or turbulence from mixers, elbows, valves, pumps, and other items that accelerate the corrosion in a specific location in the equipment removed from where the coupons were exposed.
- Coupons may be misleading in situations where the corrosion rate varies significantly over time because of unrealized process factors.

Contamination of the process fluid is an issue that must be addressed in the food, medical, and electronic equipment manufacturing industries, if coupons are introduced.

Rapid Changes in Corrosivity. The corrosion rate calculated from a coupon is an average over a specific period of time. Therefore, field coupon testing cannot detect process upsets as they occur. For real-time monitoring, electrochemical methods, such as the polarization-resistance technique, may be more appropriate (see the following section "Electrochemical Techniques").

Corrosion Rates of Coupons Compared with That of Equipment. The corrosion rate of plant equipment seldom equals that calculated on a matching test coupon because it is almost impossible to duplicate the equipment exposure with a coupon exposure. However, coupons are very helpful in many situations because they provide a clear view of the corrosion damage with information on the development of deposits, films, and localized attack. In addition, coupon testing is probably the least complicated type of in-service testing and, consequently, requires the least operator skill.

Corrosion Forms Not Detected. The principal limitation of coupon testing is the simulation of erosion-corrosion and heat-transfer effects. Careful placement of the coupons in the process equipment can slightly offset these weaknesses.

Coupon Options (Ref 2). The design of the coupon is an important part of any plant corrosion-testing program. Proper selection of the coupon shape, surface finish, metallurgical condition, and geometry allows evaluation of specific forms of corrosion. Figures 1 and 2 show examples of welded coupons for corrosion studies.

Welded Coupons. Because welding is a principal method of fabricating equipment, the use of welded coupons is often desirable. Aside from the effects of residual stresses, the primary concern is the behavior of the weld bead and the heat-affected zone (HAZ). In some alloys, the HAZ becomes sensitized to severe intergranular (sometimes called knife-line) attack, and in certain other alloys, the HAZ is anodic to the parent metal. When possible, it is more realistic to remove welded coupons from production-sized weldments than to weld the small coupons. Because the thermal conditions in both the weld metal and the HAZ are a function of the number of weld passes, the metal thickness, the weld position, and the welding technique, it is not usually considered good practice to use welded coupons to assess the possibility of sensitization from welding. It is generally better to carry out a sensitizing heat treatment on an unwelded coupon before it is tested and then look for evidence of intergranular corrosion or cracking.

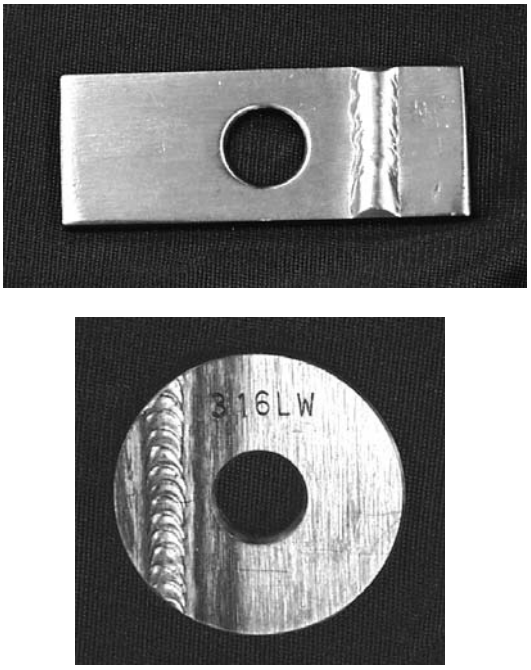

Fig. 1 Typical examples of weld coupons for corrosion monitoring and testing. Source: Metal Samples Company

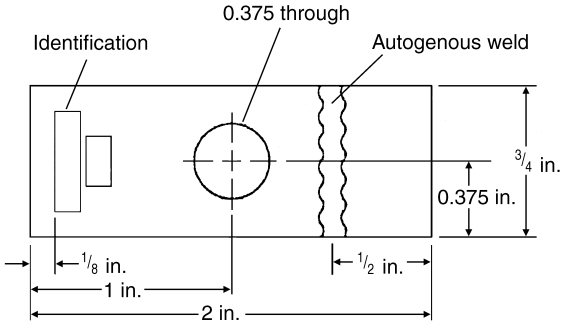

Fig. 2 Dimensions (given in inches) of a weld coupon. Standard weld is autogenous weld across end. Sanded after welding to a 120 grit finish (unless otherwise specified). Nominal thickness: ⅛ in. Source: Metal Samples Company

Sensitized Metal. Sensitization is a metallurgical change that occurs when certain austenitic stainless steels, ferritic stainless steels, nickel-base alloys, and other alloys are heated under specific conditions. This results in the precipitation of carbides or other intermetallic phases at grain boundaries, which reduces corrosion resistance. Any heat-inducing process (for example, stress relief of weldments) may cause sensitization, which is time and temperature dependent. There is a specific temperature range over which each particular alloy sensitizes rapidly. Sensitization leads to intergranular corrosion in specific environments.

Welding is the most common cause of sensitization. However, welded coupons may not exhibit sensitization because they may be given insufficient weld passes (compared with actual process equipment). As a result, they spend insufficient time in the sensitizing temperature range, and susceptibility to intergranular corrosion may not be detected.

An appropriate sensitizing heat treatment guarantees that any corrosion susceptibility induced by welding or heat treatment is detected. The optimal temperature and time ranges for sensitization vary for different alloys. For example, 30 min at 650 °C (1200 °F) is usually sufficient to sensitize type 316 stainless steel.

The advantage of using sensitized coupons is that, if corrosion occurs, they indicate a potential problem. The user is thus obliged to consider how the equipment will be welded and heat treated and to determine whether high-temperature excursions will occur during operation.

Stress-Corrosion Coupons. Typical sources of sustained tensile stress that cause SCC of equipment in service are the residual stresses resulting from forming and welding operations and the assembly stresses associated with inferference-fitted parts, especially in the case of

tapered, threaded connections. Therefore, the most suitable coupons for plant tests are the self-stressed bending and residual-stress specimens described in the section "Tests for Stress-Corrosion Cracking" in this chapter. Convenient coupons are the cup impression, U-bend, C-ring, tuning fork, and welded panel. The method of stressing for all of these coupons results in decreasing load as cracks form and begin to propagate. Therefore, complete fracture is seldom observed, and careful examination is required to detect cracking.

Crevice-Corrosion Coupons. Equipment crevices, such as weld backing rings, tube-tubesheet joints, or flanged connections, are common sites for localized corrosion in the process environment. Many metals perform differently in crevices as opposed to unshielded areas. Behavior is dependent on several factors. These factors include how strongly oxygen reduction (cathode depolarization) controls the cathode reaction or how the crevice alters the bulk process chemistry by lowering the pH or concentrating aggressive species.

The most imaginative form of coupon-corrosion testing is the simulation of crevice corrosion. The various techniques that can be used for crevice-corrosion testing include rubber brands, spot-welded lap joints, and wire wrapped around threaded bolts. Each crevice test creates a particular crevice geometry between specific materials and has a particular anode/cathode area ratio. Thus, no crevice-corrosion test is universally applicable.

The two most widely used crevice geometries in field coupon testing employ insulating spacers to separate and electrically insulate the coupons. Spacers are usually either flat washers or multiple-crevice washers. Either type of spacer can be made of materials ranging from hard ceramics to soft thermoplastic resins. Additional information can be found in the section "Tests for Pitting and Crevice Corrosion" in this chapter.

Electrochemical Techniques

A variety of electrochemical techniques are used to detect and monitor material deterioration in service or in the field. This section will briefly review some of the techniques that can be used to monitor weldment corrosion. Additional information on electrochemical methods for testing and monitoring can be found in Volume 13A, *Corrosion: Fundamentals, Testing, and Protection,* of the *ASM Handbook* and in ASTM G 96 (Ref 3).

Linear Polarization Resistance (LPR). The technique of LPR provides an estimate of the corrosion rate based on the Stern-Geary equation (Ref 4). The theory behind the technique is that the corrosion rate of a metal, in the absence of diffusional resistances, is inversely proportional to the *polarization resistance;* that is, the slope of the potential/current response curve near the corrosion potential. The equation and Tafel plots are found in the article "Electrochemical Methods of Corrosion Testing" in Volume 13A of the *ASM Handbook.* The proportionality factor, *B,* is a function of the anodic and cathodic Tafel slopes, which depend on temperature and the chemical species and concentration in the electrolyte. An external power supply gradually polarizes the specimen about 10 mV on both sides of the corrosion potential. The slope between the induced potential and the resulting current is interpreted as the polarization resistance. The time required for each resistance determination is a matter of minutes. Thus, this type of probe can provide corrosion rate feedback information with sufficient speed that it can be used in process control schemes.

The limitations to this approach include:

- A requirement that the electrolyte has a sufficiently high conductivity
- The vessel wall or pipe must be penetrated
- The use of a stable reference electrode

The latter limitation is usually not restrictive since three electrodes of the same material provides satisfactory service in most industrial applications. Even though the applied sensor perturbation is small, repeated application over a long period can lead to "artificial" surface damage. In addition, these systems cannot provide information on localized corrosion, such as pitting and SCC.

Electrochemical Impedance Spectroscopy (EIS). In principle, the same type of probe used for linear polarization resistance measurements can be used for electrochemical impedance measurements. In order to characterize certain features of corrosion behavior in detail, measurements throughout the entire frequency range are required; that is, from 0.1 Hz to 100 kHz. This approach permits the separation of the electrolyte resistance, the corrosion reaction resistance, and mass-transfer resistances. Therefore this approach is viable for highly resistive electrolytes such as steam condensate. Although EIS is usually considered to measure uniform corrosion only, the pit depth has been

found to correlate to a fitted model element, the constant phase angle (Ref 5).

Electrochemical Noise (EN). In this technique, fluctuations in potential and current between freely corroding electrodes are measured. Because of the small scale of these fluctuations of interest (in many cases <1 μV and <1 nA), sensitive instrumentation is required. A measurement frequency of 1 or 2 Hz usually suffices. For simultaneous measurement of electrochemical potential and current noise, a three-electrode sensor is required. The current is measured between two of the sensor elements with a zero-resistance circuit, and the potential is measured between the third element and the other two elements, which are at the same nominal potential. For industrial corrosion monitoring purposes, each element is usually constructed from the same material.

While measurement of EN is straightforward, data analysis can be complex. Such analysis is usually directed at distinguishing the different forms of corrosion, quantifying the noise signals, and processing the vast number of accumulated data points into a summarized format. Data processing approaches can involve both time-domain and frequency spectral analysis. A resistance parameter that is considered to be a polarization resistance and therefore a measure of the corrosion rate can be obtained from each approach (Ref 6); that is, noise resistance from the time domain and spectral noise resistance from the frequency domain.

Corrosion Potential. Measurement of corrosion potential is a relatively simple concept, and the underlying principle is widely used for monitoring the corrosion state of reinforcing steel in concrete and buried pipelines under cathodic protection. This approach can also be valuable in cases where an alloy could show both active and passive corrosion behavior in a given process stream. For example, stainless steels can provide excellent service as long as they remain passive. However, if an upset occurs that would introduce either chlorides or reducing agents into the process stream, stainless alloys may become active and exhibit excessive corrosion rates. Corrosion potential measurements can indicate the transition from passive to active corrosion.

The success of corrosion potential measurements depends on the long-term stability of a reference electrode. Such electrodes have been developed for continuous pH monitoring of process streams, and their application for measuring corrosion potentials is straightforward. However, temperature, pressure, electrolyte composition, pH, and other variables can limit the applications of these electrodes for corrosion-monitoring service. Also, while the technique may indicate changes in corrosion behavior over time, it does not provide any indication of corrosion rates.

Nondestructive Testing Techniques (Ref 7)

Different nondestructive testing (NDT) techniques like ultrasonic, eddy current, radiography, acoustic emission, and thermography are widely used for characterizing corrosion in materials and their damage during service. Of the NDT methods listed above, ultrasonic testing is the most widely used for monitoring of corrosion and will be emphasized in this section.

Ultrasonic thickness measurements can be used to monitor corrosion rates in situ. Ultrasonic thickness measurements involve placement of a transducer against the exterior of the vessel in question. The transducer produces an ultrasonic signal. This signal passes through the vessel wall, bounces off the interior surface, and returns to the transducer. The thickness is calculated by using the time that elapses between emission of the signal and its subsequent reception, along with the velocity of sound in the material. To obtain a corrosion rate, a series of measurements must be made over a time interval, and the metal loss per unit time must be determined.

One advantage of this method is that it is not necessary to penetrate the vessel to make the measurements. In addition, the results are obtained in terms of thickness. Small, handheld probes and reading devices are available for making these measurements and are relatively easy to use.

There are also several disadvantages. Ideally, a bare metal surface free of paint, thermal insulation, and corrosion products must be exposed. A coupling agent, such as grease, petroleum jelly, or oil, must be used so that the signal can pass from the probe into the metal and return. Problems may arise when vessel walls are at high or low temperatures. Serious problems may exist in equipment that has a metallurgically bonded internal lining, because it is not obvious from which surface the returning signal originates.

Despite these drawbacks, the ultrasonic thickness approach is widely practiced where it is necessary to evaluate vessel life and suitability for

further service. It must be kept in mind, however, that depending on the type of transducer used, the ultrasonic thickness method can overestimate metal thickness when the remaining thickness is under approximately 1.3 mm (0.05 in.).

Ultrasonic Testing of Welds in the By-Pass Lines of a Boiling Water Reactor. One of the typical applications of ultrasonic testing is the in-service inspection of the coolant circuit pipes and the by-pass lines in a boiling water reactor. These pipes, which are fabricated from type 316 stainless steel, are intended to serve as lines to keep minimum flow on recirculation pump outlets during start up of pumps. Detailed survey conducted earlier on various boiling water reactors around the world had indicated that the failures of the bypass line welds are due to intergranular stress corrosion cracking (IGSCC) at weld heat affected zones (Fig. 3) mainly due to stagnant water legs conditions in bypass piping which used to be kept closed after pump start up for flow control on main recirculation piping. In one of the operating reactors, after 10 years of operation, leaks were observed during hydrotesting.

In order to estimate the extent of the defects and their locations in the leaky welded joints and also to evaluate the integrity of the other 18 joints in the bypass lines, ultrasonic testing was carried out. The ultrasonic test procedure was standardized earlier in the laboratory with mock up welded pipe standards having reference defects. An ultrasonic flaw detector with a 2.25 MHz frequency, 45° angle shear wave probe was used for testing purpose. Clear defect echo patterns were observed from all the artificial defects by choosing suitable test parameters. At the standard sensitivity level, in-situ ultrasonic testing confirmed the hydrotest observations and the extent and nature of defects were determined. Based on the ultrasonic observations, it was decided to replace the four welded joints (where leaks were observed) with new joints. The consequent metallography of the removed joints confirmed the ultrasonic test observations.

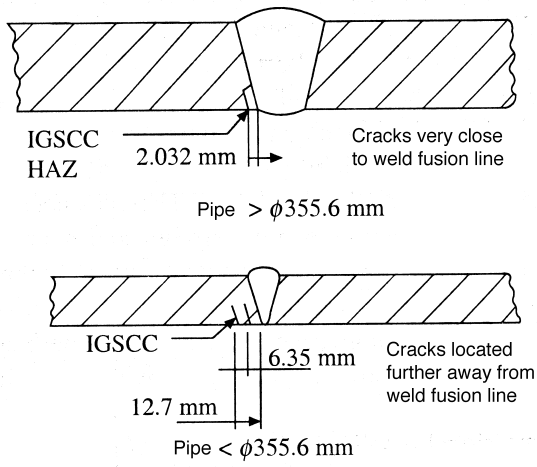

Fig. 3 Expected location of IGSCC in BWR piping. Source: Ref 7

The analysis of the study indicated that the cracks are of intergranular stress corrosion type. The failures are due to fabrication-induced stresses combined with service-induced corrosion from inside surface of the piping. Additional information on IGSCC of pipe welds in boiling water reactors can be found in Chapter 10, "Weld Corrosion in Specific Industries and Environments."

Other NDT techniques used to monitor corrosion include:

- *Eddy current testing:* In addition to its well known applications to crack and pit detection, this technique can be used to measure thickness changes caused by corrosion, build up of corrosion products in certain situations, changes in materials properties such as electrical conductivity degradation caused by intergranular corrosion.
- *Acoustic emission testing:* This technique is used to monitor SCC in wide variety of materials including sensitized austenitic stainless steels. It is also used to monitor pitting corrosion in piping and various vessels used in the chemical processing industry.
- *Radiography:* The key benefit offered by this technique is the ability to determine the extent of corrosion attack by means of measuring material loss through pipelines with insulation in the chemical and petrochemical industries.
- *Infrared thermography:* Thermal imaging techniques have been used for the detection of wall thinning in stainless steel pipes. This technique offers an alternative to ultrasonic testing, radiography, and visual inspection using a borescope.

Corrosion Testing

The majority of the test methods for evaluating corrosion of weldments have described intergranular corrosion of stainless steels and

high-nickel alloys. Other applicable tests evaluate pitting and crevice corrosion, SCC, and microbiologically influenced corrosion (MIC). Each will be briefly reviewed in this chapter.

Tests for Intergranular Corrosion

Intergranular corrosion (IGC) is preferential attack of either grain boundaries or areas immediately adjacent to grain boundaries in a material exposed to a corrosive environment but with little corrosion of the grains themselves. Intergranular corrosion is also known as intergranular attack (IGA). *End-grain attack, grain dropping,* and *"sugaring"* are additional terms that are sometimes used to describe IGC.

Tests for Stainless Steels and Nickel-Base Alloys. The austenitic and ferritic stainless steels, as well as most nickel-base alloys, are generally supplied in a heat treated condition such that they are free of carbide precipitates that are detrimental to corrosion resistance. However, these alloys are susceptible to sensitization from welding, improper heat treatment, and service in the sensitizing temperature range. The theory and application of acceptance tests for detecting the susceptibility of stainless steels and nickel-base alloys to intergranular attack are extensively reviewed in Ref 8 to 10. Corrosion tests for evaluating the susceptibility of an alloy to IGC are typically classified as either simulated-service or accelerated tests. The original laboratory tests for detecting IGC were simulated-service exposures. These were first used in 1926 when IGC was detected in an austenitic stainless steel in a copper sulfate-sulfuric acid ($CuSO_4$-H_2SO_4) pickling tank (Ref 11). Another simulated-service test for alloys intended for service in nitric acid (HNO_3) plants is described in Ref 12. In this case, for accelerated results, iron-chromium alloys were tested in a boiling 65% HNO_3 solution.

The tests described below are based on various ASTM standards and can be classified as:

- Nitric acid test
- Copper sulfate-sulfuric acid test
- Ferric sulfate-50% sulfuric acid test
- Oxalic acid etch test
- Nitric-hydrofluoric acid test

Tables 1 to 4 review the primary characteristics of these tests.

ASTM A 262. Over the years, specific accelerated tests have been developed and standardized for evaluating the susceptibility of various alloys to IGA. For example. ASTM A 262 contains six practices for detecting susceptibility to IGC in austenitic stainless steels (Ref 14). Practice A is an electrolytic oxalic-acid-etch screening test that can be performed in minutes on prepared samples followed by microscopic

Table 1 Boiling copper sulfate tests in ASTM A 262 and A 763

ASTM Designation	Solution				Testing			Alloys
			Metallic copper					
	$CuSO_4$	H_2SO_4 (By weight %)	Type	Contact	Apparatus	Evaluation	Time, h	
A 262-E	6%	16	shot or turnings (a)	yes	Allihn condenser, 1-L flask	bend test	24	austenitic stainless steels
A 262-F	72g $CuSO_4 \cdot 5H_2O$ in 600 mL	50	specimen or shot	no	Allihn condenser, 1-L flask	weight loss	120	Cast 316 Cast 316L
A763 Practice Y	72g $CuSO_4 \cdot 5H_2O$ in 600 mL	50	specimen	no	Allihn condenser, 1-L flask	weight loss, bend test, no grain dropping	120	Fe-Cr with more than 25% Cr, Type 446(96 h) Fe-26Cr-1Mo Fe-26Cr-1Mo-Ti 29Cr-4Mo 29Cr-4Mo-2Ni
Practice Z	6%	16	shot or turnings (a)	yes	Allihn condenser, 1-L flask	bend test	24	Fe-Cr with 16 to 20% Cr 430 (17Cr) 434 (17Cr-1Mo) 436 (17Cr-1Mo-Nb) 18Cr-Ti 18 Cr-2Mo-Ti

(a) Amount not specified; enough to cover the specimen. Source: Ref 13

examination of the etched microstructure for $Cr_{23}C_6$ sensitization. Practice B is a 120 h test in a boiling solution of ferric sulfate [$Fe_2(SO_4)_3$] + sulfuric acid (H_2SO_4); the weight-loss corrosion rate indicates degree of IGA due to $Cr_{23}C_6$ precipitation. A 240h test in boiling 65% HNO_3 constitutes Practice C; the degree of IGC due to $Cr_{23}C_6$ and σ-phase formation is indicated by weight-loss corrosion rates. Practice D, which was an immersion test in 10% HNO_3 + 3% HF solution at 70 °C (158 °F) has been removed from ASTM A 262 (Ref 14). Practice E is a 24 h test in boiling 6% $CuSO_4$ + 10% H_2SO_4 solution to which metallic copper is added: evaluation of IGC due to $Cr_{23}C_6$ formation is based on post-exposure visual examination of specimens for

Table 2 ASTM standard practices in A 262 for detecting susceptibility to intergranular corrosion in austenitic stainless steels

Designation	Test	Temperature	Testing time	Applicability	Evaluation method
Practice A	Oxalic acid etch screening test	ambient	1.5 min	Chromium carbide sensitization only	Microscopic examination; classification of etch structure
B	Ferric sulfate-50% sulfuric acid	boiling	120 h	Chromium carbide	Weight-loss/corrosion rate
C	65% Nitric acid	boiling	240 h	Chromium carbide and sigma phase	Weight-loss/corrosion rate
D	10% Nitric-3% hydrofluoric acids (This test is being removed from A 262)	70 °C	4 h	Chromium carbide in 316, 316L, 317, 317L	Ratio of corrosion; rates of "unknown" over that of a solution annealed specimen
E	6% Copper sulfate 10% Sulfuric acid with metallic copper	boiling	24 h	Chromium carbide	Examination for fissures after bending
F	Copper sulfate-50% sulfuric acid with metallic copper	boiling	120 h	Chromium carbide in cast 316 and 316L	Weight-loss/corrosion rate

Source: Ref 13

Table 3 ASTM standard practices in A 763 for detecting susceptibility to intergranular attack in ferritic stainless steels

Designation	Test	Temperature	Testing time	Applicability	Evaluation method
Practice W	Oxalic acid etch	ambient	1.5 min	stabilized (Ti, Nb) grades only	Classification of etch structures
X	Ferric sulfate-50% sulfuric acid	boiling	24 to 120 h	17 to 29% Cr	Weight-loss 17 to 26% Cr, microscopic examination, 29% Cr
Y	Copper sulfate 50% sulfuric acid with metallic copper	boiling	96 to 120 h	25–29% Cr	Weight-loss 26% Cr, microscopic examination, 29% Cr
Z	Copper sulfate 16% sulfuric acid with metallic copper	boiling	24 h	17–18% Cr	Check for fissures in bend test

Source: Ref 13

Table 4 ASTM standard test methods in G 28 for detecting susceptibility to intergranular attack in wrought, nickel-rich, chromium-bearing alloys

Designation	Test	Temperature	Testing time	Applicability	Evaluation method
Method A	Ferric sulfate 50% sulfuric acid	boiling	24 to 120 h	Carbides and intermetallic phases (a)	Weight-loss corrosion rate and/or microscopic examination
B	23% Sulfuric 1.2% Hydrochloric 1% Ferric chloride 1% Cupric chloride	boiling	24 h	Carbides and intermetallic phases Alloys C-276, C-22, 59	Weight-loss corrosion rate and/or microscopic examination

(a) Alloys C-4, C-276, 20 Cb-3, 600, 625, 800, 825, C-22, 59, G, G-3, G-30, and 6XN. Source: Ref 13

fissures after bending. In Practice F, a 120 h boiling test in $CuSO_4$ + 50% H_2SO_4 solution (with metallic copper present), weight-loss corrosion rates indicate the degree of sensitization due to $Cr_{23}C_6$ precipitation for molybdenum-bearing stainless steels. See Tables 1 and 2 for additional information.

Microstructural Evaluation. The oxalic acid etch test (ASTM A 262, Practice A) is used for screening specimens by classifying microstructures (Ref 13). These are obtained simply by making a polished surface anodic in 10% oxalic acid solution for 1.5 min with a current density of 1.0 amp/cm^2. This results in an "over etch" which facilitates interpretation. On specimens that are free of chromium carbides at grain boundaries the different rates of dissolution of variously oriented metal grains results in steps between grains (Fig. 4a, Step Structure). When the boundaries contain enough carbides to surround completely at least one grain there can be expected to be undermining of grains in the boiling acid tests and an increase in the corrosion rate with testing time (Fig. 4b, Ditch Structure). When the ditching does not surround grains completely the classification is Dual Structure (Fig. 4c).

Specimens with step and dual structures do not drop grains in boiling acid tests, and therefore have acceptable or "passing" corrosion rates in weight-loss tests. Materials represented by such specimens can therefore be accepted for plant use on the basis of the 1.5 min oxalic acid etch test Only those materials that have a ditch structure must be submitted for testing in the hot acid tests to determine whether or not their corrosion rates fall below or above the acceptance rate for the given alloy.

ASTM A 763 and G 28. Standardized test methods for detecting the susceptibility of ferritic stainless steels to intergranular corrosion are described in ASTM A 763 (Ref 15). The methods are similar to those described in ASTM A 262 (Ref 14) for austenitic stainless steels in that there is an oxalic acid etch test and three acid immersion tests. The principal difference between the two standards is the use of microscopic examination of samples exposed to the boiling acid solutions. The presence or absence of grain dropping becomes the acceptance criterion for these samples. See Tables 1 and 3 for additional information.

Similarly, tests for detecting susceptibility to IGC in wrought nickel-rich, chromium-bearing alloys have been incorporated into ASTM G 28 (Ref 16) See Table 4 for additional information.

Acceptance Tests. Because sensitized alloys may inadvertently be used, acceptance tests are implemented as a quality-control check to evaluate stainless steels and nickel-base alloys when:

- Different alloys, or alloys with "high" carbon content, are substituted for the low-carbon grades (for example, type 316 substituted for type 316L), and when welding or heat treatment are involved

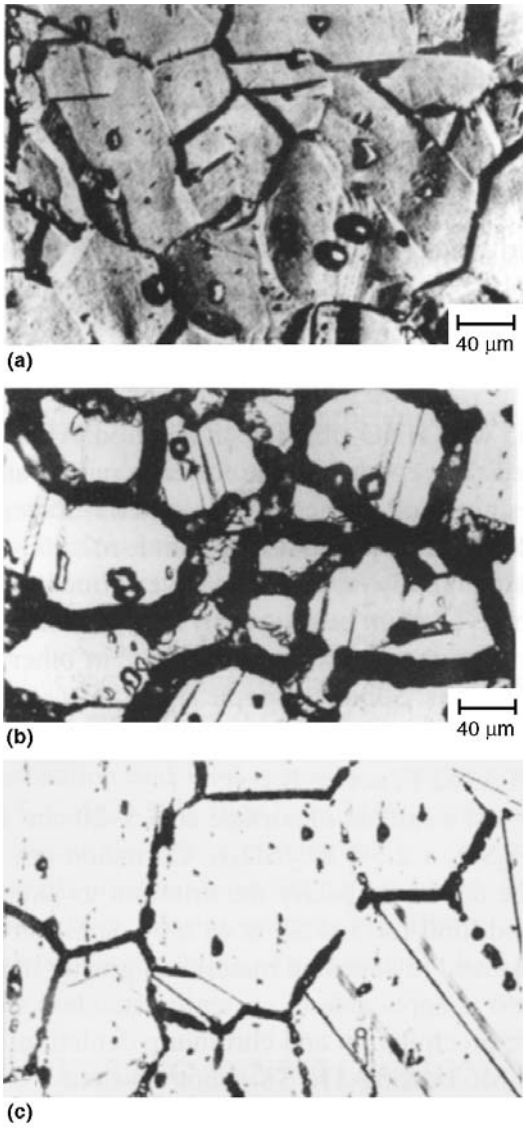

Fig. 4 Classification of etch structures after oxalic acid etching (ASTM A 262, Practice A). (a) Step structure. (b) Ditch structure. (c) Dual structure. Source: Ref 7

- An improper heat treatment during fabrication results in the formation of intermetallic phases
- The specified limits for carbon and/or nitrogen contents of an alloy are inadvertently exceeded

Some standard tests include acceptance criteria, but others do not (Ref 11, 12). Suitable criteria are needed that can clearly separate material susceptible to IGC from that resistant to attack. Table 5 lists evaluation tests and acceptance criteria for various stainless steels and nickel-base alloys. Despite establishment of "standard" acceptance/rejection criteria, the buyer and seller can agree on a different criterion that meets their particular needs.

Electrochemical Testing. ASTM G 108 describes a laboratory procedure for conducting a nondestructive electrochemical potentiokinetic reactivation (EPR) test on types 304 and 304L stainless steel to quantify the degree of sensitization (Ref 17). The metallographically mounted and highly polished test specimen is potentiodynamically polarized from the normally passive condition, in 0.5 *M* H_2SO_4 + 0.01 *M* potassium thiocyanate (KSCN) solution at 30 ± 1 °C, to active potentials—a process known as reactivation. The amount of charge passed is related to the degree of IGC associated with $Cr_{23}C_6$ precipitation, which occurs predominately at the grain boundaries. After the single loop EPR test, the microstructure is examined and:

1. The grain boundary area is calculated from the grain size and the total exposed area of the test specimen.

Table 5 Appropriate evaluation tests and acceptance criteria for wrought alloys

UNS No.	Alloy name	Sensitizing treatment	Applicable tests (ASTM standards)	Exposure time, h	Criteria for passing appearance or maximum allowable corrosion rate, mm/month (mils/month)
S43000	Type 430	None	Ferric sulfate (A 763-X)	24	1.14 (45)
S44600	Type 446	None	Ferric sulfate (A 763-X)	72	0.25 (10)
S44625	26-1	None	Ferric sulfate (A 763-X)	120	0.05 (2) and no significant grain dropping
S44626	26-1S	None	Cupric sulfate (A 763-Y)	120	No significant grain dropping
S44700	29-4	None	Ferric sulfate (A 763-X)	120	No significant grain dropping
S44800	29-4-2	None	Ferric sulfate (A 763-X)	120	No significant grain dropping
S30400	Type 304	None	Oxalic acid (A 262-A)	. . .	(a)
			Ferric sulfate (A 262-B)	120	0.1 (4)
S30403	Type 304L	1 h at 675 °C (1250 °F)	Oxalic acid (A 262-A)	. . .	(a)
			Nitric acid (A 262-C)	240	0.05 (2)
S30908	Type 309S	None	Nitric acid (A 262-C)	240	0.025 (1)
S31600	Type 316	None	Oxalic acid (A 262-A)	. . .	(a)
			Ferric sulfate (A -262-B)	120	0.1 (4)
S31603	Type 316L	1 h at 675 °C (1250 °F)	Oxalic acid (A 262-A)	. . .	(a)
			Ferric sulfate (A 262-B)	120	0.1 (4)
S31700	Type 317	None	Oxalic acid (A 262-A)	. . .	(a)
			Ferric sulfate (A 262-B)	120	0.1 (4)
S31703	Type 317L	1 h at 675 °C (1250 °F)	Oxalic acid (A 262-A)	. . .	(a)
			Ferric sulfate (A 262-B)	120	0.1 (4)
S32100	Type 321	1 h at 675 °C (1250 °F)	Nitric acid (A 262-C)	240	0.05 (2)
S34700	Type 347	1 h at 675 °C (1250 °F)	Nitric acid (A 262-C)	240	0.05 (2)
N08020	20Cb-3	1 h at 675 °C (1250 °F)	Ferric sulfate (G 28-A)	120	0.05 (2)
N08904	904L	None	Ferric sulfate (G 28-A)	120	0.05 (2)
N08825	Incoloy 825	1 h at 675 °C (1250 °F)	Nitric acid (A 262-C)	240	0.075 (3)
N06007	Hastelloy G	None	Ferric sulfate (G 28-A)	120	0.043 (1.7) sheet, plate, and bar; 0.05 (2) pipe and tubing
N06985	Hastelloy G-3	None	Ferric sulfate (G 28-A)	120	0.043 (1.7) sheet, plate, and bar; 0.05 (2) pipe and tubing
N06625	Inconel 625	None	Ferric sulfate (G 28-A)	120	0.075 (3)
N06690	Inconel 690	1 h at 540 °C (1000 °F)	Nitric acid (A 262-C)	240	0.025 (1)
N10276	Hastelloy C-276	None	Ferric sulfate (G 28-A)	24	1 (40)
N06455	Hastelloy C-4	None	Ferric sulfate (G 28-A)	24	0.43 (17)
N06110	Allcorr	None	Ferric sulfate (G 28-B)	24	0.64 (25)
N10001	Hastelloy B	None	20% hydrochloric acid	24	0.075 (3) sheet, plate, and bar; 0.1 (4) pipe and tubing
N10665	Hastelloy B-2	None	20% hydrochloric acid	24	0.05 (2) sheet, plate, and bar; 0.086 (3.4) pipe and tubing

(a) See ASTM A 262, practice A.

2. Relative proportions of grain boundary attack and non-grain-boundary pitting are determined.

A charge per unit grain-boundary area of <0.1 C/cm^2 (0.016 C/in.^{2}) generally indicates unsensitized microstructure, and >0.4 C/cm^2 (0.062 C/in.^{2}) indicates a heavily sensitized alloy. Although a double loop EPR method has been proposed (Ref 18, 19) to eliminate non-grain-boundary pitting and surface-finish effects, often observed in the single loop method, the double-loop technique is not presently included in ASTM G 108.

Additional information on the EPR test can be found in the articles "Methods for Determining Aqueous Corrosion Reaction Rates" and "Electrochemical Methods of Corrosion Testing" in Volume 13A of the *ASM Handbook.*

Tests for Pitting and Crevice Corrosion

ASTM G 48 gives procedures for determining the pitting (and crevice) corrosion resistance of stainless steels and related alloys when exposed to an oxidizing chloride environment, namely, 6% ferric chloride ($FeCl_3$ at 22 ± 2 or 50 ± 2 °C (70 ± 3.5 or 120 ± 3.5 °F) (Ref 20). Method A is a 72 h total-immersion test of small coupons that is designed to determine the relative pitting resistance of stainless steels and nickel-base chromium-bearing alloys. Method B is a crevice test under the same exposure conditions, and it can be used to determine both the pitting and crevice corrosion resistance of these alloys. These tests can be used for determining the effects of alloying additions, heat treatments, and surface finishes on pitting and crevice corrosion resistance. Methods A and B are designed to cause breakdown of type 304 stainless steel at room temperature. Methods C and D are used to determine the critical temperature to cause initiation of pitting and crevice corrosion, respectively, in 6% $FeCl_3$ + 1% HCl solution. In each of these methods, the use of $FeCl_3$ solution is justified on the basis that a similar electrolyte chemistry develops within the pits in susceptible ferrous alloys exposed to chloride-containing service environments. As a result, these tests can give misleading results for alloys intended for chloride-free service environments.

ASTM G 78 provides guidance for conducting crevice corrosion tests on stainless steels and related nickel-base alloys in seawater and, other chloride-containing environments (Ref 21). While its origins grew out of attempts to standardize the use of multiple-crevice assemblies, this guide does not promote any particular crevice former but advises the reader to be aware that crevice corrosion test results can be affected by a number of interrelated factors. In particular, crevice geometry and specimen preparation are very important aspects of testing. This standard provides guidance in the conduct of tests for flat and cylindrical specimens as well as those having irregular surfaces, such as weldments. It also reviews evaluation and reporting considerations. Importantly, Ref 21 points out that the occurrence or absence of crevice corrosion in a given test is no assurance that it will not occur under other test conditions. This is especially true if the design fails to consider those factors that may affect initiation and/or propagation behavior.

Tests for SCC

Bent-beam specimens can be used to test a variety of product forms. The bent-beam configuration is primarily used for sheet, plate, or flat extruded sections, which conveniently provide flat specimens of rectangular cross section, but it is also used for weldments. This method is applicable to specimens of any metal that are stressed to levels less than the elastic limit of the material; therefore, the applied stress can be calculated or measured accurately (ASTM G 39, Ref 22).

Welded double-beam specimens consist of two flat strips 25 to 51 mm (1 to 2 in.) wide and 127 to 254 mm (5 to 10 in.) long. The strips are bent against each other over a centrally located spacer until both ends touch. The strips are held in position by welding the ends together, as shown in Fig. 5.

In a welded double-beam specimen, the maximum stress occurs between the contact points of

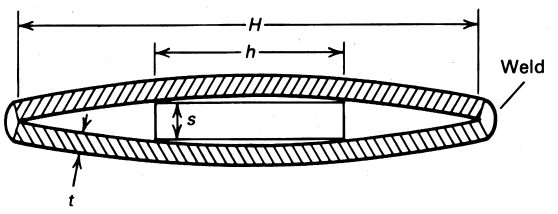

Fig. 5 Welded double-beam SCC specimen

the spacer; the stress is uniform in this area. From contact with the spacer, the stress decreases linearly toward zero at the ends of the specimen, similar to a four-point loaded specimen.

Residual-Stress Specimens. Most industrial SCC problems are associated with residual tensile stresses developed in the metal during such processes as heat treatment, fabrication, and welding. Therefore, residual-stress specimens simulating anticipated service conditions are useful for assessing the SCC performance of some materials in particular structures and in specific environments.

Weld Specimens. Residual stresses developed in and adjacent to welds are frequently a source of SCC in service. Longitudinal stresses in the vicinity of a single weld are unlikely to be as large as stresses developed in plastically deformed weldments, because stress in the weld metal is limited by the yield strength of the hot metal that shrinks as it cools. High stresses can be built up, however, when two or more weldments are joined into a more complex structure.

Test specimens containing residual welding stresses are shown in Fig. 6. In fillet welds, residual tensile stress transverse to the weld can be critical, as indicated in Fig. 6(a) for a situation in which the tension stress acts in the short-transverse direction in an Al-Zn-Mg alloy plate.

Special Considerations for Testing of Weldments. ASTM G 58 (Ref 25) covers test specimens in which stresses are developed by the welding process only (that is, residual stress, Fig. 6), an externally applied load in addition to the stresses due to welding (Fig. 5), and an externally applied load only, with residual welding stresses removed by annealing.

The National Materials Advisory Board Committee on Environmentally Assisted Cracking Test Methods for High-Strength Weldments published the following guidelines on SCC testing of weldments (Ref 26). Fracture mechanics of cracked bodies was found to be a valid and useful approach for designing against environmentally assisted cracking, although several limitations and difficulties must be taken into consideration. For static loading, K_{ISCC} and *da/dt* versus K_i are useful parameters. They are specified to a material, temperature, and metal/environment system and are functions of local chemical composition, microstructure, and so on. Fracture mechanics nomenclature is discussed in the article "Evaluating Stress-Corrosion Cracking" in Volume 13A of the *ASM Handbook.*

Superimposed minor load fluctuations and infrequent changes in load can alter environmental cracking response. This effect, which cannot be predicted from K_{ISCC} and *da/dt* values, may be significant and detrimental. Reexamination of static loading as a design premise may be required. Existing test methodology or environmentally assisted cracking tendency is applicable to the evaluation of weldments. As in other structural components, residual stress must be treated in a quantitative and realistic manner.

The National Materials Advisory Board report supports current design emphasis based on the presumption of preexisting cracklike flaws in the structure and covers testing with precracked (fracture mechanics) specimens only. It contains a critical assessment of the problems associated with environmentally assisted cracking in high-strength alloys and of state-of-the-art design and test methodology.

Fig. 6 SCC test specimen containing residual stresses from welding. (a) Sandwich specimen simulating rigid structure. Note SCC in edges of center plate. Source Ref 23. (b) Cracked ring-welded specimen. Source: Ref 24

Table 6 Electrochemical monitoring methods used for MIC

Measurement	Remarks
Corrosion potential	Easy to do, difficult to interpret without other information
Redox potential	Limited value—not selective and not directly related to corrosion: provides insight into aerobic/anaerobic status of system
Linear polarization resistance	Gives trend information for uniform corrosion: sensitive to fouling by nonconducting material such as hydrocarbons
Electrochemical impedance spectroscopy	For uniform corrosion rate and information on various corrosion-related processes; requires significant expertise to interpret; small amplitude polarization does not disturb microbial numbers or activity
Electrochemical relaxation	Fast transient techniques yield information for uniform corrosion
Electrochemical noise	No external perturbation; indicates localized corrosion events and rates; well suited to MIC
Electrical resistance	Resistance measurement reflects loss of conductor cross section by pitting or general corrosion; robust, and suited to systems with multiphase flow; fouling by electrically conducting iron sulfides can cause erroneous readings

Source: Ref 27

Tests For MIC

Electrochemical techniques used to study MIC include those in which no external signal is applied (redox potential, corrosion potential, electrochemical noise), those in which only a small potential or current perturbation is applied (polarization resistance, electrochemical impedance spectroscopy), and those in which the potential is scanned over a wide range (anodic and cathodic polarization curves, pitting scans). A number of these electrochemical techniques were discussed earlier in this chapter. Table 6 summarizes the use of electrochemical techniques to study MIC.

ACKNOWLEDGMENTS

Portions of this chapter were adapted from:

- S.W. Dean, Corrosion Monitoring for Industrial Processes, *Corrosion: Fundamentals, Testing, and Protection,* Vol 13A, *ASM Handbook,* ASM International, 2003, p 533–541
- R.M. Kain, Evaluating Crevice Corrosion, *Corrosion: Fundamentals, Testing, and Protection,* Vol 13A, *ASM Handbook,* ASM International, 2003, p 549–561
- B. Phull, Evaluating Intergranular Corrosion, *Corrosion: Fundamentals, Testing, and Protection,* Vol 13A, *ASM Handbook,* ASM International, 2003, p 568–571
- B. Phull, Evaluating Pitting Corrosion, *Corrosion: Fundamentals, Testing, and Protection,* Vol 13A, *ASM Handbook,* ASM International, 2003, p 545–548
- B. Phull, Evaluating Stress-Corrosion Cracking, *Corrosion: Fundamentals, Testing, and Protection,* Vol 13A, *ASM Handbook,* ASM International, 2003, p 575–616

REFERENCES

1. "Standard Method for Conducting Corrosion Coupon Tests in Plant Equipment," G 4, *Annual Book of ASTM Standards,* Vol 03.02, ASTM International
2. B.J. Moniz, Field Coupon Corrosion Testing, *Process Industries Corrosion—Theory and Practice,* National Association of Corrosion Engineers, 1986
3. "Standard Guide for On-Line Monitoring of Corrosion in Plant Equipment (Electrical and Electrochemical Methods)," G 96, *Annual Book of ASTM Standards,* Vol 03.02, ASTM International
4. M. Stern and R.M. Roth, *J. Electrochem. Soc.,* Vol 104, 1958, p 440t
5. P.R. Roberge and V.S. Sastri, Laboratory and Field Evaluation of Organic Corrosion Inhibitors in Sour Media, *Corros. Sci.,* Vol 35 (No. 5–8); 1993, p 1503–1513
6. R.A. Cottis, Interpretation of Electrochemical Noise Data, *Corrosion,* Vol 57 (No. 3), 2001, p 265–285
7. B. Raj, P. Kalyanasundaram, and S.K. Dewangan, Corrosion Detection and Monitoring in Austenitic Stainless Steels Using Nondestructive Testing and Evaluation Techniques, *Corrosion of Austenitic Stainless Steels: Mechanism, Mitigation and Monitoring,* H.S. Khatak and B. Raj,

Ed., ASM International and Narosa Publishing House, 2002, p 287–313
8. M. Henthorne, *Localized Corrosion—Cause of Metal Failure,* STP 516, ASTM International, 1972, p 66–119
9. M.A. Streicher, *Intergranular Corrosion of Stainless Alloys,* STP 656, ASTM International, 1978, p 3–84
10. M.A. Streicher, in *Intergranular Corrosion of Stainless Alloys,* STP 656, American Society for Testing and Materials, 1978, p 3–84
11. W.H. Hatfield, *J. Iron Steel Inst.,* Vol 127, 1993, p 380–383
12. W.R. Huey, *Trans. Am. Soc. Steel Treat.,* Vol 18, 1930, p 1126–1143
13. M.A. Streicher, Intergranular Corrosion, *Corrosion Tests and Standards: Application and Interpretation,* R. Baboian, Ed., ASTM International, 1995, p 197–217
14. "Practices for Detecting Susceptibility to Intergranular Corrosion in Austenitic Stainless Steels," A 262, *Steel—Plate, Sheet, Strip, Wire: Stainless Steel Bar, Annual Book of ASTM Standards,* Vol 1.03, ASTM International
15. "Practices for Detecting Susceptibility to Intergranular Corrosion in Ferritic Stainless Steels," A 763, *Steel—Plate, Sheet, Strip, Wire; Stainless Steel Bar, Annual Book of ASTM Standards,* Vol 1.03, ASTM International
16. "Standard Test Methods for Detecting Susceptibility to Intergranular Corrosion in Wrought, Nickel-Rich, Chromium-Bearing Alloys," G 28, *Wear and Erosion; Metal Corrosion, Annual Book of ASTM Standards,* Vol 3.02, ASTM International
17. "Standard Test Method for Electrochemical Reactivation (EPR) for Detecting Sensitization of AISI Type 304 and 304L Stainless Steel," G 108, *Wear and Erosion; Metal Corrosion, Annual Book of ASTM Standards,* Vol 3.02, ASTM International
18. A.P. Majidi and M.A. Striecher, *Corrosion,* Vol 40, 1984, p 584–592
19. M. Akashi, T. Kawamoto, and F. Umemura, *Corros. Eng.,* (Jpn.), Vol 29, 1980, p 163
20. "Standard Test Methods for Pitting and Crevice Corrosion Resistance of Stainless Steels and Related Alloys by the Use of Ferric Chloride Solution," G 48, *Wear and Erosion; Metal Corrosion,* Vol 03.02, *Annual Book of ASTM Standards,* American Society for Testing and Materials
21. "Standard Guide for Crevice Corrosion Testing of Iron-Base and Nickel-Base Stainless Alloys in Seawater and Other Chloride Containing Aqueous Environments," G 78, *Annual Book of ASTM Standards,* American Society for Testing and Materials
22. "Practice for Preparation and Use of Bent-Beam Stress-Corrosion Test Specimens," G 39, *Metal Corrosion, Erosion, and Wear,* Vol 03.02, *Annual Book of ASTM Standards,* American Society for Testing and Materials
23. M.J. Shumaker et al., Evaluation of Various Techniques for Stress Corrosion Testing Welded Aluminum Alloys, *Stress Corrosion Testing,* STP 425, American Society for Testing and Materials, 1967, p 317–341
24. A.W. Loginow, Stress Corrosion Testing of Alloys, *Mater. Prot.,* Vol 5 (No. 5), 1966, p 33–39
25. "Practice for Preparation of Stress-Corrosion Test Specimen for Weldments," G 58, *Metal Corrosion, Erosion, and Wear,* Vol 03.02, *Annual Book of ASTM Standards,* American Society for Testing and Materials
26. "Characterization of Environmentally Assisted Cracking for Design—State of the Art," National Materials Advisory Board Report No. NMAB-386, National Academy of Sciences, 1982
27. G. Schmitt, Sophisticated Electrochemical Methods for MIC Investigation and Monitoring, *Mater. Corros.,* Vol 48, 1997, p 586–601

Index

A

alloy 2205 weldments, corrosion behavior of
chemical compositions of alloy 2205 specimens tested and filler metals used in Ref 19, 109(T)
intergranular corrosion, 109
overview, 109(T)
pitting tests, 109–112(F)
stress-corrosion cracking (SCC), 112–113(T)
aluminum alloy weldments
avoiding SCC, 147
corrosion behavior, 144–155(F,T)
corrosion resistance, 144–146(F,T)
crevice corrosion, 147
effect of chemistry control, 147
filler alloy selection, 146–147(F,T)
friction stir welding (FSW), 153–154(F)
galvanic effects, 144
knife-line attack, 147
resistance spot-welding, 147–153(F)
aluminum and aluminum alloys
overview, 143
thermal conductivity, 144
welding considerations, 143–144
American Society of Mechanical Engineers (ASME) Boiler and Pressure Vessel (B&PV), 92
argon-oxygen decarburization (AOD), 99
ASTM A 53, 25
ASTM A 262, 209, 210
ASTM A 285, 25
ASTM A 763, 84, 209, 210
ASTM G 28, 210
ASTM G 48, 213
ASTM G 78, 213
austenitic stainless steel weldments, corrosion of
amounts of principal alloying elements in stainless steels tested for pitting resistance, 54(T)
chemical compositions of nonstandard austenitic stainless steels, 45–46(T)
chemical compositions of standard austenitic stainless steels, 44(T)
corrosion associated with postweld cleaning, 67–69(F)
corrosion associated with weld backing rings, 69–70(F)
corrosion behavior, 48–49
corrosion resistance (stainless steels), 47–48
crater corrosion, 56–57
crevice corrosion, 55–56(F)
effects of GTA weld shielding gas composition, 70–71(F)
effects of heat-tint oxides on corrosion, 71–73(F)
example: microbiological corrosion butt welds in water tanks, 64–66(F)
example: SCC of a type 304 stainless steel pipe caused by residual welding stresses, 59–62
example: weld craters in stainless steel heat exchanger, 57–58
example: welding conditions and corrosion resistance of heat-tinted UNS S31726 stainless steel plate, 72(T)
grade designations, 43–47(F,T)
intergranular corrosion, 49–52(F)
MIC scenarios that may play a role in the corrosion of weldments in stainless steel, 65(T)
microbiologically induced corrosion (MIC), 62–66(F,T)
molybdenum segregation, 73–74(F)
other factors influencing corrosion of weldments, 66–74(F)
overview, 43
pitting corrosion, 53–55(F,T)
preferential attack associated with weld metal precipitates, 52–53(F)
sigma precipitation in HAZs, 66–67
stress-corrosion cracking (SCC), 58–62(F)
unmixed zones, 73(F)
welding considerations, 48
austenitic stainless steels
corrosion behavior, 48–49
corrosion resistance, 47–48
intergranular corrosion, 49–52(F)
mechanical properties of, 47
nonstandard grades, 43–44
overview, 43
standard grades, 43(F)
superaustenitic steels, 44–47
welding considerations, 48

B

bent-beam specimens, 213
bimetallic inserts, 170
body-centered cubic (bcc), 99
butt welds, 65
buttering, 170(F)
BWR piping systems, 183(F)

C

carbon steel and low-alloy steel weldments, corrosion of
absorber vessel hardness results, 27(T)
carbon steel weldments, corrosion of, 19
carbon steels, 13–14(T)
classification of steels and their welding characteristics, 13–15(T)
composition and carbon equivalent of selected low-alloy steels, 18(T)
compositions of carbon steel base metals and some filler metals subject to galvanic corrosion, 24(T)
corrosion considerations, 15
corrosion rates of galvanic couples of ASTM A 53, grade B, base metal and various filler metals in a mixture of chlorinated hydrocarbons and water, 25(T)
corrosion rates of galvanic couples of ASTM A285, grade C, base metal and various filler metals at 90 °C (195 °F) in water used to wash a hydrocarbon stream, 25(T)
effect of welding practice on weldment corrosion, 35–40(F)
environmentally assisted cracking (EAC), 24–25
galvanic corrosion, 23–24(T)
geometrical factors, 19
HAZ/fusion line corrosion of welded lead pipe, 20–21
hydrogen-induced cracking (HIC), 25, 33–35(F)
industrial case studies of galvanic corrosion, 23–24(T)
influence of weld microstructure, 19
leaking carbon steel weldments in a sulfur recovery unit, 29–30(F)
low-alloy steels, 14–15(T)
overview, 13
preferential HAZ corrosion, 20(F)
preferential weld metal corrosion, 21(F,T)
preferential weldment corrosion, mitigation of, 21–23
process selection guidelines for arc welding carbon steels, 16–17(T)
residual stress, 19
stress-corrosion cracking (SCC), 25–33(F,T)
sulfide stress cracking, 25
weld cracking in oil refinery deaerator vessels, 30–33(F,T)
welding details for the preferential weld metal corrosion study, 22(T)
welds in carbon steel deaerator tanks, corrosion of, 30
wet hydrogen sulfide cracking, 25
carbon steels
carbon steel weldments, corrosion of, 19
carbon steels classified according to carbon content, 13(T)
corrosion considerations, 15
defined, 13
high-carbon steel, 14
low-carbon steels, 13–14
medium-carbon steel, 14
welding processes, 14(T)
caustic embrittlement (caustic SCC), 58–59(F)
chloride SCC, 58(F)
chromium-molybdenum steels, 15
coefficient of linear expansion
electrical conductivity, 144
melt characteristics, 144
thermal conductivity, 144
coefficient of thermal expansion, (CTE), 48
commercially pure nickel, 128
copper and copper alloys
corrosion behavior of copper weldments, 155–156
overview, 155
welding considerations, 155
corrosion associated with weld backing rings
cracking, 69
microstructure, 69
overview, 69
preferential weld corrosion, 69–70
corrosion behavior of titanium and titanium alloy weldments
hydrogen embrittlement, 158–159
overview, 158
corrosion behavior of zirconium and zirconium alloy weldments
delayed hydride cracking (DHC), 162–163(T)
overview, 162
corrosion in the pulp and paper industry
digester weld cracking, prevention of, 193
digester welds, corrosion of, 191–192(F)
pulp production, 191
washers, corrosion of, 187–197
weldments in pulp bleach plants, corrosion of, 196–200(T)
corrosion of austenitic stainless steel weldments. *see* austenitic stainless steel weldments, corrosion of
corrosion of dissimilar metal weldments. *see* dissimilar metal weldments, corrosion of
corrosion of duplex stainless steel weldments. *see* duplex stainless steel weldments, corrosion of
corrosion of ferritic stainless steel weldments. *see* ferritic stainless steel weldments, corrosion of
corrosion of high-nickel alloy weldments. *see* high-nickel alloy weldments, corrosion of
corrosion of martensitic stainless steels weldments. *see* martensitic stainless steel weldments, corrosion of
corrosion of nonferrous alloy weldments. *see* nonferrous alloy weldments, corrosion of
corrosion-resistant alloys (CRAs), 125
commercially pure nickel, 128
nickel-chromium alloys, 129
nickel-chromium-iron alloys, 130
nickel-chromium-molybdenum alloys (C-type alloys), 129–130
nickel-copper alloys, 128
nickel-iron-chromium alloys, 130

nickel-molybdenum alloys, 128–129
types of, 125–130
welding metallurgy of CRAs containing molybdenum, 132–134(F)
corrosion-resistant cladding, 188–189(F)
coupons
crevice-corrosion coupons, 206
stress-corrosion coupons, 205–206
welded coupons, 205
coupons, definition of, 203
coupons, direct testing of
advantages of, 203–204
coupon options, 204–206(F)
disadvantages of, 204
overview, 203
sensitized metal, 205
welded coupons, 205
crater corrosion, 56–57
crevice corrosion, 55–56(F)

D

dead end legs, 188
delayed cracking, 7
delayed hydride cracking (DHC), 162–163(T)
dilution, 170
dissimilar metal weldments, corrosion of
bimetallic inserts, 170
buttering, 170(F)
chemical composition of base and filler metals, wt %, 173(T)
coefficient of thermal expansion, 171
corrosion behavior, 173–174(F)
dilution, 170
galvanic corrosion and oxidation resistance, 173
hydrogen-induced cracking, 173–174(F,T)
joint integrity, factors influencing, 169
melting temperatures, 170
overview, 169
postweld heat treatment (PWHT), 174–175
property considerations, 172–173
sensitization, 174–175
suitable filler material, selection of, 171–172(F)
thermal conductivity, 170–171
weld metal, 169–170
duplex stainless steel weldments, corrosion of
comparison of mechanical properties of commonly used stainless steels in the annealed condition, 103(T)
composition and pitting resistance equivalent numbers (PREN) of wrought duplex stainless steels covered by UNS designations, 100(T)
corrosion behavior of alloy 2205 weldments, 109–113(F,T)
corrosion behavior of weldments, 105–109(F)
corrosion rate in selected chemical environments, 104(T)
corrosion resistance of Ferralium alloy 255 weldments using various nickel-base alloy-fillers and weld techniques, 112(T)
critical crevice corrosion temperatures, 104(T)
development and grade designations, 99–100(F,T)
effect of welding and pitting and SCC resistance, 107–108(F)
filler metal requirements, 104–105
fusion welding, 103–104
hydrogen-induced cracking (HIC), 108–109
influence of ferritic austenite balance on corrosion resistance, 106–107(F)
microstructure and properties, 100–102(F,T)
overview, 99
welding considerations, duplex stainless steels, 103–105
duplex stainless steels
corrosion behavior of weldments, 105–109(F)
corrosion resistance, 101–102(F,T)
development and grade designations, 99–100(F,T)
effect of welding and pitting and SCC resistance, 107–108(F)
elevated-temperature properties, 101
filler metal requirements, 104–105
hydrogen-induced cracking (HIC), 108–109
influence of ferritic austenite balance on corrosion resistance, 106–107(F)
mechanical properties, 101(T)
microstructure, 100–101(F)
overview, 99
postweld heat treatment (PWHT), 105
preheat, 105

E

electric-resistance-welded/high-frequency-induction-welded (ER/HFI) pipe, 21
electrochemical impedance spectroscopy (EIS), 206–207
electrochemical noise (EN), 207
electrogas welding processes, 15
electron microscopy/energy dispersive spectroscopy (SEM/EDS), 194(F), 197–198
electroslag welding processes, 15
end-grain attack. *see* intergranular corrosion
energy-dispersive x-ray spectros-copy (EDS), 39
environmentally assisted cracking (EAC), 24–25, 178

F

feedwater economizer
design and fabrication, 92–93
harp assembly, 92–93
performance, 93(F)
ferritic stainless steel weldments, corrosion of
corrosion behavior, 82–87(F,T)
corrosion resistance, 80
example: chemical composition of Group II ferritic stainless steels, 79(T)
example: nominal chemical composition of representative Group I standard-grade 400 series ferritic stainless steels, 78(T)
example: nominal chemical compositions of Group III intermediate-purity ferritic stainless steels, 79(T)

ferritic stainless steel weldments, corrosion of (continued)
example: nominal chemical compositions of Group III ultrahigh-purity ferritic stainless steel, 80(T)
example: results of ASTM A 763, practice Z, on representative as-welded ferritic stainless steels, 84(T)
example: results of ASTM A 763, practice Z, tests on as-welded ferritic stainless steels with titanium or niobium, 85(T)
example: typical ferritic base metal-filler metal combinations, 81(T)
ferritic stainless steel metallurgy, 90–92(F)
grade classifications, 77–79(F,T)
hydrogen embrittlement, 82–83
intergranular corrosion, 83–84
intergranular corrosion, avoiding, 84–87(F,T)
limits of interstitial element (C + N) content for acceptable as-welded intergranular corrosion resistance and as-welded ductility, 84(T)
lower interstitial levels, 84–87(F,T)
overview, 77
proper welding and PWHAT procedures, 85–87(F,T)
properties, 79–80
stabilization of carbon and nitrogen, 85(T)
welding consideration, 80–82(F,T)
ferritic stainless steels
classified as, 77(T)
corrosion behavior, 82–87(F,T)
corrosion resistance, 80
example: nominal chemical composition of representative group I, 78–79(T)
Group I alloys, 77(F)
Group II alloys, 78–79(T)
Group III alloys, 79(T)
hydrogen embrittlement, 82–83
intergranular corrosion, 83–84
intergranular corrosion, avoiding, 84–87(F,T)
lower interstitial levels, 84–87(F,T)
mechanical properties of, 79–80
metallurgy, 90–92(F)
overview, 77
weldability, 81–82(F)
welding consideration,, 80–82(F,T)
friction stir welding (FSW), 153–154(F)
fusion welding, 103–104
fusion zone, the, 2(F)

G

***Gallionella*,** 64
galvanic corrosion, 23–24(T)
industrial case studies of galvanic corrosion, 23–24(T)
galvanic couples, 3–4(F)
gas-metal arc welding (GMAW), 80, 104
gas-tungsten arc welding (GTAW), 80, 103, 186
grain dropping. *see* intergranular corrosion

H

heat-affected zone (HAZ), 1, 48
HAZ/fusion line corrosion of welded lead pipe, 20–21
preferential HAZ corrosion, 20(F)
sigma precipitation in HAZs, 66–67
heat-recovery steam generator (HRSG), 89–90(T)
heat-resistant alloys (HRAs), 125
heat-tint oxide
effects on corrosion-resistance, 71–73(F)
formation, 10
heat-treatable low-alloy (HTLA) steels, 15
high-carbon high-chromium martensitic grades, 116
high-carbon steel, 14
high-level waste, 156
high-nickel alloy weldments, corrosion of
corrosion behavior, 134–137(F,T)
corrosion-resistance alloys (CRAs), types of, 125–130(F,T)
filler metal selection, 132
nickel-chromium-molybdenum alloys, corrosion behavior, 136–137(F)
nickel-molybdenum alloys, corrosion behavior, 135–136(F)
nominal compositions of nickel alloys resistant to aqueous corrosion, 127(T)
overview, 125
phase stability of nickel-base alloys and corrosion behavior, 137–141(F,T)
welding considerations, 130–132
welding metallurgy of CRAs containing molybdenum, 132–134(F)
welding metallurgy of Ni-Cu, Ni-Cr, and Ni-Cr-Fe CRAs, 134
high-pressure (HP), 90
high-strength low-allow (HSLA) steels, 14, 181
high-temperature alloys (HTAs), 125
hydrogen embrittlement
ferritic stainless steels, 82–83
titanium and titanium alloys, 158–159(F)
hydrogen-induced cold cracking, 7(F)
hydrogen-induced cracking (HIC), 25, 33–35(F), 108–109, 177
cracks, difficulty in detecting, 34
defined, 33
description of, 33(F)
occurrences, when/where, 33(F)
steels, susceptibility to, 34–35(F)
toe cracks, 34(F)
transverse cracking, 34
hydrogen-induced disbonding, 181(F)

I

induction heating stress improvement, 189–190(F)
intergranular attack (IGA), 192. *see also* intergranular corrosion
intergranular corrosion
avoiding, 50(F)
ferritic stainless steels, 83–87(F,T)
intergranular SCC, 52
knife-line attack, 51–52
low-temperature sensitization, 51
mechanism, 49–50(F)

intergranular corrosion (continued)
sensitized HAZs in type 304 and 316 stainless steels, 50–52
intergranular SCC, 52
intergranular stress-corrosion cracking (IGSCC), 58, 183–191(F), 193–195, 198(F)

K

knife-line attack, 51–52, 147
Kraft process, 191

L

laser beam welding (LBW), 158
last-past heat sink welding, 190(F)
leaking carbon steel weldments in a sulfur recovery unit
investigation, 29–30(F)
overview, 29
preventive measures, 30
linear polarization resistance (LPR), 206
liquid metal embrittlement, 181–182(F)
low-alloy steels
chromium-molybdenum steels, 15
corrosion considerations, 15
defined, 14(T)
heat-treatable low-alloy (HTLA) steels, 15
high-strength low-allow (HSLA) steels, 14
quench-and-tempered steels, 14–15
thermal-mechanical-controlled processing (TCMP) steels, 15
welding processes, 15
low-carbon, nickel-containing martensitic grades, 115–116
low-carbon, nickel-free martensitic grades, 115
low-carbon steels, 13–14
low-pressure (LP), 90
low-temperature sensitization, 51

M

manual metal arc (MMA), 21
martensitic stainless steel weldments, corrosion of
chemical compositions of martensitic stainless steels, 117–118(T)
chemical compositions of selected supermartensitic stainless steels, 123(T)
corrosion behavior, 118–123(T)
corrosion /oxidation resistance and typical applications of martensitic stainless steels, 119–120(T)
grade designations, 115–117(F,T)
heat treat cycles and mechanical properties for type 410 stainless steel, 122(T)
overview, 115
properties, 117–118(T)
sulfide stress corrosion results for type 410 stainless steel, 123(T)
sulfide stress corrosion (SSC) resistance of type 410 weldments, 121–122(T)
supermartensitic stainless steels, 122–123
welding considerations, 118
martensitic stainless steels
corrosion resistance and oxidation resistance, 118(T)
grade designations, 115–117(F,T)
high-carbon high-chromium martensitic grades, 116
hydrogen-induced cracking, 118–121
low-carbon, nickel-containing martensitic grades, 115–116
low-carbon, nickel-free martensitic grades, 115
mechanical properties, 117–118(T)
non-standard grades, 116–117(T)
overview, 115
postweld heat treatment (PWHT), 118
standard grades, 115–116(F,T)
medium-carbon steel, 14
melting temperatures, 170
microbiologically induced corrosion (MIC), 62–66(F,T)
failure analysis, recommendations for, 63–64
improve resistance to, 63
microbiologically induced intergranular pitting, 62
overview, 9, 62
preferential attack, 62(F)
radiography or destructive testing, 64(F)
surface deposits, 64(F)
transgranular pitting, 62–63
trends, 63
mitigation of IGSCC in boiling water reactors
corrosion-resistant cladding, 188–189(F)
environmental solutions, 190–191
materials solutions, 188–189(F)
nuclear-grade stainless steels, 188
overview, 187–188
solution heat treatment, 188
weld overlay repair, 189(F)
molybdenum segregation, 73–74(F)
monitoring and testing of weld corrosion
acoustic emission testing, 208
appropriate evaluation tests and acceptance criteria for wrought alloys, 212(T)
ASTM G 48, 213
ASTM G 78, 213
ASTM standard practices in A 262 for detecting susceptibility to intergranular corrosion in austenitic stainless steels, 210(T)
ASTM standard practices in A 763 for detecting susceptibility to intergranular attack in ferritic stainless steels, 210(T)
ASTM standard test methods in G 28 for detecting susceptibility to intergranular attack in wrought, nickel-rich, chromium bearing alloys, 210(T)
bent-beam specimens, 213
boiling copper sulfate tests in ASTM A 262 and A 763, 209(T)
corrosion monitoring, 203–208(F)
corrosion testing, 208–213(F,T)
coupons, direct testing of, 203–206(F)
eddy current testing, 208
electrochemical impedance spectroscopy (EIS), 206–207
electrochemical monitoring methods used for MIC, 214(T)

monitoring and testing of weld corrosion (continued)
electrochemical noise (EN), 207
electrochemical techniques, 206–207
infrared thermography, 208
linear polarization resistance (LPR), 206
MIC, tests for, 215(T)
nondestructive testing techniques, 207–208
overview, 203
pitting and crevice corrosion, tests for, 213
radiography, 208
residual-stress specimens, 214(F)
SCC, tests for, 213–215(F)
special considerations for testing of weldments, 214–215(F)
tests for intergranular corrosion, 209–213(F,T)
tests for stainless steels and nickel-base alloys, 209–213(F,T)
ultrasonic testing of welds in the bypass lines of a boiling water reactor, 208(F)
ultrasonic thickness measurements, 207–208
weld specimens, 214(F)
welded double-beam specimens, 213–214(F)
monoethanolamine (MEA), 28

N

National Materials Advisory Board, 215
nickel-base alloys
chromium, 126
copper, 126
corrosion-resistance alloys (CRAs), types of, 125–130(F,T)
filler metal selection, 132
iron, 126
molybdenum, 126
nickel, 126
overview, 125
roles of various elements in, 126–128
tungsten, 126
welding considerations, 130–132
welding processes, 131–132
nickel-chromium alloys, 129
nickel-chromium-molybdenum alloys (C-type alloys), 129–130
nickel-molybdenum alloys, 128–129
nondestructive testing (NDT), 207
nonferrous alloy weldments, corrosion of
aluminum and aluminum alloys, 143–156(F,T)
ASME mechanical requirements for Zr702 and Zr705 used for unfired pressure vessels, 163(T)
classification of wrought aluminum alloys according to their strengthening mechanism, 144(T)
copper and copper alloys, 155–156
corrosion behavior of aluminum alloy weldments, 144–155(F,T)
corrosion behavior of tantalum and tantalum alloy weldments, 164–166
corrosion behavior of titanium and titanium alloy weldments, 158–159(F)
corrosion behavior of zirconium and zirconium alloy weldments, 162–164(T)
delayed hydride cracking (DHC), 162–163(T)
designations and nominal compositions of several titanium-base alloys, 157(T)
example: failure of pressure vessel welds due to hydrogen embrittlement, 159–160(F)
example: preferential pitting of a tantalum alloy weldment in H_2SO_4 service, 165–166
nuclear and nonnuclear grades of zirconium alloys, 161(T)
overview, 143
relative rating of selected aluminum filler alloys used to fillet weld or butt weld two compound base alloys, 148–153(T)
tantalum and tantalum alloys, 164–167
titanium and titanium alloys, 156–160(F,T)
welding considerations, 155
zirconium and zirconium alloys, 160–164(T)

P

phase stability of nickel-base alloys and corrosion behavior
changes in the corrosion rate of alloy N06022 as a consequence of second-phase precipitation, 139–141(F)
effect of intermetallic phases, 138–139(T)
second-phase precipitation, 137–138(T)
pitting, 5–7
polarization resistance, 206
postweld cleaning, corrosion associated with, 67–69(F)
postweld heat treatment (PWHT)
austenitic stainless steels, 48
carbon steel and low-allow steels, 13
duplex stainless steels, 105
ferritic stainless steels, 85–87(F,T)
martensitic stainless steels, 118
overview, 10
preferential weld metal corrosion, 21(F,T)
preferential weldment corrosion, mitigation of, 21–23
preheat and interpass temperature, 10
preheat (duplex stainless steels), 105

Q

quench-and-tempered steels, 14–15

R

radioactive waste, 156
residual-stress specimens, 214(F)

S

sensitized HAZs in type 304 and 316 stainless steels, 50–52(F)
sensitized metal, 205
service propulsion system (SPS), 159
shear-wave ultrasonic (SWU), 30
shielded metal arc welding (SMAW), 104, 186
sigma precipitation in HAZs, 66–67
spent nuclear fuel, 156
stainless steel
nuclear-grade stainless steels, 188

stainless steel (continued)
role of delta ferrite in stainless steel weld deposits, 5(F)
weld decay of, 4–5(F)
stress-corrosion coupons, 205–206
stress-corrosion cracking of C-Mn steel in a CO_2 absorber in a chemical plant
background, 26(F,T)
circumstances leading to failure, 26
conclusions and recommendations, 28
discussion, 28
impact toughness, 26–27
mechanical properties, 26–27
microstructural analysis, 26(F)
nondestructive evaluation, 26
overview, 25–26(T)
simulation tests, 27–28
stress-corrosion cracking (SCC), 3, 43
caustic embrittlement (caustic SCC), 58–59(F)
chloride SCC, 58(F)
corrosion of welds in carbon steel deaerator tanks, 30
defined, 25
due to nitrates, 28
methods for controlling, 59
in oil refineries, 28–29
overview, 58(F)
pipe weldments, 183–184(F)
SCC due to welding residual stresses, 25
stress-corrosion cracking of C-Mn steel in a CO2 absorber in a chemical plant, 25–28(F,T)
weld cracking in oil refinery deaerator vessels, 30–33(F,T)
submerged arc welding (SAW), 104, 186
sugaring. *see* intergranular corrosion
sulfate-reducing bacteria (SRB), 63
sulfide stress corrosion (SSC) resistance of type 410 weldments, 121–122(T)
sulfide stress cracking, 25, 178–179
superaustenitic steels, 44–47
supermartensitic stainless steels, 122–123

T

tantalum and tantalum alloys
corrosion behavior of weldments, 164–166
overview, 164
welding considerations, 164
tensile stress reduction solutions
heat sink welding, 189
induction heating stress improvement, 189–190(F)
last-pass heat sink welding, 190(F)
The Welding Institute (TWI), 181
thermal conductivity, 170–171
thermal-mechanical-controlled processing (TMCP) steels, 15
titanium and titanium alloys
corrosion behavior of weldments, 158–159(F)
overview, 156–157(T)
welding considerations, 157–158
toe cracks, 34(F)
transverse cracking, 34

U

unaffected base metal, 2–3
unmixed zones, 73(F)

W

weld backing rings, 69–70(F)
weld corrosion. *see* monitoring and testing of weld corrosion
weld corrosion, basic understanding of
corrosion resistance, maintaining, 1
cracking due to environments containing hydrogen sulfide, 7–9
delayed cracking, 7
factors influencing corrosion of weldments, 1
forms of weld corrosion, 3–10(F)
heat-tint oxide formation, 10
hydrogen-induced cold cracking, 7
metallurgical factors, 1
microbiologically induced corrosion (MIC), 9
overview, 1
pitting, 5–7
role of delta ferrite in stainless steel weld deposits, 5(F)
stress-corrosion cracking (SCC), 7
weld decay of stainless steel, 4–5(F)
weld microstructures, 1–3(F)
welding practice to minimize corrosion, 10
weld corrosion, forms of
cracking due to environments containing hydrogen sulfide, 7–9
delayed cracking, 7
galvanic couples, 3–4(F)
heat-tint oxide formation, 10
hydrogen-induced cold cracking, 7(F)
microbiologically influenced corrosion (MIC), 9
pitting, 5–7
role of delta ferrite in stainless steel weld deposits, 5(F)
stress-corrosion cracking (SCC), 7
weld decay of stainless steel, 4–5(F)
weld corrosion in specific industries and environments
BWR piping systems, 183(F)
dead end legs, 188
example: intergranular corrosion/cracking of a stainless steel pipe reducer section in bleached pulp stock service, 197–200(F)
fabricability considerations, 177–178
hydrogen-induced disbonding, 181(F)
IGSCC in boiling water reactors, mitigation of, 187–191(F)
intergranular stress-corrosion cracking (IGSCC), 183–184(F)
liquid metal embrittlement, 181–182(F)
maximum tensile surface residual stresses caused by surface treatments of type 304, 187(T)
mechanical properties of weldments, 186–187(F)
model for IGSCC, 184–185(F)
nuclear grades (NG), 188
overview, 177

weld corrosion in specific industries and environments (continued)
permanence of weld residual stresses, 186(F)
petroleum refining and petrochemical operations, corrosion of weldments in, 177
principle causes of corrosion of austenitic stainless steel weldments, 196(T)
pulp and paper industry, corrosion in, 191–200(F,T)
stress-corrosion cracking of pipe weldments, 183–184(F)
tensile stress reduction solutions, 189–190(F)
weld preparation method, effect of, 187
weld residual stresses, 185–187(F,T)
weldments in BWR service, stress corrosion cracking of, 183
wet H2S cracking, 178–181(F)
zinc embrittlement, prevention of, 182–183
weld corrosion, monitoring and testing of
acoustic emission testing, 208
appropriate evaluation tests and acceptance criteria for wrought alloys, 212(T)
ASTM G 48, 213
ASTM G 78, 213
ASTM standard practices in A 262 for detecting susceptibility to intergranular corrosion in austenitic stainless steels, 210(T)
ASTM standard practices in A 763 for detecting susceptibility to intergranular attack in ferritic stainless steels, 210(T)
ASTM standard test methods in G 28 for detecting susceptibility to intergranular attack in wrought, nickel-rich, chromium bearing alloys, 210(T)
bent-beam specimens, 213
boiling copper sulfate tests in ASTM A 262 and A 763, 209(T)
corrosion monitoring, 203–208(F)
corrosion testing, 208–213(F,T)
coupons, direct testing of, 203–206(F)
eddy current testing, 208
electrochemical impedance spectroscopy (EIS), 206–207
electrochemical monitoring methods used for MIC, 214(T)
electrochemical noise (EN), 207
electrochemical techniques, 206–207
infrared thermography, 208
linear polarization resistance (LPR), 206
MIC, tests for, 215(T)
nondestructive testing techniques, 207–208
overview, 203
pitting and crevice corrosion, tests for, 213
radiography, 208
residual-stress specimens, 214(F)
SCC, tests for, 213–215(F)
special considerations for testing of weldments, 214–215(F)
tests for intergranular corrosion, 209–213(F,T)
tests for stainless steels and nickel-base alloys, 209–213(F,T)
ultrasonic testing of welds in the bypass lines of a boiling water reactor, 208(F)
ultrasonic thickness measurements, 207–208
weld specimens, 214(F)
welded double-beam specimens, 213–214(F)
weld cracking in oil refinery deaerator vessels
conclusions, 32–33
discussion, 32
inspection results, 31
metallurgical analysis, 31–32(F,T)
overview, 30–31(T)
recommendations, 33
weld decay, 49
weld microstructures
fusion zone, the, 2(F)
heat-affected zone (HAZ), 2
microstructural gradients, 3
overview, 1–2(F)
unaffected base metal, 2–3
weld residual stresses
mechanical properties of weldments, 186–187(F)
overview, 185–186(F)
permanence of, 185(F)
weld preparation method, effect of, 187(T)
weldability, defined, 81–82(F)
welded coupons, 205
welded double-beam specimens, 213–214(F)
welding
butt welds, 65
example: leaking welds in a ferritic stainless steel wastewater vaporizer, 87–89(F)
friction stir welding (FSW)
gas-tungsten arc welding (GTAW), 186
heat sink welding, 189
last-pass heat sink welding, 190(F)
process selection guidelines for arc welding carbon steels, 16–17(T)
proper welding and PWHAT procedures, ferritic stainless steels, 85–87(F,T)
relative rating of selected aluminum filler alloys used to fillet weld or butt weld two compound base alloys, 148–153(T)
resistance spot-welding, 147–153(F)
shielded metal arc welding (SMAW), 186
submerged arc welding (SAW), 186
weld failure due to intergranular corrosion and cracking in a heat-recovery steam generator, 89–96(F,T)
weld metal, 169–170
welded coupons, 205
welding considerations, aluminum and aluminum alloys, 143–144
welding considerations, austenitic steels, 48
welding considerations, copper and copper alloys, 155
welding considerations, duplex stainless steels, 103–105
welding considerations, ferritic stainless steels, 80–82(F,T)
welding considerations, martensitic stainless steels, 118
welding considerations, nickel-base alloys, 130–132
welding considerations, tantalum and tantalum alloys, 164
welding considerations, titanium and titanium alloys, 157–158

welding considerations, zirconium and zirconium alloys, 161–162
welding processes, carbon steels, 14(T)
welding processes, low-alloy steels, 15
welding processes, nickel-base alloys, 131–132
welding metallurgy of CRAs containing molybdenum
fusion zone, 132–134(F)
overview, 132
welding metallurgy of Ni-Cu, Ni-Cr, and Ni-Cr-Fe CRAs
grain boundary precipitation in the HAZ, 134
microsegregation in the fusion zone of autogenous welds, 134
welding practice on weldment corrosion, effect of
conclusions and recommendations, 40
discussion, 39–40
investigation, 35–39(F)
mechanical properties, 37
overview, 35
wet H_2S cracking
environmentally assisted cracking (EAC), 25
hydrogen-induced cracking, 179(F)
refinery experience with SSC, 179–181(F)
sulfide stress cracking, 178–179

X

x-ray diffraction (XRD), 39

Z

zinc embrittlement, prevention of, 182–183
zirconium and zirconium alloys
corrosion behavior of zirconium and zirconium alloy weldments, 162–164(T)
major categories for, 160(T)
nonnuclear applications, 161
nuclear-grade zirconium, major use of, 161
nuclear/nonnuclear, differences between, 160–161
overview, 160–161(T)
welding considerations, 161–162

ASM International is the society for materials engineers and scientists, a worldwide network dedicated to advancing industry, technology, and applications of metals and materials.

ASM International, Materials Park, Ohio, USA
www.asminternational.org

Publication title	Product code
Corrosion of Weldments	05182G

To order products from ASM International:

Online Visit www.asminternational.org/bookstore

Telephone 1-800-336-5152 (US) or 1-440-338-5151 (Outside US)

Fax 1-440-338-4634

Mail Customer Service, ASM International
9639 Kinsman Rd, Materials Park, Ohio 44073-0002, USA

Email CustomerService@asminternational.org

In Europe American Technical Publishers Ltd.
27-29 Knowl Piece, Wilbury Way, Hitchin Hertfordshire SG4 0SX, United Kingdom
Telephone: 01462 437933 (account holders), 01462 431525 (credit card)
www.ameritech.co.uk

In Japan Neutrino Inc.
Takahashi Bldg., 44-3 Fuda 1-chome, Chofu-Shi, Tokyo 182 Japan
Telephone: 81 (0) 424 84 5550